FIFTH EDITION

COULSON & RICHARDSON'S CHEMICAL ENGINEERING

J M Coulson & J F Richardson
with J R Backhurst & J H Harker



VOLUME 2

Particle Technology & Separation Processes

Intas Exhibit 1032
Page 1 of 470
PGR2025-00043

Coulson and Richardson's

CHEMICAL ENGINEERING

VOLUME 2
FIFTH EDITION

Particle Technology and
Separation Processes

Intas Exhibit 1032
Page 2 of 470
PGR2025-00043

This book belongs to Bradley Loren
(bloren@mcandrews-ip.com)

Copyright Elsevier 2024

Related Butterworth-Heinemann Titles in the Chemical Engineering Series by
J. M. COULSON & J. F. RICHARDSON

Chemical Engineering, Volume 1, Sixth edition
Fluid Flow, Heat Transfer and Mass Transfer
(with J. R. Backhurst and J. H. Harker)

Chemical Engineering, Volume 3, Third edition
Chemical and Biochemical Reaction Engineering, and Control
(edited by J. F. Richardson and D. G. Peacock)

Chemical Engineering, Volume 6, Third edition
Chemical Engineering Design
(R. K. Sinnott)

Chemical Engineering, Solutions to Problems in Volume 1
(J. R. Backhurst, J. H. Harker and J. F. Richardson)

Chemical Engineering, Solutions to Problems in Volume 2
(J. R. Backhurst, J. H. Harker and J. F. Richardson)

This book belongs to Bradley Loren (bloren@mcandrews-ip.com)

Copyright Elsevier 2024

Intas Exhibit 1032
Page 4 of 470
PGR2025-00043

Coulson and Richardson's

CHEMICAL ENGINEERING

VOLUME 2
FIFTH EDITION

Particle Technology and Separation Processes

J. F. RICHARDSON

University of Wales Swansea

and

J. H. HARKER

University of Newcastle upon Tyne

with

J. R. BACKHURST

University of Newcastle upon Tyne

BUTTERWORTH HEINEMANN

OXFORD AMSTERDAM BOSTON LONDON NEW YORK PARIS
SAN DIEGO SAN FRANCISCO SINGAPORE SYDNEY TOKYO

This book belongs to Bradley Loren (bloren@mcandrews-ip.com)

Copyright Elsevier 2024

Intas Exhibit 1032
Page 5 of 470
PGR2025-00043

Butterworth-Heinemann
An imprint of Elsevier Science
Linacre House, Jordan Hill, Oxford OX2 8DP
225 Wildwood Avenue, Woburn, MA 01801-2041

First published 1955
Reprinted (with revisions) 1956, 1959, 1960
Reprinted 1962
Second edition 1968
Reprinted 1976
Third edition (SI units) 1978
Reprinted (with revisions) 1980, 1983, 1985, 1987, 1989
Fourth edition 1991
Reprinted (with revisions) 1993, 1996, 1997, 1998, 1999, 2001
Fifth edition 2002

Copyright © 1991, 2002, J. F. Richardson and J. H. Harker. All rights reserved

The right of J. F. Richardson and J. H. Harker to be identified as the authors of this work has been asserted in accordance with the Copyright, Designs and Patents Act 1988

All rights reserved. No part of this publication may be reproduced in any material form (including photocopying or storing in any medium by electronic means and whether or not transiently or incidentally to some other use of this publication) without the written permission of the copyright holder except in accordance with the provisions of the Copyright, Designs and Patents Act 1988 or under the terms of a licence issued by the Copyright Licensing Agency Ltd, 90 Tottenham Court Road, London, England W1P 0LP. Applications for the copyright holder's written permission to reproduce any part of this publication should be addressed to the publishers

British Library Cataloguing in Publication Data
A catalogue record for this book is available from the British Library

Library of Congress Cataloguing in Publication Data
A catalogue record for this book is available from the Library of Congress

ISBN 0 7506 4445 1

Typeset by Laserwords Private Limited, Chennai, India
Printed and bounded in Great Britain by the Bath Press, Bath

This book belongs to Bradley Loren (bloren@mcandrews-ip.com)
Copyright Elsevier 2024

Contents

Preface to the Fifth Edition xvii

Preface to Fourth Edition xix

Preface to the 1983 Reprint of the Third Edition xxi

Preface to Third Edition xxiii

Preface to Second Edition xxv

Preface to First Edition xxvii

Acknowledgements xxix

Introduction xxxi

1. Particulate Solids 1

1.1 Introduction 1
1.2 Particle characterisation 2
1.2.1 Single particles 2
1.2.2 Measurement of particle size 3
1.2.3 Particle size distribution 10
1.2.4 Mean particle size 11
1.2.5 Efficiency of separation and grade efficiency 17
1.3 Particulate solids in bulk 22
1.3.1 General characteristics 22
1.3.2 Agglomeration 22
1.3.3 Resistance to shear and tensile forces 23
1.3.4 Angles of repose and of friction 23
1.3.5 Flow of solids in hoppers 25
1.3.6 Flow of solids through orifices 27
1.3.7 Measurement and control of solids flowrate 27
1.3.8 Conveying of solids 29
1.4 Blending of solid particles 30
1.4.1 The degree of mixing 30
1.4.2 The rate of mixing 33
1.5 Classification of solid particles 37
1.5.1 Introduction 37
1.5.2 Gravity settling 40
1.5.3 Centrifugal separators 46
1.5.4 The hydrocyclone or liquid cyclone 48
1.5.5 Sieves or screens 55
1.5.6 Magnetic separators 58
1.5.7 Electrostatic separators 61
1.5.8 Flotation 62
1.6 Separation of suspended solid particles from fluids 67
1.6.1 Introduction 67
1.6.2 Gas cleaning equipment 72
1.6.3 Liquid washing 87

This book belongs to Bradley Loren (bloren@mcandrews-ip.com) Copyright Elsevier 2024

Intas Exhibit 1032
Page 7 of 470
PGR2025-00043

1.7 Further reading 91
1.8 References 92
1.9 Nomenclature 93

2. Particle size reduction and enlargement 95

2.1 Introduction 95
2.2 Size reduction of solids 95
2.2.1 Introduction 95
2.2.2 Mechanism of size reduction 96
2.2.3 Energy for size reduction 100
2.2.4 Methods of operating crushers 103
2.2.5 Nature of the material to be crushed 105
2.3 Types of crushing equipment 106
2.3.1 Coarse crushers 106
2.3.2 Intermediate crushers 110
2.3.3 Fine crushers 117
2.3.4 Specialised applications 137
2.4 Size enlargement of particles 137
2.4.1 Agglomeration and granulation 137
2.4.2 Growth mechanisms 138
2.4.3 Size enlargement processes 140
2.5 Further reading 143
2.6 References 143
2.7 Nomenclature 144

3. Motion of particles in a fluid 146

3.1 Introduction 146
3.2 Flow past a cylinder and a sphere 146
3.3 The drag force on a spherical particle 149
3.3.1 Drag coefficients 149
3.3.2 Total force on a particle 153
3.3.3 Terminal falling velocities 155
3.3.4 Rising velocities of light particles 161
3.3.5 Effect of boundaries 161
3.3.6 Behaviour of very fine particles 162
3.3.7 Effect of turbulence in the fluid 163
3.3.8 Effect of motion of the fluid 163
3.4 Non-spherical particles 164
3.4.1 Effect of particle shape and orientation on drag 164
3.4.2 Terminal falling velocities 166
3.5 Motion of bubbles and drops 168
3.6 Drag forces and settling velocities for particles in non-Newtonian fluids 169
3.6.1 Power-law fluids 169
3.6.2 Fluids with a yield stress 172
3.7 Accelerating motion of a particle in the gravitational field 173
3.7.1 General equations of motion 173
3.7.2 Motion of a sphere in the Stokes' law region 176
3.7.3 Vertical motion (general case) 178
3.8 Motion of particles in a centrifugal field 185
3.9 Further reading 187
3.10 References 188
3.11 Nomenclature 189

4. Flow of fluids through granular beds and packed columns 191

4.1 Introduction 191
4.2 Flow of a single fluid through a granular bed 191

This book belongs to Bradley Loren (bloren@mcandrews-ip.com)
Copyright Elsevier 2024
Intas Exhibit 1032
Page 8 of 470
PGR2025-00043

4.2.1 Darcy's law and permeability 191
4.2.2 Specific surface and voidage 192
4.2.3 General expressions for flow through beds in terms of Carman–Kozeny equations 194
4.2.4 Non-Newtonian fluids 204
4.2.5 Molecular flow 205
4.3 Dispersion 205
4.4 Heat transfer in packed beds 211
4.5 Packed columns 212
4.5.1 General description 213
4.5.2 Packings 216
4.5.3 Fluid flow in packed columns 222
4.6 Further reading 232
4.7 References 232
4.8 Nomenclature 234

5. Sedimentation 237

5.1 Introduction 237
5.2 Sedimentation of fine particles 237
5.2.1 Experimental studies 237
5.2.2 Flocculation 245
5.2.3 The Kynch theory of sedimentation 251
5.2.4 The thickener 255
5.3 Sedimentation of coarse particles 267
5.3.1 Introduction 267
5.3.2 Suspensions of uniform particles 268
5.3.3 Solids flux in batch sedimentation 274
5.3.4 Comparison of sedimentation with flow through fixed beds 277
5.3.5 Model experiments 280
5.3.6 Sedimentation of two-component mixtures 282
5.4 Further reading 286
5.5 References 286
5.6 Nomenclature 288

6. Fluidisation 291

6.1 Characteristics of fluidised systems 291
6.1.1 General behaviour of gas–solids and liquid–solids systems 291
6.1.2 Effect of fluid velocity on pressure gradient and pressure drop 293
6.1.3 Minimum fluidising velocity 296
6.1.4 Minimum fluidising velocity in terms of terminal failing velocity 300
6.2 Liquid–solids systems 302
6.2.1 Bed expansion 302
6.2.2 Non-uniform fluidisation 306
6.2.3 Segregation in beds of particles of mixed sizes 308
6.2.4 Liquid and solids mixing 312
6.3 Gas–solids systems 315
6.3.1 General behaviour 315
6.3.2 Particulate fluidisation 315
6.3.3 Bubbling fluidisation 316
6.3.4 The effect of stirring 320
6.3.5 Properties of bubbles in the bed 320
6.3.6 Turbulent fluidisation 324
6.3.7 Gas and solids mixing 326
6.3.8 Transfer between continuous and bubble phases 328
6.3.9 Beds of particles of mixed sizes 330
6.3.10 The centrifugal fluidised bed 331
6.3.11 The spouted bed 332
6.4 Gas–liquid–solids fluidised beds 333
6.5 Heat transfer to a boundary surface 334

This book belongs to Bradley Loren (bloren@mcandrews-ip.com) Copyright Elsevier 2024

Intas Exhibit 1032
Page 9 of 470
PGR2025-00043

6.5.1 Mechanisms involved 334
6.5.2 Liquid-solids systems 334
6.5.3 Gas-solids systems 338
6.6 Mass and heat transfer between fluid and particles 343
6.6.1 Introduction 343
6.6.2 Mass transfer between fluid and particles 343
6.6.3 Heat transfer between fluid and particles 347
6.6.4 Analysis of results for heat and mass transfer to particles 352
6.7 Summary of the properties of fluidised beds 357
6.8 Applications of the fluidised solids technique 358
6.8.1 General 358
6.8.2 Fluidised bed catalytic cracking 359
6.8.3 Applications in the chemical and process industries 360
6.8.4 Fluidised bed combustion 361
6.9 Further reading 364
6.10 References 364
6.11 Nomenclature 369

7. Liquid filtration 372

7.1 Introduction 372
7.2 Filtration theory 374
7.2.1 Introduction 374
7.2.2 Relation between thickness of cake and volume of filtrate 375
7.2.3 Flow of liquid through the cloth 377
7.2.4 Flow of filtrate through the cloth and cake combined 378
7.2.5 Compressible filter cakes 379
7.3 Filtration practice 382
7.3.1 The filter medium 382
7.3.2 Blocking filtration 383
7.3.3 Effect of particle sedimentation on filtration 383
7.3.4 Delayed cake filtration 384
7.3.5 Cross-flow filtration 386
7.3.6 Preliminary treatment of slurries before filtration 386
7.3.7 Washing of the filter cake 387
7.4 Filtration equipment 387
7.4.1 Filter selection 387
7.4.2 Bed filters 389
7.4.3 Bag filters 390
7.4.4 The filter press 390
7.4.5 Pressure leaf filters 400
7.4.6 Vacuum filters 405
7.4.7 The tube press 432
7.5 Further reading 434
7.6 References 435
7.7 Nomenclature 435

8. Membrane separation processes 437

8.1 Introduction 437
8.2 Classification of membrane processes 437
8.3 The nature of synthetic membranes 438
8.4 General membrane equation 442
8.5 Cross-flow microfiltration 442
8.6 Ultrafiltration 446
8.7 Reverse osmosis 452
8.8 Membrane modules and plant configuration 455
8.9 Membrane fouling 464
8.10 Electrodialysis 465
8.11 Reverse osmosis water treatment plant 467

This book belongs to Bradley Loren (bloren@mcandrews-ip.com) Copyright Elsevier 2024

Intas Exhibit 1032
Page 10 of 470
PGR2025-00043

8.12 Pervaporation 469
8.13 Liquid membranes 471
8.14 Gas separations 472
8.15 Further reading 472
8.16 References 473
8.17 Nomenclature 474

9. Centrifugal separations 475

9.1 Introduction 475
9.2 Shape of the free surface of the liquid 476
9.3 Centrifugal pressure 477
9.4 Separation of immiscible liquids of different densities 478
9.5 Sedimentation in a centrifugal field 480
9.6 Filtration in a centrifuge 485
9.7 Mechanical design 489
9.8 Centrifugal equipment 489
9.8.1 Classification of centrifuges 489
9.8.2 Simple bowl centrifuges 490
9.8.3 Disc centrifuges — general 492
9.8.4 Disc centrifuges — various types 494
9.8.5 Decanting centrifuges 495
9.8.6 Pusher-type centrifuges 497
9.8.7 Tubular-bowl centrifuge 498
9.8.8 The ultra-centrifuge 499
9.8.9 Multistage centrifuges 499
9.8.10 The gas centrifuge 500
9.9 Further reading 500
9.10 References 500
9.11 Nomenclature 501

10. Leaching 502

10.1 Introduction 502
10.1.1 General principles 502
10.1.2 Factors influencing the rate of extraction 502
10.2 Mass transfer in leaching operations 503
10.3 Equipment for leaching 506
10.3.1 Processes involved 506
10.3.2 Extraction from cellular materials 507
10.3.3 Leaching of coarse solids 510
10.3.4 Leaching of fine solids 512
10.3.5 Batch leaching in stirred tanks 515
10.4 Countercurrent washing of solids 515
10.5 Calculation of the number of stages 519
10.5.1 Batch processes 519
10.5.2 Countercurrent washing 519
10.5.3 Washing with variable underflow 522
10.6 Number of stages for countercurrent washing by graphical methods 526
10.6.1 Introduction 526
10.6.2 The use of right-angled triangular diagrams 528
10.6.3 Countercurrent systems 533
10.6.4 Non-ideal stages 539
10.7 Further reading 540
10.8 References 540
10.9 Nomenclature 540

11. Distillation 542

11.1 Introduction 542

This book belongs to Bradley Loren (bloren@mcandrews-ip.com) Copyright Elsevier 2024

Intas Exhibit 1032
Page 11 of 470
PGR2025-00043

11.2 Vapour–liquid equilibrium 542
11.2.1 Partial vaporisation and partial condensation 544
11.2.2 Partial pressures, and Dalton's, Raoult's and Henry's laws 546
11.2.3 Relative volatility 551
11.2.4 Non-ideal systems 553
11.3 Methods of distillation — two component mixtures 555
11.3.1 Differential distillation 555
11.3.2 Flash or equilibrium distillation 556
11.3.3 Rectification 558
11.3.4 Batch distillation 559
11.4 The fractionating column 559
11.4.1 The fractionating process 559
11.4.2 Number of plates required in a distillation column 561
11.4.3 The importance of the reflux ratio 571
11.4.4 Location of feed point in a continuous still 578
11.4.5 Multiple feeds and sidestreams 578
11.5 Conditions for varying overflow in non-ideal binary systems 581
11.5.1 The heat balance 581
11.5.2 Determination of the number of plates on the $H-x$ diagram 585
11.5.3 Minimum reflux ratio 586
11.5.4 Multiple feeds and sidestreams 589
11.6 Batch distillation 592
11.6.1 The process 592
11.6.2 Operation at constant product composition 593
11.6.3 Operation at constant reflux ratio 595
11.6.4 Batch or continuous distillation 599
11.7 Multicomponent mixtures 599
11.7.1 Equilibrium data 599
11.7.2 Feed and product compositions 600
11.7.3 Light and heavy key components 600
11.7.4 The calculation of the number of plates required for a given separation 601
11.7.5 Minimum reflux ratio 605
11.7.6 Number of plates at total reflux 613
11.7.7 Relation between reflux ratio and number of plates 614
11.7.8 Multiple column systems 616
11.8 Azeotropic and extractive distillation 616
11.8.1 Azeotropic distillation 618
11.8.2 Extractive distillation 619
11.9 Steam distillation 621
11.10 Plate columns 625
11.10.1 Types of trays 625
11.10.2 Factors determining column performance 628
11.10.3 Operating ranges for trays 628
11.10.4 General design methods 630
11.10.5 Plate efficiency 631
11.11 Packed columns for distillation 638
11.11.1 Packings 638
11.11.2 Calculation of enrichment in packed columns 639
11.11.3 The method of transfer units 641
11.12 Further reading 649
11.13 References 649
11.14 Nomenclature 652

12. Absorption of gases 656

12.1 Introduction 656
12.2 Conditions of equilibrium between liquid and gas 657
12.3 The mechanism of absorption 658
12.3.1 The two-film theory 658
12.3.2 Application of mass transfer theories 659

This book belongs to Bradley Loren (bloren@mcandrews-ip.com)
Copyright Elsevier 2024
Intas Exhibit 1032
Page 12 of 470
PGR2025-00043

12.3.3 Diffusion through a stagnant gas 661
12.3.4 Diffusion in the liquid phase 662
12.3.5 Rate of absorption 663
12.4 Determination of transfer coefficients 666
12.4.1 Wetted-wall columns 666
12.4.2 Coefficients in packed towers 672
12.4.3 Coefficients in spray towers 675
12.5 Absorption associated with chemical reaction 675
12.6 Absorption accompanied by the liberation of heat 681
12.7 Packed towers for gas absorption 682
12.7.1 Construction 683
12.7.2 Mass transfer coefficients and specific area in packed towers 683
12.7.3 Capacity of packed towers 684
12.7.4 Height of column based on conditions in the gas film 686
12.7.5 Height of column based on conditions in liquid film 687
12.7.6 Height based on overall coefficients 688
12.7.7 The operating line and graphical integration for the height of a column 688
12.7.8 Capacity of tower in terms of partial pressures for high concentrations 692
12.7.9 The transfer unit 692
12.7.10 The importance of liquid and gas flowrates and the slope of the equilibrium curve 698
12.8 Plate towers for gas absorption 702
12.8.1 Number of plates by use of absorption factor 704
12.8.2 Tray types for absorption 707
12.9 Other equipment for gas absorption 709
12.9.1 The use of vessels with agitators 709
12.9.2 The centrifugal absorber 712
12.9.3 Spray towers 713
12.10 Further reading 714
12.11 References 715
12.12 Nomenclature 717

13. Liquid–liquid extraction 721

13.1 Introduction 721
13.2 Extraction processes 722
13.3 Equilibrium data 725
13.4 Calculation of the number of theoretical stages 728
13.4.1 Co-current contact with partially miscible solvents 728
13.4.2 Co-current contact with immiscible solvents 730
13.4.3 Countercurrent contact with immiscible solvents 731
13.4.4 Countercurrent contact with partially miscible solvents 734
13.4.5 Continuous extraction in columns 737
13.5 Classification of extraction equipment 742
13.6 Stage-wise equipment for extraction 744
13.6.1 The mixer–settler 744
13.6.2 Baffle-plate columns 748
13.6.3 The Scheibel column 748
13.7 Differential contact equipment for extraction 750
13.7.1 Spray columns 750
13.7.2 Packed columns 756
13.7.3 Rotary annular columns and rotary disc columns 760
13.7.4 Pulsed columns 760
13.7.5 Centrifugal extractors 761
13.8 Use of specialised fluids 763
13.8.1 Supercritical fluids 763
13.8.2 Aqueous two-phase systems 765
13.9 Further reading 766
13.10 References 767
13.11 Nomenclature 769

This book belongs to Bradley Loren (bloren@mcandrews-ip.com) Copyright Elsevier 2024

Intas Exhibit 1032
Page 13 of 470
PGR2025-00043

14. Evaporation **771**

14.1 Introduction 771
14.2 Heat transfer in evaporators 771
14.2.1 Heat transfer coefficients 771
14.2.2 Boiling at a submerged surface 773
14.2.3 Forced convection boiling 775
14.2.4 Vacuum operation 777
14.3 Single-effect evaporators 778
14.4 Multiple-effect evaporators 780
14.4.1 General principles 780
14.4.2 The calculation of multiple-effect systems 782
14.4.3 Comparison of forward and backward feeds 786
14.5 Improved efficiency in evaporation 791
14.5.1 Vapour compression evaporators 791
14.5.2 The heat pump cycle 798
14.6 Evaporator operation 802
14.7 Equipment for evaporation 805
14.7.1 Evaporator selection 805
14.7.2 Evaporators with direct heating 805
14.7.3 Natural circulation evaporators 807
14.7.4 Forced circulation evaporators 810
14.7.5 Film-type units 813
14.7.6 Thin-layer or wiped-film evaporators 814
14.7.7 Plate-type units 816
14.7.8 Flash evaporators 817
14.7.9 Ancillary equipment 819
14.8 Further reading 823
14.9 References 823
14.10 Nomenclature 825

15. Crystallisation **827**

15.1 Introduction 827
15.2 Crystallisation fundamentals 828
15.2.1 Phase equilibria 828
15.2.2 Solubility and saturation 836
15.2.3 Crystal nucleation 840
15.2.4 Crystal growth 844
15.2.5 Crystal yield 850
15.2.6 Caking of crystals 852
15.2.7 Washing of crystals 852
15.3 Crystallisation from solutions 853
15.3.1 Cooling crystallisers 853
15.3.2 Evaporating crystallisers 856
15.3.3 Vacuum (adiabatic cooling) crystallisers 857
15.3.4 Continuous crystallisers 857
15.3.5 Controlled crystallisation 860
15.3.6 Batch and continuous crystallisation 862
15.3.7 Crystalliser selection 862
15.3.8 Crystalliser modelling and design 863
15.4 Crystallisation from melts 868
15.4.1 Basic techniques 868
15.4.2 Multistage-processes 870
15.4.3 Column crystallisers 872
15.4.4 Prilling and granulation 875
15.5 Crystallisation from vapours 875
15.5.1 Introduction 875
15.5.2 Fundamentals 876
15.5.3 Sublimation processes 881
15.5.4 Sublimation equipment 884

This book belongs to Bradley Loren (bloren@mcandrews-ip.com)
Copyright Elsevier 2024
Intas Exhibit 1032
Page 14 of 470
PGR2025-00043

15.6 Fractional crystallisation 885
15.6.1 Recrystallisation from solutions 887
15.6.2 Recrystallisation from melts 887
15.6.3 Recrystallisation schemes 888
15.7 Freeze crystallisation 888
15.8 High pressure crystallisation 890
15.9 Further reading 893
15.10 References 894
15.11 Nomenclature 897

16. Drying 901

16.1 Introduction 901
16.2 General principles 901
16.3 Rate of drying 904
16.3.1 Drying periods 904
16.3.2 Time for drying 907
16.4 The mechanism of moisture movement during drying 912
16.4.1 Diffusion theory of drying 912
16.4.2 Capillary theory of drying 913
16.5 Drying equipment 918
16.5.1 Classification and selection of dryers 918
16.5.2 Tray or shelf dryers 920
16.5.3 Tunnel dryers 922
16.5.4 Rotary dryers 923
16.5.5 Drum dryers 931
16.5.6 Spray dryers 933
16.5.7 Pneumatic dryers 944
16.5.8 Fluidised bed dryers 946
16.5.9 Turbo-shelf dryers 953
16.5.10 Disc dryers 954
16.5.11 Centrifuge dryers 956
16.6 Specialised drying methods 957
16.6.1 Solvent drying 957
16.6.2 Superheated steam drying 957
16.6.3 Freeze drying 959
16.6.4 Flash drying 960
16.6.5 Partial-recycle dryers 961
16.7 The drying of gases 963
16.8 Further reading 964
16.9 References 965
16.10 Nomenclature 967

17. Adsorption 970

17.1 Introduction 970
17.2 The nature of adsorbents 974
17.2.1 Molecular sieves 975
17.2.2 Activated carbon 975
17.2.3 Silica gel 978
17.2.4 Activated alumina 978
17.3 Adsorption equilibria 979
17.3.1 Single component adsorption 980
17.3.2 The Langmuir isotherm 980
17.3.3 The BET isotherm 983
17.3.4 The Gibbs isotherm 989
17.3.5 The potential theory 991
17.4 Multicomponent adsorption 993
17.5 Adsorption from liquids 994

This book belongs to Bradley Loren (bloren@mcandrews-ip.com)
Copyright Elsevier 2024
Intas Exhibit 1032
Page 15 of 470
PGR2025-00043

17.6 Structure of adsorbents 994
17.6.1 Surface area 995
17.6.2 Pore sizes 996
17.7 Kinetic effects 1002
17.7.1 Boundary film 1003
17.7.2 Intra-pellet effects 1004
17.7.3 Adsorption 1007
17.8 Adsorption equipment 1008
17.8.1 Fixed or packed beds 1009
17.8.2 Equilibrium, isothermal adsorption in a fixed bed, single adsorbate 1012
17.8.3 Non-equilibrium adsorption — isothermal operation 1017
17.8.4 Non-equilibrium adsorption — non-isothermal operation 1022
17.9 Regeneration of spent adsorbent 1026
17.9.1 Thermal swing 1026
17.9.2 Plug-flow of solids 1027
17.9.3 Rotary bed 1034
17.9.4 Moving access 1034
17.9.5 Fluidised beds 1035
17.9.6 Compound beds 1036
17.9.7 Pressure-swing regeneration 1036
17.9.8 Parametric pumping 1040
17.9.9 Cycling-zone adsorption (CZA) 1045
17.10 Further reading 1047
17.11 References 1047
17.12 Nomenclature 1049

18. Ion Exchange 1053

18.1 Introduction 1053
18.2 Ion exchange resins 1054
18.3 Resin capacity 1054
18.4 Equilibrium 1056
18.4.1 Ion exclusion and retardation 1059
18.5 Exchange kinetics 1060
18.5.1 Pellet diffusion 1060
18.5.2 Film diffusion 1064
18.5.3 Ion exchange kinetics 1065
18.5.4 Controlling diffusion 1066
18.6 Ion exchange equipment 1066
18.6.1 Staged operations 1067
18.6.2 Fixed beds 1069
18.6.3 Moving beds 1071
18.7 Further reading 1073
18.8 References 1073
18.9 Nomenclature 1074

19. Chromatographic separations 1076

19.1 Introduction 1076
19.2 Elution chromatography 1077
19.2.1 Principles 1077
19.2.2 Retention theory 1078
19.3 Band broadening and separation efficiency 1080
19.3.1 Plate height 1081
19.3.2 Band broadening processes and particle size of packing 1081
19.3.3 Resolution 1082
19.3.4 The separating power of chromatography 1083
19.4 Types of chromatography 1083
19.4.1 Comparison of gas and liquid chromatography 1083
19.4.2 Gas chromatography (GC) 1084
19.4.3 Liquid chromatography (LC) 1084

This book belongs to Bradley Loren (bloren@mcandrews-ip.com) Copyright Elsevier 2024

Intas Exhibit 1032
Page 16 of 470
PGR2025-00043

19.4.4 Supercritical fluid chromatography (SFC) 1087
19.4.5 Chiral chromatography 1087
19.5 Large–scale elution (cyclic batch) chromatography 1088
19.5.1 Introduction 1088
19.5.2 Gas chromatography equipment 1089
19.5.3 Liquid chromatography equipment 1090
19.5.4 Process design and optimisation 1091
19.6 Selective adsorption of proteins 1093
19.6.1 Principles 1093
19.6.2 Practice 1095
19.6.3 Expanded bed adsorption 1095
19.7 Simulated countercurrent techniques 1096
19.8 Combined reaction and separation 1098
19.9 Comparison with other separation methods 1099
19.10 Further reading 1100
19.11 References 1100
19.12 Nomenclature 1103

20. Product design and process intensification 1104

20.1 Product design 1104
20.1.1 Introduction 1104
20.1.2 Design of particulate products 1106
20.1.3 The role of the chemical engineer 1108
20.1.4 Green chemistry 1108
20.1.5 New processing techniques 1109
20.2 Process intensification 1110
20.2.1 Introduction 1110
20.2.2 Principles and advantages of process intensification 1111
20.2.3 Heat transfer characteristics on rotating surfaces 1113
20.2.4 Condensation in rotating devices 1119
20.2.5 Two-phase flow in a centrifugal field 1122
20.2.6 Spinning disc reactors (SDR) 1129
20.3 Further reading 1134
20.4 References 1134

Appendix 1137

A1. Steam Tables 1138
Table 1A. Properties of saturated steam (SI units) 1139
1B. Properties of saturated steam (Centigrade and Fahrenheit units) 1142
1C. Enthalpy H of dry steam (superheated) (SI units) 1144
1D. Entropy S of dry steam (superheated) (SI units) 1144
Figure 1A. Pressure-enthalpy diagram for water and steam 1145
Figure 1B. Temperature-entropy diagram for water and steam 1146
A2. Conversion Factors for common SI units 1147

Problems 1149

Index 1185

This book belongs to Bradley Loren (bloren@mcandrews-ip.com)
Copyright Elsevier 2024
Intas Exhibit 1032
Page 17 of 470
PGR2025-00043

This Page Intentionally Left Blank

This book belongs to Bradley Loren (bloren@mcandrews-ip.com)

Copyright Elsevier 2024

CHAPTER 7

Liquid Filtration

7.1. INTRODUCTION

The separation of solids from a suspension in a liquid by means of a porous medium or screen which retains the solids and allows the liquid to pass is termed filtration.

In general, the pores of the medium are larger than the particles which are to be removed, and the filter works efficiently only after an initial deposit has been trapped in the medium. In the laboratory, filtration is often carried out using a form of Buchner funnel, and the liquid is sucked through the thin layer of particles using a source of vacuum. In even simpler cases the suspension is poured into a conical funnel fitted with a filter paper. In the industrial equivalent, difficulties are encountered in the mechanical handling of much larger quantities of suspension and solids. A thicker layer of solids has to form and, in order to achieve a high rate of passage of liquid through the solids, higher pressures are needed, and a far greater area has to be provided. A typical filtration operation is illustrated in Figure 7.1, which shows the filter medium, in this case a cloth, its support and the layer of solids, or filter cake, which has already formed.

Volumes of the suspensions to be handled vary from the extremely large quantities involved in water purification and ore handling in the mining industry to relatively small quantities, as in the fine chemical industry where the variety of solids is considerable. In most industrial applications it is the solids that are required and their physical size and properties are of paramount importance. Thus, the main factors to be considered when selecting equipment and operating conditions are:

(a) The properties of the fluid, particularly its viscosity, density and corrosive properties.
(b) The nature of the solid — its particle size and shape, size distribution, and packing characteristics.
(c) The concentration of solids in suspension.
(d) The quantity of material to be handled, and its value.
(e) Whether the valuable product is the solid, the fluid, or both.
(f) Whether it is necessary to wash the filtered solids.
(g) Whether very slight contamination caused by contact of the suspension or filtrate with the various components of the equipment is detrimental to the product.
(h) Whether the feed liquor may be heated.
(i) Whether any form of pretreatment might be helpful.

Filtration is essentially a mechanical operation and is less demanding in energy than evaporation or drying where the high latent heat of the liquid, which is usually water, has to be provided. In the typical operation shown in Figure 7.1, the cake gradually builds up

This book belongs to Bradley Loren (bloren@mcandrews-ip.com) Copyright Elsevier 2024

Intas Exhibit 1032
Page 19 of 470
PGR2025-00043

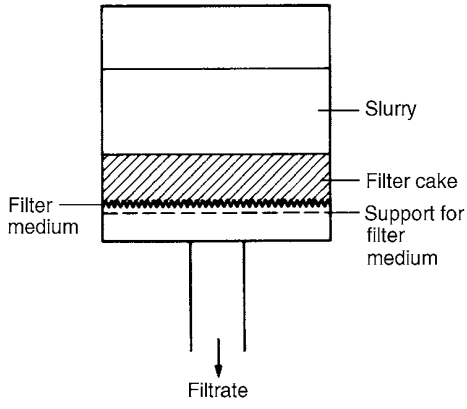


Figure 7.1. Principle of filtration

on the medium and the resistance to flow progressively increases. During the initial period of flow, particles are deposited in the surface layers of the cloth to form the true filtering medium. This initial deposit may be formed from a special initial flow of precoat material which is discussed later. The most important factors on which the rate of filtration then depends will be:

(a) The drop in pressure from the feed to the far side of the filter medium.
(b) The area of the filtering surface.
(c) The viscosity of the filtrate.
(d) The resistance of the filter cake.
(e) The resistance of the filter medium and initial layers of cake.

Two basic types of filtration processes may be identified, although there are cases where the two types appear to merge. In the first, frequently referred to as *cake filtration*, the particles from the suspension, which usually has a high proportion of solids, are deposited on the surface of a porous septum which should ideally offer only a small resistance to flow. As the solids build up on the septum, the initial layers form the effective filter medium, preventing the particles from embedding themselves in the filter cloth, and ensuring that a particle-free filtrate is obtained.

In the second type of filtration, *depth* or *deep-bed filtration*, the particles penetrate into the pores of the filter medium, where impacts between the particles and the surface of the medium are largely responsible for their removal and retention. This configuration is commonly used for the removal of fine particles from very dilute suspensions, where the recovery of the particles is not of primary importance. Typical examples here include air and water filtration. The filter bed gradually becomes clogged with particles, and its resistance to flow eventually reaches an unacceptably high level. For continued operation, it is therefore necessary to remove the accumulated solids, and it is important that this can be readily achieved. For this reason, the filter commonly consists of a bed of particulate solids, such as sand, which can be cleaned by back-flushing, often accompanied by

This book belongs to Bradley Loren (bloren@mcandrews-ip.com) Copyright Elsevier 2024

Intas Exhibit 1032
Page 20 of 470
PGR2025-00043

fluidisation. In this chapter, the emphasis is on cake filtration although deep-bed filtration, which has been discussed in detail by IVES[1,2] is considered in the section on bed filters.

There are two principal modes under which deep bed filtration may be carried out. In the first, *dead-end filtration* which is illustrated in Figure 7.1, the slurry is filtered in such a way that it is fed perpendicularly to the filter medium and there is little flow parallel to the surface of the medium. In the second, termed *cross-flow filtration* which is discussed in Section 7.3.5. and which is used particularly for very dilute suspensions, the slurry is continuously recirculated so that it flows essentially across the surface of the filter medium at a rate considerably in excess of the flowrate through the filter cake.

7.2. FILTRATION THEORY

7.2.1. Introduction

Equations are given in Chapter 4 for the calculation of the rate of flow of a fluid through a bed of granular material, and these are now applied to the flow of filtrate through a filter cake. Some differences in general behaviour may be expected, however, because the cases so far considered relate to uniform fixed beds, whereas in filtration the bed is steadily growing in thickness. Thus, if the filtration pressure is constant, the rate of flow progressively diminishes whereas, if the flowrate is to be maintained constant, the pressure must be gradually increased.

The mechanical details of the equipment, particularly of the flow channel and the support for the medium, influence the way the cake is built up and the ease with which it may be removed. A uniform structure is very desirable for good washing and cakes formed from particles of very mixed sizes and shapes present special problems. Although filter cakes are complex in their structure and cannot truly be regarded as composed of rigid non-deformable particles, the method of relating the flow parameters developed in Chapter 4 is useful in describing the flow within the filter cake. The general theory of filtration and its importance in design has been considered by SUTTLE[3]. It may be noted that there are two quite different methods of operating a batch filter. If the pressure is kept constant then the rate of flow progressively diminishes, whereas if the flowrate is kept constant then the pressure must be gradually increased. Because the particles forming the cake are small and the flow through the bed is slow, streamline conditions are almost invariably obtained, and, at any instant, the flowrate of the filtrate may be represented by the following form of equation 4.9:

$$u_c = \frac{1}{A}\frac{\mathrm{d}V}{\mathrm{d}t} = \frac{1}{5}\frac{e^3}{(1-e)^2}\frac{-\Delta P}{S^2 \mu l} \tag{7.1}$$

where V is the volume of filtrate which has passed in time t, A is the total cross-sectional area of the filter cake, u_c is the superficial velocity of the filtrate, l is the cake thickness, S is the specific surface of the particles, e is the voidage, μ is the viscosity of the filtrate, and ΔP is the applied pressure difference.

In deriving this equation it is assumed that the cake is uniform and that the voidage is constant throughout. In the deposition of a filter cake this is unlikely to be the case and the voidage, e will depend on the nature of the support, including its geometry and

This book belongs to Bradley Loren (bloren@mcandrews-ip.com) Copyright Elsevier 2024

Intas Exhibit 1032
Page 21 of 470
PGR2025-00043

surface structure, and on the rate of deposition. The initial stages in the formation of the cake are therefore of special importance for the following reasons:

(a) For any filtration pressure, the rate of flow is greatest at the beginning of the process since the resistance is then a minimum.
(b) High initial rates of filtration may result in plugging of the pores of the filter cloth and cause a very high resistance to flow.
(c) The orientation of the particle in the initial layers may appreciably influence the structure of the whole filter cake.

Filter cakes may be divided into two classes — incompressible cakes and compressible cakes. In the case of an incompressible cake, the resistance to flow of a given volume of cake is not appreciably affected either by the pressure difference across the cake or by the rate of deposition of material. On the other hand, with a compressible cake, increase of the pressure difference or of the rate of flow causes the formation of a denser cake with a higher resistance. For incompressible cakes e in equation 7.1 may be taken as constant and the quantity $e^3/[5(1-e)^2S^2]$ is then a property of the particles forming the cake and should be constant for a given material.

Thus:
$$\frac{1}{A}\frac{\mathrm{d}V}{\mathrm{d}t} = \frac{-\Delta P}{\mathbf{r}\mu l} \tag{7.2}$$

where:
$$\mathbf{r} = \frac{5(1-e)^2S^2}{e^3} \tag{7.3}$$

It may be noted that, when there is a hydrostatic pressure component such as with a horizontal filter surface, this should be included in the calculation of $-\Delta P$.

Equation 7.2 is the basic filtration equation and $\mathbf{r}$ is termed the specific resistance which is seen to depend on e and S. For incompressible cakes, $\mathbf{r}$ is taken as constant, although it depends on rate of deposition, the nature of the particles, and on the forces between the particles. $\mathbf{r}$ has the dimensions of $\mathbf{L}^{-2}$ and the units m^{-2} in the SI system.

7.2.2. Relation between thickness of cake and volume of filtrate

In equation 7.2, the variables l and V are connected, and the relation between them may be obtained by making a material balance between the solids in both the slurry and the cake as follows.

Mass of solids in filter cake $= (1-e)Al\rho_s$, where ρ_s is the density of the solids

Mass of liquid retained in the filter cake $= eAl\rho$, where ρ is the density of the filtrate. If J is the mass fraction of solids in the original suspension then:

$$(1-e)lA\rho_s = \frac{(V+eAl)\rho J}{1-J}$$

or:
$$(1-J)(1-e)Al\rho_s = JV\rho + AeJl\rho$$

so that:
$$l = \frac{JV\rho}{A\{(1-J)(1-e)\rho_s - Je\rho\}} \tag{7.4}$$

This book belongs to Bradley Loren (bloren@mcandrews-ip.com) Copyright Elsevier 2024

Intas Exhibit 1032
Page 22 of 470
PGR2025-00043

and:
$$V = \frac{\{\rho_s(1-e)(1-J) - e\rho J\}Al}{\rho J} \tag{7.5}$$

If v is the volume of cake deposited by unit volume of filtrate then:
$$v = \frac{lA}{V} \quad \text{or} \quad l = \frac{vV}{A} \tag{7.6}$$

and from equation 7.5:
$$v = \frac{J\rho}{(1-J)(1-e)\rho_s - Je\rho} \tag{7.7}$$

Substituting for l in equation 7.2:
$$\frac{1}{A}\frac{\mathrm{d}V}{\mathrm{d}t} = \frac{(-\Delta P)}{\mathbf{r}\mu}\frac{A}{vV}$$

or:
$$\frac{\mathrm{d}V}{\mathrm{d}t} = \frac{A^2(-\Delta P)}{\mathbf{r}\mu v V} \tag{7.8}$$

Equation 7.8 may be regarded as the basic relation between $-\Delta P$, V, and t. Two important types of operation are: (i) where the pressure difference is maintained constant and (ii) where the rate of filtration is maintained constant.

For a filtration at constant rate
$$\frac{\mathrm{d}V}{\mathrm{d}t} = \frac{V}{t} = \text{constant}$$

so that:
$$\frac{V}{t} = \frac{A^2(-\Delta P)}{\mathbf{r}\mu V v} \tag{7.9}$$

or:
$$\frac{t}{V} = \frac{\mathbf{r}\mu v}{A^2(-\Delta P)}V \tag{7.10}$$

and $-\Delta P$ is directly proportional to V.

For a filtration at constant pressure difference
$$\frac{V^2}{2} = \frac{A^2(-\Delta P)t}{\mathbf{r}\mu v} \tag{7.11}$$

or:
$$\frac{t}{V} = \frac{\mathbf{r}\mu v}{2A^2(-\Delta P)}V \tag{7.12}$$

Thus for a constant pressure filtration, there is a linear relation between V^2 and t or between t/V and V.

Filtration at constant pressure is more frequently adopted in practice, although the pressure difference is normally gradually built up to its ultimate value.

If this takes a time t_1 during which a volume V_1 of filtrate passes, then integration of equation 7.12 gives:
$$\frac{1}{2}(V^2 - V_1^2) = \frac{A^2(-\Delta P)}{\mathbf{r}\mu v}(t - t_1) \tag{7.13}$$

This book belongs to Bradley Loren (bloren@mcandrews-ip.com) Copyright Elsevier 2024

Intas Exhibit 1032
Page 23 of 470
PGR2025-00043

or:
$$\frac{t - t_1}{V - V_1} = \frac{\mathbf{r}\mu v}{2A^2(-\Delta P)}(V - V_1) + \frac{\mathbf{r}\mu v V_1}{A^2(-\Delta P)} \tag{7.14}$$

Thus, there where is a linear relation between V^2 and t and between $(t - t_1)/(V - V_1)$ and $(V - V_1)$, where $(t - t_1)$ represents the time of the constant pressure filtration and $(V - V_1)$ the corresponding volume of filtrate obtained.

RUTH *et al.*[4–7] have made measurements on the flow in a filter cake and have concluded that the resistance is somewhat greater than that indicated by equation 7.1. It was assumed that part of the pore space is rendered ineffective for the flow of filtrate because of the adsorption of ions on the surface of the particles. This is not borne out by GRACE[8] or by HOFFING and LOCKHART[9] who determined the relation between flowrate and pressure difference, both by means of permeability tests on a fixed bed and by filtration tests using suspensions of quartz and diatomaceous earth.

Typical values of the specific resistance **r** of filter cakes, taken from the work of CARMAN[10], are given in Table 7.1. In the absence of details of the physical properties of the particles and of the conditions under which they had been formed, these values are approximate although they do provide an indication of the orders of magnitude.

Table 7.1. Typical Values of Specific Resistance, **r**[10]

Material	Upstream filtration pressure (kN/m^2)	**r** m^{-2}
High-grade kieselguhr	—	2×10^{12}
Ordinary kieselguhr	270	1.6×10^{14}
	780	2.0×10^{14}
Carboraffin charcoal	110	4×10^{13}
	170	8×10^{13}
Calcium carbonate (precipitated)	270	3.5×10^{14}
	780	4.0×10^{14}
Ferric oxide (pigment)	270	2.5×10^{15}
	780	4.2×10^{15}
Mica clay	270	7.5×10^{14}
	780	13×10^{14}
Colloidal clay	270	8×10^{15}
	780	10×10^{15}
Gelatinous magnesium hydroxide	270	5×10^{15}
	780	11×10^{15}
Gelatinous aluminium hydroxide	270	3.5×10^{16}
	780	6.0×10^{16}
Gelatinous ferric hydroxide	270	3.0×10^{16}
	780	9.0×10^{16}
Thixotropic mud	650	2.3×10^{17}

7.2.3. Flow of liquid through the cloth

Experimental work on the flow of the liquid under streamline conditions[10] has shown that the flowrate is directly proportional to the pressure difference. It is the resistance of the cloth plus initial layers of deposited particles that is important since the latter, not only form the true medium, but also tend to block the pores of the cloth thus increasing

This book belongs to Bradley Loren (bloren@mcandrews-ip.com) Copyright Elsevier 2024

Intas Exhibit 1032
Page 24 of 470
PGR2025-00043

its resistance. Cloths may have to be discarded because of high resistance well before they are mechanically worn. No true analysis of the buildup of resistance is possible because the resistance will depend on the way in which the pressure is developed and small variations in support geometry can have an important influence. It is therefore usual to combine the resistance of the cloth with that of the first few layers of particles and suppose that this corresponds to a thickness L of cake as deposited at a later stage. The resistance to flow through the cake and cloth combined is now considered.

7.2.4. Flow of filtrate through the cloth and cake combined

If the filter cloth and the initial layers of cake are together equivalent to a thickness L of cake as deposited at a later stage in the process, and if $-\Delta P$ is the pressure drop across the cake and cloth combined, then:

$$\frac{1}{A}\frac{\mathrm{d}V}{\mathrm{d}t} = \frac{(-\Delta P)}{\mathbf{r}\mu(l+L)} \tag{7.15}$$

which may be compared with equation 7.2.

Thus:
$$\frac{\mathrm{d}V}{\mathrm{d}t} = \frac{A(-\Delta P)}{\mathbf{r}\mu\left(\dfrac{Vv}{A}+L\right)} = \frac{A^2(-\Delta P)}{\mathbf{r}\mu v\left(V+\dfrac{LA}{v}\right)} \tag{7.16}$$

This equation may be integrated between the limits $t = 0$, $V = 0$ and $t = t_1$, $V = V_1$ for constant rate filtration, and $t = t_1$, $V = V_1$ and $t = t$, $V = V$ for a subsequent constant pressure filtration.

For the period of *constant rate filtration*:

$$\frac{V_1}{t_1} = \frac{A^2(-\Delta P)}{\mathbf{r}\mu v\left(V_1+\dfrac{LA}{v}\right)}$$

or:
$$\frac{t_1}{V_1} = \frac{\mathbf{r}\mu v}{A^2(-\Delta P)}V_1 + \frac{\mathbf{r}\mu L}{A(-\Delta P)}$$

or:
$$V_1^2 + \frac{LA}{v}V_1 = \frac{A^2(-\Delta P)}{\mathbf{r}\mu v}t_1 \tag{7.17}$$

For a subsequent *constant pressure filtration*:

$$\frac{1}{2}(V^2 - V_1^2) + \frac{LA}{v}(V - V_1) = \frac{A^2(-\Delta P)}{\mathbf{r}\mu v}(t - t_1) \tag{7.18}$$

or:
$$(V - V_1 + 2V_1)(V - V_1) + \frac{2LA}{v}(V - V_1) = \frac{2A^2(-\Delta P)}{\mathbf{r}\mu v}(t - t_1)$$

or:
$$\frac{t - t_1}{V - V_1} = \frac{\mathbf{r}\mu v}{2A^2(-\Delta P)}(V - V_1) + \frac{\mathbf{r}\mu v V_1}{A^2(-\Delta P)} + \frac{\mathbf{r}\mu L}{A(-\Delta P)} \tag{7.19}$$

This book belongs to Bradley Loren (bloren@mcandrews-ip.com) Copyright Elsevier 2024

Intas Exhibit 1032
Page 25 of 470
PGR2025-00043

Thus there is a linear relation between $(t - t_1)/(V - V_1)$ and $V - V_1$, as shown in Figure 7.2, and the slope is proportional to the specific resistance, as in the case of the flow of the filtrate through the filter cake alone given by equation 7.14, although the line does not now go through the origin.

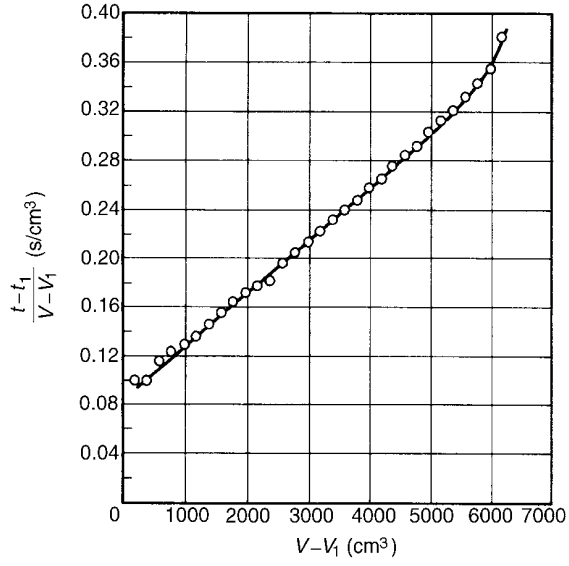


Figure 7.2. A typical filtration curve

The intercept on the $(t - t_1)/(V - V_1)$ axis should enable L, the equivalent thickness of the cloth, to be calculated although reproducible results are not obtained because this resistance is critically dependent on the exact manner in which the operation is commenced. The time at which measurement of V and t is commenced does not affect the slope of the curve, only the intercept. It may be noted that a linear relation between t and V^2 is no longer obtained when the cloth resistance is appreciable.

7.2.5. Compressible filter cakes

Nearly all filter cakes are compressible to at least some extent although in many cases the degree of compressibility is so small that the cake may, for practical purposes, be regarded as incompressible. The evidence for compressibility is that the specific resistance is a function of the pressure difference across the cake. Compressibility may be a reversible or an irreversible process. Most filter cakes are inelastic and the greater resistance offered to flow at high pressure differences is caused by the more compact packing of the particles forming the filter cake. Thus the specific resistance of the cake corresponds to that for the highest pressure difference to which the cake is subjected, even though this maximum pressure difference may be maintained for only a short time. It is therefore important that the filtration pressure should not be allowed to exceed the normal operating pressure at

This book belongs to Bradley Loren (bloren@mcandrews-ip.com) Copyright Elsevier 2024

Intas Exhibit 1032
Page 26 of 470
PGR2025-00043

any stage. In elastic filter cakes the elasticity is attributable to compression of the particles themselves. This is less usual, although some forms of carbon can give rise to elastic cakes.

As the filtrate flows through the filter cake, it exerts a drag force on the particles and this force is transmitted through successive layers of particles right up to the filter cloth. The magnitude of this force increases progressively from the surface of the filter cake to the filter cloth since at any point it is equal to the summation of the forces on all the particles up to that point. If the cake is compressible, then its voidage will decrease progressively in the direction of flow of the filtrate, giving rise to a corresponding increase in the local value of the specific resistance, $\mathbf{r}_z$, of the filter cake. The structure of the cake is, however, complex and may change during the course of the filtration process. If the feed suspension is flocculated, the flocs may become deformed within the cake, and this may give rise to a change in the effective value of the specific surface, S. In addition, the particles themselves may show a degree of compressibility. Whenever possible, experimental measurements should be made to determine how the specific resistance varies over the range of conditions which will be employed in practice.

It is usually possible to express the voidage e_z at a depth z as a function of the difference between the pressure at the free surface of the cake P_1 and the pressure P_z at that depth, that is e_z as a function of $(P_1 - P_z)$. The nomenclature is as defined in Figure 7.3.

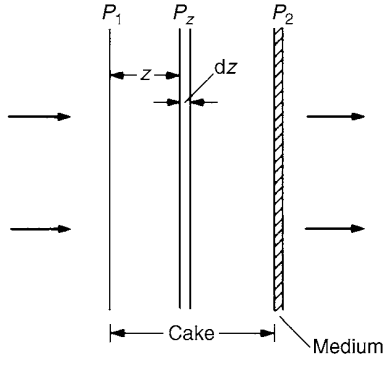


Figure 7.3. Flow through a compressible filter cake

For a compressible cake, equation 7.1 may be written as:

$$\frac{1}{A}\frac{\mathrm{d}V}{\mathrm{d}t} = \frac{e_z^3}{5(1-e_z)^2 S^2}\frac{1}{\mu}\left(-\frac{\mathrm{d}P_z}{\mathrm{d}z}\right) \tag{7.20}$$

where e_z is now a function of depth z from the surface of the cake.

In a compressible cake, the volume v of cake deposited per unit area as a result of the flow of unit volume of filtrate will not be constant, but will vary during the filtration cycle. If the particles themselves are not compressible, however, the volume of *particles* (v') will be *almost* independent of the conditions under which the cake is formed assuming a dilute feed suspension. Any small variations in v' arise because the volume of filtrate retained in the cake is a function of its voidage, although the effect will be very small,

This book belongs to Bradley Loren (bloren@mcandrews-ip.com) Copyright Elsevier 2024
Intas Exhibit 1032
Page 27 of 470
PGR2025-00043

except possibly for the filtration of very highly concentrated suspensions. The increase in cake thickness, dz resulting from the flow of a volume of filtrate dV is given by:

$$dz = dV \frac{v'}{(1 - e_z)A} \tag{7.21}$$

By comparison with equation 7.6, it may seen that:

$$\frac{v'}{v} = 1 - e_z \tag{7.22}$$

Substituting from equation 7.21 into equation 7.20 gives:

$$\frac{1}{A}\frac{dV}{dt} = \frac{e_z^3}{5(1 - e_z)^2 S^2} \frac{(1 - e_z)A}{v'} \frac{1}{\mu} \left(-\frac{dP_z}{dV}\right)$$

Thus:

$$\frac{dV}{dt} = \frac{e_z^3}{5(1 - e_z)S^2} \frac{A^2}{\mu v'} \left(-\frac{dP_z}{dV}\right) \tag{7.23}$$

$$= \frac{A^2}{\mu v' \mathbf{r}_z} \left(-\frac{dP_z}{dV}\right) \tag{7.24}$$

where:

$$\mathbf{r}_z = \frac{5(1 - e_z)S^2}{e_z^3} \tag{7.25}$$

Comparing equations 7.8 and 7.24 shows that for an incompressible cake:

$$v' \mathbf{r}_z = v \mathbf{r}$$

or:

$$\mathbf{r}_z = \mathbf{r} \frac{v}{v'}$$

At any instant in a constant pressure filtration, integration of equation 7.24 through the whole depth of the cake gives:

$$\int_0^V \frac{dV}{dt} dV = \frac{A^2}{\mu v'} \int_{P_1}^{P_2} \frac{(-dP_z)}{\mathbf{r}_z} \tag{7.26}$$

At any time t, dV/dt is approximately constant throughout the cake, unless the rate of change of holdup of liquid within the cake is comparable with the filtration rate dV/dt, such as is the case with very highly compressible cakes and concentrated slurries, and therefore:

$$V \frac{dV}{dt} = \frac{A^2}{\mu v' V} \int_{P_1}^{P_2} \frac{(-dP_z)}{\mathbf{r}_z} \tag{7.27}$$

$\mathbf{r}_z$ has been shown to be a function of the pressure difference $(P_1 - P_z)$ although it is independent of the absolute value of the pressure. Experimental studies frequently show that the relation between $\mathbf{r}_z$ and $(P_1 - P_z)$ is of the form:

$$\mathbf{r}_z = \mathbf{r}'(P_1 - P_z)^{n'} \tag{7.28}$$

where $\mathbf{r}'$ is independent of P_z and $0 < n' < 1$.

This book belongs to Bradley Loren (bloren@mcandrews-ip.com) Copyright Elsevier 2024

Intas Exhibit 1032
Page 28 of 470
PGR2025-00043

Thus:
$$\int_{P_1}^{P_2} \frac{(-\mathrm{d}P_z)}{\mathbf{r}_z} = \frac{1}{\mathbf{r}'} \int_{P_2}^{P_1} \frac{\mathrm{d}P}{(P_1 - P_z)^{n'}}$$
$$= \frac{1}{\mathbf{r}'} \frac{(P_1 - P_2)^{1-n'}}{1-n'}$$
$$= \frac{1}{\mathbf{r}'} \frac{(-\Delta P)^{1-n'}}{1-n'} \tag{7.29}$$

Thus:
$$\frac{\mathrm{d}V}{\mathrm{d}t} = \frac{A^2}{V\mu v'\mathbf{r}'} \frac{(-\Delta P)}{(1-n')(-\Delta P)^{n'}}$$
$$= \frac{A^2(-\Delta P)}{V\mu v'\mathbf{r}''(-\Delta P)^{n'}} \tag{7.30}$$

where $\mathbf{r}'' = (1 - n')\mathbf{r}'$

and:
$$\frac{\mathrm{d}V}{\mathrm{d}t} = \frac{A^2(-\Delta P)}{V\mu v'\bar{\mathbf{r}}} \tag{7.31}$$

where $\bar{\mathbf{r}}$ is the mean resistance defined by:

$$\bar{\mathbf{r}} = \bar{\mathbf{r}}''(-\Delta P)^{n'} \tag{7.32}$$

HEERTJES[11] has studied the effect of pressure on the porosity of a filter cake and suggested that, as the pressure is increased above atmospheric, the porosity decreases in proportion to some power of the excess pressure.

GRACE[8] has related the anticipated resistance to the physical properties of the feed slurry. VALLEROY and MALONEY[12] have examined the resistance of an incompressible bed of spherical particles when measured in a permeability cell, a vacuum filter, and a centrifuge, and emphasised the need for caution in applying laboratory data to units of different geometry.

TILLER and HUANG[13] give further details of the problem of developing a usable design relationship for filter equipment. Studies by TILLER and SHIRATO[14], TILLER and YEH[15] and RUSHTON and HAMEED[16] show the difficulty in presenting practical conditions in a way which can be used analytically. It is very important to note that tests on slurries must be made with equipment that is geometrically similar to that proposed. This means that specific resistance is very difficult to define in practice, since it is determined by the nature of the filtering unit and the way in which the cake is initially formed and then built up.

7.3. FILTRATION PRACTICE

7.3.1. The filter medium

The function of the filter medium is generally to act as a support for the filter cake, and the initial layers of cake provide the true filter. The filter medium should be mechanically strong, resistant to the corrosive action of the fluid, and offer as little resistance as possible

This book belongs to Bradley Loren (bloren@mcandrews-ip.com) Copyright Elsevier 2024

Intas Exhibit 1032
Page 29 of 470
PGR2025-00043

to the flow of filtrate. Woven materials are commonly used, though granular materials and porous solids are useful for filtration of corrosive liquids in batch units. An important feature in the selection of a woven material is the ease of cake removal, since this is a key factor in the operation of modern automatic units. EHLERS[17] has discussed the selection of woven synthetic materials and WROTNOWSKI[18] that of non-woven materials. Further details of some more recent materials are given in the literature[19] and a useful summary is presented in Volume 6.

7.3.2. Blocking filtration

In the previous discussion it is assumed that there is a well-defined boundary between the filter cake and the filter cloth. The initial stages in the build-up of the filter cake are important, however, because these may have a large effect on the flow resistance and may seriously affect the useful life of the cloth.

The blocking of the pores of the filter medium by particles is a complex phenomenon, partly because of the complicated nature of the surface structure of the usual types of filter media, and partly because the lines of movement of the particles are not well defined. At the start of filtration, the manner in which the cake forms will lie between two extremes — the penetration of the pores by particles and the shielding of the entry to the pores by the particles forming bridges. HEERTJES[11] considered a number of idealised cases in which suspensions of specified pore size distributions were filtered on a cloth with a regular pore distribution. First, it was assumed that an individual particle was capable on its own of blocking a single pore, then, as filtration proceeded, successive pores would be blocked, so that the apparent value of the specific resistance of the filter cake would depend on the amount of solids deposited.

The pore and particle size distributions might, however, be such that more than one particle could enter a particular pore. In this case, the resistance of the pore increases in stages as successive particles are trapped until the pore is completely blocked. In practice, however, it is much more likely that many of the pores will never become completely blocked and a cake of relatively low resistance will form over the entry to the partially blocked pore.

One of the most important variables affecting the tendency for blocking is the concentration of particles. The greater the concentration, the smaller will be the average distance between the particles, and the smaller will be the tendency for the particle to be drawn in to the streamlines directed towards the open pores. Instead, the particles in the concentrated suspension tend to distribute themselves fairly evenly over the filter surface and form bridges. As a result, suspensions of high concentration generally give rise to cakes of lower resistance than those formed from dilute suspensions.

7.3.3. Effect of particle sedimentation on filtration

There are two important effects due to particle sedimentation which may affect the rate of filtration. First, if the sediment particles are all settling at approximately the same rate, as is frequently the case in a concentrated suspension in which the particle size distribution is not very wide, a more rapid build-up of particles will occur on an

This book belongs to Bradley Loren (bloren@mcandrews-ip.com) Copyright Elsevier 2024

Intas Exhibit 1032
Page 30 of 470
PGR2025-00043

upward-facing surface and a correspondingly reduced rate of build-up will take place if the filter surface is facing downwards. Thus, there will be a tendency for accelerated filtration with downward-facing filter surfaces and reduced filtration rates for upward-facing surfaces. On the other hand, if the suspension is relatively dilute, so that the large particles are settling at a higher rate than the small ones, there will be a preferential deposition of large particles on an upward-facing surface during the initial stages of filtration, giving rise to a low resistance cake. Conversely, for a downward-facing surface, fine particles will initially be deposited preferentially and the cake resistance will be correspondingly increased. It is thus seen that there can be complex interactions where sedimentation is occurring at an appreciable rate, and that the orientation of the filter surface is an important factor.

7.3.4. Delayed cake filtration

In the filtration of a slurry, the resistance of the filter cake progressively increases and consequently, in a constant pressure operation, the rate of filtration falls. If the build-up of solids can be reduced, the effective cake thickness will be less and the rate of flow of filtrate will be increased.

In practice, it is sometimes possible to incorporate moving blades in the filter equipment so that the thickness of the cake is limited to the clearance between the filter medium and the blades. Filtrate then flows through the cake at an approximately constant rate and the solids are retained in suspension. Thus the solids concentration in the feed vessel increases until the particles are in permanent physical contact with one another. At this stage the boundary between the slurry and the cake becomes ill-defined, and a significant resistance to the flow of liquid develops within the slurry itself with a consequent reduction in the flowrate of filtrate.

By the use of this technique, a much higher rate of filtration can be achieved than is possible in a filter operated in a conventional manner. In addition, the resulting cake usually has a lower porosity because the blades effectively break down the bridges or arches which give rise to a structure in the filter cake, and the final cake is significantly drier as a result.

If the scrapers are in the form of rotating blades, the outcome differs according to whether they are moving at low or at high speed. At low speeds, the cake thickness is reduced to the clearance depth each time the scraper blade passes, although cake then builds up again until the next passage of the scraper. If the blade is operated at high speed, there is little time for solids to build up between successive passages of the blade and the cake reaches an approximately constant thickness. Since particles tend to be swept across the surface of the cake by the moving slurry, they will be trapped in the cake only if the drag force which the filtrate exerts on them is great enough. As the thickness of the cake increases the pressure gradient becomes less and there is a smaller force retaining particles in the cake surface. Thus the thickness of the cake tends to reach an equilibrium value, which can be considerably less than the clearance between the medium and the blades.

Experimental results for the effect of stirrer speed on the rate of filtration of a 10 per cent by mass suspension of clay are shown in Figure 7.4 taken from the work of Tiller and Cheng[20], in which the filtrate volume collected per unit cross-section of filter is plotted against time, for several stirrer speeds.

This book belongs to Bradley Loren (bloren@mcandrews-ip.com) Copyright Elsevier 2024

Intas Exhibit 1032
Page 31 of 470
PGR2025-00043

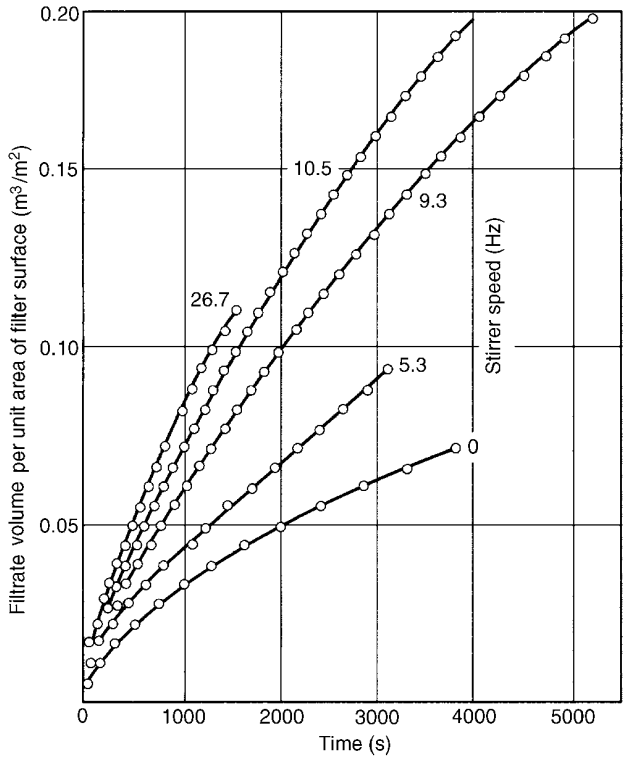


Figure 7.4. Volume as function of time for delayed cake and constant pressure filtration as a function of stirrer speed[20]

The concentration of solids in the slurry in the feed vessel to the filter at any time can be calculated by noting that the volumetric rate of feed of slurry must be equal to the rate at which filtrate leaves the vessel. For a rate of flow of filtrate of $\mathrm{d}V/\mathrm{d}t$ out of the filter, the rate of flow of slurry into the vessel must also be $\mathrm{d}V/\mathrm{d}t$ and the corresponding influx of solids is $(1 - e_0)\,\mathrm{d}V/\mathrm{d}t$, where $(1 - e_0)$ is the volume fraction of solids in the feed slurry. At any time t, the volume of solids in the vessel is $\mathbf{V}(1 - e_V)$, where $\mathbf{V}$ is its volume and $(1 - e_V)$ is the volume fraction of solids at that time. Thus a material balance on the solids gives:

$$(1 - e_0)\frac{\mathrm{d}V}{\mathrm{d}t} = \frac{\mathrm{d}}{\mathrm{d}t}[\mathbf{V}(1 - e_V)] \tag{7.33}$$

$$\frac{\mathrm{d}(1 - e_V)}{\mathrm{d}t} = \frac{1}{\mathbf{V}}(1 - e_0)\frac{\mathrm{d}V}{\mathrm{d}t} \tag{7.34}$$

For a constant filtration rate $\mathrm{d}V/\mathrm{d}t$, the fractional solids hold-up $(1 - e_V)$ increases linearly with time, until it reaches a limiting value when the resistance to flow of liquid within the slurry becomes significant. The filtration rate then drops rapidly to a near zero value.

This book belongs to Bradley Loren (bloren@mcandrews-ip.com) Copyright Elsevier 2024

Intas Exhibit 1032
Page 32 of 470
PGR2025-00043

7.3.5. Cross-flow filtration

An alternative method of reducing the resistance to filtration is to recirculate the slurry and thereby maintain a high velocity of flow parallel to the surface of the filter medium. Typical recirculation rates may be 10–20 times the filtration rate. By this means the cake is prevented from forming during the early stages of filtration. This can be particularly beneficial when the slurry is flocculated and exhibits shear-thinning non-Newtonian properties. This method of operation is discussed by MACKLEY and SHERMAN[21] and by HOLDICH, CUMMING and ISMAIL[22].

In cases where a dilute solution containing small quantities of solids which tend to blind the filter cloth is to be filtered, cross-flow filtration is extensively used. This is the normal mode of operation for ultrafiltration using membranes, a topic which is discussed in Chapter 8.

7.3.6. Preliminary treatment of slurries before filtration

If a slurry is dilute and the solid particles settle readily in the fluid, it may be desirable to effect a preliminary concentration in a thickener as discussed in Chapter 5. The thickened suspension is then fed from the thickener to the filter and the quantity of material to be handled is thereby reduced.

Theoretical treatment has shown that the nature of the filter cake has a very pronounced effect on the rate of flow of filtrate and that it is, in general, desirable that the particles forming the filter cake should have as large a size as possible. More rapid filtration is therefore obtained if a suitable agent is added to the slurry to cause coagulation. If the solid material is formed in a chemical reaction by precipitation, the particle size can generally be controlled to a certain extent by the actual conditions of formation. For example, the particle size of the resultant precipitate may be controlled by varying the temperature and concentration, and sometimes the pH, of the reacting solutions. As indicated by GRACE[8], a flocculated suspension gives rise to a more porous cake although the compressibility is greater. In many cases, crystal shape may be altered by adding traces of material which is selectively adsorbed on particular faces as noted in Chapter 15.

Filter aids are extensively used where the filter cake is relatively impermeable to the flow of filtrate. These are materials which pack to form beds of very high voidages and therefore they are capable of increasing the porosity of the filter cake if added to the slurry before filtration. Apart from economic considerations, there is an optimum quantity of filter aid which should be added in any given case. Whereas the presence of the filter aid reduces the specific resistance of the filter cake, it also results in the formation of a thicker cake. The actual quantity used will therefore depend on the nature of the material. The use of filter aids is normally restricted to operations in which the filtrate is valuable and the cake is a waste product. In some circumstances, however, the filter aid must be readily separable from the rest of the filter cake by physical or chemical means. Filter cakes incorporating filter aid are usually very compressible and care should therefore be taken to ensure that the good effect of the filter aid is not destroyed by employing too high a filtration pressure. Kieselguhr, which is a commonly used filter aid, has a voidage of about 0.85. Addition of relatively small quantities increases the voidage of most filter cakes, and the resulting porosity normally lies between that of the filter aid and that of

This book belongs to Bradley Loren (bloren@mcandrews-ip.com) Copyright Elsevier 2024

Intas Exhibit 1032
Page 33 of 470
PGR2025-00043

the filter solids. Sometimes the filter medium is "precoated" with filter aid, and a thin layer of the filter aid is removed with the cake at the end of each cycle.

In some cases the filtration time can be reduced by diluting the suspension in order to reduce the viscosity of the filtrate. This does, of course, increase the bulk to be filtered and is applicable only when the value of the filtrate is not affected by dilution. Raising the temperature may be advantageous in that the viscosity of the filtrate is reduced.

7.3.7. Washing of the filter cake

When the wash liquid is miscible with the filtrate and has similar physical properties, the rate of washing at the same pressure difference will be about the same as the final rate of filtration. If the viscosity of the wash liquid is less, a somewhat greater rate will be obtained. Channelling sometimes occurs, however, with the result that much of the cake is incompletely washed and the fluid passes preferentially through the channels, which are gradually enlarged by its continued passage. This does not occur during filtration because channels are self-sealing by virtue of deposition of solids from the slurry. Channelling is most marked with compressible filter cakes and can be minimised by using a smaller pressure difference for washing than for filtration.

Washing may be regarded as taking place in two stages. First, filtrate is displaced from the filter cake by wash liquid during the period of *displacement washing* and in this way up to 90 per cent of the filtrate may be removed. During the second stage, *diffusional washing*, solvent diffuses into the wash liquid from the less accessible voids and the following relation applies:

$$\left(\frac{\text{volume of wash liquid passed}}{\text{cake thickness}}\right) = (\text{constant}) \times \log\left(\frac{\text{initial concentration of solute}}{\text{concentration at particular time}}\right) \tag{7.35}$$

Although an immiscible liquid is seldom used for washing, air is often used to effect partial drying of the filter cake. The rate of flow of air must normally be determined experimentally.

7.4. FILTRATION EQUIPMENT

7.4.1. Filter selection

The most suitable filter for any given operation is the one which will fulfil the requirements at minimum overall cost. Since the cost of the equipment is closely related to the filtering area, it is normally desirable to obtain a high overall rate of filtration. This involves the use of relatively high pressures although the maximum pressures are often limited by mechanical design considerations. Although a higher throughput from a given filtering surface is obtained from a continuous filter than from a batch operated filter, it may sometimes be necessary to use a batch filter, particularly if the filter cake has a high resistance, since most continuous filters operate under reduced pressure and the maximum filtration pressure is therefore limited. Other features which are desirable in a filter include

This book belongs to Bradley Loren (bloren@mcandrews-ip.com) Copyright Elsevier 2024

Intas Exhibit 1032
Page 34 of 470
PGR2025-00043

ease of discharge of the filter cake in a convenient physical form, and a method of observing the quality of the filtrate obtained from each section of the plant. These factors are important in considering the types of equipment available. The most common types are filter presses, leaf filters, and continuous rotary filters. In addition, there are filters for special purposes, such as bag filters, and the disc type of filter which is used for the removal of small quantities of solids from a fluid.

The most important factors in filter selection are the specific resistance of the filter cake, the quantity to be filtered, and the solids concentration. For free-filtering materials, a rotary vacuum filter is generally the most satisfactory since it has a very high capacity for its size and does not require any significant manual attention. If the cake has to be washed, the rotary drum is to be preferred to the rotary leaf. If a high degree of washing is required, however, it is usually desirable to repulp the filter cake and to filter a second time.

For large-scale filtration, there are three principal cases where a rotary vacuum filter will not be used. Firstly, if the specific resistance is high, a positive pressure filter will be required, and a filter press may well be suitable, particularly if the solid content is not so high that frequent dismantling of the press is necessary. Secondly, when efficient washing is required, a leaf filter is effective, because very thin cakes can be prepared and the risk of channelling during washing is reduced to a minimum. Finally, where only very small quantities of solids are present in the liquid, an edge filter may be employed.

Whilst it may be possible to predict qualitatively the effect of the physical properties of the fluid and the solid on the filtration characteristics of a suspension, it is necessary in all cases to carry out a test on a sample before the large-scale plant can be designed. A simple vacuum filter with a filter area of 0.0065 m^2 is used to obtain laboratory data, as illustrated in Figure 7.5. The information on filtration rates and specific resistance obtained in this way can be directly applied to industrial filters provided due account is taken of the compressibility of the filter cake. It cannot be stressed too

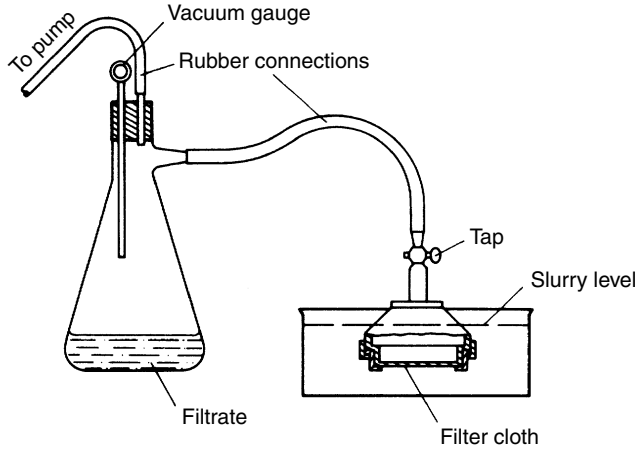


Figure 7.5. Laboratory test filter

This book belongs to Bradley Loren (bloren@mcandrews-ip.com) Copyright Elsevier 2024

Intas Exhibit 1032
Page 35 of 470
PGR2025-00043

strongly that data from any laboratory test cell must not be used without practical experience in the design of industrial units where the geometry of the flow channel is very different. The laying down of the cake influences the structure to a very a marked extent.

A "compressibility–permeability" test cell has been developed by RUTH[7] and GRACE[8] for testing the behaviour of slurries under various conditions of filtration. A useful guide to the selection of a filter type based on slurry characteristics is given in Volume 6.

7.4.2. Bed filters

Bed filters provide an example of the application of the principles of *deep bed filtration* in which the particles penetrate into the interstices of the filter bed where they are trapped following impingement on the surfaces of the material of the bed.

For the purification of water supplies and for waste water treatment where the solid content is about 10 g/m^3 or less, as noted by CLEASBY[23] granular bed filters have largely replaced the former very slow sand filters. The beds are formed from granular material of grain size 0.6–1.2 mm in beds 0.6–1.8 m deep. The very fine particles of solids are removed by mechanical action although the particles finally adhere as a result of surface electric forces or adsorption, as IVES[24] points out. This operation has been analysed by IWASAKI[25] who proposes the following equation:

$$-\frac{\partial C}{\partial l} = \lambda C \tag{7.36}$$

On integration:

$$C/C_0 = \mathrm{e}^{-\lambda l} \tag{7.37}$$

where: C is the volume concentration of solids in suspension in the filter,
C_0 is the value of C at the surface of the filter,
l is the depth of the filter, and
λ is the filter coefficient.

If u_c is the superficial flowrate of the slurry, then the rate of flow of solids through the filter at depth l is $u_c C$ per unit area. Thus the rate of accumulation of solids in a distance $\mathrm{d}l = -u_c(\partial C/\partial l)\,\mathrm{d}l$. If σ is the volume of solids deposited per unit volume of filter at a depth l, the rate of accumulation may also be expressed as $(\partial\sigma/\partial t)\,\mathrm{d}l$.

Thus:
$$-\frac{\partial C}{\partial l} = u_c\frac{\partial \sigma}{\partial t} \tag{7.38}$$

The problem is discussed further by IVES[24] and by SPIELMAN and FRIEDLANDER[26]. The backwashing of these beds has presented problems and several techniques have been adopted. These include a backflow of air followed by water, the flowrate of which may be high enough to give rise to fluidisation, with the maximum hydrodynamic shear occurring at a voidage of about 0.7.

This book belongs to Bradley Loren (bloren@mcandrews-ip.com) Copyright Elsevier 2024

Intas Exhibit 1032
Page 36 of 470
PGR2025-00043

7.4.3. Bag filters

Bag filters have now been almost entirely superseded for liquid filtration by other types of filter, although one of the few remaining types is the Taylor bag filter which has been widely used in the sugar industry. A number of long thin bags are attached to a horizontal feed tray and the liquid flows under the action of gravity so that the rate of filtration per unit area is very low. It is possible, however, to arrange a large filtering area in the plant of up to about 700 m^2. The filter is usually arranged in two sections so that each may be inspected separately without interrupting the operation.

Bag filters are still extensively used for the removal of dust particles from gases and can be operated either as pressure filters or as suction filters. Their use is discussed in Chapter 1.

7.4.4. The filter press

The filter press is one of two main types, the *plate and frame press* and the *recessed plate* or *chamber press*.

The plate and frame press

This type of filter consists of plates and frames arranged alternately and supported on a pair of rails as shown in Figure 7.6. The plates have a ribbed surface and the edges stand slightly proud and are carefully machined. The hollow frame is separated from the plate by the filter cloth, and the press is closed either by means of a hand screw or hydraulically, using the minimum pressure in order to reduce wear on the cloths. A chamber is therefore formed between each pair of successive plates as shown in Figure 7.7. The slurry is introduced through a port in each frame and the filtrate passes through the cloth on each side so that two cakes are formed simultaneously in each chamber, and these join when the frame is full. The frames are usually square and may be 100 mm–2.5 m across and 10 mm–75 mm thick.

The slurry may be fed to the press through the continuous channel formed by the holes in the corners of the plates and frames, in which case it is necessary to cut corresponding holes in the cloths which themselves act as gaskets. Cutting of the cloth can be avoided by feeding through a channel at the side although rubber bushes must then be fitted so that a leak-tight joint is formed.

The filtrate runs down the ribbed surface of the plates and is then discharged through a cock into an open launder so that the filtrate from each plate may be inspected and any plate can be isolated if it is not giving a clear filtrate. In some cases the filtrate is removed through a closed channel although it is not then possible to observe the discharge from each plate separately.

In many filter presses, provision is made for steam heating so that the viscosity of the filtrate is reduced and a higher rate of filtration obtained. Materials, such as waxes, that solidify at normal temperatures may also be filtered in steam-heated presses. Steam heating also facilitates the production of a dry cake.

Optimum time cycle. The optimum thickness of cake to be formed in a filter press depends on the resistance offered by the filter cake and on the time taken to dismantle

This book belongs to Bradley Loren (bloren@mcandrews-ip.com) Copyright Elsevier 2024

Intas Exhibit 1032
Page 37 of 470
PGR2025-00043

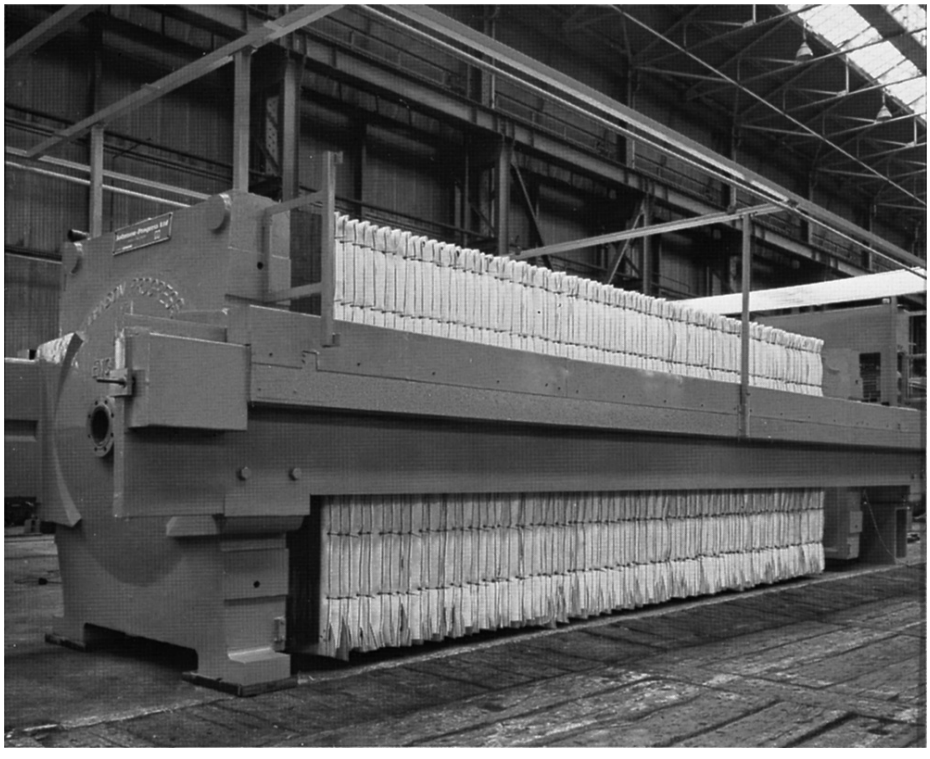


Figure 7.6. A large filter press with 2 m by 1.5 m plates

and refit the press. Although the production of a thin filter cake results in a high average rate of filtration, it is necessary to dismantle the press more often and a greater time is therefore spent on this operation. For a filtration carried out entirely at constant pressure, a rearrangement equation 7.19 gives:

$$\frac{t}{V} = \frac{\mathbf{r}\mu v}{2A^2(-\Delta P)}V + \frac{\mathbf{r}\mu L}{A(-\Delta P)} \tag{7.39}$$

$$= B_1 V + B_2 \tag{7.40}$$

where B_1 and B_2 are constants.

Thus the time of filtration t is given by:

$$t = B_1 V^2 + B_2 V \tag{7.41}$$

The time of dismantling and assembling the press, say t', is substantially independent of the thickness of cake produced. The total time of a cycle in which a volume V of filtrate is collected is then $(t + t')$ and the overall rate of filtration is given by:

$$W = \frac{V}{B_1 V^2 + B_2 V + t'}$$

W is a maximum when $\mathrm{d}W/\mathrm{d}V = 0$.

This book belongs to Bradley Loren (bloren@mcandrews-ip.com) Copyright Elsevier 2024

Intas Exhibit 1032
Page 38 of 470
PGR2025-00043

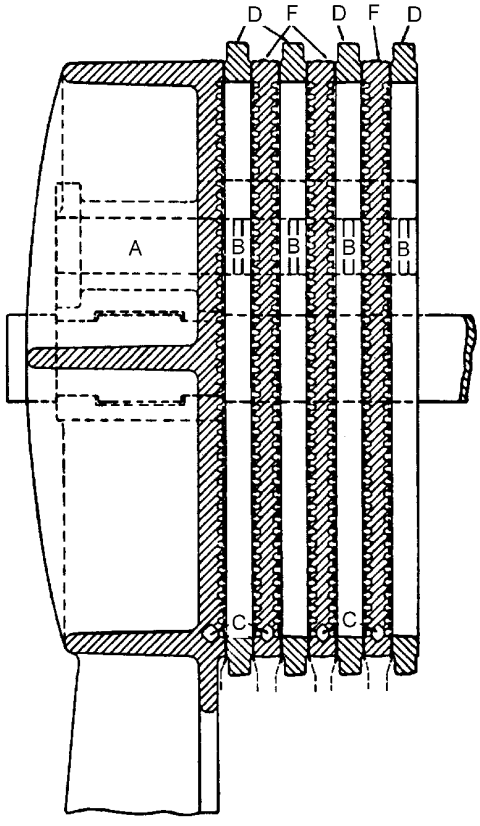


Figure 7.7. Plate and frame press. A–inlet passage. B–feed ports. C–filtrate outlet. D–frames. F–plates

Differentiating W with respect to V and equating to zero:

$$B_1V^2 + B_2V + t' - V(2B_1V + B_2) = 0$$

or:
$$t' = B_1V^2 \tag{7.42}$$

or:
$$V = \sqrt{\left(\frac{t'}{B_1}\right)} \tag{7.43}$$

If the resistance of the filter medium is neglected, $t = B_1V^2$ and the time during which filtration is carried out is exactly equal to the time the press is out of service. In practice, in order to obtain the maximum overall rate of filtration, the filtration time must always be somewhat greater in order to allow for the resistance of the cloth, represented by the term B_2V. In general, the lower the specific resistance of the cake, the greater will be the economic thickness of the frame.

The application of these equations is illustrated later in Example 7.5 which is based on the work of HARKER[27].

This book belongs to Bradley Loren (bloren@mcandrews-ip.com) Copyright Elsevier 2024

Intas Exhibit 1032
Page 39 of 470
PGR2025-00043

It is shown in Example 7.5, which appears later on the chapter, that, provided the cloth resistance is very low, adopting a filtration time equal to the downtime will give the maximum throughput. Where the cloth resistance is appreciable, then the term $B_2(t'/B_1)^{0.5}$ becomes significant and a longer filtration time is desirable. It may be seen in Figure 7.8, which is based on data from Example 7.5, that neither of these values represents the minimum cost condition however, except for the unique situation where $t' =$ (cost of shutdown)/(cost during filtering), and a decision has to be made as to whether cost or throughput is the overiding consideration. In practice, operating schedules are probably the dominating feature, although significant savings may be made by operating at the minimum cost condition.

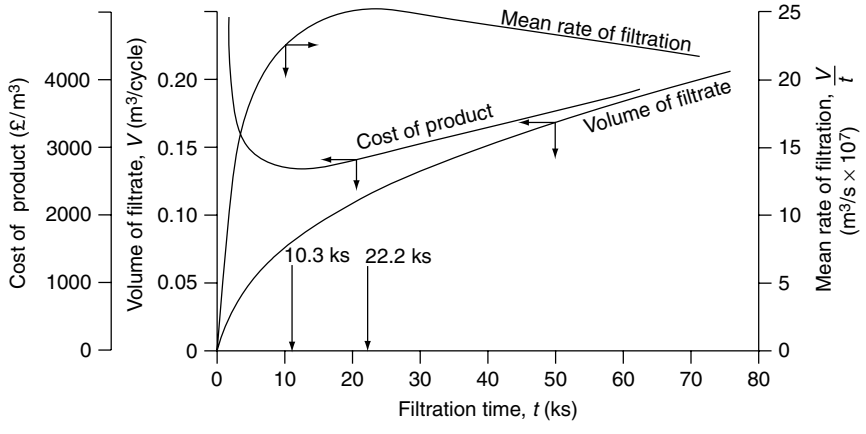


Figure 7.8. Optimisation of plate and frame press (data from Example 7.5)[27]

Washing

Two methods of washing may be employed, "simple" washing and "through" or "thorough" washing. With simple washing, the wash liquid is fed in through the same channel as the slurry although, as its velocity near the point of entry is high, erosion of the cake takes place. The channels which are thus formed gradually enlarge and uneven washing is usually obtained. Simple washing may be used only when the frame is not completely full.

In *thorough* washing, the wash liquid is introduced through a separate channel behind the filter cloth on alternate plates, known as washing plates shown in Figure 7.9, and flows through the whole thickness of the cake, first in the opposite direction and then in the same direction as the filtrate. The area during washing is one-half of that during filtration and, in addition, the wash liquid has to flow through twice the thickness, so that the rate of washing should therefore be about one-quarter of the final rate of filtration. The wash liquid is usually discharged through the same channel as the filtrate though sometimes a separate outlet is provided. Even with thorough washing some channelling occurs and several inlets are often provided so that the liquid is well distributed. If the cake is appreciably compressible, the minimum pressure should be used during washing,

This book belongs to Bradley Loren (bloren@mcandrews-ip.com) Copyright Elsevier 2024
Intas Exhibit 1032
Page 40 of 470
PGR2025-00043

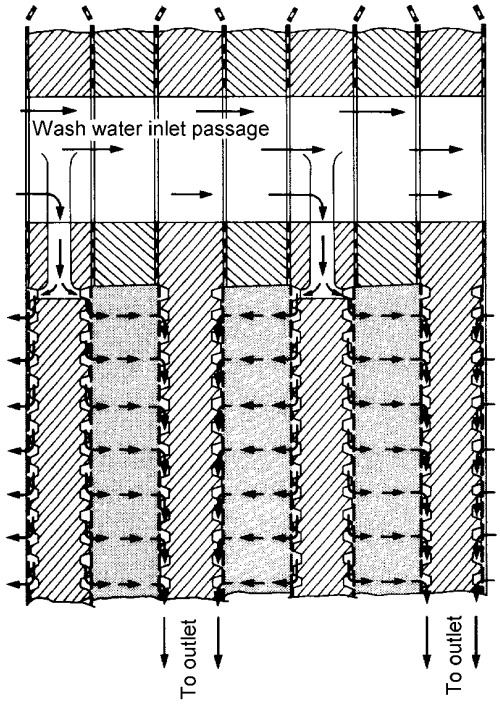


Figure 7.9. Thorough washing

and in no case should the final filtration pressure be exceeded. After washing, the cake may be made easier to handle by removing excess liquid with compressed air.

For ease in identification, small buttons are embossed on the sides of the plates and frames, one on the non-washing plates, two on the frames and three on the washing plates as shown in Figure 7.10.

Example 7.1

A slurry is filtered in a plate and frame press containing 12 frames, each 0.3 m square and 25 mm thick. During the first 180 s the pressure difference for filtration is slowly raised to the final value of 400 kN/m^2 and, during this period, the rate of filtration is maintained constant. After the initial period, filtration is carried out at constant pressure and the cakes are completely formed in a further 900 s. The cakes are then washed with a pressure difference of 275 kN/m^2 for 600 s using *thorough washing* (See the plate and frame press in Section 7.4.4). What is the volume of filtrate collected per cycle and how much wash water is used?

A sample of the slurry had previously been tested with a leaf filter of 0.05 m^2 filtering surface using a vacuum giving a pressure difference of 71.3 kN/m^2. The volume of filtrate collected in the first 300 s, was 250 cm^3 and, after a further 300 s, an additional 150 cm^3 was collected. It may be assumed that the cake is incompressible and that the cloth resistance is the same in the leaf as in the filter press.

This book belongs to Bradley Loren (bloren@mcandrews-ip.com) Copyright Elsevier 2024

Intas Exhibit 1032
Page 41 of 470
PGR2025-00043

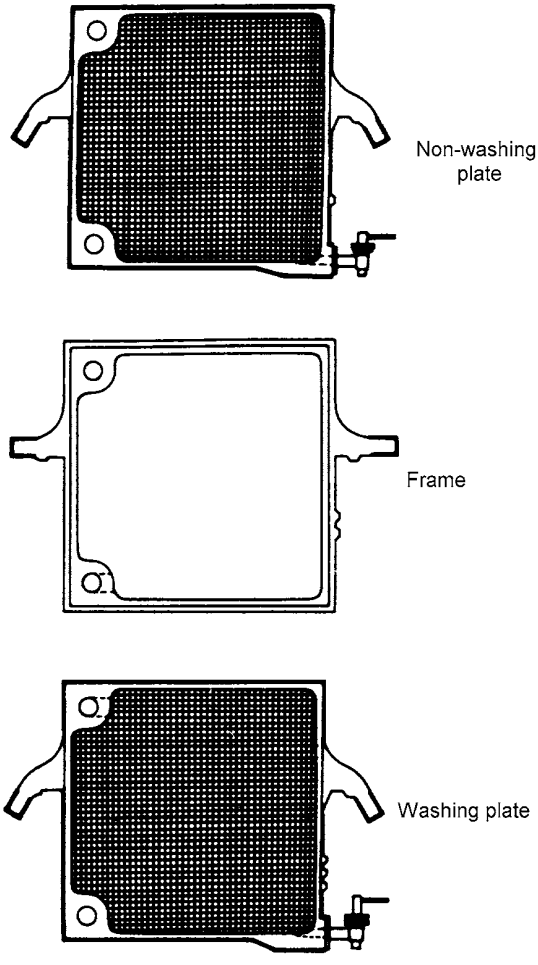


Figure 7.10. Plates and frames

Solution

In the leaf filter, filtration is at constant pressure from the start.

Thus: $$V^2 + 2\frac{AL}{\upsilon}V = 2\frac{(-\Delta P)A^2}{\mathbf{r}\mu\upsilon}t \qquad \text{(from equation 7.18)}$$

In the filter press, a volume V_1 of filtrate is obtained under constant rate conditions in time t_1, and filtration is then carried out at constant pressure.

Thus: $$V_1^2 + \frac{AL}{\upsilon}V_1 = \frac{(-\Delta P)A^2}{\mathbf{r}\mu\upsilon}t_1 \qquad \text{(from equation 7.17)}$$

This book belongs to Bradley Loren (bloren@mcandrews-ip.com) Copyright Elsevier 2024

and:

$$(V^2 - V_1^2) + 2\frac{AL}{\upsilon}(V - V_1) = 2\frac{(-\Delta P)A^2}{\mathbf{r}\mu\upsilon}(t - t_1) \qquad \text{(from equation 7.18)}$$

For the leaf filter

When $t = 300$ s, $V = 250\text{cm}^3 = 2.5 \times 10^{-4}$ m^3 and when $t = 600$ s, $V = 400$ cm$^3 = 4 \times 10^{-4}$ m^3, $A = 0.05$ m^2 and $-\Delta P = 71.3$ kN/m^2 or 7.13×10^4 N/m^2.

Thus: $(2.5 \times 10^{-4})^2 + 2(0.05L/\upsilon)2.5 \times 10^{-4} = 2(7.13 \times 10^4 \times 0.05^2/\mathbf{r}\mu\upsilon)300$

and: $(4 \times 10^{-4})^2 + 2(0.05L/\upsilon)4 \times 10^{-4} = 2(7.13 \times 10^4 \times 0.05^2/\mathbf{r}\mu\upsilon)600$

That is: $$6.25 \times 10^{-8} + 2.5 \times 10^{-5}\frac{L}{\upsilon} = \frac{1.07 \times 10^5}{\mathbf{r}\mu\upsilon}$$

and: $$16 \times 10^{-8} + 4 \times 10^{-5}\frac{L}{\upsilon} = \frac{2.14 \times 10^5}{\mathbf{r}\mu\upsilon}$$

Hence: $L/\upsilon = 3.5 \times 10^{-3}$ and $\mathbf{r}\mu\upsilon = 7.13 \times 10^{11}$

For the filter press

$A = (12 \times 2 \times 0.3^2) = 2.16$ m^2, $-\Delta P = 400$ kN/m$^2 = 4 \times 10^5$ N/m^2, $t = 180$ s. The volume of filtrate V_1 collected during the constant rate period on the filter press is given by:

$$V_1^2 + (2.16 \times 3.5 \times 10^{-3}V_1) = [(4 \times 10^5 \times 2.16^2)/(7.13 \times 10^{11})]180$$

$$V_1^2 + (7.56 \times 10^{-3}V_1) - (4.711 \times 10^{-4}) = 0$$

or: $$V_1 = -(3.78 \times 10^{-3}) + \sqrt{(1.429 \times 10^{-5} + 4.711 \times 10^{-4})} = 1.825 \times 10^{-2} \text{ m}^3$$

For the constant pressure period:

$$(t - t_1) = 900 \text{ s}$$

The total volume of filtrate collected is therefore given by:

$$(V^2 - 3.33 \times 10^{-4}) + (1.512 \times 10^{-2})(V - 1.825 \times 10^{-2}) = 5.235 \times 10^{-6} \times 900$$

or: $$V^2 + (1.512 \times 10^{-2}V) - (4.712 \times 10^{-3}) = 0$$

Thus: $$V = -0.756 \times 10^{-2} + \sqrt{(0.572 \times 10^{-4} + 4.712 \times 10^{-3})}$$

$$= 6.15 \times 10^{-2} \text{ or } \underline{\underline{0.062 \text{ m}^3}}$$

The final rate of filtration is given by:

$$\frac{-\Delta P A^2}{\mathbf{r}\mu\upsilon(V + AL/\upsilon)} = \frac{4 \times 10^5 \times 2.16^2}{7.13 \times 10^{11}(6.15 \times 10^{-2} + 2.16 \times 3.5 \times 10^{-3})} = 3.79 \times 10^{-5}\text{m}^3/\text{s}$$

(from equation 7.16)

If the viscosity of the filtrate is the same as that of the wash-water, then:

Rate of washing at 400 kN/m$^2 = \frac{1}{4} \times 3.79 \times 10^{-5} = 9.5 \times 10^{-6}$ m^3/s

Rate of washing at 275 kN/m$^2 = 9.5 \times 10^{-6} \times (275/400) = 6.5 \times 10^{-6}$ m^3/s

Thus the amount of wash-water passing in 600 s $= (600 \times 6.5 \times 10^{-6})$

$$= 3.9 \times 10^{-3}\text{m}^3 \text{ or } \underline{\underline{0.004 \text{ m}^3}}$$

This book belongs to Bradley Loren (bloren@mcandrews-ip.com) Copyright Elsevier 2024

Intas Exhibit 1032
Page 43 of 470
PGR2025-00043

The recessed plate filter press

The recessed type of press is similar to the plate and frame type except that the use of frames is obviated by recessing the ribbed surface of the plates so that the individual filter chambers are formed between successive plates. In this type of press therefore the thickness of the cake cannot be varied and it is equal to twice the depth of the recess on individual plates.

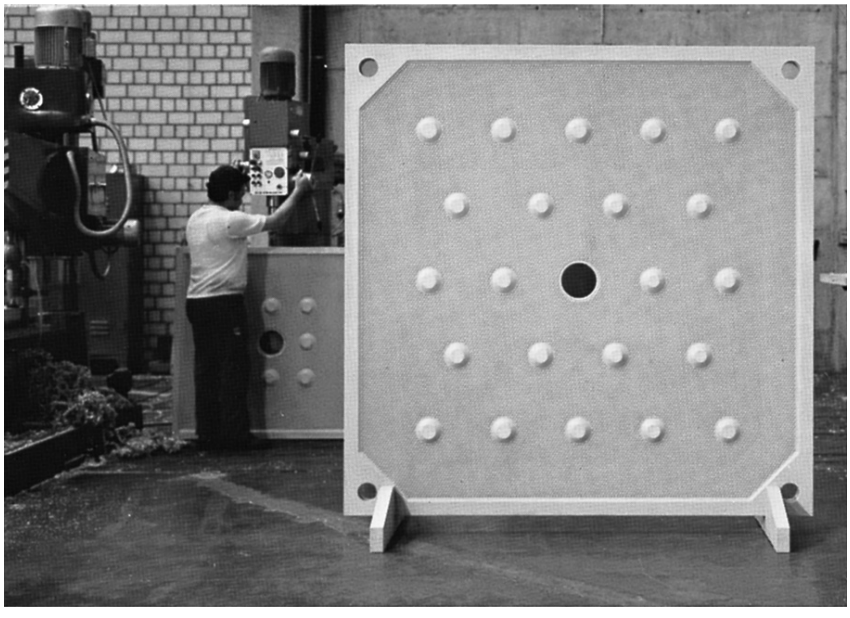


Figure 7.11. A recessed chamber plate, 2 m square

The feed channel shown in Figure 7.11 usually differs from that employed on the plate and frame press. All the chambers are connected by means of a comparatively large hole in the centre of each of the plates and the cloths are secured in position by means of screwed unions. Slurries containing relatively large solid particles may readily be handled in this type of press without fear of blocking the feed channels. As described by CHERRY[28], developments in filter presses have been towards the fabrication of larger units, made possible by mechanisation and the use of newer lighter materials of construction. The plates of wood used in earlier times were limited in size because of limitations of pressures and large cast-iron plates presented difficulty in handling. Large plates are now frequently made of rubber mouldings or of polypropylene although distortion may be a problem, particularly if the temperature is high.

The second area of advance is in mechanisation which enables the opening and closing to be done automatically by a ram driven hydraulically or by an electric motor. Plate transportation is effected by fitting triggers to two endless chains operating the plates, and labour costs have consequently been reduced very considerably. Improved designs have

This book belongs to Bradley Loren (bloren@mcandrews-ip.com) Copyright Elsevier 2024

Intas Exhibit 1032
Page 44 of 470
PGR2025-00043

given better drainage which has led to improved washing. Much shorter time cycles are now obtained and the cakes are thinner, more uniform, and drier. These advantages have been rather more readily obtained with recessed plates where the cloth is subjected to less wear.

Advantages of the filter press

(a) Because of its basic simplicity the filter press is versatile and may be used for a wide range of materials under varying operating conditions of cake thickness and pressure.
(b) Maintenance cost is low.
(c) It provides a large filtering area on a small floor space and few additional associated units are needed.
(d) Most joints are external and leakage is easily detected.
(e) High pressure operation is usually possible.
(f) It is equally suitable whether the cake or the liquid is the main product.

Disadvantages of the filter press

(a) It is intermittent in operation and continual dismantling is apt to cause high wear on the cloths.
(b) Despite the improvements mentioned previously, it is fairly heavy on labour.

Example 7.2

A slurry containing 100 kg of whiting, of density 3000 kg/m^3, per m^3 of water, and, is filtered in a plate and frame press, which takes 900 s to dismantle, clean, and re-assemble. If the cake is incompressible and has a voidage of 0.4, what is the optimum thickness of cake for a filtration pressure $(-\Delta P)$ of 1000 kN/m^2? The density of the whiting is 3000 kg/m^3. If the cake is washed at 500 kN/m^2 and the total volume of wash water employed is 25 per cent of that of the filtrate, how is the optimum thickness of the cake affected? The resistance of the filter medium may be neglected and the viscosity of water is 1 mNs/m^2. In an experiment, a pressure difference of 165 kN/m^2 produced a flow of water of 0.02 cm^3/s through a centimetre cube of filter cake.

Solution

The basic filtration equation may be written as:

$$\frac{1}{A}\frac{\mathrm{d}V}{\mathrm{d}t} = \frac{(-\Delta P)}{\mathbf{r}\mu l} \qquad \text{(equation 7.2)}$$

where **r** is defined as the specific resistance of the cake.

The slurry contains 100 kg whiting/m^3 of water.

Volume of 100 kg whiting $= (100/3000) = 0.0333$ m^3.

Volume of cake $= 0.0333/(1 - 0.4) = 0.0556$ m^3.

This book belongs to Bradley Loren (bloren@mcandrews-ip.com) Copyright Elsevier 2024

Intas Exhibit 1032
Page 45 of 470
PGR2025-00043

Volume of liquid in cake $= (0.0556 \times 0.4) = 0.0222\ \text{m}^3$.

Volume of filtrate $= (1 - 0.0222) = 0.978\ \text{m}^3$.

Thus: volume of cake/volume of filtrate $v = 0.0569$

In the experiment:

$$A = 10^{-4}\ \text{m}^2, \quad (-\Delta P) = 1.65 \times 10^5\ \text{N/m}^2, \quad l = 0.01\ \text{m},$$
$$\frac{\mathrm{d}V}{\mathrm{d}t} = 2 \times 10^{-8}\ \text{m}^3/\text{s}, \quad \mu = 10^{-3}\ \text{Ns/m}^2$$

Inserting these values in equation 7.2 gives:

$$\left(\frac{1}{10^{-4}}\right)(2 \times 10^{-8}) = \frac{1}{\mathbf{r}}\frac{(1.65 \times 10^5)}{(10^{-3})(10^{-2})}, \text{ and } \mathbf{r} = 8.25 \times 10^{13}\ \text{m}^{-2}$$

From equation 7.2:

$$V^2 = \frac{2A^2(-\Delta P)t}{\mathbf{r}\mu v} \qquad \text{(equation 7.11)}$$

But: $L =$ half frame thickness $= V\upsilon/A$ (equation 7.6)

Thus:
$$L^2 = \frac{2A(-\Delta P)vt}{\mathbf{r}\mu}$$
$$= \frac{2 \times (1 \times 10^6) \times 0.0569}{(8.25 \times 10^{13})(1 \times 10^{-3})}t_f$$
$$= 1.380 \times 10^{-6}\, t_f \text{ (where } t_f \text{ in the filtration time)}$$
$$L = 1.161 \times 10^{-3} t_f^{1/2}$$

It is shown in Section 7.4.4 that if the resistance of the filter medium is neglected, the optimum cake thickness occurs when the filtration time is equal to the downtime,

Thus: $t = 900$ s, $\quad t^{1/2} = 30$

$\therefore$ $L_{\text{opt}} = 34.8 \times 10^{-3}\ \text{m} = 34.8$ or 35 mm

and: optimum frame thickness $= \underline{\underline{70\ \text{mm}}}$

For the washing process, if the filtration pressure is halved, the rate of washing is halved. The wash water has twice the thickness to penetrate and half the area for flow that is available to the filtrate, so that, considering these factors, the washing rate is one-eighth of the final filtration rate.

The final filtration rate
$$\frac{\mathrm{d}V}{\mathrm{d}t} = \frac{A^2(-\Delta P)}{\mathbf{r}\mu\upsilon V}$$
$$= \frac{1 \times 10^6 A^2}{(8.25 \times 10^{13}) \times 10^{-3} \times 0.0569V} = \frac{(2.13 \times 10^{-4}A^2)}{V}$$

and: The washing rate $=$ (final rate of filtration/8) $= 2.66 \times 10^{-5}A^2/V$

This book belongs to Bradley Loren (bloren@mcandrews-ip.com) Copyright Elsevier 2024

Intas Exhibit 1032
Page 46 of 470
PGR2025-00043

The volume of wash water $= V/4$.

Hence: washing time $t_w = (V/4)/(2.66 \times 10^{-5} A^2/V)$

That is: $t_w = 940V^2/A^2$

$$V^2 = L^2A^2/v^2$$

Therefore: $$t_w = \left(\frac{L^2A^2}{(0.0569)^2}\right)\left(\frac{940}{A^2}\right) = 2.90 \times 10^5 L^2$$

The filtration time t_f was shown earlier to be: $t_f = L^2/1.380 \times 10^{-6} = 7.25 \times 10^5 L^2$

Thus: total cycle time $= L^2(2.90 \times 10^5 + 7.25 \times 10^5) + 900$

$$= 1.015 \times 10^6 L^2 + 900$$

The rate of cake production is then:

$$= \frac{L}{1.025 \times 10^6 L^2 + 900} = R$$

For $\mathrm{d}R/\mathrm{d}L = 0$, then: $1.025 \times 10^6 L^2 + 900 - 2.050 \times 10^6 L^2 = 0$

$$L^2 = \frac{900}{1.025 \times 10^6} \quad \text{and} \quad L = 29.6 \times 10^{-3}\ \text{m} = 29.6\ \text{mm}$$

Thus: Frame thickness $= 59.2 \approx \underline{\underline{60\ \text{mm}}}$

7.4.5. Pressure leaf filters

Pressure leaf filters are designed for final discharge of solids in either a dry or wet state, under totally enclosed conditions, with fully automatic operation.

Each type of pressure leaf filter features a pressure vessel in which are located one or more filter elements or leaves of circular or rectangular construction. The filter media may be in the form of a synthetic fibre or other fabrics, or metallic mesh. Supports and intermediate drainage members are in coarse mesh with all components held together by edge binding. Leaf outlets are connected individually to an outlet manifold which passes through the wall of the pressure vessel.

The material to be filtered is fed into the vessel under pressure, and separation takes place with the solids being deposited on the leaf surface, and the liquid passing through the drainage system and out of the filter. Cycle times are determined by pressure, cake capacity or batch quantity. Where particularly fine solids must be removed, a layer of precoat material may be deposited on the leaves prior to filtration, using diatomaceous earth, Perlite, or other suitable precoat materials.

Cake washing, for recovery of mother liquor or for removal of solubles, may be carried out before discharge of the solids as a slurry or a dry cake.

Pressure leaf filters are supplied in a wide range of size and materials of construction. One typical design is the "Verti-jet" unit with a vertical tank and vertical leaf filter, as shown in Figure 7.12, with rectangular leaves mounted individually but connected to a common outlet manifold. For sluice cleaning either a stationary or oscillating jet system

This book belongs to Bradley Loren (bloren@mcandrews-ip.com) Copyright Elsevier 2024

Intas Exhibit 1032
Page 47 of 470
PGR2025-00043

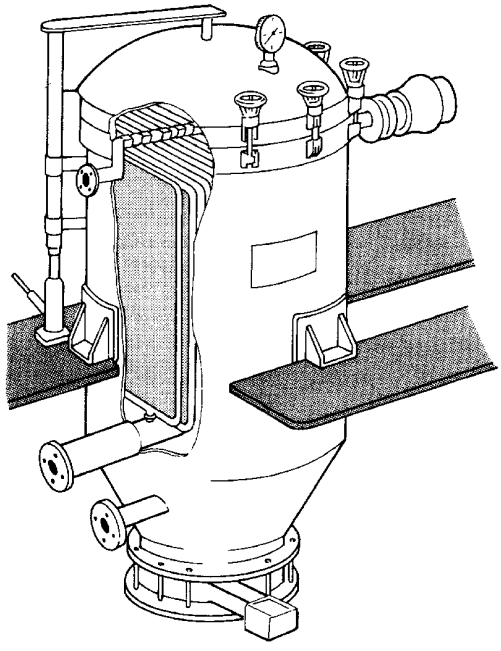


Figure 7.12. "Verti-jet" pressure leaf filter

using high efficiency spray nozzles is fitted so as to give complete cake removal. For recovery of dry solids, vibration of the leaves allows automatic discharge of the solids through a bottom discharge port provided with a quick opening door.

In the "Auto jet" design, circular leaves are mounted on a horizontal shaft which serves as the filtrate outlet manifold. The leaves are rotated during the cleaning cycle although, in addition, extra low speed continuous rotation during operation ensures uniform cake build-up in difficult applications. The leaves are of metallic or plastics construction covered with fabric or wire cloth for direct or precoat operation, and rotation of the leaves during cleaning promotes fast efficient sluice discharge with minimum power consumption. As an alternative, the leaves may be rotated over knife blades which remove the cake in a dry state. Units of this type are used for handling foodstuffs and also for the processing of minerals and effluents.

For the handling of edible oils, molten sulphur, effluents and foodstuffs, a Filtra-Matic unit is used in which either the bundle is retracted from the shell as a unit, or the filter tank is retracted leaving the filter leaves and filter cover in position. Such units are available in cylindrical, conical or trough shell configurations, and cleaning may be either wet or dry, manual or automatic. In the latter case, for dry discharge, vibration systems are used and for wet removal spray jets mounted in an overhead manifold sweep the entire leaf surface in an oscillating motion. In this design, the heavy duty leaves covered with cloth or screen are all interchangeable and, whether round or rectangular, are all the same size to give uniform precoat, cake build-up and filtration. In horizontal tray pressure filters, used in batch processes and intermittent flows, the trays are mounted horizontally with

This book belongs to Bradley Loren (bloren@mcandrews-ip.com) Copyright Elsevier 2024

Intas Exhibit 1032
Page 48 of 470
PGR2025-00043

connections to a vertical filtrate manifold at the rear, and such units are ideally suited where cake washing and positive cake drying are required. In many cases, the accumulated cake may be sluiced off without removing trays from the filter and a special recovery leaf is provided where heel filtration is required in which a thin layer of cake is left semi-permanently in contact with the filter medium to improve the clarity of the filtrate. This system is used in various clarification processes and is ideal for handling high flows of liquids with a low solids concentration. In most designs the tubes are mounted vertically from a tube sheet at the top of the tank and cleaning is provided with a self-contained internal "air-pump" backwash, thus avoiding the use of large volumes of sluicing liquid or separate pumps to provide fast and complete removal of the filter cake. The heavy gauge perforated tube cores are covered with a seamless cloth sleeve sealed at either end by a clamping device. As an alternative, heavy gauge wire is wound around the centre core, with controlled spacing to give reliable filtration and easy cake release. Tubular element units of this type are available in standard sizes up to 40 m^2.

Cartridge filters

One particular design of pressure filter is the *filter cartridge*, typified by the Metafilter which employs a filter bed deposited on a base of rings mounted on a fluted rod, and is extensively used for clarifying liquids containing small quantities of very fine suspended solids. The rings are accurately pressed from sheet metal of very uniform thickness and are made in a large number of corrosion-resistant metals, though stainless steels are usually employed. The standard rings are 22 mm in external diameter, 16 mm in internal diameter and 0.8 mm thick, and are scalloped on one side, as shown in Figure 7.13, so that the edges of the discs are separated by a distance of 0.025–0.25 mm according to

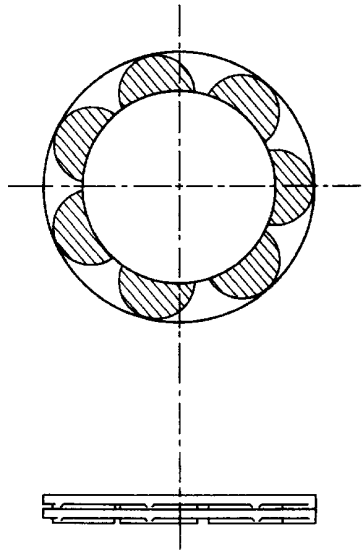


Figure 7.13. Rings for metafilter (Stella Meta)

This book belongs to Bradley Loren (bloren@mcandrews-ip.com) Copyright Elsevier 2024

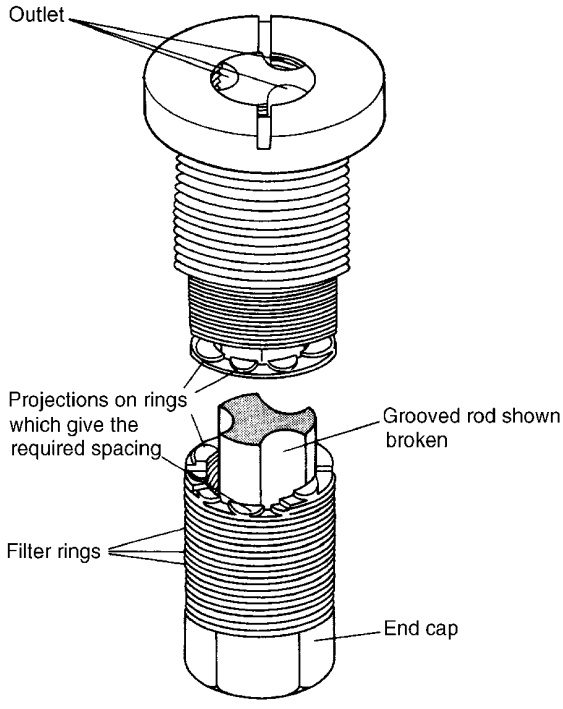


Figure 7.14. Metafilter pack (Stella Meta)

requirements. The pack is formed by mounting the rings, all the same way up, on the drainage rod and tightening them together by a nut at one end against a boss at the other as shown in Figure 7.14. The packs are mounted in the body of the filter which operates under either positive or reduced pressure.

The bed is formed by feeding a dilute suspension of material, to the filter usually a form of kieselguhr, which is strained by the packs to form a bed about 3 mm thick. Kieselguhr is available in a number of grades and forms a bed of loose structure which is capable of trapping particles much smaller than the channels. During filtration, the solids build up mainly on the surface and do not generally penetrate more than 0.5 mm into the bed. The filtrate passes between the discs and leaves through the fluted drainage rod, and operation is continued until the resistance becomes too high. The filter is then cleaned by back-flushing, which causes the filter cake to crack and peel away. In some cases the cleaning may be incomplete as a result of channelling. If for any reason the spaces between the rings become blocked, the rings may be quickly removed and washed.

The Metafilter is widely used for filtering domestic water, beer, organic solvents and oils. The filtration characteristics of clay-like materials can often be improved by the continuous introduction of a small quantity of filter aid to the slurry as it enters the filter. On the other hand, when the suspended solid is relatively coarse, the Metafilter will operate successfully as a strainer, without the use of a filter bed.

This book belongs to Bradley Loren (bloren@mcandrews-ip.com) Copyright Elsevier 2024

Intas Exhibit 1032
Page 50 of 470
PGR2025-00043

The Metafilter is very robust and is economical in use because there is no filter cloth and the bed is easily replaced and hence labour charges are low. Mono pumps or diaphragm pumps are most commonly used for feeding the filter. These are discussed in Volume 1, Chapter 8.

Example 7.3

The relation between flow and head for a certain slurry pump may be represented approximately by a straight line, the maximum flow at zero head being 0.0015 m^2/s and the maximum head at zero flow 760 m of liquid.

Using this pump to feed a particular slurry to a pressure leaf filter:

(a) How long will it take to produce 1 m^3 of filtrate?
(b) What will be the pressure across the filter after this time?

A sample of the slurry was filtered at a constant rate of 0.00015 m^3/s through a leaf filter covered with a similar filter cloth but of one-tenth the area of the full-scale unit, and after 625 s the pressure across the filter was 360 m of liquid. After a further 480 s the pressure was 600 m of liquid.

Solution

For constant rate filtration through the filter leaf:

$$V^2 + \frac{LA}{v}V = \frac{A^2(-\Delta P)t}{\mathbf{r}\mu v} \qquad \text{(equation 7.17)}$$

At a constant rate of 0.00015 m^3/s, then, when the time = 625 s:

$$V = 0.094 \text{ m}^3, (-\Delta P) = 3530 \text{ kN/m}^2$$

and, at $t = 1105$ s: $V = 0.166$ m^3 and $(-\Delta P) = 5890$ kN/m^2

Substituting these values into equation 7.17 gives:

$$(0.094)^2 + LA/v \times 0.094 = (A^2/\mathbf{r}\mu v) \times 3530 \times 625$$

or:
$$0.0088 + 0.094LA/v = 2.21 \times 10^6 A^2/\mathbf{r}\mu v \qquad \text{(i)}$$

and:
$$(0.166)^2 + LA/v \times 0.166 = (A^2/\mathbf{r}\mu v) \times 5890 \times 1105$$

or:
$$0.0276 + 0.166LA/v = 6.51 \times 10^6 A^2/\mathbf{r}\mu v \qquad \text{(ii)}$$

Equations (i) and (ii) may be solved simultaneously to give:

$$LA/v = 0.0154 \text{ and } A^2/\mathbf{r}\mu v = 4.64 \times 10^{-9}$$

As the full-size plant is 10 times that of the leaf filter, then:

$$LA/v = 0.154 \text{ and } A^2/\mathbf{r}\mu v = 4.64 \times 10^{-7}$$

This book belongs to Bradley Loren (bloren@mcandrews-ip.com) Copyright Elsevier 2024

Intas Exhibit 1032
Page 51 of 470
PGR2025-00043

If the pump develops 760 m (7460 kN/m^2) at zero flow and has zero head at $Q = 0.0015$ m^3/s, its performance may be expressed as:

$$-\Delta P = 7460 - (7460/0.0015)Q$$

or:

$$-\Delta P = 7460 - 4.97 \times 10^6 Q \text{ (kN/m}^2\text{)}$$

$$\frac{dV}{dt} = \frac{A^2(-\Delta P)}{\mathbf{r}\mu v(V + LA/v)} \qquad \text{(equation 7.16)}$$

Substituting for $(-\Delta P)$ and the filtration constants gives:

$$\frac{dV}{dt} = \frac{A^2}{\mathbf{r}\mu v}\frac{(7460 - 4.97 \times 10^6 dV/dt)}{(V + 0.154)}$$

Since $Q = dV/dt$, then:

$$\frac{dV}{dt} = \frac{4.67 \times 10^{-7}[7460 - 4.97 \times 10^6(dV/dt)]}{(V + 0.154)}$$

$$(V + 0.154)dV = 3.46 \times 10^{-3} - 2.31 dV/dt$$

The time to collect 1m^3 is then given by:

$$\int_0^1 (V + 0.154 + 2.31)dV = \int_0^t (3.46 \times 10^{-3})dt$$

and:

$$\underline{\underline{t = 857 \text{ s}}}$$

The pressure at this time is found by substituting in equation 7.17 with $V = 1$ m^3 and $t = 857$ s to give:

$$1^2 + 0.154 \times 1 = 4.64 \times 10^{-7} \times 857(-\Delta P)$$

and:

$$-\Delta P = \underline{\underline{2902 \text{ kN/m}^2}}$$

7.4.6. Vacuum filters

If in a horizontal filter both sides are open to atmosphere then, as slurry is introduced above the filter medium, filtration will occur at an adequate rate as long as the hydrostatic head of slurry above the filter medium is sufficient. The unit then operates as a gravity filter. If, however, the top of the vessel is enclosed and the slurry is introduced under pressure, then the unit operates as a pressure filter and the driving force is the amount by which the applied pressure exceeds atmospheric pressure below the filter medium. Greatly enhanced filtration rates may then be achieved. Similarly, if the pressure beneath the filter is reduced below atmospheric, the unit operates as a vacuum filter and the driving force may again be appreciably greater than that available with a gravity filter. The maximum theoretical driving force is then 101 kN/m^2 less the vapour pressure of the filtrate, and much higher flowrates may be obtained than with gravity filtration. With, for example, a head of liquor of 0.3 m in a gravity filter, the maximum driving force is about 3 kN/m^2, whereas in theory the driving force of a vacuum filter could be some thirty times greater.

Vacuum filtration has many advantages, not the least being the fact that the feed slurry, often containing abrasive solids in a corrosive liquid, can be delivered by gravity flow or by low pressure pumps which need only to overcome the resistance in the feed pipework. In addition, vacuum filtration equipment does not have to withstand high pressures

This book belongs to Bradley Loren (bloren@mcandrews-ip.com) Copyright Elsevier 2024

Intas Exhibit 1032
Page 52 of 470
PGR2025-00043

and can therefore be manufactured in a wider range of materials. When, because of corrosive conditions or the need to prevent product contamination, expensive materials of construction are required, the low pressures involved allow considerable economy in manufacturing costs. A further advantage is that, after the bulk of the mother liquor has been filtered from the solids, the cake is accessible to mechanical dewatering, flood washing and sampling, and cake removal can be carried out quickly as it is easily automated. Because of the ease of solids removal, a vacuum filter may be operated with very short cycle times of around 60 s, and the resulting thin filter cakes give very high flowrates per unit area, typically six times as great as those obtained with a pressure filter operating at the same differential pressure. Where delicate solids are handled, very low differential pressures may be used and, since the feed and the filtrate are not handled under positive pressure, there is no possibility of liquor leakage from the system as might be the case with high pressure differentials. This is an important advantage especially where corrosive or hazardous materials are involved.

Batch type vacuum filters

Batch vacuum filters were developed from gravity filters and, in essence, Buchner funnels as used in laboratories and Nutsche type filters as used in industry are similar to gravity filters, except that they feature a vacuum pump or some other vacuum generating equipment to reduce the pressure under the filter medium, thereby increasing the driving force across the filter medium.

Simple filters operating in this manner are often referred to as pan filters, and they incorporate certain features which are now being incorporated into continuously operating machines. These filters enable the initial cake formation to be made, either under gravity or at very low differential pressures, so that uniform distribution of the solids over the filter medium is obtained. Preferential settling occurs so that the heavier, and usually coarser, solids contact the filter medium first, thereby protecting it from the slower settling fine solids. Following this, the filtrate drainage section may be subjected to higher vacuum to give greater differential pressures, higher flowrates per unit area and greater total flows. A typical cycle for a batch type vacuum filter might be:

(a) Feeding of slurry,
(b) Cake formation and filtration, initially under gravity if required, followed by vacuum operation,
(c) Initial drying for maximum removal of mother liquor,
(d) Cake washing and drying,
(e) Manual discharge of solids,
(f) Cloth washing.

The advantages of such units include simplicity in both design and operation, low cost per unit area and flexibility with regard to filtration, washing and drying periods. In addition, very sharp separation of the mother liquor and various wash liquors can be obtained due to the wash liquors being completely contained within the pan. The filter cakes remain in position between batches without the necessity for power to be used for their retention. In addition, the flow through the filter medium can be stopped or be restricted to a very low rate in order to obtain leaching from the solids in the filter bed.

This book belongs to Bradley Loren (bloren@mcandrews-ip.com) Copyright Elsevier 2024

Intas Exhibit 1032
Page 53 of 470
PGR2025-00043

Against this, it may be necessary with a batch vacuum filter to provide holding vessels for feed, and possibly filtrate and wash. The discharge of solids is intermittent and this may lead to complications in feeding the solids to a continuous dryer or to some other continuous process, and cake hoppers and a feeding arrangement may have to be provided.

Since the liquor flowrate decreases as filtration proceeds, facilities to cope with this must be incorporated in the feed and filtrate handling sections of the system and the discharge of solids must be a manual operation if the solids cannot be sluiced off.

Equipment has been developed to overcome the disadvantages of manual discharge of solids from the simple batch pan type vacuum filter, and such equipment incorporates scrapers or rakes for the removal of the solids. Other pan type vacuum filters are arranged so that the pan is tipped over, when the solids are discharged, either under their own weight or sometimes with the assistance of blow-back air admitted to the underside of the filter cloth when the pan is inverted.

Further developments eliminate, or reduce to acceptable proportions, the cyclic variations noted previously and one simple development which achieves this to a limited extent involves a number of individual tipping pans arranged in parallel. For example, with three pans discharging into a common slurry tank, the operation is arranged so that whilst one pan is being charged with feed material and, whilst solids–mother liquor separation is being carried out in it, the second pan is at the washing stage and third pan is at the drying and discharging stage. This arrangement obviously reduces cyclic variations though it necessitates diversion of the feed and wash liquor from one pan to another. The operation can, however, be carried out automatically by the use of a process timer or similar control unit.

Classification of batch and continuous vacuum filters

The disadvantages of cyclic operation, attributable to the need to remove the cake from batch filters, have been largely overcome by the development of a wide range of continuous vacuum filters as summarised in Table 7.2 which includes data on the selection for a given duty. This is further detailed in Table 7.3 and is based on the work of G. H. Duffield of Stockdale Engineering and E. Davies of EDACS Ltd.

Horizontal continuous filters

One way of limiting still further cyclic variations is to use vacuum filters of the horizontal continuous type, and many designs have been developed which in the main consist of pans arranged in line or in a circle so that each in turn goes through the same cycle of operations, namely: feeding, dewatering, washing, drying, automatic solids discharge and cloth washing. The pans move past the stationary feed and wash areas where the feed and wash liquors are continuously introduced to the filter. Alternatively, a plain filter surface may be arranged as a linear belt or as a circular table, in place of pans.

All filters of this type have the distinct advantage of continuous operation and, as a result, the feed and wash liquors may be fed to the equipment at steady rates. Dense, quick settling solids can be handled, and the cake thickness — and the washing and drying times — can be varied independently between quite wide limits. The cake can be flooded with wash liquor, which can be taken away separately and re-used to obtain countercurrent

This book belongs to Bradley Loren (bloren@mcandrews-ip.com) Copyright Elsevier 2024

Intas Exhibit 1032
Page 54 of 470
PGR2025-00043

Table 7.2. Classification of vacuum filters

Type of vacuum filter	Note	Usual max. area (m^2)	Characteristics of suitable slurry (See notes below)					Performance index (See notes below)		
			A	B	C	D	E	Cake dryness	Cake washing	Filtrate clarity
(A) *Cake filters*										
Single tipping pan	1	3	X	X				4–7	8–9	8
Multi tipping pan	2	12	X	X				4–7	8–9	8
Horizontal linear tipping pan	3	25	X	X				4–7	8–9	7
Horizontal linear belt	4	20	X	X				5–8	7–8	6
Rotary tipping pan	3	200	X	X				4–7	8–9	7
Horizontal rotary table	4	15	X	X				4–7	7–8	7
Rotary drum—string discharge	5	80		X	X			5–8	6	8
Rotary drum—knife discharge	5	80		X	X			5–8	6	8
Rotary drum—roller discharge	5	80			X	X		5–6	5	8
Rotary drum—belt discharge	5	80			X	X	X	5–8	6	7
Top feed drum	6	10	X	X				1–2	1	6
Hopper/dewaterer	6	10	X					1–2	1	6
Internal drum	7	12		X	X			3–4	1	6
Single comp. drum	8	15			X			2–3	4	5
Disc	9	300		X	X			2–3	1	6
(B) *Media filters*										
Rotary drum precoat	10	80				X	X	—	6	9

NOTES

Filters

1. For small batch production. Has very wide application, is very adaptable and can be automated.
2. Usually 2 to 4 pans, for medium size batch production. Very wide application, very adaptable, can be automated.
3. For free-draining materials where very good washing is required with sharp separation between mother liquor and wash liquors.
4. For free-draining materials where very good washing is required.
5. Wide range of types and size available. Generally suitable for most slurries in categories B and C. Can usually be fitted with various mechanical devices to improve the washing and drying.
6. Restricted to very free-draining materials not requiring washing.
7. Restricted to very free-draining materials not requiring washing, but where the solids can be retained by vacuum alone.
8. Allows use of high drum speed and is capable of very high flow rates.
9. Large throughputs for small floor space.
10. Suitable for almost any clarification and for handling materials which blind normal filter media.

Slurries

A. High solids concentration, normally greater than 20 per cent, having solids which are free-draining and fast settling, giving difficulty in mechanical agitation and giving high filtration rates.
B. Rapid cake formation with reasonably fast settling solids which can be kept in suspension by mechanical agitation.
C. Lower solids concentration with solids giving slow cake formation and thin filter cakes which can be difficult to discharge.
D. Low solids concentration with solids giving slow cake formation and a filter cake having very poor mechanical strength.
E. Very low solids concentration (i.e. clarification duty), or containing solids which blind normal filter media. Filtrate usually required.
X. Slurries handled.

Performance index

9 = the highest possible performance.
1 = very poor or negligible performance.

This book belongs to Bradley Loren (bloren@mcandrews-ip.com) Copyright Elsevier 2024

Intas Exhibit 1032
Page 55 of 470
PGR2025-00043

This book belongs to Bradley Loren (bloren@mcandrews-ip.com)

Table 7.3. Operating data for some vacuum filter applications

Application	Type of vacuum filter frequently used (see note 2)	Solids content of feed (per cent by mass)	Solids handling rate kg dry solids/s m^2 filter surface (see note 3)	Moisture content of cake (per cent by mass)	Air flow	
					Filter surface (see note 4) (m^3/s m^2)	Vacuum (kN/m^2 pressure, below atmospheric)
Chemicals						
Aluminium hydrate	Top feed drum	25–50	0.12–0.2	10–17	0.025	84
Barium nitrate	”	80	0.34	5	0.13	67
Barium sulphate	Drum	40	0.013	30	0.005	33
Sodium bicarbonate	”	50	0.5	12	0.15	61
Calcium carbonate	”	50	0.03	22	0.010	33
Calcium (pptd)	”	30	0.04	40	0.010	26
Calcium sulphate	Tipping pan	35	0.16	30	0.025	41
Caustic lime mud	Drum	30	0.20	50	0.03	51
Sodium hypochlorite	Belt disch. drum	12	0.04	30	0.015	33
Titanium dioxide	Drum	30	0.03	40	0.010	33
Zinc stearate	”	5	0.007	65	0.015	33
Minerals						
Frothed coal (coarse)	Top feed drum	30	0.20	18	0.020	61
Frothed coal (fine)	Drum or Disc	35	0.10	22	0.015	51
Frothed coal tailings	Drum	40	0.05	30	0.010	26
Copper concentrates	”	50	0.07	10	0.010	30
Lead concentrates	”	70	0.27	12	0.015	26
Zinc concentrates	”	70	0.20	10	0.010	33
Flue dust (blast furnace)	”	40	0.04	20	0.015	33
Fluorspar	”	50	0.27	12	0.025	51

Copyright Elsevier 2024

Intas Exhibit 1032
Page 56 of 470
PGR2025-00043

This book belongs to Bradley Loren (bloren@mcandrews-ip.com)

Table 7.3. (*continued*)

Application	Type of vacuum filter frequently used (see note 2)	Solids content of feed (per cent by mass)	Solids handling rate kg dry solids/s m^2 filter surface (see note 3)	Moisture content of cake (per cent by mass)	Air flow	
					Filter surface (see note 4) (m^3/s m^2)	Vacuum (kN/m^2 pressure, below atmospheric)
Paper						
Kraft pulp	Deep sub. drum or Disc	1.5	0.05	90	Barometric leg	
Effluents	Drum	3	0.005	80	0.015	41
Bleach washer	”	1.0	0.20 (filtrate)	90	0.025	67
Foodstuffs						
Starch	Drum	50	0.05	40	0.015	16
Gluten	Belt discharge drum	15	0.007	48	0.010	33
Salt	Top feed drum	30	0.5	6	0.20	91
Sugar cane mud	Drum	10	0.03	30	0.005	33
Glucose (spent carbon)	”	15	0.02	50	0.0025	41
Glucose (44%)	Drum—Precoat	2	0.14 (filtrate)	50	0.0025	33
Effluents						
Primary sewage	Drum	8	0.01	65	0.008	33
Primary sewage, digested	”	6	0.005	65	0.008	33
Neutralised H_2SO_4 pickle	”	8	0.013	50	0.010	41
Plating shop effluent	Drum—Precoat	2	0.10 (filtrate)	80	0.013	33

NOTES

1. The information given should only be used as a general guide, for slight differences in the nature, size range and concentration of solids, and in the nature and temperature of liquor in which they are suspended can significantly affect the performance of any filter.
2. It should not be assumed the type of filter stated is the only suitable unit for each application. Other types may be suitable, and the ultimate selection will normally be a compromise based on consideration of many factors regarding the process and the design features of the filter.
3. The handling rate (in kg/m^2s) generally refers to dry solids except where specifically referred to as filtrate.
4. The air volumes stated are measured at the operating vacuum (i.e. they refer to attenuated air).

Copyright Elsevier 2024

Intas Exhibit 1032
Page 57 of 470
PGR2025-00043

washing of the cake if desired. Disadvantages of this equipment are the high cost per unit area, mechanical complexity, and the fact that some effectively use only 50 per cent of the total filtration area. With the horizontal linear pan and the rotary tipping pan filters, a truly continuous discharge of solids is not obtained since these units operate as short-time-cycle batch-discharge machines.

The ***horizontal pan filter*** incorporates a number of open top pans which move in a horizontal plane through the feed, filtration, washing and drying. At the discharge point the pans pass over a roller and then return to the feed end of the machine in the inverted position. The design of this type of filter varies greatly with different manufacturers, though one frequently used type has the walls of the pans built up on an open type of horizontal linear conveyor. The conveyor, within the walls of the pans, serves as the support for the filter media and for the liquor drainage system, and elsewhere the conveyor serves as the mechanical linkage between adjacent pans. The conveyor passes over vacuum boxes in the feed, filtration, washing and drying zones.

The ***horizontal rotary tipping pan filter*** has the pans located in a circle moving in a horizontal plane and, in effect, the pans are supported between the spokes of a wheel turning in a vertical shaft. Each pan is connected to a single, centrally-mounted rotary valve which controls the vacuum applied to the feed, filtration, washing and drying zones and from which the mother liquor and the various wash liquors can be diverted to individual vessels. At the discharge position, the pans are inverted through 180° and, in some designs, cake removal is assisted by the application of compressed air to the underside of the filter medium via the rotary valve. One example of this type of filter is the Prayon continuous filter, developed particularly for the vacuum filtration of the highly corrosive liquids formed in the production of phosphoric acid and phosphates. It is made in five sizes providing filtering surfaces from about 2–40 m^2 and it consists of a number of horizontal cells held in a rotating frame, and each cell passes in turn under a slurry feed pipe and a series of wash liquor inlets. Connections are arranged so as to provide three countercurrent washes. The timing of the cycle is regulated to give the required times for filtration, washing and cake drying. The discharge of the cake is by gravity as the cell is automatically turned upside-down, and can be facilitated if necessary by washing or by the application of back-pressure. The cloth is cleaned by spraying with wash liquid and is allowed to drain before it reaches the feed point again. The filter has a number of advantages including:

(a) A large filtration area, up to 85 per cent of which is effective at any instant.
(b) Low operating and maintenance costs and simple cloth replacement.
(c) Clean discharge of solids.
(d) Fabrication in a wide range of corrosion-resistant materials.
(e) Countercurrent washing.
(f) Operation at a pressure down to 15 kN/m^2.

The ***horizontal rotary table filter*** incorporates, as its name suggests, a horizontal rotary circular table divided into segments or drainage compartments, each of which is "ported" to a rotary valve underneath the table. The top surface of the table is fitted with a filter medium and walls are provided around the periphery of the table and around the hub. The feed slurry is distributed across the table through a feed box and vacuum is applied to

This book belongs to Bradley Loren (bloren@mcandrews-ip.com) Copyright Elsevier 2024

Intas Exhibit 1032
Page 58 of 470
PGR2025-00043

the segments in the feed position to extract the mother liquor. On rotation of the table, the filter cake then passes through the washing and drying zones. At the discharge position the vacuum on the segments can be broken to atmospheric pressure and the filter cake removed by a horizontal rotary scroll which lifts the solids over the periphery wall of the table. The scroll cannot be in contact with the filter medium and therefore a "heel" of solids remains on the table after passing the discharge point. This heel can either be disturbed by blow-back air and re-slurried with the incoming feed, or, in certain applications, the heel can be retained intact on the filter medium in order to obtain better retention of solids from the incoming feed than would be achieved with a clean filter cloth.

Horizontal belt or band filters

In the horizontal belt or band filter, shown in Figure 7.15, an endless belt arranged in the horizontal plane and running over pulleys at about 0.05 m/s at the feed and discharge ends (similar to the horizontal band conveyor). The principle is applied in the Landskröna band filter, as described by PARRISH and OGILVIE[29]. In the filtration, washing and drying zones, where the filter medium passes over vacuum boxes, it may be supported on a separate endless belt which also serves as the drainage member and as the valve. This belt can be provided with side walls to contain the feed slurry and wash liquors, or a flat belt can be used in conjunction with rigid static walls, against which the belt slides. Rubber, or similar, wiper blades which drag against the cake surface can be used to isolate the filtration and washing zones from each other. In some designs the belts move continuously, in others the belts are moved along in stages.

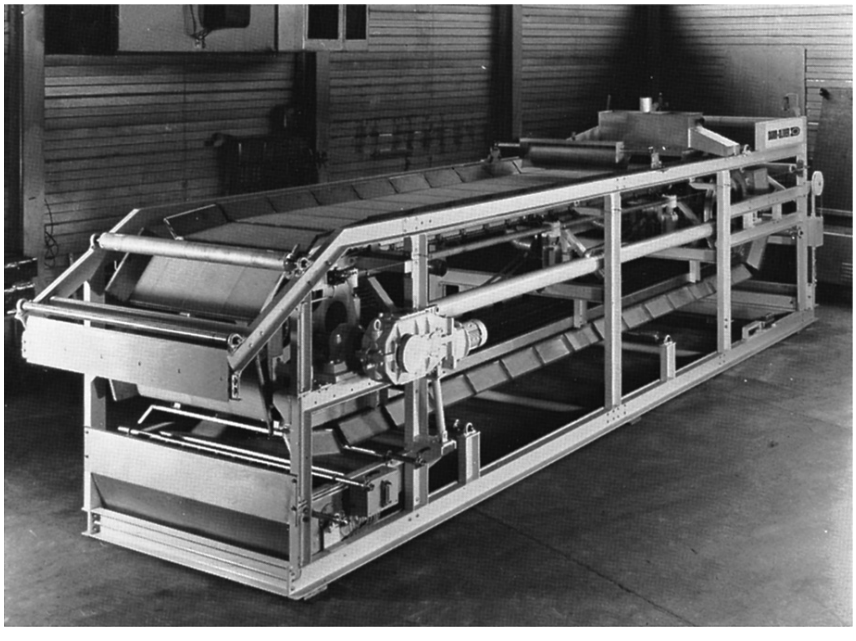


Figure 7.15. Rigid belt filter

This book belongs to Bradley Loren (bloren@mcandrews-ip.com) Copyright Elsevier 2024

Intas Exhibit 1032
Page 59 of 470
PGR2025-00043

The applications of horizontal belt filters are discussed by BLENDULF and BOND[30]. A typical filter for dewatering concentrates is shown in Figure 7.16, and it may be noted that this type of equipment is the most expensive per unit area.

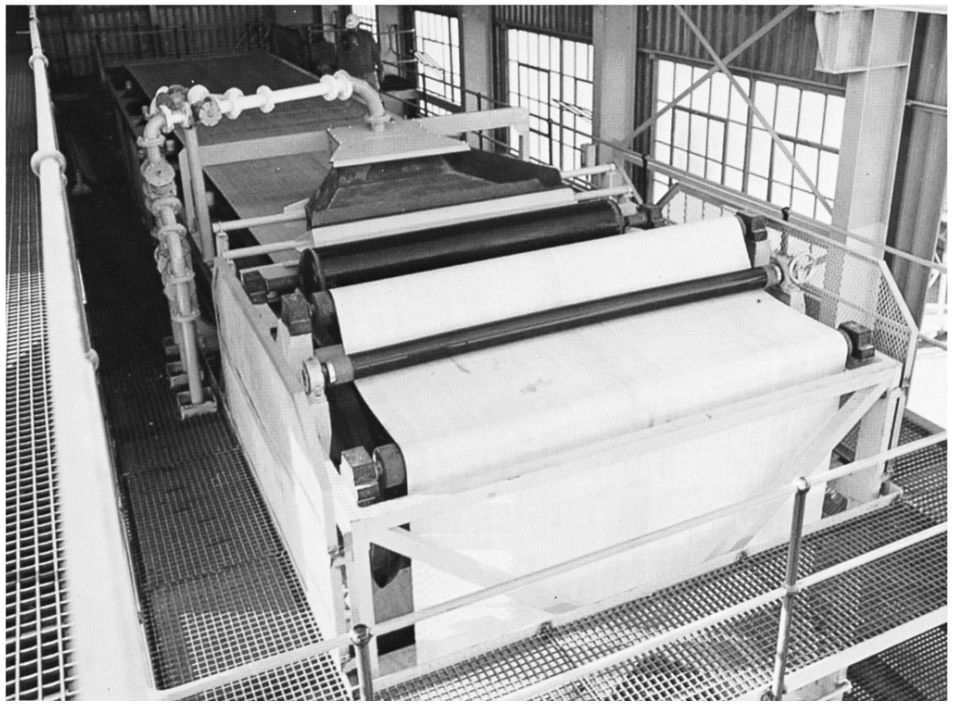


Figure 7.16. Delkor horizontal belt filter dewatering copper flotation concentrate (filter area 21 m^2)

An interesting development is the ADPEC filter described by BOSLEY[31] which has an intermittently moving belt. The slurry is fed to one end and the vacuum applied to the underside boxes and filtering occurs with the belt stationary. As the discharge roll at the other end moves inwards it trips the system so that the vacuum is relieved and the belt moved forward, thus avoiding the problem of pulling the belt continuously over the sections under vacuum.

Band filters have several advantages over rotary vacuum filters which are described in the following section. These include:

(a) Some gravitational drainage of liquid occurs because the cake and the belt are vertically separated at all stages of the filtration operation. In addition, a vacuum is not needed to keep the cake in place and this simply supplements the effect of gravity on the flow of filtrate.
(b) Because the feed is from the top, it is not necessary to agitate the suspension in the feed trough.

This book belongs to Bradley Loren (bloren@mcandrews-ip.com) Copyright Elsevier 2024

Intas Exhibit 1032
Page 60 of 470
PGR2025-00043

(c) Large particles in the slurry tend to reach the surface of the filter cloth first and to form a layer which therefore protects the cloth from the blinding effect of the fines, although this does lead to the formation of a non-uniform cake.
(d) Washing is more effective because of the improved structure of the filter cake.
(e) The fitting of an impervious cover over the cake towards its exit will reduce the loss of vacuum due to air flow through cracks in the cake.

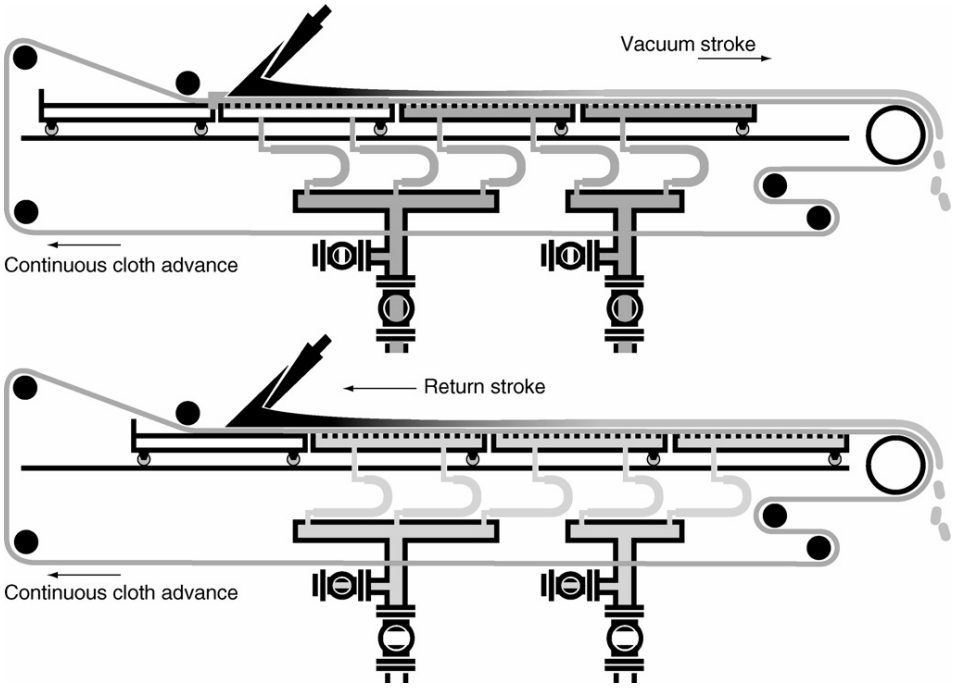


Figure 7.17. Principle of the Pannevis vacuum belt filter

Another development by Pannevis in Holland, shown in Figure 7.17, incorporates vacuum trays which support the filtercloth as it moves at a constant speed which may be varied as necessary. The vacuum tray is evacuated, filtration takes place and the tray is pulled forward by the cloth in such away that cloth and tray move at the same velocity thus offering negligible sealing problems, minimum wear, low driving power requirements and the possibility of high vacuum operation. At the end of the vacuum stroke, the vacuum is released, the tray is vented and pulled back quickly by pneumatic action to its starting position. Although an intermittent vacuum is required, the Pannevis design is in effect a continuous unit since the suspension feed, wash liquor feed and cake discharge are all fully continuous. A vacuum tray is typically 1.4 m long and 150 mm deep and the width and length of the belt are 0.25–3.0 m and 2.8–25 m, respectively.

This book belongs to Bradley Loren (bloren@mcandrews-ip.com) Copyright Elsevier 2024
Intas Exhibit 1032
Page 61 of 470
PGR2025-00043

Rotary drum filters

Because of its versatility and simplicity, one of the most widely used vacuum filters is the *rotary drum filter* and a filter of this type was patented in England in 1872 by William and James Hart. The basic design varies with different manufacturers, although essentially all drum type vacuum filters may be divided into two categories:

(a) Those where vacuum is created within compartments formed on the periphery of the drum, and
(b) Those where vacuum is applied to the whole of the interior of the drum.

The most frequently used continuous drum type filters fall into the first category. These give maximum versatility, low cost per unit area, and also allow a wide variation of the respective time periods devoted to filtration, washing and drying.

Essentially, a multi-compartment drum type vacuum filter consists of a drum rotating about a horizontal axis, arranged so that the drum is partially submerged in the trough into which the material to be filtered is fed. The periphery of the drum is divided into compartments, each of which is provided with a number of drain lines. These pass through the inside of the drum and terminate as a ring of ports covered by a rotary valve, through which vacuum is applied. The surface of the drum is covered with a filter fabric, and the drum is arranged to rotate at low speed, usually in the range 0.0016–0.004 Hz (0.1–0.25 rpm) or up to 0.05 Hz (3 rpm) for very free filtering materials.

As the drum rotates, each compartment undergoes the same cycle of operations and the duration of each of these is determined by the drum speed, the submergence of the drum and the arrangement of the valve. The normal cycle of operations consists of filtration, drying and discharge. It is also possible, however, to introduce other operations into the basic cycle, including:

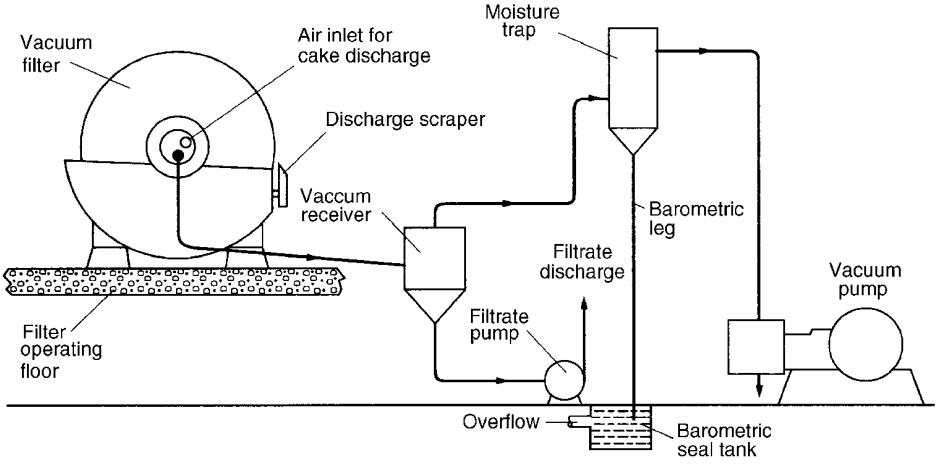
(a) Separation of initial dirty filtrate — which may be an advantage if a relatively open filter fabric is used.
(b) Washing of the filter cake.
(c) Mechanical dewatering of the filter cake.
(d) Cloth cleaning.

Figure 7.18*a* shows a typical layout of a rotary drum installation and Figure 7.18*b* shows the sequence of cake formation, washing and dewatering. A large rotary drum vacuum filter is shown in Figure 7.19.

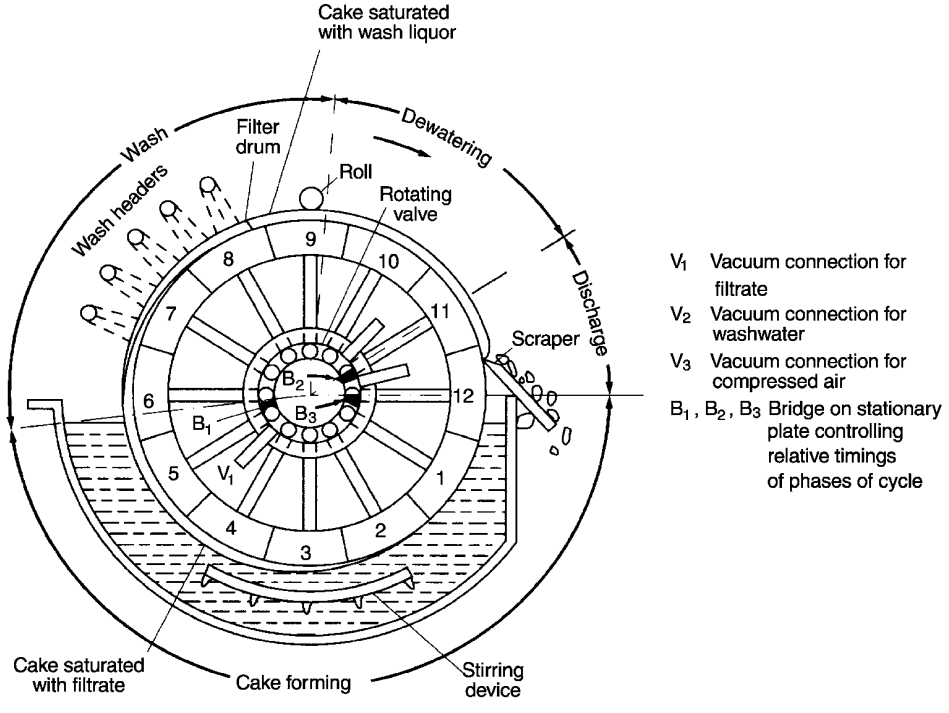
In order to achieve consistent performance of a continuous filter, it is necessary to maintain the filter medium in a clean condition. With a drum type vacuum filter this requires the complete and continuous removal of the filter cake from the drum surface, and the operating conditions are often influenced by the need to form a fully dischargeable cake. Again, in order to achieve high capacity and good cake washing and/or drying, it is very often desirable to operate with very thin cakes. Therefore, the cake discharge system of most drum type vacuum filters must be arranged so as to ensure the complete and continuous removal of extremely thin filter cakes. The most effective way of achieving this is determined to a large extent by the physical nature of the solids being handled.

This book belongs to Bradley Loren (bloren@mcandrews-ip.com) Copyright Elsevier 2024

Intas Exhibit 1032
Page 62 of 470
PGR2025-00043



(*a*)



(*b*)

Figure 7.18. Typical layout of rotary drum filter installation

This book belongs to Bradley Loren (bloren@mcandrews-ip.com)
Copyright Elsevier 2024
Intas Exhibit 1032
Page 63 of 470
PGR2025-00043

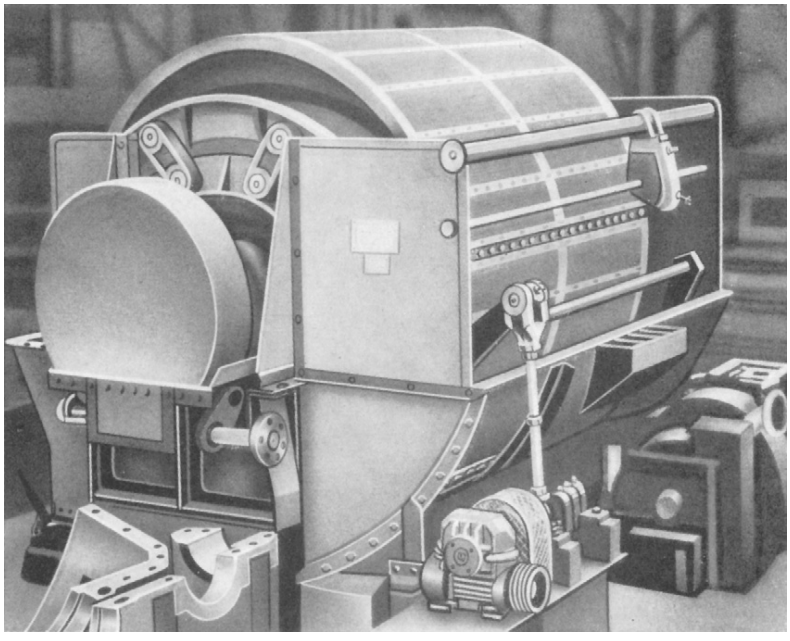


Figure 7.19. Rotary vacuum drum filter used in a zinc leaching operation

The various discharge systems that are suitable for drum type filters include the string discharge technique which is effective for an extremely wide range of materials. Essentially this involves forming the filter cake on an open type of conveyor which is in contact with the filter medium in the filtration, washing and drying zones. Consequently, the solids which are trapped by the filter medium form a cake on top of the "open" conveyor. From the discharge point on the drum the conveyor transports the filter cake to a discharge roll, at which point the cake is dislodged. The conveyor then passes through an aligning mechanism and over a return roll which guides it back into contact with the filter drum at the commencement of the cycle and just above the level of feed liquor in the filter trough.

In the string discharge system, the conveyor consists of a number of endless strings which are spaced at a pitch of approximately 12 mm over the width of the filter drum. The string spacing may, however, be in the range 6–25 mm depending on the mechanical properties of the solids.

The advantages of the string discharge system are:

(a) Thin and sticky filter cakes down to about 1.5 mm of materials such as clay may be effectively discharged.
(b) The filter cloth is almost free of mechanical wear and tear so that thin and delicate cloths may be used, and these can be selected almost solely for their filtration properties. Such cloths are usually less prone to plugging than the stronger and thicker cloths required for other discharge systems.
(c) The cloth can be attached to the drum in a simple manner so that fitting and subsequent replacement can be carried out quickly. Normally, the cloth is loosely

This book belongs to Bradley Loren (bloren@mcandrews-ip.com) Copyright Elsevier 2024

Intas Exhibit 1032
Page 64 of 470
PGR2025-00043

wrapped around the drum and it is secured to the drum at the edges and, once across the drum, at the overlap, by a simple caulking system. The use of wire winding, clamping bars, and the necessity of securing the cloth at every panel which is essential with other discharge systems, is avoided.

(d) The use of compressed air, to loosen cake from the drum surface, is avoided and consequently there is no possibility of blowing back into the filter cake moisture which has previously been removed under vacuum. This is a possibility with knife discharge filters operating with blow-back.

(e) If required, the path of the discharge strings can be altered so that the filter cake is conveyed by the strings to a convenient point for feeding a continuous dryer-extruder, or other processing equipment.

A typical string discharge mechanism is shown in Figure 7.20.



Figure 7.20. String discharge mechanism on a filter handling silica gel

The knife discharge system incorporates a knife which is arranged so that the surface of the drum runs on or near to the knife edge. The cake is dislodged from the cloth either by its own weight, with thick and heavy cakes, or by applying compressed air to the underside of the filter cloth. The blow-back air can either be admitted at low pressure for a long period, or at high pressure and instantaneously by means of a mechanical "blow-off timer". With suitable solids it is possible to operate with the knife spaced from the drum

This book belongs to Bradley Loren (bloren@mcandrews-ip.com) Copyright Elsevier 2024

Intas Exhibit 1032
Page 65 of 470
PGR2025-00043

so that not all of the cake is removed. The heel of solids is then retained on the drum and this acts as the filter media. This discharge system is particularly suitable for friable cakes that do not have the mechanical properties to bridge over the strings of a string discharge system.

With the roller cake discharge system, the cake is transferred from the drum to a discharge roll from which it is removed by a knife. This is a relatively simple method of removing thin and sticky filter cakes without having a knife rubbing against and wearing the filter cloth. Certain applications require facilities for washing the cloth either continuously or intermittently without dilution of the trough contents, and such a feature is provided by the belt discharge system where the filter cloth also acts as cake conveyor. In such a system, the cake is completely supported between the drum and the discharge roll so that thin cakes and cakes of low mechanical strength can be handled and higher drum speeds, and hence higher filtration rates, can be achieved.

The performance of drum type vacuum filters for given feed conditions can be controlled by three main variables–drum speed, vacuum (if necessary with differential vacuum applied to the filtration, washing and drying zones) and the percentage of drum surface submerged in the feed slurry. Most drum filters have facilities which allow for easy manual adjustment of these variables, although automatic adjustment of any, or all, of them can be actuated by changes in the quality and/or quantity of the feed or cake. For maximum throughput, a drum filter should be operated at the highest submergence and at the highest possible drum speed. The limiting conditions affecting submergence are:

(a) Any increase in submergence limits the proportion of the drum area available for washing and/or drying.
(b) Drum submergence above approximately 40 per cent entails the use of glands where the drum shaft and valve hub pass through the trough.
(c) High submergence may complicate the geometry of the discharge system.

Under all conditions, it is essential to operate with combinations of drum speed, submergence and vacuum, which, for the feed conditions that apply, will ensure that a fully dischargeable cake is formed. If this is not done then progressive deterioration in the effectiveness of the filter medium will occur and this will adversely affect the performance of the machine. Typical filtration cycles for drum filters are given in Table 7.4.

Drum type vacuum filters can be fitted, if required, with simple hoods to limit the escape of toxic or obnoxious vapours. These may be arranged for complete sealing, and for operation under a nitrogen or similar blanket, although this complicates access to the drum and necessitates a design in which the vacuum system and the cake receiving system are arranged to prevent gas loss. The cake moves through the washing and drying zones in the form of a continuous sheet and, because the cake and filter medium are adequately supported on the drum shell, it is possible to fit the filter with various devices that will improve the quality of the cake regarding both washing and drying, prior to discharge.

Simple rolls, extending over the full width of the filter, can be so arranged that any irregularities or cracks in the cake are eliminated, and subsequent washing and drying is therefore applied to a uniform surface. Otherwise wash liquors and air tend to short circuit, or “channel”, the deposited solids. The cake compression system may also incorporate a

This book belongs to Bradley Loren (bloren@mcandrews-ip.com) Copyright Elsevier 2024

Intas Exhibit 1032
Page 66 of 470
PGR2025-00043

This book belongs to Bradley Loren (bloren@mcandrews-ip.com)

Table 7.4. Filtration cycles for drum-type rotary vacuum filter (times in seconds)

Speed		25 per cent submergence					37.5 per cent submergence					50 per cent sub.		66.7 per cent sub.		75 per cent sub.	
		A	B	C			A	B	C			A	B	A	B	A	B
(rev/min)	(Hz)	Filter	Dewater	Initial dewater	Wash	Final dewater	Filter	Dewater	Initial dewater	Wash	Final dewater	Filter	Dewater	Filter	Dewater	Filter	Dewater
3	0.05	5	10	2	5	3	7	8	2	4	2	8	5	12	2	13	1
$2\frac{1}{2}$	0.04	6	12	2	7	3	9	10	2	5	3	11	6.5	16	2.2	17	1.8
2	0.033	7	15	3	8	4	12	14	2	9	3	13	7.5	19	3	21	2
$1\frac{1}{2}$	0.025	10	23	5	12	6	16	18	3	11	4	16	10	24	4	28	3
1	0.017	15	30	7	16	7	22	24	3	16	5	27	15	38	5	42	4
$\frac{2}{3}$	0.011	22	45	10	24	11	33	37	5	24	7	40	22	55	8	63	6
$\frac{1}{2}$	0.008	30	60	13	32	15	44	48	6	32	10	54	30	76	10	84	8
$\frac{1}{3}$	0.0055	45	91	20	48	23	66	72	9	48	15	80	44	110	16	126	12
$\frac{1}{4}$	0.004	60	120	26	64	30	88	96	12	64	20	110	60	150	21	170	17
$\frac{1}{5}$	0.0033	75	150	32	80	38	110	120	15	80	25	135	75	180	27	210	21
$\frac{1}{6}$	0.0028	90	180	39	96	45	132	144	18	96	30	160	90	220	32	280	28
$\frac{1}{7}$	0.0024	105	210	45	112	54	154	168	21	112	35	190	105	260	37	310	31
$\frac{1}{8}$	0.0200	120	240	52	128	60	176	192	24	128	40	215	120	300	42	340	34
$\frac{1}{10}$	0.0017	135	300	65	160	75	220	240	30	160	50	240	135	360	54	420	42

(Columns A + B or A + C should be used but *not* all three)

Copyright Elsevier 2024

compression or wash blanket which limits still further any tendency for the air or wash liquor to "channel". Wash blankets also avoid disturbance of the cake which might occur when high pressure sprays are directed on to the cake, and they allow the wash liquor to be applied much nearer to the point where the cake emerges from the slurry. Compression rolls, with or without blankets, can be arranged with pneumatic or hydraulically loaded cylinders or they can be weighted or fitted with springs to increase further the pressure applied to the cake as shown in Figure 7.21. In some applications, the rolls can be arranged to give a controlled cake thickness, and so give some rearrangement of the solids in the filter cake with the advantages of the elimination of cracks, compaction of the cake, and the liberation of moisture from thixotropic materials, with the liberated moisture finally being drawn into the vacuum system prior to discharge.

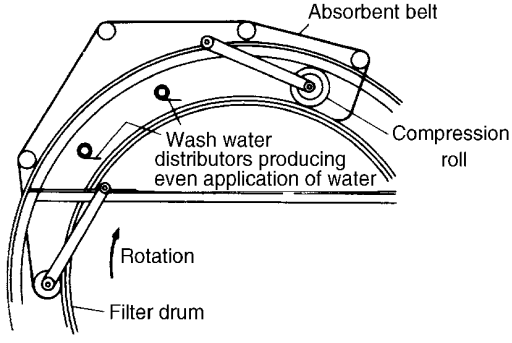


Figure 7.21. Cake compression

Other devices which find varying degrees of success in the treatment of thixotropic materials include rotary beaters and pulsating valves to interrupt the air flow in the drying zone. Both of these result in movement of the cake, giving a reduction in moisture content.

A drum type vacuum filter can easily be arranged so that the trough and hood, if fitted is thermally insulated. In addition, the filter can be equipped with heat exchange equipment, such as jackets for heating fluid or refrigerant, and electric resistance wires for heating. These features can be of particular significance in applications such as the dewaxing of lubricating oil which is normally carried out at temperatures below 263 K ($-10\,^{\circ}$C), and for salt drying which may be effected at temperatures approaching 673 K (400 °C) on a filter/dryer.

In most applications, bottom feed drum filters, that is those where the drum is partially suspended in the feed slurry, must be fitted with agitators to keep the solids in suspension. Normally, pendulum type rakes, which are pivoted on or above the drum axis, are used so as to avoid the use of glands, although rotary paddles fitted at low level in the filter trough also find application. Solids suspension may also be improved by giving careful attention to the flow pattern within the trough such as, for example, by feeding slurry into the trough at low level and at a rate in excess of that at which the material can be filtered. With this technique a constant overflow is provided so that upward movement within the trough assists in conveying solids toward the filter surface. Air sparge pipes

This book belongs to Bradley Loren (bloren@mcandrews-ip.com) Copyright Elsevier 2024
Intas Exhibit 1032
Page 68 of 470
PGR2025-00043

may also be used to prevent solids settlement, although this results in higher operating costs than with a mechanical agitation system.

Top-feed drum filters are used for the treatment of very fast settling solids that cannot easily be kept in suspension. A drum filter may be preferable, rather than a horizontal pan or similar filter, because of its low cost, simplicity and reliability, and because of the relative ease with which it can be fitted with appropriate accessory features. A top feed drum filter incorporates multi-compartments, drainlines and a rotary valve identical to those in a conventional drum filter. The feed slurry is introduced at, or just before, top dead centre, and the cake is discharged from 90° to 180° from the feed point. The feed slurry can be distributed across the drum by sprays or a weir box, or it may be contained within a 3-sided head-box which is sealed against the moving drum at each end and across the back on the ascending filter surface. For materials which do not cake together sufficiently to be self-supporting on the drum surface, a hopper-type top feed filter may

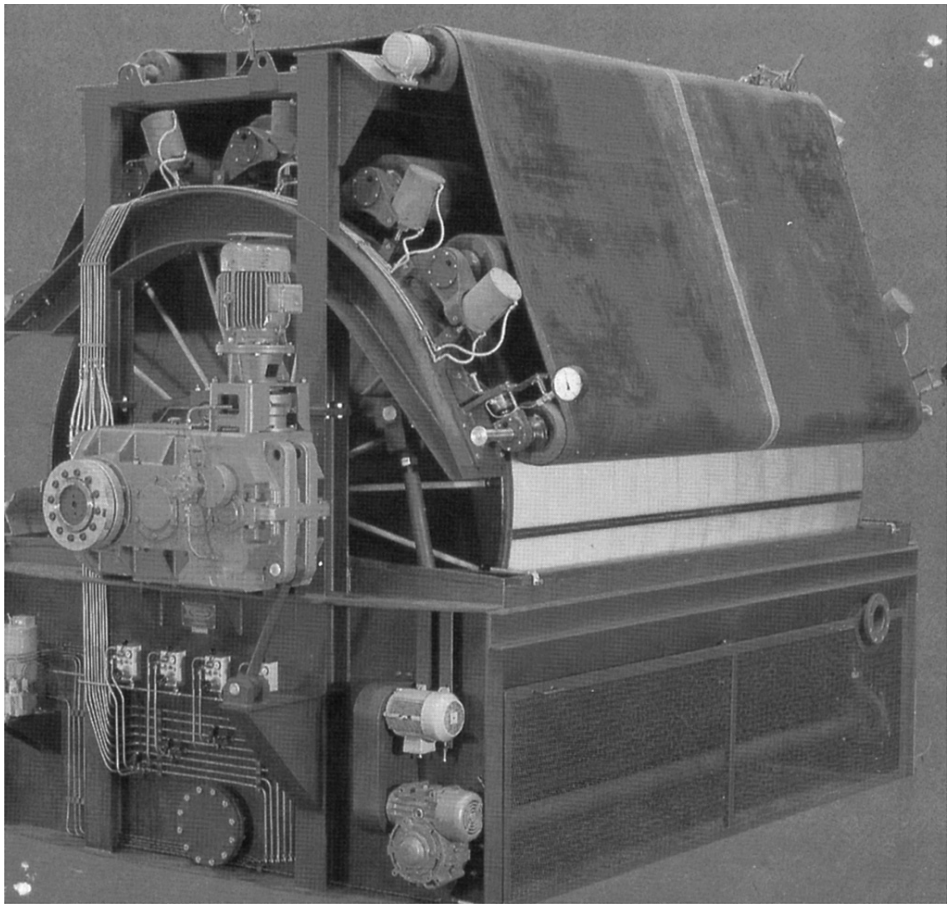


Figure 7.22. Dorr–Oliver press-belt drum filter

This book belongs to Bradley Loren (bloren@mcandrews-ip.com) Copyright Elsevier 2024

Intas Exhibit 1032
Page 69 of 470
PGR2025-00043

be used which is similar to a conventional top feed filter except that the walls extend above the drum surface around all sides of each compartment and these support the filter cake. Because larger particles settle more rapidly these are deposited near the filter cloth and smaller particles form the outer portions of the filter cake. A cake of relatively high porosity is thereby obtained and high filtration rates are achieved.

Modern plant utilises drums with surfaces of 60–100 m^2 as compared with the 20 m^2 of the older cast iron drums. Construction materials such as stainless steel, titanium, epoxy resins and plastics all give much improved corrosion resistance for many slurries and hence longer life. The replacement of the knife system by some form of belt has given better cake discharge and permitted the use of thinner filtering media, such as synthetic fibres. The belt provides some support for the cake and materially assists the effect of compressed air for lifting off the cake. Drying can be improved by totally covering the filter with a hood. Improvements have also been made in techniques for reducing cake cracking.

Recent developments in rotary filters include equipment marketed by Dorr–Oliver, illustrated in Figure 7.22, which combines vacuum filtration with pressure filtration in which filter cake moisture is reduced by 20–200 per cent. A combined filtering and drying plant has been developed in which a continuous belt, rather like a bed-spring in construction, passes round the underside of the drum filter and the filter cake is deposited on the belt to which it adheres. The belt leaves the filter towards the top and is then carried through a cabinet dryer. It then returns to the underside of the drum filter after the cake has been removed by agitation. The metal belt, which assists the drying of the material by virtue of its good heat-conducting properties, is formed into loops which are carried through the dryer on a slat conveyor. With finely divided materials the total loss of solid from the belt is as little as 1 or 2 per cent.

Example 7.4

A slurry containing 40 per cent by mass solid is to be filtered on a rotary drum filter 2 m diameter and 2 m long which normally operates with 40 per cent of its surface immersed in the slurry and under a pressure of 17 kN/m^2. A laboratory test on a sample of the slurry using a leaf filter of area 200 cm^2 and covered with a similar cloth to that on the drum produced 300 cm^3 of filtrate in the first 60 s and 140 cm^3 in the next 60 s, when the leaf was under an absolute pressure of 17 kN/m^2. The bulk density of the dry cake was 1500 kg/m^3 and the density of the filtrate was 1000 kg/m^3. The minimum thickness of cake which could be readily removed from the cloth was 5 mm.

At what speed should the drum rotate for maximum throughput and what is this throughout in terms of the mass of the slurry fed to the unit per unit time?

Solution

For the leaf filter:

$$A = 0.02 \text{ m}^2,$$

$$(-\Delta P) = (101.3 - 17) = 84.3 \text{ kN/m}^2 \text{ or } 84,300 \text{ N/m}^2$$

When $t = 60$ s: $V = 0.0003 \text{ m}^3$

When $t = 120$ s: $V = 0.00044 \text{ m}^3$

This book belongs to Bradley Loren (bloren@mcandrews-ip.com) Copyright Elsevier 2024

Intas Exhibit 1032
Page 70 of 470
PGR2025-00043

These values are substituted into the constant pressure filtration equation:

$$V^2 + \frac{2LAV}{v} = \frac{2(-\Delta P)A^2 t}{\mathbf{r}\mu v} \qquad \text{(equation 7.18)}$$

which enables the filtration constants to be determined as:

$$L/v = 2.19 \times 10^{-3} \text{ and } \mathbf{r}\mu v = 3.48 \times 10^{10}$$

For the rotary filter, equation 7.18 applies as the whole operation is at constant pressure The maximum throughput will be attained when the cake thickness is a minimum, that is 5 mm or 0.005 m.

Area of filtering surface $= (2\pi \times 2) = 4\pi$ m^2.

Bulk volume of cake deposited $= (4\pi \times 0.005) = 0.063$ m^3/revolution

If the rate of filtrate production $= w$ kg/s, then the volume flow is $0.001\ w$ m^3/s

For a 40 per cent slurry: $S/(S + w) = 0.4$, and the mass of solids $= 0.66w$.

Thus:

volume of solids deposited $= (0.66w/1500) = 4.4 \times 10^{-4} w$ m^3/s

If one revolution takes t s, then: $4.4 \times 10^{-4} wt = 0.063$

and the mass of filtrate produced per revolution $= 143$ kg.

Rate of production of filtrate $= 0.001w$ m^3/s $= V/t$

Thus: $V^2 = 1 \times 10^{-6} w^2 t^2 = 1 \times 10^{-6}(143)^2 = 0.02$ m^6

and: $V = 0.141$ m^3

Substituting $V = 0.141$ m^3 and the constants into equation 7.18, gives:

$$(0.141)^2 + 2 \times 2.19 \times 10^{-3} \times 0.141 = 2 \times 84,300 \times (4\pi)^2 t/(3.48 \times 10^{10})$$

from which $t = 26.95$ s, which is equal to time of submergence/revolution.

Thus: time for 1 revolution $= (26.9/0.4) = 67.3$ s

and: speed $= (1/67.3) =$ <u>0.015 Hz</u>

$w = (143/67.3) = 2.11$ kg/s

$S = (0.66 \times 2.11)$ kg/s

and: mass of slurry $= (1.66 \times 2.11) =$ <u>3.5 kg/s</u>

Example 7.5

A plate and frame press with a filtration area of 2.2 m^2 is operated with a pressure drop of 413 kN/m^2 and with a downtime of 21.6 ks (6 h). In a test with a small leaf filter 0.05 m^2 in area,

This book belongs to Bradley Loren (bloren@mcandrews-ip.com) Copyright Elsevier 2024

operating with a pressure difference of 70 kN/m^2, 0.00025 m^3 of filtrate was obtained in 300 s and a total of 0.00040 m^3 in 600 s. Estimate the optimum filtration time for maximum throughput.

If the operating cost during filtration is £10/ks and the cost of a shutdown is £100, what is the optimum filtration time for minimum cost?

Solution

Substituting $V = 0.00025$ m^3 at $t = 300$ s in equation 7.39 gives:

$$(300/0.00025) = 0.00025\mathbf{r}\mu v/(2 \times 0.05^2 \times 70 \times 10^3) + \mathbf{r}\mu L/(0.05 \times 70 \times 10^3)$$

or:
$$1.2 \times 10^6 = 7.14 \times 10^{-6}\mathbf{r}\mu v + 2.86 \times 10^{-4}\mathbf{r}\mu L \quad \text{(i)}$$

Substituting $V = 0.00040$ m^3 at $t = 400$ s in equation 7.39 gives:

$$1.0 \times 10^6 = 11.42 \times 10^{-6}\mathbf{r}\mu v + 2.86 \times 10^{-4}\mathbf{r}\mu L \quad \text{(ii)}$$

Solving equations (i) and (ii) simultaneously gives:

$$\mathbf{r}\mu v = 7 \times 10^{12} \text{ Ns/m}^4 \text{ and } \mathbf{r}\mu L = 4.6 \times 10^9 \text{ N/sm}^3$$

Thus, for the plate and frame filter:

$$B_1 = \frac{\mathbf{r}\mu v}{2A^2(-\Delta P)} = 7 \times 10^{12}/(2 \times 2.2^2 \times 413 \times 10^3) = 1.75 \times 10^6 \text{ s/m}^6$$

and:
$$B_2 = \frac{\mathbf{r}\mu L}{A(-\Delta P)} = 4.6 \times 10^9/(2.2 \times 413 \times 10^3) = 5.06 \times 10^3 \text{ s/m}^3$$

Substituting for V from equation 7.43 into equation 7.41, the filtration time for maximum throughput is:

$$\begin{aligned} t &= t' + B_2(t'/B_1)^{0.5} \\ &= 21.6 \times 10^3 + 5.06 \times 10^3[(21.6 \times 10^3)/(1.75 \times 10^6)]^{0.5} \\ &= 2.216 \times 10^4 \text{ s or } \underline{\underline{22.2 \text{ ks}}} \text{ (6.2 h)} \end{aligned}$$

From equation 7.43:

$$V = [(21.6 \times 10^3)/(1.75 \times 10^6)]^{0.5} = 0.111 \text{ m}^3$$

and the mean rate of filtration is:

$$V/(t + t') = 0.111/(2.216 \times 10^4 + 21.6 \times 10^3) = \underline{\underline{2.54 \times 10^{-6} \text{ m}^3/\text{s}}}$$

The total cost is:

$$C = 0.01t + 100 \text{ £/cycle}$$

or:
$$C = (0.01t + 100)/V \text{ £/m}^3$$

Substituting for t from equation 7.41 gives:

$$C = (0.01B_1V^2 + 0.01B_2V + 100)/V$$

This book belongs to Bradley Loren (bloren@mcandrews-ip.com) Copyright Elsevier 2024

Intas Exhibit 1032
Page 72 of 470
PGR2025-00043

Differentiating and putting $dC/dV = 0$:

$$V = (100/0.01B_1)^{0.5} \text{ m}^3$$

and from equation 7.41, the optimum filtration time for minimum cost is:

$$t = (100/0.01) + B_2(100/0.01B_1^{0.5}) \text{ s}$$

Substituting for B_1 and B_2:

$$t = 10^4 + 5.06 \times 10^3(10^4/1.75 \times 10^6)^{0.5}$$

$$= 1.03 \times 10^4 \text{ s or } \underline{10.3 \text{ ks}} \text{ (2.86 h)}$$

Example 7.6

A slurry, containing 0.2 kg of solid per kilogram of water, is fed to a rotary drum filter 0.6 m long and 0.6 m diameter. The drum rotates at one revolution in 360 s and 20 per cent of the filtering surface is in contact with the slurry at any instant. If filtrate is produced at the rate of 0.125 kg/s and the cake has a voidage of 0.5, what thickness of cake is produced when filtering with a pressure difference of 65 kN/m^2? The density of the solids is 3000 kg/m^3.

The rotary filter breaks down and the operation has to be carried out temporarily in a plate and frame press with frames 0.3 m square. The press takes 120 s to dismantle and 120 s to reassemble and, in addition, 120 s is required to remove the cake from each frame. If filtration is to be carried out at the same overall rate as before, with an operating pressure difference of 175 kN/m^2, what is the minimum number of frames that needs to be used and what is the thickness of each? It may be assumed that the cakes are incompressible and that the resistance of the filter medium may be neglected.

Solution

Drum filter

$$\text{Area of filtering surface} = (0.6 \times 0.6\pi) = 0.36\pi \text{ m}^2$$

$$\text{Rate of filtration} = 0.125 \text{ kg/s}$$

$$= (0.125/1000) = 1.25 \times 10^{-4} \text{ m}^3\text{/s of filtrate}$$

1 kg or 10^{-3} m^3 water is associated with 0.2 kg of solids $= 0.2/(3 \times 10^3) = 6.67 \times 10^{-5}$ m^3 of solids in the slurry.

Since the cake porosity is 0.5, 6.67×10^{-5} m^3 of water is held in the filter cake and $(10^{-3} - 6.67 \times 10^{-5}) = 9.33 \times 10^{-4}$ m^3 appears as filtrate, per kg of total water in the slurry.

Volume of cake deposited by unit volume of filtrate, $v = (6.67 \times 10^{-5} \times 2)/(9.33 \times 10^{-4}) = 0.143$.

Volumetric rate of deposition of solids $= (1.25 \times 10^{-4} \times 0.143) = 1.79 \times 10^{-5}$ m^3/s. One revolution takes 360 s. Therefore the given piece of filtering surface is immersed for $(360 \times 0.2) = 72$ s

The bulk volume of cake deposited per revolution $= (1.79 \times 10^{-5} \times 360) = 6.44 \times 10^{-3}$ m^3. Thickness of cake produced $= (6.44 \times 10^{-3})/(0.36\pi) = 5.7 \times 10^{-3}$ m or $\underline{5.7 \text{ mm}}$

This book belongs to Bradley Loren (bloren@mcandrews-ip.com) Copyright Elsevier 2024

Intas Exhibit 1032
Page 73 of 470
PGR2025-00043

Properties of filter cake

$$\frac{dV}{dt} = \frac{(-\Delta P)A}{\mathbf{r}\mu l} = \frac{(-\Delta P)A^2}{\mathbf{r}\mu V v} \qquad \text{(from equations 7.2 and 7.8)}$$

At constant pressure:

$$V^2 = \frac{2}{\mathbf{r}\mu v}(-\Delta P)A^2 t = K(-\Delta P)A^2 t \text{ (say)} \qquad \text{(from equation 7.11)}$$

Expressing pressures, areas, times and volumes in N/m^2, m^2, s and m^3 respectively, then for one revolution of the drum:

$$(1.25 \times 10^{-4} \times 360)^2 = K(6.5 \times 10^4)(0.36\pi)^2 \times 72$$

since each element of area is immersed for one-fifth of a cycle,

and: $$K = 3.38 \times 10^{-10}$$

Filter press

Using a filter press with n frames of thickness b m, the total time, for one complete cycle of the press $= (t_f + 120n + 240)$ s, where t_f is the time during which filtration is occurring.

$$\text{Overall rate of filtration} = \frac{V_f}{t_f + 120n + 240} = 1.25 \times 10^{-4} \text{ m}^3/\text{s}$$

where V_f is the total volume of filtrate per cycle.

The volume of frames/volume of cake deposited by unit volume of filtrate, v, is given by:

$$V_f = 0.3^2 nb/0.143 = 0.629nb$$

But: $$V_f^2 = (3.38 \times 10^{-10}) \times (1.75 \times 10^5)(2n \times 0.3 \times 0.3)^2 t_f \quad \text{(from equation 7.11)}$$

$$= 0.629\ nb^2$$

and: $$t_f = 2.064 \times 10^5\ b^2$$

Thus: $$1.25 \times 10^{-4} = \frac{0.629nb}{2.064 \times 10^5 b^2 + 120n + 240}$$

That is: $$25.8b^2 + 0.015n + 0.030 = 0.629nb$$

or: $$n = \frac{0.030 + 25.8b^2}{0.629b - 0.015}$$

n is a minimum when $dn/db = 0$, that is when:

$$(0.629b - 0.015) \times 51.6b - (0.030 + 25.8b^2) \times 0.629 = 0$$

$$b^2 - 0.0458b - 0.001162 = 0$$

Thus: $b = 0.0229 \pm \sqrt{(0.000525 + 0.001162)}$ and taking the positive root:

$d = 0.0640$ m or <u>64 mm</u>

This book belongs to Bradley Loren (bloren@mcandrews-ip.com) Copyright Elsevier 2024

Intas Exhibit 1032
Page 74 of 470
PGR2025-00043

Hence:
$$n = \frac{(0.030 + 25.8 \times 0.0640^2)}{(0.629 \times 0.0640 - 0.015)}$$
$$= 5.4$$

Thus a minimum of 6 frames must be used.

The sizes of frames which will give exactly the required rate of filtration when six are used are given by:

$$0.030 + 25.8b^2 = 3.774b - 0.090$$

or:
$$b^2 - 0.146b + 0.00465 = 0$$

and:
$$b = 0.073 \pm \sqrt{(0.005329 - 0.00465)}$$
$$= 0.047 \text{ or } 0.099 \text{ m}$$

Thus, 6 frames of thickness either 47 mm or 99 mm will give exactly the required filtration rate; intermediate sizes give higher rates.

Thus any frame thickness between 47 and 99 mm will be satisfactory. In practice, 50 mm (2 in) frames would probably be used.

Rotary disc filters

In essence, *the disc filter* operates in a manner similar to a bottom-feed drum filter. The principal differences to be noted are the compartments which are formed on both faces of vertical discs. These comprise eight or more segments, each of which is connected to the horizontal shaft of the machine. The filtrate and air are drawn through the filter medium, into the drainage system of the segments, and finally through passages in the rotary shaft to a valve located at one or both ends.

The discs are arranged on the shaft about 0.3 m apart as shown in Figure 7.23, resulting in economy of space, and consequently a far greater filtration area can be accommodated in a given floor space than is possible with a drum type filter. A disc filter area of approximately 80 m^2 can be achieved with eight discs, each approximately 2.5 m in diameter, in the same space as a 2.5 m diameter × 2.5 m drum filter which would have a filtration area of 20 m^2. Because of the large areas and consequently the large liquor and air flows, two rotary valves, one at each end of the main shaft, are frequently fitted. Cake discharge is usually achieved using a knife or wire, and discharge may be assisted by blow-back air. The cake falls through vertical openings in the filter trough.

In general, disc filters have the advantages that, not only is the cost per unit filtration area low and large filtration areas can be accommodated in a small floor space, but the trough can be divided into two sections so that the different slurries can be handled at the same time in the same machine. The disadvantages of these units is that heavy filter cloths are necessary, with a great tendency to "blind", and cake washing is virtually impossible due to the ease with which deposited solids can be disturbed from the vertical faces. In contrast to a drum type filter, in which all parts of the filter medium take the same path through the slurry, each part of a disc segment takes a different path, depending on its radial distance from the hub. Consequently, if homogeneous conditions cannot be maintained in the filter trough, then very uneven cakes may be formed, a situation which

This book belongs to Bradley Loren (bloren@mcandrews-ip.com) Copyright Elsevier 2024

Intas Exhibit 1032
Page 75 of 470
PGR2025-00043

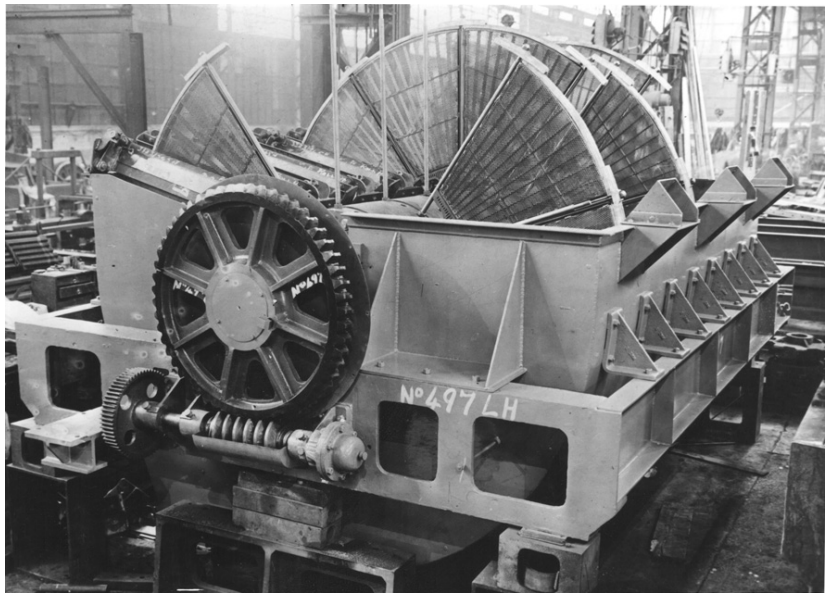


Figure 7.23. Rotary disc filter

favours preferential air flow and results in a widely variable moisture content across each segment. Disc filters also have the limitation that, because every segment must be fully submerged in slurry prior to the application of vacuum, very little variation in submergence level can be accommodated.

Precoat filters

All the filters described previously have been in the category of cake filters for they all rely on the solids present in the feed slurry having properties which are suitable for them to act as the actual filter medium and to form cakes which are relatively easily discharged. Applications arise where extremely thin filter cakes, perhaps only a fraction of a millimetre thick, have to be discharged, where extremely good filtrate clarity is essential, or where a particularly blinding substance is present, and filtration through a permanent filter medium alone, such as a filter fabric, may not be satisfactory. A much more efficient performance is achieved by utilising a bed of easily filtered material which is *precoated* on to what is otherwise a standard drum type filter.

After the precoat is established the solids to be removed from the filter feed are trapped on the surface of the precoated bed. This thin layer of slime is removed by a knife which is caused to advance slowly towards the drum. The knife also removes a thin layer of the precoated bed so that a new surface of the filter medium is exposed. This procedure allows steady filtration rates to be achieved.

A *precoated rotary drum vacuum filter* is the only filtration equipment from which extremely thin filter cakes can be positively and continuously removed in a semi-dry state.

This book belongs to Bradley Loren (bloren@mcandrews-ip.com) Copyright Elsevier 2024

Intas Exhibit 1032
Page 76 of 470
PGR2025-00043

The usual precoat materials, for most production processes, are conventional filter aids, such as diatomaceous earth and expanded Perlite, although frothed coal, calcium sulphate and other solids, which form very permeable filter cakes, may be used where such materials are compatible with the materials being processed. Wood flour and fly-ash have also been used in some applications, particularly in effluent treatment plants, where some contamination of the filtered liquor is of no great consequence. The establishment of the precoat bed should preferably be carried out using a precoat slurry of low solids concentration, at high drum speed and with low submergence, so that the bed is built up in the form of a thin layer with each revolution, thereby ensuring a uniform and compacted bed which will not easily be disturbed from the drum. For long periods of operation, the maximum bed thickness should be used. This is often determined by the mechanical design of the filter and by the cake formation properties of the precoat material. Normally the bed thickness is 75–100 mm and, with most materials this can be established on the drum in a period of about one hour. The type and grade of precoat material used, in addition to process considerations, can influence the rate at which the bed must be removed and the cost of precoat vacuum filter operation. Generally, for maximum economy, a precoat filter should operate at the highest possible submergence, consistent with the required degree of cake washing and drying, when required, and with the lowest possible knife advance rate. Some precoat filters are capable of operation at up to 70 per cent drum submergence though this, particularly with the facility to accommodate 100 mm thick beds, necessitates special design features to give adequate clearance between the drum and the trough while at the same time giving acceptable angles for the discharge knife. Knife advance rates are 0.013–0.13 mm per revolution, and drum speeds are frequently 0.002–0.03 Hz (0.1–2 rev/min). By careful control of all the variables, and by correct sizing of the equipment, it is possible to obtain precoat beds which last 60–240 hours.

To obtain maximum economy in operation, a precoat type vacuum filter should have:

(a) Easy variation of the knife advance rate.
(b) Very accurate control of the knife advance rate.
(c) A very rigid knife assembly (due to the need to advance at extremely low rates over a face width up to approximately 6 m).
(d) Rapid advance and retraction of the knife.

Mechanical and hydraulic systems for control of the knife are now used. The latter allows easy selection of the rate and direction of knife movement and the system is particularly suited to remote control or automatic operation.

Example 7.7

A sludge is filtered in a plate and frame press fitted with 25 mm frames. For the first 600 s the slurry pump runs at maximum capacity. During this period the pressure rises to 415 kN/m^2 and 25 per cent of the total filtrate is obtained. The filtration takes a further 3600 s to complete at constant pressure and 900 s is required for emptying and resetting the press.

It is found that if the cloths are precoated with filter aid to a depth of 1.6 mm, the cloth resistance is reduced to 25 per cent of its former value. What will be the increase in the overall throughput of the press if the precoat can be applied in 180 s?

This book belongs to Bradley Loren (bloren@mcandrews-ip.com) Copyright Elsevier 2024

Intas Exhibit 1032
Page 77 of 470
PGR2025-00043

Solution

Case 1

$$\frac{dV}{dt} = \frac{A^2(-\Delta P)}{v\mathbf{r}\mu\left(V + \frac{AL}{v}\right)} = \frac{a}{V+b} \qquad \text{(equation 7.16)}$$

For constant rate filtration:

$$\frac{V_0}{t_0} = \frac{a}{V_0 + b}$$

or: $$V_0^2 + bV_0 = at_0$$

For constant pressure filtration:

$$\frac{1}{2}(V^2 - V_0^2) + b(V - V_0) = a(t - t_0)$$

$$t_0 = 600 \text{ s},\ t - t_0 = 3600 \text{ s},\ V_0 = V/4$$

$$\frac{V^2}{16} + b\frac{V}{4} = 600a$$

and: $$\frac{1}{2}(V^2 - V^2/16) + b(V - V/4) = 3600a$$

Thus: $$3600a = \frac{15}{32}V^2 + \frac{3}{4}bV = \frac{3}{8}V^2 + \frac{3}{2}bV$$

and: $$b = \frac{V}{8}$$

Thus: $$a = \frac{1}{600}\left(\frac{V^2}{16} + \frac{V^2}{32}\right) = \frac{3}{19,200}V^2$$

Total cycle time $= (900 + 4200) = 5100$ s
Filtration rate $= V/5100 = 0.000196V$

Case 2

$$\frac{V_1}{t_1} = \frac{a}{V_1 + \frac{b}{4}} = \frac{V_0}{t_0} = \frac{a}{V_0 + b}$$

$$\frac{1}{2}\left(\frac{49}{64}V^2 - V_1^2\right) + \frac{b}{4}\left(\frac{7}{8}V - V_1\right) = a(t - t_1)$$

Thus: $$\frac{V}{2400} = \frac{\frac{3}{19,200}V^2}{V_1 + \frac{V}{32}}$$

and: $$t_1 = \frac{t_0}{V_0}V_1 = \frac{600}{V/4} \times \frac{11}{32}V = \frac{3300}{4} \text{ s} = 825 \text{ s}$$

This book belongs to Bradley Loren (bloren@mcandrews-ip.com) Copyright Elsevier 2024

Intas Exhibit 1032
Page 78 of 470
PGR2025-00043

Substituting gives:

$$\frac{1}{2}\left(\frac{49}{64}V^2 - \frac{121}{1024}V_1^2\right) + \frac{1}{4}\frac{V}{8}\left(\frac{7}{8}V - \frac{11}{32}V\right) = \frac{3}{19,200}V^2(t - t_1)$$

or:
$$\frac{49}{128} - \frac{121}{2048} + \frac{17}{1024} = \frac{3}{19,200}(t - t_1)$$

$$t - t_1 = \left(\frac{19,200}{3}\right)\left(\frac{784 - 121 + 34}{2048}\right)$$

$$= 2178 \text{ s}$$

$$\text{Cycle time} = (180 + 900 + 825 + 2178) = 4083 \text{ s}$$

$$\text{Filtration rate} = \left(\frac{7}{8} \times \frac{V}{4083}\right) = 0.000214V$$

$$\text{Increase} = \frac{(0.000214 - 0.000196)V}{0.000196V} \times 100 = \underline{\underline{9.1 \text{ per cent}}}$$

7.4.7. The tube press

One of the major problems in coal preparation is the dewatering of fine coal to a moisture content sufficiently low enough both to meet market requirements and to ease the problems of handlability encountered at some collieries and there is an interest in different types of dewatering equipment in addition to the conventional rotary vacuum filter. As a result, a tube press built by the former English China Clays Limited, now Imerys, was installed at a colliery where it was used to treat raw slurry which was blended into the final product. As described by GWILLIAM[32] and BROWN[33]. It was found that the product from the tube press was very low in moisture content. In the china clay industry, for which the tube press was first developed, the formation of a very dry cake reduces the load on the drying plant where the cost of removing a given quantity of water is an order of magnitude greater than in filtration.

In essence, the tube press is an automatic membrane filter press operating at pressures up to 10 MN/m^2 (100 bar) and consists of two concentric cylindrical tubes, the inner filter candle and the outer hydraulic casing. Cylindrical tubes are used as these have the ability to withstand high pressure without a reinforcing structure and are available commercially. Between the filter candle and the hydraulic casing is a flexible membrane which is fastened to both ends of the hydraulic casing. Hydraulic pressure is exerted on to the flexible membrane, applying filtration pressure to the slurry which is contained between the flexible membrane and filter candle. The membrane, being flexible, allows for the slurry feed volume to be varied to suit each individual application and this permits near optimum filter cake thicknesses to be achieved. The filter candle is perforated and around its outer circumference is fitted a drain mesh, felt backing cloth and top filter cloth forming the filter media. The backing cloth protects the filter cloth against the hydraulic high pressure whilst the mesh allows the filtrate to run into the centre of the filter candle and be drained away. Under high pressure conditions, the resistance of the filter cloth is low compared with the resistance of the filter cake. This allows a tightly woven filter cloth to be used and any imperfections in this cloth are compensated for by the felt backing cloth. In this way, clear filtrate is obtained from the tube press.

This book belongs to Bradley Loren (bloren@mcandrews-ip.com) Copyright Elsevier 2024

Intas Exhibit 1032
Page 79 of 470
PGR2025-00043

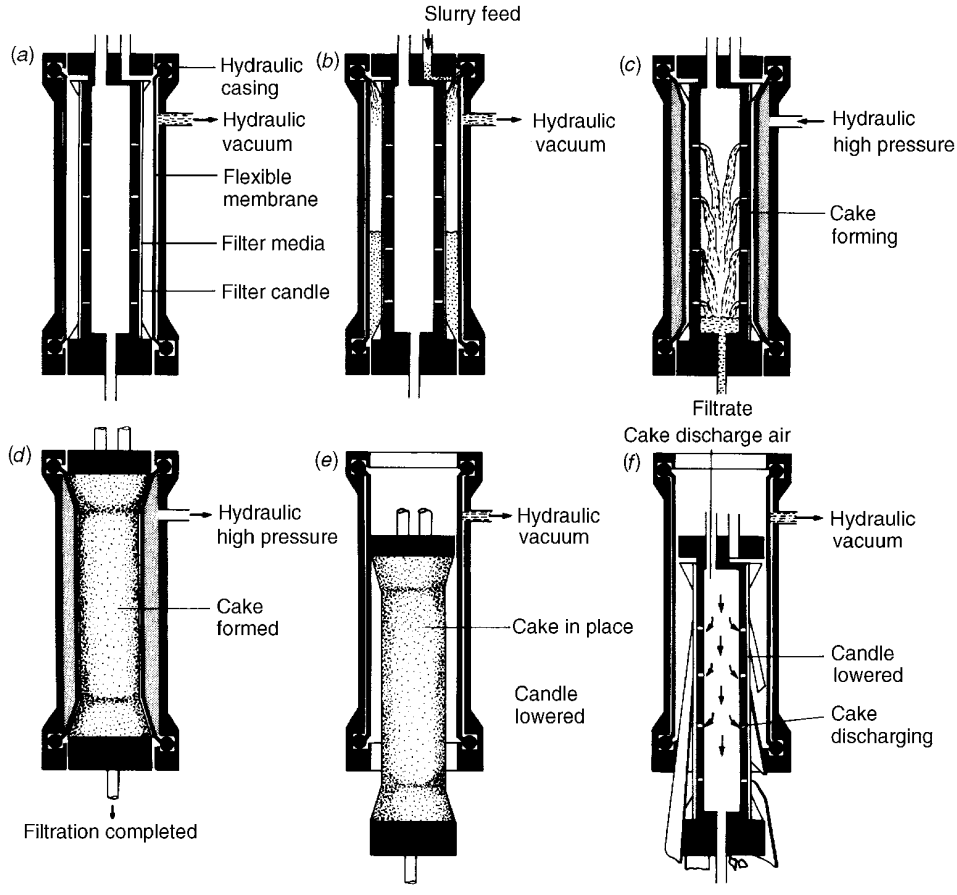


Figure 7.24. Sequence of operation of the tube press

The sequence of operation of the tube press, illustrated in Figure 7.24, is as follows. The empty tube filter press is closed and hydraulic vacuum is applied to the flexible membrane, dilating it against the outer hydraulic casing (*a*). Slurry is fed into the machine, partially filling the volume contained within the flexible membrane, the filter media and the end pieces (*b*). The exact volume of slurry fed into the tube press depends upon the characteristics of each individual slurry and corresponds to the amount required to give optimum cake thickness. The machine will automatically discharge a cake of 16–19 mm maximum thickness. The minimum thickness is dependent on the cake discharge characteristics although is normally 4–5 mm. Low pressure hydraulic fluid is fed into the tube press between the outer hydraulic casing and the flexible membrane. The membrane contracts, reducing the volume between the membrane and filter cloth and expelling the entrained air. The low pressure hydraulic flow is stopped and high pressure hydraulic fluid is applied. Filtration commences and the high pressure hydraulic fluid continues contracting the membrane, reducing the suspension volume and expelling the filtrate through the filter medium into the centre of the filter candle

This book belongs to Bradley Loren (bloren@mcandrews-ip.com) Copyright Elsevier 2024
Intas Exhibit 1032
Page 80 of 470
PGR2025-00043

and away through the filtrate drain line (*c*). Filter cake is formed around the cloth and high pressure is maintained until filtration is completed (*d*). Hydraulic vacuum is applied to the flexible membrane, dilating it against the outer hydraulic casing. When this is accomplished the filter candle is lowered to open the machine (*e*). A pulse of air admitted into the centre of the filter candle expands the filter cloth, dislodging the cake which breaks and falls out of the machine (*f*). This action, together with the candle movement, may be repeated to ensure complete discharge. The filter candle is then raised and the machine closes leaving it ready to commence the next cycle (*a*).

The unique design of the tube press allows for this cycle to be amended, however, to include air pressing and/or cake washing. With air pressing, once the initial filtration is complete, air is introduced between the membrane and the cake. The pressure cycle is then repeated. Typically an air press will further reduce the moisture content of china clay by 2.5–8 per cent. The final moisture contents with other materials are shown in Figure 7.25. Water washing, which is used for the removal of soluble salts, is similar to air pressing, except that it is water that is introduced between membrane and cake.

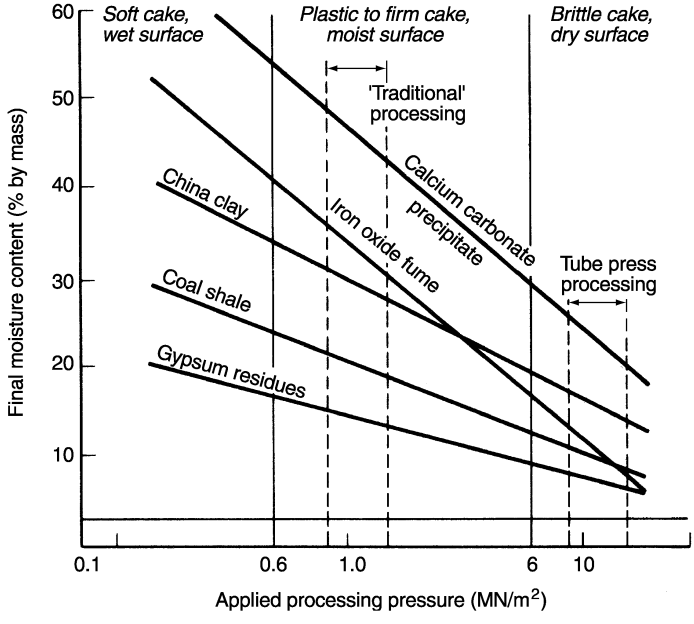


Figure 7.25. Final moisture content as a function of applied pressure

7.5. FURTHER READING

IVES, K. J. (ed.): *The Scientific Basis of Filtration* (Noordhoff, Leyden, 1975).
MATTESON, M. S. and ORR, C.: *Filtration Principles and Practice*, 2nd edn. (Marcel Dekker, New York, 1987).
PURCHAS, D. B.: *Industrial Filtration of Liquids*, 2nd edn. (Leonard Hill, London, 1971).
SUTTLE, H. K. (ed.): *Process Engineering Technique Evaluation–Filtration* (Morgan–Grampian (Publishers) Ltd., London, 1969).
SVAROVSKY, L. (ed:): *Solid–Liquid Separation*, 4th edn. (Butterworth-Heinemann, Oxford, 2000).

This book belongs to Bradley Loren (bloren@mcandrews-ip.com) Copyright Elsevier 2024
Intas Exhibit 1032
Page 81 of 470
PGR2025-00043

7.6. REFERENCES

1. IVES, K. J. (ed.): *The Scientific Basis of Filtration* (Noordhoff, Leyden, 1975).
2. IVES, K. J.: *Trans. Inst. Chem. E*. **48** (1970) T94. Advances in deep-bed filtration.
3. SUTTLE, H. K.: *The Chemical Engineer* No. 314 (Oct. 1976) 675. Development of industrial filtration.
4. RUTH, B. F., MONTILLON, G. H. and MONTONNA, R. E.: *Ind. Eng. Chem*. **25** (1933) 76 and 153. Studies in filtration. I. Critical analysis of filtration theory. II. Fundamental axiom of constant-pressure filtration.
5. RUTH, B. F.: *Ind. Eng. Chem*. **27** (1935) 708 and 806. Studies in filtration. III. Derivation of general filtration equations. IV. Nature of fluid flow through filter septa and its importance in the filtration equation.
6. RUTH, B. F. and KEMPE, L.: *Trans. Am. Inst. Chem. Eng*. **33** (1937) 34. An extension of the testing methods and equations of batch filtration practice to the field of continuous filtration.
7. RUTH, B. F.: *Ind. Eng. Chem*. **38** (1946) 564. Correlating filtration theory with practice.
8. GRACE, H. P.: *Chem. Eng. Prog*. **49** (1953) 303, 367, and 427. Resistance and compressibility of filter cakes.
9. HOFFING, E. H. and LOCKHART, F. J.: *Chem. Eng. Prog*. **47** (1951) 3. Resistance to filtration.
10. CARMAN, P. C.: *Trans. Inst. Chem. Eng*. **16** (1938) 168. Fundamental principles of industrial filtration.
11. HEERTJES, P. M.: *Chem. Eng. Sci*. **6** (1957) 190 and 269. Studies in filtration.
12. VALLEROY, V. V. and MALONEY, J. O.: *A.I.Ch.E.Jl*. **6** (1960) 382. Comparison of the specific resistances of cakes formed in filters and centrifuges.
13. TILLER, F. M. and HUANG, C. J.: *Ind. Eng. Chem*. **53** (1961) 529. Filtration equipment. Theory.
14. TILLER, F. M. and SHIRATO, M.: *A.I.Ch.E.Jl*. **10** (1964) 61. The role of porosity in filtration: Part VI. New definition of filtration resistance.
15. TILLER, F. M. and YEH, C. S.: *A.I.Ch.E.Jl*. **31** (1985) 1241. The role of porosity in filtration: Part X. Deposition of compressible cakes on external radial surfaces.
16. RUSHTON, A. and HAMEED, M. S.: *Filtn. and Sepn*. **6** (1969) 136. The effect of concentration in rotary vacuum filtration.
17. EHLERS, S.: *Ind. Eng. Chem*. **53** (1961) 552. The selection of filter fabrics re-examined.
18. WROTNOWSKI, A. C.: *Chem. Eng. Prog*. **58** No. 12 (Dec. 1962) 61. Nonwoven filter media.
19. PURCHAS, D. B.: *Industrial Filtration of Liquids*, 2nd edn. (Leonard Hill, London, 1971).
20. TILLER, F. M. and CHENG, K. S.: *Filt. and Sepn*. **14** (1977) 13. Delayed cake filtration.
21. MACKLEY, M. R. and SHERMAN, N. E.: *Chem. Eng. Sci.* **47** (1997) 3067. Cross-flow cake filtration mechanics and kinetics.
22. HOLDICH, R. G., CUMMING, I. W. and ISMAIL, B.: *Chem. Eng. Res. Des.* **73** (1995) 20. The variation of cross-flow filtration rate with wall shear stress and the effect of deposit thickness.
23. CLEASBY, J. L.: *The Chemical Engineer* No. 314 (Oct. 1976) 663. Filtration with granular beds.
24. IVES, K. J.: *Proc. Int. Water Supply Assn. Eighth Congress*, Vienna. Vol. 1. (Internatl. Water Supply Assn., London, 1969). Special Subject No. 7. Theory of Filtration.
25. IWASAKI, T.: *J. Am. Water Works Assn*. **29** (1937) 1591. Some notes on sand filtration.
26. SPIELMAN, L. A. and FRIEDLANDER, S. K.: *J. Colloid and Interface. Sci*. **46** (1974) 22. Role of the electrical double layer in particle deposition by convective diffusion.
27. HARKER, J. H.: *Processing* **2** (1979) 35. Getting the best out of batch filtration.
28. CHERRY, G. B.: *Filtn. and Sepn*. **11** (1974) 181. New developments in filter plates and filter presses.
29. PARRISH, P. and OGILVIE, H.: *Calcium Superphosphates and Compound Fertilisers. Their Chemistry and Manufacture* (Hutchison, 1939).
30. BLENDULF, K. A. G. and BOND, A. P.: *I. Chem. E. Symposium Series* No. 59, (1980) 1 : 5/1. The development and application of horizontal belt filters in the mineral, processing and chemical industries.
31. BOSLEY, R.: *Filtn. and Sepn*. **11** (1974) 138. Vacuum filtration equipment innovations.
32. GWILLIAM, R. D.: *Filt. and Sepn*. **8** (1971) 173. The E.C.C. tube filter press.
33. BROWN, A.: *Filt. and Sepn*. **16** (1979) 468. The tube press.

7.7. NOMENCLATURE

		Units in SI System	Dimensions in **M**, **L**, **T**
A	Cross-sectional area of bed or filtration area	m^2	$\mathbf{L}^2$
B_1	Coefficient	s/m^6	$\mathbf{L}^{-6}\mathbf{T}$
B_2	Coefficient	s/m^3	$\mathbf{L}^{-3}\mathbf{T}$
b	Frame thickness	m	**L**
C	Volume concentration of solids in the filter	—	—

This book belongs to Bradley Loren (bloren@mcandrews-ip.com) Copyright Elsevier 2024

Intas Exhibit 1032
Page 82 of 470
PGR2025-00043

		Units in SI System	Dimensions in **M**, **L**, **T**
C'	Total cost of filtration per unit volume	£/m^3	$\mathbf{L}^{-3}$
C_0	Value of C at filter surface	—	—
e	Voidage of bed or filter cake	—	—
e_0	Liquid fraction in feed slurry	—	—
e_V	Liquid fraction in slurry in vessel	—	—
e_z	Voidage at distance z from surface	—	—
J	Mass fraction of solids in slurry	—	—
L	Thickness of filter cake with same resistance as cloth	m	$\mathbf{L}$
l	Thickness of filter cake or bed	m	$\mathbf{L}$
n'	Compressibility index	—	—
P_1	Pressure at downstream face of cake	N/m^2	$\mathbf{ML}^{-1}\mathbf{T}^{-2}$
P_2	Pressure at upstream face of cake	N/m^2	$\mathbf{ML}^{-1}\mathbf{T}^{-2}$
P_z	Pressure at distance z from surface	N/m^2	$\mathbf{ML}^{-1}\mathbf{T}^{-2}$
$-\Delta P$	Total drop in pressure	N/m^2	$\mathbf{ML}^{-1}\mathbf{T}^{-2}$
$-\Delta P'$	Drop in pressure across cake	N/m^2	$\mathbf{ML}^{-1}\mathbf{T}^{-2}$
$-\Delta P''$	Pressure drop across cloth	N/m^2	$\mathbf{ML}^{-1}\mathbf{T}^{-2}$
R	Rate of cake production	m/s	$\mathbf{LT}^{-1}$
$\mathbf{r}$	Specific resistance of filter cake	m^{-2}	$\mathbf{L}^{-2}$
$\bar{\mathbf{r}}$	Mean value of $\mathbf{r}_z$	m^{-2}	$\mathbf{L}^{-2}$
$\mathbf{r}_z$	Specific resistance of compressible cake at distance z from surface (equation 7.25)	m^{-2}	$\mathbf{L}^{-2}$
$\bar{\mathbf{r}}', \bar{\mathbf{r}}''$	Functions of $\mathbf{r}_z$ independent of ΔP	m^{-2}/(N/m^2)$^{n'}$	$\mathbf{M}^{-n'}\mathbf{L}^{n'-2}\mathbf{T}^{2n'}$
S	Specific surface	m^{-1}	$\mathbf{L}^{-1}$
t	Time	s	$\mathbf{T}$
t$'$	Time of dismantling filter press	s	$\mathbf{T}$
t_1	Time at beginning of operation	s	$\mathbf{T}$
u_c	Mean velocity of flow calculated over the whole area	m/s	$\mathbf{LT}^{-1}$
V	Volume of liquid flowing in time t	m^3	$\mathbf{L}^3$
V_1	Volume of liquid passing in time t_1	m^3	$\mathbf{L}^3$
$\mathbf{V}$	Volume of vessel	m^3	$\mathbf{L}^3$
v	Volume of cake deposited by unit volume of filtrate	—	—
v'	Volume of solids deposited by unit volume of filtrate	—	—
w	Mass rate of production of filtrate	kg/s	$\mathbf{MT}^{-1}$
W	Overall volumetric rate of filtration	m^3/s	$\mathbf{L}^3\mathbf{T}^{-1}$
z	Distance from surface of filter cake	m	$\mathbf{L}$
λ	Filter coefficient	m^{-1}	$\mathbf{L}^{-1}$
μ	Viscosity of fluid	Ns/m^2	$\mathbf{ML}^{-1}\mathbf{T}^{-1}$
ρ	Density of fluid	kg/m^3	$\mathbf{ML}^{-3}$
ρ_s	Density of solids	kg/m^3	$\mathbf{ML}^{-3}$
σ	Volume of solids deposited per unit volume of filter	—	—

This book belongs to Bradley Loren (bloren@mcandrews-ip.com) Copyright Elsevier 2024

Intas Exhibit 1032
Page 83 of 470
PGR2025-00043

CHAPTER 9

Centrifugal Separations

9.1. INTRODUCTION

There is now a wide range of situations where centrifugal force is used in place of the gravitational force in order to effect separations. The resulting accelerations may be several thousand times that attributable to gravity. Some of the benefits include far greater rates of separation; the possibility of achieving separations which are either not practically feasible, or actually impossible, in the gravitational field; and a substantial reduction of the size of the equipment. Recent developments in the use of centrifugal fields in *process intensification* are discussed in Chapter 20.

Centrifugal fields can be generated in two distinctly different ways:

(a) By introducing a fluid with a high tangential velocity into a cylindrical or conical vessel, as in the *hydrocyclone* and in the *cyclone separator* (Chapter 1). In this case, the flow pattern in the body of the separator approximates to a *free vortex* in which the tangential velocity varies *inversely* with the radius (see Volume 1, Chapter 2). Generally, the larger and heavier particles will collect and be removed near the walls of the separator, and the smaller and lighter particles will be taken off through an outlet near the axis of the vessel.
(b) By the use of the *centrifuge*. In this case the fluid is introduced into some form of rotating bowl and is rapidly accelerated. Because the frictional drag within the fluid ensures that there is very little *rotational slip* or relative motion between fluid layers within the bowl, all the fluid tends to rotate at a constant angular velocity ω and a *forced vortex* is established. Under these conditions, the tangential velocity will be *directly* proportional to the radius at which the fluid is rotating.

In this chapter, attention is focused on the operation of the centrifuge. Some of the areas where it is extensively used are as follows:

(a) *For separating particles on the basis of their size or density*. This is effectively using a centrifugal field to achieve a higher rate of sedimentation than could be achieved under gravity.
(b) *For separating immiscible liquids of different densities*, which may be in the form of dispersions or even emulsions in the feed stream. This is the equivalent of a gravitational decantation process.
(c) *For filtration of a suspension*. In this case centrifugal force replaces the force of gravity or the force attributable to an applied pressure difference across the filter.

This book belongs to Bradley Loren (bloren@mcandrews-ip.com) Copyright Elsevier 2024

Intas Exhibit 1032
Page 84 of 470
PGR2025-00043

(d) *For the drying of solids and, in particular, crystals*. Liquid may be adhering to the surface of solid particles and may be trapped between groups of particles. Drainage may be slow in the gravitational field, especially if the liquid has a high viscosity. Furthermore, liquid is held in place by surface tension forces which must be exceeded before liquid can be freed. This is particularly important with fine particles. Thus, processes which are not possible in the gravitational field can be carried out in the centrifuge.

(e) *For breaking down of emulsions and colloidal suspensions*. A colloid or emulsion may be quite stable in the gravitational field where the dispersive forces, such as those due to Brownian motion, are large compared with the gravitational forces acting on the fine particles or droplets. In a centrifugal field which may be several thousand times more powerful, however, the dispersive forces are no longer sufficient to maintain the particles in suspension and separation is effected.

(f) *For the separation of gases*. In the nuclear industry isotopes are separated in the gas centrifuge in which the accelerating forces are sufficiently great to overcome the dispersive effects of molecular motion. Because of the very small difference in density between isotopes and between compounds of different isotopes, fields of very high intensity are needed.

(g) *For mass transfer processes*. Because far greater efficiencies and higher throughputs can be obtained before flooding occurs, centrifugal packed bed contactors are finding favour and are replacing ordinary packed columns in situations where compactness is important, or where it is desirable to reduce the holdup of materials undergoing processing because of their hazardous properties. An important application is the use of inert gases in the desorption of oxygen from sea water in order to reduce its corrosiveness; in North Sea oil rigs the sea water is used as a coolant in heat exchangers. In addition, centrifugal contactors for liquid–liquid extraction processes now have important applications discussed in Chapter 13. These are additional areas where centrifugal fields, and the employment of centrifuges, is gaining in importance.

9.2. SHAPE OF THE FREE SURFACE OF THE LIQUID

For an element of liquid in a centrifuge bowl which is rotating at an angular velocity of ω, the centrifugal acceleration is $r\omega^2$, compared with the gravitational acceleration of g. The ratio $r\omega^2/g$ is one measure of the separating effect obtained in a centrifuge relative to that arising from the gravitational field; values of $r\omega^2/g$ may be very high (up to 10^4) in some industrial centrifuges and more than an order of magnitude greater in the ultra-centrifuge, discussed in Section 9.8. In practice, the axis of rotation may be vertical, horizontal, or intermediate, and the orientation is usually determined by the means adopted for introducing feed and, removing product streams, from the centrifuge.

Figure 9.1 shows an element of the free surface of the liquid in a bowl which is rotating at a radius r_0 about a vertical axis at a very low speed; the centrifugal and gravitational fields will then be of the same order of magnitude. The centrifugal force per unit mass is $r_0\omega^2$ and the corresponding gravitational force is g. These two forces are perpendicular

This book belongs to Bradley Loren (bloren@mcandrews-ip.com) Copyright Elsevier 2024
Intas Exhibit 1032
Page 85 of 470
PGR2025-00043

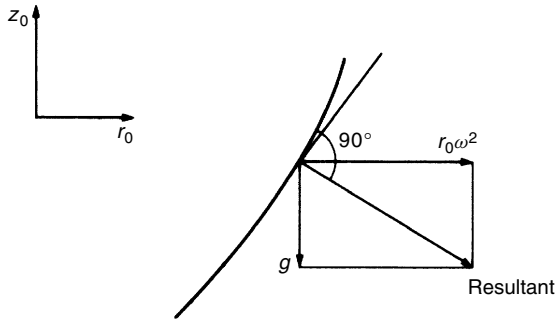


Figure 9.1. Element of surface of liquid

to one another and may be combined as shown to give the resultant force which must, at equilibrium, be at right angles to the free surface. Thus, the slope at this point is given by:

$$\frac{dz_0}{dr_0} = \frac{\text{radial component of force}}{\text{axial component of force}} = \frac{r_0\omega^2}{g} \tag{9.1}$$

where z_0 is the axial coordinate of the free surface of the liquid.

Equation 9.1 may be integrated to give:

$$z_0 = \frac{\omega^2}{2g}r_0^2 + \text{constant}$$

If z_a is the value of z_0 which corresponds to the position where the free surface is at the axis of rotation ($r_0 = 0$), then:

$$z_0 - z_a = \frac{\omega^2}{2g}r_0^2 \tag{9.2}$$

Equations 9.1 and 9.2 correspond with equations 2.80 and 2.79 in Volume 1, Chapter 2. Taking the base of the bowl as the origin for the measurement of z_0, positive values of z_a correspond to conditions where the whole of the bottom of the bowl is covered by liquid. Negative values of z_a imply that the paraboloid of revolution describing the free surface would cut the axis of rotation below the bottom, and therefore the central portion of the bowl will be dry.

Normally $r_0\omega^2 \gg g$, the surface is nearly vertical, and z_0 has a very large negative value. Thus, in practice, the free surface of the liquid will be effectively concentric with the walls of the bowl. It is seen therefore that the operation of a high speed centrifuge is independent of the orientation of the axis of rotation.

9.3. CENTRIFUGAL PRESSURE

A force balance on a sector of fluid in the rotating bowl, carried out as in Volume 1, Chapter 2, gives the pressure gradient at a radius r:

$$\frac{\partial P}{\partial r} = \rho\omega^2 r \tag{9.3}$$

This book belongs to Bradley Loren (bloren@mcandrews-ip.com) Copyright Elsevier 2024

Intas Exhibit 1032
Page 86 of 470
PGR2025-00043

Unlike the vertical pressure gradient in a column of liquid which is constant at all heights, the centrifugal pressure gradient is a function of radius of rotation r, and increases towards the wall of the basket. Integration of equation 9.3 at a given height gives the pressure P exerted by the liquid on the walls of the bowl of radius R when the radius of the inner surface of the liquid is r_0 as:

$$P = \tfrac{1}{2}\rho\omega^2(R^2 - r_0^2) \tag{9.4}$$

9.4. SEPARATION OF IMMISCIBLE LIQUIDS OF DIFFERENT DENSITIES

The problem of the continuous separation of a mixture of two liquids of different densities is most readily understood by first considering the operation of a gravity settler, as shown in Figure 9.2. For equilibrium, the hydrostatic pressure exerted by a height z of the denser liquid must equal that due to a height z_2 of the heavier liquid and a height z_1 of the lighter liquid in the separator.

Thus: $$z\rho_2 g = z_2\rho_2 g + z_1\rho_1 g$$

or: $$z = z_2 + z_1\frac{\rho_1}{\rho_2} \tag{9.5}$$

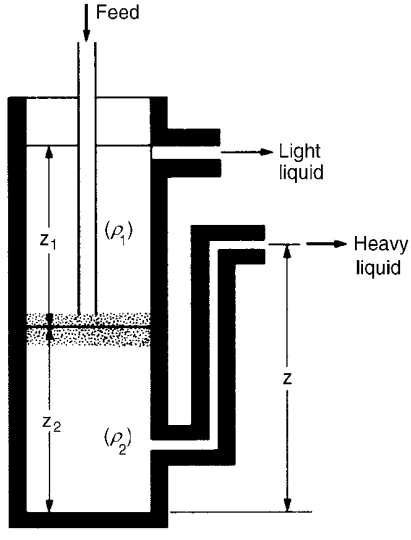


Figure 9.2. Gravity separation of two immiscible liquids

For the centrifuge it is necessary to position the overflow on the same principle, as shown in Figure 9.3. In this case the radius r_i of the weir for the less dense liquid will correspond approximately to the radius of the inner surface of the liquid in the bowl. That

This book belongs to Bradley Loren (bloren@mcandrews-ip.com) Copyright Elsevier 2024

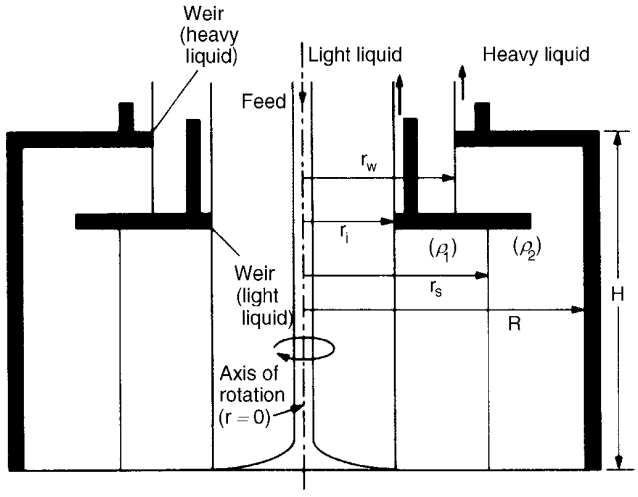


Figure 9.3. Separation of two immiscible liquids in a centrifuge

of the outer weir r_w must be such that the pressure developed at the wall of the bowl of radius R by the heavy liquid alone as it flows over the weir is equal to that due to the two liquids within the bowl. Thus, applying equation 9.4 and denoting the densities of the light and heavy liquids by ρ_1 and ρ_2 respectively and the radius of the interface between the two liquids in the bowl as r_s:

$$\tfrac{1}{2}\rho_2\omega^2(R^2 - r_w^2) = \tfrac{1}{2}\rho_2\omega^2(R^2 - r_s^2) + \tfrac{1}{2}\rho_1\omega^2(r_s^2 - r_i^2)$$

or:
$$\frac{r_s^2 - r_i^2}{r_s^2 - r_w^2} = \frac{\rho_2}{\rho_1} \tag{9.6}$$

If Q_1 and Q_2 are the volumetric rates of feed of the light and heavy liquids respectively, on the assumption that there is no slip between the liquids in the bowl and that the same, then residence time is required for the two phases, then:

$$\frac{Q_1}{Q_2} = \frac{r_s^2 - r_i^2}{R^2 - r_s^2} \tag{9.7}$$

Equation 9.7 enables the value of r_s to be calculated for a given operating condition.

The retention time t_R necessary to give adequate separation of the liquids will depend on their densities and interfacial tension, and on the form of the dispersion, and can only be determined experimentally for that mixture. The retention time is given by:

$$t_R = \frac{V'}{Q_1 + Q_2} = \frac{V'}{Q} \tag{9.8}$$

where Q is the total feed rate of liquid, Q_1 and Q_2 refer to the light and heavy liquids respectively, and V' is the volumetric holdup of liquid in the bowl.

Approximately:
$$V' \approx \pi(R^2 - r_i^2)H \tag{9.9}$$

This book belongs to Bradley Loren (bloren@mcandrews-ip.com) Copyright Elsevier 2024

Intas Exhibit 1032
Page 88 of 470
PGR2025-00043

where H is the axial length (or clarifying length) of the bowl.

Thus:
$$t_R = \frac{Q}{\pi(R^2 - r_i^2)H} \tag{9.10}$$

Equation 9.10 gives the relation between Q and r_i for a given retention time, and determines the required setting of the weir. In practice the relative values of r_i and r_w are adjusted to modify the relative residence times of the individual phases to give extra separating time for the more difficult phase. In the decanter centrifuge, r_i is adjusted to influence either discharged cake dryness or the conveying efficiency.

In equations 9.6 and 9.7, ρ_2/ρ_1 and Q_1/Q_2 are determined by the properties and composition of the mixture to be separated, and R is fixed for a given bowl; r_i and r_w are governed by the settings of the weirs. The radius r_s of the interface between the two liquids is then the only unknown and this may be eliminated between the two equations. Substitution of the value r_i from equation 9.10 then permits calculation of the required radius r_w of the weir for the heavy liquid.

This treatment gives only a simplified approach to the design of a system for the separation of two liquids. It will need modification to take account of the geometric configuration of the centrifuge — a topic which is discussed in Section 9.8.

9.5. SEDIMENTATION IN A CENTRIFUGAL FIELD

Centrifuges are extensively used for separating fine solids from suspension in a liquid. As a result of the far greater separating power compared with that available using gravity, fine solids and even colloids may be separated. Furthermore, it is possible to break down emulsions and to separate dispersions of fine liquid droplets, though in this case the suspended phase is in the form of liquid droplets which will coalesce following separation. Centrifuges may be used for batch operation when dealing with small quantities of suspension although, on the large scale, arrangements must sometimes be incorporated for the continuous removal of the separated constituents. Some of the methods of achieving this are discussed along with the various types of equipment in Section 9.8. When centrifuges are used for *polishing*, the removal of the very small quantities of finely divided solids needs be carried out only infrequently, and manual techniques are then often used.

Because centrifuges are normally used for separating fine particles and droplets, it is necessary to consider only the Stokes' law region in calculating the drag between the particle and the liquid.

It is seen in Chapter 3 that, as a particle moves outwards towards the walls of the bowl of a centrifuge, the accelerating force progressively increases and therefore the particle never reaches an equilibrium velocity as is the case in the gravitational field. Neglecting the inertia of the particle, then:

$$\frac{\mathrm{d}r}{\mathrm{d}t} = \frac{d^2(\rho_s - \rho)r\omega^2}{18\mu} \tag{9.11}$$

(equation 3.109)

This book belongs to Bradley Loren (bloren@mcandrews-ip.com) Copyright Elsevier 2024

Intas Exhibit 1032
Page 89 of 470
PGR2025-00043

$$= u_0 \frac{r\omega^2}{g} \tag{9.12}$$

(equation 3.110)

At the walls of the bowl of radius r, $\mathrm{d}r/\mathrm{d}t$ is given by:

$$\left(\frac{\mathrm{d}r}{\mathrm{d}t}\right)_{r=R} = \frac{d^2(\rho_s - \rho)R\omega^2}{18\mu} \tag{9.13}$$

The time taken to settle through a liquid layer of thickness h at the walls of the bowl is given by integration of equation 9.11 between the limits $r = r_0$ (the radius of the inner surface of the liquid), and $r = R$ to give equation 3.121. This equation may be simplified where $R - r_0 (= h)$ is small compared with R, as in equation 3.122.

Then:
$$t_R = \frac{18\mu h}{d^2(\rho_s - \rho)R\omega^2} \tag{9.14}$$

(equation 3.100)

It may be seen that equation 9.14 is the time taken to settle through the distance h at a velocity given by equation 9.13. t_R is then the minimum retention time required for all particles of size greater than d to be deposited on the walls of the bowl. Thus, the maximum throughput Q at which all particles larger than d will be retained is given by substitution for t_R from equation 9.8 to give:

$$Q = \frac{d^2(\rho_s - \rho)R\omega^2 V'}{18\mu h} \tag{9.15}$$

or:
$$Q = \frac{d^2(\rho_s - \rho)g}{18\mu} \frac{R\omega^2 V'}{hg} \tag{9.16}$$

From equation 3.24:
$$\frac{d^2(\rho_s - \rho)g}{18\mu} = u_0$$

where u_0 is the terminal falling velocity of the particle in the gravitational field and hence:

$$Q = u_0 \frac{R\omega^2 V'}{hg} \tag{9.17}$$

Writing the capacity term as:

$$\begin{aligned} \Sigma &= \frac{R\omega^2 V'}{hg} \\ &= \frac{\pi R(R^2 - r_0^2)H\omega^2}{hg} \\ &= \pi R(R + r_0)H\frac{\omega^2}{g} \end{aligned} \tag{9.18}$$

Then:
$$Q = u_0 \Sigma \tag{9.19}$$

This book belongs to Bradley Loren (bloren@mcandrews-ip.com) Copyright Elsevier 2024

Intas Exhibit 1032
Page 90 of 470
PGR2025-00043

Equation 9.18 implies that the greater the depth h of liquid in the bowl, that is the lower the value of r_0, the smaller will be the value of Σ, but this is seldom borne out in practice in decanter centrifuges. This is probably due to high turbulence experienced and the effects of the scrolling mechanism. Σ is independent of the properties of the fluid and the particles and depends only on the dimensions of the centrifuge, the location of the overflow weir and the speed of rotation. It is equal to the cross-sectional area of a gravity settling tank with the same clarifying capacity as the centrifuge. Thus, Σ is a measure of the capacity of the centrifuge and gives a quantification of its performance for clarification. This treatment is attributable to the work of AMBLER[1].

For cases where the thickness h of the liquid layer at the walls is comparable in order of magnitude with the radius R of the bowl, it is necessary to use equation 3.121 in place of equation 9.14 for the required residence time in the centrifuge or:

$$t_R = \frac{18\mu}{d^2(\rho_s - \rho)\omega^2} \ln \frac{R}{r_0} \tag{9.20}$$

(from equation 3.121)

Then:
$$Q = \frac{d^2(\rho_s - \rho)\omega^2 V'}{18\mu \ln(R/r_0)} \tag{9.21}$$

$$= \frac{d^2(\rho_s - \rho)g}{18\mu} \frac{\omega^2 V'}{g \ln(R/r_0)} \tag{9.22}$$

$$= u_0 \Sigma \tag{9.23}$$

In this case:
$$\Sigma = \frac{\omega^2 V'}{g \ln(R/r_0)}$$

$$= \frac{\pi(R^2 - r_i^2)H}{\ln(R/r_0)} \frac{\omega^2}{g} \tag{9.24}$$

A similar analysis can be carried out with various geometrical arrangements of the bowl of the centrifuge. Thus, for example, for a disc machine (described later) the value of Σ is very much greater than for a cylindrical bowl of the same size. Values of Σ for different arrangements are quoted by HAYTER[2] and by TROWBRIDGE[3].

This treatment leads to the calculation of the condition where all particles larger than a certain size are retained in the centrifuge. Other definitions are sometimes used, such as for example, the size of the particle which will just move half the radial distance from the surface of the liquid to the wall, or the condition when just half of the particles of the specified size will be removed from the suspension.

Example 9.1

In a test on a centrifuge all particles of a mineral of density 2800 kg/m^3 and of size 5 μm, equivalent spherical diameter, were separated from suspension in water fed at a volumetric throughput rate of 0.25 m^3/s. Calculate the value of the capacity factor Σ.

This book belongs to Bradley Loren (bloren@mcandrews-ip.com) Copyright Elsevier 2024

Intas Exhibit 1032
Page 91 of 470
PGR2025-00043

What will be the corresponding size cut for a suspension of coal particles in oil fed at the rate of 0.04 m^3/s? The density of coal is 1300 kg/m^3 and the density of the oil is 850 kg/m^3 and its viscosity is 0.01 Ns/m^2.

It may be assumed that Stokes' law is applicable.

Solution

The terminal falling velocity of particles of diameter 5 μm in water, of density $\rho = 1000$ kg/m^3 and, of viscosity $\mu = 10^{-3}$ Ns/m^2, is given by:

$$u_0 = \frac{d^2(\rho_s - \rho)g}{18\mu} = \frac{25 \times 10^{-12} \times (2800 - 1000) \times 9.81}{18 \times 10^{-3}} \qquad \text{(equation 3.24)}$$

$$= 2.45 \times 10^{-5} \text{ m/s}$$

From the definition of Σ:

$$Q = u_0 \Sigma \qquad \text{(equation 9.19)}$$

and:

$$\Sigma = \frac{0.25}{(2.45 \times 10^{-5})} = 1.02 \times 10^4 \text{ m}^2.$$

For the coal-in-oil mixture:

$$u_0 = \frac{Q}{\Sigma} = \frac{0.04}{(1.02 \times 10^4)} = 3.92 \times 10^{-6} \text{ m/s}.$$

From equation 3.24:

$$d^2 = \frac{18\mu u_0}{(\rho_s - \rho)g}$$

$$= \frac{18 \times 10^{-2} \times 3.92 \times 10^{-6}}{(1300 - 850) \times 9.81}$$

and:

$$d = 4.0 \times 10^{-6} \text{ m or } \underline{\underline{4\ \mu\text{m}}}.$$

Example 9.2

A centrifuge is fitted with a conical disc stack with an included angle of 2θ, and there are n flow passages between the discs. A suspension enters at radius r_1 and leaves at radius r_2. Obtain an expression for the separating power Σ of the centrifuge. It may be assumed that the resistance force acting on the particles is given by Stokes' law.

Solution

For two discs AA′ and BB′, as shown in Figure 9.4, the particle which is most unfavourably placed for collection will enter at point A at radius r_1, and be deposited on the upper plate at point B′ at

This book belongs to Bradley Loren (bloren@mcandrews-ip.com) Copyright Elsevier 2024

Intas Exhibit 1032
Page 92 of 470
PGR2025-00043

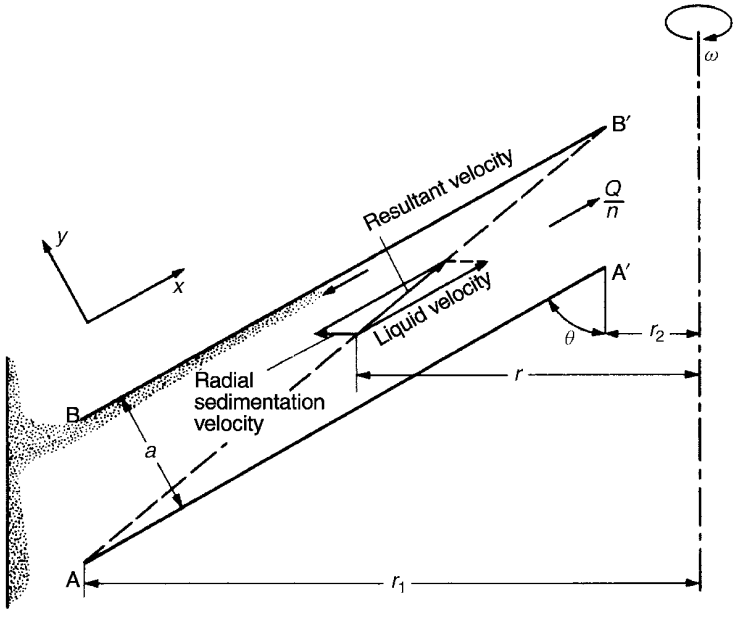


Figure 9.4. Path of limit particle through separation channel

radius r_2. It is assumed that the suspension is evenly divided between the discs. The particles will move in not quite in a straight line because both velocity components are a function of r.

At radius r, the velocity of the liquid in the flow channel is:

$$\frac{Q}{2\pi r a n} = \frac{\mathrm{d}x}{\mathrm{d}t} \tag{i}$$

where x is the distance parallel to the discs and a is the spacing.

At radius r, the centrifugal sedimentation velocity of a particle, whose diameter is d is given by:

$$\frac{\mathrm{d}r}{\mathrm{d}t} = \frac{d^2 r\omega^2(\rho_s - \rho)}{18\mu} \qquad \text{(equation 9.11)}$$

$$= u_0 \frac{r\omega^2}{g} \qquad \text{(equation 9.12) (ii)}$$

From the geometry of the system:

$$-\frac{\mathrm{d}r}{\mathrm{d}x} = \sin\theta$$

Thus from equation (i):

$$-\frac{\mathrm{d}r}{\mathrm{d}t} = \frac{Q}{2\pi r a n}\sin\theta \tag{iii}$$

and:

$$\frac{\mathrm{d}y}{\mathrm{d}r} = \cos\theta$$

This book belongs to Bradley Loren (bloren@mcandrews-ip.com) Copyright Elsevier 2024

Intas Exhibit 1032
Page 93 of 470
PGR2025-00043

Thus from equation (ii):

$$\frac{dy}{dt} = u_0 \frac{r\omega^2}{g} \cos\theta \tag{iv}$$

Dividing equation (iv) by equation (iii) gives:

$$-\frac{dy}{dr} = \left(\frac{u_0 r\omega^2 \cos\theta}{g}\right) \cdot \left(\frac{2\pi r a n}{Q \sin\theta}\right)$$

$$= \frac{2\pi n a u_0 \omega^2 \cot\theta}{Qg} r^2$$

The particle must move through distance a in the y direction as its radial position changes from r_1 to r_2.

Thus:

$$-\int_0^a dy = \frac{2\pi n a u_0 \omega^2 \cot\theta}{Qg} \int_{r_1}^{r_2} r^2 \, dr$$

$$a = \frac{2\pi n a u_0 \omega^2 \cot\theta}{3Qg}(r_1^3 - r_2^3)$$

$$Q = u_0 \frac{2\pi n \omega^2 \cot\theta}{3g}(r_1^3 - r_2^3)$$

$$= u_0 \Sigma \qquad \text{(from the definition of } \Sigma\text{, equation 9.19)}$$

or:

$$\Sigma = \underline{\underline{\frac{2\pi \omega^2 n \cot\theta (r_1^3 - r_2^3)}{3g}}}$$

9.6. FILTRATION IN A CENTRIFUGE

When filtration is carried out in a centrifuge, it is necessary to use a perforated bowl to permit removal of the filtrate. The driving force is the centrifugal pressure due to the liquid and suspended solids, and this will not be affected by the presence of solid particles deposited on the walls. The resulting force must overcome the friction caused by the flow of liquid through the filter cake, the cloth, and the supporting gauze and perforations. The resistance of the filter cake will increase as solids are deposited although the other resistances will remain approximately constant throughout the process. Considering filtration in a bowl of radius R and supposing that the suspension is introduced at such a rate that the inner radius of the liquid surface remains constant as shown in Figure 9.5, then at some time t after the commencement of filtration, a filter cake of thickness l will have been built up and the radius of the interface between the cake and the suspension will be r'.

If dP' is the pressure difference across a small thickness dl of cake, the velocity of flow of the filtrate is given by equation 7.2, and:

$$\frac{1}{A}\frac{dV}{dt} = u_c = \frac{1}{\mathbf{r}\mu}\left(\frac{-dP'}{dl}\right) \tag{9.25}$$

where $\mathbf{r}$ is the specific resistance of the filter cake and μ is the viscosity of the filtrate.

This book belongs to Bradley Loren (bloren@mcandrews-ip.com) Copyright Elsevier 2024

Intas Exhibit 1032
Page 94 of 470
PGR2025-00043

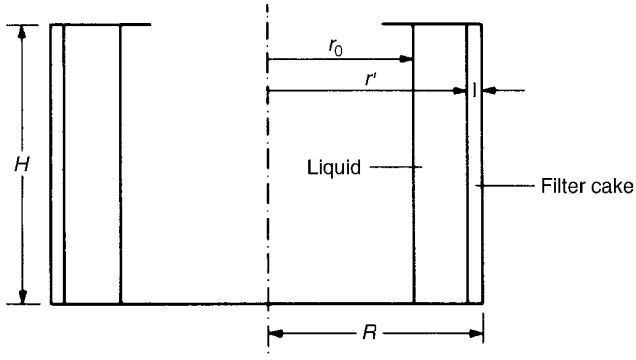


Figure 9.5. Filtration in a centrifuge

If the centrifugal force is large compared with the gravitational force, the filtrate will flow in an approximately radial direction, and will be evenly distributed over the axial length of the bowl. The area available for flow will increase towards the walls of the bowl. If dV is the volume of filtrate flowing through the filter cake in time dt, then:

$$u_c = \frac{1}{2\pi r' H}\frac{dV}{dt}$$

Thus:

$$\frac{1}{\mathbf{r}\mu}\left(\frac{-dP'}{dl}\right) = \frac{1}{2\pi r' H}\frac{dV}{dt} \tag{9.26}$$

$$-dP' = \frac{\mathbf{r}\mu\, dl}{2\pi r' H}\frac{dV}{dt}$$

and thus the total pressure drop through the cake at time t is given by:

$$\begin{aligned} -\Delta P' &= \frac{\mathbf{r}\mu}{2\pi H}\frac{dV}{dt}\int_0^l \frac{dl}{r'} \\ &= \frac{\mathbf{r}\mu}{2\pi H}\frac{dV}{dt}\int_{r'}^R \frac{dr'}{r'} \\ &= \frac{\mathbf{r}\mu}{2\pi H}\frac{dV}{dt}\ln\frac{R}{r'} \end{aligned} \tag{9.27}$$

If the resistance of the cloth is negligible, $-\Delta P'$ is equal to the centrifugal pressure. More generally, if the cloth, considered together with the supporting wall of the basket, is equivalent in resistance to a cake of thickness L, situated at the walls of the basket, the pressure drop $-\Delta P''$ across the cloth is given by:

$$\frac{-\Delta P''}{\mathbf{r}\mu L} = \frac{1}{2\pi H R}\frac{dV}{dt}$$

$$-\Delta P'' = \frac{\mathbf{r}\mu}{2\pi H}\frac{dV}{dt}\frac{L}{R} \tag{9.28}$$

This book belongs to Bradley Loren (bloren@mcandrews-ip.com) Copyright Elsevier 2024

Intas Exhibit 1032
Page 95 of 470
PGR2025-00043

Thus the total pressure drop across the filter cake and the cloth $(-\Delta P)$, say, is given by:

$$(-\Delta P) = (-\Delta P') + (-\Delta P'')$$

Thus:
$$-\Delta P = \frac{\mathbf{r}\mu}{2\pi H}\frac{\mathrm{d}V}{\mathrm{d}t}\left(\ln\frac{R}{r'} + \frac{L}{R}\right) \tag{9.29}$$

Before this equation can be integrated it is necessary to establish the relation between r' and V. If v is the bulk volume of incompressible cake deposited by the passage of unit volume of filtrate, then:

$$v\,\mathrm{d}V = -2\pi r' H\,\mathrm{d}r'$$
$$\frac{\mathrm{d}V}{\mathrm{d}t} = -\frac{2\pi H r'}{v}\frac{\mathrm{d}r'}{\mathrm{d}t} \tag{9.30}$$

and substituting for $\mathrm{d}V/\mathrm{d}t$ in the previous equation gives:

$$-\Delta P = -\frac{\mathbf{r}\mu}{2\pi H}\frac{2\pi H r'}{v}\frac{\mathrm{d}r'}{\mathrm{d}t}\left(\ln\frac{R}{r'} + \frac{L}{R}\right) \tag{9.31}$$

Thus:
$$\frac{v(-\Delta P)}{\mathbf{r}\mu}\,\mathrm{d}t = \left(\ln\frac{r'}{R} - \frac{L}{R}\right) r'\,\mathrm{d}r'$$

This may be integrated between the limits $r' = R$ and $r' = r'$ as t goes from 0 to t. $-\Delta P$ is constant because the inner radius r_0 of the liquid is maintained constant:

$$\frac{(-\Delta P)vt}{\mathbf{r}\mu} = \int_R^{r'}\left\{\left(\ln\frac{r'}{R} - \frac{L}{R}\right) r'\right\}\mathrm{d}r'$$
$$= \frac{1}{4}(R^2 - r'^2) + \frac{L}{2R}(R^2 - r'^2) + \tfrac{1}{2}r'^2\ln\frac{r'}{R} \tag{9.32}$$

and:
$$(R^2 - r'^2)\left(1 + 2\frac{L}{R}\right) + 2r'^2\ln\frac{r'}{R} = \frac{4(-\Delta P)vt}{\mathbf{r}\mu}$$
$$= \frac{2vt\rho\omega^2}{\mathbf{r}\mu}(R^2 - r_0^2) \tag{9.33}$$

since:
$$-\Delta P = \tfrac{1}{2}\rho\omega^2(R^2 - r_0^2) \qquad \text{(from equation 9.4)}$$

From this equation, the time t taken to build up the cake to a given thickness r' may be calculated. The corresponding volume of cake is given by:

$$Vv = \pi(R^2 - r'^2)H \tag{9.34}$$

and the volume of filtrate is:

$$V = \frac{\pi}{v}(R^2 - r'^2)H \tag{9.35}$$

HARUNI and STORROW[4] have carried out an extensive investigation into the flow of liquid through a cake formed in a centrifuge and have concluded that, although the results of tests on a filtration plant and a centrifuge are often difficult to compare because of the effects of the compressibility of the cake, it is frequently possible to predict the flowrate

This book belongs to Bradley Loren (bloren@mcandrews-ip.com) Copyright Elsevier 2024

Intas Exhibit 1032
Page 96 of 470
PGR2025-00043

in a centrifuge to within 20 per cent. They have also shown that, when the thickness varies with height in the basket, the flowrate can be calculated on the assumption that the cake has a uniform thickness equal to the mean value; this gives a slightly high value in most cases.

Example 9.3

When an aqueous slurry is filtered in a plate and frame press, fitted with two 50 mm thick frames each 150 mm square, operating with a pressure difference of 350 kN/m^2, the frames are filled in 3600 s (1 h). How long will it take to produce the same volume of filtrate as is obtained from a single cycle when using a centrifuge with a perforated basket, 300 mm diameter and 200 mm deep? The radius of the inner surface of the slurry is maintained constant at 75 mm and the speed of rotation is 65 Hz (3900 rpm).

It may be assumed that the filter cake is incompressible, that the resistance of the cloth is equivalent to 3 mm of cake in both cases, and that the liquid in the slurry has the same density as water.

Solution

In the filter press

Noting that $V = 0$ when $t = 0$, then:

$$V^2 + 2\frac{AL}{v}V = \frac{2(-\Delta P)A^2 t}{\mathbf{r}\mu v} \qquad \text{(from equation 7.18)}$$

and:

$$V = \frac{lA}{v} \qquad \text{(from equation 7.6)}$$

Thus:

$$\frac{l^2A^2}{v^2} + \left(\frac{2AL}{v}\right)\left(\frac{lA}{v}\right) = \frac{2(-\Delta P)A^2 t}{\mathbf{r}\mu v}$$

or:

$$l^2 + 2Ll = \frac{2(-\Delta P)vt}{\mathbf{r}\mu}$$

For one cycle

$$l = 25 \text{ mm} = 0.025 \text{ m}; \quad L = 3 \text{ mm} = 0.003 \text{ m}$$

$$-\Delta P = 350 \text{ kN/m}^2 = 3.5 \times 10^5 \text{ N/m}^2$$

$$t = 3600 \text{ s}$$

$\therefore$

$$0.025^2 + (2 \times 0.003 \times 0.025) = 2 \times 3.5 \times 10^5 \times 3600 \times \left(\frac{v}{\mathbf{r}\mu}\right)$$

and:

$$\left(\frac{\mathbf{r}\mu}{v}\right) = 3.25 \times 10^{12}$$

In the centrifuge

$$(R^2 - r'^2)\left(1 + 2\frac{L}{R}\right) + 2r'^2 \ln\frac{r'}{R} = \frac{2vt\rho\omega^2}{r\mu}(R^2 - r_0^2) \qquad \text{(equation 9.33)}$$

$R = 0.15$ m, $H = 0.20$ m, and the volume of cake $= 2 \times 0.050 \times 0.15^2 = 0.00225$ m^3

This book belongs to Bradley Loren (bloren@mcandrews-ip.com) Copyright Elsevier 2024

Intas Exhibit 1032
Page 97 of 470
PGR2025-00043

Thus: $\pi(R^2 - r'^2) \times 0.20 = 0.00225$

and: $(R^2 - r^2) = 0.00358$

Thus: $r'^2 = (0.15^2 - 0.00358) = 0.0189 \text{ m}^2$

and: $r' = 0.138 \text{ m}$

$r_0 = 75 \text{ mm} = 0.075 \text{ m}$

and: $\omega = 65 \times 2\pi = 408.4 \text{ rad/s}$

The time taken to produce the same volume of filtrate or cake as in one cycle of the filter press is therefore given by:

$$(0.15^2 - 0.138^2)(1 + 2 \times 0.003/0.15) + 2(0.0189)\ln(0.138/0.15) = \frac{2 \times t \times 1000 \times 408.4^2}{3.25 \times 10^{12}}(0.15^2 - 0.075^2)$$

or: $0.00359 - 0.00315 = 1.732 \times 10^{-6} t$

from which: $t = \dfrac{4.4 \times 10^{-4}}{1.732 \times 10^{-6}}$

$= \underline{\underline{254 \text{ s or } 4.25 \text{ min.}}}$

9.7. MECHANICAL DESIGN

Features of the mechanical design of centrifuges are discussed in Volume 6, where, in particular, the following items are considered:

(a) The mechanical strength of the bowl, which will be determined by the dimensions of the bowl, the material of construction and the speed of operation.
(b) The implications of the critical speed of rotation, which can cause large deflections of the shaft and vibration.
(c) The slow gyratory motion, known as *precession*, which can occur when the bowl or basket is tilted.

9.8. CENTRIFUGAL EQUIPMENT

9.8.1. Classification of centrifuges

Centrifuges may be grouped into two distinct categories–those that utilise the principle of filtration and those that utilise the principle of sedimentation, both enhanced by the use of a centrifugal field. These two classes may be further subdivided according to the method of discharge, particularly the solids discharge. This may be batch, continuous or a combination of both. Further subdivisions may be made according to source of manufacture or mechanical features, such as the method of bearing suspension, axis orientation or containment. In size, centrifuges vary from the small batch laboratory tube spinner to the

This book belongs to Bradley Loren (bloren@mcandrews-ip.com) Copyright Elsevier 2024

Intas Exhibit 1032
Page 98 of 470
PGR2025-00043

large continuous machines with several tons of rotating mass, developing a few thousands of g relative centrifugal force. RECORDS[5] has suggested the following classification.

Filtration centrifuges

(a) Batch discharge, vertical axis, perforate basket.
(b) Knife discharge, pendulum suspension, vertical axis, perforate basket.
(c) Peeler: horizontal axis, knife discharge at speed.
(d) Pusher.
(e) Scroll discharge.

Sedimentation centrifuges

(a) Bottle spinner.
(b) Tubular bowl.
(c) Decanter — scroll discharge.
(d) Imperforate bowl — skimmer pipe discharge, sometimes also a knife.
(e) Disc machine.
  (i) Batch.
  (ii) Nozzle discharge.
  (iii) Opening bowl (solids ejecting).
  (iv) Valve discharge.

Liquid–liquid separation centrifuges

(a) Tubular bowl.
(b) Three phase scroll discharge decanter.
(c) Disc machine.

Clearly with such a wide range of equipment it is not realistic to describe examples of machinery in each category. Discussion will therefore be limited to the more important types of machine and the conditions under which they may be used.

9.8.2. Simple bowl centrifuges

Most batch centrifuges are mounted with their axes vertical and, because of the possibility of uneven loading of the machine, the bowl is normally supported in bearings and the centrifuge itself is supported by resilient mountings. In this way the inevitable out-of-balance forces on the supporting structure are reduced to, typically, 5 per cent or less.

In the case of the underdriven batch machine, where the drive and bearings are underneath, as shown in Figure 9.6, access to the bowl is direct, while product is discharged from the top in manual machines and from the bottom in automatically controlled machines. In the case of the overdriven batch centrifuge, where the bowl is suspended from above, a valve is often incorporated in the bottom of the bowl for easy discharge of the solids. With a purpose designed drive, the unit can handle higher

This book belongs to Bradley Loren (bloren@mcandrews-ip.com) Copyright Elsevier 2024

Intas Exhibit 1032
Page 99 of 470
PGR2025-00043



Figure 9.6. Underdriven batch centrifuge

throughputs of freely filtering feed slurry by cycling more quickly than the underdriven machine.

Batch centrifuges with imperforate bowls are used either for producing an accelerated separation of solid particles in a liquid, or for separating mixtures of two liquids. In the former case, the solids are deposited on the wall of the bowl and the liquid is removed through an overflow or skimming tube. The suspension is continuously fed in until a suitable depth of solids has been built up on the wall; this deposit is then removed either by hand or by a mechanical scraper. With the bowl mounted about a horizontal axis, solids are more readily discharged because they can be allowed to fall directly into a chute.

In the centrifuge shown in Figure 9.7, the liquid is taken off through a skimming tube and the solids, which may be washed before discharge if desired, are removed by a cutter. This machine is often mounted vertically and the cutter knife sometimes extends over the full depth of the bowl.

Perforated bowls are used when relatively large particles are to be separated from a liquid, as for example in the separation of crystals from a mother liquor. The mother liquor passes through the bed of particles and then through the perforations in the bowl. When the centrifuge is used for filtration, a coarse gauze is laid over the inner surface of the bowl and the filter cloth rests on the gauze. Space is thus provided behind the cloth for the filtrate to flow to the perforations.

When a mixture of liquids is to be separated, the denser liquid collects at the imperforate bowl wall and the less dense liquid forms an inner layer. Overflow weirs are arranged

This book belongs to Bradley Loren (bloren@mcandrews-ip.com) Copyright Elsevier 2024

Intas Exhibit 1032
Page 100 of 470
PGR2025-00043

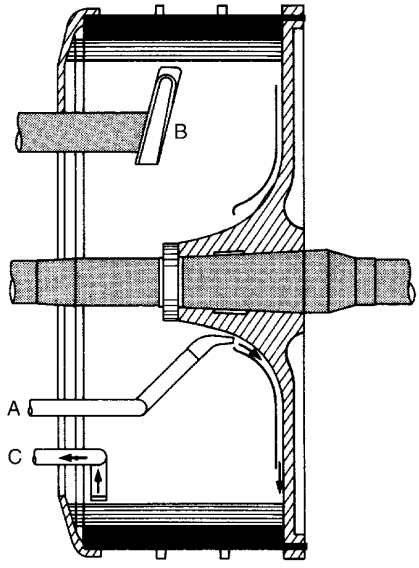


Figure 9.7. Horizontally mounted bowl with automatic discharge of solids. A–Feed, B–Cutter, C–Skimming tube

so that the two constituents are continuously removed. The design of the weirs has been considered in a previous section.

9.8.3. Disc centrifuges — general

For a given rate of feed to the centrifuge, the degree of separation obtained will depend on the thickness of the liquid layer formed at the wall of the bowl and on the total depth of the bowl, since both these factors control the time the mixture remains in the machine. A high degree of separation could therefore be obtained with a long bowl of small diameter, although the speed required would then need to be very high. By comparison the introduction of conical discs into the bowl, as illustrated in Figure 9.8, enables the liquid stream to be split into a large number of very thin layers and permits a bowl of greater diameter. The separation of a mixture of water and dirt from a relatively low density oil takes place as shown in Figure 9.9 with the dirt and water collecting close to the undersides of the discs and moving radially outwards, and with the oil moving inwards along the top sides.

A disc bowl, although still a high speed machine, can thus be run at lower speeds relative to the excessive speeds required for a long bowl of small diameter. Also its size is very much smaller relative to a bowl without discs, as may be seen from Figure 9.10. The separation of two liquids in a disc-type bowl is illustrated in the left-hand side of Figure 9.8. Liquid enters through the distributor AB, passes through C, and is distributed between the discs E through the holes D. The denser liquid is taken off through F and I and the less dense liquid through G.

This book belongs to Bradley Loren (bloren@mcandrews-ip.com) Copyright Elsevier 2024

Intas Exhibit 1032
Page 101 of 470
PGR2025-00043

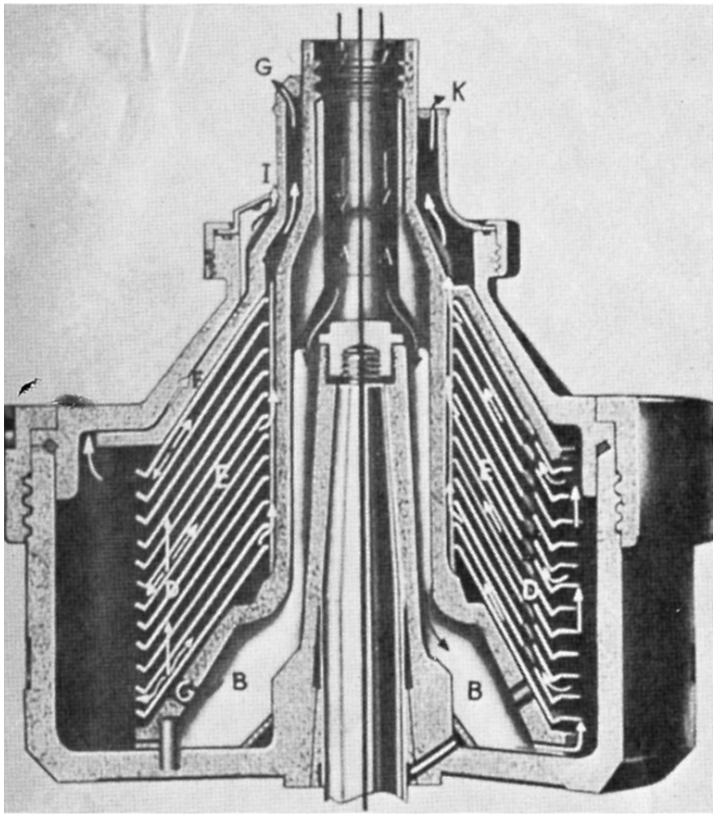


Figure 9.8. Bowl with conical discs (left-hand side for separating liquids, right-hand side for separating solid from liquid)

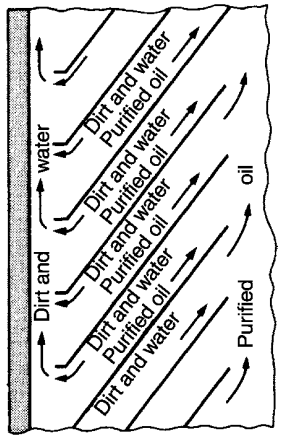


Figure 9.9. Separation of water and dirt from oil in disc bowl

This book belongs to Bradley Loren (bloren@mcandrews-ip.com) Copyright Elsevier 2024

Intas Exhibit 1032
Page 102 of 470
PGR2025-00043

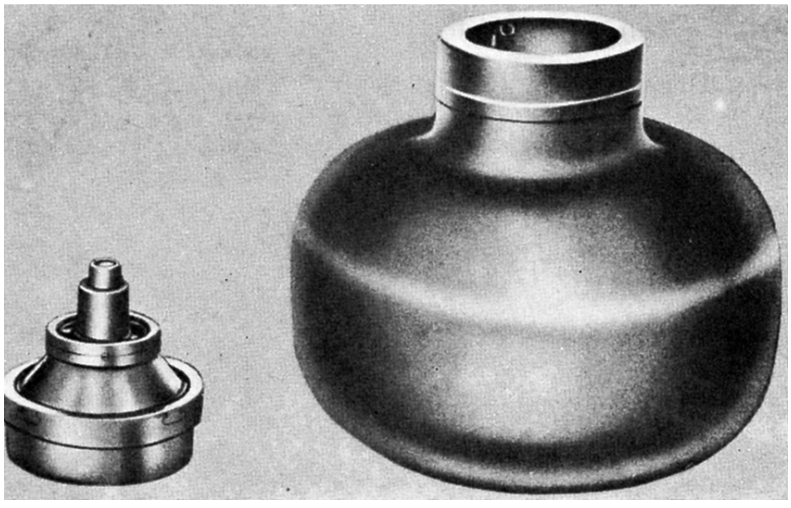


Figure 9.10. Two bowls of equal capacity; with discs (left) and without discs (right)

A disc-type bowl is often used for the separation of fine solids from a liquid and its construction is shown in the right-hand side of Figure 9.8. Here there is only one liquid outlet K, and the solids are retained in the space between the ends of the discs and the wall of the bowl.

9.8.4. Disc centrifuges — various types

Disc centrifuges vary considerably according to the type of discharge. The liquid(s) can discharge freely or through centrifugal pumps. The solids may be allowed to accumulate within the bowl and then be discharged manually ("batch bowl"). A large number of disc machines ("opening bowl") discharge solids intermittently when ports are opened automatically at the periphery of the bowl on a timed basis or are actuated from a signal from a liquid clarity meter. The opening on sophisticated machines may be adjusted to discharge only the compacted solids.

Another type of disc centrifuge has nozzles or orifices at the periphery where thickened solids are discharged continuously, and sometimes a fraction of this discharge is recycled to ensure that the nozzles are able to prevent breakthrough of the clarified supernatant liquid. Sometimes these nozzles are internally fitted to the bowl. Others are opened and closed electrically or hydrostatically from a build up of the sludge within the bowl.

Centrifuges of these types are used in the processing of yeast, starch, meat, fish products and fruit juices. They form essential components of the process of rendering in the extraction of oils and fats from cellular materials. The raw material, consisting of bones, animal fat, fish offal, or vegetable seeds is first disintegrated and then, after a preliminary gravitational separation, the final separation of water, oil, and suspended solids is carried out in a number of valve nozzle centrifuges.

This book belongs to Bradley Loren (bloren@mcandrews-ip.com) Copyright Elsevier 2024

Intas Exhibit 1032
Page 103 of 470
PGR2025-00043

9.8.5. Decanting centrifuges

The widely used decanting type continuous centrifuge, shown in Figure 9.11, is mounted on a horizontal axis. The mixture of solids and liquids is fed to the machine through a stationary pipe which passes through one of the support bearings, shown in Figure 9.12. The feed pipe discharges the mixture near the centre of the machine. The heavier solids settle on to the wall of the imperforate or solid bowl under the influence of the centrifugal

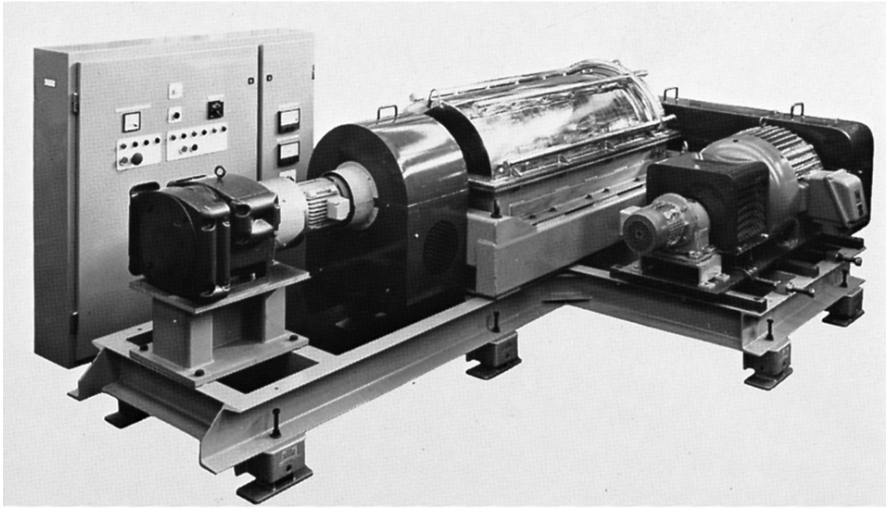


Figure 9.11. Solid-bowl decanter centrifuge

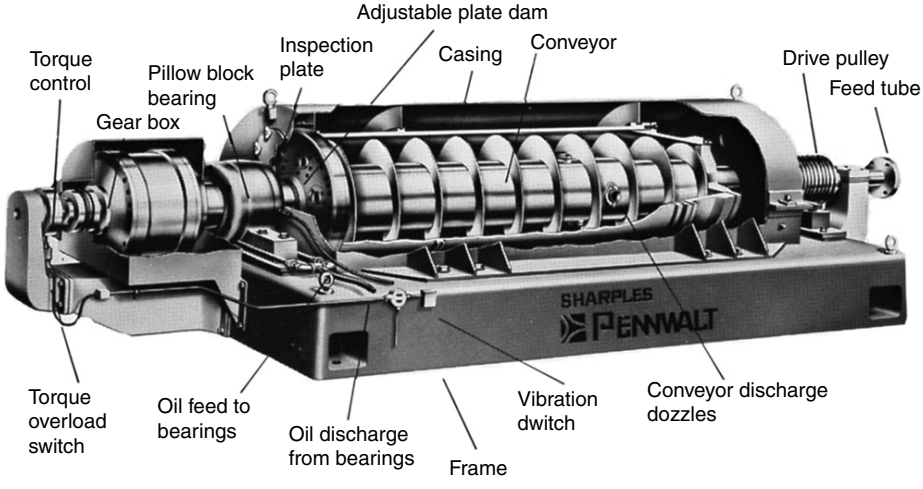


Figure 9.12. Solid-bowl decanter centrifuge–principles of operation

This book belongs to Bradley Loren (bloren@mcandrews-ip.com) Copyright Elsevier 2024

Intas Exhibit 1032
Page 104 of 470
PGR2025-00043

force. Inside the bowl is a close fitting helical scroll which rotates at a slightly different speed from the solid bowl. Typically the speed differential is in the range 0.5 to 100 rpm (0.01–2 Hz).

At one end of the bowl a conical section is attached giving a smaller diameter. The liquid runs round the helical scroll and is discharged over weir plates fitted at the parallel end of the bowl. The solids are moved by the conveying action of the helical scroll up the gentle slope of the conical section, out of the liquid and finally out of the machine. Decanters of this type are known as solid bowl decanters.

A variant of the decanting centrifuge is the screen bowl decanter, shown in Figures 9.13 and 9.14. In this unit a further perforated section is attached to the smaller diameter end of the conical section. This is known as the screen and allows further drying and/or washing of the solids to take place.

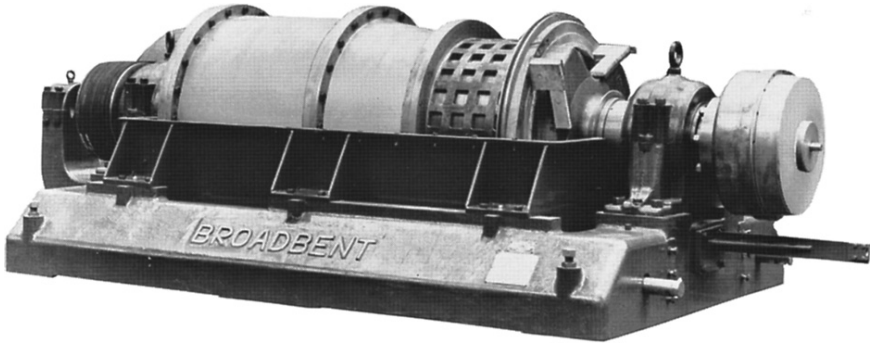


Figure 9.13. Screen bowl decanter centrifuge (cover removed)

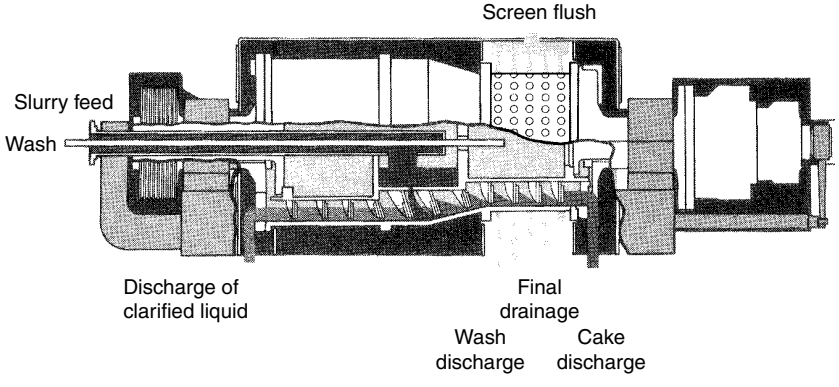


Figure 9.14. Screen bowl decanter centrifuge-principles of operation

Machines may be tailored to meet specific process requirement by altering the diameter of the liquid discharge, the differential speed of the helical scroll, the position at which the

This book belongs to Bradley Loren (bloren@mcandrews-ip.com) Copyright Elsevier 2024

Intas Exhibit 1032
Page 105 of 470
PGR2025-00043

feed enters the machine and the rotational speed of the bowl. Decanting centrifuges are available in a wide range of diameters and lengths. Diameters are 0.2–1.5 m, and lengths are typically 1.5–5 times the diameter. The longer machines are used when clear liquids are required. Shorter bowl designs are used to produce the driest solids. Continuous throughputs in excess of 250 tonnes/h (70 kg/s) of feed can be handled by a single machine.

9.8.6. Pusher-type centrifuges

This type of centrifuge is used for the separation of suspensions and is fitted either with a perforated or imperforate bowl. The feed is introduced through a conical funnel and the cake is formed in the space between the flange and the end of the bowl. The solids are intermittently moved along the surface of the bowl by means of a reciprocating pusher. The pusher comes forward and returns immediately and then waits until a further layer of solids has been built up before advancing again. In this machine the thickness of filter cake cannot exceed the distance between the surface of the bowl and the flange of the funnel. The liquid either passes through the holes in the bowl or, in the case of an imperforate bowl, is taken away through an overflow. The solids are washed by means of a spray, as shown in Figure 9.15.

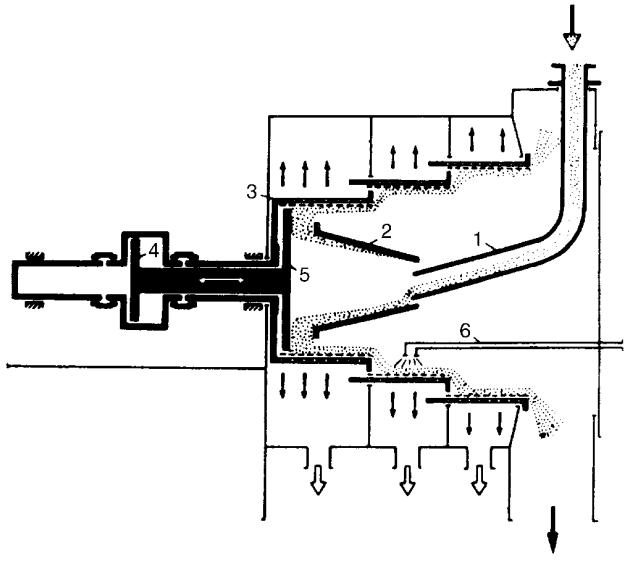


Figure 9.15. Pusher-type centrifuge. 1. Inlet; 2. Inlet funnel; 3. Bowl; 4. Piston; 5. Pusher disc; 6. Washing spray

A form of pusher type centrifuge which is particularly suitable for filtering slurries of low concentrations is shown in Figure 9.16. A perforated pusher cone gently accelerates the feed and secures a large amount of preliminary drainage near the apex of the cone. The

This book belongs to Bradley Loren (bloren@mcandrews-ip.com) Copyright Elsevier 2024
Intas Exhibit 1032
Page 106 of 470
PGR2025-00043

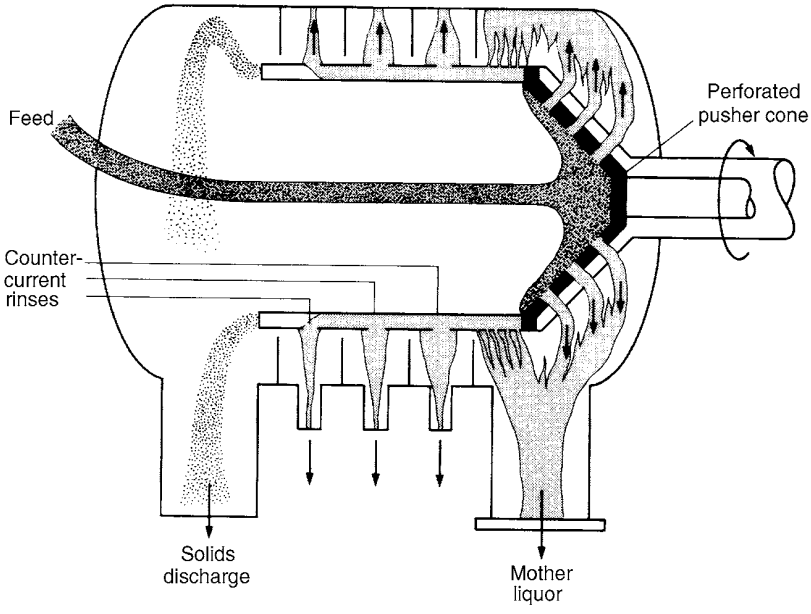


Figure 9.16. Pusher-type centrifuge

solids from the partially concentrated suspension are then evenly laid on the cylindrical surface and, in this way, the risk of the solids being washed out of the bowl is minimised.

9.8.7. Tubular-bowl centrifuge

Because, for a given separating power, the stress in the wall is a minimum for machines of small radius, machines with high separating powers generally use very tall bowls of small diameters. A typical centrifuge, shown in Figure 9.17, would consist of a bowl about 100 mm diameter and 1 m long incorporating longitudinal plates to act as accelerator blades to bring the liquid rapidly up to speed. On laboratory machines speeds up to 50,000 rpm (1000 Hz) are used to give accelerations 60,000 times the gravitational acceleration. A wide range of materials of construction can be used.

The position of the liquid interface is determined by balancing centrifugal forces as in Figure 9.3. The lip, of radius r_w, over which the denser liquid leaves the bowl is part of a removable ring. Various sizes maybe fitted to provide for the separation of liquids of various relative densities.

Often the material fed to these machines contains traces of denser solids in addition to the two liquid phases. These solids are deposited on the inner wall of the bowl, and the machine is dismantled periodically to remove them. A common application is the removal of water and suspended solids from lubricating oil.

The super-centrifuge is used for clarification of oils and fruit juices and for the removal of oversize and undersize particles from pigmented liquids. The liquid is continuously discharged, but the solids are retained in the bowl and must be removed periodically.

This book belongs to Bradley Loren (bloren@mcandrews-ip.com) Copyright Elsevier 2024

Intas Exhibit 1032
Page 107 of 470
PGR2025-00043

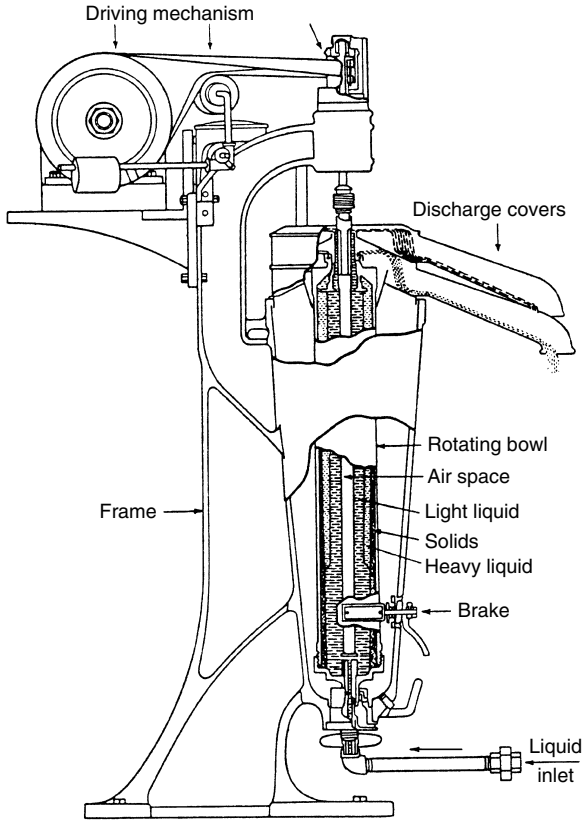


Figure 9.17. Sectional view of the super-centrifuge

9.8.8. The ultra-centrifuge

For separation of colloidal particles and for breaking down emulsions, the ultra-centrifuge is used. This operates at speeds up to 30 rpm (1600 Hz) and produces a force of 100,000 times the force of gravity for a continuous liquid flow machine, and as high as 500,000 times for gas phase separation, although these machines are very small. The bowl is usually driven by means of a small air turbine. The ultra-centrifuge is often run either at low pressures or in an atmosphere of hydrogen in order to reduce frictional losses, and a fivefold increase in the maximum speed can be attained by this means.

9.8.9. Multistage centrifuges

Among many specialist types of centrifuge is the multistage machine which consists of series of bowls mounted concentrically on a vertical axis. The feed suspension is introduced into the innermost bowl and the overflow then passes successively to each larger bowl in turn. As the separating force is directly proportional to the radius of

This book belongs to Bradley Loren (bloren@mcandrews-ip.com) Copyright Elsevier 2024

Intas Exhibit 1032
Page 108 of 470
PGR2025-00043

rotation, the largest particles are separated out at the first stage, and progressively finer particles are recovered at each subsequent stage. The finest particles are collected in the outermost vessel from which the remaining liquid or suspension is discharged. The multistage system may also incorporate a series of concentric vertical baffles in a single bowl, with the suspension flowing upwards and downwards through successive annular channels. Both the design and operation are complex, and the machines are somewhat inflexible.

9.8.10. The gas centrifuge

A specialised, though nevertheless highly important, function for which the centrifuge has been developed is the separation of radioactive isotopes as described by FISHMAN[6]. The concentration of uranium-235 from less than 1 per cent up to about 5 per cent is achieved by subjecting uranium hexafluoride (UF_6) to an intense centrifugal field. The small differences in density of the components of the mixture necessitate the use of very high accelerations in order to obtain the desired separation. Mechanical considerations dictate the use of small diameter rotors (0.1–0.2 m) rotating at speeds up to 2000 Hz (10^5 rpm), giving velocities of up to 700 m/s and accelerations of up to 10^6 *g* at the periphery. Under these conditions the gas flow can vary from free molecular flow in the low pressure region at the centre, to a high Mach number flow at the periphery. Furthermore, pressure will change by a factor of 10 over a distance of about 2 mm as compared with a distance of about 20 km in the earth's gravitational field.

For use in a radioactive environment the gas centrifuge must be completely maintenance free. It has been used for the separation of xenon isotopes and consideration has been given to its application for separation of fluorohydrocarbons. Worldwide, in the region of a quarter of a million gas centrifuges have been manufactured. As an order of magnitude figure, an investment of £1000 is necessary to obtain 0.3 g/s (10 g/h) of product.

Further information is given in the papers by WHITLEY[7,8].

9.9. FURTHER READING

AMBLER, C. M.: In *Encyclopedia of Chemical Processing and Design*, Vol. 7. MCKETTA, J. J. ed. (Marcel Dekker, New York, 1978).

HSU, H-W.: *Ind. Eng. Chem. Fundamentals* **25** (1986) 588. Separations by liquid centrifugation.

LAVANCHY, A. C. and KEITH, F. W.: In *Encyclopedia of Chemical Technology*, KIRK, R. E. and OHMER, D. F. (eds.) Vol. 4, (Wiley-Interscience, 1979) 710 Centrifugal separation.

MULLIN, J. W.: In *Chemical Engineering Practice*, CREMER, H. W. and DAVIES, T. (eds.) Vol. 6, (Butterworths, 1958) p 528. Centrifuging.

ZEITSCH, K. *Centrifugal Filtration* (Butterworth & Co, 1981).

9.10. REFERENCES

1. AMBLER, C. A.: *Chem. Eng. Prog.* **48** (1952) 150. The evaluation of centrifuge performance.
2. HAYTER, A. J.: *J. Soc. Cosmet. Chem.* (1962) 152. Progress in centrifugal separations.
3. TROWBRIDGE, M. E. O'K.: *The Chemical Engineer* No. 162 (Aug. 1962) A73. Problems in the scaling-up of centrifugal separation equipment.
4. HARUNI, M. M. and STORROW, J. A.: *Ind. Eng. Chem.* **44** (1952) 2751: *Chem. Eng. Sci.* **1** (1952) 154: **2** (1953) 97, 108, 164 and 203. Hydroextraction.

This book belongs to Bradley Loren (bloren@mcandrews-ip.com) Copyright Elsevier 2024

Intas Exhibit 1032
Page 109 of 470
PGR2025-00043

5. RECORDS, F. A.: Alfa Laval Sharples Ltd, Private communication (March 1990).
6. FISHMAN, A. M.: *A. I. Chem. E. Symposium Series* No. 169, 73 (1977). Developments in Uranium enrichment, 43. The centar gas centrifuge enrichment project: Economics and engineering considerations.
7. WHITLEY, S.: *A Summary of the Development of the Gas Centrifuge* British Nuclear Fuels plc, Enrichment Division, Capenhurst, (June 1988).
8. WHITLEY, S.: *Reviews of Modern Physics* **56** (1984) 41, 67. Review of the gas centrifuges until 1962. Part I: Principles of separation physics. Part II: Principles of high-speed rotation.

9.11. NOMENCLATURE

		Units in SI System	Dimensions in **M**, **L**, **T**
A	Cross-sectional area of filter	m^2	$\mathbf{L}^2$
a	Distance between discs in stack	m	**L**
d	Diameter (or equivalent diameter of particle)	m	**L**
g	Acceleration due to gravity	m/s^2	$\mathbf{LT}^{-2}$
H	Length (axial) of centrifuge bowl	m	**L**
h	Depth of liquid at wall of bowl	m	**L**
L	Thickness of filter cake with same resistance as cloth	m	**L**
l	Thickness of filter cake	m	**L**
n	Number of passages between discs in bowl	—	—
P	Pressure	N/m^2	$\mathbf{ML}^{-1}\mathbf{T}^{-2}$
P'	Pressure in cake	N/M^2	$\mathbf{ML}^{-1}\mathbf{T}^{-2}$
P''	Pressure in cloth	N/m^{-2}	$\mathbf{ML}^{-1}\mathbf{T}^{-2}$
$-\Delta P$	Pressure drop (total)	N/M^2	$\mathbf{ML}^{-1}\mathbf{T}^{-2}$
$-\Delta P'$	Pressure drop over filter cake	N/M^2	$\mathbf{ML}^{-1}\mathbf{T}^{-2}$
$-\Delta P''$	Pressure drop over filter cloth	N/M^2	$\mathbf{ML}^{-1}\mathbf{T}^{-2}$
Q	Volumetric feed rate to centrifuge	m^3/s	$\mathbf{L}^3\mathbf{T}^{-1}$
R	Radius of bowl of centrifuge	m	**L**
r	Specific resistance of filter cake	m^{-2}	$\mathbf{L}^{-2}$
r	Radius of rotation	m	**L**
r_0	Radius of inner surface of liquid in bowl	m	**L**
r_1	Radius at inlet to disc bowl centrifuge	m	**L**
r_2	Radius at outlet of disc bowl centrifuge	m	**L**
r_i	Radius of weir for lighter liquid	m	**L**
r_s	Radius of interface between liquids in bowl	m	**L**
r_w	Radius of overflow weir for heavier liquid	m	**L**
r'	Radius at interface between liquid and filter cake	m	**L**
t	Time	s	**T**
t_R	Retention time in centrifuge	s	**T**
u_0	Terminal falling velocity of particle	m/s	$\mathbf{LT}^{-1}$
u_c	Superficial filtration velocity $\left[\frac{1}{A}\frac{dV}{dt}\right]$	m/s	$\mathbf{LT}^{-1}$
V	Volume of filtrate passing in time t	m^3	$\mathbf{L}^3$
V'	Volumetric capacity of centrifuge bowl	m^3	$\mathbf{L}^3$
v	Volume of cake deposited by passage of unit volume of filtrate	—	—
x	Distance parallel to discs in disc bowl centrifuge	m	**L**
y	Distance perpendicular to discs in disc bowl centrifuge	m	**L**
z	Vertical height	m	**L**
z_0	Vertical height of free surface of liquid (at radius r_0)	m	**L**
z_a	Value of z_0 at vertical axis of rotation ($r_0 = 0$)	m	**L**
μ	Viscosity of liquid	Ns/m^2	$\mathbf{ML}^{-1}\mathbf{T}^{-1}$
ρ	Density of liquid	kg/m^3	$\mathbf{ML}^{-3}$
ρ_s	Density of particles	kg/m^3	$\mathbf{ML}^{-3}$
θ	Half included angle between discs	—	—
ω	Angular velocity	rad/s	$\mathbf{s}^{-1}$
Σ	Capacity term for centrifuge	m^2	$\mathbf{L}^2$

This book belongs to Bradley Loren (bloren@mcandrews-ip.com) Copyright Elsevier 2024

Intas Exhibit 1032
Page 110 of 470
PGR2025-00043

CHAPTER 13

Liquid–Liquid Extraction

13.1. INTRODUCTION

The separation of the components of a liquid mixture by treatment with a solvent in which one or more of the desired components is preferentially soluble is known as liquid–liquid extraction — an operation which is used, for example, in the processing of coal tar liquids and in the production of fuels in the nuclear industry, and which has been applied extensively to the separation of hydrocarbons in the petroleum industry. In this operation, it is essential that the liquid-mixture feed and solvent are at least partially if not completely immiscible and, in essence, three stages are involved:

(a) Bringing the feed mixture and the solvent into intimate contact,
(b) Separation of the resulting two phases, and
(c) Removal and recovery of the solvent from each phase.

It is possible to combine stages (a) and (b) into a single piece of equipment such as a column which is then operated continuously. Such an operation is known as differential contacting. Liquid–liquid extraction is also carried out in stagewise equipment, the prime example being a mixer–settler unit in which the main features are the mixing of the two liquid phases by agitation, followed by settling in a separate vessel by gravity. This mixing of two liquids by agitation is of considerable importance and the topic is discussed in some detail in Volume 1, Chapter 7.

Extraction is in many ways complementary to distillation and is preferable in the following cases:

(a) Where distillation would require excessive amounts of heat, such as, for example, when the relative volatility is near unity.
(b) When the formation of azeotropes limits the degree of separation obtainable in distillation.
(c) When heating must be avoided.
(d) When the components to be separated are quite different in nature.

Important applications of liquid–liquid extraction include the separation of aromatics from kerosene-based fuel oils to improve their burning qualities and the separation of aromatics from paraffin and naphthenic compounds to improve the temperature-viscosity characteristics of lubricating oils. It may also be used to obtain, for example, relatively

This book belongs to Bradley Loren (bloren@mcandrews-ip.com) Copyright Elsevier 2024

Intas Exhibit 1032
Page 111 of 470
PGR2025-00043

pure compounds such as benzene, toluene, and xylene from catalytically produced reformates in the oil industry, in the production of anhydrous acetic acid, in the extraction of phenol from coal tar liquors, and in the metallurgical and biotechnology industries.

In all extraction processes, the important feature is the selective nature of the solvent, in that the separation of compounds is based on differences in solubilities, rather than differences in volatilities as in distillation. In recent years, it has become possible to use computerised techniques to aid in the choice of a solvent with the required selectivity and to "design" appropriate molecular structures.

A recent and extremely important development lies in the application of the technique of liquid extraction to *metallurgical processes*. The successful development of methods for the purification of uranium fuel and for the recovery of spent fuel elements in the nuclear power industry by extraction methods, mainly based on packed, including pulsed, columns as discussed in Section 13.5 has led to their application to other metallurgical processes. Of these, the recovery of copper from acid leach liquors and subsequent electro-winning from these liquors is the most extensive, although further applications to nickel and other metals are being developed. In many of these processes, some form of chemical complex is formed between the solute and the solvent so that the kinetics of the process become important. The extraction operation may be either a physical operation, as discussed previously, or a chemical operation. Chemical operations have been classified by HANSON[1] as follows:

(a) Those involving cation exchange such as, for example, the extraction of metals by carboxylic acids;
(b) Those involving anion exchange, such as the extraction of anions involving a metal with amines, and
(c) Those involving the formation of an additive compound, for example, extraction with neutral organo-phosphorus compounds. An important operation of this type is the purification of uranium from the nitrate with tri-*n*-butyl phosphate.

This process of metal purification is of particular interest in that it involves the application of principles of both chemistry and chemical engineering and necessitates the cost evaluation of alternatives.

A whole new technology with respect to extraction, developed within the last decade, has been the use of *supercritical* or *near supercritical fluids* as solvent.

In *biotechnology*, many of the usual organic solvents will degrade a sensitive product, such as a protein; this has led to the use of "mild" aqueous-based extractants, such as water–polyethyleneglycol–phosphate mixtures, which will partition and concentrate the product in one of the two aqueous layers which are formed.

The use of supercritical fluids and aqueous-based extractants is discussed in Section 13.8

13.2. EXTRACTION PROCESSES

The three steps outlined in Section 13.1, necessary in all liquid–liquid extraction operations, may be carried out either as a batch or as a continuous process.

This book belongs to Bradley Loren (bloren@mcandrews-ip.com) Copyright Elsevier 2024

Intas Exhibit 1032
Page 112 of 470
PGR2025-00043

In the single-stage batch process illustrated in Figure 13.1, the solvent and solution are mixed together and then allowed to separate into the two phases — the *extract* E containing the required solute in the added solvent and the *raffinate* R, the weaker solution with some associated solvent. With this simple arrangement mixing and separation occur in the same vessel.

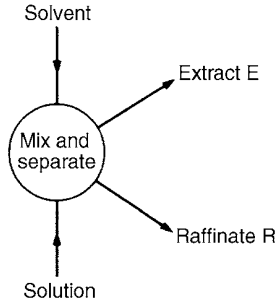


Figure 13.1. Single-stage batch extraction

A continuous two-stage operation is shown in Figure 13.2, where the mixers and separators are shown as separate vessels. There are three main forms of equipment. First there is the mixer-settler as shown in Figure 13.1, secondly, there is the column type of design with trays or packing as in distillation and, thirdly, there are a variety of units incorporating rotating devices such as the Scheibel and the Podbielniak extractors. In all cases, the extraction units are followed by distillation or a similar operation in order to recover the solvent and the solute. Some indication of the form of these alternative arrangements may be seen by considering two of the processes referred to in Section 13.1.

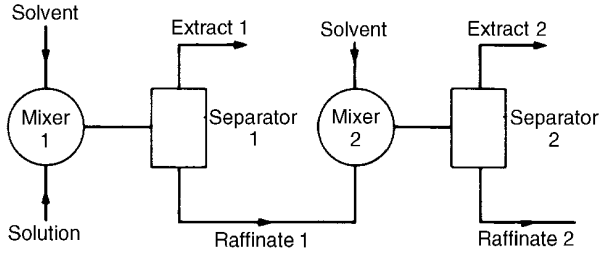


Figure 13.2. Multiple-contact system with fresh solvent

One system for separating benzene, toluene, and xylene groups from light feed-stocks is shown in Figure 13.3, where n-methylpyrolidone (NMP) with the addition of some glycol is used as the solvent. The feed is passed to a multistage extractor arranged as a tower from which an aromatics-free raffinate is obtained at the top. The extract stream containing the solvent, aromatics, and low boiling non-aromatics is distilled to provide the extractor recycle stream as a top product, and a mixture of aromatics and solvent at the bottom. This stream passes to a stripper from which the glycol and the aromatics

This book belongs to Bradley Loren (bloren@mcandrews-ip.com) Copyright Elsevier 2024
Intas Exhibit 1032
Page 113 of 470
PGR2025-00043

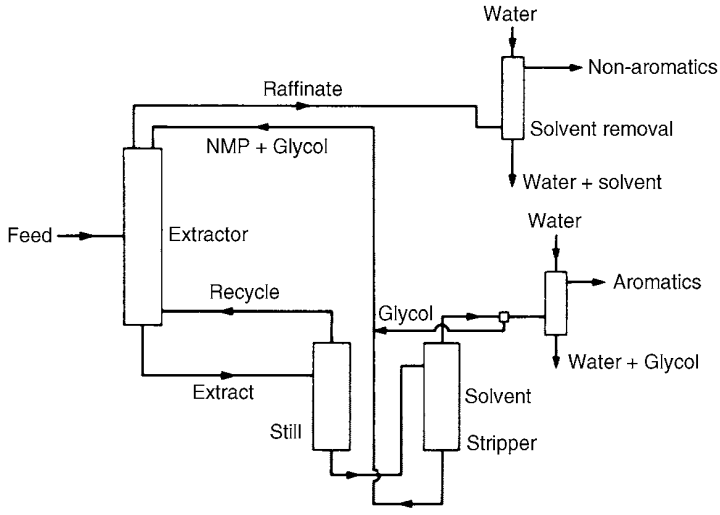


Figure 13.3. Process for benzene, toluene and xylene recovery

are recovered. This is a complex system illustrating the need for careful recycling and recovery of solvent.

The concentration of acrylic acid by extraction with ethyl acetate[2] is a rather different illustration of this technique. As shown in Figure 13.4, the dilute acrylic acid solution of concentration about 20 per cent is fed to the top of the extraction column 1, the ethyl acetate solvent being fed in at the base. The acetate containing the dissolved acrylic acid and water leaves from the top and is fed to the distillation column 2, where the acetate is removed as an azeotrope with water and the dry acrylic acid is recovered as product from the bottom.

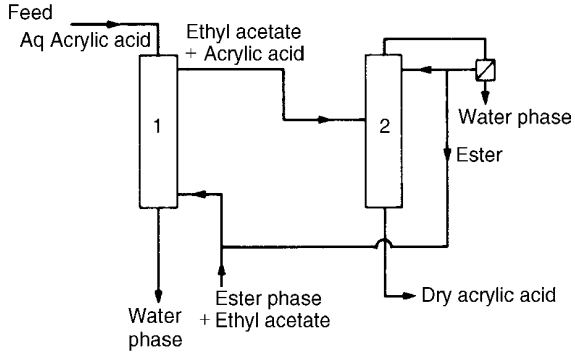


Figure 13.4. Concentration of acrylic acid by extraction with ethyl acetate[2]

It may be seen from these illustrations that successful extraction processes should not be judged simply by the performance of the extraction unit alone, but by assessment of

This book belongs to Bradley Loren (bloren@mcandrews-ip.com) Copyright Elsevier 2024
Intas Exhibit 1032
Page 114 of 470
PGR2025-00043

the recovery achieved by the whole plant. This aspect of the process may be complex if chemical reactions are involved. The sections of the plant for mixing and for separation must be considered together when assessing capital cost. The cost of the organic solvents used in the metallurgical processes may also be high.

The mechanism of transfer of solute from one phase to the second is one of molecular and eddy diffusion and the concepts of phase equilibrium, interfacial area, and surface renewal are all similar in principle to those met in distillation and absorption, even though, in liquid–liquid extraction, dispersion is effected by mechanical means including pumping and agitation, except in standard packed columns.

In formulating design criteria for extraction equipment, it is necessary to take into account the equilibrium conditions for the distribution of solute between the phases as this determines the maximum degree of separation possible in a single stage. The resistance to diffusion and, in the case of chemical effects, the kinetics are also important in that these determine the residence time required to bring about near equilibrium in a stage-wise unit, or the height of a transfer unit in a differential contactor. The transfer rate is given by the accepted equation:

$$\text{Rate per unit interfacial area} = k\Delta C \tag{13.1}$$

where k is a mass transfer coefficient and ΔC a concentration driving force. A high value of k can be obtained only if turbulent or eddy conditions prevail and, although these may be readily achieved in the continuous phase by some form of agitation, it is very difficult to generate eddies in the drops which constitute the dispersed phase.

13.3. EQUILIBRIUM DATA

The equilibrium condition for the distribution of one solute between two liquid phases is conveniently considered in terms of the distribution law. Thus, at equilibrium, the ratio of the concentrations of the solute in the two phases is given by $C_E/C_R = K'$, where K' is the distribution constant. This relation will apply accurately only if both solvents are immiscible, and if there is no association or dissociation of the solute. If the solute forms molecules of different molecular weights, then the distribution law holds for each molecular species. Where the concentrations are small, the distribution law usually holds provided no chemical reaction occurs.

The addition of a new solvent to a binary mixture of a solute in a solvent may lead to the formation of several types of mixture:

(a) A homogeneous solution may be formed and the selected solvent is then unsuitable.
(b) The solvent may be completely immiscible with the initial solvent.
(c) The solvent may be partially miscible with the original solvent resulting in the formation of one pair of partially miscible liquids.
(d) The new solvent may lead to the formation of two or three partially miscible liquids.

Of these possibilities, types (b), (c), and (d) all give rise to systems that may be used, although those of types (b) and (c) are the most promising. With conditions of type (b), the equilibrium relation is conveniently shown by a plot of the concentration of solute in one

This book belongs to Bradley Loren (bloren@mcandrews-ip.com) Copyright Elsevier 2024

Intas Exhibit 1032
Page 115 of 470
PGR2025-00043

phase against the concentration in the second phase. Conditions given by (c) and (d) are usually represented by triangular diagrams. Equilateral triangles are used, although it is also possible to use right-angled isosceles triangles, which are discussed in Chapter 10.

The system, acetone (**A**)–Water (**B**)–methyl isobutyl ketone (**C**), as shown in Figure 13.5, is of type (c). Here the solute **A** is completely miscible with the two solvents **B** and **C**, although the two solvents are only partially miscible with each other. A mixture indicated by point H consists of the three components **A**, **B** and **C** in the ratio of the perpendiculars HL, HJ, HK. The distance BN represents the solubility of solvent **C** in **B**, and MC that of **B** in **C**. The area under the curved line NPFQM, the binodal solubility curve, represents a two-phase region which will split up into two layers in equilibrium with each other. These layers have compositions represented by points P and Q, and PQ is known as a "tie line". Such lines, two of which are shown in the diagram, connect the compositions of two phases in equilibrium with each other, and these compositions must be found by practical measurement. There is one point on the binodal curve at F which represents a single phase that does not split into two phases. F is known as a *plait* point, and this must also be found by experimental measurement. The plait point is fixed if either the temperature or the pressure is fixed. Within the area under the curve, the temperature and composition of one phase will fix the composition of the other. Applying the phase rule to the three-components system at constant temperature and pressure, the number of degrees of freedom is equal to 3 minus the number of phases. In the area where there is only one liquid phase, there are two degrees of freedom and two compositions must be stated. In a system where there are two liquid phases, there is only one degree of freedom.

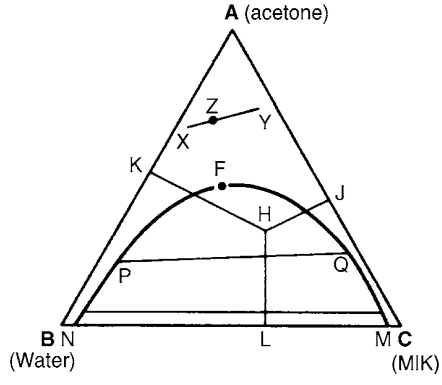


Figure 13.5. Equilibrium relationship for acetone distributed between water and methyl isobutyl ketone

One of the most useful features of this method of representation is that, if a solution of composition X is mixed with one of composition Y, then the resulting mixture will have a composition shown by Z on a line XY, such that:

$$XZ/ZY = (\text{amount of Y})/(\text{amount of X}).$$

Similarly, if an extract Y is removed, from a mixture Z the remaining liquor will have composition X.

This book belongs to Bradley Loren (bloren@mcandrews-ip.com) Copyright Elsevier 2024

Intas Exhibit 1032
Page 116 of 470
PGR2025-00043

In Figure 13.6 two separate two-phase regions are formed, whilst in Figure 13.7 the two-phase regions merge on varying the temperature. Aniline (**A**), water (**B**), and phenol (**C**) represent a system of the latter type. Under the conditions shown in Figures 13.6 and 13.7, **A** and **C** are miscible in all proportions, although **B** and **A**, and **B** and **C** are only partially miscible.

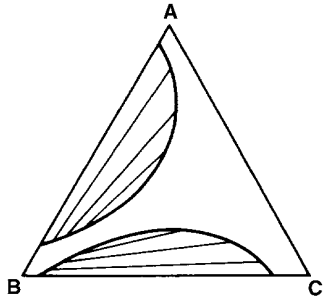


Figure 13.6. Equilibrium relationship for the aniline–water–phenol system

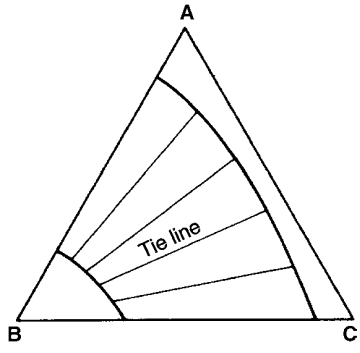


Figure 13.7. Equilibrium relationship for the aniline–water–phenol system at a higher temperature

Whilst these diagrams are of considerable use in presenting equilibrium data, Figure 13.8 is in many ways more useful for determining the selectivity of a solvent, and the number of stages that are likely to be required. In Figure 13.8 the percentage of solute in one phase is plotted against the percentage in the second phase in equilibrium with it. This is equivalent to plotting the compositions at either end of a tie line. The important factor in assessing the value of a solvent is the ratio of the concentrations of the desired component in the two phases, rather than the actual concentrations. A selectivity ratio may be defined in terms of either mass or mole fractions as:

$$\beta = \left[\frac{x_A}{x_B}\right]_E \Big/ \left[\frac{x_A}{x_B}\right]_R \tag{13.2}$$

where x_A and x_B are the mass or mole fractions of **A** and **B** in the two phases E and R.

This book belongs to Bradley Loren (bloren@mcandrews-ip.com) Copyright Elsevier 2024
Intas Exhibit 1032
Page 117 of 470
PGR2025-00043

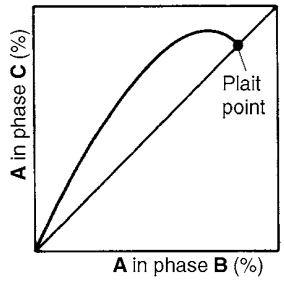


Figure 13.8. Equilibrium distribution of solute **A** in phases **B** and **C**

For a few systems β tends to be substantially constant, although it more usually varies with concentration. The selectivity ratio has the same significance in extraction as relative volatility has in distillation, so that the ease of separation is directly related to the numerical value of β. As β approaches unity, a larger number of stages is necessary for a given degree of separation and the capital and operating costs increase correspondingly. When $\beta = 1$ any separation is impossible.

13.4. CALCULATION OF THE NUMBER OF THEORETICAL STAGES

13.4.1. Co-current contact with partially miscible solvents

In calculating the number of ideal stages required for a given degree of separation, the conditions of equilibrium expressed by one of the methods discussed in Section 13.3 is used. The number of stages where single or multiple contact equipment is involved is considered first, and then the design of equipment where the concentration change is continuous is discussed.

For the general case where the solvents are partially miscible, the feed solution F is brought into contact with the selective solvent **S**, to give raffinate R_1 and an extract E_1. The addition of streams F and **S** is shown on the triangular diagram in Figure 13.9, by the point M, where FM/MS $= S/F$. This mixture M breaks down to give extract E_1 and raffinate R_1, at opposite ends of a tie line through M.

If a second stage is used, then the raffinate R_1 is treated with a further quantity of solvent **S**, and extract E_2 and raffinate R_2 are obtained as shown in the same figure.

The complete process consists in carrying out the extraction, and recovering the solvent from the raffinate and extract obtained. Thus, for a single-stage system as shown in Figure 13.10, the raffinate R is passed into the distillation column where it is separated to give purified raffinate R′ and solvent S_R. The extract E is passed to another distillation unit to give extract E′ and a solvent stream S_E. These recovered solvents S_R and S_E are pumped back to the extraction process as shown. This cycle may be represented on a diagram, as shown in Figure 13.11, by showing the removal of S_R from R to give composition R′, and the removal of S_E from E to give composition E′. It has been assumed in this case that perfect separation is obtained in the stills, so that pure solvent

This book belongs to Bradley Loren (bloren@mcandrews-ip.com) Copyright Elsevier 2024

Intas Exhibit 1032
Page 118 of 470
PGR2025-00043

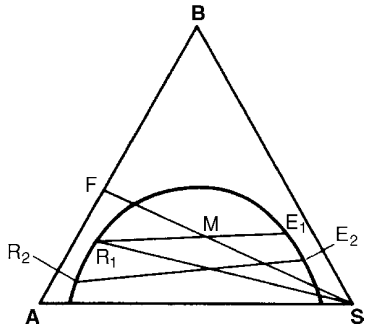


Figure 13.9. Multiple contact with fresh solvent used at each stage

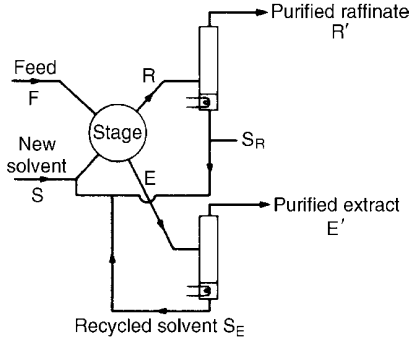


Figure 13.10. Single-stage process with solvent recovery

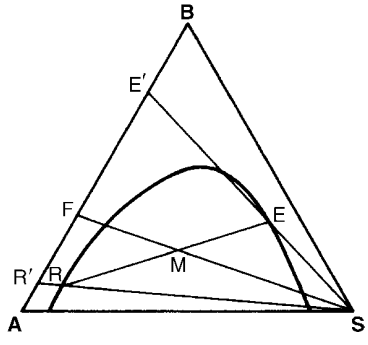


Figure 13.11. Representation of process shown in Figure 13.10

is obtained in the streams S_R and S_E, although the same form of diagram can be used where imperfect separation is obtained. It may be noted that, when ES is a tangent to the binodal curve, then the maximum concentration of solute **B** in the extract E′ is obtained. It also follows that E′ then represents the maximum possible concentration of **B** in the feed. Sufficient solvent **S** must be used to bring the mixture M within the two-phase area.

This book belongs to Bradley Loren (bloren@mcandrews-ip.com) Copyright Elsevier 2024

Intas Exhibit 1032
Page 119 of 470
PGR2025-00043

13.4.2. Co-current contact with immiscible solvents

In this case, which is illustrated in Figure 13.12, triangular diagrams are not required. If the initial solution contains a mass A of solvent **A** with a mass ratio X_f of solute, then the selective solvent to be added will be a mass S of solvent **S**. On mixing and separating, a raffinate is obtained with the solvent **A** containing a mass ratio X_1 of solute, and an extract with the solvent **S** containing a mass ratio Y_1 of solute. A material balance on the solute gives:

$$AX_f = AX_1 + SY_1$$

or:

$$\frac{Y_1}{X_1 - X_f} = -\frac{A}{S} \tag{13.3}$$

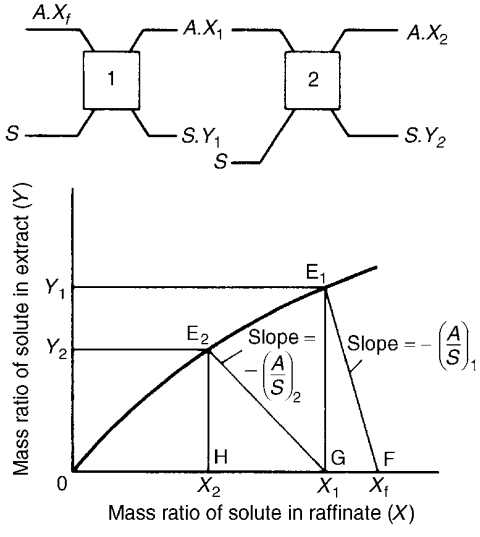


Figure 13.12. Calculation of number of stages for co-current multiple-contact process, using immiscible solvents

This process may be illustrated by allowing the point F to represent the feed solution and drawing a line FE_1, of slope $-(A/S)_1$, to cut the equilibrium curve at E_1. This then gives composition Y_1 of the extract and X_1 of the raffinate. If a further stage is then carried out by the addition of solvent **S** to the stream AX_1, then point E_2 is found on the equilibrium curve by drawing GE_2 of slope $-(A/S)_2$. Point E_2 then gives the compositions X_2 and Y_2 of the final extract and raffinate. This system may be used for any number of stages, with any assumed variation in the proportion of solvent **S** to raffinate from stage to stage.

If the distribution law is followed, then the equilibrium curve becomes a straight line given by $Y = mX$. The material balance on the solute may then be rewritten as:

$$AX_f = AX_1 + SY_1 = AX_1 + SmX_1 = (A + Sm)X_1$$

This book belongs to Bradley Loren (bloren@mcandrews-ip.com) Copyright Elsevier 2024

Intas Exhibit 1032
Page 120 of 470
PGR2025-00043

or:
$$X_1 = \left[\frac{A}{A + Sm}\right] X_f. \tag{13.4}$$

If a further mass S of **S** is added to raffinate AX_1 to give an extract of composition Y_2 and a raffinate X_2 in a second stage, then:

$$AX_1 = AX_2 + SmX_2 = X_2(A + Sm)$$

and:
$$X_2 = \left[\frac{A}{A + Sm}\right] X_1 = \left[\frac{A}{A + Sm}\right]^2 X_f \tag{13.5}$$

For n stages:
$$X_n = \left[\frac{A}{A + Sm}\right]^n X_f \tag{13.6}$$

and the number of stages is given by:
$$n = \frac{\log X_n/X_f}{\log\left[\dfrac{A}{A + Sm}\right]} \tag{13.7}$$

13.4.3. Countercurrent contact with immiscible solvents

If a series of mixing and separating vessels is arranged so that the flow is countercurrent, then the conditions of flow may be represented as shown in Figure 13.13, where each circle corresponds to a mixer and a separator. The initial solution F of the solute **B** in solvent **A** is fed to the first unit and leaves as raffinate R_1. This stream passes through the units and leaves from the nth unit as stream R_n. The fresh solvent **S** enters the nth unit and passes in the reverse direction through the units, leaving as extract E_1.

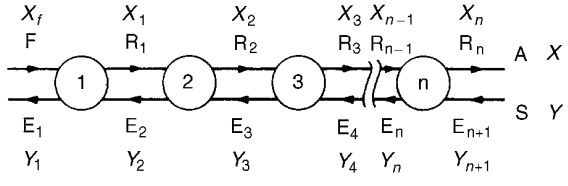


Figure 13.13. Arrangement for multiple-contact extraction in countercurrent flow

The following definitions may be made:

X = the ratio of solute to solvent in the raffinate streams, and

Y = the ratio of the solute to solvent in the extract streams.

If the two solvents are immiscible, the solvent in the raffinate streams remains as A, and the added solvent in the extract streams as S. The material balances for the solute may then be written as

This book belongs to Bradley Loren (bloren@mcandrews-ip.com) Copyright Elsevier 2024

Intas Exhibit 1032
Page 121 of 470
PGR2025-00043

(a) For the 1st stage: $AX_f + SY_2 = AX_1 + SY_1$

(b) For the nth stage: $AX_{n-1} + SY_{n+1} = AX_n + SY_n$

(c) For the whole unit: $AX_f + SY_{n+1} = AX_n + SY_1$

or:
$$Y_{n+1} = \frac{A}{S}(X_n - X_f) + Y_1 \tag{13.8}$$

This is the equation of a straight line of slope A/S, known as the *operating line*, which passes through the points (X_f, Y_1) and (X_n, Y_{n+1}). In Figure 13.14, the equilibrium relation, Y_n against X_n, and the operating line are drawn in, and the number of stages required to pass from X_f to X_n is found by drawing in steps between the operating line and the equilibrium curve. In this example, four stages are required, and (X_n, Y_{n+1}) corresponds to (X_4, Y_5). It may be noted that the operating line connects the compositions of the raffinate stream leaving and the fresh solvent stream entering a unit, X_n and Y_{n+1}, respectively.

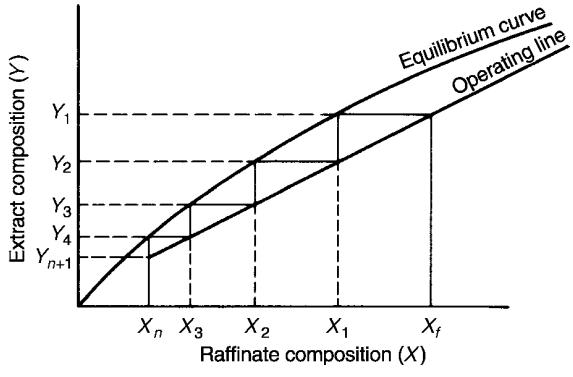


Figure 13.14. Graphical method for determining the number of stages for the process shown in Figure 13.13, using immiscible solvents

Example 13.1

160 cm^3/s of a solvent **S** is used to treat 400cm^3/s of a 10 per cent by mass solution of **A** in **B**, in a three-stage countercurrent multiple-contact liquid–liquid extraction plant. What is the composition of the final raffinate?

Using the same total amount of solvent, evenly distributed between the three stages, what would be the composition of the final raffinate if the equipment were used in a simple multiple-contact arrangement?

Equilibrium data:

kg **A**/kg **B**:	0.05	0.10	0.15
kg **A**/kg **S**:	0.069	0.159	0.258
Densities (kg/m^3):	$\rho_{\mathbf{A}} = 1200$,	$\rho_{\mathbf{B}} = 1000$,	$\rho_{\mathbf{S}} = 800$

This book belongs to Bradley Loren (bloren@mcandrews-ip.com) Copyright Elsevier 2024

Intas Exhibit 1032
Page 122 of 470
PGR2025-00043

Solution

(a) *Countercurrent operation*

Considering the solvent **S**, $160\text{cm}^3/\text{s} = 1.6 \times 10^{-4}\text{m}^3/\text{s}$

and: mass flowrate $= (1.6 \times 10^{-4} \times 800) = 0.128$ kg/s

Considering the solution, $400\text{cm}^3/\text{s} = 4 \times 10^{-4}$ m^3/s
containing, say, a m^3/s **A** and $(5 \times 10^{-4} - a)$ m^3 /s **B**.

Thus: mass flowrate of **A** $= 1200a$ kg/s

and: mass flowrate of **B** $= (4 \times 10^{-4} - a)1000 = (0.4 - 1000a)$ kg/s

a total of: $(0.4 + 200a)$ kg/s

The concentration of the solution is:

$$0.10 = 1200a/(0.4 + 200a)$$

Thus: $$a = 3.39 \times 10^{-5}\text{m}^3/\text{s}$$

mass flowrate of **A** $= 0.041$ kg/s, mass flowrate of **B** $= 0.366$ kg/s

and: ratio of **A**/**B** in the feed, $X_f = (0.041/0.366) = 0.112$ kg/kg

The equilibrium data are plotted in Figure 13.15 and the value of $X_f = 0.112$ kg/kg is marked in. The slope of the equilibrium line is:

$$(\text{mass flowrate of } \mathbf{B})/(\text{mass flowrate of } \mathbf{S}) = (0.366/0.128) = 2.86$$

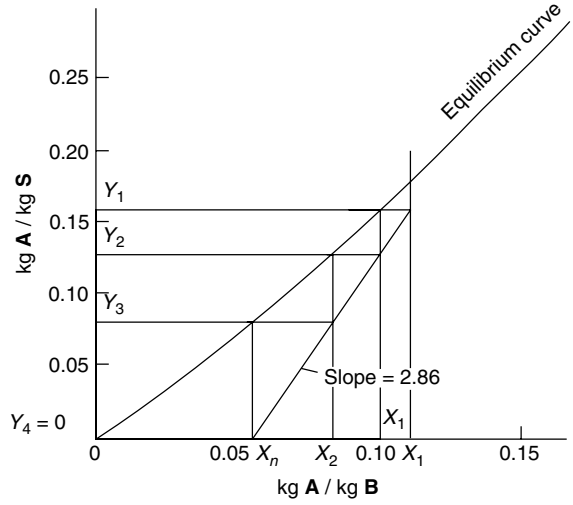


Figure 13.15. Construction for Example 13.1

This book belongs to Bradley Loren (bloren@mcandrews-ip.com) Copyright Elsevier 2024

Intas Exhibit 1032
Page 123 of 470
PGR2025-00043

Since pure solvent is added, $Y_{n+1} = Y_4 = 0$ and a line of slope 2.86 is drawn in such that stepping off from $X_f = 0.112$ kg/kg to $Y_4 = 0$ gives exactly three stages.

When $Y_4 = 0$, $X_n = X_3 = 0.057$ kg/kg,

Thus: the composition of final raffinate is $\underline{\underline{0.057 \text{ kg } \mathbf{A}/\text{kg } \mathbf{B}}}$

(b) *Multiple contact*

In this case, $(0.128/3) = 0.0427$ kg/s of pure solvent **S** is fed to each stage.

Stage 1

$$X_f = (0.041/0.366) = 0.112\text{kg/kg}$$

and from the equilibrium curve, the extract contains 0.18 **A**/kg **S** and $(0.18 \times 0.0427) = 0.0077$ kg/s **A**.

Thus: raffinate from stage 1 contains $(0.041 - 0.0077) = 0.0333$ kg/s **A** and 0.366 kg/s **B**

and: $$X_1 = (0.0333/0.366) = 0.091\text{kg/kg}$$

Stage 2

$$X_1 = 0.091\text{kg/kg}$$

and from Figure 13.15 the extract contains 0.14 kg **A**/kg **S**

or: $$(0.14 \times 0.0427) = 0.0060 \text{ kg/s } \mathbf{A}$$

Thus: the raffinate from stage 2 contains $(0.0333 - 0.0060) = 0.0273$ kg/s **A** and 0.366 kg/s **B**

Thus: $$X_2 = (0.0273/0.366) = 0.075 \text{ kg/kg}$$

Stage 3

$$X_2 = 0.075 \text{ kg/kg}$$

and from Figure 13.15, the extract contains 0.114 kg **A**/kg **S**

or: $$(0.114 \times 0.0427) = 0.0049 \text{ kg/s } \mathbf{A}.$$

Thus: the raffinate from stage 3 contains $(0.0273 - 0.0049) = 0.0224$ kg/s **A** and 0.366 kg/s **B**

and: $$X_3 = (0.0224/0.366) = 0.061 \text{ kg/kg}$$

Thus: the composition of final raffinate $= \underline{\underline{0.061\text{kg } \mathbf{A}/\text{kg } \mathbf{B}}}$

13.4.4. Countercurrent contact with partially miscible solvents

In this case the arrangement of the equipment is the same as for immiscible solvents although, as the amounts of solvent in the extract and raffinate streams are varying, the material balance is taken for the total streams entering and leaving each stage.

This book belongs to Bradley Loren (bloren@mcandrews-ip.com) Copyright Elsevier 2024

With the notation as shown in Figure 13.13, if the feed F, the final extract E_1, the fresh solvent **S** = stream E_{n+1} and, the final raffinate R_n are fixed, then making material balances:

(a) *Over the first unit*

$$F + E_2 = R_1 + E_1$$

and:
$$F - E_1 = R_1 - E_2 = P, \text{ say} — \text{the difference stream} \tag{13.9}$$

(b) *Over stages* 1 *to n*

$$F + E_{n+1} = R_n + E_1 = M, \text{ say} \tag{13.10}$$

and:
$$F - E_1 = R_n - E_{n+1} = P. \tag{13.11}$$

(c) *Over the unit n*

$$R_{n-1} + E_{n+1} = E_n + R_n$$

and:
$$R_{n-1} - E_n = R_n - E_{n+1} = P \tag{13.12}$$

Thus the difference in quantity between the raffinate leaving a stage R_n, and the extract entering from next stage E_{n+1}, is constant. Similarly, it can be shown that the difference between the amounts of each component in the raffinate and the extract streams is constant. This means that, with the notation of a triangular diagram, lines joining any two points representing R_n and E_{n+1} pass through a common pole. The number of stages required to so from an initial concentration F to a final raffinate concentration R_n may then be found using a triangular diagram, shown in Figure 13.16.

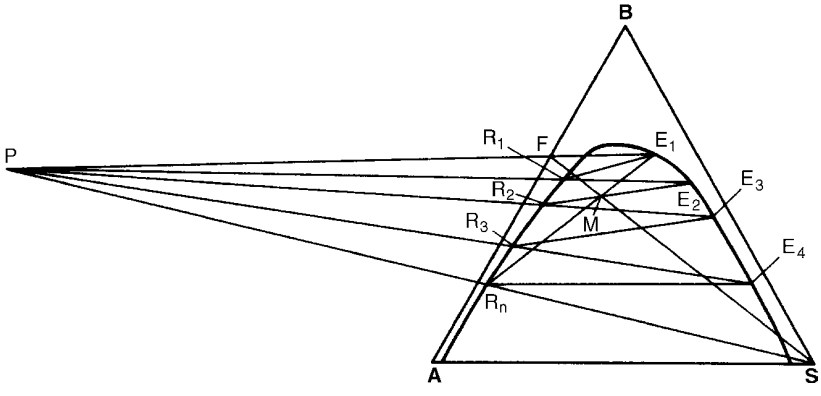


Figure 13.16. Graphical method for determining the number of stages for the process shown in Figure 13.13, using partially miscible solvents

If the points F and S representing the compositions of the feed and fresh solvent **S** are joined, then the composition of a mixture of F and **S** is shown by point M where:

$$\frac{\text{MS}}{\text{MF}} = \frac{\text{mass of F}}{\text{mass of } \mathbf{S}}$$

This book belongs to Bradley Loren (bloren@mcandrews-ip.com) Copyright Elsevier 2024

Intas Exhibit 1032
Page 125 of 470
PGR2025-00043

A line is drawn from R_n through M to give E_1 on the binodal curve and E_1F and SR_n to meet at the pole P. It may be noted that P represents an imaginary mixture, as described for the leaching problems discussed in Chapter 10.

In an ideal stage, the extract E_1 leaves in equilibrium with the raffinate R_1, so that the point R_1 is at the end of the tie line through E_1. To determine the extract E_2, PR_1 is drawn to cut the binodal curve at E_2. The points R_2, E_3, R_3, E_4, and so on, may be found in the same way. If the final tie line, say ER_4, does not pass through R_n, then the amount of solvent added is incorrect for the desired change in composition. In general, this does not invalidate the method, since it gives the required number of ideal stages with sufficient accuracy.

Example 13.2

A 50 per cent solution of solute **C** in solvent **A** is extracted with a second solvent **B** in a counter-current multiple contact extraction unit. The mass of **B** is 25 per cent of that of the feed solution, and the equilibrium data are as given in Figure 13.17.

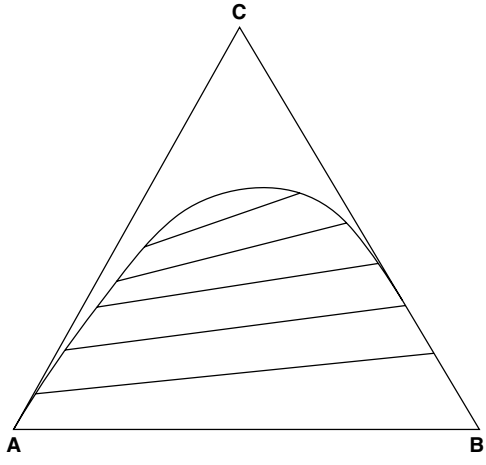


Figure 13.17. Equlibrium data for Example 13.2.

Determine the number of ideal stages required and the mass and concentration of the first extract if the final raffinate contains 15 per cent of solute **C.**

Solution

The equilibrium data are replotted in Figure 13.18 and F, representing the feed, is drawn in on AC at $C = 0.50$, $A = 0.50$. FB is joined and M located such that FM/MB $= 0.25$. R_n is located on the equilibrium curve such that $C = 0.15$. In fact $B = 0.01$ and $A = 0.84$. E_1 is located by projecting R_nM on to the curve and the pole P by projecting E_1F and BR_n. R_1 is found by projecting from

This book belongs to Bradley Loren (bloren@mcandrews-ip.com) Copyright Elsevier 2024

Intas Exhibit 1032
Page 126 of 470
PGR2025-00043

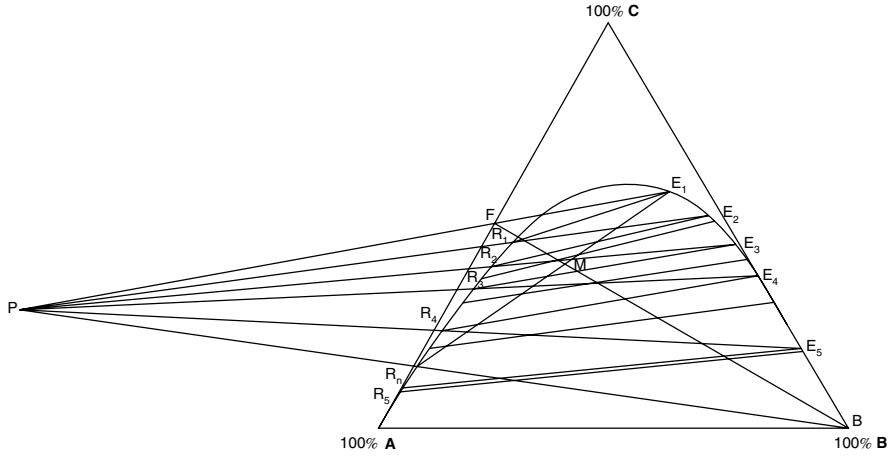


Figure 13.18. Graphical construction for Example 13.2.

E_1 along a tie-line and E_2 as the projection of PR_1. The working is continued in this way and it is found that R_5 is below R_n and hence 5 ideal stages are required.

From Figure 13.18 the concentration of extract E_1 is 9 per cent **A,** 58 per cent **C,** and 33 per cent **B.**

13.4.5. Continuous extraction in columns

As SHERWOOD and PIGFORD[3] point out, the use of spray towers, packed towers or mechanical columns enables continuous countercurrent extraction to be obtained in a similar manner to that in gas absorption or distillation. Applying the two-film theory of mass transfer, explained in detail in Volume 1, Chapter 10, the concentration gradients for transfer to a desired solute from a raffinate to an extract phase are as shown in Figure 13.19, which is similar to Figure 12.1 for gas absorption.

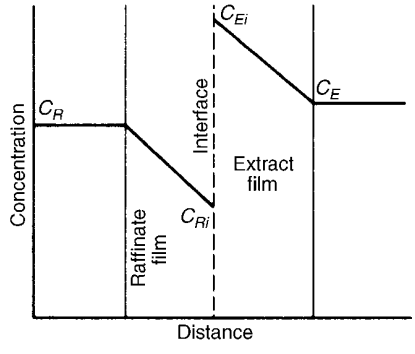


Figure 13.19. Concentration profile near an interface

This book belongs to Bradley Loren (bloren@mcandrews-ip.com) Copyright Elsevier 2024

The transfer through the film on the raffinate side of the interface is brought about by a concentration difference $C_R - C_{Ri}$, and through the film on the extract side by a concentration difference $C_{Ei} - C_E$.

The rate of transfer across these films may be expressed, as in absorption, as:

$$N' = k_R(C_R - C_{Ri}) = k_E(C_{Ei} - C_E) \tag{13.13}$$

where: C_R, C_E are the molar concentrations of the solute in the raffinate and extract phases.
k_R, k_E are the transfer coefficients for raffinate and extract films, respectively, and
N' is the molar rate of transfer per unit area.

Then:

$$\frac{k_R}{k_E} = \frac{C_{Ei} - C_E}{C_R - C_{Ri}} = \frac{\Delta C_E}{\Delta C_R} \tag{13.14}$$

If the equilibrium curve may be taken as a straight line of slope m, then assuming equilibrium at the interface gives:

$$C_{Ei} = mC_{Ri} \tag{13.15}$$

$$C_E = mC_R^* \tag{13.16}$$

and:

$$C_E^* = mC_R \tag{13.17}$$

where C_E^* is the concentration in phase E in equilibrium with C_R in phase R, and C_R^* is the concentration in phase R in equilibrium with C_E in phase E.

The relations for mass transfer may also be written in terms of overall transfer coefficients K_R and K_E defined by:

$$N' = K_R(C_R - C_R^*) = K_E(C_E^* - C_E) \tag{13.18}$$

and by a similar reasoning to that used for absorption, as discussed in Chapter 12 (equation 12.22):

$$\frac{1}{K_R} = \frac{1}{k_R} + \frac{1}{mk_E} \tag{13.19}$$

and:

$$\frac{1}{K_E} = \frac{1}{k_E} + \frac{m}{k_R} \tag{13.20}$$

Capacity of a column operating as continuous countercurrent unit

The capacity of a column operating as a countercurrent extractor, as shown in Figure 13.20, may be derived as follows.

If L'_R, L'_E are the volumetric flowrates of raffinate and extract phases per unit area,
a is the interfacial surface per unit volume, and
Z is the height of packing,

This book belongs to Bradley Loren (bloren@mcandrews-ip.com) Copyright Elsevier 2024

Intas Exhibit 1032
Page 128 of 470
PGR2025-00043

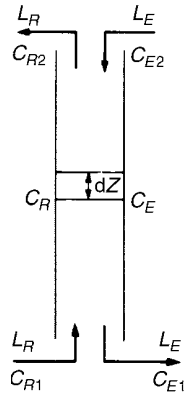


Figure 13.20. Countercurrent flow in a packed column

then, over a small height $\mathrm{d}Z$, a material balance gives:

$$L'_R \,\mathrm{d}C_R = L'_E \,\mathrm{d}C_E \tag{13.21}$$

From equation 13.13:

$$L'_R \,\mathrm{d}C_R = k_R(C_R - C_{Ri})a \,\mathrm{d}Z$$

and:

$$\int_{C_{R2}}^{C_{R1}} \frac{\mathrm{d}C_R}{C_R - C_{Ri}} = \frac{k_R a}{L'_R} Z \tag{13.22}$$

The integral on the left-hand side of this equation is known as the number of raffinate-film transfer units, $\mathbf{N}_R$, and the height of the raffinate-film transfer unit is:

$$\mathbf{H}_R = \frac{L'_R}{k_R a} \tag{13.23}$$

In a similar manner, and by analogy with absorption (equations 12.80, 12.81, 12.82):

$$\mathbf{H}_E = \frac{L'_E}{k_E a} = \text{height of extract-film transfer unit} \tag{13.24}$$

$$\mathbf{H}_{OR} = \frac{L'_R}{K_R a} = \text{height of overall transfer unit based on concentration in raffinate phase} \tag{13.25}$$

$$\mathbf{H}_{OE} = \frac{L'_E}{K_E a} = \text{height of overall transfer unit based on concentration in extract phase} \tag{13.26}$$

Since:

$$\frac{1}{K_R} = \frac{1}{k_R} + \frac{1}{mk_E} \qquad \text{(equation 13.18)}$$

$$\frac{L'_R}{K_R} = \frac{L'_R}{k_R} + \left(\frac{L'_R}{mk_E} \times \frac{L'_E}{L'_E}\right)$$

This book belongs to Bradley Loren (bloren@mcandrews-ip.com) Copyright Elsevier 2024

Intas Exhibit 1032
Page 129 of 470
PGR2025-00043

Thus:
$$\mathbf{H}_{OR} = \mathbf{H}_R + \frac{L'_R}{mL'_E}\mathbf{H}_E \tag{13.27}$$

and:
$$\mathbf{H}_{OE} = \mathbf{H}_E + \frac{mL'_E}{L'_R}\mathbf{H}_R \tag{13.28}$$

These equations are the same form of relation as already obtained for distillation (Chapter 11, equations 11.148 and 11.149) and for absorption (Chapter 12), although it is only with dilute solutions that the group mL'_E/L'_R is constant. If equations 13.27 and 13.28 are combined, then:

$$\mathbf{H}_{OR} = \frac{L'_R}{mL'_E}\mathbf{H}_{OE} \tag{13.29}$$

The group L'_R/mL'_E is the ratio of the slope of the operating line to that of the equilibrium curve so that, when these two are parallel, it follows that $\mathbf{H}_{OR}$ and $\mathbf{H}_{OE}$ are numerically equal.

In deriving these relationships, it is assumed that L'_R and L'_E are constant throughout the tower. This is not the case if a large part of the solute is transferred from a concentrated solution to the other phase.

It is also assumed that the transfer coefficients are independent of concentration. For dilute solutions and where the equilibrium relation is a straight line, a simple expression may be obtained for determining the required height of a column, by the same method as given in Chapter 12.

Thus $L'_R\,\mathrm{d}C_R = K_R(C_R - C_R^*)a\,\mathrm{d}Z$ may be integrated over the height Z and expressed as:

$$L'_R(C_{R1} - C_{R2}) = K_R(\Delta C_R)_{\mathrm{lm}} aZ \tag{13.30}$$

where $(\Delta C_R)_{\mathrm{lm}}$ is the logarithmic mean of $(C_R - C_R^*)_1$ and $(C_R - C_R^*)_2$. This simple relation has been used by workers in the determination of K_R or K_E in small laboratory columns, although care should be taken when applying these results to other conditions.

Equations 13.27 and 13.28 have been used as a basis of correlating mass transfer measurements in continuous countercurrent contactors. For example, LEIBSON and BECKMANN[4] plotted $\mathbf{H}_{OE}$ against mL'_E/L'_R, as shown in Figure 13.21, for a variety of column packings and obtained good straight lines. Caution must, be exercised, however, in drawing conclusions from such plots. Although equation 13.28 suggests that the intercepts and slopes of the lines are numerically equal to $\mathbf{H}_E$ and $\mathbf{H}_R$ respectively, this is true only provided that both these quantities are independent of the flow ratio L'_E/L'_R. This is not always the case and, with packed towers, the height of the continuous phase film transfer unit does in fact depend upon the flow ratio, as discussed by GAYLER and PRATT[5]. Under these conditions neither equation 13.27 nor 13.28 can be used to apportion the individual resistances to mass transfer between the two phases, and the film coefficients have to be determined by direct measurement.

Example 13.3

In the extraction of acetic acid from an aqueous solution with benzene in a packed column of height 1.4 m and of cross-sectional area 0.0045 m^2, the concentrations measured at the inlet and outlet of the column are as shown in Figure 13.22.

This book belongs to Bradley Loren (bloren@mcandrews-ip.com) Copyright Elsevier 2024

Intas Exhibit 1032
Page 130 of 470
PGR2025-00043

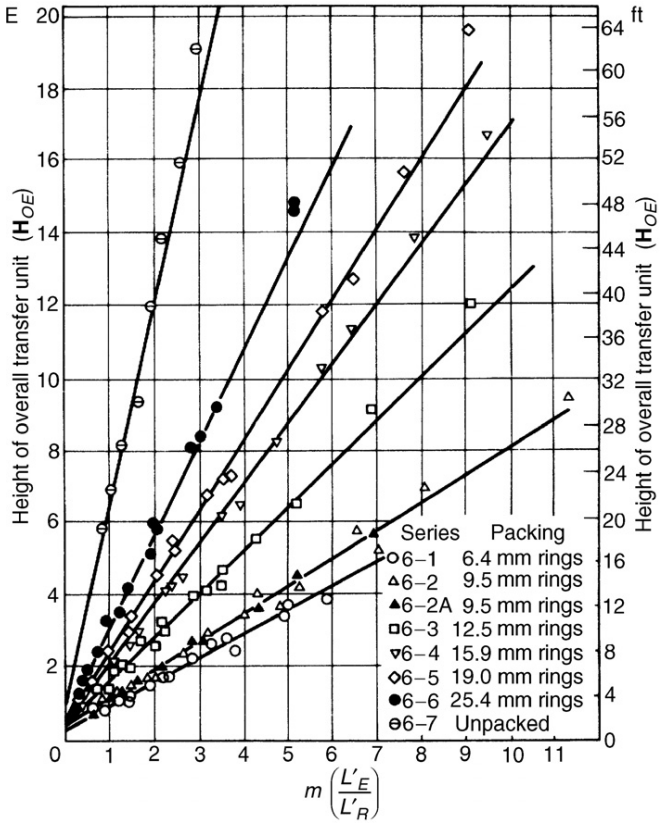


Figure 13.21. Height of the transfer unit $\mathbf{H}_{OE}$ as a function of mL_E/L_R for the transfer of diethylamine from water to dispersed toluene using various packings[4]

Determine the overall transfer coefficient and the height of the transfer unit.

Acid concentration in inlet water phase, C_{W2}	=	0.690 kmol/m^3
Acid concentration in outlet water phase, C_{W1}	=	0.685 kmol/m^3
Flowrate of benzene phase	=	5.7 cm^{3}s or 1.27×10^{-3} m^3/m^{2}s
Inlet benzene phase concentration, C_{B1}	=	0.0040 kmol/m^3
Outlet benzene phase concentration, C_{B2}	=	0.0115 kmol/m^3
The equilibrium relationship for this system is: $\frac{C_B^*}{C_W^*}$	=	0.0247

Solution

The acid transferred to the benzene phase is:

$$5.7 \times 10^{-6}(0.0115 - 0.0040) = 4.275 \times 10^{-8} \text{ kmol/s}$$

This book belongs to Bradley Loren (bloren@mcandrews-ip.com) Copyright Elsevier 2024

Intas Exhibit 1032
Page 131 of 470
PGR2025-00043

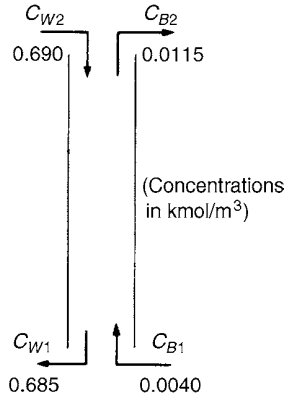


Figure 13.22. Data for Example 13.3

From the equilibrium relationship:

$$\mathbf{C}^*_{B1} = (0.0247 \times 0.685) = 0.0169 \text{ kmol/m}^3$$

and: $$C^*_{B2} = (0.0247 \times 0.690) = 0.0170 \text{ kmol/m}^3$$

Thus: Driving force at bottom, $\Delta C_1 = (0.0169 - 0.0040) = 0.0129$ kmol/m^3

and: Driving force at top, $\Delta C_2 = (0.0170 - 0.0115) = 0.0055$ kmol/m^3

Thus: Log mean driving force, $\Delta C_{\text{lm}} = 0.0087$ kmol/m^3

Thus:
$$K_B a = \frac{\text{moles transferred}}{\text{volume of packing} \times \Delta C_{\text{lm}}} = \frac{(4.275 \times 10^{-8})}{(0.0063 \times 0.0087)}$$
$$= 7.8 \times 10^{-4} \text{ kmol/s m}^3\text{(kmol/m}^3\text{)}$$

and: $$\mathbf{H}_{OB} = (1.27 \times 10^{-3})/(7.8 \times 10^{-4}) = \underline{\underline{1.63 \text{ m}}}$$

13.5. CLASSIFICATION OF EXTRACTION EQUIPMENT

In most industrial applications, multistage countercurrent contacting is required. The hydrodynamic driving force necessary to induce countercurrent flow and subsequent phase separation may be derived from the differential effects of either gravity or centrifugal force on the two phases of different densities. Essentially there are two types of design by which effective multistage operation may be obtained:

(a) *stage-wise contactors*, in which the equipment includes a series of physical stages in which the phases are mixed and separated, and
(b) *differential contactors*, in which the phases are continuously brought into contact with complete phase separation only at the exits from the unit.

This book belongs to Bradley Loren (bloren@mcandrews-ip.com) Copyright Elsevier 2024

Intas Exhibit 1032
Page 132 of 470
PGR2025-00043

The three factors, the inducement of countercurrent flow, stage-wise or differential contacting and the means of effecting phase separation are the basis of a classification of contactors proposed by HANSON[1] which is summarised in Table 13.1.

Table 13.1. Classification of contactors

Countercurrent flow produced by	Phase interdispersion by	Differential contactors	Stagewise contactors
Gravity	Gravity	GROUP A Spray column Packed column	GROUP B Perforated plate column
	Pulsation	GROUP C Pulsed packed column Pulsating plate column	GROUP D Pulsed sieve plate column Controlled cycling column
	Mechanical agitation	GROUP E Rotating disc contactor Oldshue-Rushton column Zeihl column Graesser contractor	GROUP F Scheibel column Mixer-settlers
Centrifugal force	Centrifugal force	GROUP G Podbielniak Quadronic De Laval	GROUP H Westfalia Robatel

Typical regions for application of contactors of different types are given in Table 13.2. The choice of a contactor for a particular application requires the consideration of several factors including chemical stability, the value of the products and the rate of phase separation. Occasionally, the extraction system may be chemically unstable and the contact time must then be kept to a minimum by using equipment such as a centrifugal contactor.

Table 13.2. Typical regions of application of contactor groups listed in Table 13.1[1]

	System criterion	Modest throughput	High throughput
Small number of stages required	Chemically stable Easy phase separation Low value	A, B or mixer–settler	E or F
	Chemically stable Appreciable value	C or D	E or F (not mixer–settler)
	Chemically unstable Slow phase separation	G or H	G or H
Large number of stages required	Chemically stable Easy phase separation Low value	B, C, D or mixer–settler	E or F
	Chemically stable Appreciable value	C or D	E or F (not mixer–settler)
	Chemically unstable Slow phase separation	G or H	G or H

The more important types of stage-wise and differential contactors are discussed in Sections 13.6 and 13.7 respectively.

This book belongs to Bradley Loren (bloren@mcandrews-ip.com) Copyright Elsevier 2024

Intas Exhibit 1032
Page 133 of 470
PGR2025-00043

13.6. STAGE-WISE EQUIPMENT FOR EXTRACTION

13.6.1. The mixer–settler

In the mixer-settler, the solution and solvent are mixed by some form of agitator in the *mixer*, and then transferred to the *settler* where the two phases separate to give an extract and a raffinate. The mixer unit, which is usually a circular or square vessel with a stirrer, may be designed on the principles given in Volume 1, Chapter 7. In the settler the separation is often gravity-controlled, and the liquid densities and the form of the dispersion are important parameters. It is necessary to establish the principles which determine the size of these units and to have an understanding of the criteria governing their internal construction. Whilst the mixer and settler are first considered as separate items, it is important to appreciate that they are essential component parts of a single processing unit.

The mixer. As a result of the agitation achieved in a mixer, the two phases are brought to, or near to, equilibrium so that one theoretical stage is frequently obtained in a single mixer where a physical extraction process is taking place. Where a chemical reaction occurs, the kinetics must be established so that the residence time and the hold-up may be calculated. The hold-up is the key parameter in determining size, and scale-up is acceptably reliable, although a reasonably accurate estimate of the power required is important with large units. For a circular vessel, baffles are required to give the optimum degree of agitation and the propeller, which should be about one-third of the diameter of the vessel, should be mounted just below the interface and operate with a tip speed of 3–15 m/s, depending on the nature of the propeller or turbine. A shroud around the propeller helps to give good initial mixing of the streams, and it also provides some pumping action and hence improves circulation.

As discussed in Volume 1, Chapter 7, the two key parameters determining power are the Reynolds number for the agitator and the power number. The Reynolds number should exceed 10^4 for optimum agitation. This gives a power number of about 6 for a fully baffled tank. It is important to note that the power number and the tip speed cannot both be kept constant in scale-up.

The settler. In this unit, gravitational settling frequently occurs and, in addition, coalescence of droplets must take place. Baffles are fitted at the inlet in order to aid distribution. The rates of sedimentation and coalescence increase with drop size, and therefore excessive agitation resulting in the formation of very small drops should be avoided. The height of the dispersion band Z_B is influenced by the throughput since a minimum residence time is required for coalescence to occur. This height Z_B is related to the dispersed and continuous phase superficial velocities, u_d and u_c by:

$$Z_B = \text{constant } (u_d + u_c) \tag{13.31}$$

Pilot tests may be necessary to achieve satisfactory design, although the sizing of the settler is a difficult problem when the throughputs are large.

Combined mixer–settler units

Recent work has emphasised the need to consider the combined mixer–settler operation, particularly in metal extraction systems where the throughput may be very large. Thus

This book belongs to Bradley Loren (bloren@mcandrews-ip.com) Copyright Elsevier 2024

Intas Exhibit 1032
Page 134 of 470
PGR2025-00043

WARWICK and SCUFFHAM[6] give details of a design, shown in Figure 13.23, in which the two operations are effected in the one combined unit. The impeller has swept-back vanes with double shrouds, and the two phases meet in the draught tube. A baffle on top of the agitator reduces air intake and a baffle on the inlet to the settler is important in controlling the flow pattern. This arrangement gives a good performance and is mechanically neat. Raising the impeller above the draught tube increases internal recirculation which in turn improves the stage efficiency, as shown in Figure 13.24. The effect of agitation on the thickness of the dispersion band is shown in Figure 13.25. The depth of the dispersion

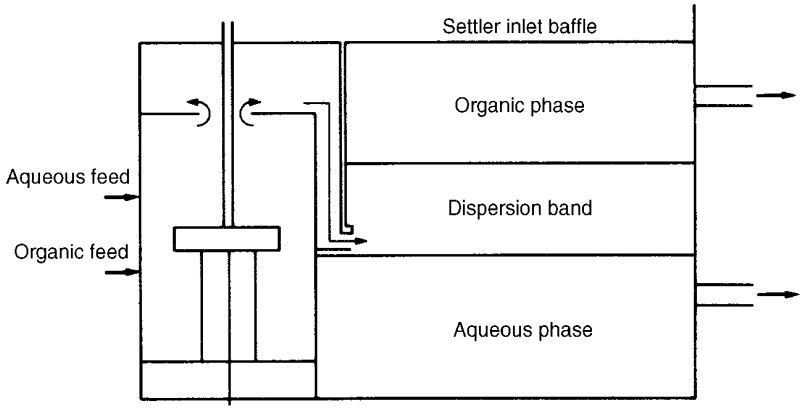


Figure 13.23. Mixer–settler

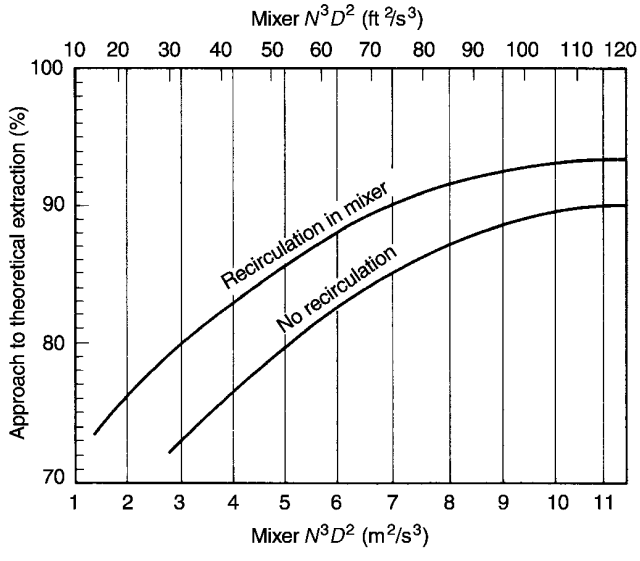


Figure 13.24. The effect of variation of mixer internal recirculation on extraction efficiency[6]

This book belongs to Bradley Loren (bloren@mcandrews-ip.com) Copyright Elsevier 2024
Intas Exhibit 1032
Page 135 of 470
PGR2025-00043

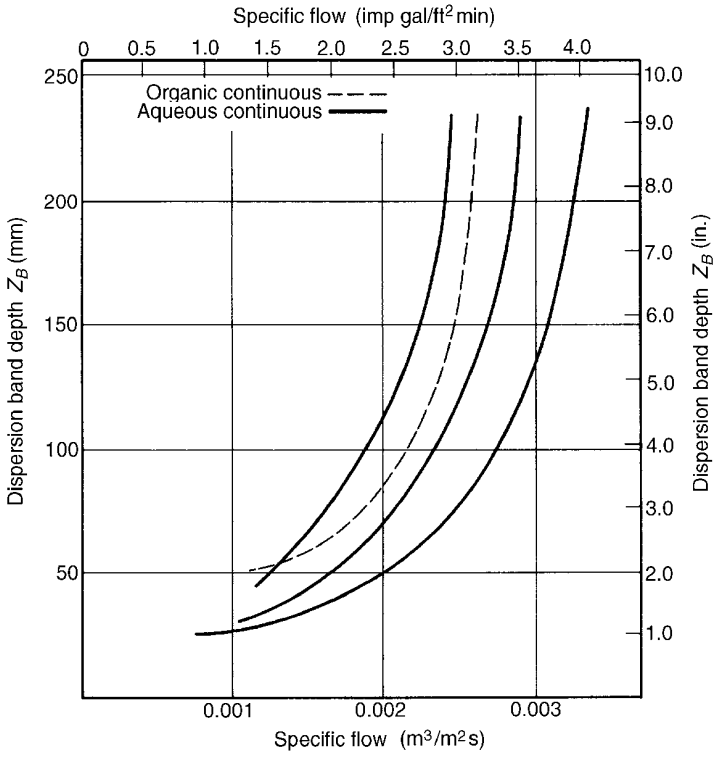


Figure 13.25. The effect of variation of phase continuity and mixer N^3D^2 on settler dispersion band depth[6]

band Z_B varies with the total flow per unit area. Whilst this work was primarily aimed at a design for copper-extraction processes, it is clear that there is scope for further important applications of these units.

The segmented mixer–settler. Novel features for a combined mixer–settler are incorporated in a unit from Davy International, described by JACKSON *et al.*[7] and illustrated in Figure 13.26, where specially designed KnitMesh pads are used to speed up the rate of coalescence. The centrally situated mixer is designed to give the required holdup, and the mixture is pumped at the required rate to the settler which is formed in segments around the mixer, each fed by individual pipework. The KnitMesh pads which are positioned in each segment are 0.75–1.5 m in depth. One key advantage of this design is that the holdup of the dispersed phase in the settler is reduced to about 20 per cent of that in the mixer, as compared with 50 per cent with simple gravity settlers.

The use of KnitMesh in a coalescer for liquid–liquid separation applications is illustrated in Figure 13.27 where an oil–water mixture enters the unit and passes through the coalescer element. As it does so, the water droplets coalesce and separation occurs between the oil and the water. After passing through the KnitMesh, the two phases are readily removed from the top and bottom of the unit.

This book belongs to Bradley Loren (bloren@mcandrews-ip.com) Copyright Elsevier 2024

Intas Exhibit 1032
Page 136 of 470
PGR2025-00043

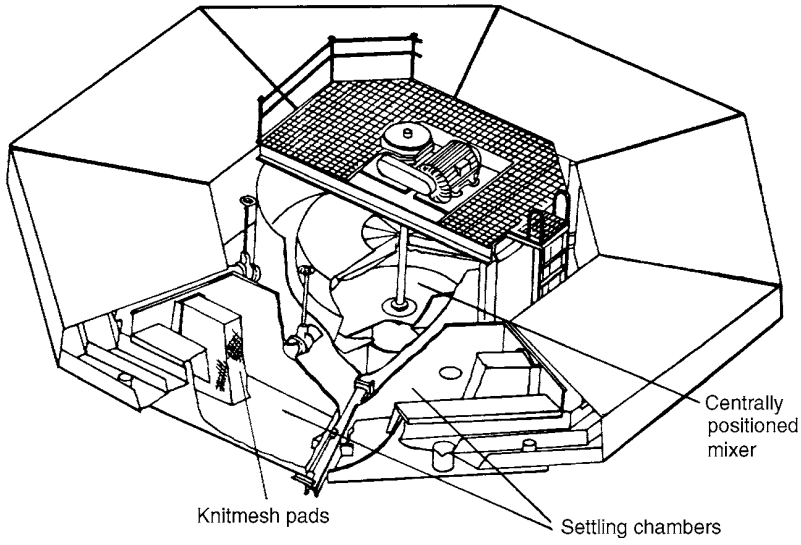


Figure 13.26. Segmented mixer–settler[7]

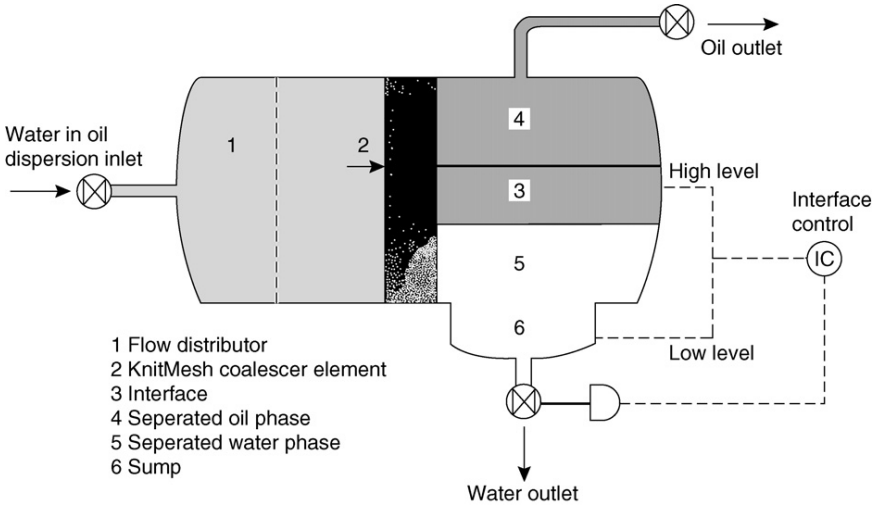


Figure 13.27. Flow in a KnitMesh separator

Kühni have recently developed a mixer-settler column which, as its name suggests is a series of mixer–settlers in the form of a column. The unit consists of a number of stages installed one on top of another, each hydraulically separated, and each with a mixing and settling zone as shown in Figure 13.28. With this design, it is possible to eliminate some of the main disadvantages of conventional mixer–settlers whilst maintaining stagewise

This book belongs to Bradley Loren (bloren@mcandrews-ip.com) Copyright Elsevier 2024
Intas Exhibit 1032
Page 137 of 470
PGR2025-00043

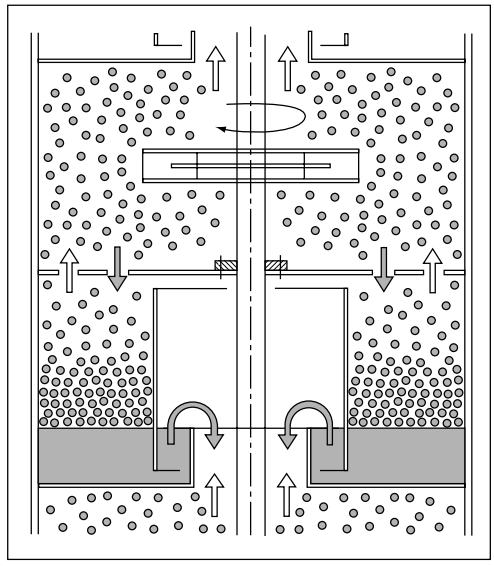


Figure 13.28. Kühni mixer–settler column.

phase contact. As the mixer turbines do not need to transport the liquids from stage to stage, the speed of rotation can be adjusted so as to achieve optimum droplet sizes. Because it is necessary to settle the liquid phase in every stage, the specific throughput is only 0.003 m^3/m^2s which is considerably lower than with more conventional columns. Residence times are of the order of 900 s and extraction may be controlled by the residence time and pH. It is possible to combine extraction with reaction in such a system.

13.6.2. Baffle-plate columns

These are simple cylindrical columns provided with baffles to direct the flow of the dispersed phase, as shown in Figure 13.29. The efficiency of each plate is very low, though since the baffles can be positioned very close together at 75–150 mm, it is possible to obtain several theoretical stages in a reasonable height.

13.6.3. The Scheibel column

One of the problems with perforated plate and indeed packed columns is that redispersion of the liquids after each stage is very poor. To overcome this, SCHEIBEL and KARR[8] introduced a unit, shown in Figure 13.30, in which a series of agitators is mounted on a central rotating shaft. Between the agitators is fitted a wire mesh section which successfully breaks up any emulsions. Some results for a column 292 mm diameter, with 100 mm diameter agitators and with packing sections 230 and 340 mm, are shown in Figure 13.31. It is found that one theoretical stage is obtained in a height of 0.45–0.75 m. This is a

This book belongs to Bradley Loren (bloren@mcandrews-ip.com) Copyright Elsevier 2024

Intas Exhibit 1032
Page 138 of 470
PGR2025-00043

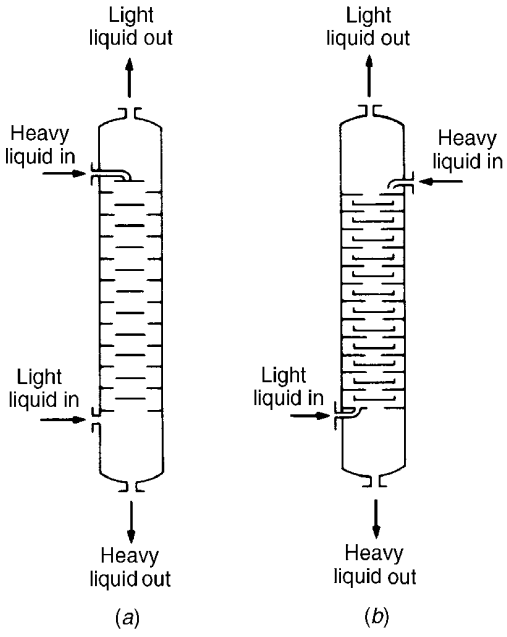


Figure 13.29. Baffle-plate column

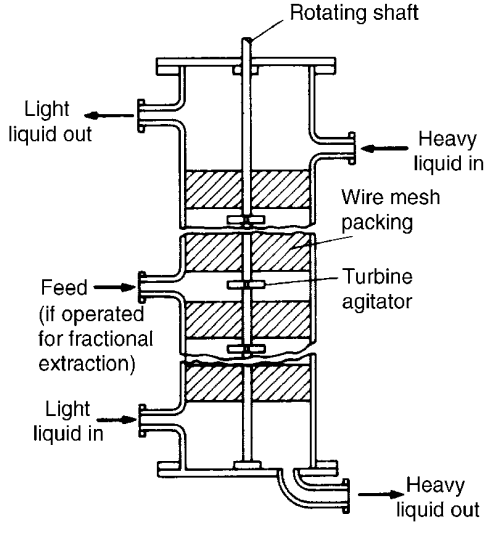


Figure 13.30. Scheibel column[8]

This book belongs to Bradley Loren (bloren@mcandrews-ip.com) Copyright Elsevier 2024

Intas Exhibit 1032
Page 139 of 470
PGR2025-00043

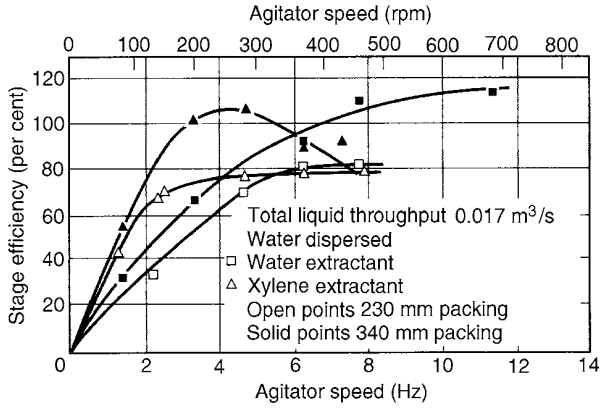


Figure 13.31. Effect of agitator speed on efficiency for the system acetone–xylene–ester[8]

significant improvement on that usually obtained in a packed column. Although there are few data on large units, there should be no fall in efficiency as the diameter is increased.

13.7. DIFFERENTIAL CONTACT EQUIPMENT FOR EXTRACTION

13.7.1. Spray columns

Two methods of operating spray columns are shown in Figure 13.32. Either the light or heavy phase may be dispersed. In the former case (*a*) the light phase enters from a

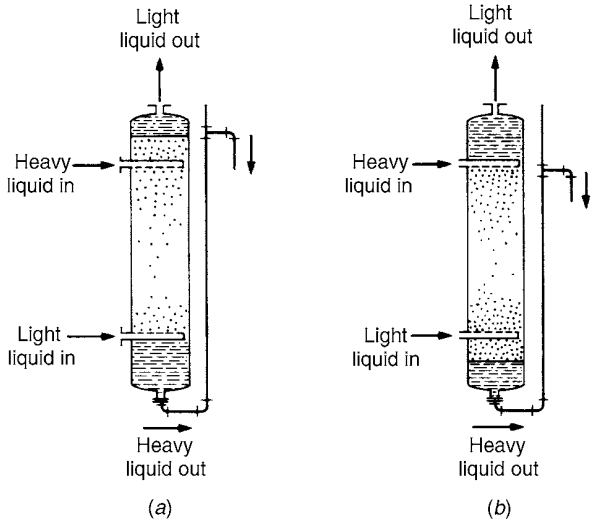


Figure 13.32. Spray towers

This book belongs to Bradley Loren (bloren@mcandrews-ip.com) Copyright Elsevier 2024

distributor at the bottom of the column and the droplets rise through the heavier phase, finally coalescing to form a liquid–liquid interface at the top of the tower. Alternatively, the heavier phase may be dispersed, in which case the interface is held at the bottom of the tower as shown in (*b*). Although spray towers are simple in construction, they are inefficient because considerable recirculation of the continuous phase takes place. As a result, true countercurrent flow is not maintained and up to 6 m may be required for the height of one theoretical stage. There is very little turbulence in the continuous phase and lack of interface renewal, and appreciable axial mixing results in poor performance.

Because the droplets of dispersed phase rise or fall through the continuous phase under the influence of gravity, it will be apparent that there is a limit to the amount of dispersed phase that can pass through the tower for any given flowrate of continuous phase. Thus referring to Figure 13.32(*a*), any additional light phase fed to the bottom of the tower, in excess of that which can pass upwards under the influence of gravity, will be rejected from the bottom of the unit and the tower is then said to be flooded, as discussed by BLANDING and ELGIN[9]. It is therefore important to be able to predict the conditions under which flooding will occur, so that the diameter of tower may be calculated for any required throughput. Although no complete analysis of this problem has, as yet, been achieved, it may be treated approximately in the following way.

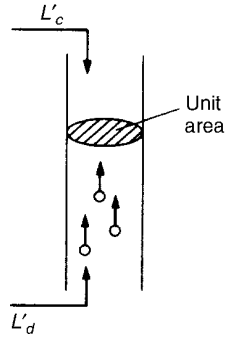


Figure 13.33. Section of a spray tower

Dispersed phase hold-up. Figure 13.33 represents a section of a spray tower of unit cross-sectional area. The light phase is assumed to be dispersed, and the volumetric flowrates per unit area of the two phases are L'_d and L'_c respectively. The superficial velocities u_d, u_c of the phases are therefore also equal to L'_d and L'_c. Under steady-state conditions the amount of dispersed phase held up in the tower in the form of droplets is conveniently expressed in terms of the fractional hold-up j, that is the fractional volume of the two-phase dispersion occupied by the dispersed phase. This may also be thought of as the fraction of the cross-sectional area of the tower occupied by the dispersed phase. The velocity of the dispersed phase relative to the tower is therefore L'_d/j. Similarly, the relative velocity of the continuous phase is equal to $L'_c/(1-j)$. If the overall flow is regarded as strictly countercurrent, the sum of these two velocities will be equal to the

This book belongs to Bradley Loren (bloren@mcandrews-ip.com) Copyright Elsevier 2024
Intas Exhibit 1032
Page 141 of 470
PGR2025-00043

velocity of the dispersed phase relative to the continuous phase, u_r or:

$$\frac{L'_d}{j} + \frac{L'_c}{(1-j)} = u_r \tag{13.32}$$

In the case of spray towers it has been shown by THORNTON[10] that u_r is well represented by $\bar{u}_0(1-j)$ where $\bar{u}_0$ is the velocity of a single droplet relative to the continuous phase, and is termed the droplet characteristic velocity. The term $(1-j)$ is a correction to $\bar{u}_0$ which takes into account the way in which the characteristic velocity is modified when there is a finite population of droplets present, as opposed to a single droplet. It must be seen therefore that for very dilute dispersions, that is as $j \to 0$, $\bar{u}_0(1-j) \to \bar{u}_0$. On the other hand, as the fractional hold-up increases, the relative velocity of the dispersed phase decreases due to interactions between the droplets. Substituting for u_r, equation 13.32 may be written as:

$$\frac{u_d}{j} + \frac{u_c}{1-j} = \bar{u}_0(1-j) \tag{13.33}$$

This equation relates the hold-up to the flowrates of the phases and column diameter through the characteristic velocity, $\bar{u}_0$. It therefore gives a method of calculating the hold-up for a given set of flowrates if $\bar{u}_0$ is known. Conversely, equation 13.33 may be used to calculate $\bar{u}_0$ from experimental hold-up measurements made at different flowrates. Thus, if hold-up data are plotted with $L'_d + (j/(1-j))L'_c$ as the ordinate against $j(1-j)$ as the abscissa, a linear plot is obtained which passes through the origin and which has a slope equal to $\bar{u}_0$[10].

Flooding-point condition. A plot of equation 13.33 in the form of u_d and u_c against j for a typical value of $\bar{u}_0 = 0.042$ m/s is shown in Figure 13.34. Although equation 13.33 is cubic, only the root which lies between zero and the flooding-point values of u_d and u_c is realisable in practice. These portions of the hold-up curves are shown by full lines in Figure 13.34. If the flowrate of one of the phases is kept constant, an increase in the flowrate of the other phase will result in an increased value of the hold-up until the flooding-point is reached. The latter corresponds to the maxima in the two curves shown in Figure 13.34, so that the flooding-point condition is given by $\mathrm{d}u_d/\mathrm{d}j = \mathrm{d}u_c/\mathrm{d}j = 0$. Since those portions of the hold-up curves beyond the flooding-point are unrealistic in practice, the value of j corresponding to the maximum flowrates also represents the limiting hold-up at flooding, although this condition is not obtainable mathematically from equation 13.33.

Carrying out the differentiation described previously gives:

$$u_{df} = 2\bar{u}_0 j_f^2(1-j_f) \qquad \text{when } \mathrm{d}u_c/\mathrm{d}j = 0 \tag{13.34}$$

and:

$$u_{cf} = \bar{u}_0(1-j_f)^2(1-2j_f) \text{ when } \mathrm{d}u_d/\mathrm{d}j = 0 \tag{13.35}$$

The value of j_f, the limiting hold-up at the flooding-point, may be obtained by eliminating $\bar{u}_0$ between equations 13.34 and 13.35 and solving for j_f.

Thus:

$$j_f = \frac{(r^2+8r)^{0.5} - 3r}{4(1-r)} \tag{13.36}$$

where:

$$r = u_{df}/u_{cf}. \tag{13.37}$$

This book belongs to Bradley Loren (bloren@mcandrews-ip.com) Copyright Elsevier 2024

Intas Exhibit 1032
Page 142 of 470
PGR2025-00043

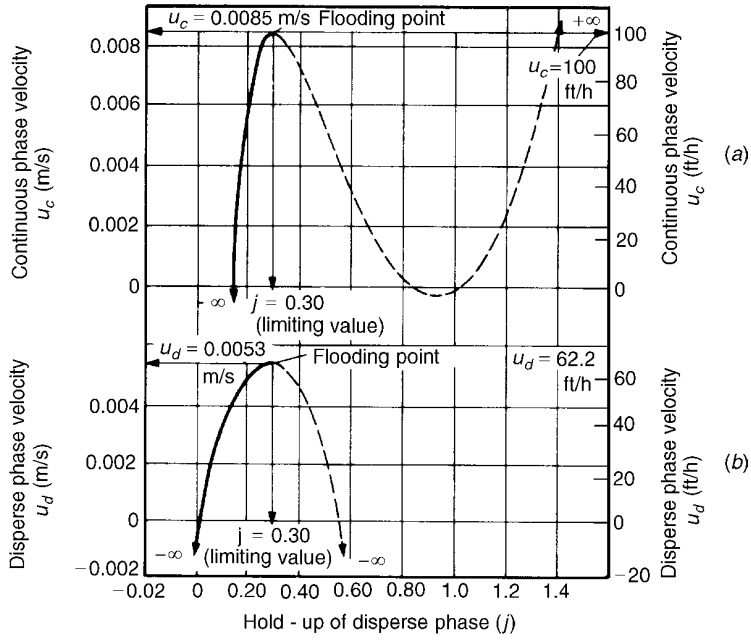


Figure 13.34. Spray tower (*a*) Continuous phase velocity (u_c) as function of hold-up of disperse phase (j)($u_c = 0.0085$ m/s, $\bar{u}_0 = 0.042$ m/s) (*b*) Disperse phase velocity (u_d) as a function of hold-up of disperse phase (j) ($u_d = 0.0053$ m/s, $\bar{u}_0 = 0.0042$ m/s)

The derivation of equations 13.34 and 13.35 has been carried out assuming that $\bar{u}_0$ is constant and independent of the flowrates, up to and including the flooding-point. This in turn assumes that the droplet size is constant and that no coalescence occurs as the hold-up increases. Whilst this assumption is essentially valid in properly designed spray towers, this is certainly not the case with packed towers. Equations 13.34 and 13.35 cannot therefore be used to predict the flooding-point in packed towers and a more empirical procedure must be adopted.

A typical form of flooding-point curve for spray towers is shown in Figure 13.35 where values of u_{df} are plotted against u_{cf}. The limiting values of each flowrate as the other approaches zero may be determined readily from equations 13.34 and 13.35. Thus, when

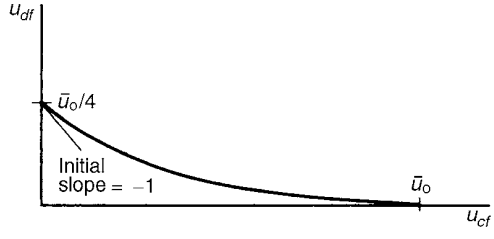


Figure 13.35. Flooding-point curve for spray tower

This book belongs to Bradley Loren (bloren@mcandrews-ip.com) Copyright Elsevier 2024

Intas Exhibit 1032
Page 143 of 470
PGR2025-00043

$u_{df} \to 0$, $j_f \to 0$ and in the limit $u_{cf} = \bar{u}_0$. Similarly, as $u_{cf} \to 0$, $j_f \to 0.50$ and in the limit $u_{df} = \bar{u}_0/4$. In addition, by combining equations 13.34 and 13.35 and differentiating u_{df} with respect to u_{cf}, it is seen that the slope of the flooding-point curve is given by:

$$\frac{\mathrm{d}u_{df}}{\mathrm{d}u_{cf}} = -\frac{j_f}{(1 - j_f)} \tag{13.38}$$

It is apparent therefore that the curve meets the abscissa tangentially as $u_{df} \to 0$, and meets the ordinate with a slope of -1 as $u_{cf} \to 0$.

Equations 13.34 and 13.35 may be used for correlating or extending incomplete flooding-point data. Thus, for example, if flooding-point–hold-up data are available for a range of flowrates, a plot of u_{df} as ordinate against $j_f^2(1 - j_f)$ as abscissa will result in a straight line through the origin, of slope $2\bar{u}_0$. Alternatively, if $\bar{u}_0$ is known, either equations 13.34 or 13.35 may be used to calculate the tower diameter for a required throughput. The actual area of tower to be used is then taken as twice this area to ensure that the unit operates at below 50 per cent of the flooding-point flowrates.

Droplet characteristic velocity and droplet size. The characteristic velocity may be calculated from hold-up measurements below the flooding-point using equation 13.33, or from hold-up measurements at the flooding-point using equations 13.34 or 13.35. In many instances, however, such data are not available and it is then necessary to be able to predict $\bar{u}_0$ from a knowledge of the physical properties of the extraction system. This involves predicting firstly the mean droplet size which is present in the tower, and then the corresponding mean droplet velocity. A full discussion of the problem is beyond the scope of this chapter although for low nozzle velocities, the mean droplet size may be established by means of the correlation proposed by HAYWORTH and TREYBAL[11]. The corresponding droplet velocity may then be calculated by the methods of HU and KINTNER[12] or KLEE and TREYBAL[13].

Interfacial area. The interfacial area per unit volume of tower, or specific area, is given by:

$$a = \frac{\text{Total area}}{\text{Volume}} = \frac{\pi d_s^2}{\pi \frac{d_s^3}{6} \frac{1}{j}} = \frac{6j}{d_s} \tag{13.39}$$

where j is the fractional hold-up and d_s is the mean droplet size, defined in Chapter 1, equation 1.14, as:

$$d_s = \frac{\Sigma n_1 d_1^3}{\Sigma n_1 d_1^2} \tag{13.40}$$

where n_1 is the number of droplets of diameter d_1 in a population.

Example 13.4

The number and size of droplets in a given population are:

diameter (mm)	2	3	4	5	6
number (−)	30	120	200	80	20

Estimate the surface mean droplet size.

This book belongs to Bradley Loren (bloren@mcandrews-ip.com) Copyright Elsevier 2024

Intas Exhibit 1032
Page 144 of 470
PGR2025-00043

Solution

The mean droplet size is given by equations 13.40 and 1.14 as:

$$d_s = \Sigma n_1 d_1^3 / \Sigma n_1 d_1^2$$

where n_1 is the number of droplets of diameter d_1 in a population.
Thus:

Table 13.3. Calculation of mean droplet Diameter

n_1	d_1 mm	d_1^2	d_1^3	$n_1 d_1^3$	$n_1 d_1^2$
30	2	4	8	240	120
120	3	9	27	3240	1080
200	4	16	64	12800	3200
80	5	25	125	100000	2000
200	6	36	216	4320	720
Total				30600	7120

Thus: $\Sigma n_1 d_1^3 = 30600$ and $\Sigma n_1 d_1^2 = 7120$

and: $d_s = (30600/7120) = \underline{\underline{4.30 \text{ mm}}}$

Mass transfer. It is not yet possible to predict the mass transfer coefficient with a high degree of accuracy because the mechanisms of solute transfer are but imperfectly understood as discussed LIGHT and CONWAY[14], COULSON and SKINNER[15] and GARNER and HALE[16]. In addition, the flow in spray towers is not strictly countercurrent due to recirculation of the continuous phase, and consequently the effective overall driving force for mass transfer is not the same as that for true countercurrent flow.

As a first approximation, the dispersed-phase film coefficients may be calculated using the HANDLOS and BARON[17] model for circulating liquid spheres. The continuous phase film coefficients may be estimated from the correlation of RUBY and ELGIN[18], and the overall coefficients then calculated using equations 13.20 or 13.21. Such procedures are, however, only approximate at best, and further work is required before generalised correlations can be developed which take into account the effect of recirculation and the different mass transfer rates at the dispersed phase entry nozzles, during droplet rise and during coalescence at the top of the tower. Typical data[18–21] and standard texts[22–24] for HTU values covering a range of extraction systems are available in the literature. In this respect, scale-up from pilot data raises problems. Reference may also be made to the work of HANSON[1] for further discussion on mass transfer in liquid–liquid systems.

Hitherto no mention has been made of interfacial effects accompanying the mass transfer process. Under certain conditions the presence of an undistributed solute gives rise to the Marangoni effect, discussed by DAVIES and RIDEAL[25] and GROOTHUIS and ZUIDERWEG[26], which results in interfacial turbulence and droplet coalescence. These effects are generally more obvious when solute transfer takes place from an organic solvent droplet into an aqueous continuous phase. In the reverse direction of transfer, interfacial disturbances of this nature are frequently absent. The existence of interfacial phenomena of this type presents yet one more obstacle to a quantitative interpretation of

This book belongs to Bradley Loren (bloren@mcandrews-ip.com) Copyright Elsevier 2024

Intas Exhibit 1032
Page 145 of 470
PGR2025-00043

the mass transfer process. In addition, when coalescence is marked, the droplet size is no longer constant up the tower and the derivations of equations 13.34 and 13.35, which are based upon constant $\bar{u}_0$ values, are no longer valid. From a practical point of view, these equations may still be used for design purposes, since the effect of droplet coalescence is to enhance the flooding-point beyond the value predicted by equations 13.34 and 13.35, so that the tower operates in practice below 50 per cent of the flooding-point.

13.7.2. Packed columns

Although packed columns are similar to those used for distillation and absorption, it must be noted that the flowrates of the phases are very different and two liquid phases are always present. The packing increases the interfacial area, and considerably increases mass transfer rates compared with those obtained with spray columns because of the continuous coalescence and break-up of the drops, though the HTU values are still high. Packed columns are unsuitable for use with dirty liquids, suspensions, or high viscosity liquids. They have proved to be satisfactory in the petroleum industry, though at present they cannot be scaled-up to cope with the very high flows encountered in metallurgical processes. They are economical in the use of ground space.

Minimum packing size. For reproducible results the minimum packing size should be such that the mean void height is not less than the mean droplet diameter. As reported by GAYLER *et al.*[27], this critical packing size is given by:

$$d_{\text{crit}} = 2.42 \left(\frac{\sigma}{\Delta \rho g} \right)^{0.5} \tag{13.41}$$

Dispersed phase hold-up. Three regimes of flow may be distinguished with packings greater than the critical size:

(a) Region of linear hold-up. At low dispersed phase flowrates the droplets move freely within the interstices of the packing and the hold-up increases linearly with dispersed phase flowrate.
(b) Region of rapidly increasing hold-up. Above a hold-up of approximately 10 per cent, corresponding to the lower transition point, the hold-up increases more rapidly with increasing dispersed phase flow. This is due to the onset of hindered movement of the droplets within the packing voids.
(c) Region of constant hold-up. At higher dispersed phase flowrates, the upper transition point is encountered above which droplet coalescence occurs. In this region the hold-up remains constant as the flowrate is increased until the flooding-point is reached. It is apparent therefore that a plot of u_d against j is of similar form to that shown in Figure 13.34, except that the point corresponding to the flooding point for spray towers coincides with the upper transition point for packed towers.

Below the upper transition point, hold-up data may be correlated by an equation analogous to that used for spray towers, except as GAYLER *et al.*[27] and GAYLER and PRATT[28] point

This book belongs to Bradley Loren (bloren@mcandrews-ip.com) Copyright Elsevier 2024

Intas Exhibit 1032
Page 146 of 470
PGR2025-00043

out, a correction must be introduced to take the packing voidage e into account. Thus:

$$\frac{u_d}{j} + \frac{u_c}{(1-j)} = e\bar{u}_0(1-j) \tag{13.42}$$

Droplet size and interfacial area. In the absence of interfacial effects accompanying mass transfer, the droplets break down by impact with elements of packing and finally reach an equilibrium size which is independent of the packing size. Conversely, small droplets gradually coalesce until the equilibrium size is attained. PRATT and his coworkers[5,29] showed that the mean droplet size attained in the tower is well represented by:

$$d_0 = 0.92\left(\frac{\sigma}{\Delta\rho g}\right)^{0.50}\left(\frac{\bar{u}_0 ej}{u_d}\right) \tag{13.43}$$

Correcting equation 13.39 for the packing voidage, the specific area in the tower is given by:

$$a = \frac{6ej}{d_0} \tag{13.44}$$

Droplet characteristic velocity. GAYLER, ROBERTS and PRATT[27] proposed a graphical correlation for $\bar{u}_0$ which takes into account the fact that the droplets are periodically halted by collisions with elements of packing and then accelerate to some fraction of their terminal velocity, u_0, before being deflected or stopped again by a further collision. Figure 13.36 enables u_0 to be determined from a knowledge of the physical properties of the system. This value is then used in conjunction with Figure 13.37 to evaluate $\bar{u}_0$ for any given column diameter d_c and nominal packing size d_p.

Once $\bar{u}_0$ has been determined, the hold-up for any particular set of flowrates may be calculated from equation 13.42, the mean droplet size from equation 13.43, and the specific area from equation 13.44.

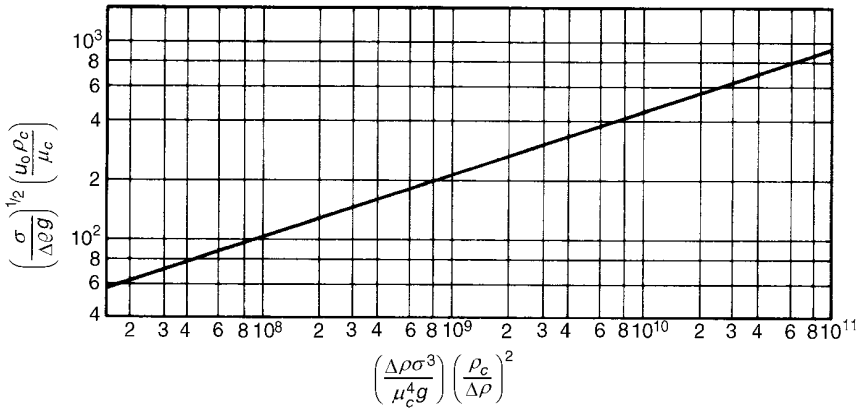


Figure 13.36. Chart for calculation of droplet terminal velocity, u_0[27]

This book belongs to Bradley Loren (bloren@mcandrews-ip.com) Copyright Elsevier 2024

Intas Exhibit 1032
Page 147 of 470
PGR2025-00043

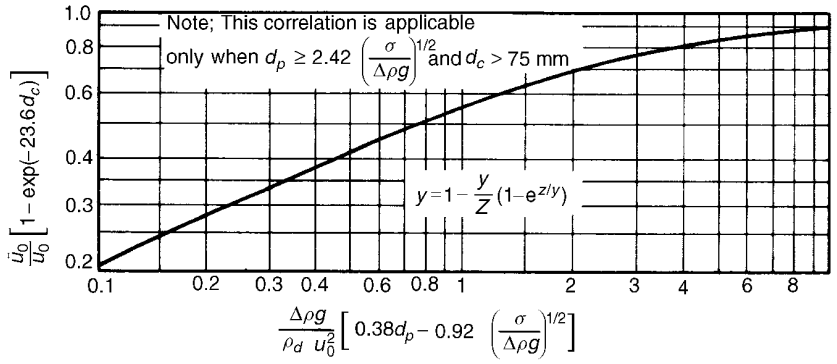


Figure 13.37. Chart for calculation of velocity ($\bar{u}_0$) of a single droplet relative to continuous phase (d_c and d_p are in m)[27]

Flooding-point. Because the flooding-point is no longer synonymous with that for spray towers, equations 13.34 and 13.35 predict only the upper transition point. DELL and PRATT[30] adopted a semi-empirical approach for the flooding-point by consideration of the forces acting on the separate dispersed and continuous phase channels which form when coalescence sets in just below the flooding-point. The following expression correlates data to within ±20 per cent:

$$1 + 0.835\left(\frac{\rho_d}{\rho_c}\right)^{1/4}\left(\frac{u_d}{u_c}\right)^{1/2} = J\left[\frac{u_c^2 a_p}{g e^3}\left(\frac{\rho_c}{\Delta\rho}\right)\left(\frac{\sigma}{\sigma_T}\right)^{1/4}\right]^{-1/4} \tag{13.45}$$

Values of the constant J are given in Table 13.4.

Table 13.4. Values of constant J for use in equation 13.45[30]

Type of packing	Nominal packing size, d_p (mm)					
	6	9	12.5	19	25	57.5
Raschig rings*	0.49	0.53	0.57	0.61	0.63	0.63
Lessing rings	—	0.61	0.61	—	—	—
Berl saddles	0.52	—	0.67	0.67	—	—
Spheres	—	—	0.61	—	—	—

*For values of the LHS of equation 13.45 <1.6 the exponent on the RHS becomes −0.20 and the constant 1.10 $J^{0.8}$.

Mass transfer. As in the case of spray columns, it is not yet possible to predict mass transfer rates from first principles. In the absence of any reliable correlations, use may be made of typical values of overall[20,31] and film[32,33] coefficients. A comprehensive summary is given in Perry's Chemical Engineers' Handbook[22].

Example 13.5

In order to extract acetic acid from dilute aqueous solution with isopropyl ether, the two immiscible phases are passed countercurrently through a packed column 3 m in length and 75 mm in diameter.

This book belongs to Bradley Loren (bloren@mcandrews-ip.com) Copyright Elsevier 2024

Intas Exhibit 1032
Page 148 of 470
PGR2025-00043

It is found that, if 0.5 kg/m^{2}s of the pure ether is used to extract 0.25 kg/m^{2}s of 4.0 per cent acid by mass, then the ether phase leaves the column with a concentration of 1.0 per cent acid by mass.

Calculate:

(a) the number of overall transfer units based on the raffinate phase, and
(b) the overall extraction coefficient based on the raffinate phase.

The equilibrium relationship is given by:

$$(\text{kg acid/kg isopropyl ether}) = 0.3\ (\text{kg acid/kg water}).$$

Solution

$$\text{Cross-sectional area of packing} = (\pi/4)0.075^2 = 0.0044\ \text{m}^2$$

and:
$$\text{volume of packing} = (0.0044 \times 3) = 0.0133\ \text{m}^3.$$

$$\text{The concentration of acid in the extract} = 1.0 \text{ per cent or } 0.01\ \text{kg/kg}.$$

Thus: mass of acid transferred to the ether $= 0.05(0.01 - 0) = 0.005$ kg/m^{2}s

or:
$$(0.005 \times 0.0044) = 0.000022\ \text{kg/s}.$$

$$\text{Acid in the aqueous feed} = (0.25 \times 0.04) = 0.01\ \text{kg/m}^3\ \text{s}.$$

Thus:
$$\text{acid in raffinate} = (0.01 - 0.005) = 0.005\ \text{kg/m}^2\ \text{s}$$

and: concentration of acid in the raffinate $= (0.005/0.25) = 0.02$ kg/kg or 2.0 per cent.

At the top of the column:

$$C_{R_2} = 0.040\ \text{kg/kg and } C^*_{R_2} = (0.040 \times 0.3) = 0.012\text{kg/kg}$$

Thus:
$$\Delta C_2 = (0.012 - 0.010) = 0.002\ \text{kg/kg}$$

At the bottom of the column:

$$C_{R_1} = 0.20\ \text{kg/kg and } C^*_{E_1} = (0.020 \times 0.3) = 0.006\ \text{kg/kg}$$

Thus:
$$\Delta C_1 = (0.006 - 0) = 0.006\ \text{kg/kg}$$

and the logarithmic mean driving force is:

$$(\Delta C_R)_{\text{lm}} = (0.006 - 0.002)/\ln(0.006/0.002) = 0.0036\ \text{kg/kg}$$

$$K_R a = \text{mass transferred/[volume of packing} \times (\Delta C_R)_{\text{lm}}]$$

$$= 0.000022/(0.0133 \times 0.0036) = \underline{0.461\ \text{kg/m}^3\text{s(kg/kg)}}$$

From equation 13.25:

the height of an overall transfer unit,
$$\mathbf{H}_{OR} = L'_R/K_R a$$

$$= (0.25/0.461) = 0.54\ \text{m}$$

and:
$$\text{the number of overall transfer units} = (3/0.54) = \underline{5.53}$$

This book belongs to Bradley Loren (bloren@mcandrews-ip.com) Copyright Elsevier 2024

Intas Exhibit 1032
Page 149 of 470
PGR2025-00043

13.7.3. Rotary annular columns and rotary disc columns

With these columns as described by THORNTON and PRATT[34] and VERMIJS and KRAMERS[35], mechanical energy is provided to form the dispersed phase. The equipment is particularly suitable for installations where a moderate number of stages is required, and where the throughput is considerable. A well dispersed system is obtained with this arrangement. Figure 13.38 shows a rotary annular column.

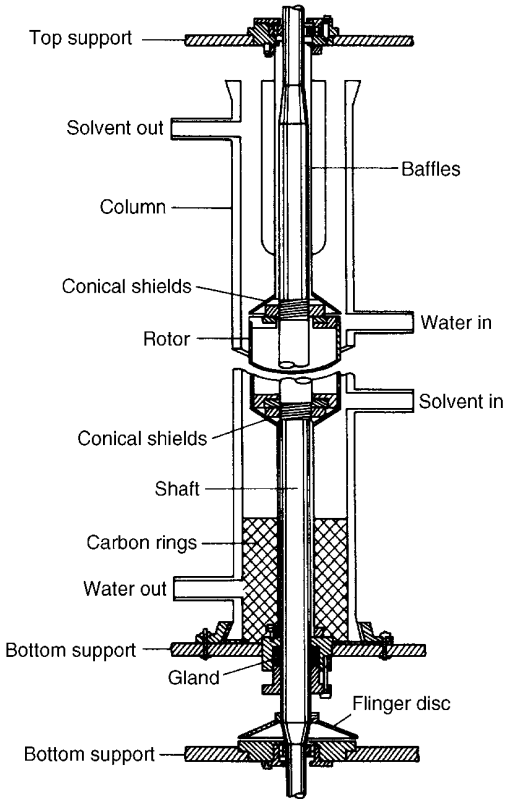


Figure 13.38. Rotary annular column

Flooding-point data may be correlated by equations 13.34 and 13.35 using the droplet characteristic velocity concept as discussed by THORNTON and PRATT[34], since coalescence is absent.

13.7.4. Pulsed columns

In order to prevent coalescence of the dispersed drops, VAN DIJCK[36] and others have devised methods of providing the whole of the continuous phase with a pulsed motion. This may be done, either by some mechanical device, or by the introduction of compressed air.

This book belongs to Bradley Loren (bloren@mcandrews-ip.com) Copyright Elsevier 2024

The pulsation markedly improves performance of packed columns and the HTU is about half that of an unpulsed column. There are advantages in using gauze-type packings since the pulsation operation often breaks ceramic rings. Perforated plates, as used in distillation, may also be used for pulsed extraction. Pulsed packed columns have been used in the nuclear industry though they are limited in size since the pulsation system is difficult to arrange and the pulsation itself demands strengthening of the column.

Flooding-point data have been correlated by equations analogous to 13.34 and 13.35. This procedure is permissible since, as THORNTON[37] and LOGSDAIL and THORNTON[38] report, pulsed columns can be operated up to the flooding-point with no droplet coalescence.

13.7.5. Centrifugal extractors

If separation is difficult in a mixer–settler unit, a centrifugal extractor may be used in which the mixing and the separation stages are contained in the same unit which operates as a differential contactor.

In the *Podbielniak* contactor, the first of the rotating machines to be developed, the heavy phase is driven outwards by centrifugal force and the light phase is displaced inwards. Referring to Figure 13.39 which illustrates a unit produced by Baker Perkins, the heavy phases enters at D, passes to J and is driven out at B. The light phase enters at A and is displaced inwards towards the shaft and leaves at C. The two liquids intermix in zone E where they are flowing countercurrently through the perforated concentric elements and are separated in the spaces between. In zones F and G the perforated elements are surfaces on which the small droplets of entrained liquid can coalesce, the large drops then being driven out by centrifugal force.

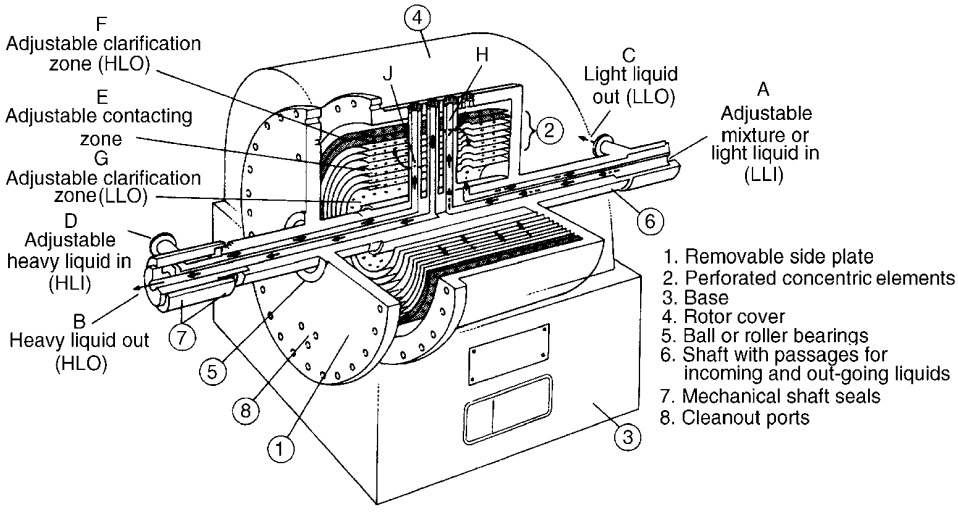


Figure 13.39. Podbielniak contactor

This book belongs to Bradley Loren (bloren@mcandrews-ip.com) Copyright Elsevier 2024

Intas Exhibit 1032
Page 151 of 470
PGR2025-00043

The contactor finds extensive use where high performance phase separation and countercurrent extraction or washing in the one unit are required. Particularly important applications are the removal of acid sludges from hydrocarbons, shown in Figure 13.40, hydrogen peroxide extraction, sulphonate soap and antibiotics extraction, the extraction of rare earths such as uranium and vanadium from leach liquors, and the washing of refined edible oils.

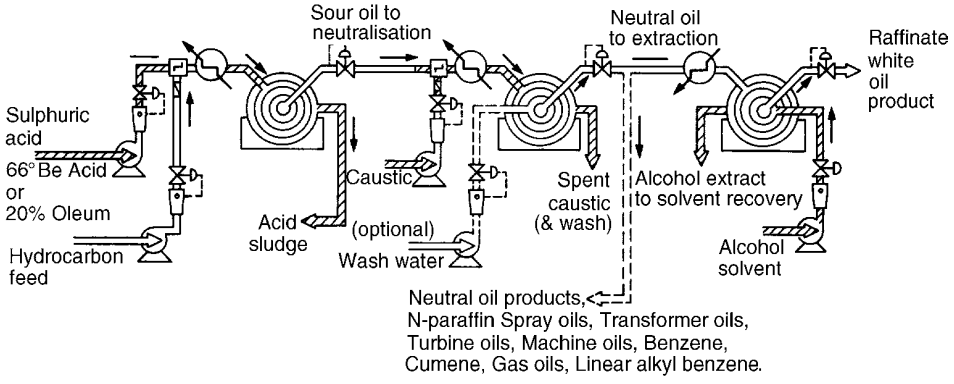


Figure 13.40. Application of the Podbielniak contactor to the acid treatment of hydrocarbon feeds

The *Alfa-Laval* contactor shown in Figure 13.41, has a vertical spindle and the rotor is fitted with concentric cylindrical inserts with helical wings forming a series of spiral

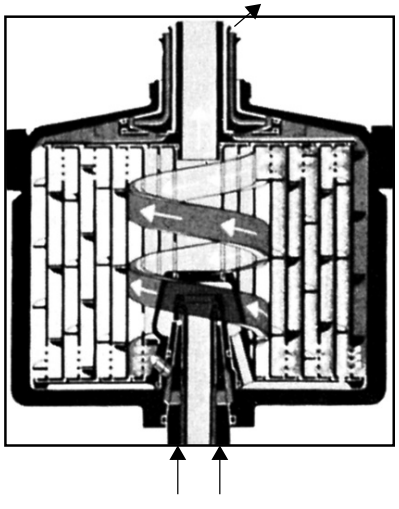


Figure 13.41. Working principle of Alfa-Laval centrifugal extractor

This book belongs to Bradley Loren (bloren@mcandrews-ip.com)
Copyright Elsevier 2024
Intas Exhibit 1032
Page 152 of 470
PGR2025-00043

passages. The two phases are fed into the bottom, the light phase being led to the periphery from which it flows inwards along the spiral, with the heavy phase flowing countercurrently. High shear forces are thus generated giving high extraction rates.

These units give many ideal stages, run continuously and take up a minimum space. For these reasons they have been adopted in many drug extractions, though they are unsuitable for medium or large throughputs.

To some extent, the *Scheibel column* may be considered as a centrifugal device, although as coalescence takes place between the layers of mesh packing, in that sense it is a stage-wise contactor, and it has therefore been described in Section 13.6.3.

13.8. USE OF SPECIALISED FLUIDS

With the widening use of the liquid–liquid extraction for the separation of complex mixtures into their components, it has been necessary to develop fluids with highly selective characteristics. The metallurgical, nuclear, biotechnolgy and food industries are now major users of the technique, and many of the recent developments have originated in those fields. Some of the characteristics and properties of two classes of fluids of increasing importance–supercritical fluids and aqueous two-phase systems are described in this section.

Supercritical fluids can be highly selective and their solvent power can be controlled by adjustment of the operating pressure. With fluids such as carbon dioxide, there is no residual contamination of the product as the solvent evaporates completely at the end of the operation.

The application of two aqueous phase systems is largely confined to the biotechnology industry where the highly complex fragile molecules would be degraded by the action of most of the solvents in common use in the chemical industry. Because biochemical and micrbiological products are normally produced in the aqueous phase, the solvent is very benign because interfacial tensions are very low.

13.8.1. Supercritical fluids

A supercritical fluid is a substance that is above its critical point, that is above the highest temperature and pressure at which its vapour and liquid can co-exist at equilibrium. Although some materials decompose at a temperature below what would be their critical temperature, the supercritical regions of many common gases and liquids are easily attained. The two most popular and inexpensive fluids in this respect are carbon dioxide and water, which are non-toxic and non-flammable and therefore, as pointed out by BRENECKE[39], essentially environmentally benign solvents that can be used even for food processing without undue regulatory restrictions. As presented by REID *et al.*[40], the critical point of carbon dioxide, 304.3 K and 7.3 MN/m^2, is readily accessible although that of water at 647.2 K and 22.09 MN/m^2 is somewhat more challenging. Data for other

This book belongs to Bradley Loren (bloren@mcandrews-ip.com) Copyright Elsevier 2024

supercritical fluids are:

	T_c (K)	P_c (MN/m^2)
ethane	305.4	4.88
ethylene	282.9	5.04
propane	369.9	4.25
ammonia	405.7	11.28

Since the densities of these fluids change dramatically with very small changes in temperature or applied pressure, any density-dependent property such as the solubility of a heavy organic solute for example, may be manipulated, as FRIEDRICH *et al.*[41] have pointed out, over wide ranges. This feature can be utilised in simple separation schemes in which a compound is extracted at high pressure where its solubility is high and then a reduction of the pressure causes the solute to come out of solution with the supercritical fluid being recycled by repressurisation.

The dependence of solubility on pressure can be exploited in the separation of complex mixtures. If the pressure is initially high enough for all the components to be dissolved and is then reduced in stages, precipitation of successive components may be achieved in each stage. Other advantages of supercritical fluids include the fact that their viscosities are less than those of typical liquids and, as the diffusivities of the solutes are closer to those of gases rather than liquids, mass transfer resistances are considerably less than those in normal liquids. Thus, in general, supercritical fluids combine the advantages of having the diffusivities of gases and the solvent power of liquids.

One of the main commercial applications of supercritical fluids is in food processing where supercritical carbon dioxide, which is used on a large scale in the de-caffeination of tea and coffee, is particularly favoured as it leaves no residue in the product. In addition, MCHUGH and KRUKONIS[42] have described the extraction of hops, spices and flavours using supercritical carbon dioxide, which may also be used for the extraction of a whole range of natural products, including pharmaceutical compounds, health supplements and fragrances. JENNINGS *et al.*[43] have described the extraction of taxol, an anti-cancer agent, from a slow-growing variety of the yew tree; FAVATI *et al.*[44] have found that gamma-linolenic acid, a health aid, can be extracted from evening primrose oil seeds; and BORCH-JENSEN *et al.*[45] have shown that the valuable eicosapentaenoic and docosahexaenoic acids in fish oils may be fractionated with supercritical carbon dioxide. MOYLER[46] lists over 80 varieties of seeds, roots, leaves, flowers and fruits which may be extracted with either liquid or supercritical carbon dioxide, and many supercritical carbon dioxide extracts are currently available including celery, ginger, paprika, rosemary, sage and vanilla.

Supercritical fluids also find application in the areas of pollution prevention and remediation, and supercritical carbon dioxide is used as a replacement solvent for many hazardous solvents in both extraction and separation processes and also as a reaction medium and in materials processing. Although carbon dioxide is considered as a 'greenhouse gas', there is actually no net increase in the amount of the gas if it is removed from the environment, used as the solvent instead of a hazardous substance, and returned to the environment. In this way, most of the uses of supercritical carbon dioxide may be considered as environmentally friendly. Because the solubilities of oils and greases in carbon dioxide are high, it is particularly suited to the cleaning of machinery[47] and, as discussed in the literature[48], it is used as a solvent in textile dyeing operations where it is used to treat any dye-laden

This book belongs to Bradley Loren (bloren@mcandrews-ip.com) Copyright Elsevier 2024

Intas Exhibit 1032
Page 154 of 470
PGR2025-00043

wastewater. With the addition of appropriate chelating agents, as described by SAITO *et al.*[49], metals can be effectively extracted from solutions and soils with supercritical carbon dioxide which is also used, as discussed by YAZDI and BEEKMAN[50] to recover uranium from the aqueous solutions produced in the reprocessing of spent nuclear fuels. The main application of supercritical water has been in the oxidation of hazardous organic materials since water is readily miscible with both oxygen and organics and very high degrees of destruction can be achieved with very short residence times. This technology also finds use in the destruction of chemical weapons and stockpiled explosives, as well as in the clean-up of industrial and municipal wastes.

In the use of supercritical carbon dioxide for bioseparations, JOHNSTON *et al.*[51] have reported that proteins can be solublised in reverse micelles formed in carbon dioxide. In general, bioseparations can offset the high cost of attaining the necessary pressures since the products are of high value, they are present in the broth in low concentrations and conventional solvents often lead to recovery problems.

Although perhaps beyond the area of solvent extraction, it may be noted that various processes have been developed in which the solute is dissolved in the supercritical fluid and then the solution is expanded through a nozzle. This gives very high degree of supersaturation and results in the growth and nucleation of very fine particles, as discussed in Chapter 15. Products formed in this way include drug-polymers and materials which promote the gradual release of flavours and fragrances, as discussed by HUTCHENSON and FORSTER[52]. The selective precipitation of solutes is used for a wide variety of products including foods, proteins and explosives, as described by CHANG and RANDOLPH[53]. Spray drying of a solution in a supercritical liquid has been used for the production of microspheres and microporous fibres[54]. Again, beyond the field of solvent extraction, it may be noted that supercritical fluids have found increasing use in providing benign solvents in which to carry out chemical reactions. A review of this work has been provided by SAVAGE *et al.*[55], and the processes described include the polymerisation of highly fluorinated acrylic polymers, the production of formic acid, brominations of alkylaromatics and phase-transfer catalysis. A general review of the exploitation of supercritical fluids in reaction chemistry has been provided by CLIFFORD and BARTLE[56].

13.8.2. Aqueous two-phase systems

The possibility of a three component system consisting of water and two organic components separating into two phases has been known for some time, though it is only since biochemical processes, including fermentation, have been used for the production of expensive highly complex molecules that it has assumed such a great industrial importance. Two-phase aqueous systems are now extensively used for the separation of product from the associated cell debris. Essentially, the addition of a polymer, such a polyethylene glycol or dextran, usually with a phosphate, to a fermentation product causes phase separation to occur, and the way in which the phases separate is determined by the structure and molecular weight of the polymer, and its concentration. A good separation depends on operating under conditions where the tie-line on the phase equilibrium diagram is long. One of the inevitable problems with a system in which both interfacial tension and difference in density of the phases are low lies in the difficulty of obtaining a sharp separation of the liquid layers.

This book belongs to Bradley Loren (bloren@mcandrews-ip.com) Copyright Elsevier 2024

Intas Exhibit 1032
Page 155 of 470
PGR2025-00043

One of the most useful sources of information about these systems is the work of ZASLAVSKY[57]. The partition of proteins and other compounds in aqueous two-phase systems is influenced by a large number of parameters including the types of polymer composing the two-phase system, the mean molecular weight of the polymers, the molecular weight distribution of the polymers, the length of a tie-line, the types of ions composing or added to the system, ionic strength, pH and temperature. Most of these factors do not act independently and, in the main, conditions for a desired partition have to be determined experimentally, as discussed by KULA *et al.*[58], although a thermodynamic interpretation has been presented by BROOKS *et al.*[59]. Where an efficient separation of different substances in an aqueous two-phase system cannot be achieved in a single step, a multi-stage procedure, known as countercurrent distribution, is used. The equipment consists of a series of compartments containing defined volumes of top and bottom phases, in which a substrate partitions itself accordingly. Phase-mixing is followed by phase-settling, and moving the top phases to the adjacent bottom phases. MATTIASSON and KAUL[60] have proposed that a centrifugal separation step be introduced so as to reduce the phase settling time, and a continuous cross-current extraction unit has been developed by HUSTEDT *et al.*[61]. On comparing the large-scale recovery of enzymes by partitioning in aqueous phase systems with other separation processes such as solid–liquid separation by centrifugation, filtration using a drum filter and cross-flow filtration, it is found that partitioning requires larger amounts of chemicals when operating without a recycle, although, as KRONER *et al.*[62] have reported that labour and investment costs are considerably lower. One disadvantage of using two-phase aqueous extraction for many separations is the need for highly purified dextran as one of the phase-forming polymers which is very expensive. KRONER *et al.*[63] have investigated the use of crude dextran as a cheaper alternative and found only a small change in the partition coefficients for a number of enzymes, all of which were recovered with high yields. Crude dextran also gave a wider variation in system parameters and operating costs were some times reduced as shorter residence times were required. Polyethylene glycol–salt systems are preferred for large-scale enzyme extractions even though most proteins partition strongly into the salt-rich bottom phase. Protein isolation and purification are now carried out on a large-scale and HUDSTEDT and PAPAMICHAEL[64] have developed a two-stage aqueous two-phase extraction system for the isolation of β-D-Galactosidase from Escherichia Coli. WOODROW and QUIRK[65] have investigated the partitioning behaviour of acylamidase using a polyethylene glycol–dextran system. Other extractive bioconversions and fermentations with aqueous-phase systems include the production of toxin factor, production of butanol and acetone, cyclic fermentation production of alcohol, the production of glucose-6-phosphate from glucose, the production of L-methionine from racemic mixtures, the production of glucose from starch, deacetylation of penicillin-G, saccharification of cellulose and the production of ethanol and fermentable sugars from cellulose.

13.9. FURTHER READING

BACKHURST, J. R., HARKER, J. H. and PORTER, J. E.: *Problems in Heat and Mass Transfer* (Edward Arnold, London, 1974).
BLUMBERG, R.: *Liquid–Liquid Extraction* (Harcourt Brace Jovanovich, London, 1988).
FAHIEN, R.: *Transport Operations* (McGraw-Hill, New York, 1982).

This book belongs to Bradley Loren (bloren@mcandrews-ip.com) Copyright Elsevier 2024
Intas Exhibit 1032
Page 156 of 470
PGR2025-00043

FRANCIS, A. W.: *Handbook for Components in Solvent Extraction* (Gordon & Breach, New York, 1972).
GODFREY, J. C. and SLATER, M. J.: *Liquid–liquid Extraction Equipment* (Wiley, New York, 1994).
HANSON, C. (ed.): *Recent Advances in Liquid–Liquid Extraction* (Pergamon Press, Oxford, 1971).
HINES, A. L. and MADDOX, R. N.: *Mass Transfer Fundamentals and Applications* (Prentice-Hall, Englewood Cliffs, 1985).
HOLLAND, F. A. and CHAPMAN, F. S.: *Liquid Mixing and Processing in Stirred Tanks* (Reinhold, New York, 1966).
JAMRACK, W. D.: *Base Metal Extraction by Chemical Engineering Techniques* (Pergamon Press, Oxford, 1963).
KING, C. J.: *Separation Processes* 2nd. edn. (McGraw-Hill, New York, 1980).
LO, T. C., BAIRD, M. I. and HANSON, C. (eds): *Handbook of Solvent Extraction* (John Wiley, 1983).
MARCUS, Y. (ed): *Solvent Extraction Reviews* (Marcel Dekker, New York, 1971).
MCCABE, W. L., SMITH, J. C. and HARRIOTT, P.: *Unit Operations in Chemical Engineering*. 4th edn. (McGraw-Hill, New York, (1984)).
MCHUGH, M. A. and KRUKONIS, V. J.: *Supercritical Fluid Extraction — Principles and Practice* (Butterworths, Boston, 1986).
PAUL, P. M. F. and WISE, W. S.: *The Principles of Gas Extraction* (Mills and Boon, London, 1971).
PAULAITIS, M. E., PENNINGER, S. M. L., GRAY, R. D. and DAVIDSON, P. (eds): *Chemical Engineering at Supercritical Fluid Conditions* (Ann Arbor Science, Ann Arbon, 1983).
PRATT, H. R. C.: *Countercurrent Separation Processes* (Elsevier, Amsterdam, 1967).
SCHWEITZER, M. (ed): *Handbook of Separation Techniques for Chemical Engineers* (McGraw-Hill, New York, 1979).
SHERWOOD, T. K., PIGFORD, R. L. and WILKE, C. R.: *Mass Transfer* (McGraw-Hill, New York, 1975).
SQUIRES, T. G. and PAULAITIS, M. E. (eds): *Supercritical Fluids — Chemical and Engineering Principles and Applications*. ACS Symposium Series 329 (American Chemical Society, Washington, 1987).
TREYBAL, R. E.: *Mass Transfer Operations*. 3rd edn. (McGraw-Hill, New York, 1980).
WALTER, H., BROOKS, D. E. and FISHER, D.: *Partitioning in Aqueous Two-Phase Systems*. (Academic Press, New York, 1985).
WANKAT, P. C.: *Equilibrium Staged Separations: Separations for Chemical Engineers* (Elsevier, New York, 1988).
ZASLAVSKY, B. Y.: *Aqueous Two-Phase Partitioning* (Marcel Dekker, 1994). Solvent Extraction, Proc. of the Int. Solvent Extraction Conference. The Hague, 1971. (Soc. Chem. Ind., London, 1971).

13.10. REFERENCES

1. HANSON, C.: *Het Ingenieursblad* **41**, 15–16 (Aug. 1972) 408–17. The technology of solvent extraction in metallurgical processes.
2. British Patent No. 995472: Distillers Company Limited (29 April 1964). Acrylic acid recovery.
3. SHERWOOD, T. K. and PIGFORD, R. L.: *Absorption and Extraction*, 2nd edn. (McGraw-Hill, New York, 1952).
4. LEIBSON, I and BECKMANN, R. B.: *Chem. Eng. Prog.* **49** (1953) 405. The effect of packing size and column diameter on mass transfer in liquid–liquid extraction.
5. GAYLER, R. and PRATT, H. R. C.: *Trans. Inst. Chem. Eng.* **31** (1953) 69. Liquid–liquid extraction. Part V — Further studies of droplet behaviour in packed columns.
6. WARWICK, G. C. I. and SCUFFHAM, J. B.: *Het Ingenieursblad* **41,** 15–16 (Aug. 1972) 442–449. The design for mixer–settlers for metallurgical duties.
7. JACKSON, I. D., NEWRICK, G. M. and WARWICK, G. C. I.: *I. Chem. E.* Symposium Series **42**, 15.1–15.8. A recent development in the design of hydrometallurgical mixer–settlers.
8. SCHEIBEL, E. G. and KARR, A. E.: *Ind. Eng. Chem.* **42** (1950) 1048. Semicommercial multistage extraction columns.
9. BLANDING, F. H. and ELGIN, J. C.: *Trans. Am. Inst. Chem. Eng.* **38** (1942) 305. Limiting flow in liquid–liquid extraction columns.
10. THORNTON, J. D.: *Chem. Eng. Sci.* **5** (1956) 201. Spray liquid–liquid extraction columns.
11. HAYWORTH, C. B. and TREYBAL, R. E.: *Ind. Eng. Chem.* **42** (1950) 1174. Drop formation in two-liquid-phase systems.
12. HU, S. and KINTNER, R. C.: *A.I.Ch.E.Jl.* **1** (1955) 42. The fall of single liquid drops through water.
13. KLEE, A. J. and TREYBAL, R. E.: *A.I.Ch.E.Jl.* **2** (1956) 44. Rate of rise or fall of liquid drops.
14. LICHT, W. and CONWAY, J. B.: *Ind. Eng. Chem.* **42** (1950) 1151. Mechanism of solute transfer in spray towers.

This book belongs to Bradley Loren (bloren@mcandrews-ip.com) Copyright Elsevier 2024

Intas Exhibit 1032
Page 157 of 470
PGR2025-00043

15. COULSON, J. M. and SKINNER, S. J.: *Chem. Eng. Sci.* **1** (1952) 197. The mechanism of liquid–liquid extraction across stationary and moving interfaces. Part 1. Mass transfer into single dispersed drops.
16. GARNER, F. H. and HALE, A. A.: *Chem. Eng. Sci.* **2** (1953) 157. The effect of surface agents in liquid extraction processes.
17. HANDLOS, A. E. and BARON, T.: *A.I.Ch.E.Jl.* **3** (1957) 127. Mass and heat transfer from drops in liquid–liquid extraction.
18. RUBY, C. L. and ELGIN, J. C.: Mass transfer — Transport properties. *Chem. Eng. Prog.* Symp. Series No. 16, **51** (1955) 17. Mass transfer between liquid drops and a continuous liquid phase in a countercurrent fluidized system. Liquid–liquid extraction in a spray tower.
19. APPEL, F. J. and ELGIN, J. C.: *Ind. Eng. Chem.* **29** (1973) 451. Countercurrent extraction of benzoic acid between toluene and water.
20. SHERWOOD, T. K., EVANS, J. E. and LONGCOR, J. V. A.: *Trans. Am. Inst. Chem. Eng.* **35** (1939) 597. Extraction in spray and packed columns.
21. ROW, S. B., KOFFOLT, J. H., and WITHROW, J. R.: *Trans. Am. Inst. Chem. Eng.* **37** (1941) 559. Characteristics and performance of a nine-inch liquid–liquid extraction column.
22. PERRY, R. H., GREEN, D. W. and MALONEY, J. O. (eds.): *Perry's Chemical Engineers' Handbook.* 7th edn. (McGraw-Hill Book Company, New York, 1997).
23. TREYBAL, R. E.: *Liquid Extraction.* 2nd edn. (McGraw-Hill, New York, 1963).
24. SHERWOOD, T. K., PIGFORD, R. L. WILKE, C. R.: *Mass Transfer* (McGraw-Hill, New York, 1975).
25. DAVIES, J. T. and RIDEAL, E. K.: *Interfacial Phenomena* (Academic Press, 1961).
26. GROOTHUIS, H. and ZUIDERWEG, F. J.: *Chem. Eng. Sci.* **12** (1960) 288. Influence of mass transfer on coalescence of drops.
27. GAYLER, R., ROBERTS, N. W. and PRATT, H. R. C.: *Trans. Inst. Chem. Eng.* **31** (1953) 57. Liquid–liquid extraction. Part IV. A further study of hold-up in packed columns.
28. GAYLER, R. and PRATT, H. R. C.: *Trans. Inst. Chem. Eng.* **29** (1951) 110. Symposium on liquid–liquid extraction. Part II. Hold-up and pressure drop in packed columns.
29. LEWIS, J. B., JONES, I. and PRATT, H. R. C.: *Trans. Inst. Chem. Eng.* **29** (1951) 126. Symposium on liquid–liquid extraction. Part III. A study of droplet behaviour in packed columns.
30. DELL, F. R. and PRATT, H. R. C.: *Trans. Inst. Chem. Eng.* **29** (1951) 89 Symposium on liquid–liquid extraction. Part I. Flooding rates for packed columns.
31. PRATT, H. R. C. and GLOVER, S. T.: *Trans. Inst. Chem. Eng.* **24** (1946) 54. Liquid–liquid extraction: Removal of acetone and acetaldehyde from vinyl acetate with water in a packed column.
32. COLBURN, A. P. and WELSH, D. G.: *Trans. Am. Inst. Chem. Eng.* **38** (1942) 179. Experimental study of individual transfer resistances in countercurrent liquid–liquid extraction.
33. LADDHA, G. S. and SMITH, J. M.: *Chem. Eng. Prog.* **46** (1950) 195. Mass transfer resistances in liquid–liquid extraction.
34. THORNTON, J. D. and PRATT, H. R. C.: *Trans. Inst. Chem. Eng.* **31** (1953) 289. Liquid–liquid extraction. Part VII. Flooding rates and mass transfer data for rotary annular columns.
35. VERMIJS, H. J. A. and KRAMERS, H.: *Chem. Eng. Sci.* **3** (1954) 55. Liquid–liquid extraction in a "rotating disc contactor".
36. VAN DIJCK, W. J. D.: *U.S. Patent* 2,011,186 (1935). Intimately contacting fluids (immiscible liquids).
37. THORNTON, J. D.: *Trans. Inst. Chem. Eng.* **35** (1957) 316. Liquid–liquid extraction. Part XIII. The effect of pulse wave-form and plate geometry on the performance and throughput of a pulsed column.
38. LOGSDAIL, D. H. and THORNTON, J. D.: *Trans. Inst. Chem. Eng.* **35** (1957) 331. Liquid–liquid extraction. Part XIV. The effect of column diameter upon the performance and throughput of pulsed plate columns.
39. BRENECKE, J. F.: *Chem. & Industry* (4 November 1996) 831. New applications of supercritical fluids.
40. REID, R. C., PRAUSNITZ, J. M. and POLING, B. E.: *The Properties of Liquids and Gases*. 4th. edn. (McGraw-Hill, New York, 1987)
41. FRIEDRICH, J. P., LIST, G. R. and HEAKIN, A. J.: *J. Am. Oil. Chem. Soc.* **59** (1982) 288–292. Petroleum-free extraction of oil from soybeans with supercritical CO_2.
42. MCHUGH, M. A. and KRUKONIS, V. J.: *Supercritical Fluid Extraction - Principles and Practice*. 2nd. edn. (Butterworth-Heinemann, Oxford, 1994)
43. JENNINGS, D. W., CHANG, F., BAZOOK, V.: *J. Chem. Eng. Data*. **37** (1992) 337–338. Vapor-liquid equilibria for carbon dioxide plus 1-pentanol.
44. FAVATI, F., KING, J. W. and MAZZANTI, M.: *J. Am. Oil. Chem. Soc.* **68** (1991) 422–427. Supercritical carbon dioxide extraction of evening primrose oil.
45. BORCH-JENSEN, C., STABY, A. and MOLLERUP, J. M.: *Ind. Eng. Chem. Res.* **33** (1994) 1574–1579. Phase equilibria of urea-fractioned fish oil fatty acid ethyl esters and supercritical carbon dioxide.
46. MOYLER, D. A. in KING, M. B. and BOTT, T. R. (eds): *Extraction of Natural Products using near-critical Solvents*. (Chapman & Hall, Glasgow, 1993)
47. *Electronic Materials Technology News* **9** (March 1995) No. 3.
48. STEINER, R.: *Chemical Engineering* **100** (3) (March 1993) 114–119. Carbon dioxide's expanding role.

This book belongs to Bradley Loren (bloren@mcandrews-ip.com) Copyright Elsevier 2024

Intas Exhibit 1032
Page 158 of 470
PGR2025-00043

49. SAITO, N., IKUSHIMA, Y. and GOTO, T.: *Bull. Chem. Soc. Japan* **63** (1990) 1532–1534. Liquid-solid extraction of acetylacetone chelates with supercritical carbon dioxide.
50. YAZDI, A. V. and BEEKMAN, E. J.: *Mater. Res.* **10** (1995) 530–537. Design of highly CO_2-soluble chelating agents for carbon dioxide extraction of heavy metals.
51. JOHNSTON, K. P., HARRISON, K. L., CLARKE, M. J.: *Science* **271** (1996) 624–626. Water in carbon dioxide microemulsions: An environment for hydrophiles including proteins.
52. HUTCHENSON, K. W. and FOSTER, N. R. in HUTCHENSON, K. W. and FOSTER, N. R.: *Innovations in Supercritical Fluids*. ACS Symposium Series 608, (American Chemical Society, Washington, 1995)
53. CHANG, C. M. J., RANDOLPH, A. D. and CROFT, N. E.: *Biotech. Prog.* **7** (1991) 275. Separation of beta-caretone mixtures precipitated from liquid solvents with high pressure CO_2.
54. DIXON, D. J., JOHNSTON, K. P. and BODMEIER, R. A.: *AIChE Jl.* **39** (1993) 127. Polymeric materials formed by precipitation with a compressed fluid antisolvent.
55. SAVAGE, P. E., GOPLAN, S., MIZAN, T. I., MARTINO, C. J. and BROCK, E. E.: *AIChE Jl.* **41** (1995) 1723–1778. Reactions at supercritical conditions - applications and fundamentals.
56. CLIFFORD, T. and BARTLE, K.: *Chem. Ind.* (17 June, 1996) 449–452. Chemical reactions in supercritical fluids.
57. ZASLAVSKY, B. Y.: *Aqueous Two-phase Partitioning*. (Marcel Dekker, London, 1994)
58. KULA, M-R. in WINGARD, L. B., KATCHALSKI-KATZIRE, E. and GOLDSTEIN, L. (eds.): *Applied Biochemistry and Bioengineering. Vol 2: Enzyme Technology*. (Academic Press, New York, 1979) 71–95.
59. BROOKS, D. E., SHARP, K. A. and FISHER, D. in WALTER, H., BROOKS, D. E. and FISHER, D. (eds.): *Partitioning in Aqueous Two Phase Systems, Theory, Methods, Uses and Applications to Biotechnology*. (Academic Press, New York, 1985) 11–84.
60. MATTIASSON, B. and KAUL, R.: *Jl. Am. Chem. Soc.* **314** (1986) 79–92. Use of aqueous 2-phase systems for recovery and purification in biotechnology.
61. HUSTEDT, H., KRONER, K. H. and PAPMICHAEL, N.: *Proc. Biochem.* (October, 1988) 129–137. Continuous cross-current aqueous 2-phase extraction of enzymes from biomass - automated recovery in production scale.
62. KRONER, K. H., HUSTEDT, H. and KULA, M-R.: *Proc. Biochem.* No. 10 (1984) 170–179. Extractive enzyme recovery - economic considerations.
63. KRONER, K. H., HUSTEDT, H. and KULA, M-R.: *Biotech. Bioeng.* **24** (1982) 1015–1045. Evaluation of crude dextrain as phase-forming polymer for the extraction of enzymes in aqueous 2-phase systems in large scale.
64. HUDSTEDT, H. and PAPAMICHAEL, N.: *Abstr. Pap. Am. Chem. Soc.* **195** (June, 1988) 198. IEC Part 1. Design of economical aqueous 2-phase extraction processes.
65. WOODROW, J. R. and QUIRK, A. V.: *Enzyme. Microb. Tech.* **8** (1986) 183–187. Anomalous partitioning of aryl acylamidase in aqueous 2-phase systems.

13.11. NOMENCLATURE

		Units in SI System	Dimensions in **M**, **N**, **L**, **T**
A	Mass of solvent **A**	kg	**M**
a	Interfacial area per unit volume of tower	m^2/m^3	$\mathbf{L}^{-1}$
a_p	Superficial area of packing per unit volume of tower	m^2/m^3	$\mathbf{L}^{-1}$
B	Mass of solvent **B**	kg	**M**
b	index	—	—
C	Concentration of solute	$kmol/m^3$	$\mathbf{NL}^{-3}$
C^*	Value of concentration in equilibrium with second phase	$kmol/m^3$	$\mathbf{NL}^{-3}$
D_T	Diameter of tank	m	**L**
d	Particle size	m	**L**
d_c	Diameter of column	m	**L**
d_p	Nominal size of packing	m	**L**
d_s	Surface mean (Sauter mean) diameter of drop	m	**L**
d_{crit}	Critical packing size	m	**L**
E	Mass of extract	kg	**M**
e	Voidage of packing	—	—
F	Mass of feed	kg	**M**
g	Acceleration due to gravity	m/s^2	$\mathbf{LT}^{-2}$

This book belongs to Bradley Loren (bloren@mcandrews-ip.com) Copyright Elsevier 2024

Intas Exhibit 1032
Page 159 of 470
PGR2025-00043

		Units in SI System	Dimensions in **M**, **N**, **L**, **T**
H	Height of the transfer unit	m	**L**
J	Coefficient in equation 13.45 for flooding data	—	—
j	Fractional hold-up of dispersed phase	—	—
K	Overall mass transfer coefficient	m/s	$\mathbf{LT}^{-1}$
K'	Constant	—	—
k	Mass transfer coefficient	m/s	$\mathbf{LT}^{-1}$
L'	Volumetric rate of flow per unit area	m^3/m^2s	$\mathbf{LT}^{-1}$
M	Total flow of material through the system	kg	**M**
m	Slope of the equilibrium line	—	—
N	Revolutions per unit time	s^{-1}	$\mathbf{T}^{-1}$
N'	Molar rate of transfer per unit area	$kmol/m^2s$	$\mathbf{NL}^{-2}\ \mathbf{T}^{-1}$
N	Number of transfer units	—	—
n	Number of stages	—	—
$n_1, n_2, \ldots$	Numbers of particles or droplets	—	—
P	Difference stream	kg	**M**
R	Mass of raffinate	kg	**M**
r	Ratio u_{df}/u_{cf}	—	—
S	Added solvent in extract stream	kg	**M**
u	Volumetric flowrate per unit area	m^3/m^2s	$\mathbf{LT}^{-1}$
u_r	Velocity of dispersed phase relative to continuous phase	m/s	$\mathbf{LT}^{-1}$
u_0	Terminal falling velocity of droplet	m/s	$\mathbf{LT}^{-1}$
$\bar{u}_0$	Velocity of single droplet relative to continuous phase	m/s	$\mathbf{LT}^{-1}$
X_f	Mass ratio of solute in feed	kg/kg (kmol/kmol)	—
$X_1,\ X_2$	Mass ratio of solute in raffinate	kg/kg (kmol/kmol)	—
$x_A,\ x_B$	Mass (or mole) fraction of **A**, **B**	kg/kg (kmol/kmol)	—
$Y_1,\ Y_2$	Mass ratio of solute in extract	kg/kg (kmol/kmol)	—
Z	Height of packing	m	**L**
Z_B	Height of dispersion band	m	**L**
β	Selectivity ratio (equation 13.2)	—	—
ρ	Density	kg/m^3	$\mathbf{ML}^{-3}$
$\Delta\rho$	Density difference between phases	kg/m^3	$\mathbf{ML}^{-3}$
σ	Interfacial tension	J/m^2 or N/m	$\mathbf{MT}^{-2}$
σ_T	Interfacial tension, water-air at 288 K (0.073 N/m)	J/m^2 or N/m	$\mathbf{MT}^{-2}$

Suffixes

c, d	continuous and disperse phases
E, R	extract and raffinate phases
O	overall (transfer units)
f	limiting value at flooding point
i	value of interface
lm	logarithmic mean value
1, 2	values at bottom, top of column

This book belongs to Bradley Loren (bloren@mcandrews-ip.com) Copyright Elsevier 2024

Intas Exhibit 1032
Page 160 of 470
PGR2025-00043

CHAPTER 14

Evaporation

14.1. INTRODUCTION

Evaporation, a widely used method for the concentration of aqueous solutions, involves the removal of water from a solution by boiling the liquor in a suitable vessel, an evaporator, and withdrawing the vapour. If the solution contains dissolved solids, the resulting strong liquor may become saturated so that crystals are deposited. Liquors which are to be evaporated may be classified as follows:

(a) Those which can be heated to high temperatures without decomposition, and those that can be heated only to a temperature of about 330 K.
(b) Those which yield solids on concentration, in which case crystal size and shape may be important, and those which do not.
(c) Those which, at a given pressure, boil at about the same temperature as water, and those which have a much higher boiling point.

Evaporation is achieved by adding heat to the solution to vaporise the solvent. The heat is supplied principally to provide the latent heat of vaporisation, and, by adopting methods for recovery of heat from the vapour, it has been possible to achieve great economy in heat utilisation. Whilst the normal heating medium is generally low pressure exhaust steam from turbines, special heat transfer fluids or flue gases are also used.

The design of an evaporation unit requires the practical application of data on heat transfer to boiling liquids, together with a realisation of what happens to the liquid during concentration. In addition to the three main features outlined above, liquors which have an inverse solubility curve and which are therefore likely to deposit scale on the heating surface merit special attention.

14.2. HEAT TRANSFER IN EVAPORATORS

14.2.1. Heat transfer coefficients

The rate equation for heat transfer takes the form:

$$Q = U A \Delta T \tag{14.1}$$

where: Q is the heat transferred per unit time,
U is the overall coefficient of heat transfer,
A is the heat transfer surface, and
ΔT is the temperature difference between the two streams.

This book belongs to Bradley Loren (bloren@mcandrews-ip.com) Copyright Elsevier 2024

Intas Exhibit 1032
Page 161 of 470
PGR2025-00043

In applying this equation to evaporators, there may be some difficulty in deciding the correct value for the temperature difference because of what is known as the *boiling point rise* (BPR). If water is boiled in an evaporator under a given pressure, then the temperature of the liquor may be determined from steam tables and the temperature difference is readily calculated. At the same pressure, a solution has a boiling point greater than that of water, and the difference between its boiling point and that of water is the BPR. For example, at atmospheric pressure (101.3 kN/m^2), a 25 per cent solution of sodium chloride boils at 381 K and shows a BPR of 8 deg K. If steam at 389 K were used to concentrate the salt solution, the overall temperature difference would not be $(389 - 373) = 16$ deg K, but $(389 - 381) = 8$ deg K. Such solutions usually require more heat to vaporise unit mass of water, so that the reduction in capacity of a unit may be considerable. The value of the BPR cannot be calculated from physical data of the liquor, though Dühring's rule is often used to find the change in BPR with pressure. If the boiling point of the solution is plotted against that of water at the same pressure, then a straight line is obtained, as shown for sodium chloride in Figure 14.1. Thus, if the pressure is fixed, the boiling point of water is found from steam tables, and the boiling point of the solution from Figure 14.1. The boiling point rise is much greater with strong electrolytes, such as salt and caustic soda.

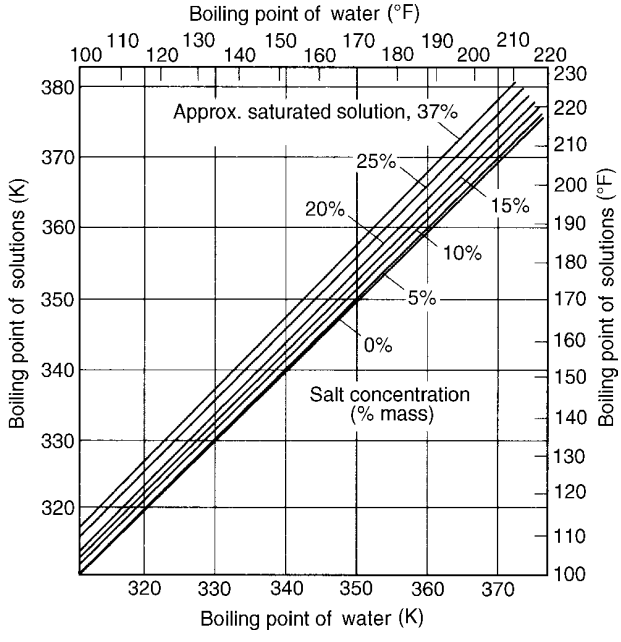


Figure 14.1. Boiling point of solutions of sodium chloride as a function of the boiling point of water. Dühring lines

Overall heat transfer coefficients for any form of evaporator depend on the value of the film coefficients on the heating side and for the liquor, together with allowances for scale deposits and the tube wall. For condensing steam, which is a common heating medium, film coefficients are approximately 6 kW/m^2 K. There is no entirely satisfactory

This book belongs to Bradley Loren (bloren@mcandrews-ip.com) Copyright Elsevier 2024

Intas Exhibit 1032
Page 162 of 470
PGR2025-00043

general method for calculating transfer coefficients for the boiling film. Design equations of sufficient accuracy are available in the literature, however, although this information should be used with caution.

14.2.2. Boiling at a submerged surface

The heat transfer processes occurring in evaporation equipment may be classified under two general headings. The first of these is concerned with boiling at a submerged surface. A typical example of this is the horizontal tube evaporator considered in Section 14.7, where the basic heat transfer process is assumed to be nucleate boiling with convection induced predominantly by the growing and departing vapour bubbles. The second category includes two-phase forced-convection boiling processes occurring in closed conduits. In this case convection is induced by the flow which results from natural or forced circulation effects.

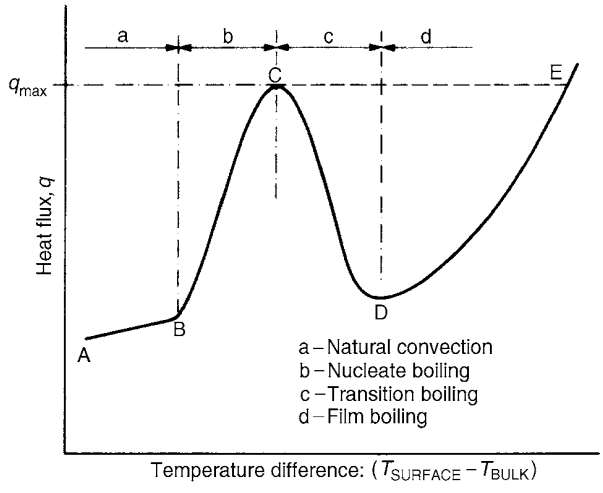


Figure 14.2. Typical characteristic for boiling at a submerged surface

As detailed in Volume 1, Chapter 9 and in Volume 6, the heat flux–temperature difference characteristic observed when heat is transferred from a surface to a liquid at its boiling point, is as shown in Figure 14.2. In the range AB, although the liquid in the vicinity of the surface will be slightly superheated, there is no vapour formed and heat transfer is by natural convection with evaporation from the free surface. Boiling commences at B with bubble columns initiated at preferred sites of nucleation centres on the surface. Over the nucleate boiling region, BC, the bubble sites become more numerous with increasing flux until, at C, the surface is completely covered. In the majority of commercial evaporation processes the heating medium is a fluid and therefore the controlling parameter is the overall temperature difference. If an attempt is made to increase the heat flux beyond that at C, by increasing the temperature difference,

This book belongs to Bradley Loren (bloren@mcandrews-ip.com) Copyright Elsevier 2024
Intas Exhibit 1032
Page 163 of 470
PGR2025-00043

the nucleate boiling mechanism will partially collapse and portions of the surface will be exposed to vapour blanketing. In the region of transition boiling CD the average heat transfer coefficient, and frequently the heat flux, will decrease with increasing temperature difference, due to the increasing proportion of the surface exposed to vapour. This self-compensating behaviour is not exhibited if heat flux rather than temperature difference is the controlling parameter. In this case an attempt to increase the heat flux beyond point C will cause the nucleate boiling regime to collapse completely, exposing the whole surface to a vapour film. The inferior heat transfer characteristics of the vapour mean that the surface temperature must rise to E in order to dissipate the heat. In many instances this temperature exceeds the melting point of the surface and results can be disastrous. For obvious reasons the point C is generally known as *burnout*, although the terms *departure from nucleate boiling (DNB point)* and *maximum heat flux* are in common usage. In the design of evaporators, a method of predicting the heat transfer coefficient in nucleate boiling h_b, and the maximum heat flux which might be expected before h_b begins to decrease, is of extreme importance. The complexity of the nucleate boiling process has been the subject of many studies. In a review of the available correlations for nucleate boiling, WESTWATER[1] has presented some fourteen equations. PALEN and TABOREK[2] reduced this list to seven and tested these against selected experimental data[3,4]. As a result of this study two equations, those due to MCNELLY[5] and GILMOUR[6], were selected as the most accurate. Although the modified form of the Gilmour equation is somewhat more accurate, the relative simplicity of the McNelly equation is attractive and this equation is given in dimensionless form as:

$$\left[\frac{h_b d}{k}\right] = 0.225\left[\frac{C_p \mu_L}{k}\right]^{0.69}\left[\frac{qd}{\lambda \mu_L}\right]^{0.69}\left[\frac{Pd}{\sigma}\right]^{0.31}\left[\frac{\rho_L}{\rho_v} - 1\right]^{0.31} \tag{14.2}$$

The inclusion of the characteristic dimension d is necessary dimensionally, though its value does not affect the result obtained for h_b.

This equation predicts the heat transfer coefficient for a single isolated tube and is not applicable to tube bundles, for which PALEN and TABOREK[2] showed that the use of this equation would have resulted in 50–250 per cent underdesign in a number of specific cases. The reason for this discrepancy may be explained as follows. In the case of a tube bundle, only the lowest tube in each vertical row is completely irrigated by the liquid with higher tubes being exposed to liquid–vapour mixtures. This partial vapour blanketing results in a lower average heat transfer coefficient for tube bundles than the value given by equation 14.2. In order to calculate these average values of h for a tube bundle, equations of the form $h = C_s h_b$ have been suggested[2] where the surface factor C_s is less than 1 and is, as might be expected, a function of the number of tubes in a vertical row, the pitch of the tubes, and the basic value of h_b. The factor C_s can only be determined by statistical analysis of experimental data and further work is necessary before it can be predicted from a physical model for the process.

The single tube values for h_b have been correlated by equation 14.2, which applies to the true nucleate boiling regime and takes no account of the factors which eventually lead to the maximum heat flux being approached. As discussed in Volume 1, Chapter 9, equations for *maximum flux*, often a limiting factor in evaporation processes, have been tested by PALEN and TABOREK[2], though the simplified equation of ZUBER[7] is recommended. This

This book belongs to Bradley Loren (bloren@mcandrews-ip.com) Copyright Elsevier 2024

Intas Exhibit 1032
Page 164 of 470
PGR2025-00043

takes the form:

$$q_{\max} = \frac{\pi}{24}\lambda\rho_v\left[\frac{\sigma g(\rho_L - \rho_v)}{\rho_v^2}\right]^{1/4}\left[\frac{\rho_L + \rho_v}{\rho_L}\right]^{1/2} \tag{14.3}$$

where: $q_{\max}$ is the maximum heat flux,
λ is the latent heat of vaporisation,
ρ_L is the density of liquid,
ρ_v is the density of vapour,
σ is the interfacial tension, and
g is the acceleration due to gravity.

14.2.3. Forced convection boiling

The performance of evaporators operating with forced convection depends very much on what happens when a liquid is vaporised during flow through a vertical tube. If the liquid enters the tube below its boiling point, then the first section operates as a normal heater and the heat transfer rates are determined by the well-established equations for single phase flow. When the liquid temperature reaches the boiling point corresponding to the local pressure, boiling commences. At this stage the vapour bubbles are dispersed in the continuous liquid phase although progressive vaporisation of the liquid gives rise to a number of characteristic flow patterns which are shown in Figure 14.3. Over the initial boiling section convective heat transfer occurs with vapour bubbles dispersed in the liquid. Higher up, the tube bubbles become more numerous and elongated, and bubble coalescence occurs and eventually the bubbles form slugs which later collapse to give an annular flow regime in which vapour forms the central core with a thin film of liquid carried up the wall. In the final stage, dispersed flow with liquid entrainment in the vapour core occurs. In general, the conditions existing in the tube are those of annular flow. With further evaporation, the rising liquid film becomes progressively thinner and this thinning, together with the increasing vapour core velocity, eventually causes breakdown of the liquid film, leading to dry wall conditions.

For boiling in a tube, there is therefore a contribution from nucleate boiling arising from bubble formation, together with forced convection boiling due to the high velocity liquid–vapour mixture. Such a system is inherently complex since certain parameters influence these two basic processes in different ways.

Dengler and Addoms[8] measured heat transfer to water boiling in a 6 m tube and found that the heat flux increased steadily up the tube as the percentage of vapour increased, as shown in Figure 14.4. Where convection was predominant, the data were correlated using the ratio of the observed two-phase heat transfer coefficient (h_{tp}) to that which would be obtained had the same total mass flow been all liquid (h_L) as the ordinate. As discussed in Volume 6, Chapter 12, this ratio was plotted against the reciprocal of X_{tt}, the parameter for two-phase turbulent flow developed by Lockhart and Martinelli[9]. The liquid coefficient h_L is given by:

$$h_L = 0.023\left[\frac{k}{d_t}\right]\left[\frac{4W}{\pi d_t \mu_L}\right]^{0.8}\left[\frac{C_p\mu_L}{k}\right]^{0.4} \tag{14.4}$$

This book belongs to Bradley Loren (bloren@mcandrews-ip.com) Copyright Elsevier 2024
Intas Exhibit 1032
Page 165 of 470
PGR2025-00043

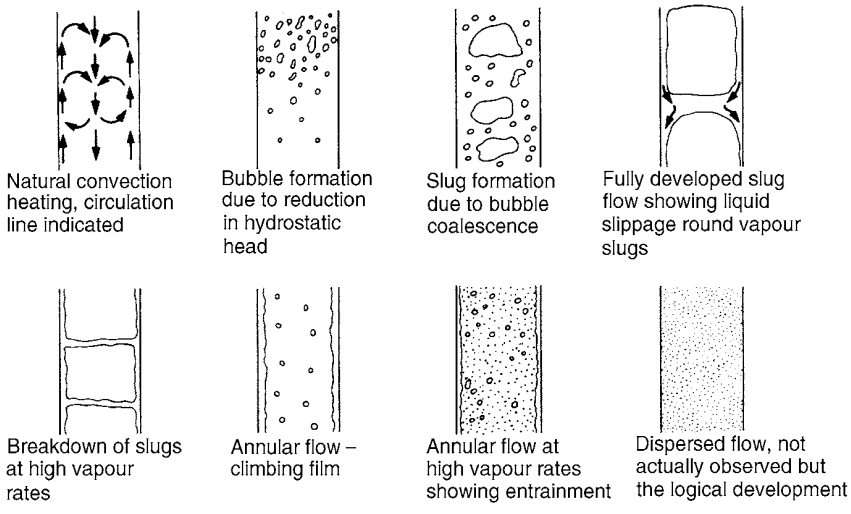


Figure 14.3. The nature of two-phase flow in an evaporator tube

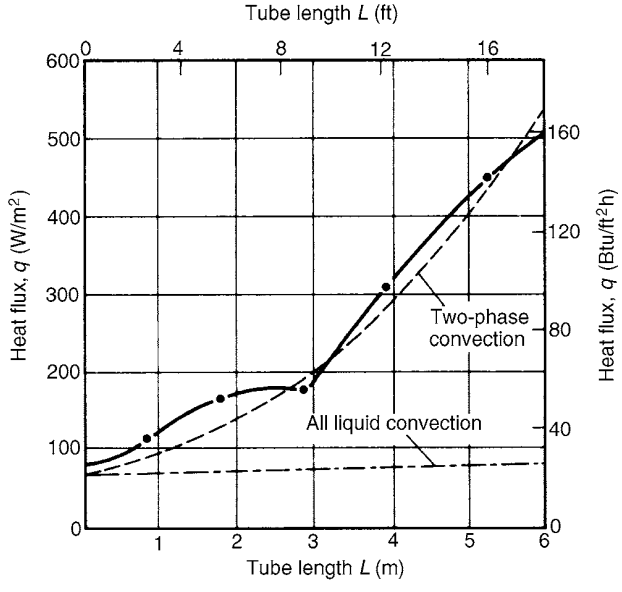


Figure 14.4. Variation of the heat flux to water in an evaporator tube[8]

where W is the total mass rate of flow. The parameter $1/X_{tt}$ is given by:

$$\frac{1}{X_{tt}} = \left[\frac{y}{1-y}\right]^{0.9} \left[\frac{\rho_L}{\rho_v}\right]^{0.5} \left[\frac{\mu_v}{\mu_L}\right]^{0.1} \tag{14.5}$$

This book belongs to Bradley Loren (bloren@mcandrews-ip.com) Copyright Elsevier 2024
Intas Exhibit 1032
Page 166 of 470
PGR2025-00043

$1/X_{tt}$ is strongly dependent on the mass fraction of vapour y. The density and viscosity terms give a quantitative correction for the effect of pressure in the absence of nucleate boiling.

Eighty-five per cent of the purely convective data for two-phase flow were correlated to within 20 per cent by the expression:

$$\frac{h_{tp}}{h_L} = 3.5\left[\frac{1}{X_{tt}}\right]^{0.5} \qquad \text{where } 0.25 < \frac{1}{X_{tt}} < 70 \tag{14.6}$$

Similar results for a range of organic liquids are reported by GUERRIERI and TALTY[10], though, in this work, h_L is based on the point mass flowrate of the unvaporised part of the stream, that is, W is replaced by $W(1-y)$ in equation 14.4.

One unusual characteristic of equation 14.2 is the dependence of h_b on the heat flux q. The calculation of h_b presents no difficulty in situations where the controlling parameter is the heat flux, as is the case with electrical heating. If a value of q is selected, this together with a knowledge of operating conditions and the physical properties of the boiling liquid permits the direct calculation of h_b. The surface temperature of the heater may now be calculated from q and h_b and the process is described completely. Considering the evaluation of a process involving heat transfer from steam condensing at temperature T_c to a liquid boiling at temperature T_b, assuming that the condensing coefficient is constant and specified as h_c, and also that the thermal resistance of the intervening wall is negligible, an initial estimate of the wall temperature T_w may be made. The heat flux q for the condensing film may now be calculated since $q = h_c(T_c - T_w)$, and the value of h_b may then be determined from equation 14.2 using this value for the heat flux. A heat balance across the wall tests the accuracy of the estimated value of T_w since $h_c(T_c - T_w)$ must equal $h_b(T_w - T_b)$, assuming the intervening wall to be plane. If the error in this heat balance is unacceptable, further values of T_w must be assumed until the heat balance falls within specified limits of accuracy.

A more refined design procedure would include the estimation of the steam-side coefficient h_c by one of the methods discussed in Volume 1, Chapter 9. Whilst such iterative procedures are laborious when carried out by hand, they are ideally handled by computers which enable a rapid evaluation to any degree of accuracy to be easily achieved.

14.2.4. Vacuum operation

With a number of heat sensitive liquids it is necessary to work at low temperatures, and this is effected by boiling under a vacuum, as indeed is the case in the last unit of a multi-effect system. Operation under a vacuum increases the temperature difference between the steam and boiling liquid as shown in Table 14.1 and therefore tends to increase the heat flux. At the same time, the reduced boiling point usually results in a more viscous material and a lower film heat transfer coefficient.

For a standard evaporator using steam at 135 kN/m^2 and 380 K with a total heat content of 2685 kJ/kg, evaporating a liquor such as water, the capacity under vacuum is $(101.3/13.5) = 7.5$ times great than that at atmospheric pressure. The advantage in capacity for the same unit is therefore considerable, though there is no real change in the consumption of steam in the unit. In practice, the advantages are not as great as this since

This book belongs to Bradley Loren (bloren@mcandrews-ip.com) Copyright Elsevier 2024

Intas Exhibit 1032
Page 167 of 470
PGR2025-00043

Table 14.1. Advantages of vacuum operation

	Atmospheric pressure (101.3 kN/m^2)	Vacuum Operation (13.5 kN/m^2)
Boiling point	373 K	325 K
Temperature drop to liquor	7 deg K	55 deg K
Heat lost in condensate	419 kJ/kg	216 kJ/kg
Heat used	2266 kJ/kg	2469 kJ/kg

operation at a lower boiling point reduces the value of the heat transfer coefficient and additional energy is required to achieve and maintain the vacuum.

14.3. SINGLE-EFFECT EVAPORATORS

Single-effect evaporators are used when the throughput is low, when a cheap supply of steam is available, when expensive materials of construction must be used as is the case with corrosive feedstocks and when the vapour is so contaminated so that it cannot be reused. Single effect units may be operated in batch, semi-batch or continuous batch modes or continuously. In strict terms, batch units require that filling, evaporating and emptying are consecutive steps. Such a method of operation is rarely used since it requires that the vessel is large enough to hold the entire charge of feed and that the heating element is low enough to ensure that it is not uncovered when the volume is reduced to that of the product. Semi-batch is the more usual mode of operation in which feed is added continuously in order to maintain a constant level until the entire charge reaches the required product density. Batch-operated evaporators often have a continuous feed and, over at least part of the cycle, a continuous discharge. Often a feed drawn from a storage tank is returned until the entire contents of the tank reach the desired concentration. The final evaporation is then achieved by batch operation. In essence, continuous evaporators have a continuous feed and discharge and concentrations of both feed and discharge remain constant.

The heat requirements of single-effect continuous evaporators may be obtained from mass and energy balances. If enthalpy data or heat capacity and heat of solution data are not available, heat requirements may be taken as the sum of the heat needed to raise the feed from feed to product temperature and the heat required to evaporate the water. The latent heat of water is taken at the vapour head pressure instead of the product temperature in order to compensate, at least to some extent, for the heat of solution. If sufficient vapour pressure data are available for the liquor, methods are available for calculating the true latent heat from the slope of the Dühring line and detailed by Othmer[11]. The heat requirements in batch operation are generally similar to those in continuous evaporation. Whilst the temperature and sometimes the pressure of the vapour will change during the course of the cycle which results in changes in enthalpy, since the enthalpy of water vapour changes only slightly with temperature, the differences between continuous and batch heat requirements are almost negligible for all practical purposes. The variation of the fluid properties, such as viscosity and boiling point rise, have a much greater effect on heat transfer, although these can only be estimated by a step-wise calculation. In

This book belongs to Bradley Loren (bloren@mcandrews-ip.com) Copyright Elsevier 2024

Intas Exhibit 1032
Page 168 of 470
PGR2025-00043

estimating the boiling temperature, the effect of temperature on the heat transfer characteristics of the type of unit involved must be taken into account. At low temperatures some evaporator types show a marked drop in the heat transfer coefficient which is often more than enough to offset any gain in available temperature difference. The temperature and cost of the cooling water fed to the condenser are also of importance in this respect.

Example 14.1

A single-effect evaporator is used to concentrate 7 kg/s of a solution from 10 to 50 per cent solids. Steam is available at 205 kN/m^2 and evaporation takes place at 13.5 kN/m^2. If the overall coefficient of heat transfer is 3 kW/m^2 deg K, estimate the heating surface required and the amount of steam used if the feed to the evaporator is at 294 K and the condensate leaves the heating space at 352.7 K. The specific heats of 10 and 50 per cent solutions are 3.76 and 3.14 kJ/kg deg K respectively.

Solution

Assuming that the steam is dry and saturated at 205 kN/m^2, then from the Steam Tables in the Appendix, the steam temperature = 394 K at which the total enthalpy = 2530 kJ/kg.

At 13.5 kN/m^2, water boils at 325 K and, in the absence of data on the boiling point elevation, this will be taken as the temperature of evaporation, assuming an aqueous solution. The total enthalpy of steam at 325 K is 2594 kJ/kg.

Thus the feed, containing 10 per cent solids, has to be heated from 294 to 325 K at which temperature the evaporation takes place.

$$\text{In the feed, mass of dry solids} = (7 \times 10)/100 = 0.7 \text{ kg/s}$$

and, for x kg/s of water in the product:

$$(0.7 \times 100)/(0.7 + x) = 50$$

from which:

$$x = 0.7 \text{ kg/s}$$

Thus:

$$\text{water to be evaporated} = (7.0 - 0.7) - 0.7 = 5.6 \text{ kg/s}$$

Summarising:

Stream	Solids (kg/s)	Liquid (kg/s)	Total (kg/s)
Feed	0.7	6.3	7.0
Product	0.7	0.7	1.4
Evaporation		5.6	5.6

Using a datum of 273 K:

Heat entering with the feed = $(7.0 \times 3.76)(294 - 273) = 552.7$ kW

Heat leaving with the product = $(1.4 \times 3.14)(325 - 273) = 228.6$ kW

Heat leaving with the evaporated water = $(5.6 \times 2594) = 14,526$ kW

Thus:

Heat transferred from the steam = $(14526 + 228.6) - 552.7 = 14,202$ kW

This book belongs to Bradley Loren (bloren@mcandrews-ip.com) Copyright Elsevier 2024

Intas Exhibit 1032
Page 169 of 470
PGR2025-00043

The enthalpy of the condensed steam leaving at 352.7 K $= 4.18(352.7 - 273) = 333.2$ kJ/kg

The heat transferred from 1 kg steam $= (2530 - 333.2) = 2196.8$ kJ/kg

and hence:

$$\text{Steam required} = (14,202/2196.8) = \underline{\underline{6.47 \text{ kg/s}}}$$

As the preheating of the solution and the sub-cooling of the condensate represent but a small proportion of the heat load, the temperature driving force may be taken as the difference between the temperatures of the condensing steam and the evaporating water, or:

$$\Delta T = (394 - 325) = 69 \text{ deg K}$$

Thus: Heat transfer area, $A = Q/U\Delta T$ (equation 14.1)

$$= 14,202/(3 \times 69) = \underline{\underline{68.6 \text{ m}^2}}$$

14.4. MULTIPLE-EFFECT EVAPORATORS

The single effect evaporator uses rather more than 1 kg of steam to evaporate 1 kg of water. Three methods have been introduced which enable the performance to be improved, either by direct reduction in the steam consumption, or by improved energy efficiency of the whole unit. These are:

(a) Multiple effect operation
(b) Recompression of the vapour rising from the evaporator
(c) Evaporation at low temperatures using a heat pump cycle.

The first of these is considered in this section and (b) and (c) are considered in Section 14.5.

14.4.1. General principles

If an evaporator, fed with steam at 399 K with a total heat of 2714 kJ/kg, is evaporating water at 373 K, then each kilogram of water vapour produced will have a total heat content of 2675 kJ. If this heat is allowed to go to waste, by condensing it in a tubular condenser or by direct contact in a jet condenser for example, such a system makes very poor use of steam. The vapour produced is, however, suitable for passing to the calandria of a similar unit, provided the boiling temperature in the second unit is reduced so that an adequate temperature difference is maintained. This, as discussed in Section 14.2.4, can be effected by applying a vacuum to the second effect in order to reduce the boiling point of the liquor. This is the principle reached in the multiple effect systems which were introduced by Rillieux in about 1830.

For three evaporators arranged as shown in Figure 14.5, in which the temperatures and pressures are T_1, T_2, T_3, and P_1, P_2, P_3, respectively, in each unit, if the liquor has no

This book belongs to Bradley Loren (bloren@mcandrews-ip.com) Copyright Elsevier 2024

Intas Exhibit 1032
Page 170 of 470
PGR2025-00043

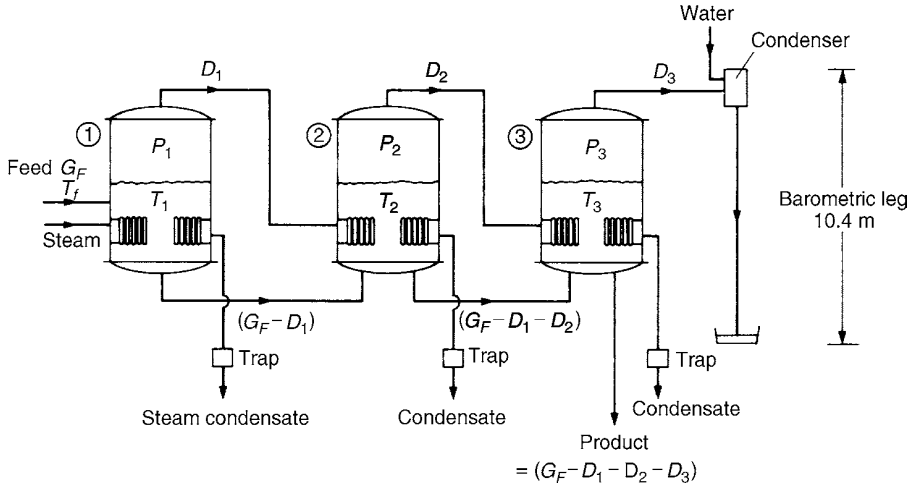


Figure 14.5. Forward-feed arrangement for a triple-effect evaporator

boiling point rise, then the heat transmitted per unit time across each effect is:

Effect 1 $\quad Q_1 = U_1 A_1 \Delta T_1, \quad$ where $\Delta T_1 = (T_0 - T_1)$,

Effect 2 $\quad Q_2 = U_2 A_2 \Delta T_2, \quad$ where $\Delta T_2 = (T_1 - T_2)$,

Effect 3 $\quad Q_3 = U_3 A_3 \Delta T_3, \quad$ where $\Delta T_3 = (T_2 - T_3)$.

Neglecting the heat required to heat the feed from T_f to T_1, the heat Q_1 transferred across where A_1 appears as latent heat in the vapour D_1 and is used as steam in the second effect, and:

$$Q_1 = Q_2 = Q_3$$

So that:
$$U_1 A_1 \Delta T_1 = U_2 A_2 \Delta T_2 = U_3 A_3 \Delta T_3 \tag{14.7}$$

If, as is commonly the case, the individual effects are identical, $A_1 = A_2 = A_3$, and:

$$U_1 \Delta T_1 = U_2 \Delta T_2 = U_3 \Delta T_3 \tag{14.8}$$

On this analysis, the difference in temperature across each effect is inversely proportional to the heat transfer coefficient. This represents a simplification, however, since:

(a) the heat required to heat the feed from T_f to T_1 has been neglected, and
(b) the liquor passing from stages ① to ② carries heat into the second effect, and this is responsible for some evaporation. This is also the case in the third effect.

The latent heat required to evaporate 1 kg of water in ①, is approximately equal to the heat obtained in condensing 1 kg of steam at T_0.

This book belongs to Bradley Loren (bloren@mcandrews-ip.com) Copyright Elsevier 2024

Intas Exhibit 1032
Page 171 of 470
PGR2025-00043

Thus 1 kg of steam fed to ① evaporates 1 kg of water in ①. Again the 1 kg of steam from ① evaporates about 1 kg of steam in ②. Thus, in a system of N effects, 1 kg of steam fed to the first effect will evaporate in all about N kg of liquid. This gives a simplified picture, as discussed later, although it does show that one of the great attractions of a multiple-effect system is that considerably more evaporation per kilogram of steam is obtained than in a single-effect unit. The economy of the system, measured by the kilograms of water vaporised per kilogram of steam condensed, increases with the number of effects.

The water evaporated in each effect is proportional to Q, since the latent heat is approximately constant. Thus the total capacity is:

$$\begin{aligned} Q &= Q_1 + Q_2 + Q_3 \\ &= U_1 A_1 \Delta T_1 + U_1 A_2 \Delta T_2 + U_3 A_3 \Delta T_3 \end{aligned} \tag{14.9}$$

If an average value of the coefficients U_{av} is taken, then:

$$Q = U_{av}(\Delta T_1 + \Delta T_2 + \Delta T_3)A \tag{14.10}$$

assuming the area of each effect is the same. A single-effect evaporator operating with a temperature difference $\Sigma\Delta T$, with this average coefficient U_{av}, would, however, have the same capacity $Q = U_{av} A \Sigma\Delta T$. Thus, it is seen that the capacity of a multiple-effect system is the same as that of a single effect, operating with the same total temperature difference and having an area A equal to that of one of the multiple-effect units. The value of the multiple-effect system is that better use is made of steam although, in order to achieve this, a much higher capital outlay is required for the increased number of units and accessories.

14.4.2. The calculation of multiple-effect systems

In the equations considered in Section 14.4.1, various simplifying assumptions have been made which are now considered further in the calculation of a multiple-effect system. In particular, the temperature distribution in such a system and the heat transfer area required in each effect are determined. The method illustrated in Example 14.2 is essentially based on that of HAUSBRAND[12].

Example 14.2A (Forward-feed)

4 kg/s (14.4 tonne/hour) of a liquor containing 10 per cent solids is fed at 294 K to the first effect of a triple-effect unit. Liquor with 50 per cent solids is to be withdrawn from the third effect, which is at a pressure of 13 kN/m^2 (~0.13 bar). The liquor may be assumed to have a specific heat of 4.18 kJ/kg K and to have no boiling point rise. Saturated dry steam at 205 kN/m^2 is fed to the heating element of the first effect, and the condensate is removed at the steam temperature in each effect as shown in Figure 14.5.

If the three units are to have equal areas, estimate the area, the temperature differences and the steam consumption. Heat transfer coefficients of 3.1, 2.0 and 1.1 kW/m^2 K for the first, second, and third effects respectively, may be assumed.

This book belongs to Bradley Loren (bloren@mcandrews-ip.com) Copyright Elsevier 2024

Intas Exhibit 1032
Page 172 of 470
PGR2025-00043

Solution 1

A precise theoretical solution is neither necessary nor possible, since during the operation of the evaporator, variations of the liquor levels, for example, will alter the heat transfer coefficients and hence the temperature distribution. It is necessary to assume values of heat transfer coefficients, although, as noted previously, these will only be approximate and will be based on practical experience with similar liquors in similar types of evaporators.

Temperature of dry saturated steam at 205 kN/m^2 = 394 K.

At a pressure of 13 kN/m^2 (0.13 bar), the boiling point of water is 325 K, so that the total temperature difference $\Sigma\Delta T = (394 - 325) = 69$ deg K.

First Approximation.

Assuming that: $U_1\Delta T_1 = U_2\Delta T_2 = U_3\Delta T_3$ (equation 14.8)

then substituting the values of U_1, U_2 and U_3 and $\Sigma\Delta T = 69$ deg K gives:

$$\Delta T_1 = 13 \text{ deg K}, \quad \Delta T_2 = 20 \text{ deg K}, \quad \Delta T_3 = 36 \text{ deg K}$$

Since the feed is cold, it will be necessary to have a greater value of ΔT_1 than given by this analysis. It will be assumed that $\Delta T_1 = 18$ deg K, $\Delta T_2 = 17$ deg K, $\Delta T_3 = 34$ deg K.

If the latent heats are given by λ_0, λ_1, λ_2 and λ_3, then from the Steam Tables in the Appendix:

For steam to 1:	$T_0 = 394$ K and $\lambda_0 = 2200$ kJ/kg
For steam to 2:	$T_1 = 376$ K and $\lambda_1 = 2249$ kJ/kg
For steam to 3:	$T_2 = 359$ K and $\lambda_2 = 2293$ kJ/kg
	$T_3 = 325$ K and $\lambda_3 = 2377$ kJ/kg

Assuming that the condensate leaves at the steam temperature, then heat balances across each effect may be made as follows:

Effect 1:

$$D_0\lambda_0 = G_F C_p(T_1 - T_f) + D_1\lambda_1, \text{ or } 2200\ D_0 = 4 \times 4.18(376 - 294) + 2249\ D_1$$

Effect 2:

$$D_1\lambda_1 + (G_F - D_1)C_p(T_1 - T_2) = D_2\lambda_2, \text{ or } 2249\ D_1 + (4 - D_1)4.18(376 - 359) = 2293\ D_2$$

Effect 3:

$$D_2\lambda_2 + (G_F - D_1 - D_2)C_p(T_2 - T_3) = D_3\lambda_3,$$

$$\text{or } 2293\ D_2 + (4 - D_1 - D_2)4.18(359 - 325) = 2377\ D_3$$

where G_F is the mass flowrate of liquor fed to the system, and C_p is the specific heat capacity of the liquid, which is assumed to be constant.

A material balance over the evaporator is:

	Solids (kg/s)	Liquor (kg/s)	Total (kg/s)
Feed	0.4	3.6	4.0
Product	0.4	0.4	0.8
Evaporation		3.2	3.2

This book belongs to Bradley Loren (bloren@mcandrews-ip.com) Copyright Elsevier 2024

Intas Exhibit 1032
Page 173 of 470
PGR2025-00043

Making use of the previous equations and the fact that $(D_1 + D_2 + D_3) = 3.2$ kg/s, the evaporation in each unit is, $D_1 \approx 0.991$, $D_2 \approx 1.065$, $D_3 \approx 1.144$, $D_0 \approx 1.635$ kg/s. The area of the surface of each calandria necessary to transmit the necessary heat under the given temperature difference may then be obtained as:

$$A_1 = \frac{D_0\lambda_0}{U_1\Delta T_1} = \frac{(1.635 \times 2200)}{(3.1 \times 18)} = 64.5 \text{ m}^2$$

$$A_2 = \frac{D_1\lambda_1}{U_2\Delta T_2} = \frac{(0.991 \times 2249)}{(2.0 \times 17)} = 65.6 \text{ m}^2$$

$$A_3 = \frac{D_2\lambda_2}{U_3\Delta T_3} = \frac{(1.085 \times 2293)}{(1.1 \times 34)} = 65.3 \text{ m}^2$$

These three calculated areas are approximately equal, so that the temperature differences assumed may be taken as nearly correct. In practice, ΔT_1 would have to be a little larger since A_1 is the smallest area. It may be noted that, on the basis of these calculations, the economy is given by $e = (3.2/1.635) = \underline{\underline{2.0}}$. Thus, a triple effect unit working under these conditions gives a reduction in steam utilisation compared with a single effect, though not as large an economy as might be expected.

A simplified method of solving problems of multiple effect evaporation, suggested by STORROW[13], is particularly useful for systems with a large number of effects because it obviates the necessity for solving many simultaneous equations. Essentially the method depends on obtaining only an approximate value for those heat quantities which are a small proportion of the whole. Example 14.2A is now solved by this method.

Solution 2

From Figure 14.5 it may be seen that for a feed G_F to the first effect, vapour D_1 and liquor $(G_F - D_1)$ are fed forward to the second effect. In the first effect, steam is condensed partly in order to raise the feed to its boiling point and partly to effect evaporation. In the second effect, further vapour is produced mainly as a result of condensation of the vapour from the first effect and to a smaller extent by flash vaporisation of the concentrated liquor which is fed forward. As the amount of vapour produced by the latter means is generally only comparatively small, this may be estimated only approximately. Similarly, the vapour produced by flash evaporation in the third effect will be a small proportion of the total and only an approximate evaluation is required.

Vapour production by flash vaporisation — approximate evaluation

If the heat transferred in each effect is the same, then:

$$U_1\Delta T_1 = U_2\Delta T_2 = U_3\Delta T_3 \qquad \text{(equation 14.8)}$$

or: $$3.1\Delta T_1 = 2.0\Delta T_2 = 1.1\Delta T_3$$

Steam temperature = 394 K. Temperature in condenser = 325 K.

Thus: $$\Sigma\Delta T = (394 - 325) = 69 \text{ deg K}$$

Solving: $$\Delta T_1 = 13 \text{ deg K} \quad \Delta T_2 = 20 \text{ deg K} \quad \Delta T_3 = 36 \text{ deg K}$$

These values of ΔT will be valid provided the feed is approximately at its boiling point.

This book belongs to Bradley Loren (bloren@mcandrews-ip.com) Copyright Elsevier 2024

Intas Exhibit 1032
Page 174 of 470
PGR2025-00043

Weighting the temperature differences to allow for the fact that the feed enters at ambient temperature gives:

$$\Delta T_1 = 18 \text{ deg K} \quad \Delta T_2 = 18 \text{ deg K} \quad \Delta T_3 = 33 \text{ deg K}$$

and the temperatures in each effect are:

$$T_1 = 376 \text{ K} \quad T_2 = 358 \text{ K} \quad \text{and} \quad T_3 = 325 \text{ K}$$

The total evaporation $(D_1 + D_2 + D_3)$ is obtained from a material balance:

	Solids (kg/s)	Liquor (kg/s)	Total (kg/s)
Feed	0.4	3.6	4.0
Product	0.4	0.4	0.8
Evaporation		3.2	3.2

Assuming, as an approximation, equal evaporation in each effect, or $D_1 = D_2 = D_3 = 1.07$ kg/s, then the latent heat of flash vaporisation in the second effect is given by:

$$4.18(4.0 - 1.07)(376 - 358) = 220.5 \text{ kW}$$

and latent heat of flash vaporisation in the third effect is:

$$4.18(4.0 - 2 \times 1.07)(358 - 325) = 256.6 \text{ kW}$$

Final calculation of temperature differences

Subsequent calculations are considerably simplified if it is assumed that the latent heat of vaporisation is the same at all temperatures in the multiple-effect system, since under these conditions the condensation of 1 kg of steam gives rise to the formation of 1 kg of vapour.

Thus:

$$\text{At 394 K, the latent heat} = 2200 \text{ kJ/kg}$$

$$\text{At 325 K, the latent heat} = 2377 \text{ kJ/kg}$$

$$\text{Mean value, } \lambda = 2289 \text{ kJ/kg}$$

The amounts of heat transferred in each effect (Q_1, Q_2, Q_3) and in the condenser (Q_c) are related by:

$$Q_1 - G_F C_p (T_1 - T_f) = Q_2 = (Q_3 - 220.5) = (Q_c - 220.5 - 256.6)$$

or:

$$Q_1 - 4.0 \times 4.18(394 - \Delta T_1 - 294) = Q_2 = (Q_3 - 220.5) = (Q_c - 477.1) \text{ kW}$$

$$\text{Total evaporation} = (Q_2 + Q_3 + Q_c)/2289 = 3.2 \text{ kg/s}$$

Thus:

$$Q_2 + (Q_2 + 220.5) + (Q_2 + 477.1) = 7325 \text{ kW}$$

or:

$$Q_2 = 2209 \text{ kW}$$

$$Q_3 = 2430 \text{ kW}$$

This book belongs to Bradley Loren (bloren@mcandrews-ip.com) Copyright Elsevier 2024

Intas Exhibit 1032
Page 175 of 470
PGR2025-00043

and:
$$Q_1 = 2209 + 4.0 \times 4.18(394 - \Delta T_1 - 294)$$
$$= (3881 - 16.72\Delta T_1) \text{ kW}$$

Applying the heat transfer equations, then:

$$3881 - 16.72\Delta T_1 = 3.1A\Delta T_1, \quad \text{or} \quad A\Delta T_1 = (1252 - 5.4\Delta T_1) \text{ m}^2\text{K}$$
$$2209 = 2.0A\Delta T_2, \quad \text{or} \quad A\Delta T_2 = 1105 \text{ m}^2\text{K}$$
$$2430 = 1.1A\Delta T_3, \quad \text{or} \quad A\Delta T_3 = 2209 \text{ m}^2\text{K}$$

Further:
$$\Delta T_1 + \Delta T_2 + \Delta T_3 = 69 \text{ deg K}$$

Values of ΔT_1, ΔT_2, ΔT_3 are now chosen by trial and error to give equal values of A in each effect, as follows:

ΔT_1 (deg K)	A_1 (m^2)	ΔT_2 (deg K)	A_2 (m^2)	ΔT_3 (deg K)	A_3 (m^2)
18	64.2	18	61.4	33	66.9
19	60.5	17	65.0	33	66.9
18	64.2	17.5	63.1	33.5	65.9
18	64.2	17	65.0	34	64.9

The areas, as calculated in the last line, are approximately equal, so that the assumed temperature differences are acceptable and:

$$\text{Steam consumption} = (Q_1/2289) = (3580/2289) = 1.56 \text{ kg/s}$$
$$\text{Economy} = (3.2/1.56) \approx \underline{\underline{2.0}} \text{ kg/kg}$$

The calculation of areas in multiple-effect systems is relatively straightforward for one or two configurations, although it becomes tedious in the extreme where a wide range of operating conditions is to be investigated. Fortunately the calculations involved lend themselves admirably to processing by computer, and in this respect reference should be made to work such as that by STEWART and BEVERIDGE[14].

14.4.3. Comparison of forward and backward feeds

In the unit considered in Example 14.2A, the weak liquor is fed to effect ① and flows on to ② and then to ③. The steam is also fed to ①, and the process is known as forward-feed since the feed is to the same unit as the steam and travels down the unit in the same direction as the steam or vapour. It is possible, however, to introduce the weak liquor to effect ③ and cause it to travel from ③ to ② to ①, whilst the steam and vapour still travel in the direction of ① to ② to ③. This system, shown in Figure 14.6, is known as backward-feed. A further arrangement for the feed is known as parallel-feed, which is shown in Figure 14.7. In this case, the liquor is fed to each of the three effects in parallel although the steam is fed only to the first effect. This arrangement is commonly used in the concentration of salt solutions, where the deposition of crystals makes it difficult to use

This book belongs to Bradley Loren (bloren@mcandrews-ip.com) Copyright Elsevier 2024
Intas Exhibit 1032
Page 176 of 470
PGR2025-00043

the standard forward-feed arrangement. The effect of backward-feed on the temperature distribution, the areas of surface required, and the economy of the unit is of importance, and Example 14.2A is now considered for this flow arrangement.

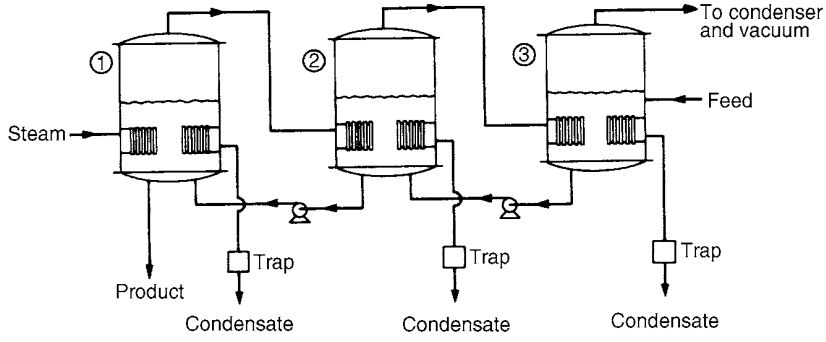


Figure 14.6. Backward-feed arrangement for a triple-effect evaporator

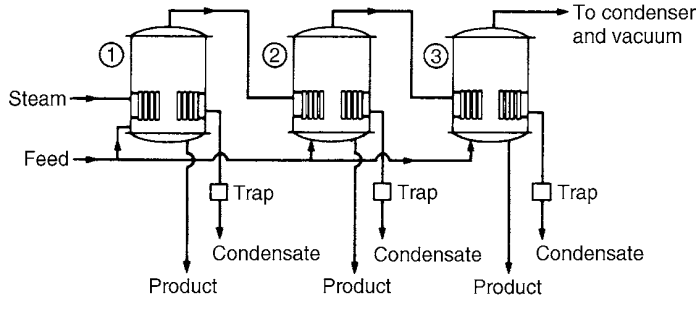


Figure 14.7. Parallel-feed arrangement for a triple-effect evaporator

Example 14.2B (Backward-Feed)

Since the dilute liquor is now at the lowest temperature and the concentrated liquor at the highest, the heat transfer coefficients will not be the same as in the case of forward-feed. In effect ①, the liquor is now much more concentrated than in the former case, and hence U_1 will not be as large as before. Again, on the same argument, U_3 will be larger than before. Although it is unlikely to be exactly the same, U_2 will be taken as being unaltered by the arrangement. Taking values of $U_1 = 2.5$, $U_2 = 2.0$ and $U_3 = 1.6$ kW/m^2 K, the temperature distribution may be determined in the same manner as for forward feed, by taking heat balances across each unit.

Solution 1

In this case, it is more difficult to make a reasonable first estimate of the temperature differences because the liquid temperature is increasing as it passes from effect to effect ($3 \rightarrow 2 \rightarrow 1$) and

This book belongs to Bradley Loren (bloren@mcandrews-ip.com) Copyright Elsevier 2024

Intas Exhibit 1032
Page 177 of 470
PGR2025-00043

sensible heat must be added at each stage. It may therefore be necessary to make several trial and error solutions before achieving the conditions for equal areas. In addition, the values of U_1, U_2 and U_3 may be different from those in forward-feed, depending as they do on concentration as well as on temperature.

Taking: $\Delta T_1 = 20$ deg K, $\Delta T_2 = 24$ deg K, $\Delta T_3 = 25$ deg K

The temperatures in the effect and the corresponding latent heats are:

$$T_0 = 394 \text{ K and } \lambda_0 = 2200 \text{ kJ/kg}$$
$$T_1 = 374 \text{ K and } \lambda_1 = 2254 \text{ kJ/kg}$$
$$T_2 = 350 \text{ K and } \lambda_2 = 2314 \text{ kJ/kg}$$
$$T_3 = 325 \text{ K and } \lambda_3 = 2377 \text{ kJ/kg}$$

The heat balance equations are then:

Effect 3:

$$D_2\lambda_2 = G_F C_p(T_3 - T_f) + D_3\lambda_3, \text{ or } 2314\ D_2 = 4 \times 4.18(325 - 294) + 2377\ D_3$$

Effect 2:

$$D_1\lambda_1 = (G_F - D_3)C_p(T_2 - T_3) + D_2\lambda_2, \text{ or } 2254\ D_1 = (4 - D_3)4.18(350 - 325) + 2314\ D_2$$

Effect 1:

$$D_0\lambda_0 = (G_F - D_3 - D_2)C_p(T_1 - T_2) + D_1\lambda_1,$$
$$\text{or } 2200\ D_0 = (4 - D_3 - D_2)4.18(374 - 350) + 2254\ D_1$$

Again taking $(D_1 + D_2 + D_3) = 3.2$ kg/s, these equations may be solved to give:

$$D_1 \approx 1.261,\ D_2 \approx 1.086,\ D_3 \approx 0.853,\ D_0 \approx 1.387 \text{ kg/s}$$

The areas of transfer surface are then:

$$A_1 = \frac{D_0\lambda_0}{U_1\Delta T_1} = \frac{(1.387 \times 2200)}{(2.5 \times 20)} = 61.0 \text{ m}^2$$
$$A_2 = \frac{D_1\lambda_1}{U_2\Delta T_2} = \frac{(1.261 \times 2254)}{(2.00 \times 24)} = 59.2 \text{ m}^2$$
$$A_3 = \frac{D_2\lambda_2}{U_3\Delta T_3} = \frac{(1.086 \times 2314)}{(1.6 \times 25)} = 62.8 \text{ m}^2$$

These three areas are approximately equal, so that the temperature differences suggested are sufficiently acceptable for design purposes. The economy for this system is $(3.2/1.387) = \underline{\underline{2.3}}$ kg/kg.

Solution 2

Using Storrow's method, as in Example 14.2A, the temperatures in the effects will be taken as:

$$T_1 = 374 \text{ K}, \quad T_2 = 350 \text{ K}, \quad T_3 = 325 \text{ K}$$

This book belongs to Bradley Loren (bloren@mcandrews-ip.com) Copyright Elsevier 2024

Intas Exhibit 1032
Page 178 of 470
PGR2025-00043

With backward-feed, as shown in Figure 14.6, the liquid has to be raised to its boiling point as it enters each effect.

The heat required to raise the feed to the second effect to its boiling point is:

$$= 4.18(4.0 - 1.07)(350 - 325)$$

$$= 306.2 \text{ kW}$$

The heat required to raise the feed to the first effect to its boiling point is:

$$= 4.18(4.0 - 2 \times 1.07)(374 - 350)$$

$$= 186.6 \text{ kW}$$

Assuming a constant value of 2289 kJ/kg for the latent heat in all the stages, the relation between the heat transferred in each effect and in the condenser is:

$$Q_1 - 186.6 = Q_2 = (Q_3 + 306.2) = (Q_c + 306.2 + 4 \times 4.18(325 - 294))$$

$$= Q_c + 824.5$$

$$\text{Total evaporation} = (Q_2 + Q_3 + Q_c)/2289 = 3.2 \text{ kg/s}$$

and: $$Q_2 + (Q_2 - 306.2) + (Q_2 - 824.5) = 7325 \text{ kW}$$

Thus: $$Q_2 = 2819 = A\Delta T_2 \times 2.0 \text{ kW}$$

$$Q_3 = 2512 = A\Delta T_3 \times 1.6 \text{ kW}$$

and: $$Q_1 = 3006 = A\Delta T_1 \times 2.5 \text{ kW}$$

or: $$A\Delta T_1 = 1202 \text{ m}^2 \text{ K}$$

$$A\Delta T_2 = 1410 \text{ m}^2 \text{ K}$$

$$A\Delta T_3 = 1570 \text{ m}^2 \text{ K}$$

and: $$\Delta T_1 + \Delta T_2 + \Delta T_3 = 69 \text{ deg K}$$

Thus:

ΔT_1 (deg K)	A_1 (m^2)	ΔT_2 (deg K)	A_2 (m^2)	ΔT_3 (deg K)	A_3 (m^2)
20	60.1	24	58.9	25	62.8

The areas are approximately equal and the assumed values of ΔT are therefore acceptable.

$$\text{Economy} = \frac{3.2}{(3006/2289)} = \underline{\underline{2.4}} \text{ kg/kg}$$

On the basis of heat transfer area and thermal considerations, a comparison of the two methods of feed is:

	Forward	Backward
Total steam used D_0 (kg)	1.635	1.387
Economy (kg/kg)	2.0	2.3
Condenser load D_3 (kg)	1.44	0.853
Heat transfer surface per effect A (m^2)	65.1	61.0

This book belongs to Bradley Loren (bloren@mcandrews-ip.com) Copyright Elsevier 2024

Intas Exhibit 1032
Page 179 of 470
PGR2025-00043

For the conditions of Example 14.2, the backward feed system shows a reduction in steam consumption, an improved economy, a reduction in condenser load, and a small reduction in heat transfer area.

Effect of feed system on economy

In the case of forward feed systems, all the liquor has to be heated from T_f to T_1 by steam although, in the case of backward feed, the heating of the feed in the last effect is done with steam that has already evaporated $(N - 1)$ times its own mass of water, assuming ideal conditions. The feed temperature must therefore be regarded as a major feature in this class of problem. WEBRE[15] has examined the effect of feed temperature on the economy and the evaporation in each effect, for the case of a liquor fed at the rate of 12.5 kg/s to a triple-effect evaporator in which a concentrated product was obtained at a flowrate of 8.75 kg/s. Neglecting boiling-point rise and working with a fixed vacuum on the third effect, the curves shown in Figures 14.8 and 14.9 for the three methods of forward, backward and parallel feed were prepared.

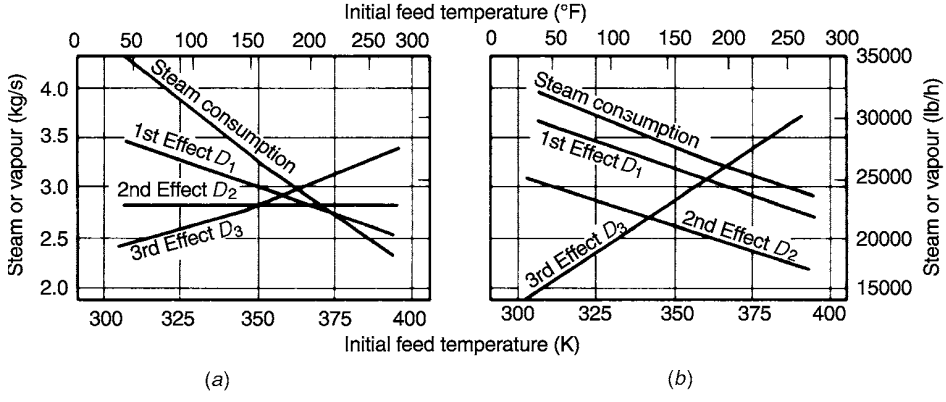


Figure 14.8. Effect of feed temperature on the operation of a triple effect evaporator (*a*) Forward feed (*b*) Backward feed

Figure 14.8*a* illustrates the drop in steam consumption as the feed temperature is increased with forward feed. It may be seen that, for these conditions, D_1 falls, D_2 remains constant and D_3 rises with increase in the feed temperature T_f. With backward feed shown in Figure 14.8*b*, the fall in steam consumption is not so marked and it may be seen that, whereas D_1 and D_2 fall, the load on the condenser D_3 increases. The results are conveniently interpreted in Figure 14.9, which shows that the economy increases with T_f for a forward-feed system to a marked extent, whilst the corresponding increase with the backward-feed system is relatively small. At low values of T_f, the backward feed gives the higher economy. At some intermediate value, the two systems give the same value of economy, whilst for high values of T_f the forward-feed system is more economical in steam.

These results, whilst showing the influence of T_f on the economy, should not be interpreted too rigidly, since the values for the coefficients for the two systems and

This book belongs to Bradley Loren (bloren@mcandrews-ip.com) Copyright Elsevier 2024

Intas Exhibit 1032
Page 180 of 470
PGR2025-00043

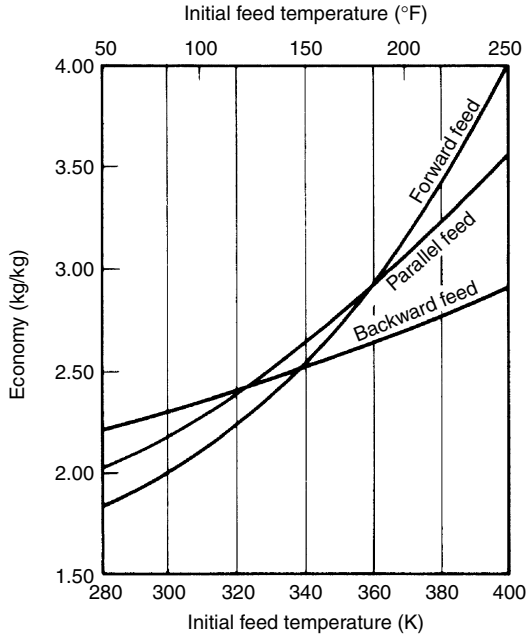


Figure 14.9. Economy of triple-effect evaporators

the influence of boiling-point rise may make a substantial difference to these curves. In general, however, it will be found that with cold feeds the backward-feed system is more economical. Despite this fact, the forward-feed system is the most common, largely because it is the simplest to operate, whilst backward feed requires the use of pumps between each effect.

The main criticism of the forward-feed system is that the most concentrated liquor is in the last effect, where the temperature is lowest. The viscosity is therefore high and low values of U are obtained. In order to compensate for this, a large temperature difference is required, and this limits the number of effects. It is sometimes found, as in the sugar industry, that it is preferable to run a multiple-effect system up to a certain concentration, and to run a separate effect for the final stage where the crystals are formed.

14.5. IMPROVED EFFICIENCY IN EVAPORATION

14.5.1. Vapour compression evaporators

Considering an evaporator fed with saturated steam at 387 K, equivalent to 165 kN/m^2, concentrating a liquor boiling at 373 K at atmospheric pressure, if the condensate leaves at 377 K, then:

1 kg of steam at 387 K has a total heat of 2698 kJ.
1 kg of condensate at 377 K has a total heat of 437 kJ and
the heat given up is 2261 kJ/kg steam.

This book belongs to Bradley Loren (bloren@mcandrews-ip.com) Copyright Elsevier 2024
Intas Exhibit 1032
Page 181 of 470
PGR2025-00043

If this condensate is returned to the boiler, then at least 2261 kJ/kg must be added to yield 1 kg of steam to be fed back to the evaporator. In practice, of course, more heat per kilogram of condensate will be required. 2261 kJ will vaporise 1 kg of liquid at atmospheric pressure to give vapour with a total heat of 2675 kJ/kg. To regenerate 1 kg of steam in the original condition from this requires the addition of only 23 kJ. The idea of vapour compression is to make use of the vapour from the evaporator, and to upgrade it to the condition of the original steam. Such a system offers enormous advantages in thermal economy, though it is by no means easy to add the 23 kJ to each kilogram of vapour in an economical manner. The two methods available are:

(a) the use of steam-jet ejectors as shown in Figure 14.10, and:
(b) the use of mechanical compressors as shown in Figure 14.11.

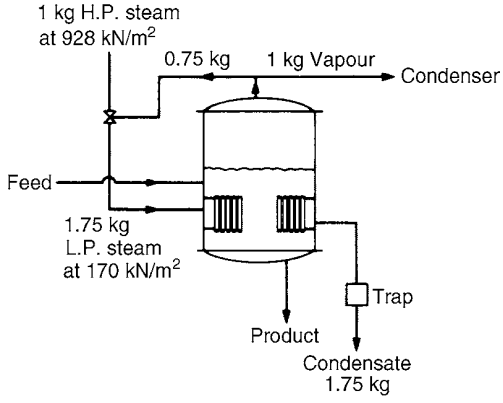


Figure 14.10. Vapour compression evaporator with high pressure steam-jet compression

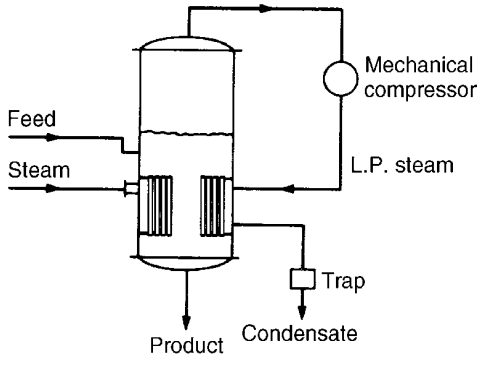


Figure 14.11. Vapour compression evaporator with a mechanical compressor

This book belongs to Bradley Loren (bloren@mcandrews-ip.com) Copyright Elsevier 2024

Intas Exhibit 1032
Page 182 of 470
PGR2025-00043

In selecting a compressor for this type of operation, the main difficulty is the very large volume of vapour to be handled. Rotary compressors of the Rootes type, described in Volume 1, Chapter 8, are suitable for small and medium size units, though these have not often been applied to large installations. Mechanical compressors have been used extensively in evaporation systems for the purification of sea water.

The use of an ejector, fed with high-pressure steam, is illustrated in Figure 14.10. High-pressure steam is injected through a nozzle and the low-pressure vapours are drawn in through a second inlet at right angles, the issuing jet of steam passing out to the calandria, as shown. These units are relatively simple in construction and can be made of corrosion-resistant material. They have no moving parts and for this reason will have a long life. They have the great advantage over mechanical compressors in that they can handle large volumes of vapour and can therefore be arranged to operate at very low pressures. The disadvantage of the steam-jet ejector is that it works at maximum efficiency at only one specific condition. Some indication of the performance of these units is shown in Figure 14.12, where the pressure of the mixture, for different amounts of vapour compressed per kilogram of live steam, is shown for a series of different pressures. With an ejector of these characteristics using steam at 965 kN/m^2, 0.75 kg vapour/kg steam can be compressed to give 1.75 kg of vapour at 170 kN/m^2. An evaporator unit, as shown in Figure 14.11, will therefore give 1.75 kg of vapour/kg high pressure steam. Of the 1.75 kg of vapour, 0.75 kg is taken to the compressor and the remaining 1 kg to the condenser. Ideally, this single-effect unit gives an economy of 1.75, or approximately the economy of a double-effect unit.

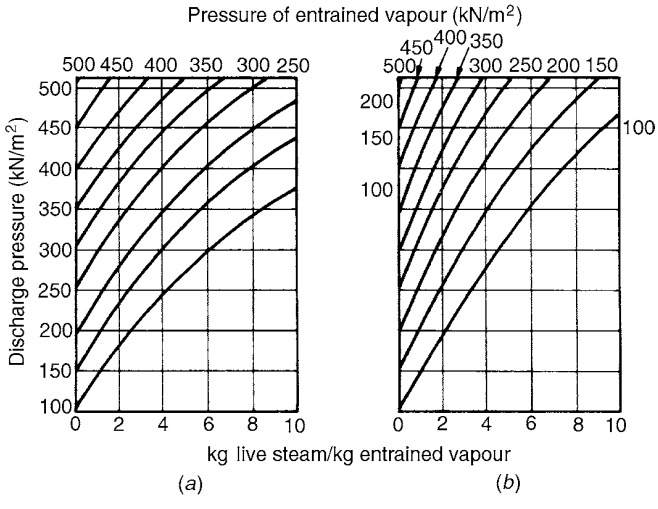


Figure 14.12. Performance of a steam jet ejector, (*a*) 790 kN/m^2 operating pressure, (*b*) 1135 kN/m^2 operating pressure

Vapour compression may be applied to the vapour from the first effect of a multiple-effect system, thus giving increased utilisation of the steam. Such a device is not suitable for use with liquors with a high boiling-point rise, for in these cases the vapour, although

This book belongs to Bradley Loren (bloren@mcandrews-ip.com) Copyright Elsevier 2024
Intas Exhibit 1032
Page 183 of 470
PGR2025-00043

initially superheated, has to be compressed to such a great degree, in order to give the desired temperature difference across the calandria, that the efficiency is reduced. The application of these compressors depends on the steam load of the plant. If there is plenty of low-pressure steam available, then the use of vapour compression can rarely be advocated. If, however, high-pressure steam is available, then it may be used to advantage in a vapour compression unit. It will, in fact, be far superior to the practice of passing high-pressure steam through a reducing valve to feed an evaporator.

Example 14.3

Saturated steam leaving an evaporator at atmospheric pressure is compressed by means of saturated steam at 1135 kN/m^2 in a steam jet to a pressure of 135 kN/m^2. If 1 kg of the high-pressure steam compresses 1.6 kg of the vapour produced at atmospheric pressure, comment on the efficiency of the compressor.

Solution

The efficiency of an ejector η' is given by:

$$\eta' = (m_1 + m_2)(H_4 - H_3)/[m_1(H_1 - H_2)]$$

where m_1 is the mass of high-pressure steam (kg), m_2 is the mass of entrained steam (kg), H_1 is the enthalpy of high-pressure steam (kJ/kg), H_2 is the enthalpy of steam after isentropic expansion in the nozzle to the pressure of the entrained vapours (kJ/kg), H_3 is the enthalpy of the mixture at the start of compression in the diffuser section (kJ/kg), and H_4 is the enthalpy of the mixture after isentropic compression to the discharge pressure (kJ/kg).

The high-pressure steam is saturated at 1135 kN/m^2 at which $H_1 = 2780$ kJ/kg. If this is allowed to expand isentropically to 101.3 kN/m^2, then from the entropy–enthalpy chart, given in the Appendix, $H_2 = 2375$ kJ/kg and the dryness faction is 0.882.

Making an enthalpy balance across the system, then:

$$m_1 H_1 + m_2 H_e = (m_1 + m_2) H_4$$

where H_e is the enthalpy of entrained steam. Since this is saturated at 101.3 kN/m^2, then:

$$H_e = 2690 \text{ kJ/kg} \quad \text{and } (1 \times 2780) + (1.6 \times 2690) = (1.0 + 1.6) H_4$$

from which: $$H_4 = 2725 \text{ kJ/kg}$$

Again assuming isentropic compression from 101.3 to 135 kN/m^2, then:

$$H_3 = 2640 \text{ kJ/kg (from the chart)}$$

and: $$\eta' = (1.0 + 1.6)(2725 - 2640)/[1.0(2780 - 2375)] = \underline{\underline{0.55}}$$

This value is low, since in good design overall efficiencies approach 0.75–0.80. Obviously the higher the efficiency the greater the entrainment ratio or the higher the saving in live steam. The low efficiency is borne out by examination of Figure 14.12*b*, which applies for an operating pressure of 1135 kN/m^2.

This book belongs to Bradley Loren (bloren@mcandrews-ip.com) Copyright Elsevier 2024

Intas Exhibit 1032
Page 184 of 470
PGR2025-00043

Since the pressure of entrained vapour = 101.3 kN/m^2 and the discharge pressure = 135 kN/m^2, the required flow of live steam = 0.5 kg/kg entrained vapour.

In this case the ratio is (1.0/1.6) = 0.63 kg/kg.

Example 14.4

Distilled water is produced from sea water by evaporation in a single-effect evaporator working on the vapour compression system. The vapour produced is compressed by a mechanical compressor at 50 per cent efficiency and then returned to the calandria of the evaporator. Additional steam, dry and saturated at 650 kN/m^2, is bled into the steam space through a throttling valve. The distilled water is withdrawn as condensate from the steam space. 50 per cent of the sea water is evaporated in the plant. The energy supplied in addition to that necessary to compress the vapour may be assumed to appear as superheat in the vapour.

Using the following data, calculate the quantity of additional steam required in kg/s.

Production of distillate = 0.125 kg/s, pressure in vapour space = 101.3 kN/m^2, temperature difference from steam to liquor = 8 deg K, boiling point rise of sea water = 1.1 deg K, specific heat capacity of sea water = 4.18 kJ/kg deg K. The sea water enters the evaporator at 344 K from an external heater.

Solution

The pressure in the vapour space is 101.3 kN/m^2 at which pressure, water boils at 373 K. The sea water is therefore boiling at (373 + 1.1) = 374.1 K and the temperature in the steam space is (374.1 + 8) = 382.1 K. At this temperature, steam is saturated at 120 kN/m^2 and has sensible and total enthalpies of 439 and 2683 kJ/kg respectively.

Making a *mass balance*, there are two inlet streams — the additional steam, say G_x kg/s, and the sea water feed, say G_y kg/s. The two outlet streams are the distilled water product, 0.125 kg/s, and the concentrated sea water, 0.5 G_y kg/s.

Thus: $$(G_x + G_y) = (0.125 + 0.5\ G_y) \text{ or } (G_x + 0.5\ G_y) = 0.125 \quad \text{(i)}$$

Making an *energy balance*, energy is supplied by the compressor and in the steam and inlet sea water and is removed by the sea water and the product. At 650 kN/m^2, the total enthalpy of the steam = 2761 kJ/kg. Thus the energy in this stream = 2761G_x kW. The sea water enters at 344 K.

Thus: $$\text{enthalpy of feed} = [G_y \times 4.18(344 - 273)] = 296.8G_y \text{ kW}$$

The sea water leaves the plant at 374.1 K and hence:

the enthalpy of the concentrated sea water = $(0.5G_y \times 4.18)(374.1 - 273) = 211.3G_y$ kW

The product has an enthalpy of 439 kJ/kg or $(439 \times 0.125) = 54.9$ kW

Making a balance:

$$(E + 2761G_x + 296.8G_y) = (211.3G_y + 54.9)$$

and: $$(E + 2761G_x + 85.5G_y) = 54.9 \quad \text{(ii)}$$

where E is the power supplied to the compressor.

This book belongs to Bradley Loren (bloren@mcandrews-ip.com) Copyright Elsevier 2024

Intas Exhibit 1032
Page 185 of 470
PGR2025-00043

Substituting from equation (i) into equation (ii) gives:

$$(E + 2761G_x) + 85.5(0.25 - 2G_x) = 54.9$$

and:
$$(E + 2590G_x) = 33.5 \quad \text{(iii)}$$

For a single-stage isentropic compression, the work done in compressing a volume V_1 of gas at pressure P_1 to a volume V_2 at pressure P_2 is given by equation 8.32 in Volume 1 as:

$$[P_1V_1/(\gamma - 1)][(P_2/P_1)^{\gamma-1/\gamma} - 1]$$

In the compressor, $0.5G_y$ kg/s vapour is compressed from $P_1 = 101.3$ kN/m^2, the pressure in the vapour space, to $P_2 = 120$ kN/m^2, the pressure in the calandria.

At 101.3 kN/m^2 and 374.1 K, the density of steam $= (18/22.4)(273/374.1) = 0.586$ kg/m^3

and hence the volumetric flowrate at pressure P_1 is $(0.5\ G_y/0.586) = 0.853\ G_y$ m^3/s

Taking $\gamma = 1.3$ for steam, then:

$$(E' \times 0.5G_y) = [(101.3 \times 0.853G_y)/(1.3 - 1)][(120/101.3)^{0..3/1..3} - 1]$$

$$0.5E'G_y = 288.0G_y(1.185^{0.231} - 1) = 11.5G_y$$

and:
$$E' = 23.0 \text{ kW/(kg/s)}$$

As the compressor is 50 per cent efficient, then:

$$E = (E/0.5) = 46.0 \text{ kW/(kg/s)}$$

$$= (46.0 \times 0.5G_y) = 23.0G_y \text{ kW}$$

Substituting in equation (ii) gives:

$$(E + 2761G_x) + 85.5(E/23.0) = 54.9$$

Thus:
$$2761G_x = (54.9 + 4.72E)$$

From equation (iii):
$$E = (33.5 - 2590G_x)$$

and in equation (iv):
$$2761G_x = 54.9 + 4.72(33.5 - 2590G_x)$$

from which:
$$G_x = \underline{\underline{0.014 \text{ kg/s}}}$$

Example 14.5

An evaporator operating on the thermo-recompression principle employs a steam ejector to maintain atmospheric pressure over the boiling liquid. The ejector uses 0.14 kg/s of steam at 650 kN/m^2 and superheated by 100 deg K and produces a pressure in the steam chest of 205 kN/m^2. A condenser removes surplus vapour from the atmospheric pressure line.

What is the capacity and economy of the system and how could the economy be improved?

Data

Properties of the ejector:

nozzle efficiency = 0.95, efficiency of momentum transfer = 0.80, efficiency of compression = 0.90.

The feed enters the evaporator at 295 K and concentrated liquor is withdrawn at the rate of 0.025 kg/s. This concentrated liquor exhibits a boiling-point rise of 10 deg K. The plant is sufficiently well lagged so that heat losses to the surroundings are negligible.

This book belongs to Bradley Loren (bloren@mcandrews-ip.com) Copyright Elsevier 2024

Intas Exhibit 1032
Page 186 of 470
PGR2025-00043

Solution

It is assumed that P_1 is the pressure of live steam = 650 kN/m^2 and P_2 is the pressure of entrained steam = 101.3 kN/m^2.

The enthalpy of the live steam at 650 kN/m^2 and (435 + 100) = 535 K, $H_1 = 2970$ kJ/kg.

Therefore H_2, the enthalpy after isentropic expansion from 650 to 101.3 kN/m^2, using an enthalpy–entropy chart, is $H_2 = 2605$ kJ/kg and the dryness fraction, $x_2 = 0.97$. The enthalpy of the steam after actual expansion to 101.3 kN/m^2 is given by H_2', where:

$$(H_1 - H_2') = 0.95(2970 - 2605) = 347 \text{ kJ/kg}$$

and:

$$H_2' = (2970 - 347) = 2623 \text{ kJ/kg}$$

At $P_2 = 101.3$ kN/m^2, $\lambda = 2258$ kJ/kg

and the dryness after expansion but before entrainment x_2' is given by:

$$(x_2' - x_2)\lambda = (1 - e_1)(H_1 - H_2)$$

or:

$$(x_2' - 0.97)2258 = (1 - 0.95)(2970 - 2605) \text{ and } x_2' = 0.978.$$

If x_2'' is the dryness after expansion *and* entrainment, then:

$$(x_2'' - x_2')\lambda = (1 - e_3)(H_1 - H_2')$$

or:

$$(x_2'' - 0.978)2258 = (1 - 0.80)(2970 - 2623) \text{ and } x_2'' = 1.00$$

Assuming that the steam at the discharge pressure $P_3 = 205$ kN/m^2 is also saturated, that is $x_3 = 1.00$, then from the steam chart in the Appendix, H_3 the enthalpy of the mixture at the start of compression in the diffuser section at 101.3 kN/m^2 is $H_3 = 2675$ kJ/kg. Again assuming the entrained steam is also saturated, the enthalpy of the mixture after isentropic compression in the diffuser from 101.3 to 205 kN/m^2, $H_4 = 2810$ kJ/kg.

The entrainment ratio is given by:

$$(m_2/m_1) = \{[(H_1 - H_2)/(H_4 - H_3)]\eta_1\eta_2\eta_3 - 1\}$$

where η_1, η_2 and η_3 are the efficiency of the nozzle, momentum transfer and compression, respectively.

Thus:

$$(m_2/m_1) = \{[(2970 - 2605)/(2810 - 2675)]0.95 \times 0.80 \times 0.90 - 1\}$$

$$= 0.85 \text{ kg vapour entrained/kg live steam}$$

It was assumed that $x_3 = 1.0$. This may be checked as follows:

$$x_3 = [x_2 + x_4(m_2/m_1)]/(1 + m_2/m_1)$$

$$= (1.0 + 1.0 \times 0.85)/(1 + 0.85) = 1.0$$

Thus with a flow of 0.14 kg/s live steam, the vapour entrained at 101.3 kN/m^2 is $(0.14 \times 0.85) = 0.12$ kg/s, giving 0.26 kg/s steam saturated at 205 kN/m^2 to the calandria.

Allowing for a 10 deg K boiling-point rise, the temperature of boiling liquor in the unit is $T_1' = 383$ K and taking the specific heat capacity as 4.18 kJ/kg K, then:

$$D_0\lambda_0 = G_F C_p(T_1' - T_f) + D_1\lambda_1$$

or:

$$0.26 \times 2200 = (G_F \times 4.18)(393 - 295) + (D_1 \times 2258)$$

This book belongs to Bradley Loren (bloren@mcandrews-ip.com) Copyright Elsevier 2024

Intas Exhibit 1032
Page 187 of 470
PGR2025-00043

$$572 = (368G_F + 2258D_1)$$

But: $(G_F - D_1) = 0.025$ kg/s and $D_1 = 0.214$ kg/s

Thus: the economy of system $= (0.214/0.14) = \underline{1.53}$

The capacity, in terms of the throughput of solution, is:

$$G_F = (0.214 + 0.025) = \underline{0.239 \text{ kg/s}}$$

Apart from increasing the efficiency of the ejector, the economy of the system might be improved by operating with a higher live-steam pressure, increasing the pressure in the vapour space, and by using the vapour not returned to the ejector to preheat the feed solution.

14.5.2. The heat pump cycle

The evaporation of citrus juices at temperatures up to 328 K, or of pharmaceutical products at even lower temperatures, has led to the development of an evaporator incorporating a heat-pump cycle using a separate working fluid. The use of the heat pump cycle, with ammonia as the working fluid is shown in Figure 14.13. In this arrangement, ammonia

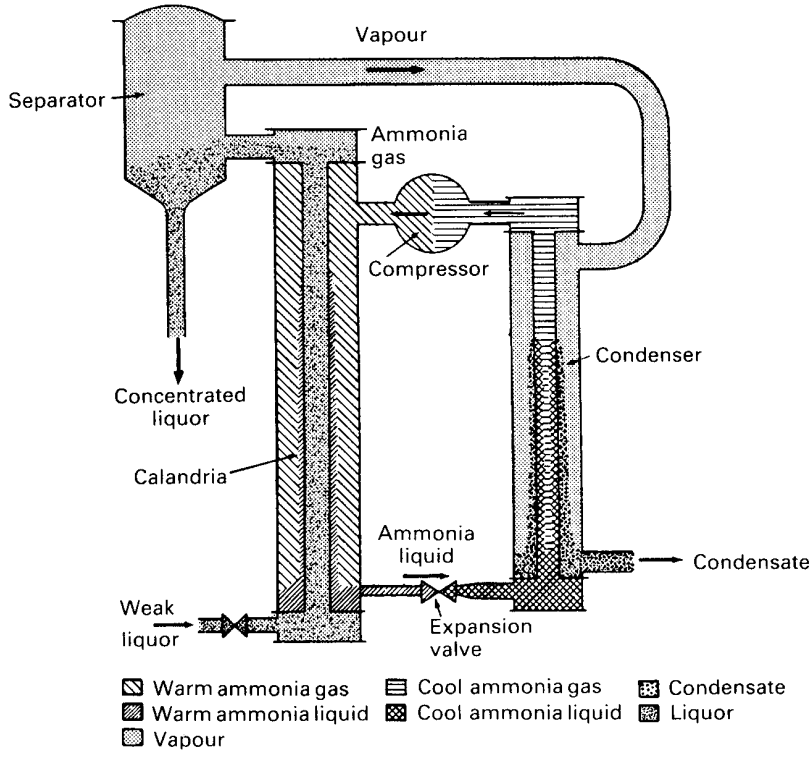


Figure 14.13. Heat pump cycle using ammonia

This book belongs to Bradley Loren (bloren@mcandrews-ip.com) Copyright Elsevier 2024

Intas Exhibit 1032
Page 188 of 470
PGR2025-00043

gas vaporises the feed liquor at 288–313 K. The ammonia is condensed and the liquid ammonia is then passed through an expansion valve, where it is cooled to a much lower temperature. The cooled liquid ammonia then enters the condenser where it condenses the vapour leaving the separator. The ammonia is vaporised and leaves as low pressure gas, to be compressed in a mechanical compressor and then passed to the evaporator for a second cycle. The excess heat introduced by the compressor must be removed from the ammonia by means of a cooler.

The main advantage of this form of unit is the very great reduction in the volume of gas handled by the compressor. Thus, 1 kg of water vapour at, say, 311 K, with a volume of 22 m^3 and latent heat about 2560 kJ/kg, passes this heat to ammonia at a temperature of say 305 K. About 2.1 kg of ammonia will be vaporised to give a vapour with a volume of only about 0.22 m^3 at the high pressure used in the ammonia cycle.

SCHWARZ[16] gives a comparison of the various units used for low temperature evaporation. The three types in general use are the single-effect single-pass, the single-effect with recirculation, and the multiple-effect with recirculation. Each of these types may involve vapour compression or the addition of a second heat transfer medium. Schwarz suggests that multiple-effect units are the most economical, in terms of capital and operating costs. It is important to note that the single-effect, single-pass system offers the minimum hold-up, and hence a very short transit time. With film-type units, there seems little to be gained by recirculation, since over 70 per cent vaporisation can be achieved in one pass. The figures in Table 14.2 show the comparison between a double-effect unit with vapour compression on the first effect, and a unit with an ammonia refrigeration cycle, both units giving 1.25 kg/s (4.5 tonne/h) of evaporation.

Table 14.2. Comparison of refrigeration and vapour compression systems

System	Steam at 963 kN/m^2 (kg/s)	Water at 300 K (m^3/s)	Power (kW)
Refrigeration cycle	0.062	0.019	320*
Vapour compression	0.95	0.076	20
Ratio of steam system to refrigeration	15.1	4	0.06

*Includes 300 kW compressor.

The utilities required for the refrigeration system other than power are therefore very much less than for recompression with steam, although the capital cost and the cost of power will be much higher.

REAVELL[17] has given a comparison of costs for the concentration of a feed of a heat-sensitive protein liquor at 1.70 kg/s from 10 per cent to 50 per cent solids, on the basis of a 288 ks (160 hour) week. These data are shown in Table 14.3. It may be noted that, when using the double-effect evaporation with vapour compression, a lower temperature can be used in the first effect than when a triple-effect unit is used. In determining these figures no account has been taken of depreciation, although if this is 15 per cent of the capital costs it does not make a significant difference to the comparison.

The use of a heat pump cycle is the subject of Problem 14.22 at the end of this Volume, and a detailed discussion of the topic is given in the Solutions Manual.

This book belongs to Bradley Loren (bloren@mcandrews-ip.com) Copyright Elsevier 2024

Intas Exhibit 1032
Page 189 of 470
PGR2025-00043

Table 14.3. Comparison of various systems for the concentration of a protein liquid

Type	Approx. installed cost (£)	Cost of steam (£/year)	Net saving compared with single effect (£/year)
Single effect	50,000	403,000	—
Double effect	70,000	214,000	189,000
Double effect with vapour compression	90,000	137,000	266,000
Triple effect	100,000	143,000	260,000

Example 14.6

For the concentration of fruit juice by evaporation it is proposed to use a falling-film evaporator and to incorporate a heat pump cycle with ammonia as the medium. The ammonia in vapour form will enter the evaporator at 312 K and the water will be evaporated from the juices at 287 K. The ammonia in the vapour–liquid mixture will enter the condenser at 278 K and the vapour will then pass to the compressor. It is estimated that the work for compressing the ammonia will be 150 kJ/kg of ammonia and that 2.28 kg of ammonia will be cycled/kg water evaporated. The following proposals are available for driving the compressor:

(a) to use a diesel engine drive taking 0.4 kg of fuel/MJ; the calorific value being 42 MJ/kg and the cost £0.02/kg;
(b) to pass steam, costing £0.01/10 kg through a turbine which operates at 70 per cent isentropic efficiency, between 700 and 101.3 kN/m^2.

Explain by means of a diagram how this plant will work, and include all necessary major items of equipment required. Which method should be adopted for driving the compressor?

A simplified flow diagram of the plant is given in Figure 14.14.

Solution

Considering the ammonia cycle

Ammonia gas will leave the condenser, probably saturated at low pressure, and enter the compressor which it leaves at high pressure and 312 K. In the calandria heat will be transferred to the liquor and the ammonia gas will be cooled to saturation, condense, and indeed may possibly leave the unit at 278 K as slightly sub-cooled liquid though still at high pressure. This liquid will then be allowed to expand adiabatically in the throttling valve to the lower pressure during which some vaporisation will occur and the vapour — liquid mixture will enter the condenser with a dryness fraction of, say, 0.1–0.2. In the condenser heat will be transferred from the condensing vapours, and the liquid ammonia will leave the condenser, probably just saturated, though still at the low pressure. The cycle will then be repeated.

Considering the liquor stream

Weak liquor will enter the plant and pass to the calandria where it will be drawn up as a thin film by the partial vacuum caused by ultimate condensation of vapour in the condenser. Vaporisation will take place due to heat transfer from condensing ammonia in the calandria, and the vapour and concentrated liquor will then pass to a separator from which the concentrated liquor will be

This book belongs to Bradley Loren (bloren@mcandrews-ip.com) Copyright Elsevier 2024

Intas Exhibit 1032
Page 190 of 470
PGR2025-00043

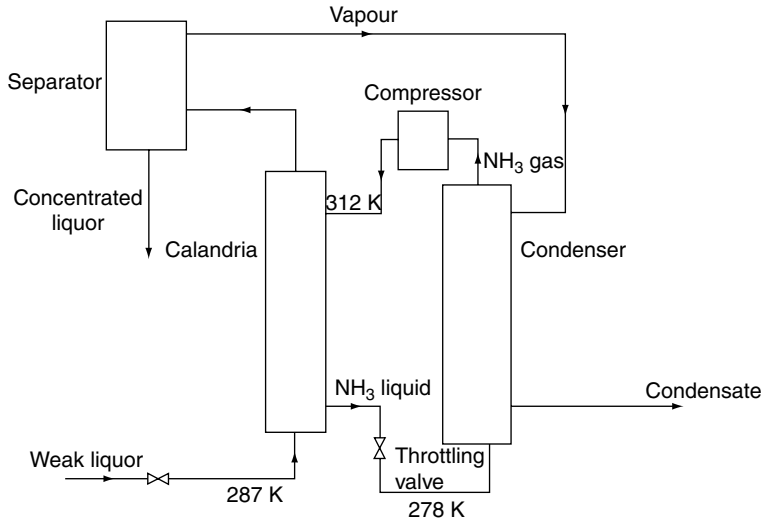


Figure 14.14. Flow diagram for Example 14.6

drawn off as product. The vapours will pass to the condenser where they will be condensed by heat transfer to the evaporating ammonia and leave the plant as condensate. A final point is that any excess heat introduced by the compressor must be removed from the ammonia by means of a cooler.

Fuller details of the cycle and salient features of operation are given in Section 14.5.2.

Choice of compressor drive (basis 1 kg water evaporated)

(a) *Diesel engine*

For 1 kg evaporation, ammonia circulated = 2.28 kg and the work done in compressing the ammonia

$$= (150 \times 2.28)$$

$$= 342 \text{ kJ or } 0.342 \text{ MJ/kg evaporation}$$

For an output of 1 MJ, the engine consumes 0.4 kg fuel.

Thus: fuel consumption $= (0.4 \times 0.342) = 0.137$ kg/kg water evaporated

and: cost $= (0.02 \times 0.137) = \underline{0.00274}$ £/kg water evaporated

(b) *Turbine*

The work required is 0.342 MJ/kg evaporation.

Therefore with an efficiency of 70 per cent:

$$\text{energy required from steam} = (0.342 \times 100/70) = 0.489 \text{ MJ/kg.}$$

Enthalpy of steam saturated at 700 kN/m^2 = 2764 kJ/kg.

This book belongs to Bradley Loren (bloren@mcandrews-ip.com) Copyright Elsevier 2024

Intas Exhibit 1032
Page 191 of 470
PGR2025-00043

Enthalpy of steam saturated at 101.3 kN/m^2 = 2676 kJ/kg.

Thus: energy from steam = (2764 − 2676) = 88 kJ/kg or 0.088 MJ/kg

and: steam required = (0.489/0.088) = 5.56 kg/kg evaporation

at a cost of: $(0.01 \times 5.56)/10 =$ 0.0056 £/kg water evaporated

and hence: the *Diesel engine would be used for driving the compressor.*

14.6. EVAPORATOR OPERATION

In evaporation, solids may come out of solution and form a deposit or scale on the heat transfer surfaces. This causes a gradual increase in the resistance to heat transfer and, if the same temperature difference is maintained, the rate of evaporation decreases with time and it is necessary to shut down the unit for cleaning at periodic intervals. The longer the boiling time, the lower is the number of shutdowns which are required in a given period although the rate of evaporation would fall to very low levels and the cost per unit mass of material handled would become very high. A far better approach is to make a balance which gives a minimum number of shutdowns whilst maintaining an acceptable throughput.

It has long been established[18] that, with scale formation, the overall coefficient of heat transfer may be expressed as a function of the boiling time by an equation of the form:

$$1/U^2 = at_b + b \tag{14.11}$$

where t_b is the boiling time. If Q_b is the total heat transferred in this time, then:

$$\frac{\mathrm{d}Q_b}{\mathrm{d}t_\mathrm{b}} = UA\Delta T$$

and substituting for U from equation 14.11 gives:

$$\frac{\mathrm{d}Q_b}{\mathrm{d}t_b} = \frac{A\Delta T}{(at_b + b)^{0.5}} \tag{14.12}$$

Integrating between 0 and Q_b and 0 and t_b gives:

$$Q_b = (2A\Delta T/a)[(at_b + b)^{0.5} - b^{0.5}] \tag{14.13}$$

There are two conditions for which an optimum value of the boiling time may be sought–the time whereby the heat transferred and hence the solvent evaporated is a maximum and secondly, the time for which the cost per unit mass of solvent evaporated is a minimum. These are now considered in turn.

Maximum heat transfer

If the time taken to empty, clean and refill the unit is t_c, then the total time for one cycle is $t = (t_b + t_c)$ and the number of cycles in a period t_P is $t_P/(t_b + t_c)$. The total

This book belongs to Bradley Loren (bloren@mcandrews-ip.com) Copyright Elsevier 2024

Intas Exhibit 1032
Page 192 of 470
PGR2025-00043

heat transferred during this period is the product of the heat transferred per cycle and the number of cycles in the period or:

$$Q_P = (2A\Delta T/a)[(at_b + b)^{0.5} - b^{0.5}][t_P/(t_b + t_c)] \tag{14.14}$$

The optimum value of the boiling time which gives the maximum heat transferred per cycle is obtained by differentiating equation 14.14 and equating to zero which gives:

$$t_{b\text{opt}} = t_c + (2/a)(abt_c)^{0.5} \tag{14.15}$$

Minimum cost

Taking C_c as the cost of a shutdown and the variable cost during operation including a labour component as C_b, then the total cost during period t_P is:

$$C_T = (C_c + t_b C_b)t_P/(t_b + t_c)$$

and substituting from equation 14.14:

$$C_T = [aQ_P(C_c + t_b C_b)]/2A\Delta T[at_b + b)^{0.5} - b^{0.5}] \tag{14.16}$$

The optimum value of the boiling time to give minimum cost is obtained by differentiating equation 14.16 and equating to zero to give:

$$t_{b\text{opt}} = (C_c/C_b) + 2(abC_cC_b)^{0.5}/(aC_b) \tag{14.17}$$

In using this equation, it must be ensured that the required evaporation is achieved. If this is greater than that given by equation 14.17, then it is not possible to work at minimum cost conditions. The use of these equations is illustrated in the following example which is based on the work of HARKER[19].

Example 14.7

In an evaporator handling an aqueous salt solution, the overall coefficient U (kW/m^2 deg K) is given by a form of equation 14.14 as:

$$1/U^2 = 7 \times 10^{-5}t_b + 0.2,$$

the heat transfer area is 40 m^2, the temperature driving force is 40 deg K and the latent heat of vaporisation of water is 2300 kJ/kg. If the down-time for cleaning is 15 ks (4.17 h), the cost of a shutdown is £600 and the operating cost during boiling is £18/ks (£64.6/h), estimate the optimum boiling times to give a) maximum throughput and b) minimum cost.

Solution

(a) *Maximum throughput*

The boiling time to give maximum heat transfer and hence maximum throughput is given by equation 14.15:

$$t_{b\text{opt}} = (15 \times 10^3) + (2/(7 \times 10^{-5}))(7 \times 10^{-5} \times 0.2 \times 15 \times 10^3)^{0.5}$$

$$= 2.81 \times 10^4 \text{ s or } \underline{\underline{28.1 \text{ ks}}} \text{ (7.8 h)}$$

This book belongs to Bradley Loren (bloren@mcandrews-ip.com) Copyright Elsevier 2024

Intas Exhibit 1032
Page 193 of 470
PGR2025-00043

The heat transferred during boiling is given by equation 14.13:

$$Q_b = (2 \times 40 \times 40)(7 \times 10^{-5})[((7 \times 10^{-5} \times 2.81 \times 10^4) + 0.2)^{0.5} - 0.2^{0.5}] = 4.67 \times 10^7 \text{ kJ}$$

and the water vaporated $= (4.67 \times 10^7)/2300 = 2.03 \times 10^4$ kg

Rate of evaporation during boiling $= (2.03 \times 10^4)/(2.81 \times 10^4) = 0.723$ kg/s

Mean rate of evaporation during the cycle $= 2.03/[(2.8 \times 10^4) + (15 \times 10^3)] =$ 0.471kg/s.

Cost of the operation $= ((2.81 \times 10^4 \times 18)/1000) + 600 = 1105.8$ £/cycle

or: $(1105.8/(2.03 \times 10^4) = 0.055$ £/kg.

(b) *Minimum cost*

The boiling time to give minimum cost is given by equation 14.17:

$$t_{b\text{opt}} = (600/0.018) + [2(7 \times 10^{-5} \times 0.2 \times 600 \times 0.018)^{0.5}]/(7 \times 10^{-5} \times 0.018)$$
$$= 5.28 \times 10^4 \text{ s or } 52.8 \text{ ks}(14.7 \text{ h})$$

The heat transferred during one boiling period is given by equation 14.13:

$$Q_b = [(2 \times 40 \times 40)/(7 \times 10^{-5})][7 \times 10^{-5} \times 5.28 \times 10^4 + 0.2)^{0.5} - 0.2^{0.5}] = 6.97 \times 10^7 \text{ kJ}$$

and the water evaporated $= (6.97 \times 10^7)/2300 = 3.03 \times 10^4$ kg

Rate of evaporation during boiling $= (3.03 \times 10^4)/(5.28 \times 10^4) = 0.574$ kg/s

Mean rate of evaporation during the cycle $= (3.03 \times 10^4)/[(5.28 \times 10^4) + (15 \times 10^3)] =$ 0.45 kg/s

In this case, cost of one cycle $= (5.28 \times 10^4 \times 0.018) + 600 = £1550.4$

or: $1550.4/(3.03 \times 10^4) =$ 0.0512 £/kg

Thus, the maximum throughput is 0.471 kg/s and the throughput to give minimum cost, 0.0512 £/kg, is 0.45 kg/s. If the desired throughput is between 0.45 and 0.471 kg/s, then this can be achieved although minimum cost operation is not possible. If a throughput of less than 0.45 kg/s is required, say 0.35 kg/s, then a total cycle time of $(3.03 \times 10^4)/0.35 = 8.65 \times 10^4$ s or 86.5 ks is required. This could be achieved by boiling at 0.423 kg/s for 71.5 ks followed by a shutdown of 15 ks, which gives a cost of 0.0624 £/kg. This is not the optimum boiling time for minimum cost and an alternative approach might be to boil for 52.8 ks at the optimum value, 0.45 kg/s, and, with a shutdown of 15 ks, a total cost of 0.0654 £/kg is estimated which is again higher than the minimum value. It would be, in fact, more cost effective to operate with the optimum boiling time of 52.8 ks and the down-time of 15 ks and to *close the plant down* for the remaining 18.7 ks of the 86.5 ks cycle. In this way, the minimum cost of 0.0512 £/kg would be achieved. In practice, the plant would probably not be closed down each cycle but rather for the equivalent period say once per month or indeed once a year. In all such considerations, it should be noted that, when a plant is shut down, there is no return on the capital costs and overheads which still have to be paid and this may affect the economics.

Whilst calculated optimum cycle times may not exactly correspond to convenient operating schedules, this is not important as slight variations in the boiling times will not affect the economics greatly.

This book belongs to Bradley Loren (bloren@mcandrews-ip.com) Copyright Elsevier 2024

Intas Exhibit 1032
Page 194 of 470
PGR2025-00043

14.7. EQUIPMENT FOR EVAPORATION

14.7.1. Evaporator selection

The rapid development of the process industries and of new products has provided many liquids with a wide range of physical and chemical properties all of which require concentration by evaporation. The type of equipment used depends largely on the method of applying heat to the liquor and the method of agitation. Heating may be either direct or indirect. Direct heating is represented by solar evaporation and by submerged combustion of a fuel. In indirect heating, the heat, generally provided by the condensation of steam, passes through the heating surface of the evaporator.

Some of the problems arising during evaporation include:

(a) High product viscosity.
(b) Heat sensitivity.
(c) Scale formation and deposition.

Equipment has been developed in an attempt to overcome one or more of these problems. In view of the large number of types of evaporator which are available, the selection of equipment for a particular application can only be made after a detailed analysis of all relevant factors has been made. These will, of course, include the properties of the liquid to be evaporated, capital and running costs, capacity, holdup, and residence time characteristics. Evaporator selection considered in detail in Volume 6, has been discussed by MOORE and HESLER[20] and PARKER[21]. Parker has attempted to test the suitability of each basic design for dealing with the problems encountered in practice, and the basic information is presented in the form shown in Figure 14.15. The factors considered include the ability to handle liquids in three viscosity ranges, to deal with foaming, scaling or fouling, crystal production, solids in suspension, and heat sensitive materials. A comparison of residence time and holding volume relative to the wiped film unit is also given. It is of interest to note that the agitated or wiped film evaporator is the only one which is shown to be applicable over the whole range of conditions covered.

14.7.2. Evaporators with direct heating

The use of solar heat for the production of Glauber's salt has been described by HOLLAND[22,23]. Brine is pumped in hot weather to reservoirs of 100,000 m^2 in area to a depth of 3–5 m, and salt is deposited. Later in the year, the mother liquor is drained off and the salt is stacked mechanically, and conveyed to special evaporators in which hot gases enter at 1150–1250 K through a suitable refractory duct and leave at about 330 K. The salt crystals melt in their water of crystallisation and are then dried in the stream of hot gas. BLOCH *et al.*[24], who examined the mechanism of evaporation of salt brines by direct solar energy, found that the rate of evaporation increased with the depth of brine. The addition of dyes, such as 2-naphthol green, enables the solar energy to be absorbed in a much shallower depth of brine, and this technique has been used to obtain a significant increase in the rate of production in the Dead Sea area.

This book belongs to Bradley Loren (bloren@mcandrews-ip.com) Copyright Elsevier 2024

Intas Exhibit 1032
Page 195 of 470
PGR2025-00043

This book belongs to Bradley Loren (bloren@mcandrews-ip.com)

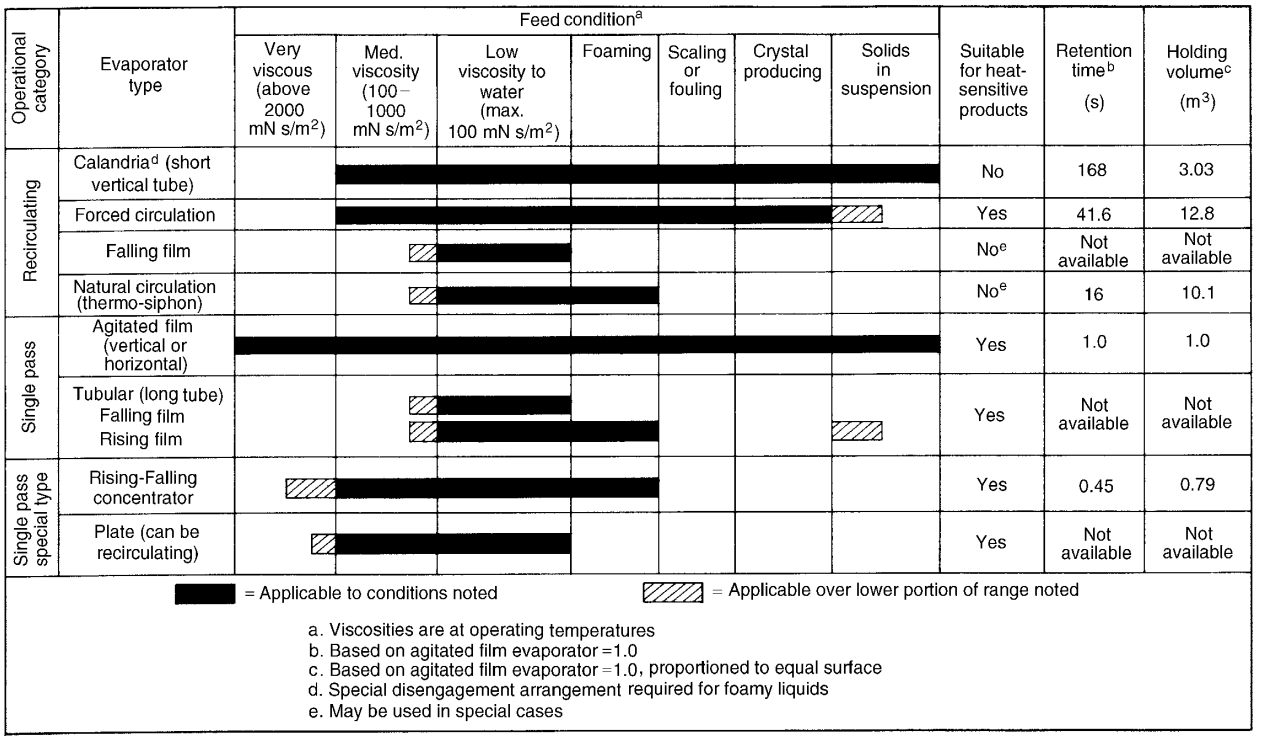


Figure 14.15. Evaporator selection (after PARKER[21])

Copyright Elsevier 2024

The submerged combustion of a gas, such as natural gas, has been used for the concentration of very corrosive liquors, including spent pickle liquors, weak phosphoric and sulphuric acids. A suitable burner for direct immersion in the liquor, as developed by SWINDIN[25], is shown in Figure 14.16. The depth of immersion of the burner is determined by the time of heat absorption and, for example, a 50 mm burner may be immersed by 250 mm and a 175 mm burner by about 450 mm. The efficiency of heat absorption is measured by the difference between the temperature of the liquid and that of the gases leaving the surface, values of 2–5 deg K being obtained in practice. The great attraction of this technique, apart from the ability to handle corrosive liquors, is the very great heat release obtained and the almost instantaneous transmission of the heat to the liquid, typically 70 MW/m^3.

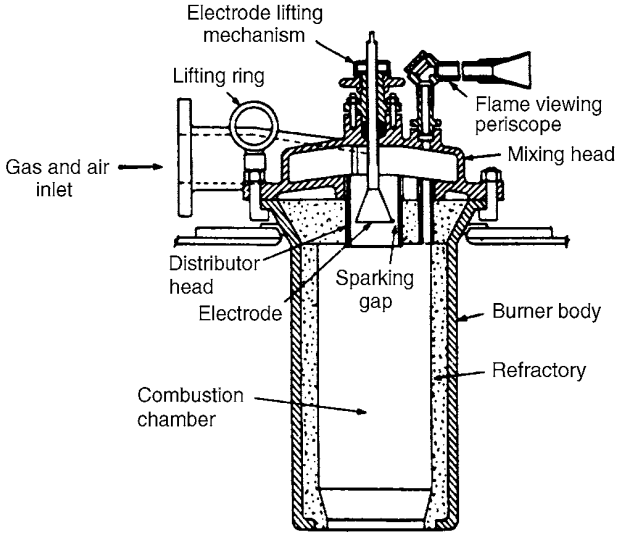


Figure 14.16. Burner for submerged combustion[25]

14.7.3. Natural circulation evaporators

Whilst each of the previous types of evaporator is of considerable importance in a given industry, it is the steam-heated evaporator that is the most widely used unit in the process industries and this is now considered in detail. In Chapter 9 of Volume 1, it is shown that the movement of the liquid over the heating surface has a marked influence on the rate of heat transfer, and it is thus convenient to classify evaporators according to the method of agitation or the nature of the circulation of the liquor over the heating surface. On this basis evaporators may be divided into three main types:

(a) Natural circulation units.
(b) Forced circulation units.
(c) Film-type units.

This book belongs to Bradley Loren (bloren@mcandrews-ip.com) Copyright Elsevier 2024
Intas Exhibit 1032
Page 197 of 470
PGR2025-00043

The developments that have taken place have, in the main, originated from the sugar and salt industries where the cost of evaporation represents a major factor in the process economics. In recent years, particular attention has been given to obtaining the most efficient use of the heating medium, and the main techniques that have been developed are the use of the multiple-effect unit, and of various forms of vapour compression units. With natural-circulation evaporators, circulation of the liquor is achieved by convection currents arising from the heating surface. This group of evaporators may be subdivided according to whether the tubes are horizontal with the steam inside, or vertical with the steam outside.

Rillieux is usually credited with first using *horizontal tubes*, and a unit of this type is shown in Figure 14.17. The horizontal tubes extend between two tube plates to which they are fastened either by packing plates or, more usually, by expansion. Above the heating section is a cylindrical portion in which separation of the vapour from the liquid takes place. The vapour leaves through some form of de-entraining device to prevent the carry-over of liquid droplets with the vapour stream. The steam enters one steam chest, passes through the tubes and out into the opposite chest, and the condensate leaves through a steam trap. Horizontal evaporators are relatively cheap, require low head room, are easy to install, and are suitable for handling liquors that do not crystallise. They can be used either as batch or as continuous units, and the shell is generally 1–3.5 m diameter and 2.5–4 m high. The liquor circulation is poor, and for this reason such units are unsuitable for viscous liquors.

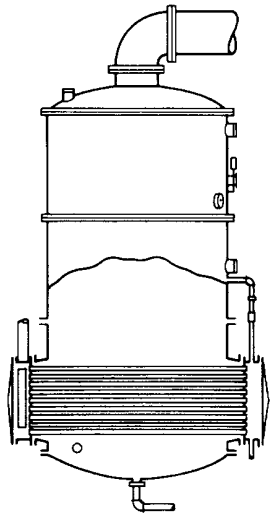


Figure 14.17. Natural circulation evaporator with horizontal tubes

The use of *vertical tubes* is associated with Robert, and this type is sometimes known as the Robert or Standard Evaporator. A typical form of vertical evaporator is illustrated in Figure 14.18, in which a vertical cylindrical body is used, with the tubes held between two horizontal tube plates which extend right across the body. The lower portion of the evaporator is frequently spoken of as the calandria section shown in Figure 14.19. Tubes

This book belongs to Bradley Loren (bloren@mcandrews-ip.com) Copyright Elsevier 2024

Intas Exhibit 1032
Page 198 of 470
PGR2025-00043

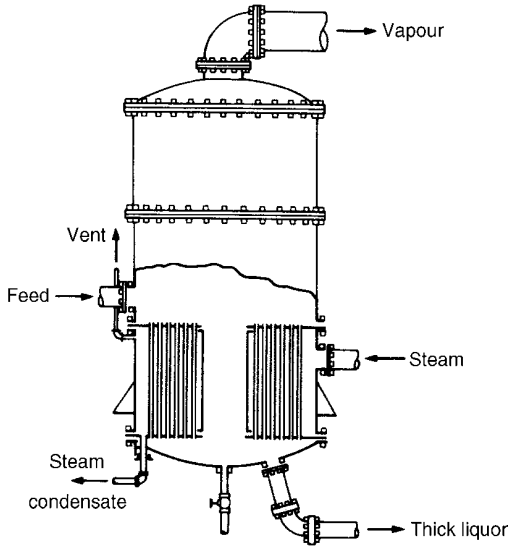


Figure 14.18. Evaporator with vertical tubes and a large central downcomer

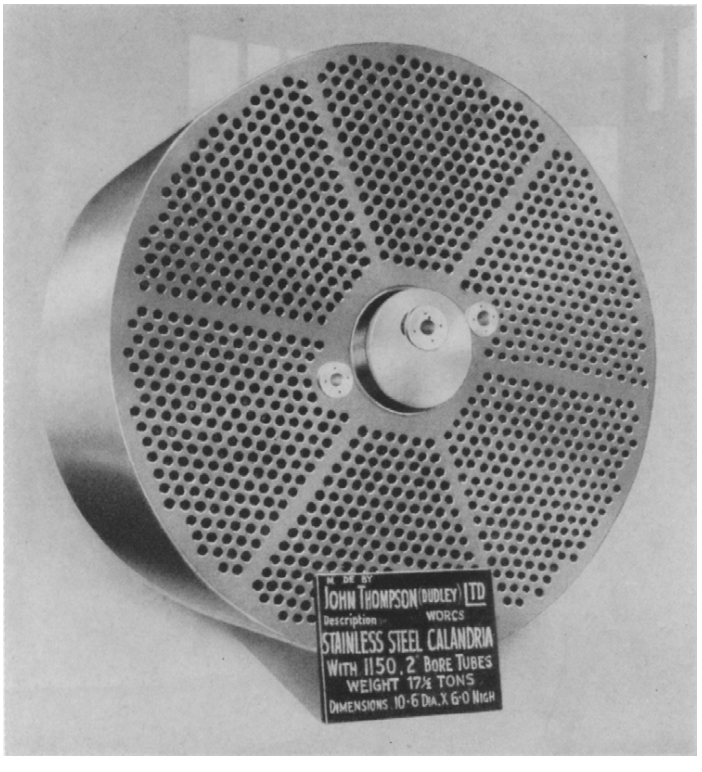


Figure 14.19. Calandria for an evaporator

This book belongs to Bradley Loren (bloren@mcandrews-ip.com)
Copyright Elsevier 2024
Intas Exhibit 1032
Page 199 of 470
PGR2025-00043

are 1–2 m in length and 37–75 mm diameter, giving ratio of length to inside diameter of the tubes of 20–40. In the basket type shown in Figure 14.20 vertical tubes are used with the steam outside, though the heating element is suspended in the body so as to give an annular downtake. The advantages claimed for this design are that the heating unit is easily removed for repairs, and that crystals formed in the downcomer do not break up. As the circulation of the liquor in the tubes is better, the vertical tube evaporator is used widely in the sugar and salt industries where throughputs are very large.

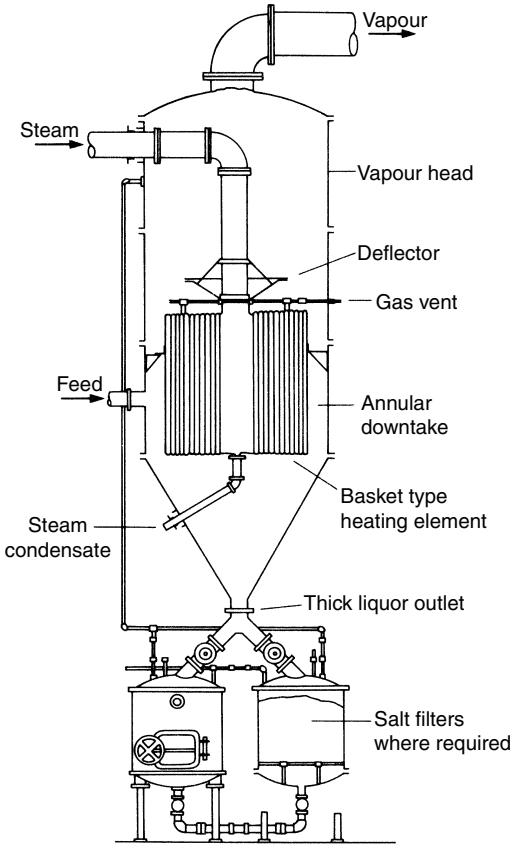


Figure 14.20. Basket type of evaporator

14.7.4. Forced circulation evaporators

Increasing the velocity of flow of the liquor through tubes results in a significant increase in the liquid-film transfer coefficient. This is achieved in the forced circulation units where a propeller or other impeller is mounted in the central downcomer, or a circulating pump is mounted outside the evaporator body. In the concentration of strong brines, for example, an internal impeller, often a turbine impeller, is fitted in the downtake, and this form

This book belongs to Bradley Loren (bloren@mcandrews-ip.com) Copyright Elsevier 2024

of construction is particularly useful where crystallisation takes place. Forced circulation enables higher degrees of concentration to be achieved, since the heat transfer rate can be maintained in spite of the increased viscosity of the liquid. Because pumping costs increase roughly as the cube of the velocity, the added cost of operation of this type of unit may make it uneconomic, although many forced circulation evaporators are running with a liquor flow through the tubes of 2–5 m/s which is a marked increase on the value for natural circulation. Where stainless steel or expensive alloys such as Monel are to be used, forced circulation is favoured because the units can be made smaller and cheaper than those relying on natural circulation. In the type illustrated in Figure 14.21, there is an external circulating pump, usually of the centrifugal type when crystals are present, though otherwise vane types may be used. The liquor is either introduced at the bottom and pumped straight through the calandria, or it is introduced in the separating section. In most units, boiling does not take place in the tubes, because the hydrostatic head of liquid raises the boiling point above that in the separating space. Thus the liquor enters the bottom of the tubes and is heated as it rises and at the same time the pressure falls. In the separator the pressure is sufficiently low for boiling to occur. Forced circulation evaporators work well on materials such as meat extracts, salt, caustic soda, alum and other crystallising materials and also with glues, alcohols, and foam-forming materials.

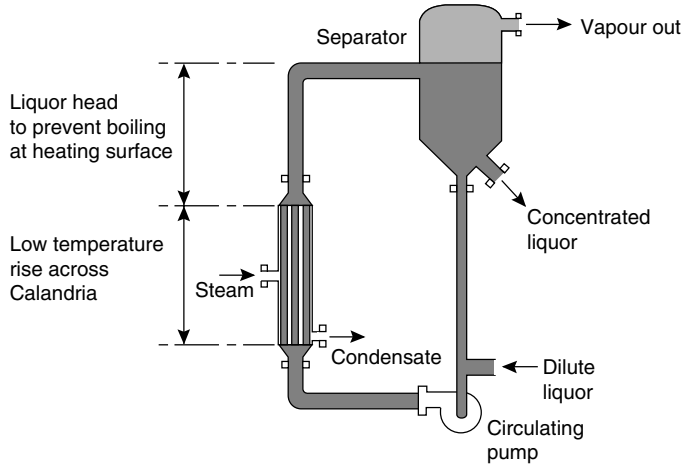


Figure 14.21. Forced circulation evaporator with an external pump

For certain applications multi-pass arrangements are used. When a plate heat exchanger is used instead of the tubular unit, boiling on the heating surfaces is avoided by increasing the static head using a line restriction between the plate pack and the separator. Compared with tubular units, lower circulation rates and reduced liquid retention times are important advantages. Plate-type units are discussed further in Section 14.7.7.

For the handling of corrosive fluids, forced-circulation evaporators have been constructed in a variety of inert materials, and particularly in graphite where the unique combination of chemical inertness coupled with excellent thermal conductivity gives the

This book belongs to Bradley Loren (bloren@mcandrews-ip.com) Copyright Elsevier 2024
Intas Exhibit 1032
Page 201 of 470
PGR2025-00043

material important advantages. Graphite differs from most constructional materials in its high anisotropy which results in directionally preferred thermal conductivity, and in the difference between its relatively good compressive strength and its poor tensile or torsional strength. Although it is easily machinable, it is not ductile or malleable and cannot be cast or welded. The use of cements in assembly is undesirable because they are usually less chemically or thermally stable. There are also problems of differential expansion. In order to exploit the advantages of this material and to avoid the foregoing problems, special constructional techniques are necessary. The Polybloc system, which is described by HILLIARD[26–28], is based on the use of robust blocks assembled exclusively under compression. Heat transfer occurs between fluids passing through holes drilled in the blocks and positioned so as to exploit preferred anisotropic crystal orientation for the highest thermal conductivity in the direction of heat flow. Inert gaskets eliminate the need for cements and enable units of varying size to be assembled simply by stacking the required number of blocks as shown in Figure 14.22. A similar form of construction has been adopted by the Powell Duffryn Company. In commercial installations high values of overall transfer coefficients have been achieved and, for example, a value of 1.1 kW/m^{2}K has been obtained for concentrating thick fruit juice containing syrup, and also for concentrating 40 per cent sulphuric acid to 60 per cent. A value of 0.8 kW/m^{2}K has been obtained for sulphuric acid concentration from 60 per cent to 74 per cent at a pressure of 1.5 kN/m^2, and similar values have been obtained with spinning-bath liquors and some pharmaceuticals.

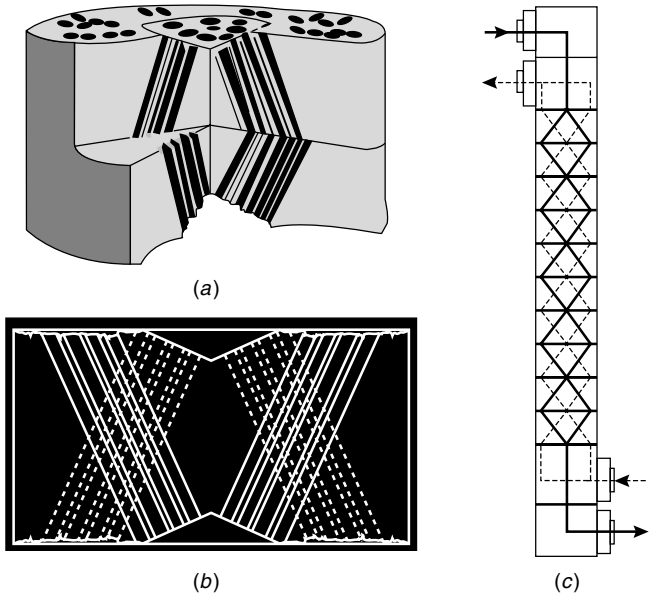


Figure 14.22. The Polybloc system (after HILLIARD[27]). (*a*) Cutaway section of x-flow block as used for two corrosive fluids. (*b*) Section through x-flow block. (*c*) Stacked Polybloc exchanger

This book belongs to Bradley Loren (bloren@mcandrews-ip.com) Copyright Elsevier 2024

Intas Exhibit 1032
Page 202 of 470
PGR2025-00043

14.7.5. Film-type units

In all the units so far discussed, the liquor remains for some considerable time in the evaporator, up to several hours with batch operation, and this may be undesirable as many liquors decompose if kept at temperatures at or near their boiling points for any length of time. The temperature can be reduced by operating under a vacuum, as discussed previously, though there are many liquors which are very heat-sensitive, such as orange juice, blood plasma, liver extracts and vitamins. If a unit is designed so that the residence time is only a few seconds, then these dangers are very much reduced. This is the principle of the Kestner long tube evaporator, introduced in 1909, which is fitted with tubes of 38 to 50 mm diameter, mounted in a simple vertical steam chest. The liquor enters at the bottom, and a mixture of vapour and entrained liquor leaves at the top and enters a separator, usually of the tangential type. The vapour passes out from the top and the liquid from the bottom of the separator. In the early models the thick liquid was recirculated through the unit, although the once-through system is now normally used.

An alternative name for the long-tube evaporator is the *climbing film evaporator*. The progressive evaporation of a liquid, whilst it passes through a tube, gives rise to a number of flow regimes discussed in Section 14.2.3. In the long-tube evaporator the annular flow or climbing-film regime is utilised throughout almost all the tube length, the climbing film being maintained by drag induced by the vapour core which moves at a high velocity relative to the liquid film. With many viscous materials, however, heat transfer rates in this unit are low because there is little turbulence in the film, and the thickness of the film is too great to permit much evaporation from the film as a result of conduction through it. In evaporators of this type it is essential that the feed should enter the tubes as near as possible to its boiling point. If the feed is subcooled, the initial sections will act merely as a feed heater thus reducing the overall performance of the unit. Pressure drop over the tube length will be attributable to the hydrostatic heads of the single-phase and two-phase regions, friction losses in these regions, and losses due to the acceleration of the vapour phase. The first published analysis of the operation of this type of unit was given by BADGER and his associates[29–31] who fitted a small thermocouple inside the experimental tube, 32 mm outside diameter and 5.65 m long, so that the couple could be moved up and down the centre of the tube. In this way, it was found that the temperature rose slightly from the bottom of the tube to the point where boiling commenced, after which the change in temperature was relatively small. Applying this technique, it was possible to determine the heat transfer coefficients in the non-boiling and boiling sections of the tube.

A *falling-film evaporator* with the liquid film moving downwards, operates in a similar manner, as shown in Figure 14.23. The falling-film evaporator is the simplest and most commonly used type of film-evaporator in which the liquid flows under gravitational force as a thin film on the inside of heated vertical tubes and the resulting vapour normally flows co-currently with the liquid in the centre of the tubes. A complete evaporator stage consists of the evaporator, a separator to separate the vapours from the residual liquid, and a condenser. Where high evaporation ratios are required, part of the concentrated liquid is recycled back to the evaporator inlet in order to ensure that the tubes are sufficiently wetted. An essential part of every falling film evaporator is the liquid distribution system since the liquid feed must not only be evenly distributed to all the tubes, but also form a

This book belongs to Bradley Loren (bloren@mcandrews-ip.com) Copyright Elsevier 2024

Intas Exhibit 1032
Page 203 of 470
PGR2025-00043

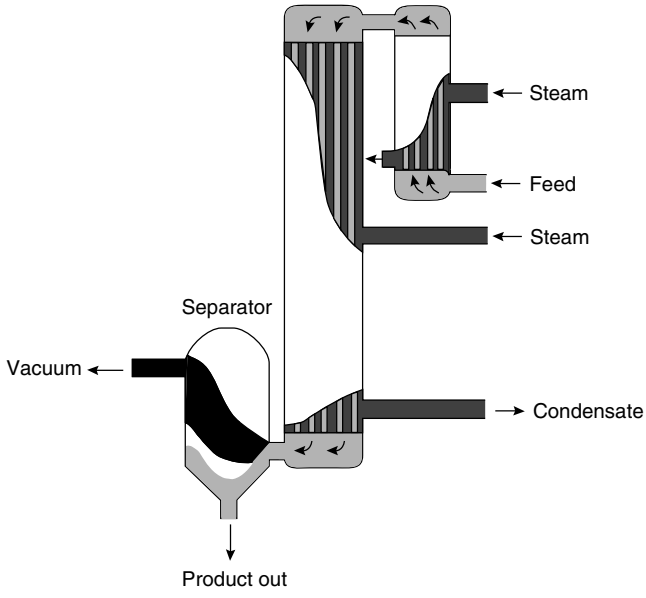


Figure 14.23. Single-effect falling-film evaporator

continuous film of the inner circumference of the tubes. Kuhni has developed a two-stage unit in which, after an initial pre-distribution, the liquid is directed tangentially onto the tubes through slits in specially designed tube inserts. The advantages of falling film evaporators include:

(a) high heat transfer coefficients, 2000–5000 W/m^{2}K for water and 500–1000 W/m^{2}K for organics,
(b) short residence times on the heated surface, 5–10 s without recirculation,
(c) low pressure drops, 0.2–0.5 kN/m^2,
(d) suitablity for vacuum operation,
(e) high evaporation ratios, c. 70 per cent without and 95 per cent with recirculation,
(f) wide operating range, up to 400 per cent of the minimum throughput,
(g) low susceptibility to fouling,
(h) minimum cost operation.

14.7.6. Thin-layer or wiped-film evaporators

This type of unit, known also as a thin-film evaporator is shown in Figure 14.24. It consists of a vertical tube, the lower portion of which is surrounded by a jacket which contains the heating medium. The upper part of the tube is not jacketed and this acts as a separator. A rotor, driven by an external motor, has blades which extend nearly to the bottom of the tube, mounted so that there is a clearance of only about 1.3 mm between their tips and the inner surface of the tube. The liquor to be concentrated is picked up as it enters by the

This book belongs to Bradley Loren (bloren@mcandrews-ip.com) Copyright Elsevier 2024

Intas Exhibit 1032
Page 204 of 470
PGR2025-00043

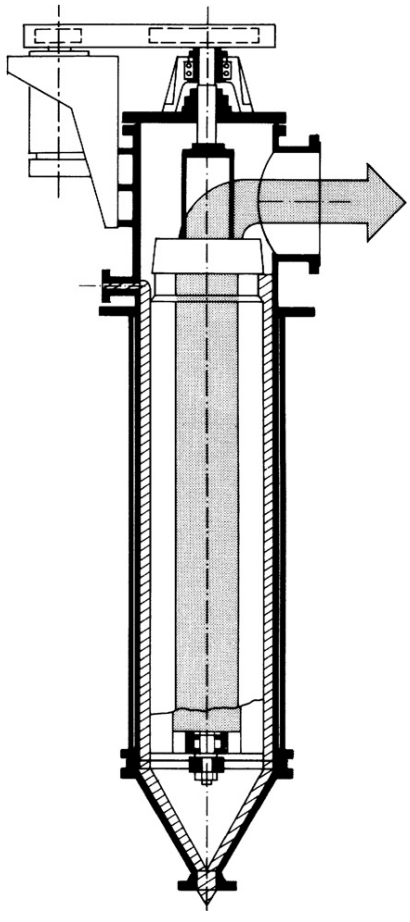


Figure 14.24. Thin-film evaporator

rotating blades and thrown against the tube wall. This action provides a thin film of liquid and sufficient agitation to give good heat transfer, even with very viscous liquids. The film flows down by gravity, becoming concentrated as it falls. The concentrated liquor is taken off at the bottom by a pump, and the vapour leaves the top of the unit where it is passed to a condenser. Development of this basic design has been devoted mainly to the modification of the blade system. An early alternative was the use of a hinged blade. In this type of unit the blade is forced on to the wall under centrifugal action, the thickness of the film being governed by a balance between this force and the hydrodynamic forces produced in the liquid film on which the blade rides. The first experimental comparison of the fixed and hinged blade wiped-film evaporators was that of BRESSLER[32]. For each type of blade there appeared to be an optimum wiper speed beyond which an increase had no further effect on heat transfer. This optimum was reached at a lower speed with the hinged blade. Other agitator designs in which the blades, usually made from rubber,

This book belongs to Bradley Loren (bloren@mcandrews-ip.com) Copyright Elsevier 2024

Intas Exhibit 1032
Page 205 of 470
PGR2025-00043

graphite or synthetic materials, actually scrape the wall have been studied. The use of nylon brushes as the active agitator elements has been investigated by McManus[33] using a small steam heated evaporator, 63 mm internal diameter and 762 mm long. Water and various aqueous solutions of sucrose and glycerol were tested in the evaporator. A notable feature of the unit was the high heat fluxes obtained with the viscous solutions. Values as high as 70 kW/m^2 were obtained when concentrating a 60 per cent sucrose feedstock to 73 per cent, at a film temperature difference of 16.5 deg K with a wiper speed of 8.3 Hz. The fluxes obtained for the evaporation of water under similar conditions were nearly 4.5 times higher. A detailed analysis of the heat transfer mechanism, based on unsteady-state conduction to the rapidly renewed film, was presented. Similar analyses are to be found in the work of Harriott[34] and Kool[35]. Close agreement between the theory and experimental data confirmed the appropriateness of the model chosen to represent the heat transfer process. The theory has one main disadvantage, however, in that a satisfactory method for the estimation of liquid film thickness is not available. The most important factor influencing the evaporation coefficient is the thermal conductivity of the film material, and that the effects of viscosity and wiper speed which is inversely proportional to the heating time t, are of less significance.

A comprehensive discussion of the main aspects of the wiped-film evaporator technique covering thin-film technology in general, the equipment, and its economics and process applications is given by Mutzenburg[36], Parker[37], Fischer[38], and Ryley[39]. An additional advantage of wiped-film evaporators, especially those producing a scraped surface, is the reduction or complete suppression of scale formation though, in processes where the throughput is very high, this type of unit obviously becomes uneconomic and the traditional way of avoiding scale formation, by operating a flash evaporation process, is more suitable.

14.7.7. Plate-type units

A plate evaporator consists of a series of gasketted plates mounted within a support frame. Film-type plate evaporators can be climbing-film, falling-film or a combination of these. Figure 14.25 shows the flow and plate arrangement of an APV falling-film plate evaporator. Each unit comprises a product plate and a steam plate, and this arrangement is repeated to provide the required heat transfer area. Product flow down each side of the plate may be in series where this is advantageous in terms of wetting rates.

Both the vapour evaporated from the boiling film and the concentrated product are discharged from the evaporator to a vapour–liquid separator from which the product is pumped, the vapour passing to the next effect of the evaporator, or the condenser. Compared with tubular evaporators, plate evaporators can offer important advantages in terms of headroom, floorspace, accessibility and flexibility.

APV, whose "Paraflow" plate heat exchanger is illustrated in Volume 1, Chapter 9, supply climbing and falling-film plate evaporators with evaporative capacities up to 10 kg/s. Such units offer the advantages of short contact and residence times and low liquor hold-up, and hence are widely used for the concentration of heat-sensitive materials.

For applications where viscosities or product concentrations are high, APV have developed the "Paravap" evaporator in which corrugated-plate heat exchanger plates are

This book belongs to Bradley Loren (bloren@mcandrews-ip.com) Copyright Elsevier 2024

Intas Exhibit 1032
Page 206 of 470
PGR2025-00043

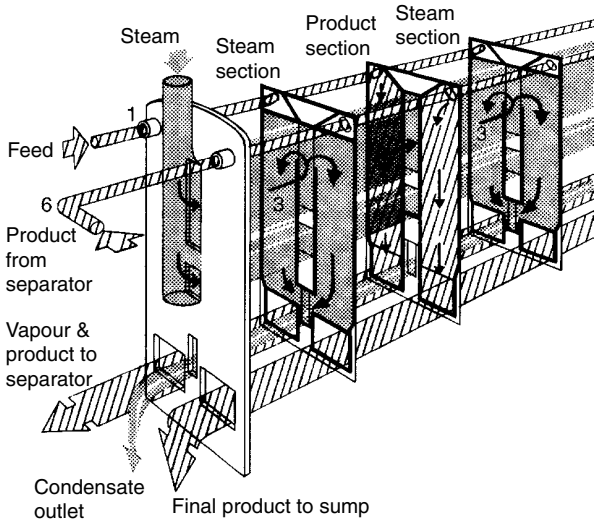


Figure 14.25. Flow and plate arrangement for two-stage operation

used in a climbing-film arrangement, thereby increasing turbulence in the liquid film compared with standard plate evaporators. A typical arrangement of an APV "Paravap" plant is shown in Figure 14.26. Feed liquor from balance tank 1 is pumped 2 through the feed preheater 3 to the evaporator 4 where it boils. Concentrated product and evaporated vapour are discharged to the separator 5 from which product is pumped 6. Vapour passes to the condenser 7 from which condensate is pumped 8, vacuum being maintained by a liquid ring pump 9. Single-pass operation is used for low concentration ratios between feed and product, whilst higher ratios require the recirculation of some of the product. This can be to the balance tank or feed pipework, although in some cases it is necessary to use in-line devices to achieve satisfactory mixing.

For some products it has been found advantageous to pressurise the plate heat exchanger, with an orifice or valve preventing boiling until the liquor enters the separator, in what is known as the APV "Paraflash" system. This is a special case of the forced circulation evaporator described earlier.

APV "Paravap" and "Paraflash" evaporators are used for products with viscosities up to 5 Ns/m^2 and concentrations in excess of 99 per cent by mass. Evaporation rates are up to 4 kg/s.

It may be noted that the gasket is a key component in plate heat exchangers, and this may limit the maximum temperature which can be used and may indeed prevent the use of this type of equipment with some corrosive fluids.

14.7.8. Flash evaporators

In the flash evaporator, boiling in the actual tubes is suppressed and the superheated liquor is flashed into a separator operating at reduced pressure. Whilst the high heat transfer rates

This book belongs to Bradley Loren (bloren@mcandrews-ip.com) Copyright Elsevier 2024

Intas Exhibit 1032
Page 207 of 470
PGR2025-00043

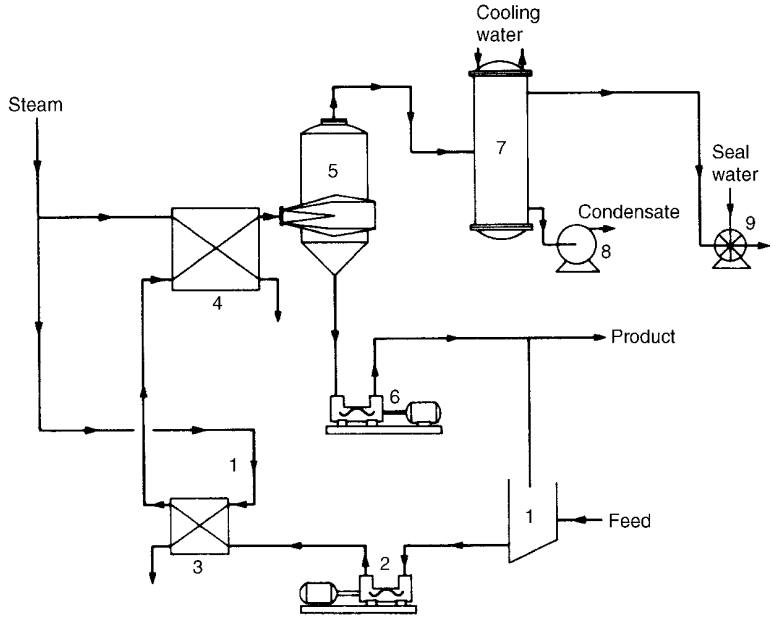


Figure 14.26. Flowsheet for a typical "Paravap" evaporator installation

associated with boiling in tubes cannot be utilised, the thermodynamic and economical advantages of the system when operated in a multistage configuration outweigh this consideration. These advantages, stated independently by FRANKEL[40] and SILVER[41], have been important in the past decade in the intensive effort to devise economic processes for the desalination of sea water. This topic is discussed further by BAKER[42], who considers multistage flash evaporation with heat input supplied by a conventional steam boiler, by a gas-turbine cycle, or by vapour recompression. The combined power–water plant is also considered. Attempts to reduce scale formation in flash evaporators to even lower levels have resulted in a number of novel developments. In one unit described by WOODWARD[43], sea water is heated by a countercurrent spray of hot immiscible oil. In this respect the process is similar to liquid–liquid extraction, the extracted quantity being heat in this case. The sea water is heated under pressure and subsequently flashed into a low pressure chamber. A similar direct contact system is discussed by WILKE *et al.*[44]. Yet another arrangement which avoids the intervening metallic wall of the conventional heat exchanger is described by OTHMER *et al.*[45]. In this process direct mass transfer between brine and pure water is utilised in the desalination operation.

The formation of solids in evaporators is not always undesirable and, indeed, this is precisely what is required in the *evaporator-crystalliser* discussed in Chapter 15. The evaporator–crystalliser is a unit in which crystallisation takes place largely as a result of the removal of solvent by evaporation. Cooling of the liquor may, in some cases, produce further crystallisation thus establishing conditions similar to those in vacuum crystallisation. The true evaporator–crystalliser is distinguished, however, by its use of an external heat source. Crystallisation by evaporation is practised on salt solutions having

This book belongs to Bradley Loren (bloren@mcandrews-ip.com) Copyright Elsevier 2024

Intas Exhibit 1032
Page 208 of 470
PGR2025-00043

a small change of solubility with temperature, such as sodium chloride and ammonium sulphate, which cannot be dealt with economically by other means, as well as those with inverted solubility curves. It is also widely used in the production of many other crystalline materials, as outlined by BAMFORTH[46]. The problem of design for crystallising equipment is extremely complicated and consequently design data are extremely meagre and unreliable. This topic is discussed further in Chapter 15.

The *development of unwanted foams* is a problem that evaporation has in common with a number of processes, and a considerable amount of effort has been devoted to the study of defoaming techniques using chemical, thermal, or mechanical methods. Chemical techniques involve the addition of substances, called antifoams, to foam-producing solutions to eliminate completely, or at least to reduce drastically, the resultant foam. Antifoams are, in general, slightly soluble in foaming solutions and can cause a decrease in surface tension. Their ability to produce an expanded surface film is, however, one explanation of their foam-inhibiting characteristic, as discussed by BECKERMAN[47]. Foams may be caused to collapse by raising or lowering the temperature. Many foams collapse at high temperature due to a decrease in surface tension, solvent evaporation, or chemical degradation of the foam-producing agents; at low temperatures freezing or a reduction in surface elasticity may be responsible. Other methods which are neither chemical nor thermal may be classified as mechanical. Tensile, shear, or compressive forces may be used to destroy foams, and such methods are discussed in some detail by GOLDBERG and RUBIN[48]. The ultimate choice of defoaming procedure depends on the process under consideration and the convenience with which a technique may be applied.

14.7.9. Ancillary equipment

One important component of any evaporator installation is the *equipment for condensing the vapour* leaving the last effect of a multiple-effect unit, achieved either by direct contact with a jet of water, or in a normal tubular exchanger. If M is the mass of cooling water used per unit mass of vapour in a jet condenser, and H is the enthalpy per unit mass of vapour, then a heat balance gives:

$$\underset{\text{(Heat in)}}{H + MC_pT_i} = \underset{\text{(Heat out)}}{C_pT_e + MC_pT_e} \tag{14.18}$$

where T_i and T_e are the inlet and outlet temperatures of the water, above a standard datum temperature, and where the condensate is assumed to leave at the same temperature as the cooling water. From equation 14.18:

$$M = \frac{H - C_pT_e}{C_p(T_e - T_i)} \tag{14.19}$$

If, for example, $T_e = 316$ K, $T_i = 302$ K, and the pressure $= 87.8$ kN/m^2, then:

$$M = \frac{2596 - 4.18(316 - 273)}{4.18(316 - 302)} = 41.5 \text{ kg/kg}$$

This book belongs to Bradley Loren (bloren@mcandrews-ip.com) Copyright Elsevier 2024

Intas Exhibit 1032
Page 209 of 470
PGR2025-00043

The water is then conveniently discharged at atmospheric pressure, without the aid of a pump, by allowing it to flow down a vertical pipe, known as a barometric leg, of sufficient length for the pressure at the bottom to be slightly in excess of atmospheric pressure. For a jet condenser with a barometric leg, a chart for determining the water requirement has been prepared by ARROWSMITH[49], and this is shown in Figure 14.27.

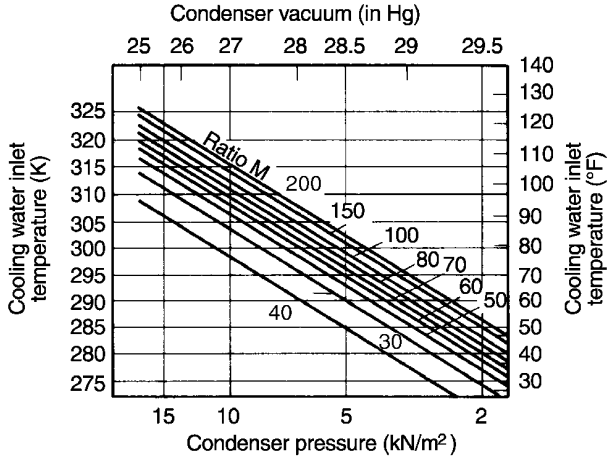


Figure 14.27. Ratio (M) of cooling water to vapour required under various conditions[49]

Jet condensers may be either of the countercurrent or parallel flow type. In the countercurrent unit, the water leaves at the bottom through a barometric leg, and any entrained gases leave at the top. This provides what is known as a *dry vacuum system*, since the pump has to handle only the non-condensable gases. The cooling water will generally be heated to within 3–6 deg K of the vapour temperature. With the parallel flow system, the temperature difference will be rather greater and, therefore, more cooling water will be required. In this case, the water and gas will be withdrawn from the condenser and passed through a wet vacuum system. As there is no barometric leg, the unit can be mounted at floor level, although the pump displacement is about one and a half times that for the dry vacuum system.

Air is introduced into a jet condenser from the cooling water, as a result of the evolution of non-condensable gases in the evaporator, and as a result of leakages. The volume of air to be removed is frequently about 15 per cent of that of the cooling water. The most convenient way of obtaining a vacuum is usually by means of a steam jet ejector. Part of the momentum of a high velocity steam jet is transferred to the gas entering the ejector, and the mixture is then compressed in the diverging portion of the ejector by conversion of kinetic energy into pressure energy. Good performance by the ejector is obtained largely by correct proportioning of the steam nozzle and diffuser, and poor ejectors will use much more high pressure steam than a well designed unit. The amount of steam required increases with the compression ratio. Thus, a single-stage ejector will remove air from a system at a pressure of 17 kN/m^2 where a compression ratio of 6 is required. To remove air from a system at 3.4 kN/m^2 would involve a compression ratio

This book belongs to Bradley Loren (bloren@mcandrews-ip.com) Copyright Elsevier 2024
Intas Exhibit 1032
Page 210 of 470
PGR2025-00043

of 30, and a single-stage unit would be uneconomic in steam consumption. A two-stage ejector is shown in Figure 14.28. The first stage withdraws air from the high vacuum vessel and compresses it to say 20 kN/m^2, and the second stage compresses the discharge from the first ejector to atmospheric pressure. A further improvement is obtained if a condenser is inserted after the first stage, as this will reduce the amount of vapour to be handled in the final stage. An indication of the number of stages required for various conditions is shown in Figure 14.29[49]. The higher the steam pressure the smaller is the consumption, and pressures of 790–1135 kN/m^2 are commonly used in multistage units. Typical performance curves are shown in Figure 14.30[49], where the air duty for a given steam consumption and given steam pressure is shown as a function of the number of stages and the operating pressure.

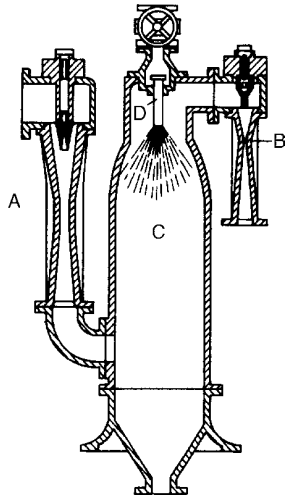


Figure 14.28. Two-stage ejector with condenser: *A* — First stage. *B* — Second stage. *C* — Condenser. *D* — Water spray

In operating an evaporator, it is important to minimise entrainment of the liquid in the vapour passing over to the condenser. Entrainment is reduced by having a considerable headroom, of say 1.8 m, above the boiling liquid, though the addition of some form of de-entrainer is usually essential. Figure 14.31 shows three *methods of reducing entrainment*. The simplest is to take the vapour from an upturned pipe as in *a*, and this has been found to give quite good results in small units. The deflector type *b* is a common form of de-entrainer and the tangential separator *c* is the type usually fitted to climbing-film units. This problem is particularly important in the concentration of radioactive waste liquors and has been discussed by McCULLOUGH[50], who cites the case of a batch evaporator of the forced-circulation type in which the vapours are passed to a 3.6 m diameter separator and then through four bubble cap trays to give complete elimination of entrained liquor. A good entrainment separator will reduce the amount of liquid carried over to 10–20 kg/10^6 kg of vapour.

This book belongs to Bradley Loren (bloren@mcandrews-ip.com) Copyright Elsevier 2024

Intas Exhibit 1032
Page 211 of 470
PGR2025-00043

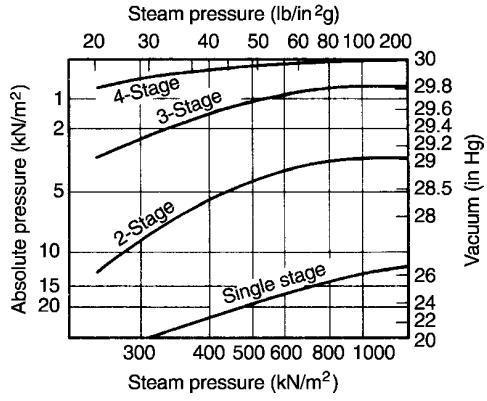


Figure 14.29. Recommended number of stages for various operating conditions[49]

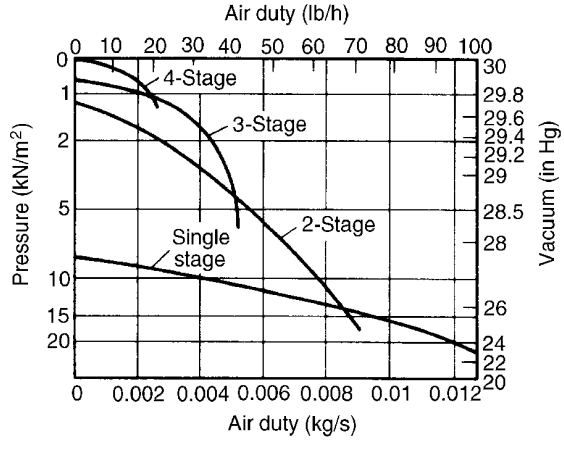


Figure 14.30. Air duty of steam jet ejectors, for a given steam consumption and steam pressure[49]

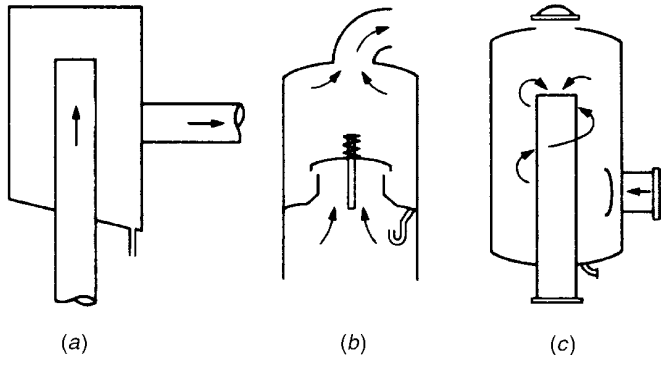


Figure 14.31. Entrainment separators: (*a*) Upturned pipe, (*b*) Deflector type, (*c*) Tangential type

This book belongs to Bradley Loren (bloren@mcandrews-ip.com) Copyright Elsevier 2024
Intas Exhibit 1032
Page 212 of 470
PGR2025-00043

14.8. FURTHER READING

AZBEL, D. S.: *Fundamentals of Heat Transfer in Process Engineering* (Noyes, New York, 1984).
AZBEL, D. S.: *Heat Transfer Applications in Process Engineering* (Noyes, New York, 1984).
BACKHURST, J. R. and HARKER, J. H.: *Process Plant Design* (Heinemann, London, 1973).
BADGER, W. L.: *Heat Transfer and Evaporation* (Chemical Catalog Co., 1926).
BILLET, R.: *Evaporation Technology*: *Principles*, *Applications*, *Economics*. (VCH, London, 1989).
HAUSBRAND, E.: *Evaporating*, *Condensing and Cooling Apparatus*. Translated from the second revised German edition by A. C. WRIGHT, Fifth English edition revised by B. HEASTIE (E. Benn, London, 1933).
HOLLAND, F. A., MOORES, R. M., WATSON, F. A., and WILKINSON, J. K.: *Heat Transfer* (Heinemann, London, 1970).
KERN, D. Q.: *Process Heat Transfer* (McGraw-Hill, New York, 1950).
KING, C. J.: *Separation Processes* 2nd edn. (McGraw-Hill, New York, 1980).
KREITH, F.: *Principles of Heat Transfer*, 2nd edn. (International Textbook Co., London, 1965).
MCADAMS, W. H.: *Heat Transmission*, 3rd edn. (McGraw-Hill, New York, 1954).
MCCABE, W. L., SMITH, J. C. and HARRIOTT, P.: *Unit Operations of Chemical Engineering*, 4th edn. (McGraw-Hill, New York, 1984).
MCKENNA, B. M. (ed): *Engineering and Food*, Vol. 2. *Process Applications* (Elsevier Applied Science, New York, 1984).
MINTON, P. E.: *Handbook of Evaporation Technology*. (Noyes, New York, 1987).
PERRY, R. H. and GREEN, D. W. (eds): *Perry's Chemical Engineers' Handbook*. 6th edn. (McGraw-Hill Book Company, New York, 1984).
PETERS, M. S. and TIMMERHAUS, K. D.: *Plant Design and Economics for Chemical Engineers*, 3rd edn. (McGraw-Hill, New York, 1984).
SMITH, R. A.: *Vaporisors, Selection, Design and Operation*. (Longman, London, 1987).
TYNER, M.: *Process Engineering Calculations* (Ronald Press, New York, 1960).

14.9. REFERENCES

1. WESTWATER, J. W.: *Petro/Chem. Engr.* **33**, No. 9 (Aug. 1961) 186–9 and **33**, No. 10 (Sept. 1961) 219–26. Nucleate pool boiling.
2. PALEN, J. W. and TABOREK, J. J.: *Chem. Eng. Prog.* **58**, No. 7 (July 1962) 37–46. Refinery kettle reboilers: proposed method for design and optimization.
3. CRYDER, D. S. and GILLILAND, E. R.: *Ind. Eng. Chem.* **24** (1932) 1382–7. Heat transmission from metal surfaces to boiling liquids. I. Effect of physical properties of boiling liquid on liquid film coefficient.
4. CICHELLI, M. T. and BONILLA, C. F.: *Trans. Am. Inst. Chem. Eng.* **41** (1945) 755–87. Heat transfer to liquids boiling under pressure.
5. MCNELLY, M. J.: *J. Imp. Coll. Chem. Eng. Soc.* **7** (1953) 18. A correlation of the rates of heat transfer to nucleate boiling liquids.
6. GILMOUR, C. H.: *Chem. Eng. Prog.* Symp. Ser. No. 29, **55** (1959) 67–78. Performance of vaporizers: Heat transfer analysis of plant data.
7. ZUBER, N.: *Trans. Am. Soc. Mech. Eng.* **80** (1958) 711–20. On the stability of boiling heat transfer.
8. DENGLER, C. E. and ADDOMS, J. N.: *Chem. Eng. Prog.* Symp. Ser. No. 18, **52** (1956) 95–103. Heat transfer mechanism for vaporization of water in a vertical tube.
9. LOCKHART, R. W. and MARTINELLI, R. C.: *Chem. Eng. Prog.* **45** (1949) 39–48. Proposed correlation of data for isothermal two-phase, two-component flow in pipes.
10. GUERRIERI, S. A. and TALTY, R. D.: *Chem. Eng. Prog.* Symp. Ser. No. 18, **52** (1956) 69–77. A study of heat transfer to organic liquids in single-tube, natural-circulation, vertical-tube boilers.
11. OTHMER, D.F.: *Ind. Eng. Chem.* **32** (1940) 841. Correlating vapor pressure and latent heat date. A new plot.
12. HAUSBRAND, E.: *Evaporating, Condensing and Cooling Apparatus.* Translated from the second revised German edition by A. C. Wright. Fifth English edition revised by B. HEASTIE (E. Benn, London. 1933).
13. STORROW, J. A.: *Ind. Chemist* **27** (1951) 298. Design calculations for multiple-effect evaporators — Part 3.
14. STEWART, G. and BEVERIDGE, G. S. G.: *Computers and Chemical Engineering* **1** (1977). 3. Steady-state cascade simulation in multiple effect evaporation.

This book belongs to Bradley Loren (bloren@mcandrews-ip.com) Copyright Elsevier 2024

Intas Exhibit 1032
Page 213 of 470
PGR2025-00043

15. WEBRE, A. L.: *Chem. Met. Eng.* **27** (1922) 1073. Evaporation — A study of the various operating cycles in triple effect units.
16. SCHWARZ, H. W.: *Food Technol.* **5** (1951) 476. Comparison of low temperature (e.g. 15–24 citrus juice) evaporators.
17. REAVELL, B. N.: *Ind. Chemist* **29** (1953) 475. Developments in evaporation with special reference to heat sensitive liquors.
18. MCCABE, W.L. and ROBINSON, C.S.: *Ind. Eng. Chem.* **16** (1924) 478. Evaporator scale formation.
19. HARKER, J.H.: *Processing* **12** (December 1978) 31–32. Finding the economic balance in evaporator operation.
20. MOORE, J. G. and HESLER, W. E.: *Chem. Eng. Prog.* **59**, No. 2 (Feb. 1963) 87–92. Equipment for the food industry — 2: Evaporation of heat sensitive materials.
21. PARKER, N. H.: *Chem. Eng., Albany* **70**, No. 15 (22 July 1963) 135–40. How to specify evaporators.
22. HOLLAND, A. A.: *Chem. Eng., Albany* **55** (xii) (1948) 121. More Saskatchewan salt cake.
23. HOLLAND, A. A.: *Chem. Eng., Albany* **58** (i) (1951) 106. New type evaporator.
24. BLOCH, M. R., FARKAS, L., and SPIEGLER, K. S.: *Ind. Eng. Chem.* **43** (1951) 1544. Solar evaporation of salt brines.
25. SWINDIN, N.: *Trans. Inst. Chem. Eng.* **27** (1949) 209. Recent developments in submerged combustion.
26. HILLIARD, A.: *Brit. Chem. Eng.* **4** (1959) 138–43. Considerations on the design of graphite heat exchangers.
27. HILLIARD, A.: *Brit. Chem. Eng.* **8** (1963) 234–7. The X-flow Polybloc system of construction for graphite.
28. HILLIARD, A.: *Ind. Chemist* **39** (1963) 525–31. Effect of anisotropy on design considerations for graphite.
29. BROOKS, C. H. and BADGER, W. L.: *Trans. Am. Inst. Chem. Eng.* **33** (1937) 392. Heat transfer coefficients in the boiling section of a long-tube, natural circulation evaporator.
30. STROEBE, G. W., BAKER, E. M., and BADGER, W. L.: *Trans. Am. Inst. Chem. Eng.* **35** (1939) 17. Boiling film heat transfer coefficients in a long-tube vertical evaporator.
31. CESSNA, O. C., LIENTZ, J. R., and BADGER, W. L.: *Trans. Am. Inst. Chem. Eng.* **36** (1940) 759. Heat transfer in a long-tube vertical evaporator.
32. BRESSLER, R.: *Z. Ver. deut. Ing.* **100**, No. 15 (1958) 630–8. Versuche über die Verdampfung von dünnen Flüssigkeitsfilmen.
33. MCMANUS, T.: University of Durham, Ph.D. Thesis (1963). The influence of agitation on the boiling of liquids in tubes.
34. HARRIOTT, P.: *Chem. Eng. Prog.* Symp. Ser. No. 29, **55** (1959) 137–9. Heat transfer in scraped surface exchangers.
35. KOOL, J.: *Trans. Inst. Chem. Eng.* **36** (1958) 253–8. Heat transfer in scraped vessels and pipes handling viscous materials.
36. MUTZENBURG, A. B.: *Chem. Eng., Albany* **72**, No. 19 (13 Sept. 1965) 175–8. Agitated thin film evaporators. Part I. Thin film technology.
37. PARKER, N.: *Chem. Eng., Albany* **72**, No. 19 (13 Sept. 1965) 179–85. Agitated thin film evaporators. Part 2. Equipment and economics.
38. FISCHER, R.: *Chem. Eng., Albany* **72**, No. 19 (13 Sept. 1965) 186–90. Agitated thin film evaporators. Part 3. Process applications.
39. RYLEY, J. T.: *Ind. Chemist* **38** (1962) 311–19. Controlled film processing.
40. FRANKEL, A.: *Proc. Inst. Mech. Eng.* **174**, No. 7 (1960) 312–24. Flash evaporators for the distillation of sea-water.
41. SILVER, R. S.: *Proc. Inst. Mech. Eng.* **179**, Pt. 1. No. 5 (1964–5) 135–54. Nominated Lecture: Fresh water from the sea.
42. BAKER, R. A.: *Chem. Eng. Prog.* **59**, No. 6 (June 1963) 80–3. The flash evaporator.
43. WOODWARD, T.: *Chem. Eng. Prog.* **57**, No. 1 (Jan. 1961) 52–7. Heat transfer in a spray column.
44. WILKE, C. R., CHENG, C. T., LEDESMA, V. L., and PORTER, J. W.: *Chem. Eng. Prog.* **59**, No. 12 (Dec. 1963) 69–75. Direct contact heat transfer for sea water evaporation.
45. OTHMER, D. F., BENENATI, R. F., and GOULANDRIS, G. C.: *Chem. Eng. Prog.* **57**, No. 1 (Jan. 1961) 47–51. Vapour reheat flash evaporation without metallic surfaces.
46. BAMFORTH, A. W.: *Industrial Crystallization* (Leonard Hill, London, 1965).
47. BECKERMAN, J. J.: *Foams, Theory and Industrial Applications* (Reinhold, New York, 1953).
48. GOLDBERG, M. and RUBIN, E.: *Ind. Eng. Chem. Process Design and Development* **6** (1967) 195–200. Mechanical foam breaking.
49. ARROWSMITH, G.: *Trans. Inst. Chem. Eng.* **27** (1949) 101. Production of vacuum for industrial chemical processes.
50. MCCULLOUGH, G. E.: *Ind. Eng. Chem.* **43** (1951) 1505. Concentration of radioactive liquid waste by evaporation.

This book belongs to Bradley Loren (bloren@mcandrews-ip.com) Copyright Elsevier 2024

Intas Exhibit 1032
Page 214 of 470
PGR2025-00043

14.10. NOMENCLATURE

		Units in SI System	Dimensions in **M, L, T, θ**
A	Heat transfer surface	m^2	$\mathbf{L}^2$
a	Constant in Equation 14.11	m^4K^2/W^2	$\mathbf{M}^{-2}\mathbf{T}^5\boldsymbol{\theta}^2$
b	Constant in Equation 14.11	m^4K^2/W^2	$\mathbf{M}^{-2}\mathbf{T}^6\boldsymbol{\theta}^2$
C_b	Variable cost during operation	£/s	$\mathbf{T}^{-1}$
C_c	Total cost of a shutdown	£	—
C_p	Specific heat of liquid at constant pressure	J/kg K	$\mathbf{L}^2\mathbf{T}^{-2}\boldsymbol{\theta}^{-1}$
C_s	Surface factor	—	—
C_T	Total cost during period t_P	£	—
D	Liquid evaporated or steam condensed per unit time	kg/s	$\mathbf{MT}^{-1}$
d	A characteristic dimension	m	**L**
d_t	Tube diameter	m	**L**
E	Power to compressor	W	$\mathbf{ML}^2\mathbf{T}^{-3}$
E'	Net work done on unit mass	J/kg	$\mathbf{L}^2\mathbf{T}^{-2}$
G_F	Mass rate of feed	kg/s	$\mathbf{MT}^{-1}$
G_x	mass flow of extra steam dryness fraction	kg/s	$\mathbf{MT}^{-1}$
G_y	mass flow of sea water	kg/s	$\mathbf{MT}^{-1}$
g	Acceleration due to gravity	m/s^2	$\mathbf{LT}^{-2}$
H	Enthalpy per unit mass of vapour	J/kg	$\mathbf{L}^2\mathbf{T}^{-2}$
h	Average value of h_b for a tube bundle	W/m^2 K	$\mathbf{MT}^{-3}\boldsymbol{\theta}^{-1}$
h_b	Film heat transfer coefficient for boiling liquid	W/m^2 K	$\mathbf{MT}^{-3}\boldsymbol{\theta}^{-1}$
h_c	Film heat transfer coefficient for condensing steam	W/m^2 K	$\mathbf{MT}^{-3}\boldsymbol{\theta}^{-1}$
h_L	Liquid-film heat transfer coefficient	W/m^2 K	$\mathbf{MT}^{-3}\boldsymbol{\theta}^{-1}$
h_{tp}	Heat transfer coefficient for two phase mixture	W/m^2 K	$\mathbf{MT}^{-3}\boldsymbol{\theta}^{-1}$
k	Thermal conductivity of liquid	W/m K	$\mathbf{MLT}^{-3}\boldsymbol{\theta}^{-1}$
m	Mass	kg	**M**
M	Mass of cooling water per unit mass of vapour	kg/kg	—
N	Number of effects	—	—
P	Pressure	N/m^2	$\mathbf{ML}^{-1}\mathbf{T}^{-2}$
Q	Heat transferred per unit time	W	$\mathbf{ML}^2\mathbf{T}^{-3}$
Q_b	Total heat transferred during boiling time	J	$\mathrm{ML}^2\mathrm{T}^{-2}$
q	Heat flux per unit area	W/m^2	$\mathbf{MT}^{-3}$
T	Temperature	K	$\boldsymbol{\theta}$
T_b	Boiling temperature of liquid	K	$\boldsymbol{\theta}$
T_c	Condensing temperature of steam	K	$\boldsymbol{\theta}$
T_f	Feed temperature	K	$\boldsymbol{\theta}$
T_w	Heater wall temperature	K	$\boldsymbol{\theta}$
ΔT	Temperature difference	K	$\boldsymbol{\theta}$
t	Time	s	**T**
t_b	Boiling time	s	**T**
t_c	Time for emptying, cleaning and refilling unit	s	**T**
t_P	Total production time	s	**T**
U	Overall heat transfer coefficient	W/m^2 K	$\mathbf{MT}^{-3}\boldsymbol{\theta}^{-1}$
V	Volume	m^3	$\mathbf{L}^3$
G_F	Feed rate	kg/s	$\mathbf{MT}^{-1}$
X_{tt}	Lockhart and Martinelli's parameter(equations 14.5 and 14.6)	—	—
y	Mass fraction of vapour	—	—
Z	Hydrostatic head	m	**L**
γ	Ratio of specific heat at constant pressure to specific heat at constant volume	—	—
λ	Latent heat of vaporisation per unit mass	J/kg	$\mathbf{L}^2\mathbf{T}^{-2}$
η	Economy	—	—

This book belongs to Bradley Loren (bloren@mcandrews-ip.com) Copyright Elsevier 2024

Intas Exhibit 1032
Page 215 of 470
PGR2025-00043

		Units in SI System	Dimensions in **M, L, T, θ**
η'	Efficiency of ejector	—	—
μ_L	Viscosity of liquid	Ns/m^2	$\mathbf{ML^{-1}T^{-1}}$
μ_v	Viscosity of vapour	Ns/m^2	$\mathbf{ML^{-1}T^{-1}}$
ρ_L	Density of liquid	kg/m^3	$\mathbf{ML^{-3}}$
ρ_v	Density of vapour	kg/m^3	$\mathbf{ML^{-3}}$
σ	Interfacial tension	J/m^2	$\mathbf{MT^{-2}}$

Suffixes

0	refers to the steam side of the first effect
1, 2, 3	refer to the first, second and third effects
av	refers to an average value
c	refers to the condenser
i and e	refer to the inlet and exit cooling water

This book belongs to Bradley Loren (bloren@mcandrews-ip.com)
Copyright Elsevier 2024
Intas Exhibit 1032
Page 216 of 470
PGR2025-00043

CHAPTER 15

Crystallisation

15.1. INTRODUCTION

Crystallisation, one of the oldest of unit operations, is used to produce vast quantities of materials, including sodium chloride, sodium and aluminium sulphates and sucrose which all have production rates in excess of 10^8 tonne/year on a world basis. Many organic liquids are purified by crystallisation rather than by distillation since, as shown by MULLIN[1] in Table 15.1, enthalpies of crystallisation are generally much lower than enthalpies of vaporisation and crystallisation may be carried out closer to ambient temperature thereby reducing energy requirements. Against this, crystallisation is rarely the last stage in a process and solvent separation, washing and drying stages are usually required. Crystallisation is also a key operation in the freeze-concentration of fruit juices, the desalination of sea water, the recovery of valuable materials such as metal salts from electroplating processes, the production of materials for the electronic industries and in biotechnological operations such as the processing of proteins.

Table 15.1. Energy requirements for crystallisation and distillation[1]

Substance	Melting point (K)	Enthalpy of crystallisation (kJ/kg)	Boiling point (K)	Enthalpy of vaporisation (kJ/kg)
o-cresol	304	115	464	410
m-cresol	285	117	476	423
p-cresol	306	110	475	435
o-xylene	246	128	414	347
m-xylene	225	109	412	343
p-xylene	286	161	411	340
o-nitrotoluene	268.9	120	495	344
m-nitrotoluene	288.6	109	506	364
p-nitrotoluene	325	113	511	366
water	273	334	373	2260

Although crystals can be grown from the liquid phase — either a solution or a melt — and also from the vapour phase, a degree of supersaturation, which depends on the characteristics of the system, is essential in all cases for crystal formation or growth to take place. Some solutes are readily deposited from a cooled solution whereas others crystallise only after removal of solvent. The addition of a substance to a system in order to alter equilibrium conditions is often used in precipitation processes where supersaturation is sometimes achieved by chemical reaction between two or more substances and one of the reaction products is precipitated.

This book belongs to Bradley Loren (bloren@mcandrews-ip.com)

Copyright Elsevier 2024

Intas Exhibit 1032
Page 217 of 470
PGR2025-00043

15.2. CRYSTALLISATION FUNDAMENTALS

In evaluating a crystallisation operation, data on phase equilibria are important as this indicates the composition of product which might be anticipated and the degree of supersaturation gives some idea of the driving force available. The rates of nuclei formation and crystal growth are equally important as these determine the residence time in, and the capacity of a crystalliser. These parameters also enable estimates to be made of crystal sizes, essential for the specification of liquor flows through beds of crystals and also the mode and degree of agitation required. It is these considerations that form the major part of this Section.

15.2.1. Phase equilibria

One-component systems

Temperature and pressure are the two variables that affect phase equilibria in a one-component system. The phase diagram in Figure 15.1 shows the equilibria between the solid, liquid, and vapour states of water where all three phases are in equilibrium at the *triple point*, 0.06 N/m^2 and 273.3 K. The *sublimation curve* indicates the vapour pressure of ice, the *vaporisation curve* the vapour pressure of liquid water, and the *fusion curve* the effect of pressure on the melting point of ice. The fusion curve for ice is unusual in that, in most one component systems, increased pressure increases the melting point, whilst the opposite occurs here.

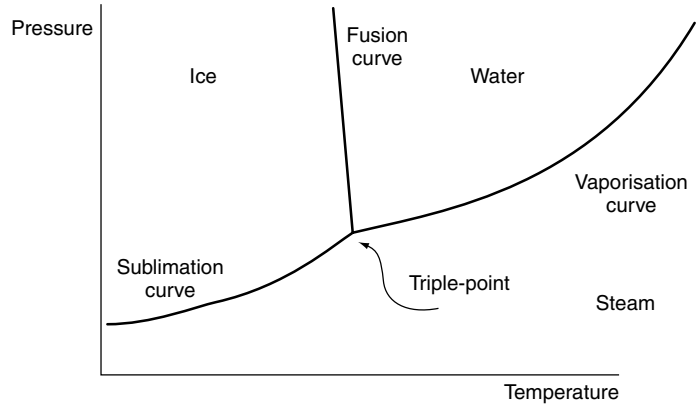


Figure 15.1. Phase diagram for water

A single substance may crystallise in more than one of seven crystal systems, all of which differ in their lattice arrangement, and exhibit not only different basic shapes but also different physical properties. A substance capable of forming more than one different crystal is said to exhibit *polymorphism*, and the different forms are called *polymorphs*. Calcium carbonate, for example, has three polymorphs — calcite (hexagonal),

This book belongs to Bradley Loren (bloren@mcandrews-ip.com) Copyright Elsevier 2024

Intas Exhibit 1032
Page 218 of 470
PGR2025-00043

aragonite (tetragonal), and vaterite (trigonal). Although each polymorph is composed of the same single substance, it constitutes a separate phase. Since only one polymorph is thermodynamically stable at a specified temperature and pressure, all the other polymorphs are potentially capable of being transformed into the stable polymorph. Some polymorphic transformations are rapid and reversible and polymorphs may be *enantiotropic* (interconvertible) or *monotropic* (incapable of transformation). Graphite and carbon, for example, are monotropic at ambient temperature and pressure, whereas ammonium nitrate has five enantiotropic polymorphs over the temperature range 255–398 K. Figure 15.2*a*, taken from MULLIN[2], shows the phase reactions exhibited by two enantiotropic forms, α and β, of the same substance. The point of intersection of the two vapour pressure curves is the transition point at which the two forms can co-exist in equilibrium at the specified temperature and pressure. The triple point at which vapour, liquid and β solid can co-exist may be considered as the melting point of the β form. On slow heating, solid α changes into solid β and finally melts with the reverse process taking place on slow cooling. Rapid heating or cooling can, however, result in

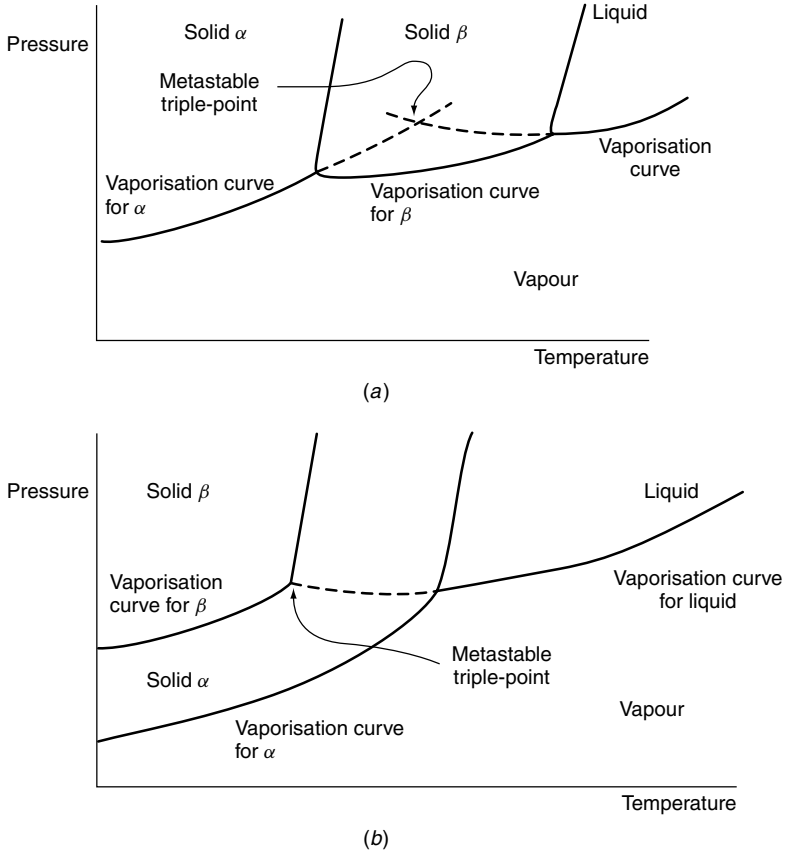


Figure 15.2. Phase diagram for polymorphic substances[2]

This book belongs to Bradley Loren (bloren@mcandrews-ip.com) Copyright Elsevier 2024

Intas Exhibit 1032
Page 219 of 470
PGR2025-00043

different behaviour where the vapour pressure of the α form follows a continuation of the vaporisation curve, and changes in the liquid are represented by the liquid vaporisation curve. The two curves intersect at a *metastable triple point* where the liquid, vapour, and a solid can coexist in metastable equilibrium. Figure 15.2*b* shows the pressure–temperature curves for a monotropic substance for which the vapour pressure curves of the α and β forms do not intersect, and hence there is no transition point. In this case, solid β is the metastable form, and the metastable triple point is as shown.

Two-component systems

Temperature, pressure, and concentration can affect phase equilibria in a two-component or binary system, although the effect of pressure is usually negligible and data can be shown on a two-dimensional temperature–concentration plot. Three basic types of binary system — eutectics, solid solutions, and systems with compound formation — are considered and, although the terminology used is specific to melt systems, the types of behaviour described may also be exhibited by aqueous solutions of salts, since, as MULLIN[3] points out, there is no fundamental difference in behaviour between a melt and a solution.

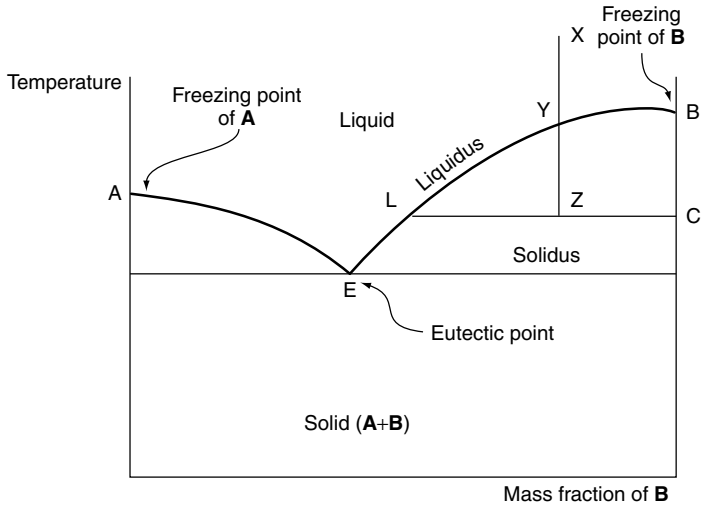
An example of a binary *eutectic system* **AB** is shown in Figure 15.3*a* where the eutectic is the mixture of components that has the lowest crystallisation temperature in the system. When a melt at X is cooled along XZ, crystals, theoretically of pure **B**, will start to be deposited at point Y. On further cooling, more crystals of pure component **B** will be deposited until, at the eutectic point E, the system solidifies completely. At Z, the crystals C are of pure **B** and the liquid L is a mixture of **A** and **B** where the mass proportion of solid phase (crystal) to liquid phase (residual melt) is given by ratio of the lengths LZ to CZ; a relationship known as the *lever arm rule*. Mixtures represented by points above AE perform in a similar way, although here the crystals are of pure **A**. A liquid of the eutectic composition, cooled to the eutectic temperature, crystallises with unchanged composition and continues to deposit crystals until the whole system solidifies. Whilst a eutectic has a fixed composition, it is not a chemical compound, but is simply a physical mixture of the individual components, as may often be visible under a low-power microscope.

The second common type of binary system is one composed of a continuous series of *solid solutions*, where the term *solid solution* or *mixed crystal* refers to an intimate mixture on the molecular scale of two or more components. The components of a solid-solution system cannot be separated as easily as those of a eutectic system. This is shown in Figure 15.3*b*, where the liquidus represents the temperature at which mixtures of **A** and **B** begin to crystallise on cooling and the solidus represents temperatures at which mixtures begin to melt on heating. A melt at X begins to crystallise at Y and then at Z, the system consists of a mixture of crystals of a composition represented by C and a liquid of a composition represented by L, where the ratio of crystals to liquid is again given by the lever arm rule. The crystals do not, however, consist of a single pure component as in a simple eutectic system but are an intimate mixture of components **A** and **B** which must be heated and re-crystallised, perhaps many times, in order to achieve further purification. In this way, a simple eutectic system may be purified in a single-stage crystallisation operation, whereas a solid-solution system always needs multistage operation.

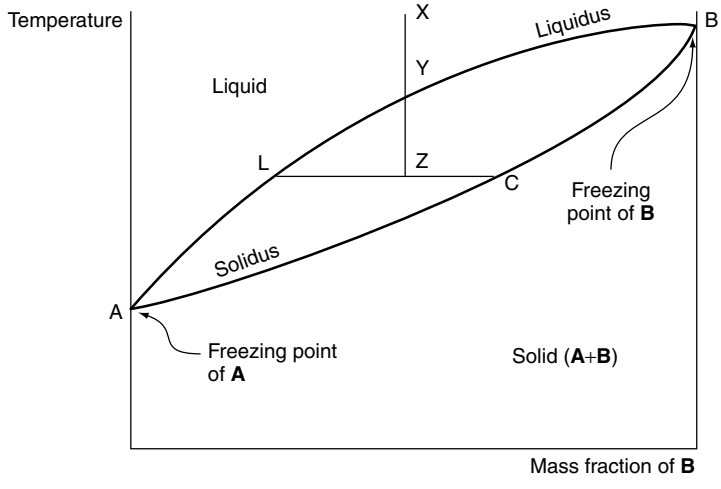
The solute and solvent of a binary system can combine to form one or more different *compounds* such as, for example, hydrates in aqueous solutions. If the compound can

This book belongs to Bradley Loren (bloren@mcandrews-ip.com) Copyright Elsevier 2024

Intas Exhibit 1032
Page 220 of 470
PGR2025-00043



(*a*) Eutectic



(*b*) Solid solution

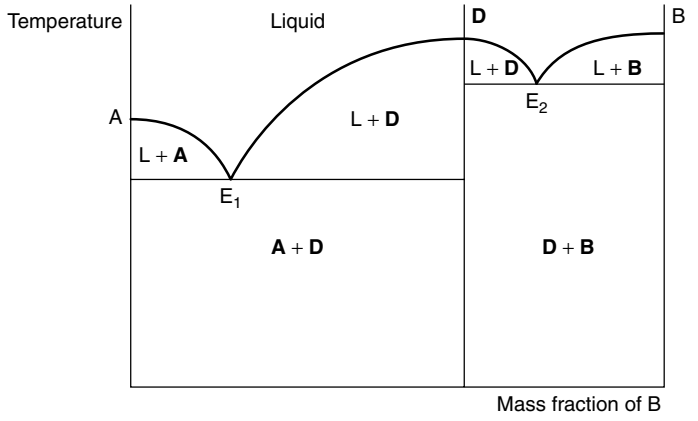
(AE, EB - Crystallisation temperatures of all mixtures of **A** and **B**)

Figure 15.3. Phase diagrams for binary systems

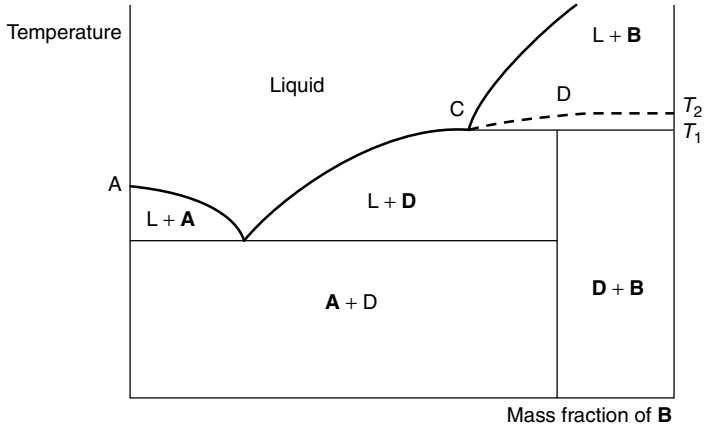
co-exist in stable equilibrium with a liquid phase of the same composition, then it has a *congruent* melting point, that is where melting occurs without change in composition. If this is not the case, then the melting point is *incongruent*. In Figure 15.4*a*, the heating–cooling cycle follows the vertical line through point D since melting and crystallisation occur without any change of composition. In Figure 15.4*b*, however, compound **D** decomposes at a temperature T_1 which is below its theoretical melting point T_2. Thus, if

This book belongs to Bradley Loren (bloren@mcandrews-ip.com) Copyright Elsevier 2024

Intas Exhibit 1032
Page 221 of 470
PGR2025-00043



(*a*) Congruent melting point



(*b*) Incongruent melting point

Figure 15.4. Phase diagrams for binary systems (E - eutectic, L - liquid)

D is heated, melting begins at T_1, though is not complete. At T_1, a system of composition D contains crystals of pure **B** in a melt of composition C. If this mixture is cooled, then a solid mixture of **B** and that represented by point C is obtained and subsequent heating and cooling cycles result in further decomposition of the compound represented by D.

There is current interest in the use of inorganic-salt hydrates as heat-storage materials, particularly for storage of solar heat in domestic and industrial space heating, where, ideally, the hydrate should have a congruent melting point so that sequences of crystallisation–melting–crystallisation can be repeated indefinitely. Incongruently melting hydrate systems tend to stratify on repeated temperature cycling with a consequent loss of efficiency as melting gives a liquid phase that contains crystals of a lower hydrate or of the anhydrous salt, which settle to the bottom of the container and fail to re-dissolve on subsequent heating. Calcium chloride hexahydrate, whilst not a true congruently melting

This book belongs to Bradley Loren (bloren@mcandrews-ip.com) Copyright Elsevier 2024
Intas Exhibit 1032
Page 222 of 470
PGR2025-00043

hydrate, appears to be one of the most promising materials[4,5] as are sodium sulphate deca-hydrate, sodium acetate tri-hydrate, and sodium thiosulphate penta-hydrate which all do have incongruent melting points[6,7].

Three-component systems

Phase equilibria in three-component systems are affected by temperature, pressure, and the concentrations of any two of the three components. Since the effect of pressure is usually negligible, phase equilibria may be plotted on an isothermal triangular diagram and, as an example, the temperature–concentration space model for *o*-, *m*-, and *p*-nitrophenol is shown in Figure 15.5*a*[3]. The three components are **O**, **M**, and **P**, respectively and points O′, M′, and P′ represent the melting points of the pure components *o*- (318 K), *m*- (370 K) and *p*-nitrophenol (387 K). The vertical faces of the prism represent temperature–concentration diagrams for the three binary eutectic systems **O-M**, **O-P**, and **M-P**, which are all similar to that shown in Figure 15.4. The binary eutectics are represented by points A (304.7 K; 72.5 per cent **O**, 27.5 per cent **M**), B (306.7 K; 75.5 per cent **O**, 24.5 per cent **P**), and C (334.7 K; 54.8 per cent **M**, 45.2 per cent **P**) and AD within the prism represents the effect of adding **P** to the **O-M** binary eutectic at A. Similarly, curves BD and CD denote the lowering of freezing points of the binary eutectics represented by points B and C, respectively, upon adding the third component. Point D is a ternary eutectic point (294.7 K; 57.7 per cent **O**, 23.2 per cent **M**, 19.1 per cent **P**) at which the liquid freezes to form a solid mixture of the three components. The section above the freezing point surfaces formed by the liquidus curves represents the homogeneous liquid phase, the section below these surfaces down to a temperature, D denotes solid and liquid phases in equilibrium and the section below this temperature represents a completely solidified system.

Figure 15.5*b* is the projection of AD, BD, and CD in Figure 15.5*a* on to the triangular base of the prism. Again **O**, **M** and **P** are the pure components, points A, B, and C represent the three binary eutectic points and D is the ternary eutectic point. The diagram is divided by AD, BD, and CD into three regions which denote the three liquidus surfaces in the space model and the temperature falls from the apexes and sides of the triangle toward the eutectic point D. Several isotherms showing points on the liquidus surfaces are shown. When, for example, a molten mixture with a composition X is cooled, solidification starts when the temperature is reduced to 353 K and since X lies in the region ADCM, pure *m*-nitrophenol is deposited. The composition of the remaining melt changes along line MX′ and at X′, equivalent to 323 K, *p*-nitrophenol also starts to crystallise. On further cooling, both *m* and *p*-nitrophenol are deposited and the composition of the liquid phase changes in the direction X′D. When the melt composition and temperature reach point D, *o*-nitrophenol also crystallises out and the system solidifies without further change in composition.

Many different types of phase behaviour are encountered in ternary systems that consist of water and two solid solutes. For example, the system $KNO_3-NaNO_3-H_2O$ which does not form hydrates or combine chemically at 323 K is shown in Figure 15.6, which is taken from MULLIN[3]. Point A represents the solubility of KNO_3 in water at 323 K (46.2 kg/100 kg solution), C the solubility of $NaNO_3$ (53.2 kg/100 kg solution), AB is the composition of saturated ternary solutions in equilibrium with solid KNO_3 and BC

This book belongs to Bradley Loren (bloren@mcandrews-ip.com) Copyright Elsevier 2024

Intas Exhibit 1032
Page 223 of 470
PGR2025-00043

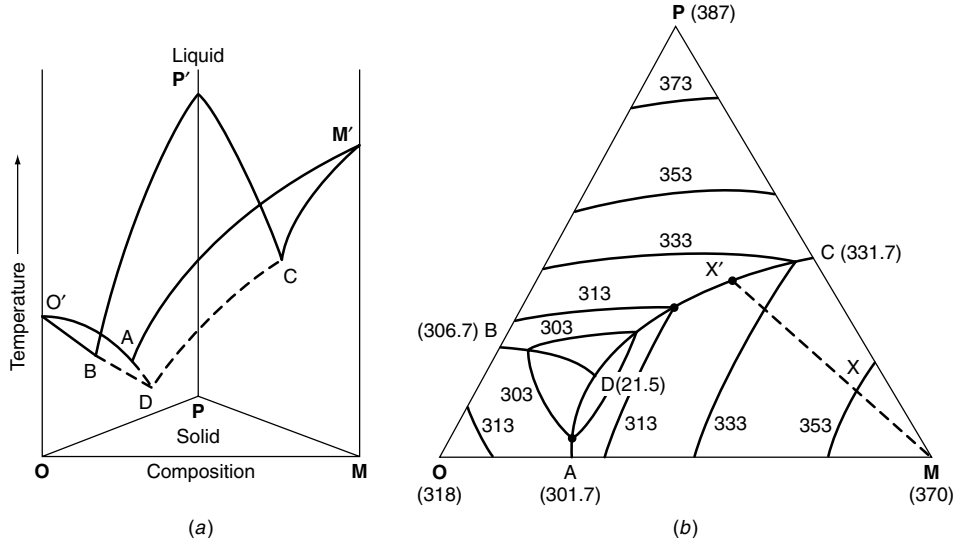


Figure 15.5. Eutectic formation in the ternary system *o*-, *m*- and *p*-nitrophenol[3] a) Temperature–concentration space model; b) Projection on a triangular diagram. (Numerical values represent temperatures in K)

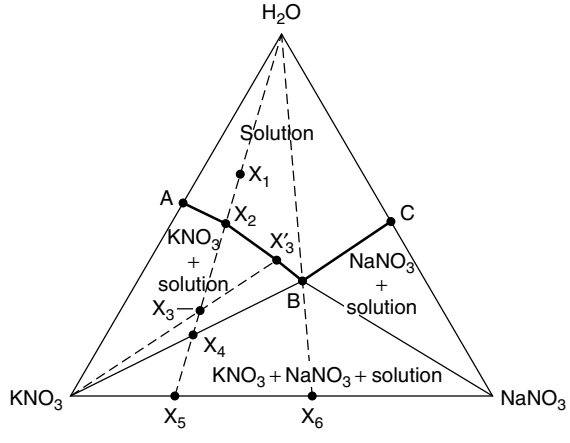


Figure 15.6. Phase diagram for the ternary system $KNO_3-NaNO_3-H_2O$ at 323 K[3]

those in equilibrium with solid $NaNO_3$. The area above the line ABC is the region of unsaturated homogeneous solutions. At point B, the solution is saturated with both KNO_3 and $NaNO_3$. If, for example, water is evaporated isothermally from an unsaturated solution at X_1, the solution concentration increases along X_1X_2 and pure KNO_3 is deposited when the concentration reaches X_2. If more water is evaporated to give a system of composition X_3, the solution composition is represented by X_3' on the saturation curve AB, and by point B when composition X_4 is reached. Further removal of water causes deposition

This book belongs to Bradley Loren (bloren@mcandrews-ip.com) Copyright Elsevier 2024
Intas Exhibit 1032
Page 224 of 470
PGR2025-00043

of $NaNO_3$. After this, all solutions in contact with solid have a constant composition B, which is referred to as the *eutonic point* or *drying-up point* of the system. After complete evaporation of water, the composition of the solid residue is indicated by X_5. Similarly, if an unsaturated solution, represented by a point to the right of B is evaporated isothermally, only $NaNO_3$ is deposited until the solution composition reaches B. KNO_3 is then also deposited and the solution composition remains constant until evaporation is complete. If water is removed isothermally from a solution of composition B, the composition of deposited solid is given by X_6 and it remains unchanged throughout the evaporation process.

Multi-component systems

The more components in a system, the more complex are the phase equilibria and it is more difficult to represent phases graphically. Descriptions of multi-component solid–liquid diagrams and their uses have been given by MULLIN[3], FINDLAY and CAMPBELL[8], RICCI[9], NULL[10] and NYVLT[11] and techniques for predicting multi-component solid–liquid phase equilibria have been presented by HORMEYER *et al.*[12], KUSIK *et al.*[13], and SANDER *et al.*[14].

Phase transformations

Metastable crystalline phases frequently crystallise to a more stable phase in accordance with Ostwald's rule of stages, and the more common types of phase transformation that occur in crystallising and precipitating systems include those between polymorphs and solvates. Transformations can occur in the solid state, particularly at temperatures near the melting point of the crystalline solid, and because of the intervention of a solvent. A stable phase has a lower solubility than a metastable phase, as indicated by the solubility curves in Figures 15.7*a* and 15.7*b* for enantiotropic and monotropic systems respectively and,

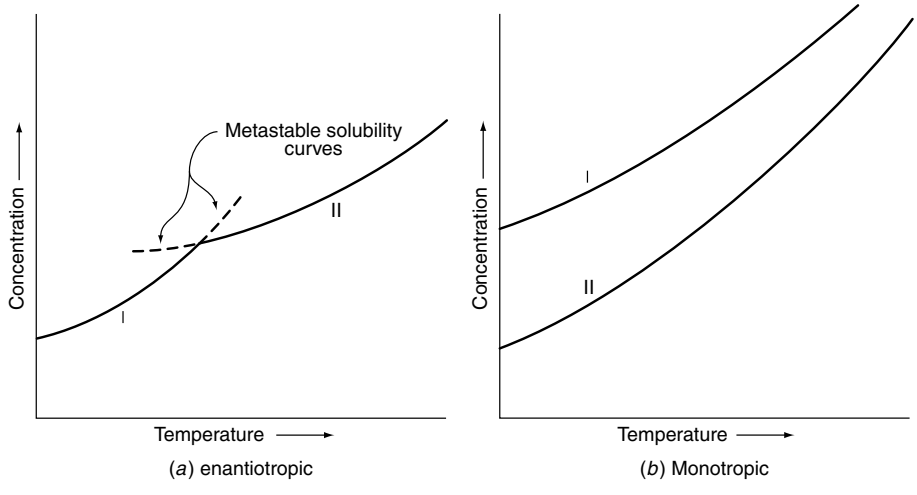


Figure 15.7. Solubility curves for substances with two polymorphs I and II[2]

This book belongs to Bradley Loren (bloren@mcandrews-ip.com) Copyright Elsevier 2024

Intas Exhibit 1032
Page 225 of 470
PGR2025-00043

whilst transformation cannot occur between the metastable (I) and stable (II) phases in the monotropic system in the temperature range shown, it is possible above the transition temperature in an enantiotropic system. Polymorphic transformation adds complexity to a phase diagram, as illustrated by NANCOLLAS *et al.*[15] and NANCOLLAS and REDDY[16] who have studied dissolution–recrystallisation transformations in hydrate systems, and CARDEW *et al.*[17] and CARDEW and DAVEY[18] who have presented theoretical analyses of both solid state and solvent-mediated transformations in an attempt to predict their kinetics.

15.2.2. Solubility and saturation

Supersaturation

A solution that is in thermodynamic equilibrium with the solid phase of its solute at a given temperature is a saturated solution, and a solution containing more dissolved solute than that given by the equilibrium saturation value is said to be supersaturated. The degree of supersaturation may be expressed by:

$$\Delta c = c - c^* \tag{15.1}$$

where c and c^* are the solution concentration and the equilibrium saturation value respectively. The supersaturation ratio, S, and the relative supersaturation, φ are then:

$$S = c/c^* \tag{15.2}$$

and:

$$\varphi = \Delta c/c^* = S - 1 \tag{15.3}$$

Solution concentrations may be expressed as mass of anhydrate/mass of solvent or as mass of hydrate/mass of free solvent, and the choice affects the values of S and φ as shown in the following example which is based on the data of MULLIN[3].

Example 15.1

At 293 K, a supersaturated solution of sucrose contains 2.45 kg sucrose/kg water. If the equilibrium saturation value is 2.04 kg/kg water, what is the supersaturation ratio in terms of kg/kg water and kg/kg solution?

Solution

For concentrations in kg sucrose/kg water:

$$c = 2.45 \text{ kg/kg}, c^* = 2.04 \text{ kg/kg}$$

and:

$$S = c/c^* = (2.45/2.04) = \underline{\underline{1.20}}$$

For concentrations in kg sucrose/kg solution:

$$c = 2.45/(2.45 + 1.0) = 0.710 \text{ kg/kg solution},$$

$$c^* = 2.04/(2.04 + 1.0) = 0.671 \text{ kg/kg solution}$$

and:

$$S = (0.710/0.671) = \underline{\underline{1.06}}$$

This book belongs to Bradley Loren (bloren@mcandrews-ip.com) Copyright Elsevier 2024

Intas Exhibit 1032
Page 226 of 470
PGR2025-00043

Whilst the fundamental driving force for crystallisation, the true thermodynamic supersaturation, is the difference in chemical potential, in practice supersaturation is generally expressed in terms of solution concentrations as given in equations 15.1–15.3. MULLIN and SÖHNEL[19] has presented a method of determining the relationship between concentration-based and activity-based supersaturation by using concentration-dependent activity-coefficients.

In considering the state of supersaturation, OSTWALD[20] introduced the terms *labile* and *metastable* supersaturation to describe conditions under which spontaneous (primary) nucleation would or would not occur, and MIERS and ISAAC[21] have represented the metastable zone by means of a solubility–supersolubility diagram, as shown in Figure 15.8.

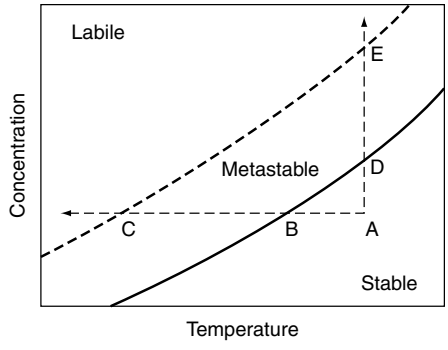


Figure 15.8. Solubility supersolubility diagram

Whilst the (continuous) solubility curve can be determined accurately, the position of the (broken) supersolubility curve is less certain as it is influenced by factors such as the rate at which the supersaturation is generated, the degree of agitation and the presence of crystals or impurities. In the stable unsaturated zone, crystallisation is impossible. In the metastable supersaturated zone, spontaneous nucleation is improbable although a crystal would grow, and in the unstable or labile saturated zone, spontaneous nucleation is probable but not inevitable. If a solution at A is cooled without loss of solvent along ABC, spontaneous nucleation cannot occur until C is reached. Although the tendency to nucleate increases once the labile zone is reached, some solutions become too viscous to permit nucleation and set to a glass. Supersaturation can also be achieved by removing solvent and ADE represents such an operation carried out at constant temperature. Because the solution near the evaporating surface is more highly supersaturated than the bulk solution, penetration into the labile zone rarely occurs and crystals at the surface fall into the solution and induce nucleation, often before bulk conditions at E have been reached. Industrial crystallisers often combine cooling and evaporation. The width of the metastable zone is often expressed as a temperature difference, ΔT which is related to the corresponding concentration difference, Δc by the point slope of the solubility curve, $\mathrm{d}c^*/\mathrm{d}T$ or:

$$\Delta c \simeq \frac{\mathrm{d}c^*}{\mathrm{d}T}\Delta T \tag{15.4}$$

This book belongs to Bradley Loren (bloren@mcandrews-ip.com) Copyright Elsevier 2024
Intas Exhibit 1032
Page 227 of 470
PGR2025-00043

Table 15.2. Maximum allowable supercooling ΔT_{max} for aqueous salt Solutions at 298 K[3]

Substance	deg K	Substance	deg K	Substance	deg K
NH_4Cl	0.7	$Na_2CO_3.10H_2O$	0.6	$Na_2S_2O_3.5H_2O$	1.0
NH_4NO_3	0.6	$Na_2CrO_4.10H_2O$	1.6	K alum	4.0
$(NH_4)_2SO_4$	1.8	NaCl	4.0	KBr	1.1
$NH_4H_2PO_4$	2.5	$Na_2B_4O_7.10H_2O$	4.0	KCl	1.1
$CuSO_4.5H_2O$	1.4	NaI	1.0	KI	0.6
$FeSO_4.7H_2O$	0.5	$NaHPO_4.12H_2O$	0.4	KH_2PO_4	9.0
$MgSO_4.7H_2O$	1.0	$NaNO_3$	0.9	KNO_3	0.4
$NiSO_4.7H_2O$	4.0	$NaNO_2$	0.9	KNO_2	0.8
$NaBr.2H_2O$	0.9	$Na_2SO_4.10H_2O$	0.3	K_2SO_4	6.0

Data measured in the presence of crystals with slow cooling and moderate agitation. The working value for a normal crystalliser may be 50 per cent of these values or less.

The measurement of the width of the metastable zone is discussed in Section 15.2.4, and typical data are shown in Table 15.2. Provided the actual solution concentration and the corresponding equilibrium saturation concentration at a given temperature are known, the supersaturation may be calculated from equations 15.1–15.3. Data on the solubility for two- and three-component systems have been presented by SEIDELL and LINKE[22], STEPHEN *et al.*[23] and BROUL *et al.*[24]. Supersaturation concentrations may be determined by measuring a concentration-dependent property of the system such as density or refractive index, preferably in situ on the plant. On industrial plant, both temperature and feedstock concentration can fluctuate, making the assessment of supersaturation difficult. Under these conditions, the use of a mass balance based on feedstock and exit-liquor concentrations and crystal production rates, averaged over a period of time, is usually an adequate approach.

Prediction of solubilities

Techniques are available for estimating binary and multi-component solubility behaviour. One example is the van't Hoff relationship which, as stated by MOYERS and ROUSSEAU[25], takes the following form for an ideal solution:

$$\ln x = \frac{H_f}{\mathbf{R}T}\left(\frac{T}{T_M} - 1\right) \tag{15.5}$$

where x is the mole fraction of solute in solution, H_f is the heat of fusion and T_M is the melting point of the pure component. One interesting consequence of this equation is that solubility depends only on the properties of the solute occurring in the equation. Another equation frequently used for ideal systems incorporates cryoscopic constants, values of which have been obtained empirically for a wide variety of materials in the course of the American Petroleum Research Project 44[26]. This takes the form:

$$\ln(1/x) = z_1(T_M - T)[1 + z_2(T_M - T)\ldots..] \tag{15.6}$$

where:

$$z_1 = \frac{H_f}{\mathbf{R}T_M^2} \text{ and } z_2 = \frac{1}{T_M} - \frac{C_p}{2H_f}\Big/2H_f.$$

MOYERS and ROUSSEAU[25] have used equations 15.5 and 15.6. to calculate the freezing point data for *o*- and *p*-xylene shown in Table 15.3.

This book belongs to Bradley Loren (bloren@mcandrews-ip.com) Copyright Elsevier 2024

Intas Exhibit 1032
Page 228 of 470
PGR2025-00043

Table 15.3. Calculated freezing point curves for *o*- and *p*-xylene[25]

	Data		*p*-xylene	*o*-xylene
	T_M (K)		286.41	247.97
	ΔH_f (kJ/kmol)		17120	13605
	A (mole fraction/deg K)		0.02599	0.02659
	B (mole fraction/deg K)		0.0028	0.0030
Temperature (K)	Mole fraction in solution *p*-xylene		*o*-xylene	
	Eqn. 15.5	Eqn. 15.6	Eqn. 15.5	Eqn. 15.6
286.41	1.00	1.00		
280	0.848	0.844		
270	0.646	0.640		
260	0.482	0.478		
249.97			1.00	1.00
240	0.249	0.256	0.803	0.805
235			0.695	0.699
230	0.172	0.183		

Crystal size and solubility

If *very small* solute particles are dispersed in a solution, the solute concentration may exceed the normal equilibrium saturation value. The relationship between particle size and solubility first applied to solid–liquid systems by OSTWALD[20] may be expressed as:

$$\ln \frac{c_r}{c^*} = \frac{2\,M\sigma}{n_i \mathbf{R} T \rho_s r} \tag{15.7}$$

where c_r is the solubility of particles of radius r, ρ_s the density of the solid, M the relative molecular mass of the solute in solution, σ the interfacial tension of the crystallisation surface in contact with its solution and n_i the moles of ions formed from one mole of electrolyte. For a non-electrolyte, $n_i = 1$ and for most inorganic salts in water, the solubility increase is really only significant for particles of less than 1 μm. The use of this equation is illustrated in the following example which is again based on data from MULLIN[3].

Example 15.2

Compare the increase in solubility above the normal equilibrium values of 1, 0.1 and 0.01 μm particles of barium sulphate and sucrose at 298 K. The relevant properties of these materials are:

	barium sulphate	sucrose
relative molecular mass (kg/kmol)	233	342
number of ions (−)	2	1
solid density (kg/m^3)	4500	1590
interfacial tension (J/m^2)	0.13	0.01

Solution

Taking the gas constant, **R** as 8314 J/kmol K, then in equation 15.7:

This book belongs to Bradley Loren (bloren@mcandrews-ip.com) Copyright Elsevier 2024

Intas Exhibit 1032
Page 229 of 470
PGR2025-00043

For barium sulphate:

$$\ln(c_r/c^*) = (2 \times 233 \times 0.13)/(2 \times 8314 \times 298 \times 4500r) = 2.72 \times 10^{-9}/r$$

For sucrose:

$$\ln(c_r/c^*) = (2 \times 342 \times 0.01)/(1 \times 8314 \times 298 \times 1590\, r) = 1.736 \times 10^{-9}/r$$

Substituting 0.5×10^{-7}, 0.5×10^{-8} and 0.5×10^{-9} m for r gives the following data:

	particle size d(μm)	r(μm)	c_r/c^*	increase (per cent)
barium sulphate	1	0.5	1.005	0.5
	0.1	0.05	1.06	6
	0.01	0.005	1.72	72
sucrose	1	0.5	1.004	0.4
	0.1	0.05	1.035	3.5
	0.01	0.005	1.415	41.5

Effect of impurities

Industrial solutions invariably contain dissolved impurities that can increase or decrease the solubility of the prime solute considerably, and it is important that the solubility data used to design crystallisation processes relate to the actual system used. Impurities can also have profound effects on other characteristics, such as nucleation and growth.

15.2.3. Crystal nucleation

Nucleation, the creation of crystalline bodies within a supersaturated fluid, is a complex event, since nuclei may be generated by many different mechanisms. Most nucleation classification schemes distinguish between *primary nucleation* - in the absence of crystals and *secondary nucleation* - in the presence of crystals. STRICKLAND-CONSTABLE[27] and KASHCHIEV[28] have reviewed nucleation, and GARSIDE and DAVEY[29] have considered secondary nucleation in particular.

Primary nucleation

Classical theories of primary nucleation are based on sequences of bimolecular collisions and interactions in a supersaturated fluid that result in the build-up of lattice-structured bodies which may or may not achieve thermodynamic stability. Such primary nucleation is known as *homogeneous*, although the terms *spontaneous* and *classical* have also been used. As discussed by UBBELHODE[30] and GARTEN and HEAD[31], ordered solute-clustering can occur in supersaturated solutions prior to the onset of homogeneous nucleation, and BERGLUND *et al.*[32] has detected the presence of quasi-solid-phase species even in unsaturated solutions. MULLIN and LECI[33] discussed the development of concentration gradients in supersaturated solutions of citric acid under the influence of gravity, and LARSON and GARSIDE[34] estimated the size of the clusters at 4–10 nm. Primary nucleation may also be initiated by suspended particles of foreign substances, and this mechanism is generally

This book belongs to Bradley Loren (bloren@mcandrews-ip.com) Copyright Elsevier 2024

Intas Exhibit 1032
Page 230 of 470
PGR2025-00043

referred to as *heterogeneous* nucleation. In industrial crystallisation, most primary nucleation is almost certainly heterogeneous, rather than homogeneous, in that it is induced by foreign solid particles invariably present in working solutions. Although the mechanism of heterogeneous nucleation is not fully understood, it probably begins with adsorption of the crystallising species on the surface of solid particles, thus creating apparently crystalline bodies, larger than the critical nucleus size, which then grow into macro-crystals.

Homogeneous nucleation. A consideration of the energy involved in solid-phase formation and in creation of the surface of an arbitrary spherical crystal of radius r in a supersaturated fluid gives:

$$\Delta G = 4\pi r^2\sigma + (4\pi/3)r^3\Delta G_v \tag{15.8}$$

where ΔG is the overall excess free energy associated with the formation of the crystalline body, σ is the interfacial tension between the crystal and its surrounding supersaturated fluid, and ΔG_v is the free energy change per unit volume associated with the phase change. The term $4\pi r^2\sigma$, which represents the surface contribution, is positive and is proportional to r^2 and the term $(4\pi/3)r^3\Delta G_v$ which represents the volume contribution, is negative and is proportional to r^3. Any crystal smaller than the critical nucleus size r_c is unstable and tends to dissolve whilst any crystal larger than r_c is stable and tends to grow. Combining equations 15.7 and 15.8, and expressing the rate of nucleation J in the form of an Arrhenius reaction rate equation, gives the nucleation rate as:

$$J = F\exp\left[-\frac{16\pi\sigma^3 v^2}{3\,\mathbf{k}^3T^3(\ln S)^2}\right] \tag{15.9}$$

where F is a pre-exponential factor, v is molar volume, $\mathbf{k}$ is the Boltzmann constant and S is the supersaturation ratio. Since equation 15.9 predicts an explosive increase in the nucleation rate beyond some so-called critical value of S, it not only demonstrates the powerful effect of supersaturation on homogeneous nucleation, but also indicates the possibility of nucleation at any level of supersaturation.

Heterogeneous nucleation. The presence of foreign particles or heteronuclei enhances the nucleation rate of a given solution, and equations similar to those for homogeneous nucleation have been proposed to express this enhancement. The result is simply a displacement of the nucleation rate against supersaturation curve, as shown in Figure 15.9, indicating that nucleation occurs more readily at a lower degree of supersaturation. For primary nucleation in industrial crystallisation, classical relationships similar to those based on equation 15.9 have little use, and all that can be justified is a simple empirical relationship such as:

$$J = K_N(\Delta c)^n \tag{15.10}$$

which relates the primary nucleation rate J to the supersaturation Δc from equation 15.1. The primary nucleation rate constant K_N, and the order of the nucleation process n, which is usually greater than 2, depend on the physical properties and hydrodynamics of the system.

Secondary nucleation

Secondary nucleation can, by definition, take place only if crystals of the species under consideration are already present. Since this is usually the case in industrial crystallisers, secondary nucleation has a profound influence on virtually all industrial crystallisation processes.

This book belongs to Bradley Loren (bloren@mcandrews-ip.com) Copyright Elsevier 2024

Intas Exhibit 1032
Page 231 of 470
PGR2025-00043

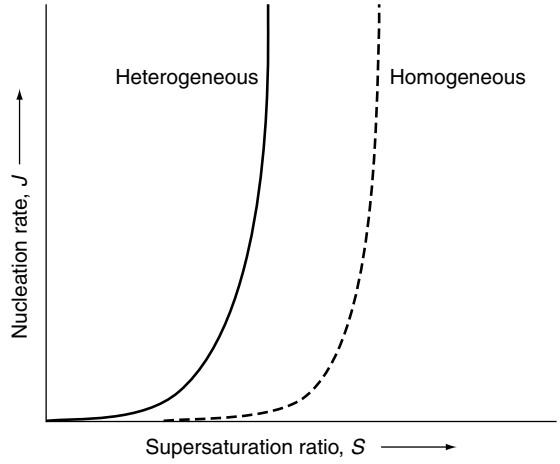


Figure 15.9. Effect of supersaturation on the rates of homogeneous and heterogeneous nucleation.

Apart from deliberate or accidental introduction of tiny seed crystals to the system, and productive interactions between existing crystals and quasi-crystalline embryos or clusters in solution, the most influential mode of new crystal generation in an industrial crystalliser is contact secondary nucleation between the existing crystals themselves, between crystals and the walls or other internal parts of the crystalliser, or between crystals and the mechanical agitator. Secondary nucleation rates (in $m^{-3}s^{-1}$) are most commonly correlated by empirical relationships such as:

$$B = K_b \rho_m^j N^l \Delta c^b \tag{15.11}$$

where B is the rate of secondary nucleation or birthrate, K_b *is* the birthrate constant, ρ_m is the slurry concentration or magma density and N is a term that gives some measure of the intensity of agitation in the system such as the rotational speed of an impeller. The exponents j, l, and b vary according to the operating conditions.

Nucleation measurements

One of the earliest attempts to derive nucleation kinetics for solution crystallisation was proposed by Nyvlt[35] and Nyvlt *et al.*[36] whose method is based on the measurement of metastable zone widths shown in Figure 15.8, using a simple apparatus, shown in Figure 15.10, consisting of a 50 ml flask fitted with a thermometer and a magnetic stirrer, located in an external cooling bath. Nucleation is detected visually and both primary and secondary nucleation can be studied in this way. Typical results[3] shown in Figure 15.11 demonstrate that seeding has a considerable influence on the nucleation process, and the difference between the slopes of the two lines indicates that primary and secondary nucleation occur by different mechanisms. Solution turbulence also affects nucleation and, in general, agitation reduces the metastable zone width. For example, the metastable zone width for gently agitated potassium sulphate solutions is about 12 deg K whilst vigorous agitation reduces this to around 8 deg K. The presence of crystals also induces secondary

This book belongs to Bradley Loren (bloren@mcandrews-ip.com) Copyright Elsevier 2024

Intas Exhibit 1032
Page 232 of 470
PGR2025-00043

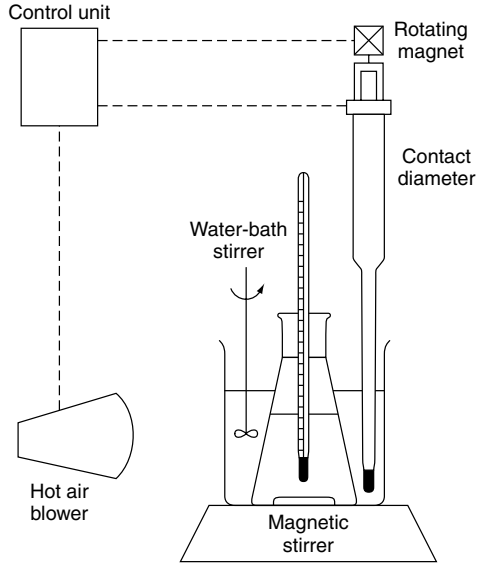


Figure 15.10. Simple apparatus for measuring metastable zone widths[36]

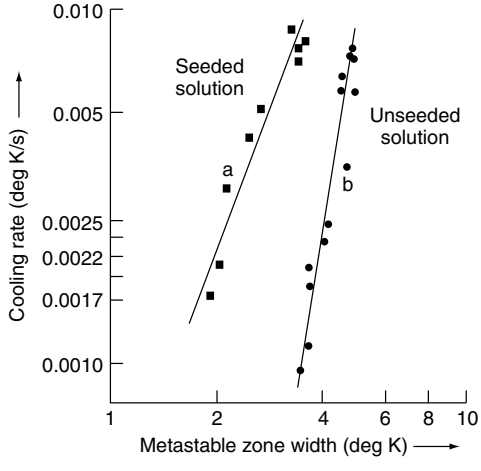


Figure 15.11. Metastable zone width of aqueous ammonium[3]

nucleation at a supercooling of around 4 deg K. The relation between supercooling ΔT and supersaturation Δc is given by equation 15.4. Useful information on secondary nucleation kinetics for crystalliser operation and design can be determined only from model experiments that employ techniques such as those developed for MSMPR (mixed-suspension mixed-product removal) crystallisers. As discussed by, NYVLT *et al.*[36] and RANDOLPH and LARSON[37], in a real crystalliser, both nucleation and growth proceed together and interact with other system parameters in a complex manner.

This book belongs to Bradley Loren (bloren@mcandrews-ip.com) Copyright Elsevier 2024
Intas Exhibit 1032
Page 233 of 470
PGR2025-00043

Induction periods

A delay occurs between attainment of supersaturation and detection of the first newly created crystals in a solution, and this so-called *induction period*, t_i is a complex quantity that involves both nucleation and growth components. If it is assumed that t_i is essentially concerned with nucleation, that is $t_i \propto 1/J$, then MULLIN[3] has shown, from equation 15.9, that:

$$\frac{1}{t_i} \propto \exp \frac{\sigma^3}{T^3(\log S)^2} \tag{15.12}$$

Thus, for a given temperature, a logarithmic plot of t_i against $(\log S)^{-2}$ should yield a straight line which, if the data truly represent homogeneous nucleation, will allow the calculation of the interfacial tension σ and the evaluation of the effect of temperature on σ. NIELSEN and SÖHNEL[38] has attempted to derive a general correlation between interfacial tension and the solubility of inorganic salts as shown in Figure 15.12*a*, although the success of this method depends on precise measurement of the induction period t_i, which presents problems if t_i is less than a few seconds.

SÖHNEL and MULLIN[39] have shown that short induction periods can be determined by a technique that detects rapid changes in the conductivity of a supersaturated solution. Typical results for $CaCO_3$, $SrCO_3$, and $BaCO_3$, produced by mixing an aqueous solution of Na_2CO_3 with a solution of the appropriate chloride, are shown in Figure 15.12*b*. The slopes of the linear, high-supersaturation regions are used to calculate the interfacial tensions ($0.08-0.12$ J/m^2), which compare reasonably well with the values predicted from the interfacial tension–solubility relationship in Figure 15.12*a*. Although interfacial tensions evaluated from experimentally measured induction periods are somewhat unreliable, measurements of the induction period can provide useful information on other crystallisation phenomena, particularly the effect of impurities.

15.2.4. Crystal growth

Fundamentals

As with nucleation, classical theories of crystal growth[3,20,21,35,40–42] have not led to working relationships, and rates of crystallisation are usually expressed in terms of the supersaturation by empirical relationships. In essence, overall mass deposition rates, which can be measured in laboratory fluidised beds or agitated vessels, are needed for crystalliser design, and growth rates of individual crystal faces under different conditions are required for the specification of operating conditions.

In simple terms, the crystallisation process may be considered to take place in two stages — a diffusional step in which solute is transported from the bulk fluid through the solution boundary layer adjacent to the crystal surface, and a deposition step in which adsorbed solute ions or molecules at the crystal surface are deposited and integrated into the crystal lattice. These two stages which are shown in Figure 15.13, may be described by:

$$\mathrm{d}m/\mathrm{d}t = k_d A(c - c_i) = k_r A(c_i - c^*)^i \tag{15.13}$$

where m is the mass deposited in time t, A is the crystal surface area, c, c_i and c^* are the solute concentrations in the bulk solution, at the interface and at equilibrium saturation and k_d and k_r are the diffusion and deposition or reaction mass transfer coefficients.

This book belongs to Bradley Loren (bloren@mcandrews-ip.com) Copyright Elsevier 2024

Intas Exhibit 1032
Page 234 of 470
PGR2025-00043

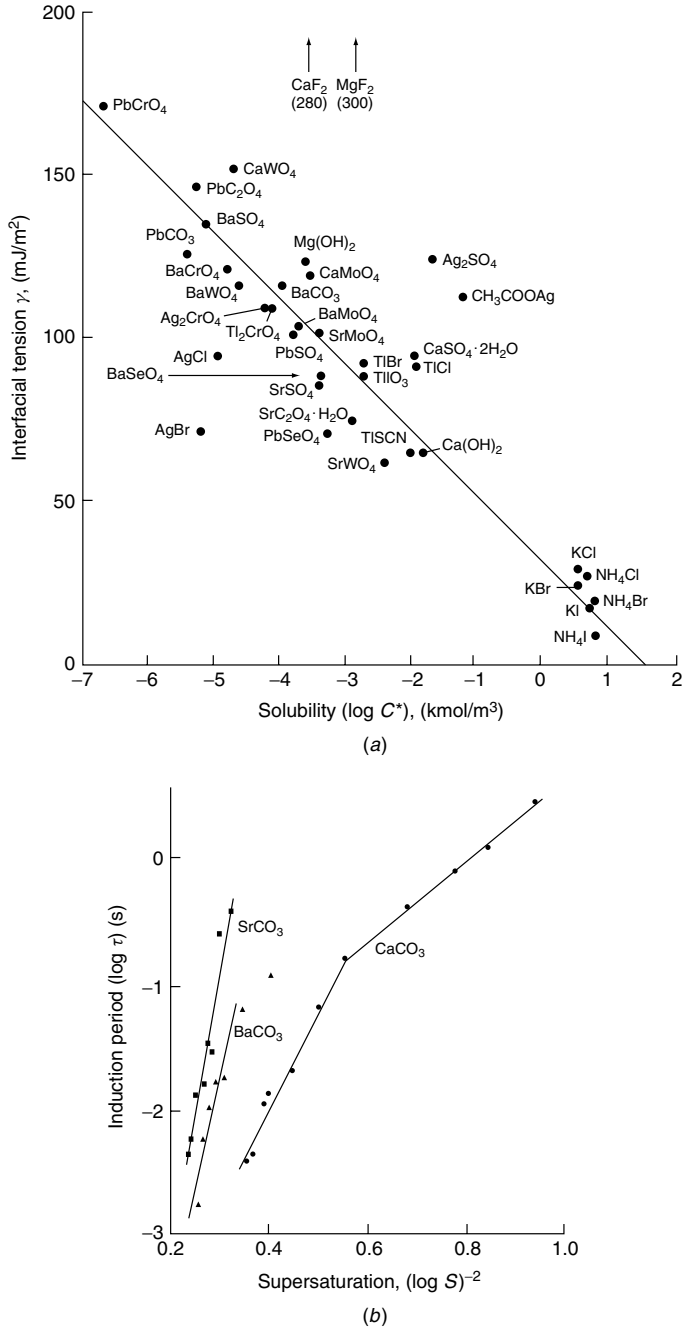


Figure 15.12. (*a*) Interfacial tension as a function of solubility[38] (*b*) Induction period as a function of initial supersaturation[39]

This book belongs to Bradley Loren (bloren@mcandrews-ip.com)
Copyright Elsevier 2024
Intas Exhibit 1032
Page 235 of 470
PGR2025-00043

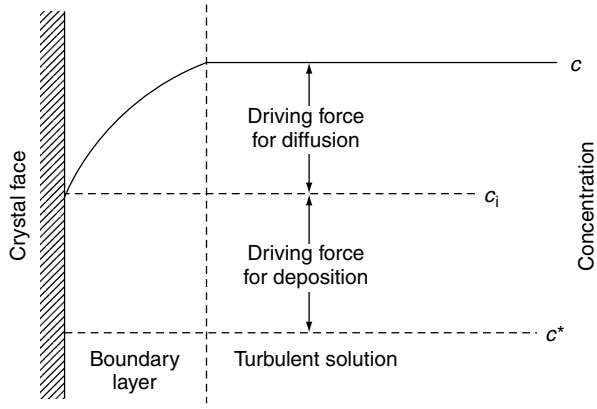


Figure 15.13. Concentration driving forces for crystal growth from solution

Because it is not possible to determine the interfacial concentration, this is eliminated by using the overall concentration driving force $\Delta c = (c - c^*)$, where:

$$(c - c^*) = \left(\frac{1}{k_d}\right)\frac{\mathrm{d}m}{\mathrm{d}t} + \left(\frac{1}{k_r}\right)\left(\frac{\mathrm{d}m}{\mathrm{d}t}\right)^{\frac{1}{i}}$$

Eliminating c and introducing an overall crystal growth coefficient, K_G gives the approximate relation:

$$\mathrm{d}m/\mathrm{d}t = K_G(\Delta c)^s \tag{15.14}$$

The exponents i and s in equations 15.13 and 15.14, referred to as the order of integration and overall crystal growth process, should not be confused with their more conventional use in chemical kinetics where they always refer to the power to which a concentration should be raised to give a factor proportional to the rate of an elementary reaction. As MULLIN[3] points out, in crystallisation work, the exponent has no fundamental significance and cannot give any indication of the elemental species involved in the growth process. If $i = 1$ and $s = 1$, c_i may be eliminated from equation 15.13 to give:

$$\frac{1}{K_G} = \frac{1}{k_D} + \frac{1}{k_r} \tag{15.15}$$

Where the rate of integration is very high, K_G is approximately equal to k_d and the crystallisation is diffusion controlled. When the diffusional resistance is low, K_G is approximately equal to k_r and the process is controlled by the deposition step. Whilst the diffusional step is generally proportional to the concentration driving force, the *integration* process is rarely first-order and for many inorganic salts crystallising from aqueous solution, s lies in the range 1– 2.

Comprehensive reviews of theories of crystal growth have been presented by GARSIDE[43], NIELSEN[44], PAMPLIN[45] and KALDIS and SCHEEL[46].

This book belongs to Bradley Loren (bloren@mcandrews-ip.com) Copyright Elsevier 2024

Intas Exhibit 1032
Page 236 of 470
PGR2025-00043

Measurement of growth rate

Methods used for the measurement of crystal growth rates are either a) direct measurement of the linear growth rate of a chosen crystal face or b) indirect estimation of an overall linear growth rate from mass deposition rates measured on individual crystals or on groups of freely suspended crystals[3,35,41,47,48].

Face growth rates. Different crystal faces grow at different rates and faces with a high value of s grow faster than faces with low values. Changes in growth environment such as temperature, supersaturation pH, and impurities can have a profound effect on growth, and differences in individual face growth rates give rise to habit changes in crystals. For the measurement of individual crystal-face growth-rates, a fixed crystal in a glass cell is observed with a travelling microscope under precisely controlled conditions of solution temperature, supersaturation and liquid velocity[3]. The solution velocity past the fixed crystal is often an important growth-determining parameter, sometimes responsible for the so-called size-dependent growth effect often observed in agitated and fluidised-bed crystallisers. Large crystals have higher settling velocities than small crystals and, if their growth is diffusion-controlled, they tend to grow faster. Salts that exhibit solution velocity dependent growth rates include the alums, nickel ammonium sulphate, and potassium sulphate, although salts such as ammonium sulphate and ammonium or potassium dihydrogen phosphate are not affected by solution velocity.

Overall growth rates. In the laboratory, growth rate data for crystalliser design can be measured in fluidised beds or in agitated vessels, and crystal growth rates measured by growing large numbers of carefully sized seeds in fluidised suspension under strictly controlled conditions. A warm undersaturated solution of known concentration is circulated in the crystalliser and then supersaturated by cooling to the working temperature. About 5 g of closely sized seed crystals with a narrow size distribution and a mean size of around 500 μm is introduced into the crystalliser, and the upward solution velocity is adjusted so that the crystals are maintained in a reasonably uniform fluidised state in the growth zone. The crystals are allowed to grow at a constant temperature until their total mass is some 10 g, when they are removed, washed, dried, and weighed. The final solution concentration is measured, and the mean of the initial and final supersaturations is taken as the average for the run, an assumption which does not involve any significant error because the solution concentration is usually not allowed to change by more than about 1 per cent during a run. The overall crystal growth rate is then calculated in terms of mass deposited per unit area per unit time at a specified supersaturation.

Expression of growth rate

Because the rate of growth depends, in a complex way, on temperature, supersaturation, size, habit, system turbulence and so on, there is no simple was of expressing the rate of crystal growth, although, under carefully defined conditions, growth may be expressed as an overall mass deposition rate, R_G (kg/m^2 s), an overall linear growth rate, $G_d (= \mathrm{d}d/\mathrm{d}t)$ (m/s) or as a mean linear velocity, $u' (= \mathrm{d}r/\mathrm{d}t)$ (m/s). Here d is some characteristic size of the crystal such as the equivalent aperture size, and r is the radius corresponding to the

This book belongs to Bradley Loren (bloren@mcandrews-ip.com) Copyright Elsevier 2024

Intas Exhibit 1032
Page 237 of 470
PGR2025-00043

equivalent sphere where $r = 0.5d$. The relationships between these quantities are:

$$R_G = K_G \Delta c^s = \left(\frac{1}{A}\right)\frac{\mathrm{d}m}{\mathrm{d}t} = \frac{3\alpha\rho\dfrac{\mathrm{d}d}{\mathrm{d}t}}{\beta} = \left(\frac{6\alpha\rho}{\beta}\right)\frac{\mathrm{d}r}{\mathrm{d}t} = \frac{6\alpha\rho u'}{\beta} \tag{15.16}$$

where ρ is the density of the crystal and the volume and surface shape factors, α and β, are related to particle mass m and surface area A, respectively, by:

$$m = \alpha\rho d^3 \tag{15.17}$$

and:

$$A = \beta d^2 \tag{15.18}$$

Values of $6\alpha/\beta$ are 1 for spheres and cubes and 0.816 for octahedra and typical values of the mean linear growth velocity, $u'(= 0.5\ G_d)$ for crystals 0.5–1 mm growing in the presence of other crystals are given in Table 15.4 which is taken from MULLIN[3].

Table 15.4. Mean over-all crystal growth rates expressed as a linear velocity[3]

	Supersaturation ratio		
Substance	deg K	S	u' (m/s)
NH_4NO_3	313	1.05	8.5×10^{-7}
$(NH_4)_2SO_4$	303	1.05	2.5×10^{-7}
	333	1.05	4.0×10^{-7}
$MgSO_4.7H_2O$	293	1.02	4.5×10^{-8}
	303	1.01	8.0×10^{-8}
	303	1.02	1.5×10^{-7}
KCl	313	1.01	6.0×10^{-7}
KNO_3	293	1.05	4.5×10^{-8}
	313	1.05	1.5×10^{-7}
K_2SO_4	293	1.09	2.8×10^{-8}
	293	1.18	1.7×10^{-7}
	303	1.07	4.2×10^{-8}
	323	1.06	7.0×10^{-8}
	323	1.12	3.2×10^{-7}
NaCl	323	1.002	2.5×10^{-8}
	323	1.003	6.5×10^{-8}
	343	1.002	9.0×10^{-8}
	343	1.003	1.5×10^{-7}

Dependence of growth rate on crystal size

Experimental evidence indicates that crystal growth kinetics often depend on crystal size, possibly because the size depends on the surface deposition kinetics and different crystals of the same size can also have different growth rates because of differences in surface structure or perfection. In addition, as discussed by WHITE *et al.*[49], JONES and MULLIN[50], JANSE and DE JONG[51] and GARSIDE and JANČIČ[52], small crystals of many substances grow much more slowly than larger crystals, and some do not grow at all. The behaviour of very small crystals has considerable influence on the performance of continuously operated crystallisers because new crystals with a size of 1–10 μm are constantly generated by secondary nucleation and these then grow to populate the full crystal size distribution.

This book belongs to Bradley Loren (bloren@mcandrews-ip.com) Copyright Elsevier 2024

Intas Exhibit 1032
Page 238 of 470
PGR2025-00043

Growth - nucleation interactions

Crystal nucleation and growth in a crystalliser cannot be considered in isolation because they interact with one another and with other system parameters in a complex manner. For a complete description of the crystal size distribution of the product in a continuously operated crystalliser, both the nucleation and the growth processes must be quantified, and the laws of conservation of mass, energy, and crystal population must be applied. The importance of population balance, in which all particles are accounted for, was first stressed in the pioneering work of RANDOLPH and LARSON[37].

Crystal habit modification

Differences in the face growth-rates of crystals give rise to changes in their habit or shape. Although the growth kinetics of individual crystal faces usually depend to various extents on supersaturation so that crystal habit can sometimes be controlled by adjusting operating conditions, the most common cause of habit modification is the presence of impurities. Although a soluble impurity will often remain in the liquid phase so that pure crystals are formed, in many cases, both the rate of nucleation and the crystal growth rate are affected. More usually, the effect is one of retardation, thought to be due to the adsorption of the impurity on the surface of the nucleus or crystal. Materials with large molecules such as tannin, dextrin or sodium hexametaphosphate, added in small quantities to boiler feed water, prevent the nucleation and growth of calcium carbonate crystals and hence reduce scaling. In a similar way, the addition of 0.1 per cent of HCl and 0.1 per cent $PbCl_2$ prevent the growth of sodium chloride crystals. In some cases the adsorption occurs preferentially on one particular face of the crystal, thus modifying the crystal shape. One example is that sodium chloride crystallised from solutions containing traces of urea forms octohedral instead of the usual cubic crystals. In a similar way, dyes are preferentially adsorbed on inorganic crystals[53], although the effect is not always predictable. GARRETT[54] has described a number of uses of additives as habit modifiers, and industrial applications of habit modification are reported in several reviews[3,55,56] in which the factors that must be considered in selecting a suitable habit modifier are discussed. In the main, solid impurities act as condensation nuclei and cause dislocations in the crystal structure.

Inclusions in crystals

Inclusions are small pockets of solid, liquid, or gaseous impurities trapped in crystals that usually occur randomly although a regular pattern may be sometimes observed. As described by MULLIN[3], a simple technique for observing inclusions is to immerse the crystal in an inert liquid of similar refractive index or, alternatively, in its own saturated solution when, if the inclusion is a liquid, concentration streamlines will be seen as the two fluids meet and, if it is a vapour, a bubble will be released. Industrial crystals may contain significant amounts of included mother liquor that can significantly affect product purity and stored crystals may cake because of liquid seepage from inclusions in broken crystals. In order to minimise inclusions, the crystallising system should be free of dirt and other solid debris, vigorous agitation or boiling should be avoided, and ultrasonic irradiation may be used to suppress adherence of bubbles to a growing crystal face. As fast crystal growth is probably the

This book belongs to Bradley Loren (bloren@mcandrews-ip.com) Copyright Elsevier 2024

Intas Exhibit 1032
Page 239 of 470
PGR2025-00043

most common cause of inclusion formation, high supersaturation levels should be avoided. DEICHA[57], POWERS[58], WILCOX and KUO[59] and SASKA and MYERSON[60] have published detailed accounts of crystal inclusion.

15.2.5. Crystal yield

The yield of crystals produced by a given degree of cooling may be estimated from the concentration of the initial solution and the solubility at the final temperature, allowing for any evaporation, by making solvent and solute balances. For the solvent, usually water, the initial solvent present is equal to the sum of the final solvent in the mother liquor, the water of crystallisation within the crystals and any water evaporated, or:

$$w_1 = w_2 + y\frac{R-1}{R} + w_1 E \tag{15.19}$$

where w_1 and w_2 are the initial and final masses of solvent in the liquor, y is the yield of crystals, R is the ratio (molecular mass of hydrate/molecular mass of anhydrous salt) and E is the ratio (mass of solvent evaporated/mass of solvent in the initial solution). For the solute:

$$w_1 c_1 = w_2 c_2 + y/R \tag{15.20}$$

where c_1 and c_2 are the initial and final concentrations of the solution expressed as (mass of anhydrous salt/mass of solvent). Substituting for w_2 from equation 15.19:

$$w_1 c_1 = c_2\left[w_1(1-E) - y\frac{R-1}{R}\right] + \frac{y}{R} \tag{15.21}$$

from which the yield for aqueous solutions is given by:

$$y = R w_1 \frac{c_1 - c_2(1-E)}{1 - c_2(R-1)} \tag{15.22}$$

The actual yield may differ slightly from that given by this equation since, for example, when crystals are washed with fresh solvent on the filter, losses may occur through dissolution. On the other hand, if mother liquor is retained by the crystals, an extra quantity of crystalline material will be deposited on drying. Since published solubility data usually refer to pure solvents and solutes that are rarely encountered industrially, solubilities should always be checked against the actual working liquors.

Before equation 15.22 can be applied to vacuum or adiabatic cooling crystallisation, the quantity E must be estimated, where, from a heat balance:

$$E = \frac{qR(c_1 - c_2) + C_p(T_1 - T_2)(1 + c_1)[1 - c_2(R-1)]}{\lambda[1 - c_2(R-1)] - qRc_2} \tag{15.23}$$

In this equation, λ is the latent heat of evaporation of the solvent (J/kg), q is the heat of crystallisation of the product (J/kg), T_1 is the initial temperature of the solution (K), T_2 is the final temperature of the solution (K) and C_p is the specific heat capacity of the solution (J/kg K).

This book belongs to Bradley Loren (bloren@mcandrews-ip.com) Copyright Elsevier 2024

Intas Exhibit 1032
Page 240 of 470
PGR2025-00043

Example 15.3

What is the theoretical yield of crystals which may be obtained by cooling a solution containing 1000 kg of sodium sulphate (molecular mass = 142 kg/kmol) in 5000 kg water to 283 K? The solubility of sodium sulphate at 283 K is 9 kg anhydrous salt/100 kg water and the deposited crystals will consist of the deca-hydrate (molecular mass = 322 kg/kmol). It may be assumed that 2 per cent of the water will be lost by evaporation during cooling.

Solution

The ratio, $R = (322/142) = 2.27$

The initial concentration, $c_1 = (1000/5000) = 0.2$ kg Na_2SO_4/kg water

The solubility, $c_2 = (9/100) = 0.09$ kg Na_2SO_4/kg water

The initial mass of water, $w_1 = 5000$ kg and the water lost by evaporation, $E = (2/100) = 0.02$ kg/kg

Thus, in equation 15.22:

$$\text{yield, } y = (5000 \times 2.27)[0.2 - 0.09(1 - 0.02)]/[1 - 0.09(2.27 - 1)]$$

$$= \underline{\underline{1432 \text{ kg } Na_2SO_4.10H_2O}}$$

Example 15.4

What is the yield of sodium acetate crystals ($CH_3COONa.3H_2O$) obtainable from a vacuum crystalliser operating at 1.33 kN/m^2 when it is supplied with 0.56 kg/s of a 40 per cent aqueous solution of the salt at 353 K? The boiling point elevation of the solution is 11.5 deg K.

Data:

Heat of crystallisation, $q = 144$ kJ/kg trihydrate
Heat capacity of the solution, $C_p = 3.5$ kJ/kg deg K
Latent heat of water at 1.33 kN/m^2, $\lambda = 2.46$ MJ/kg
Boiling point of water at 1.33 kN/m^2 = 290.7 K
Solubility of sodium acetate at 290.7 K, $c_2 = 0.539$ kg/kg water.

Solution

Equilibrium liquor temperature = (290.7 + 11.5) = 302.2 K.
Initial concentration, $c_1 = 40/(100 - 40) = 0.667$ kg/kg water
Final concentration, $c_2 = 0.539$ kg/kg water
Ratio of molecular masses, $R = (136/82) = 1.66$

Thus, in equation 15.23:

$$E = \{144 \times 1.66(0.667 - 0.539) + 3.5(353 - 302.2)(1 + 0.667)[1 - 0.539(1.66 - 1)]\}/$$

$$\{2460[1 - 0.539(1.66 - 1)] - (144 \times 1.66 \times 0.539)\}$$

$$= 0.153 \text{ kg/kg water originally present.}$$

This book belongs to Bradley Loren (bloren@mcandrews-ip.com) Copyright Elsevier 2024

Intas Exhibit 1032
Page 241 of 470
PGR2025-00043

The yield is then given by equation 15.22 as:

$$y = (0.56(100 - 40)/100)1.66[0.667 - 0.539(1 - 0.153)]/[1 - 0.539(1.66 - 1)]$$
$$= \underline{\underline{0.183 \text{ kg/s}}}$$

15.2.6. Caking of crystals

Crystalline materials frequently cake or cement together on storage and crystal size, shape, moisture content, and storage conditions can all contribute to the caking tendency. In general, caking is caused by a dampening of the crystal surfaces in storage because of inefficient drying or an increase in atmospheric humidity above some critical value that depends on both substance and temperature. The presence of a hygroscopic trace impurity in the crystals, can also greatly influence their tendency to absorb atmospheric moisture. Moisture may also be released from inclusions if crystals fracture under storage conditions and, if crystal surface moisture later evaporates, adjacent crystals become firmly joined together with a cement of re-crystallised solute. Caking may be minimised by efficient drying, packaging in airtight containers, and avoiding compaction on storage. In addition, crystals may be coated with an inert dust that acts as a moisture barrier. Small crystals are more prone to cake than large crystals because of the greater number of contact points per unit mass, although actual size is less important than size distribution and shape and the narrower the size distribution and the more granular the shape, the lower is the tendency of crystals to cake. Crystal size distribution can be controlled by adjusting operating conditions in a crystalliser and crystal shape may be influenced by the use of habit modifiers. A comprehensive account of the inhibition of caking by trace additives has been given by PHOENIX[61].

15.2.7. Washing of crystals

The product from a crystalliser must be subjected to efficient solid–liquid separation in order to remove mother liquor and, whilst centrifugal filtration can reduce the liquor content of granular crystals to 5–10 per cent, small irregular crystals may retain more than 50 per cent. After filtration, the product is usually washed to reduce the amount of liquor retained still further and, where the crystals are very soluble in the liquor, another liquid in which the substance is relatively insoluble is used for the washing, although this two-solvent method means that a solvent recovery unit is required. When simple washing is inadequate, two stages may be required for the removal of mother liquor with the crystals removed from the filter, re-dispersed in wash liquor and filtered again. This may cause a loss of yield although this is much less than the loss after a complete re-crystallisation.

If, for simplicity, it is assumed that the soluble impurity is in solution and that solution concentrations are constant throughout the dispersion vessel, then wash liquor requirements for decantation washing may be estimated as follows.

If, in *batch operation*, c_{io} and c_{in} denote the impurity concentrations in the crystalline material (kg impurity/kg product) initially and after washing stage n respectively, and F

This book belongs to Bradley Loren (bloren@mcandrews-ip.com) Copyright Elsevier 2024

Intas Exhibit 1032
Page 242 of 470
PGR2025-00043

is the fraction of liquid removed at each decantation, then a mass balance gives:

$$c_{in} = c_{io}(1 - F)^n \tag{15.24}$$

or:
$$\ln(c_{in}/c_{io}) = n \ln(1 - F) \tag{15.25}$$

For *continuous operation*, where fresh wash-liquid enters the vessel continuously and liquor is withdrawn through a filter screen, then a mass balance gives:

$$V_L \, \mathrm{d}c = -c_\mathrm{i} \, \mathrm{d}V_W \tag{15.26}$$

or:
$$\ln(c_{in}/c_{io}) = -V_W/V_L \tag{15.27}$$

where c_{io} and c_{in} are the initial and final concentrations and V_L and V_W are the volumes of liquor in the vessel and of the wash-water respectively. Combining equations 15.25 and 15.27:

$$n \ln(1 - F) = -V_W/V_L \tag{15.28}$$

or:
$$\frac{1}{nF}\frac{V_w}{V_L} = -\ln\frac{1 - F}{F} \tag{15.29}$$

As MULLIN[3] points out, this equation can be used for comparing batch and continuous processing since V_W and nFV_L represent the wash liquor requirements for both cases.

15.3. CRYSTALLISATION FROM SOLUTIONS

Solution crystallisers are usually classified according to the method by which supersaturation is achieved, that is by cooling, evaporation, vacuum, reaction and salting out. The term *controlled* denotes supersaturation control whilst *classifying* refers to classification of product size.

15.3.1. Cooling crystallisers

Non-agitated vessels

The simplest type of cooling crystalliser is an unstirred tank in which a hot feedstock solution is charged to an open vessel and allowed to cool, often for several days, by natural convection. Metallic rods may be suspended in the solution so that large crystals can grow on them thereby reducing the amount of product that sinks to the bottom of the unit. The product is usually removed manually. Because cooling is slow, large interlocked crystals are usually produced. These retain mother liquor and thus the dried crystals are generally impure. Because of the uncontrolled nature of the process, product crystals range from a fine dust to large agglomerates. Labour costs are high, but the method is economical for small batches since capital, operating, and maintenance costs are low, although productivity is low and space requirements are high.

Agitated vessels

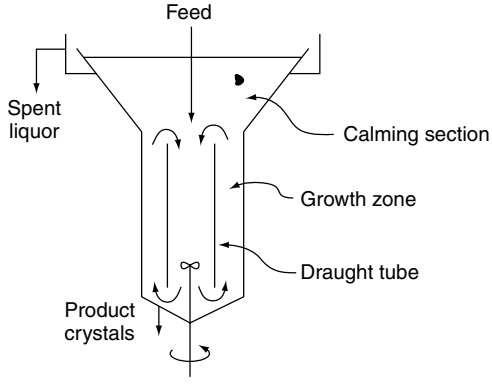
Installation of an agitator in an open-tank crystalliser gives smaller and more uniform crystals and reduces batch times. Because less liquor is retained by the crystals after filtration

This book belongs to Bradley Loren (bloren@mcandrews-ip.com) Copyright Elsevier 2024

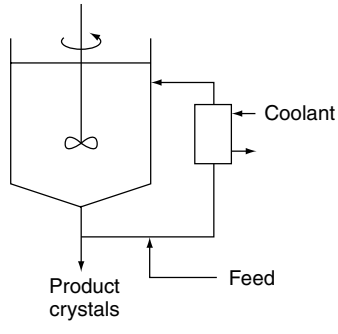
Intas Exhibit 1032
Page 243 of 470
PGR2025-00043

and more efficient washing is possible, the final product has a higher purity. Water jackets are usually preferred to coils for cooling because the latter often become encrusted with crystals and the inner surfaces of the crystalliser should be smooth and flat to minimise encrustation. Operating costs of agitated coolers are higher than for simple tanks and, although the productivity is higher, product handling costs are still high. Tank crystallisers vary from shallow pans to large cylindrical tanks.

The typical agitated cooling crystalliser, shown in Figure 15.14*a*, has an upper conical section which reduces the upward velocity of liquor and prevents the crystalline product from being swept out with the spent liquor. An agitator, located in the lower region of a draught tube circulates the crystal slurry through the growth zone of the crystalliser; cooling surfaces may be provided if required. External circulation, as shown in Figure 15.14*b*, allows good mixing inside the unit and promotes high rates of heat transfer between liquor and coolant, and an internal agitator may be installed in the crystallisation tank if required. Because the liquor velocity in the tubes is high, low temperature differences are usually adequate, and encrustation on heat transfer surfaces is reduced considerably. Batch or continuous operation may be employed.



(*a*) Internal circulation through a draught tube



(*b*) External circulation through a heat exchanger

Figure 15.14. Cooling crystallisers

This book belongs to Bradley Loren (bloren@mcandrews-ip.com) Copyright Elsevier 2024
Intas Exhibit 1032
Page 244 of 470
PGR2025-00043

Scraped-surface crystallisers

The Swenson-Walker scraped-surface unit, which is used for processing inorganic salts that have a high temperature solubility coefficient with water, is a shallow semi-cylindrical trough, about 600 mm wide and 3–12 m long, fitted with a water-cooled jacket. A helical scraper rotating at 0.8–1.6 Hz, keeps the cooling surfaces clean and enhances growth of crystals by moving them through the solution which flows down the sloping trough. Several units may be connected in series and the capacity is determined by the heat transfer rate which should exceed 60 kW[(1)] for economic operation, with heat transfer coefficients in the range 50–150 W/m^2 deg K. High coefficients and hence high production rates are obtained with double-pipe, scraped-surface units such as Votator and Armstrong crystallisers in which spring-loaded internal agitators scrape the heat transfer surfaces. With turbulent flow in the tube, coefficients of 50–700 W/m^2 deg K are achieved. Such units range from 75 to 600 mm in diameter and 0.3 to 3 m long. They are used mainly for processing fats, waxes and other organic melts, as outlined in Section 15.4, although the processing of inorganic solutions such as sodium sulphate from viscose spin-bath liquors, has been reported by ARMSTRONG[(62)].

Example 15.5

A solution containing 23 per cent by mass of sodium phosphate is cooled from 313 to 298 K in a Swenson-Walker crystalliser to form crystals of $Na_3PO_4.12H_2O$. The solubility of Na_3PO_4 at 298 K is 15.5 kg/100 kg water, and the required product rate of crystals is 0.063 kg/s. The mean heat capacity of the solution is 3.2 kJ/kg deg K and the heat of crystallisation is 146.5 kJ/kg. If cooling water enters and leaves at 288 and 293 K, respectively, and the overall coefficient of heat transfer is 140 W/m^2 deg K, what length of crystalliser is required?

Solution

The molecular mass of hydrate/molecular mass of anhydrate, $R = (380/164) = 2.32$

It will be assumed that the evaporation is negligible and that $E = 0$.

The initial concentration, $c_1 = 0.23$ kg/kg solution or $0.23/(1 - 0.23) = 0.30$ kg/kg water

The final concentration, $c_2 = 15.5$ kg/kg water or 0.155 kg/kg water

In 1 kg of the initial feed solution, there is 0.23 kg salt and 0.77 kg water and hence $w_1 = 0.77$ kg

The yield is given by equation 15.22:

$$y = 2.32 \times 0.77[0.30 - 0.155(1 - 0)]/[1 - 0.155(2.32 - 1)]$$
$$= 0.33 \text{ kg}$$

In order to produce 0.063 kg/s of crystals, the required feed is:

$$= (1 \times 0.063/0.33) = 0.193 \text{ kg/s}$$

The heat required to cool the solution $= 0.193 \times 3.2(313 - 298) = 9.3$ kW

This book belongs to Bradley Loren (bloren@mcandrews-ip.com) Copyright Elsevier 2024

Intas Exhibit 1032
Page 245 of 470
PGR2025-00043

Heat of crystallisation = (0.063 × 146.5) = 9.2 kW; a total of (9.3 + 9.2) = 18.5 kW

Assuming countercurrent flow, $\Delta T_1 = (313 - 293) = 20$ deg K

$\Delta T_2 = (298 - 288) = 10$ deg K

and the logarithmic mean, $\Delta T_m = (20 - 10)/\ln(20/10) = 14.4$ deg K

The heat transfer area required, $A' = Q/U\Delta T_m = 18.5/(0.14 \times 14.4) = 9.2$ m^2

Assuming that the area available is, typically, 1 m^2/m length, the length of exchanger required = 9.2 m. In practice 3 lengths, each of 3 m length would be specified.

Direct-contact cooling

The occurrence of crystal encrustation in conventional heat exchangers can be avoided by using direct-contact cooling (DCC) in which supersaturation is achieved by allowing the process liquor to come into contact with a cold heat-transfer medium. Other potential advantages of DCC include better heat transfer and lower cooling loads, although disadvantages include product contamination from the coolant and the cost of extra processing required to recover the coolant for further use. Since a solid, liquid, or gaseous coolant can be used with transfer of sensible or latent heat, the coolant may or may not boil during the operation, and it can be either miscible or immiscible with the process liquor, several types of DCC crystallisation are possible:

(a) immiscible, boiling, solid or liquid coolant where heat is removed mainly by transfer of latent heat of sublimation or vaporisation;
(b) immiscible, non-boiling, solid, liquid, or gaseous coolant with mainly sensible heat transfer;
(c) miscible, boiling, liquid coolant with mainly latent heat transfer; and
(d) miscible, non-boiling, liquid coolant with mainly sensible heat transfer.

Crystallisation processes employing DCC have been used successfully in the de-waxing of lubricating oils[63], the desalination of water[64], and the production of inorganic salts from aqueous solution[65].

15.3.2. Evaporating crystallisers

If the solubility of a solute in a solvent is not appreciably decreased by lowering the temperature, the appropriate degree of solution supersaturation can be achieved by evaporating some of the solvent and the oldest and simplest technique, the use of solar energy, is still employed commercially throughout the world[66]. Common salt is produced widely from brine in steam-heated evaporators, multiple-effect evaporator-crystallisers are used in sugar refining and many types of forced-circulation evaporating crystallisers are in large-scale use[3,40,67]. Evaporating crystallisers are usually operated under reduced pressure to aid solvent removal, minimise heat consumption, or decrease the operating temperature of the solution, and these are described as *reduced-pressure evaporating crystallisers*.

This book belongs to Bradley Loren (bloren@mcandrews-ip.com) Copyright Elsevier 2024

Intas Exhibit 1032
Page 246 of 470
PGR2025-00043

15.3.3. Vacuum (adiabatic cooling) crystallisers

A vacuum crystalliser operates on a slightly different principle from the reduced-pressure unit since supersaturation is achieved by simultaneous evaporation and adiabatic cooling of the feedstock. A hot, saturated solution is fed into an insulated vessel maintained under reduced pressure. If the feed liquor temperature is higher than the boiling point of the solution under the low pressure existing in the vessel, the liquor cools adiabatically to this temperature and the sensible heat and any heat of crystallisation liberated by the solution evaporate solvent and concentrate the solution.

15.3.4. Continuous crystallisers

The majority of continuously operated crystallisers are of three basic types: forced-circulation, fluidised-bed and draft-tube agitated units.

Forced-circulation crystallisers

A *Swenson forced-circulation crystalliser* operating at reduced pressure is shown in Figure 15.15. A high recirculation rate through the external heat exchanger is used to provide good heat transfer with minimal encrustation. The crystal magma is circulated from the lower conical section of the evaporator body, through the vertical tubular heat exchanger, and reintroduced tangentially into the evaporator below the liquor level to create a swirling action and prevent flashing. Feed-stock enters on the pump inlet side of the circulation system and product crystal magma is removed below the conical section.

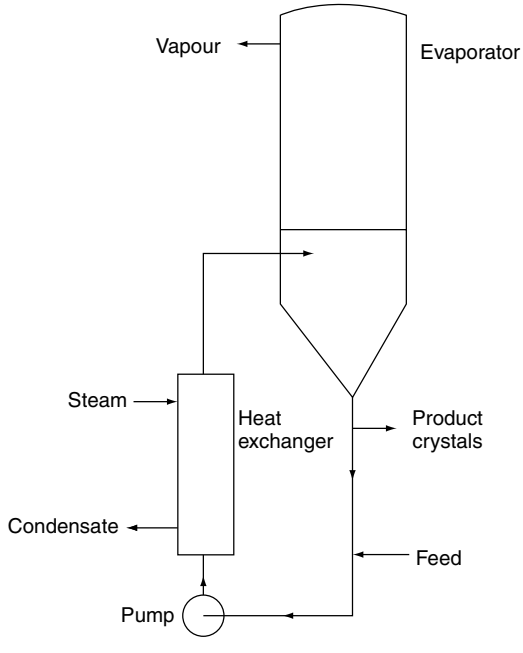


Figure 15.15. Forced-circulation Swenson crystalliser

This book belongs to Bradley Loren (bloren@mcandrews-ip.com)
Copyright Elsevier 2024
Intas Exhibit 1032
Page 247 of 470
PGR2025-00043

Fluidised-bed crystallisers

In an *Oslo fluidised-bed crystalliser*, a bed of crystals is suspended in the vessel by the upward flow of supersaturated liquor in the annular region surrounding a central downcomer, as shown in Figure 15.16. Although originally designed as classifying crystallisers, fluidised-bed Oslo units are frequently operated in a mixed-suspension mode to improve productivity, although this reduces product crystal size[68]. With the classifying mode of operation, hot, concentrated feed solution is fed into the vessel at a point directly above the inlet to the circulation pipe. Saturated solution from the upper regions of the crystalliser, together with the small amount of feedstock, is circulated through the tubes of the heat exchanger and cooled by forced circulation of water or brine. In this way, the solution becomes supersaturated although care must be taken to avoid spontaneous nucleation. Product crystal magma is removed from the lower regions of the vessel.

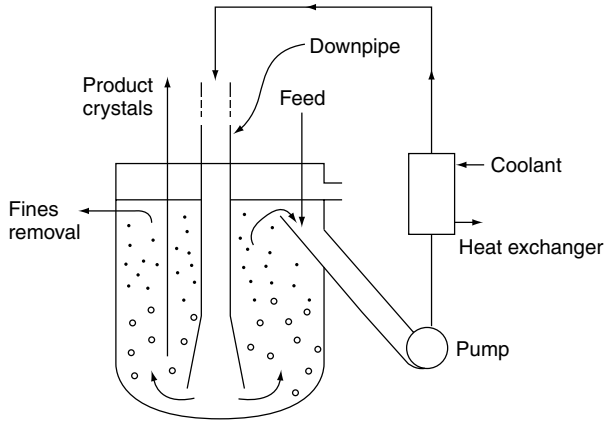


Figure 15.16. Oslo cooling crystalliser

Draught-tube agitated vacuum crystallisers

A *Swenson draught-tube-baffled (DTB) vacuum unit* is shown in Figure 15.17. A relatively slow-speed propellor agitator is located in a draught tube that extends to a small distance below the liquor level. Hot, concentrated feed-stock, enters at the base of the draught tube, and the steady movement of magma and feed-stock to the surface of the liquor produces a gentle, uniform boiling action over the whole cross-sectional area of the crystalliser. The degree of supercooling thus produced is less than 1 deg K and, in the absence of violent vapour flashing, both excessive nucleation and salt build-up on the inner walls are minimised. The internal baffle forms an annular space free of agitation and provides a settling zone for regulating the magma density and controlling the removal of excess nuclei. An integral elutriating leg may be installed below the crystallisation zone to effect some degree of product classification.

The *Standard-Messo turbulence crystalliser*, Figure 15.18, is a draught-tube vacuum unit in which two liquor flow circuits are created by concentric pipes: an outer ejector

This book belongs to Bradley Loren (bloren@mcandrews-ip.com) Copyright Elsevier 2024
Intas Exhibit 1032
Page 248 of 470
PGR2025-00043

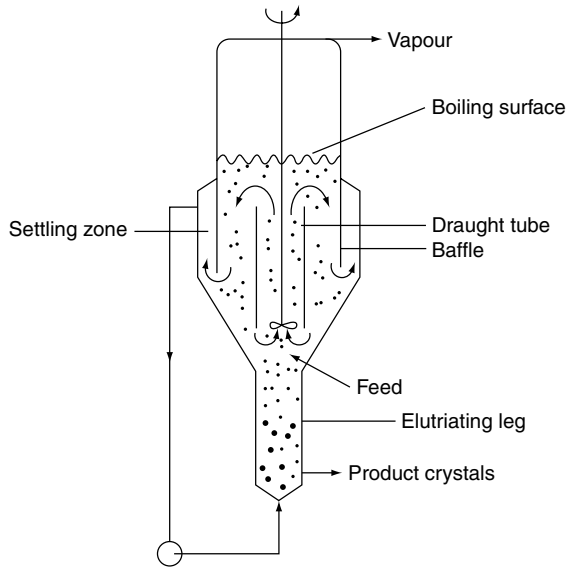


Figure 15.17. Swenson draught-tube-baffled (DTB) crystalliser

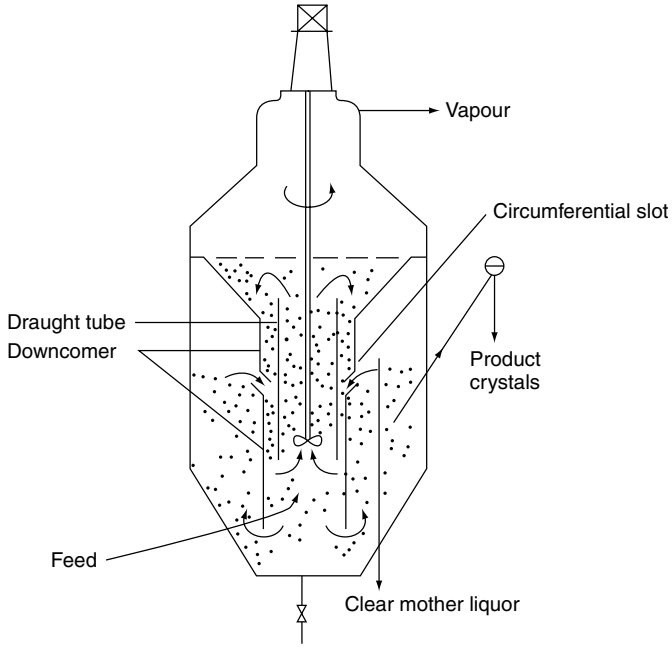


Figure 15.18. Standard-Messo turbulence crystalliser

This book belongs to Bradley Loren (bloren@mcandrews-ip.com)
Copyright Elsevier 2024
Intas Exhibit 1032
Page 249 of 470
PGR2025-00043

tube with a circumferential slot, and an inner guide tube in which circulation is effected by a variable-speed agitator. The principle of the Oslo crystalliser is utilised in the growth zone, partial classification occurs in the lower regions, and fine crystals segregate in the upper regions. The primary circuit is created by a fast upward flow of liquor in the guide tube and a downward flow in the annulus. In this way, liquor is drawn through the slot between the ejector tube and the baffle, and a secondary flow circuit is formed in the lower region of the vessel. Feedstock is introduced into the draught tube and passes into the vaporiser section where flash evaporation takes place. In this way, nucleation occurs in this region, and the nuclei are swept into the primary circuit. Mother liquor may be drawn off by way of a control valve that provides a means of controlling crystal slurry density.

The *Escher-Wyss Tsukishima double-propeller* (DP) *crystalliser*, shown in Figure 15.19, is essentially a draught-tube agitated crystalliser. The DP unit contains an annular baffled zone and a double-propellor agitator which maintains a steady upward flow inside the draught tube and a downward flow in the annular region, thus giving very stable suspension characteristics.

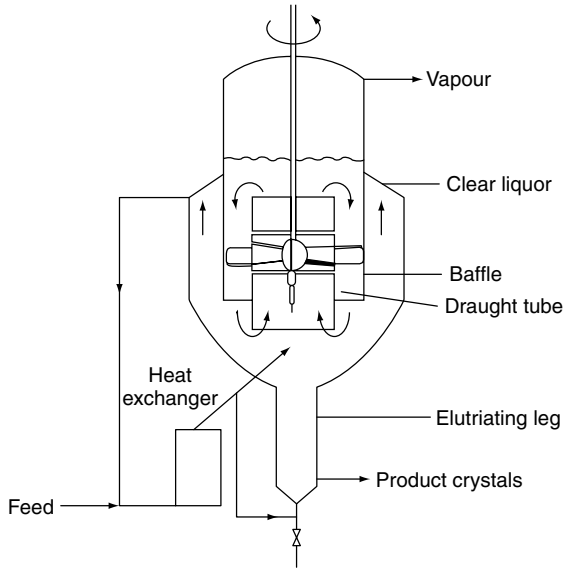


Figure 15.19. Escher-Wyss Tsukishima double-propeller (DP) crystalliser

15.3.5. Controlled crystallisation

Carefully selected seed crystals are sometimes added to a crystalliser to control the final product crystal size. The rapid cooling of an unseeded solution is shown in Figure 15.20*a* in which the solution cools at constant concentration until the limit of the metastable zone is reached, where nucleation occurs. The temperature increases slightly due to the release of latent heat of crystallisation, but on cooling more nucleation occurs. The temperature and concentration subsequently fall and, in such a process, nucleation and growth cannot

This book belongs to Bradley Loren (bloren@mcandrews-ip.com) Copyright Elsevier 2024
Intas Exhibit 1032
Page 250 of 470
PGR2025-00043

be controlled. The slow cooling of a seeded solution, in which temperature and solution composition are controlled within the metastable zone throughout the cooling cycle, is shown in Figure 15.20*b*. Crystal growth occurs at a controlled rate depositing only on the added seeds and spontaneous nucleation is avoided because the system is never allowed to become labile. Many large-scale crystallisers are operated on this batch operating method that is known as *controlled crystallisation*.

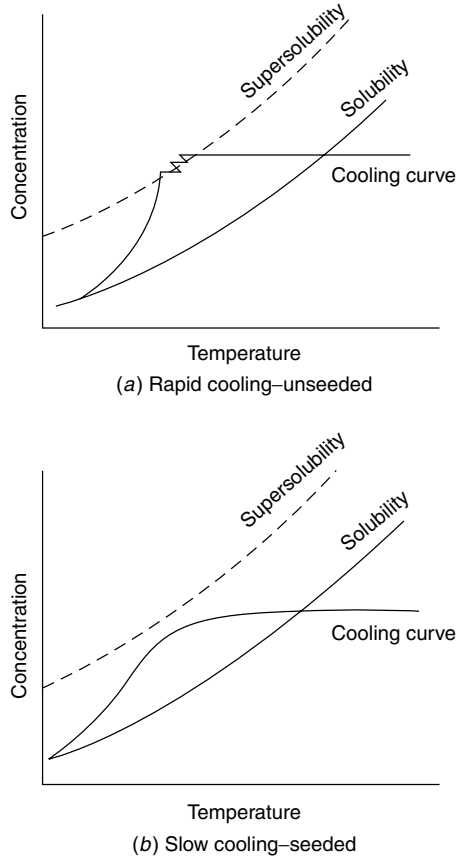


Figure 15.20. Effect of seeding on cooling crystallisation

If crystallisation occurs only on the added seeds, the mass m, of seeds of size d_s that can be added to a crystalliser depends on the required crystal yield y and the product crystal size d_p, as follows:

$$m_s = y\left(\frac{d_s^3}{d_p^3 - d_s^3}\right) \tag{15.30}$$

The product crystal size from a batch crystalliser can also be controlled by adjusting the rates of cooling or evaporation. Natural cooling, for example, produces a supersaturation

This book belongs to Bradley Loren (bloren@mcandrews-ip.com) Copyright Elsevier 2024

Intas Exhibit 1032
Page 251 of 470
PGR2025-00043

peak in the early stages of the process when rapid, uncontrolled heavy nucleation inevitably occurs, although nucleation can be controlled within acceptable limits by following a cooling path that maintains a constant low level of supersaturation. As MULLIN and NYVLT[69] has pointed out, the calculation of optimum cooling curves for different operating conditions is complex, although the following simplified relationship is usually adequate for general application:

$$T_t = T_0 - (T_0 - T_f)(t/t_b)^3 \tag{15.31}$$

where T_0, T_f, and T_t are the temperatures at the beginning, end and any time t during the process, respectively, and t_b is the overall batch time.

15.3.6. Batch and continuous crystallisation

Continuous, steady-state operation is not always the ideal mode for the operation of crystallisation processes, and batch operation often offers considerable advantages such as simplicity of equipment and reduced encrustation on heat-exchanger surfaces. Whilst only a batch crystalliser can, in certain cases, produce the required crystal form, size distribution, or purity, the operating costs can be significantly higher than those of a comparable continuous unit, and problems of product variation from batch to batch may be encountered. The particular attraction of a continuous crystalliser is its built-in flexibility for control of temperature, supersaturation nucleation, crystal growth, and other parameters that influence the size distribution of the crystals. The product slurry may have to be passed to a holding tank, however, to allow equilibrium between the crystals and the mother liquor to be reached if unwanted deposition in the following pipelines and effluent tanks is to be avoided. One important advantage of batch operation, especially in the pharmaceutical industry, is that the crystalliser can be cleaned thoroughly at the end of each batch, thus preventing contamination of the next charge with any undesirable products that might have been formed as a result of transformations, rehydration, dehydration, air oxidation and so on during the batch cycle. In continuous crystallisation systems, undesired self-seeding may occur after a certain operating time, necessitating frequent shutdowns and washouts.

Semi-continuous crystallisation processes which often combine the best features of both batch and continuous operation are described by NYVLT[35], RANDOLPH[37], ROBINSON and ROBERTS[70] and ABBEG and BALAKRISHNAM[71]. It may be possible to use a series of tanks which can then be operated as individual units or in cascade. MULLIN[3] suggests that for production rates in excess of 0.02 kg/s (70 kg/h) or liquor feeds in excess of 0.005 m^3/s, continuous operation is preferable although sugar may be produced batch-wise at around 0.25 kg/s (900 kg/h) per crystalliser.

15.3.7. Crystalliser selection

The temperature–solubility relationship for solute and solvent is of prime importance in the selection of a crystalliser and, for solutions that yield appreciable amounts of crystals on cooling, either a simple cooling or a vacuum cooling unit is appropriate. An evaporating crystalliser would be used for solutions that change little in composition on cooling and

This book belongs to Bradley Loren (bloren@mcandrews-ip.com) Copyright Elsevier 2024

Intas Exhibit 1032
Page 252 of 470
PGR2025-00043

salting-out would be used in certain cases. The shape, size and size distribution of the product is also an important factor and for large uniform crystals, a controlled suspension unit fitted with suitable traps for fines, permitting the discharge of a partially classified product, would be suitable. This simplifies washing and drying operations and screening of the final product may not be necessary. Simple cooling-crystallisers are relatively inexpensive, though the initial cost of a mechanical unit is fairly high although no costly vacuum or condensing equipment is required. Heavy crystal slurries can be handled in cooling units without liquor circulation, though cooling surfaces can become coated with crystals thus reducing the heat transfer efficiency. Vacuum crystallisers with no cooling surfaces do not have this disadvantage but they cannot be used when the liquor has a high boiling point elevation. In terms of space, both vacuum and evaporating units usually require a considerable height.

Once a particular class of unit has been decided upon, the choice of a specific unit depends on initial and operating costs, the space available, the type and size of the product, the characteristics of the feed liquor, the need for corrosion resistance and so on. Particular attention must be paid to liquor mixing zones since the circulation loop includes many regions where flow streams of different temperature and composition mix. These are all points at which temporary high supersaturations may occur causing heavy nucleation and hence encrustation, poor performance and operating instabilities. As TOUSSAINT and DONDERS[72] stresses, it is essential that the compositions and enthalpies of mixer streams are always such that, at equilibrium, only one phase exists under the local conditions of temperature and pressure.

15.3.8. Crystalliser modelling and design

Population balance

Growth and nucleation interact in a crystalliser in which both contribute to the final crystal size distribution (CSD) of the product. The importance of the population balance[37] is widely acknowledged. This is most easily appreciated by reference to the simple, idealised case of a mixed-suspension, mixed-product removal (MSMPR) crystalliser operated continuously in the steady state, where no crystals are present in the feed stream, all crystals are of the same shape, no crystals break down by attrition, and crystal growth rate is independent of crystal size. The crystal size distribution for steady state operation in terms of crystal size d and population density n' (number of crystals per unit size per unit volume of the system), derived directly from the population balance over the system[37] is:

$$n' = n^{\circ} \exp(-d/G_d t_r) \tag{15.32}$$

where n° is the population density of nuclei and t_r is the residence time. Rates of nucleation B and growth $G_d (= \mathrm{d}d/\mathrm{d}t)$ are conventionally written in terms of supersaturation as:

$$B = k_1 \Delta c^b \tag{15.33}$$

and:

$$G_d = k_2 \Delta c^s \tag{15.34}$$

This book belongs to Bradley Loren (bloren@mcandrews-ip.com) Copyright Elsevier 2024

Intas Exhibit 1032
Page 253 of 470
PGR2025-00043

These empirical expressions may be combined to give:

$$B = k_3 G^i \tag{15.35}$$

where:

$$i = b/s \text{ and } k_3 = k_1/k_2^i \tag{15.36}$$

where b and s are the kinetic orders of nucleation and growth, respectively, and i is the relative kinetic order. The relationship between nucleation and growth may be expressed as:

$$B = n^\circ G_d \tag{15.37}$$

or:

$$n^\circ = k_4 {G_d}^{i-1} \tag{15.38}$$

In this way, experimental measurement of crystal size distribution, recorded on a number basis, in a steady-state MSMPR crystalliser can be used to quantify nucleation and growth rates. A plot of log n against d should give a straight line of slope $-(G_d t_r)^{-1}$ with an intercept at $d = 0$ equal to n° and, if the residence time t_r is known, the crystal growth rate G_d can be calculated. Similarly, a plot of log n° against log G_d should give a straight line of slope $(i - 1)$ and, if the order of the growth process s is known, the order of nucleation b may be calculated. Such plots are shown in Figure 15.21.

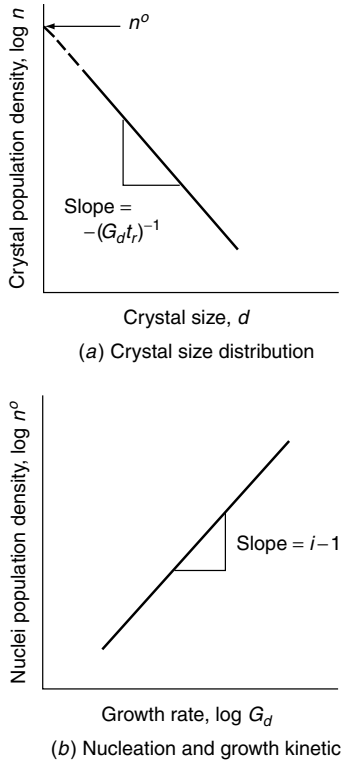


Figure 15.21. Population plots for a continuous mixed-suspension mixed-product removal (MSMPR) crystalliser

This book belongs to Bradley Loren (bloren@mcandrews-ip.com) Copyright Elsevier 2024

Intas Exhibit 1032
Page 254 of 470
PGR2025-00043

The mass of crystals per unit volume of the system, the so-called magma density, ρ_m is given by:

$$\rho_m = 6\alpha\rho n^\circ (G_d t_r)^4 \tag{15.39}$$

where α is the volume shape factor defined by $\alpha = \text{volume}/d^3$ and ρ is the crystal density.

The peak of the mass distribution, the dominant size d_D of the CSD, is given by MULLIN[1] as:

$$d_D = 3\ G_d t_r \tag{15.40}$$

and this can be related to the crystallisation kinetics by:

$$d_D \propto t_r^{(i-1)/(i+3)} \tag{15.41}$$

This interesting relationship[37] enables the effect of changes in residence time to be evaluated. For example, if $i = 3$, a typical value for many inorganic salt systems, a doubling of the residence time would increase the dominant product crystal size by only 26 per cent. This could be achieved either by doubling the volume of the crystalliser or by halving the volumetric feed rate, and hence the production rate. Thus, residence time adjustment is usually not a very effective means of controlling product crystal size.

CSD modelling based on population balance considerations may be applied to crystalliser configurations other than MSMPR[37] and this has become a distinct, self-contained branch of reaction engineering[56,59,60,73].

Example 15.6

An MSMPR crystalliser operates with a steady nucleation rate of $n^\circ = 10^{13}/\text{m}^4$, a growth rate, $G_d = 10^{-8}$ m/s and a mixed-product removal rate, based on clear liquor of 0.00017 m^3/s. The volume of the vessel, again based on clear liquor, is 4 m^3, the crystal density is 2660 kg/m^3 and the volumetric shape factor is 0.7. Determine:

(a) the solids content in the crystalliser
(b) the crystal production rate
(c) the percent of nuclei removed in the discharge by the time they have grown to 100 μm.
(d) the liquor flowrate which passes through a trap which removes 90 per cent of the original nuclei by the time they have grown to 100 μm

Solution

Draw-down time = (4/0.00017) = 23530 s

(a) From a mass balance, the total mass of solids is:

$$\begin{aligned} c_s &= 6\alpha\rho n^\circ (G_d t_r)^4 \qquad \text{(equation 15.39)} \\ &= (6 \times 0.6 \times 2660 \times 10^{13})(10^{-8} \times 23530)^4 \\ &= \underline{\underline{343\ \text{kg/m}^3}} \end{aligned}$$

(b) The production rate = (343 × 0.00017) = <u>0.058 kg/s (200 kg/h)</u>

This book belongs to Bradley Loren (bloren@mcandrews-ip.com) Copyright Elsevier 2024

Intas Exhibit 1032
Page 255 of 470
PGR2025-00043

(c) The crystal population decreases exponentially with size or:

$$n/n^{\circ} = \exp(-L/G_d t_r) \qquad \text{(equation 15.32)}$$
$$= \exp[(-100 \times 10^{-6})/(10^{-8} \times 23530)]$$
$$= 0.66 \text{ or } 66 \text{ per cent}$$

Thus: $(100 - 66) = \underline{34 \text{ per cent have been discharged by the time they reach } 100\ \mu\text{m.}}$

(d) If $(100 - 90) = 10$ per cent of the nuclei remain and grow to $>100\ \mu$m, then in equation 15.32:

$$(1/0.10) = \exp[(-100 \times 10^{-6})/(10^{-8} t_r)]$$

and: $t_r = 4343$ s

Thus: $4343 = 4/(0.00017 + Q_F)$

and: $Q_F = \underline{0.00075 \text{ m}^3/\text{s } (2.68 \text{ m}^3/\text{h})}$

Design procedures

MULLIN[3] has given details of a procedure for the design of classifying crystallisers in which the calculation steps are as follows.

(a) The maximum allowable supersaturation is obtained and hence the working saturation, noting that this is usually about 30 per cent of the maximum.
(b) The solution circulation rate is obtained from a materials balance.
(c) The maximum linear growth-rate is obtained based on the supersaturation in the lowest layer which contains the product crystals and assuming that $(\beta/\alpha) = 6$.
(d) The crystal growth time is calculated from the growth rate for different relative desupersaturations (100 per cent desuperation corresponding to the reduction of the degree of supersaturation to zero).
(e) The mass of crystals in suspension and the suspension volume are calculated assuming a value for the voidage which is often about 0.85.
(f) The solution up-flow velocity is calculated for very small crystals (< 0.1 mm) using Stokes' Law although strictly this procedure should not be used for particles other than spheres or for Re > 0.3. In a real situation, laboratory measurements of the velocity are usually required.
(g) The crystalliser area and diameter are first calculated and then the height which is taken as (volume of suspension/cross-sectional area).
(h) A separation intensity (S.I.), defined by GRIFFITHS[74] as the mass of equivalent 1 mm crystals produced in 1 m^3 of crystalliser volume in 1 s, is calculated. Typical values are 0.015 kg/m^3 s at 300 K and up to 0.05 at higher temperatures and, for crystals >1 mm, the intensity is given by:

$$\text{S.I.} = d_p P'/V \qquad (15.42)$$

where d_p is the product crystal size, P' (kg/s) is the crystal production rate and V (m^3) is the suspension volume.

This book belongs to Bradley Loren (bloren@mcandrews-ip.com) Copyright Elsevier 2024

Intas Exhibit 1032
Page 256 of 470
PGR2025-00043

MULLIN[3] has used this procedure for the design of a unit for the crystallisation of potassium sulphate at 293 K. The data are given in Table 15.5 from which it will be noted that the cross-sectional area depends linearly on the relative degree of de-supersaturation and the production rate depends linearly on the area but is independent of the height. If the production rate is fixed, then the crystalliser height may be adjusted by altering the sizes of the seed or product crystals. MULLIN and NYVLT[75] have proposed a similar procedure for mixed particle-size in a crystalliser fitted with a classifier at the product outlet which controls the minimum size of product crystals.

Table 15.5. Design of a continuous classifying crystalliser[3]

Basic Data:
Substance: potassium sulphate at 293 K
Product: 0.278 kg/s of 1 mm crystals
Growth constant: $k_d = 0.75\Delta c^{-2}$ kg/m^{2}s
Nucleation constant: $k_n = 2 \times 10^8 \Delta c^{-7.3}$ kg/s
Crystal size: Smallest in fluidised bed = 0.3 mm, (free settling velocity = 40 mm/s)
Smallest in system = 0.1 mm
Crystal density = 2660 kg/m^3, Solution density = 1082 kg/m^3
Solution viscosity = 0.0012 Ns/m^2, Solubility, c^* = 0.1117 kg/kg water

Desupersaturation	1.0	0.9	0.5	0.1
Maximum growth rate (μm/s)	5.6	5.6	5.6	5.6
Up-flow velocity (m/s)	0.04	0.04	0.04	0.04
Circulation rate (m^3/s)	0.029	0.032	0.058	0.286
Crystal residence time (ks)	1469	907	51.8	12.6
Mass of crystals (Mg)	145	90	5.1	1.25
Volume of crystal suspension (m^3)	364	225	12.8	3.15
Cross-sectional area of crystalliser (m^2)	0.72	0.80	1.45	7.2
Crystalliser diameter (m)	0.96	1.01	1.36	3.02
Crystalliser height (m)	505	281	8.8	0.44
Height/diameter	525	280	6.5	0.15
Separation intensity	3.0	4.5	78	320
Economically possible	no	no	yes	no

Scale-up problems

Crystalliser design is usually based on data measured on laboratory or pilot-scale units or, in difficult cases, both. One of the main problems in scaling up is characterisation of the particle–fluid hydrodynamics and the assessment of its effects on the kinetics of nucleation and crystal growth. In fluidised-bed crystallisers, for example, the crystal suspension velocity must be evaluated — a parameter which is related to crystal size, size distribution, and shape, as well as bed voidage and other system properties — such as density differences between particles and liquid and viscosity of the solution. Possible ways of estimating suspension velocity are discussed in the literature[3,41,43,76,77], although, as MULLIN[3] points out, determination of suspension velocities on actual crystal samples is often advisable. In agitated vessels, the 'just-suspended' agitator speed N_{JS}, that is the minimum rotational speed necessary to keep all crystals in suspension, must be determined since, not only do all the crystals have to be kept in suspension, but the development of 'dead spaces' in the vessel must also be avoided as these are unproductive zones and regions of high supersaturation in which vessel surfaces can become encrusted. Fluid and crystal

This book belongs to Bradley Loren (bloren@mcandrews-ip.com) Copyright Elsevier 2024
Intas Exhibit 1032
Page 257 of 470
PGR2025-00043

properties, together with vessel and agitator geometries, are important in establishing N_{JS} values[3,43]. As discussed in Volume 1, Section 7.3, agitated vessel crystallisers are often scaled up successfully on the crude basis of either *constant power input per unit volume* or *constant agitator tip speed*, although BENNETT *et al.*[78] have suggested that, in draught-tube agitated vessels, the quantity (tip speed)^2/(vessel volume/volumetric circulation rate) should be kept constant.

15.4. CRYSTALLISATION FROM MELTS

15.4.1. Basic techniques

A *melt* is a liquid or a liquid mixture at a temperature near its freezing point and *melt crystallisation* is the process of separating the components of a liquid mixture by cooling until crystallised solid is deposited from the liquid phase. Where the crystallisation process is used to separate, or partially separate, the components, the composition of the crystallised solid will differ from that of the liquid mixture from which it is deposited. The ease or difficulty of separating one component from a multi-component mixture by crystallisation may be represented by a phase diagram as shown in Figures 15.4 and 15.5, both of which depict binary systems — the former depicts a eutectic, and the latter a continuous series of solid solutions. These two systems behave quite differently on freezing since a eutectic system can deposit a pure component, whereas a solid solution can only deposit a mixture of components.

Two basic techniques of melt crystallisation are:

(a) gradual deposition of a crystalline layer on a chilled surface in a static or laminar-flowing melt, and
(b) fast generation of discrete crystals in the body of an agitated vessel.

Gradual deposition (a) occurs in the Proabd refiner[79] which essentially utilises a batch cooling process in which a static liquid feedstock is progressively crystallised on to extensive cooling surfaces, such as fin-tube heat-exchangers, supplied with a cold heat-transfer fluid located inside a crystallisation tank. As crystallisation proceeds, the liquid becomes increasingly impure and crystallisation may be continued until virtually the entire charge has solidified. When the crystallised mass is then slowly melted by circulating a hot fluid through the heat exchanger, the impure fraction melts first and drains out of the tank. As melting proceeds, the melt run-off becomes progressively richer in the desired component, and fractions may be taken off during the melting stage. A typical flow diagram, based on a scheme for the purification of naphthalene, is shown in Figure 15.22 where the circulating fluid is usually cold water that is heated during the melting stage by steam injection. Another example of gradual deposition occurs in the rotary drum crystalliser which consists of a horizontal cylinder, partially immersed in the melt, or otherwise supplied with feedstock. The coolant enters and leaves the inside of the hollow drum through trunnions and, as the drum rotates, a crystalline layer forms on the cold surface and is removed with a scraper knife. Two feed and discharge arrangements are shown in Figure 15.23. Rotary drum behaviour and design have been discussed by GELPERIN and

This book belongs to Bradley Loren (bloren@mcandrews-ip.com) Copyright Elsevier 2024

Intas Exhibit 1032
Page 258 of 470
PGR2025-00043

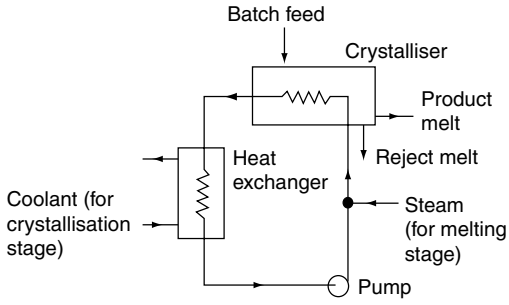


Figure 15.22. Batch cooling crystallisation of melts: flow diagram for the Proabd refiner

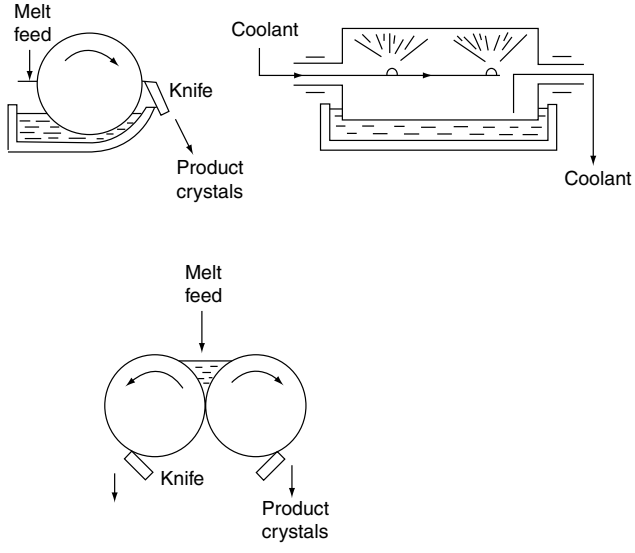


Figure 15.23. Feed and discharge arrangements for drum crystallisers

NOSOV[80] and PONOMARENKO *et al.*[81]. WINTERMANTEL[82] has shown that the structure and impurity levels of growing crystal layers are determined primarily by mass-transfer effects at the layer front.

Fast-melt crystallisation (b) takes place in the scraped-surface heat exchanger, which consists of a cylindrical tube surrounded by a heat-exchange jacket. The tube is surrounded by close-clearance scraper blades and rotates at relatively low speed. Two basic types are available: the large (>200 mm in diameter, >3 m long) slow-speed (< 0.15 Hz) unit, and the small (<150 mm in diameter, <1.5 m long) high-speed (> 8 Hz) machine. Both types can handle viscous magmas, operating at temperatures as low as 190 K, and are widely used in the manufacture of margarine (crystallisation of triglycerides), de-waxing of lubricating oils (crystallisation of higher n-alkanes), and large-scale processing of many organic substances, such as naphthalene, *p*-xylene, chlorobenzenes and so on. The magma

This book belongs to Bradley Loren (bloren@mcandrews-ip.com) Copyright Elsevier 2024
Intas Exhibit 1032
Page 259 of 470
PGR2025-00043

emerging from a scraped-surface crystalliser generally contains very small crystals, often less than 10 μm, which are difficult to separate and can subsequently cause reprocessing problems unless the crystals are first grown to a larger size in a separate holdup tank.

15.4.2. Multistage-processes

A single-stage crystallisation process may not always achieve the required product purity and further separation, melting, washing, or refining may be required. Two approaches are used:

a) a repeating sequence of crystallisation, melting, and re-crystallisation;
b) a single crystallisation step followed by countercurrent contacting of the crystals with a relatively pure liquid stream.

The first approach is preferred if the concentration of impurities in the feedstock is high, and is essential if the system forms a continuous series of solid solutions. The second approach is used where the concentration of impurities is low, although some industrial operations require a combination of both systems. ATWOOD[83] has offered an analysis of different types of multistage crystallisation schemes.

As described by MULLIN[3], BENNETT *et al.*[78] and RITTNER and STEINER[84], many industrial melt-crystallisation processes have been developed, and further interest is being stimulated by the energy-saving potential in large scale processing, as compared with distillation. One example is the *Newton-Chambers process*, described by MOLINARI *et al.*[79], in which benzene is produced from a coal-tar benzole fraction by contacting the impure feedstock with brine. The slurry is centrifuged, yielding benzene crystals (freezing point 278.6 K) and a mixture of brine and mother liquor which is then allowed to settle. The brine is returned for refrigeration and the mother liquor is reprocessed to yield motor fuel. The process efficiency depends to a large extent on the efficient removal of impure mother liquor that adheres to the benzene crystals, and several modes of operation are possible. In the thaw–melt method shown in Figure 15.24, benzene crystals are washed in the centrifuge with brine at a temperature above 279 K. Some of the benzene crystals partially melt, which helps to wash away the adhering mother liquor. The thawed liquor may then be recycled. Multistage operation can be employed, in which the first crop of crystals is removed as product and the second, from the liquor, is melted for recycle. The *Sulzer MWB process*, described by FISCHER *et al.*[85], involves crystallisation on a cold surface and, since it may be operated effectively as a multistage separation device, it can be used to purify solid solutions. In an effective multistage countercurrent scheme, only one crystalliser, a vertical multi-tube heat exchanger, is required and the crystals do not have to be transported since they remain deposited on the internal heat-exchange surfaces in the vessel until they are melted for further processing. The intermediate storage tanks and crystalliser are linked by a control system consisting of a programme timer, actuating valves, pumps, and cooling loop, as shown in Figure 15.25. This process has been used on a large scale for the purification of organics, such as chloronitrobenzenes, nitrotoluenes, cresols, and xylenols, and in the separation of fatty acids.

This book belongs to Bradley Loren (bloren@mcandrews-ip.com) Copyright Elsevier 2024

Intas Exhibit 1032
Page 260 of 470
PGR2025-00043

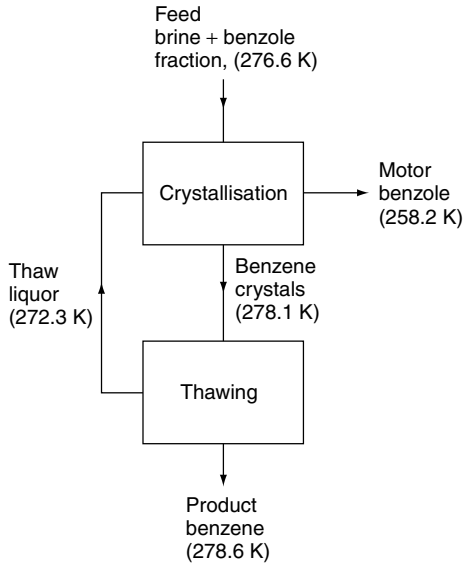


Figure 15.24. Newton — Chambers process for the purification of benzene

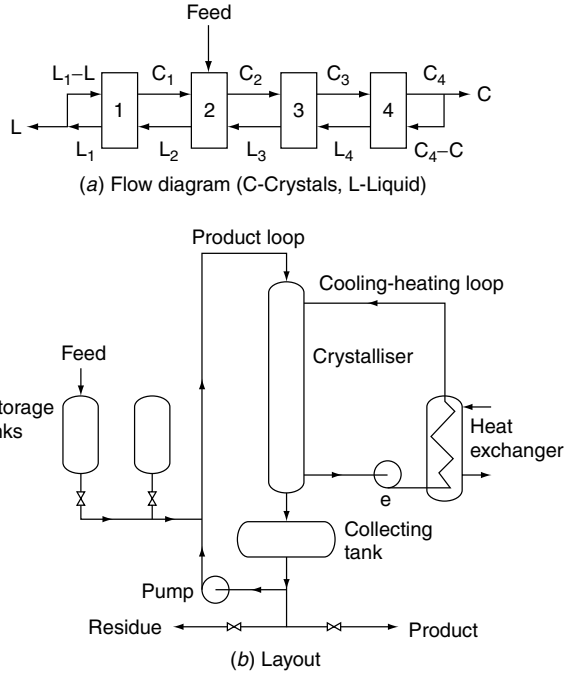


Figure 15.25. Sulzer MWB process

This book belongs to Bradley Loren (bloren@mcandrews-ip.com)
Copyright Elsevier 2024
Intas Exhibit 1032
Page 261 of 470
PGR2025-00043

15.4.3. Column crystallisers

Because the components of the melt feedstock components can form both eutectic and solid-solution systems with one another, sequences of washing, partial or complete melting, and re-crystallisation are often necessary to produce one of the components in near-pure form. Because the operation of a sequence of melt crystallisation steps can be time-consuming and costly, many attempts have been made to carry out some of these operations in a single unit, such as a column crystalliser. One example is the *Schildknecht column* developed in the 1950's which is shown in Figure 15.26. Liquid feedstock enters the column continuously at an intermediate point and freezing at the bottom of the column and melting at the top are achieved using, respectively, a suitable refrigerant and a hot fluid or an electrical heating element. Crystals and liquid pass through the column countercurrently, and the solid phase is transported downward by a helical conveyor fixed on a central shaft. The purification zone is usually operated at a virtually constant temperature, intermediate between the temperatures of the freezing and melting sections. Crystals are formed mainly in the freezing section, although some may also be deposited on the inner surface of the column and removed by the helical conveyor. During this operation, crystals make contact with the counter-flowing liquid melt and are thereby surface-washed. A system in which an upward flowing liquid is in contact with crystals being conveyed downward has also been used and, in this case, the locations of the freezer and melter are the reverse of those shown in Figure 15.26. Gates and Powers[86] and Henry and Powers[87] have discussed the modelling of column crystallisers.

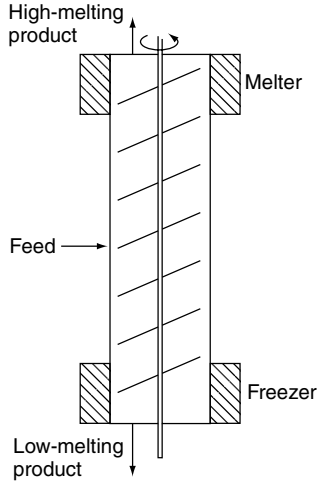


Figure 15.26. Schildknecht column

Whilst the Schildknecht column is essentially a laboratory-scale unit, a melt-crystalliser of the wash-column type was developed by Phillips Petroleum Company in the 1960s for large-scale production of *p*-xylene. The key features of this *Phillips pulsed-column crystalliser*, as described by McKay *et al.*[88], are shown in Figure 15.27. A cold slurry

This book belongs to Bradley Loren (bloren@mcandrews-ip.com) Copyright Elsevier 2024
Intas Exhibit 1032
Page 262 of 470
PGR2025-00043

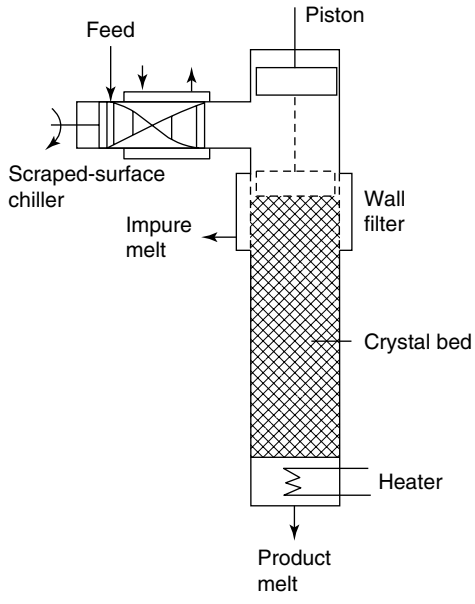


Figure 15.27. Phillips pulsed-column crystalliser[88]

feed, produced in a scraped-surface chiller, enters at the top of the column and crystals are pulsed downward in the vertical bed by a piston, whilst impure mother liquor leaves through a filter. The upward-flowing wash liquor is generated at the bottom by a heater that melts pure crystals before they are removed from the column.

Whilst the *Brodie purifier*[89] developed in the late 1960s incorporates several features of the column crystallisers described previously, it also has the potential to deal effectively with solid-solution systems. As shown in Figure 15.28, it is essentially a centre-fed column that can convey crystals from one end to the other. As the crystals move through the unit, their temperature is gradually increased along the flow path and thus they are subjected to partial melting which encourages the release of low-melting impurities. The interconnected scraped-surface heat exchangers are of progressively smaller diameter so as to maintain reasonably constant axial flow velocities and to prevent back-mixing. The vertical purifying column acts as a countercurrent washer in which descending, nearly pure, crystals meet an upward stream of pure melt. The Brodie purifier has been used in the large-scale production of high-purity 1,4-dichlorobenzene and naphthalene.

The *Tsukishima Kikai (TSK) countercurrent cooling crystallisation process* described by Takegami[90] is, in effect, a development of Brodie technology. A typical system, consisting of three conventional cooling crystallisers connected in series is shown in Figure 15.29. Feed enters the first-stage vessel and partially crystallises, and the slurry is then concentrated in a hydrocyclone before passing into a Brodie purifying column. After passage through a settling zone in the crystalliser, clear liquid overflows to the next stage. Slurry pumping and overflow of clear liquid in each stage result in countercurrent flow of liquid and solid. This process has been applied in the large-scale production of *p*-xylene.

This book belongs to Bradley Loren (bloren@mcandrews-ip.com) Copyright Elsevier 2024
Intas Exhibit 1032
Page 263 of 470
PGR2025-00043

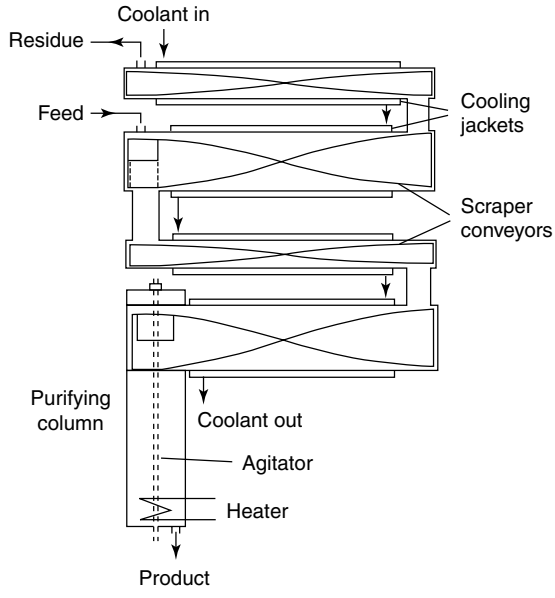


Figure 15.28. Brodie purifier[89]

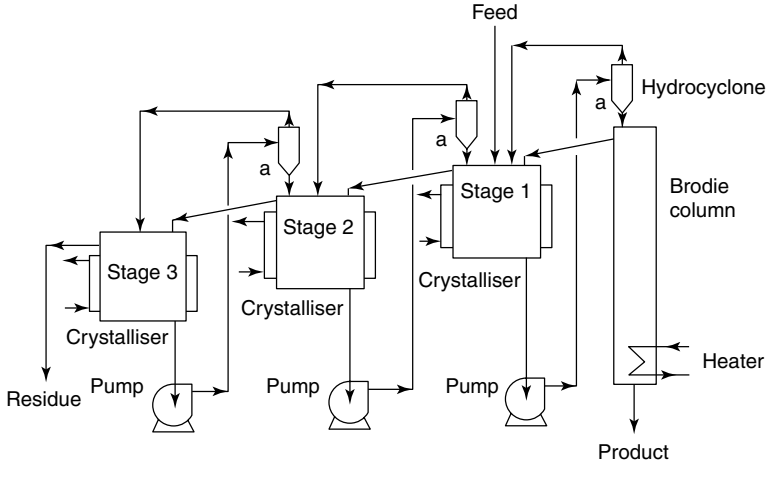


Figure 15.29. Tsukishima Kikai (TSK) countercurrent cooling crystallisation process[90]

Units have been developed by Sulzer Chemtech which consist of vertical tubes where the product flows as a film down the inside surface of the tubes, and the liquid used for cooling and heating is distributed so as to wet the external surface of the tubes. During the initial freezing stage, the heat transfer medium chills the tubes, partial melting is then induced by raising the temperature of the heat transfer medium and higher temperatures are

This book belongs to Bradley Loren (bloren@mcandrews-ip.com) Copyright Elsevier 2024
Intas Exhibit 1032
Page 264 of 470
PGR2025-00043

then applied for the final melting stage. A distribution system equalises the flow through the tubes and optimum performance is achieved by accurate control of the heating and cooling profiles. Sulzer also produce a unit for static melt crystallisation which employs cooled plates immersed in a stagnant melt. After a crystal layer has formed, sweating is induced, as with the falling-film device, and the sweated fraction is removed. The remaining crystal layer is then melted and passed to storage. A higher degree of purity may be obtained by using the intermediate product as feedstock and repeating the procedure and, in a similar way, the residue drained from the first phase of operation may be further depleted by additional melt-freezing processes to give an enhanced yield. A relatively new development is the use of a heat pump in which one crystalliser operates in the crystallisation mode as an evaporator, and a further identical unit operates in the sweating or melting mode as a condenser. In this way, energy costs are reduced due to the use of the enthalpy of condensation for crystal melting. Auxiliary exchangers are required only for the elimination of excess energy and for the start-up operation.

A further development, discussed by Moritoki[91], is *high-pressure crystallisation*, which is considered in Section 15.9.

15.4.4. Prilling and granulation

Prilling, a melt-spray crystallisation process in which solid spherical granules are formed, is used particularly in the manufacture of fertilisers such as ammonium nitrate and urea. Shearon and Dunwoody[92] describe the prilling of ammonium nitrate, in which a very concentrated solution containing about 5 per cent of water is sprayed at 415 K into the top of a 30 m high, 6 m diameter tower, and the droplets fall countercurrently through an upwardly flowing air stream that enters the base of the tower at 293 K. The solidified droplets, which leave the tower at 353 K and contain about 4 per cent water, must be dried to an acceptable moisture content at a temperature below 353 K in order to prevent any polymorphic transitions. Nunnelly and Cartney[93] describe a melt granulation technique for urea in which molten urea is sprayed at 420 K on to cascading granules in a rotary drum. Seed granules of less than 0.5 mm diameter can be built up to the product size of 2–3 mm. Heat released by the solidifying melt is removed by the evaporation of a fine mist of water sprayed into the air as it passes through the granulation drum.

An important application of granulation is in improving the 'flowability' of very fine (submicron) particles which stick together because of the large surface forces acting in materials with very high surface/volume ratios.

15.5. CRYSTALLISATION FROM VAPOURS

15.5.1. Introduction

The term *sublimation* strictly refers to the phase change: solid → vapour, with no intervention of a liquid phase. In industrial applications, however, the term usually includes the reverse process of condensation or *desublimation*: solid → vapour → solid. In practice, it is sometimes desirable to vaporise a substance from the liquid state and hence the

This book belongs to Bradley Loren (bloren@mcandrews-ip.com) Copyright Elsevier 2024

Intas Exhibit 1032
Page 265 of 470
PGR2025-00043

complete series of phase changes is then: solid → liquid → vapour → solid, and, on the condensation side of the process, with the supersaturated vapour condensing directly to the crystalline solid state without the creation of a liquid phase.

Common organic compounds that can be purified led by sublimation include[94]:

> 2-aminophenol, anthracene, anthranilic acid, anthraquinone, benzanthrone, benzoic acid, 1,4-benzoquinone, camphor, cyanuric chloride, *iso*-phthalic acid, naphthalene, 2-napththol, phthalic anhydride, phthalimide, pyrogallol, salicylic acid, terephthalic acid and thymol

and the following elemental and inorganic substances for which the process is suitable include:

> aluminum chloride, arsenic, arsenic(III) oxide, calcium, chromium(III) chloride, hafnium tetrachloride, iodine, iron(III) chloride, magnesium, molybdenum trioxide, sulphur, titanium tetrachloride, uranium hexafluoride and zirconium tetrachloride.

In addition, the sublimation of ice in freeze-drying, discussed in Chapter 16, has become an important operation particularly in the biological and food industries. The various industrial applications of sublimation techniques are discussed by several authors[3,40,95,96,97], and the principles underlying vaporisation and condensation[98] and the techniques for growing crystals from the vapour phase[99] are also presented in the literature.

15.5.2. Fundamentals

Phase equilibria

A sublimation process is controlled primarily by the conditions under which phase equilibria occur in a single-component system, and the phase diagram of a simple one-component system is shown in Figure 15.30 where the *sublimation curve* is dependent on the vapour pressure of the solid, the *vaporisation curve* on the vapour pressure of the liquid, and the *fusion curve* on the effect of pressure on the melting point. The slopes of these three curves can be expressed quantitatively by the Clapeyron equation:

$$(\mathrm{d}P/\mathrm{d}T)_{\mathrm{sub}} = \lambda_s/T(v_g - v_s) \tag{15.43}$$

$$(\mathrm{d}P/\mathrm{d}T)_{\mathrm{vap}} = \lambda_v/T(v_g - v_l) \tag{15.44}$$

$$(\mathrm{d}P/\mathrm{d}T)_{\mathrm{fus}} = \lambda_f/T(v_l - v_s) \tag{15.45}$$

where P is the vapour pressure, and v_s, v_l and v_g are the molar volumes of the solid, liquid, and gas phases, respectively. The molar latent heats (enthalpies) of sublimation, vaporisation, and fusion (λ_s, λ_v and λ_f respectively) are related at a given temperature by:

$$\lambda_s = \lambda_v + \lambda_f \tag{15.46}$$

This book belongs to Bradley Loren (bloren@mcandrews-ip.com) Copyright Elsevier 2024

Intas Exhibit 1032
Page 266 of 470
PGR2025-00043

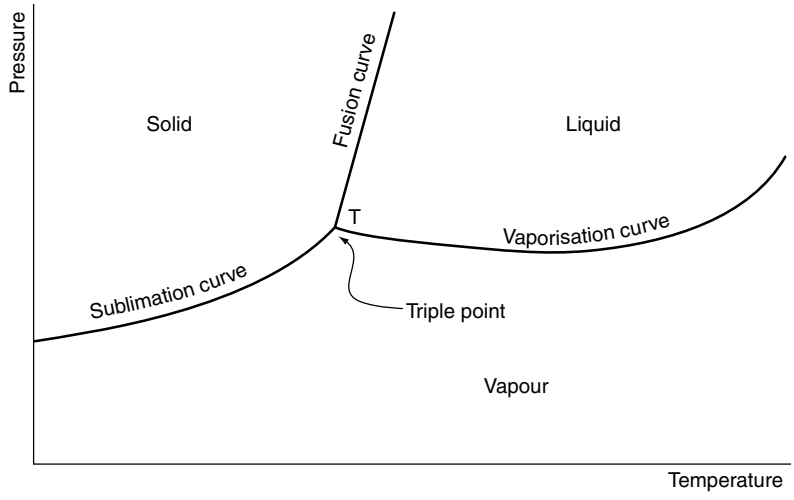


Figure 15.30. Phase diagram for a single-component system

Although there are few data available on sublimation-desublimation, a considerable amount of information can be calculated using the Clausius-Clapeyron equation provided that information on vapour pressure is available at two or more temperatures. In this way:

$$\ln \frac{P_1}{P_2} = \frac{\lambda'_v}{\mathbf{R}} \left(\frac{1}{T_2} - \frac{1}{T_1} \right) \tag{15.47}$$

where λ'_v is latent heat of vaporisation per mole.

Example 15.7

The vapour pressures of naphthalene at 463 and 433 K are 0.780 and 0.220 kN/m^2 respectively. If λ'_v does not vary greatly over the temperature range considered, what is the vapour pressure at 393 K?

Solution

In equation 15.47: $\ln(780/220) = [\lambda'_v(463 - 433)]/[8314 \times 463 \times 433]$

and: $\lambda'_v = 70340$ kJ/kmol

Thus: $\ln(220/P) = [70340(433 - 393)]/[8.314 \times 433 \times 393]$

and: $P = \underline{\underline{30 \text{ kN/m}^2}}$

The position of the *triple point* T, which represents the temperature and pressure at which the solid, liquid, and gas phases co-exist in equilibrium, is of the utmost importance in

This book belongs to Bradley Loren (bloren@mcandrews-ip.com) Copyright Elsevier 2024

Intas Exhibit 1032
Page 267 of 470
PGR2025-00043

sublimation-desublimation processes. If it occurs at a pressure above atmospheric, the solid cannot melt under normal atmospheric conditions, and true sublimation (solid → vapour) is easily achieved. For example, since the triple point for carbon dioxide is at 216 K and 500 kN/m^2, liquid CO_2 is not formed when solid CO_2 is heated at atmospheric pressure and the solid simply vaporises. If the triple point occurs at a pressure less than atmospheric, certain precautions are necessary if the phase changes solid → vapour and vapour → solid are to be controlled. For example, since the triple point for water is 273.21 K and 0.6 kN/m^2, ice melts when it is heated above 273.2 K at atmospheric pressure. For ice to sublime, both the temperature and the pressure must be kept below the triple-point values. If the solid → liquid stage takes place before vaporisation, the operation is often called *pseudo-sublimation*. Both true sublimation and pseudo-sublimation cycles are depicted in Figure 15.31. For a substance with a triple point at a pressure greater than atmospheric, true sublimation occurs. The solid at A is heated to a temperature B and the increase in vapour pressure is given by AB. The condensation is given by BCDE. Since the vapour passing to the condenser may cool slightly and be diluted with an inert gas such as air, C can be taken as the condition at the condenser inlet. After entering the condenser, the vapour is mixed with more inert gas, and the partial pressure and temperature drop to D. The vapour then cools at essentially constant pressure to E which is the condenser temperature. When the triple point of the substance occurs at a pressure lower than atmospheric, heating may result in the temperature and vapour pressure of the solid exceeding the values at the triple-point, and the solid will then melt in the vaporiser along AB′. In the condensation stage, the partial pressure in the vapour stream entering the condenser must be reduced below the pressure at the triple-point to prevent initial condensation to a liquid by diluting the vapour with an inert gas, although the frictional pressure drop in the vapour line is often sufficient to effect the required drop in partial pressure. C′ then represents the conditions at the entry into the condenser and the condensation path is C′DE.

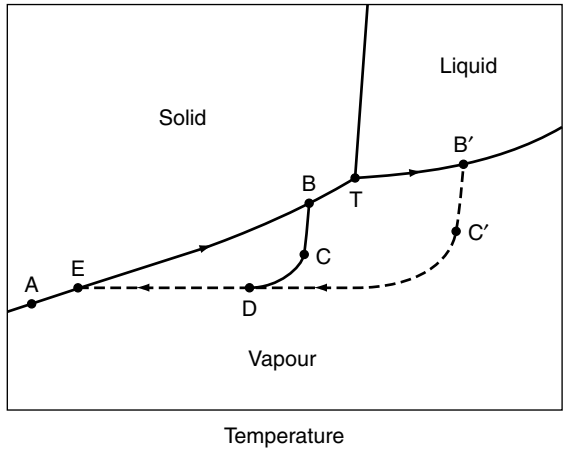


Figure 15.31. Phase diagram showing true sublimation (ABCDE) and pseudosublimation (AB′C′DE) cycles.[94]

This book belongs to Bradley Loren (bloren@mcandrews-ip.com) Copyright Elsevier 2024
Intas Exhibit 1032
Page 268 of 470
PGR2025-00043

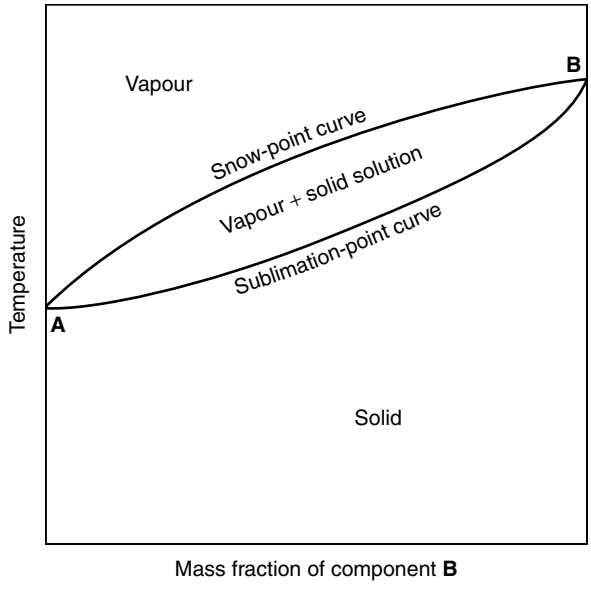


Figure 15.32. Phase diagram for a two-component solid-solution system at a pressure below the triple points of the two components **A** and **B**

Fractional sublimation. If two or more sublimable substances form true solid solutions, their separation by fractional sublimation is theoretically possible. The phase diagram for a binary solid-solution system at a pressure below the triple-point pressures of the two components is shown in Figure 15.32, where points A and B represent the equilibrium sublimation temperatures of pure components **A** and **B**, respectively, at a given pressure. The lower curve represents the sublimation temperatures of mixtures of **A** and **B**, while the upper curve represents the solid-phase condensation temperatures, generally called *snow points*. Figure 15.33 shows that if a solid solution at S is heated to some temperature X, the resulting vapour phase at Y and residual solid solution at Z contain different proportions of the original components, quantified by the *lever arm rule*. The sublimate and the residual solid may then each be subjected again to this procedure and, therefore, the possibility of fractionation exists, although the practical difficulties may be considerable. GILLOT and GOLDBERGER[100], VITOVEC *et al.*[101] and EGGERS *et al.*[102] have described experimental studies of fractional sublimation, and nucleation and growth rates, of organic condensates. MATSOUKA *et al.*[103] has also applied the procedure to the fractionation of mixed vapours.

Vaporisation and condensation

Vaporisation. The maximum theoretical vaporisation rate v' (kg/m^2 s) from the surface of a pure liquid or solid is limited by its vapour pressure and is given by the Hertz-Knudsen equation[104], which can be derived from the kinetic theory of gases:

$$v' = P_s(M'/2\pi \mathbf{R} T_s)^{0.5} \tag{15.48}$$

This book belongs to Bradley Loren (bloren@mcandrews-ip.com) Copyright Elsevier 2024

Intas Exhibit 1032
Page 269 of 470
PGR2025-00043

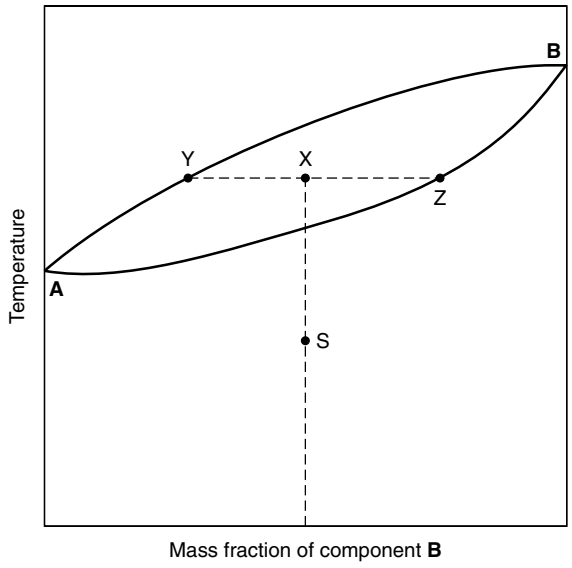


Figure 15.33. Fractional sublimation of two components **A** and **B** demonstrated on a solid-solution phase diagram

where P_s is the vapour pressure at the surface temperature T_s, M' is the molecular weight and **R** is the gas constant. In practice, the actual vaporisation rate may be lower than predicted by equation 15.48, and a correction factor e, generally referred to as an evaporation coefficient, is included to give:

$$v' = eP_s(M'/2\pi \mathbf{R}T_s)^{0.5} \tag{15.49}$$

A laboratory technique used to measure values of e for sublimable solid materials is described by PLEWES and KLASSEN[105].

Sublimation rates of pure solids into turbulent air streams have been successfully correlated by the Gilliland–Sherwood equation[102]:

$$d'/x' = 0.023Re^{0.38}Sc^{0.44} \tag{15.50}$$

where d' *is* a characteristic dimension of the vaporisation chamber, x' is the effective film thickness for mass transfer at the vapour–solid interface, and *Re* and *Sc* are the dimensionless Reynolds and Schmidt numbers, respectively.

Condensation is generally a transient operation in which, as discussed by UEDA and TAKASHIMA[106], simultaneous heat and mass transfer are further complicated by the effects of spontaneous condensation in the bulk gaseous phase. After the creation of supersaturation in the vapour phase, nucleation normally occurs which may be homogeneous in special circumstances, but more usually heterogeneous. This process is followed by both crystal growth and agglomeration which lead to the formation of the final crystal product. As a rate process, the condensation of solids from vapours is less well understood than vaporisation[98]. STRICKLAND-CONSTABLE[107] has described a simple laboratory technique

This book belongs to Bradley Loren (bloren@mcandrews-ip.com) Copyright Elsevier 2024
Intas Exhibit 1032
Page 270 of 470
PGR2025-00043

for measuring kinetics in subliming systems which has been used to compare the rates of solid evaporation and crystal growth of benzophenone under comparable conditions. The two most common ways of creating the supersaturation necessary for crystal nucleation and subsequent growth are: (a) cooling by a metal surface to give either a glassy or multi-crystalline deposit that requires mechanical removal and (b) dilution with an inert gas to produce a loose crystalline mass that is easy to handle. BILIK and KRUPICZKA[108] have described the measurement and correlation of heat transfer rates during condensation of phthalic anhydride in a pilot plant connected to an industrial desublimation unit, CIBOROWSKI and WRENSKI[109] have reported on the condensation of several sublimable materials in a fluidised bed, and KNUTH and WEINSPACH[110] have summarised an extensive study on heat- and mass-transfer processes in a fluidised-bed desublimation unit.

15.5.3. Sublimation processes

Simple and vacuum sublimation

Simple sublimation is a batch-wise process in which the solid material is vaporised and then diffuses towards a condenser under the action of a driving force attributable to difference in partial pressures at the vaporising and condensing surfaces. The vapour path between the vaporiser and the condenser should be as short as possible in order to reduce mass-transfer resistance. Simple sublimation has been used for centuries, often in very crude equipment, for the commercial production of ammonium chloride, iodine, and flowers of sulphur.

Vacuum sublimation is a development of simple sublimation, which is particularly useful if the pressure at the triple-point is lower than atmospheric, where the transfer of vapour from the vaporiser to the condenser is enhanced by the increased driving force attributable to the lower pressure in the condenser. Iodine, pyrogallol, and many metals have been purified by vacuum sublimation processes in which the exit gases from the condenser are usually passed through a cyclone or scrubber to protect the vacuum equipment and to minimise product loss.

Entrainer sublimation

In entrainer sublimation, an entrainer gas is blown into the vaporisation chamber of a sublimer in order to increase the vapour flowrate to the condensing equipment, thereby increasing the yield. Air is the most commonly used entrainer, though superheated steam can be employed for substances such as anthracene that are relatively insoluble in water. If steam is used, the vapour may be cooled and condensed by direct contact with a spray of cold water. Although the recovery of the sublimate is efficient, the product is wet. The use of an entrainer gas in a sublimation process also provides the heat needed for sublimation and an efficient means of temperature control. If necessary, it may also provide dilution for the fractional condensation at the desublimation stage. Entrainer sublimation, whether by gas flow over a static bed of solid particles or through a fluidised bed, is ideally suited to continuous operation.

A general-purpose, continuous entrainer–sublimation plant is shown in Figure 15.34. The impure feedstock is pulverised in a mill and, if necessary, a suitable entrainer gas,

This book belongs to Bradley Loren (bloren@mcandrews-ip.com) Copyright Elsevier 2024

Intas Exhibit 1032
Page 271 of 470
PGR2025-00043

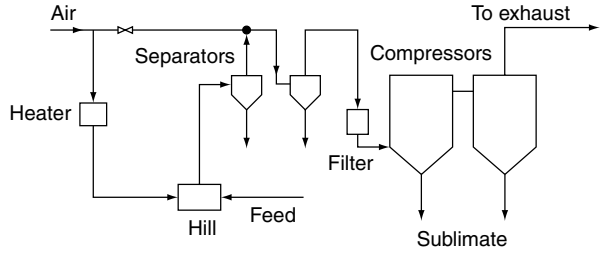


Figure 15.34. General-purpose continuous sublimation unit[3]

such as hot air, is used to blow the fine particles, which volatilise readily, into a series of separators, such as cyclones, where nonvolatile solid impurities are removed. A filter may also be located in the vapour line to remove final traces of inert, solid impurities. The vapour then passes to a series of condensers from which the sublimate is subsequently discharged. The exhaust gases may be recycled, or passed to the atmosphere through a cyclone or wet scrubber to recover any entrained product.

Although the application of fluidisation techniques to sublimation–desublimation processes was first proposed by MATZ[111], the technique has not yet been widely adopted for large-scale commercial use, despite its obvious advantage of improving both heat and mass transfer rates. CEDRO[112] has, however, reported on a fluidised-bed de-sublimation unit operating in the United States for the production of aluminum chloride at the rate of 3 kg/s (11 tonne/h).

The *product yield* from an entrainer–sublimation process may be estimated as follows. The mass flowrate G' of the inert gas and the mass sublimation rate S' are related by:

$$\frac{G'}{S'} = \frac{\rho_g P_g}{\rho_s P'_s} \tag{15.51}$$

where P_g and P'_s are the partial pressures of the inert gas and vaporised material, respectively, in the vapour stream, and ρ_g and ρ_s are their respective vapour densities. The total pressure P_t of the system is the sum of the partial pressures of the components or:

$$P_t = P_g + P'_s \tag{15.52}$$

From equation 15.51:

$$S' = G' \left(\frac{\rho_s}{\rho_g}\right) \left(\frac{P'_s}{P_t - P'_s}\right) \tag{15.53}$$

or, in terms of the molecular weights of the inert gas, M_g and of the material being sublimed, M_s:

$$S' = G' \left(\frac{M_s}{M_g}\right) \left(\frac{P'_s}{P_t - P'_s}\right) \tag{15.54}$$

The theoretical maximum yield from an entrainer sublimation process is the difference between the calculated sublimation rates corresponding to the conditions in the vaporisation and condensation stages.

This book belongs to Bradley Loren (bloren@mcandrews-ip.com) Copyright Elsevier 2024

Intas Exhibit 1032
Page 272 of 470
PGR2025-00043

Example 15.8

Salicylic acid ($M_s = 138$ kg/kmol) is to be purified by entrainer sublimation with air ($M_g = 29$ kg/kmol) at 423 K. The vapour is fed at 101.5 kN/m^2 to a series of condensers, the internal temperature and pressure of the last condenser being 313 K and 100 kN/m^2 respectively. The air flowrate is 0.56 kg/s and the pressure drop between the vaporiser and the last condenser is 1.5 kN/m^2. The vapour pressures of salicylic acid at 423 and 313 K are 1.44 and 0.0023 kN/m^2 respectively. What are the mass sublimation rates in the vaporiser and condenser?

Solution

Under saturated conditions:

Vaporisation stage: $P_t = 101.5$ kN/m^2, $P'_s = 1.44$ kN/m^2

Thus, in equation 15.54:

$$S'_v = 0.56(138/29)(1.44/(101.5 - 1.44)) = 0.038 \text{ kg/s } (38 \text{ g/s})$$

Condensation stage: $P_t = 100$ kN/m^2, $P'_s = 0.0023$ kN/m^2

Thus, in equation 15.54:

$$S' = 0.56(138/29)(0.0023/(100 - 0.0023)) = \underline{0.000061 \text{ kg/s } (0.061 \text{ g/s})}$$

In this example, the loss from the condenser exit gases is only 0.061 g/s whilst the theoretical maximum yield is 38 g/s. This maximum yield is obtained, however, only if the air is saturated with salicylic acid vapour at 423 K, and saturation is approached only if the air and salicylic acid are in contact for a sufficiently long period of time at the required temperature. A fluidised-bed vaporiser may achieve these optimum conditions though, if air is simply blown over bins or trays containing the solid, saturation will not be achieved and the actual rate of sublimation will be lower than that calculated. In some cases, the degree of saturation achieved may be as low as 10 per cent of the calculated value. The actual loss of product in the exit gases from the condenser is then greater than the calculated value. There are other losses which can be minimised by using an efficient scrubber.

Comparison of entrainer-sublimation and crystallisation

An analysis by KUDELA and SAMPSON[97] of the processes for commercial purification of naphthalene suggests that sublimation is potentially more economical than conventional melt crystallisation. In the sublimation method, the feedstock is completely vaporised in a nitrogen stream and then partially condensed. Heat is removed by vaporising water at the top of the condenser and, in order to prevent deposition of sublimate on the vessel walls, the inner wall of the condenser is sufficiently permeable to allow it to pass some of the entrainer gas. Impurities remain in the vapour stream and are subsequently condensed in a cooler located after the compressor used to circulate the entrainer. The stream carrying impurities and wastewater from the separator is washed with benzene in an extractor. Sublimation gives a higher yield of naphthalene at a lower cost, and with a smaller space requirement, than crystallisation[94]. Although steam and electricity consumption is higher for sublimation, this is offset by a much lower cooling-water requirement.

This book belongs to Bradley Loren (bloren@mcandrews-ip.com) Copyright Elsevier 2024

Intas Exhibit 1032
Page 273 of 470
PGR2025-00043

Fractional sublimation

As discussed in Section 15.5.2, the separation of two or more sublimable substances by fractional sublimation is theoretically possible if the substances form true solid solutions. GILLOT and GOLDBERGER[100] have reported the development of a laboratory-scale process known as thin-film fractional sublimation which has been applied successfully to the separation of volatile solid mixtures such as hafnium and zirconium tetrachlorides, 1,4-dibromobenzene and 1-bromo-4-chlorobenzene, and anthracene and carbazole. A stream of inert, non-volatile solids fed to the top of a vertical fractionation column falls countercurrently to the rising supersaturated vapour which is mixed with an entrainer gas. The temperature of the incoming solids is maintained well below the snow-point temperature of the vapour, and thus the solids become coated with a thin film (10 μm) of sublimate which acts as a reflux for the enriching section of the column above the feed entry point.

15.5.4. Sublimation equipment

Very few standard forms of sublimation or de-sublimation equipment are in common use and most industrial units, particularly on the condensation side of the process, have been developed on an ad hoc basis for a specific substance and purpose. The most useful source of information on sublimation equipment is the patent literature, although as HOLDEN and BRYANT[95] and KEMP *et al.*[96] point out, it is not clear whether a process has been, or even can be, put into practice.

Vaporisers

A variety of types of vaporisation units has been used or proposed for large-scale operation[95], the design depending on the manner in which the solid feedstock is to be vaporised. These include:

(a) a bed of dry solids without entrainer gas,
(b) dry solids suspended in a dense non-volatile, liquid;
(c) solids suspended in a boiling (entrainer) liquid where the entrainer vapour is formed in situ;
(d) entrainer gas flowing through a fixed bed of solid particles;
(e) entrainer gas bubbling through molten feedstock such that vaporisation takes place above the triple-point pressure;
(f) entrainer gas flowing through a dense phase of solid particles in a fluidised bed;
(g) entrainer gas flowing through a dilute phase of solid particles, such as in a transfer-line vaporiser where the solid and gas phases are in co-current flow, or in a raining solids unit where the solids and entrainer may be in countercurrent flow.

Condensers

Sublimate condensers are usually large, air-cooled chambers which tend to have very low heat-transfer coefficients (5–10 W/m^2 deg K) because sublimate deposits on the condenser walls act as an insulator, and vapour velocities in the chambers are generally very low.

This book belongs to Bradley Loren (bloren@mcandrews-ip.com) Copyright Elsevier 2024

Intas Exhibit 1032
Page 274 of 470
PGR2025-00043

Quenching the vapour with cold air in the chamber may increase the rate of heat removal although excessive nucleation is likely and the product crystals will be very small. Condenser walls may be kept free of solid by using internal scrapers, brushes, and other devices, and all vapour lines in sublimation units should be of large diameter, be adequately insulated, and if necessary, be provided with supplementary heating to minimise blockage due to the buildup of sublimate. One of the main hazards of air-entrainment sublimation is the risk of explosion since many solids that are considered safe in their normal state can form explosive mixtures with air. All electrical equipment should therefore be flame-proof, and all parts of the plant should be efficiently earthed to avoid build-up of static electricity.

The method of calculating the density of deposited layers of sublimate and of other variables and the optimisation of sublimate condenser design, has been discussed by WINTERMANTEL *et al.*[113]. It is generally assumed that the growth rate of sublimate layers is governed mainly by heat and mass transfer. The model which is based on conditions in the diffusion boundary layer takes account of factors such as growth rate, mass transfer, and concentrations in the gas. The model shows a reasonably good fit to experimental data.

In a variant of the large-chamber de-sublimation condenser, the crystallisation chamber may be fitted with gas-permeable walls as described by VITOVEC *et al.*[101]. The vapour and the entrainer gas are cooled by evaporation of water dispersed in the pores of the walls, and an inert gas passes through the porous walls into the cooling space and protects the internal walls from solid deposits. Crystallisation takes place in the bulk vapour–gas mixture as a result of direct contact with the dispersed water. This arrangement has been used, for example, for the partial separation of a mixture of phthalic anhydride and naphthalene by using nitrogen as the entrainer. Although fluidised-bed condensers have been considered for large-scale application, most of the published reports are concerned with laboratory-scale investigations[110].

15.6. FRACTIONAL CRYSTALLISATION

A single crystallisation operation performed on a solution or a melt may fail to produce a pure crystalline product for a variety of reasons including:

(a) the impurity may have solubility characteristics similar to those of the desired pure component, and both substances consequently co-crystallise,
(b) the impurity may be present in such large amounts that the crystals inevitably become contaminated.
(c) a pure substance cannot be produced in a single crystallisation stage if the impurity and the required substance form a solid solution.

Re-crystallisation from a solution or a melt is, therefore, widely employed to increase crystal purity.

Example 15.9

Explain how fractional crystallisation may be applied to a mixture of sodium chloride and sodium nitrate given the following data. At 293 K, the solubility of sodium chloride is 36 kg/100 kg water

This book belongs to Bradley Loren (bloren@mcandrews-ip.com) Copyright Elsevier 2024

Intas Exhibit 1032
Page 275 of 470
PGR2025-00043

and of sodium nitrate 88 kg/100 kg water. Whilst at this temperature, a saturated solution comprising both salts will contain 25 kg sodium chloride and 59 kg of sodium nitrate per 100 kg of water. At 373 K, these values, again per 100 kg of water, are 40 and 176 and 17 and 160, respectively.

Solution

The data enable a plot of kg NaCl/100 kg of water to be drawn against kg $NaNO_3$/100 kg of water as shown in Figure 15.35. On the diagram, points C and E represent solutions saturated with respect to both NaCl and $NaNO_3$ at 293 K and 373 K respectively. Fractional crystallisation may then be applied to this system as follows:

(a) A solution saturated with both NaCl and $NaNO_3$ is made up at 373 K. This is represented by point E, and, on the basis of 100 kg water, this contains 17 kg NaCl and 160 kg $NaNO_3$.
(b) The solution is separated from any residual sold and then cooled to 293 K. In so doing, the composition of the solution moves along EG.
(c) Point G lies on CB which represents solutions saturated with $NaNO_3$ but not with NaCl. Thus the solution still contains 17 kg NaCl and in addition is saturated with 68 kg $NaNO_3$. That is $(168 - 68) = 92$ kg of pure $NaNO_3$ crystals have come out of solution and this may be drained and washed.

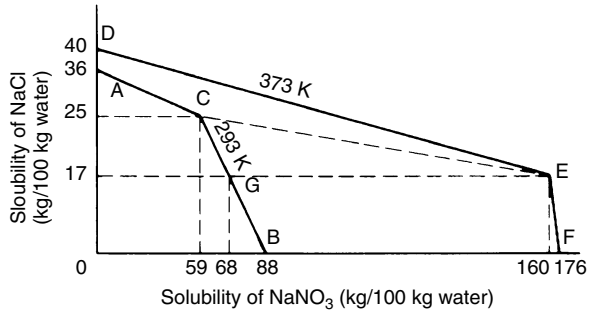


Figure 15.35. Effect of sodium chloride on the solubility of sodium nitrate

In this way, relatively pure $NaNO_3$, depending on the choice of conditions and particle size, has been separated from a mixture of $NaNO_3$ and NaCl.

The amount of $NaNO_3$ recovered from the saturated solution at 373 K is:

$$(92 \times 100)/160 = \underline{57.5\%}$$

An alternative approach is to note that points C and B represent 59 and 88 kg $NaNO_3$/100 kg water and assuming CB to be a straight line, then by similar triangles:

$$\text{concentration of } NaNO_3 = 59 + [(88 - 59)(25 - 17)]/24$$

$$= 68.3 \text{ kg/100 kg water}$$

and:

$$\text{yield of } NaNO_3 = (160 - 68.3) = \underline{91.7 \text{ kg/100 kg water}}.$$

whilst all the sodium chloride remains in solution.

This book belongs to Bradley Loren (bloren@mcandrews-ip.com) Copyright Elsevier 2024

Intas Exhibit 1032
Page 276 of 470
PGR2025-00043

If the cycle is then repeated, during the evaporation stage the sodium chloride is precipitated (and removed!) whilst the concentration of the nitrate re-attains 160 kg/100 kg water. On cooling again, the amount of sodium nitrate which crystallises out is 91.7 kg/100 kg water,

or: $(91.7 \times 100)/160 = \underline{\underline{57.3 \text{ per cent of the nitrate in solution}}}$, as before.

The same percentage of the chloride will be precipitated on re-evaporation.

15.6.1. Recrystallisation from solutions

Most of the impurities from a crystalline mass can often be removed by dissolving the crystals in a small amount of fresh hot solvent and cooling the solution to produce a fresh crop of purer crystals. The solubility of the impurities in the solvent must, however, be greater than that of the main product. Re-crystallisation may have to be repeated many times before crystals of the desired purity are obtained. A simple recrystallisation scheme is:

$$\begin{array}{ccccccc} \mathrm{S} & & \mathrm{S} & & & & \\ \downarrow & & \downarrow & & & & \\ \mathbf{AB} & \rightarrow & \mathrm{X_1} & \rightarrow & \mathrm{X_2} & \rightarrow & \mathrm{X_3} \\ & \downarrow & & \downarrow & & \downarrow & \\ & \mathrm{L_1} & & \mathrm{L_2} & & \mathrm{L_3} & \end{array}$$

An impure crystalline mass **AB**, where **A** is the less soluble, desired component, is dissolved in the minimum amount of hot solvent **S** and then cooled. The first crop of crystals X_1 will contain less impurity **B** than the original mixture, and **B** is concentrated in the liquor L_1. To achieve a higher degree of crystal purity, the procedure can be repeated. In each stage of such a sequence, losses of the desired component **A** can be considerable, and the final amount of 'pure' crystals may easily be a small fraction of the starting mixture **AB**. Many schemes have been designed to increase both the yield and the separation efficiency of fractional re-crystallisation. The choice of solvent depends on the characteristics of the required substance **A** and the impurity **B**. Ideally, **B** should be very soluble in the solvent at the lowest temperature employed and **A** should have a high temperature coefficient of solubility, so that high yields of **A** can be obtained from operation within a small temperature range.

15.6.2. Recrystallisation from melts

Schemes for recrystallisation from melts are similar to those for solutions, although a solvent is not normally added. Usually, simple sequences of heating (melting) and cooling (partial crystallisation) are followed by separation of the purified crystals from the residual melt. Selected melt fractions may be mixed at intervals according to the type of scheme employed, and fresh feed-stock may be added at different stages if necessary. As BAILEY[114] reports, several such schemes have been proposed for purification of fats and waxes.

As described in Section 15.2.1, eutectic systems can be purified in theory by single-stage crystallisation, whereas solid solutions always require multistage operations. Countercurrent fractional crystallisation processes in column crystallisers are described in Section 15.4.3.

This book belongs to Bradley Loren (bloren@mcandrews-ip.com) Copyright Elsevier 2024

Intas Exhibit 1032
Page 277 of 470
PGR2025-00043

15.6.3. Recrystallisation schemes

A number of fractional crystallisation schemes have been devised by MULLIN[3] and GORDON *et al.*[115], and the use of such schemes has been discussed by JOY and PAYNE[116] and SALUTSKY and SITES[117].

15.7. FREEZE CRYSTALLISATION

Crystallisation by freezing, or *freeze crystallisation*, is a process in which heat is removed from a solution to form crystals of the solvent rather than of the solute. This is followed by separation of crystals from the concentrated solution, washing the crystals with near-pure solvent, and finally melting the crystals to produce virtually pure solvent. The product of freeze crystallisation can be either the melted crystals, as in water desalination, or the concentrated solution, as in the concentration of fruit juice or coffee extracts. Freeze crystallisation is applicable in principle to a variety of solvents and solutions although, because it is most commonly applied to aqueous systems, the following comments refer exclusively to the freezing of water.

One of the more obvious advantages of freezing over evaporation for removal of water from solutions is the potential for saving heat energy resulting from the fact that the enthalpy of crystallisation of ice, 334 kJ/kg, is only one-seventh of the enthalpy of vaporisation of water, 2260 kJ/kg, although it has to be acknowledged that the cost of producing 'cold' is many times more than the cost of producing 'heat'. Process energy consumption may be reduced below that predicted by the phase-change enthalpy, however, by utilising energy recycle methods, such as multiple-effect or vapour compression, as commonly employed in evaporation as discussed in Chapter 14. In freeze-crystallisation plants operating by direct heat exchange, vapour compression has been used to recover refrigeration energy by using the crystals to condense the refrigerant evaporated in the crystalliser. Another advantage of freeze crystallisation, important in many food applications, is that the volatile flavour components normally lost during conventional evaporation can be retained in the freeze-concentrated product. Despite earlier enthusiasm, large-scale applications in desalination, effluent treatment, dilute liquor concentration and solvent recovery and so on have not been developed as yet.

All freeze separation processes depend on the formation of pure solvent crystals from solution, as described for eutectic systems in Section 15.2.1. which allows single-stage operation. Solid-solution systems, requiring multistage-operation, are not usually economic. Several types of freeze crystallisation processes may be designated according to the kind of refrigeration system used as follows:.

(a) In *indirect-contact freezing*, the liquid feedstock is crystallised in a scraped-surface heat exchanger as described in Section 15.4, fitted with internal rotating scraper blades and an external heat-transfer jacket through which a liquid refrigerant is passed. The resulting ice-brine slurry passes to a wash column where the ice crystals are separated and washed before melting. VAN PELT and VAN NISTELROOY[118] have described one of the commercial systems which are based on this type of freezing process.

This book belongs to Bradley Loren (bloren@mcandrews-ip.com) Copyright Elsevier 2024

Intas Exhibit 1032
Page 278 of 470
PGR2025-00043

(b) *Direct-contact freezing* processes utilise inert, immiscible refrigerants and are suitable for desalination. A typical scheme taken from BARDUHN[64] is shown in Figure 15.36. Sea-water, at a temperature close to its freezing point, is fed continuously into the crystallisation vessel where it comes in direct contact with a liquid refrigerant such as *n*-butane which vaporises and causes ice crystals to form due to the exchange of latent heat. The ice-brine slurry is fed to a wash column where it is washed countercurrently with fresh water. The emerging brine-free ice is melted by the enthalpy of the condensation of the vapour released from the compressed refrigerant. A major part of the energy input is that required for the compressors.

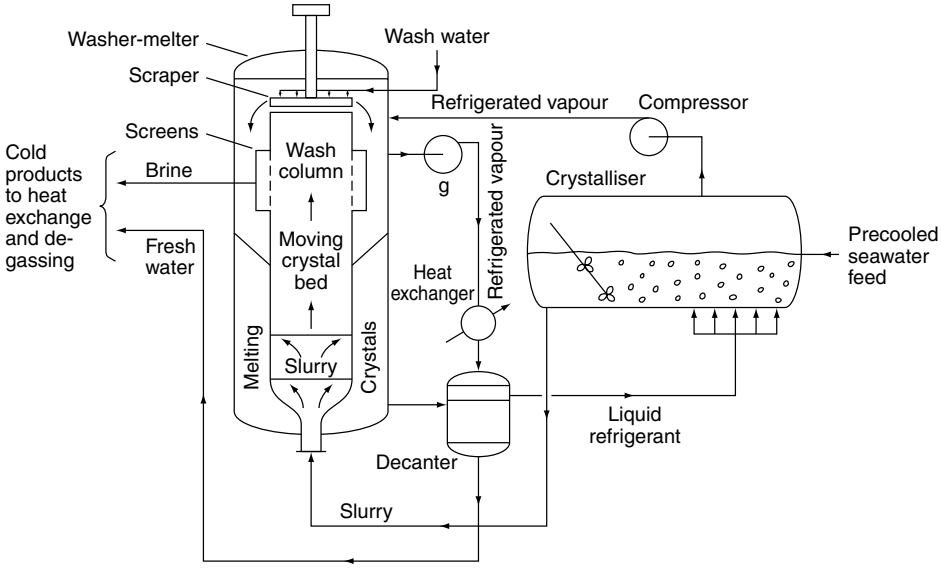


Figure 15.36. Desalination of seawater by freezing[64]

(c) *Vacuum freezing processes* do not require a conventional heat exchanger, and the problems of scale formation on heat-transfer surfaces are avoided. Cooling is effected by flash evaporating some of the solvent as the liquid feedstock enters a crystallisation vessel maintained at reduced pressure. Although vacuum freezing is potentially attractive for aqueous systems it has not, as yet, achieved widespread commercial success.

THIJSSEN and SPICER[119] has given a general review of freeze concentration as an industrial separation process and BUSHNELL and EAGEN[63] have discussed the status of freeze desalination. The potential of freeze crystallisation in the recycling and re-use of wastewater has been reviewed by HEIST[120], and the kinetics of ice crystallisation in aqueous sugar solutions and fruit juice are considered by OMRAN and KING[121].

This book belongs to Bradley Loren (bloren@mcandrews-ip.com) Copyright Elsevier 2024
Intas Exhibit 1032
Page 279 of 470
PGR2025-00043

15.8. HIGH PRESSURE CRYSTALLISATION

As noted previously, high pressure crystallisation in which an impure liquid feedstock is subjected to pressures of up to 300 MN/m^2 in a relatively small chamber, 0.001 m^3 in volume, under adiabatic conditions is a relatively recent development. As the pressure and temperature of the charge increase, fractional crystallisation takes place and the impurities are concentrated in the liquid phase which is then discharged from the pressure chamber. At the end of the cycle, further purification is possible since residual impurities in the compressed crystalline plug may then be 'sweated out' when the pressure is released. MORITOKI[91] has claimed that a single-cycle operation lasting less than 300 s is capable of substantially purifying a wide range of organic binary melt systems.

The principle of operation is illustrated in Figure 15.37 which shows the pressure-volume relationship. Curve a shows the phase change of a pure liquid as it is pressurised isothermally. Crystallisation begins at point A_1 and proceeds by compression without any pressure change until it is complete at point A_2. Beyond this point, the solid phase is compressed resulting in a very sharp rise in pressure. If the liquid contains impurities, these nucleate at point B_1. As the crystallisation of the pure substance progresses, the impurities are concentrated in the liquid phase and a higher pressure is required to continue the crystallisation process. As a result, the equilibrium pressure of the liquid–solid system rises exponentially with increase of the solid fraction, as shown by curve *b* which finally approaches

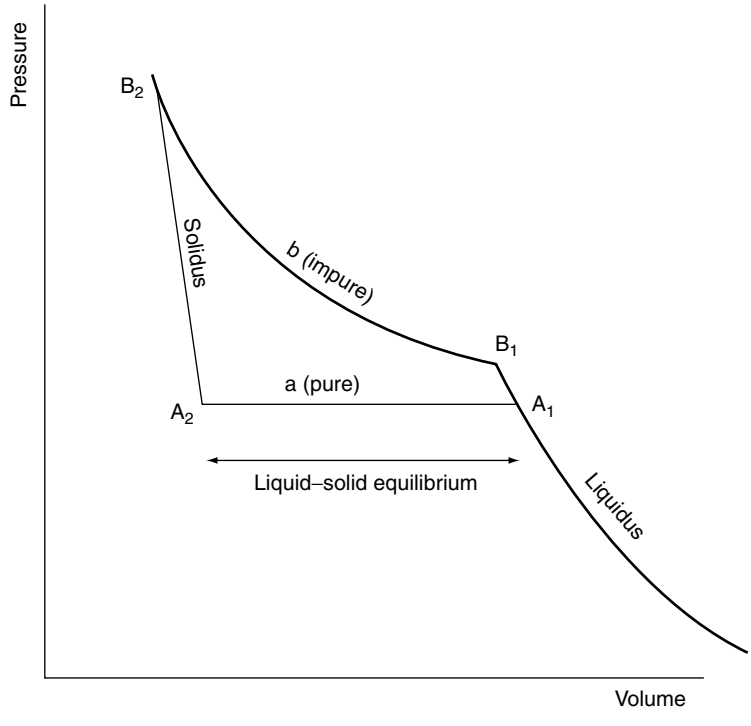


Figure 15.37. Relationship between pressure and volume for isothermal conditions

This book belongs to Bradley Loren (bloren@mcandrews-ip.com) Copyright Elsevier 2024

the solidus curve. A liquid–solid equilibrium line in terms of pressure and temperature is shown in Figure 15.38*a*. The liquid–solid equilibrium line moves from line a to line b with increase in impurities and line c represents the liquid–solid equilibrium for eutectic composition. On the industrial scale, a liquid is adiabatically compressed first from point A to point B, accompanied by heat generation and then to point C at which nucleation occurs accompanied by a temperature rise due to the release of the latent heat. Again, it is during this step that the impurities are concentrated into the mother liquor. At this stage, the liquid is separated from the solid phase and removed from the vessel at point C which is at a slightly lower pressure than the eutectic line. When the greater part of the liquid has been removed, its pressure decreases at first gradually and then rapidly to atmospheric pressure whilst the crystals are maintained at the initial separation pressure. In this way, the crystals are compacted and their surfaces are purified by slight melting, or by the so-called 'sweating' phenomenon. After the separation at point D, the crystals are highly purified and the line representing the equilibrium state gradually approaches line a. The basic pattern of operation as a function of time is shown in Figure 15.38*b*.

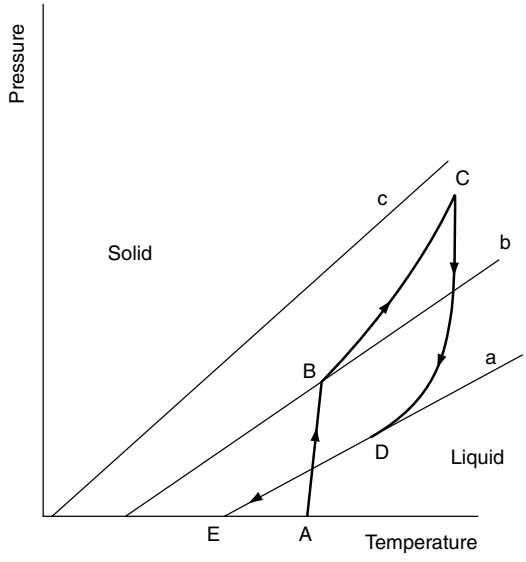
Pilot scale investigations by Kobe Steel have shown, for example, that the impurity level in a feed of mesitylene is reduced from 0.52 to 0.002 per cent in a single operating cycle at 15 MN/m^2 and a concentration of greater than 99 per cent *p*-xylene is obtained from a mixture of *p*-xylene and mesitylene containing 80 per cent *p*-xylene. It has also been shown that whilst crystals of cumenealdehyde are very difficult to obtain by cooling, nucleation and crystal growth occur at pressures of 50–70 MN/m^2 and, where the crystals obtained are then used as seed material, cumenealdehyde is then easily crystallised and purified at pressures below 20 MN/m^2. In this work, even though the capacity of the pilot unit was only 0.0015 m^3, some 360 tonne/year of raw material could be processed in 120 s cycles over a period of 8000 h.

Kobe Steel claim that, in terms of running costs, not only is the energy consumption low, being 10–50 per cent compared with conventional processes, but high pressure operation is ideally suited to the separation of isomers which are difficult to purify by other processes. These substances may have close boiling points or may be easily decomposed by temperature elevation. In this respect, recent work on supercritical fluids, as described by POLOAKOFF *et al.*[122], is of great importance.

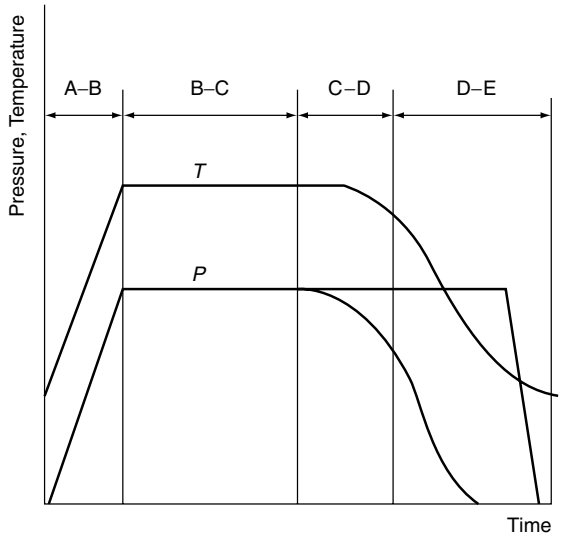
As discussed in Chapter 14, supercritical fluids are gases that are compressed until their densities are close to those of liquids. They are extremely non-ideal gases in which interactions between molecules of a supercritical fluid and a potential solute can provide a 'solvation energy' for many solids to dissolve. The higher the pressure and hence the density of the supercritical fluid, the greater are the solvent–solute interactions and hence the higher the solubility of the solid. In other words the solvent power of a supercritical fluid is 'tunable' and this is the key factor in the use of supercritical fluids for a wide range of processes. As discussed in Chapter 14, supercritical fluids in common use include ethene, ethane and propane together with supercritical carbon dioxide and these have all been widely discussed in the literature[123–127]. Although supercritical fluids have considerable advantages in the field of process intensification and can also replace environmentally undesirable solvents and indeed most organics, their most important property as far as crystallisation is concerned is that they can be tuned to dissolve the desired product, or indeed any impurities, which are then separated by crystallisation at high pressure. It is in this way that crystallisation is moving from the simple production of

This book belongs to Bradley Loren (bloren@mcandrews-ip.com) Copyright Elsevier 2024

Intas Exhibit 1032
Page 281 of 470
PGR2025-00043



(*a*) Adiabatic application of pressure



A–B–C: Pressurising step
C: Liquid-phase discharge
C–D–E: Solid phase compaction/sweating step

(*b*) Pressure and temperature variation during a cycle

Figure 15.38. High pressure crystallisation

This book belongs to Bradley Loren (bloren@mcandrews-ip.com)
Copyright Elsevier 2024
Intas Exhibit 1032
Page 282 of 470
PGR2025-00043

hydrates from salt solutions towards a fully fledged separation technique which has and will have many advantages in comparison with more traditional operations in the years to come.

15.9. FURTHER READING

BAILEY, A. E.: *Solidification of Fats and Waxes* (Interscience, New York, 1950).
BAMFORTH, A. W.: *Industrial Crystallisation* (Leonard Hill, London, 1965).
BARTOLOMAI, A. (ed.): *Food Factories: Processes, Equipment and Costs* (VCH, New York, 1987).
BUCKLEY, H. E.: *Crystal Growth* (Wiley, New York, 1951).
BRUIN, S. (ed.): *Preconcentration and Drying of Food Materials* (Elsevier, New York, 1988).
FAKTOR, M. M. and GARRETT, D. E.: *Growth of Crystals from the Vapour* (Chapman and Hall, London, 1974).
FINDLAY, A. and CAMPBELL, A. N.: *The Phase Rule and its Applications* 9th. edition. (Longman, London, 1951).
JANCIC, S. J. and GROOTSCHOLTEN, A. M.: *Industrial Crystallisation* (Reidel, Dordrecht, 1984)
KALDIS, E. and SCHEEL, H. J.: *Crystal Growth and Materials* (North-Holland, Amsterdam, 1977).
LARSON, R.: *Constitutive Equations for Polymer Melts and Solutions* (Butterworth, London, 1988).
LAWSON, W. D. and NIELSEN, S.: *Preparation of Single Crystals* (Butterworths, London, 1958).
LUI, Y. A., MCGEE, H. A. and EPPERLY, W. R. (eds.): *Recent Developments in Chemical Process and Plant Design* (Wiley, New York, 1987).
MATZ, G.: *Kristallisation* 2nd. edition (Springer Verlag, Berlin, 1969).
MERSTMANN, A. (ed.): *Crystallization Technology Handbook* (Marcel Dekker, New York, 1995).
MOYERS, C. G. and ROUSSEAU, R. W. in ROUSSEAU, R. W.: *Handbook of Separation Process Technology* (John Wiley, New York)
MULLIN, J. W.: *Crystallization* 3rd. edition (Butterworth-Heinemann, Oxford, 1993, 1997).
MULLIN, J. W.: *Crystallization* 4th edition (Butterworth-Heinemann, Oxford, 2001).
MULLIN, J. W.: 'Crystallisation' in Kirk-Othmer: *Encyclopedia of Chemical Technology*, Volume 7, 3rd. edition (John Wiley & Sons, New York, 1979).
MULLIN, J. W. 'Crystallisation and Precipitation' in *Ullmann's Encyclopedia of Industrial Chemistry*, Volume B2 (VCH Verlagsgesellschaft mbH, Weinheim, 1988)
MYERSON, A. S.: *Handbook of Industrial Crystallization*, 2nd edition (Butterworth-Heinemann, Oxford, 2000)
NULL, H. R.: *Phase Equilibrium in Process Design* (Wiley-Interscience, New York, 1970).
NYVLT, J.: *Industrial Crystallisation from Solutions* (Butterworths, London, 1971)
NYVLT, J.: *Solid–Liquid Phase Equilibria* (Elsevier-North Holland, New York, 1977).
NYVLT, J.: *Industrial Crystallisation* (Verlag Chemie, Weinheim, NY. 1978).
PAMPLIN, B. R. (ed.): *Crystal Growth*, 2nd. edition (Pergamon Press, Oxford, 1980).
RANDOLPH, D. and LARSON, M. A.: *Theory of Particulate Processes* (Academic Press, New York, 1971).
RUTNER, E., GOLDFINGER, P. and HIRTH, J. P. (eds.): *Condensation and Evaporation of Solids* (Gordon and Breach, New York, 1964).
SCHWEITZER, P. A. (ed.): *Handbook of Separation Techniques for Chemical Engineers* 2nd. edition (McGraw-Hill, New York, 1988).
STRICKLAND-CONSTABLE, R. F.: *Kinetics and Mechanism of Crystallisation* (Academic Press, London, 1968).
THIJSSEN, H. A. in SPICER, A. (ed.): *Advances in Preconcentration and Dehydration of Foods* (Wiley-Interscience, New York, 1974).
UBBELOHDE, A. R.: *Melting and Crystal Structure* (OUP, Oxford, 1965).
WALTON, A. G.: *The Formation and Properties of Precipitates* (Interscience, New York, 1967).
WALAS, S. M.: *Chemical Process Equipment:Selection and Design* (Butterworth, London, 1989).
WISNIAK, J.: *Phase Diagrams.* Physical Sciences Data 10 (Elsevier-North Holland, New York, 1981).
ZETTLEMOYER, A. C. (ed.): *Nucleation* (Marcel Dekker, New York, 1969).
AIChE Symp. Ser. (a) 65 (1969) no. 95, Crystallization from solutions and melts; (b) 67 (1971) no. 110, Factors affecting size distribution; (c) 68 (1972) no. 121, Crystallization from solutions: Nucleation phenomena in growing crystal systems; (d) 72 (1976) no. 153, Analysis and design of crystallisation processes; (e) 76 (1980) no. 193, Design, control and analysis of crystallisation processes; (f) 78 (1982) no. 215, Nucleation, growth and impurity effects in crystallisation process engineering; (g) 80 (1984) no. 240, Advances in crystallisation from solutions.

This book belongs to Bradley Loren (bloren@mcandrews-ip.com) Copyright Elsevier 2024

Intas Exhibit 1032
Page 283 of 470
PGR2025-00043

15.10. REFERENCES

1. MULLIN, J. W.: 'Crystallization' in Kirk-Othmer: *Encyclopedia of Chemical Technology*, Volume 7, 3rd. edition (John Wiley & Sons, New York, 1979)
2. MULLIN, J. W. 'Crystallization and Precipitation' in *Ullmann's Encyclopedia of Industrial Chemistry*, Volume B2 (VCH Verlagsgesellschaft mbH, Weinheim, 1988)
3. MULLIN, J. W.: *Crystallization* 4th. edn. (Butterworth-Heinemann, Oxford, 2001)
4. FEILCHENFELD, H. and SARIG, S.: *Ind. Eng. Chem. Process. Prod. Res. Dev*. **24** (1985) 130–133. Calcium chloride hexahydrate: A phase-changing material for energy storage.
5. KIMURAH, H.: *J. Cryst. Growth* **73** (1985) 53–62. Impurity effect on growth rates of $CaCl_2.6H_2O$ crystals.
6. GRONVOLD, F. and MEISINGSET, K. K.: *J. Chem. Thermodyn*. **14** (1982) 1083–1098. Thermodynamic properties and phase transitions of salt hydrates between 270 and 400K: $NH_4Al(SO_4)_2.12H_2O$, $KAl(SO_4)_2.12H_2O$, $Al_2(SO_4)_3.17H_2O$, $ZnSO_4.7H_2O$, $NaSO_4.10H_2O$ and $Na_2S_2O_3.5H_2O$.
7. KIMURA, H. and KAI, J.: *Solar Energy* **35** (1985) 527–534. Phase change stability of sodium acetate trihydrate and its mixtures.
8. FINDLAY, A. and CAMPBELL, A. N.: *The Phase Rule and its Applications*, 9th. edition (Longman, London, 1951).
9. RICCI, J. E.: *The Phase Rule and Heterogeneous Equilibrium* (van Nostrand, New York, 1951).
10. NULL, H. R.: *Phase Equilibrium in Process Design* (Wiley-Interscience, New York, 1970).
11. NYVLT, J.: *Solid-Liquid Phase Equilibrium* (Academia, Prague, Elsevier, Amsterdam, 1977).
12. HÖRMEYER, H.: *Germ. Chem. Eng.* **6** (1983) 277–281. Calculation of crystallisation equilibria.
13. KUSIK, C. L., MEISSNER, H. P. and FIELD, E. L.: *A.I.Ch.E. Jl.* **25** (1979) 759–762. Estimation of phase diagrams and solubilities for aqueous multi-ion systems.
14. SANDER, B., RASMUSSEN, P. and FREDENSLUND, A.: *Chem. Eng. Sci.* **41** (1986) 1197–1202. Calculation of solid-liquid equilibria in aqueous solutions of nitrate salts using an extended uniquac equation.
15. NANCOLLAS, G. H., REDDY, M. M. and TSAI, F.: *J. Cryst. Growth* **20** (1973) 125–134. Crystal growth kinetics of minerals encountered in water treatment processes.
16. NANCOLLAS, G. H. and REDDY, M. M.: *Soc. Pet. Eng. J.* (April 1974) 117–123. The kinetics of crystallisation of scale-forming materials.
17. CARDEW, P. T., DAVEY, R. J. and RUDDICK, A. J.: *J. Chem. Soc. Faraday Trans. 2*, **80** (1984) 659–668. Kinetics of polymorphic solid-state transformations.
18. CARDEW, P. T. and DAVEY, R. J.: *Proc. R. Soc. London Ser. A* **398** (1985) 415–428. The kinetics of solvent-mediated phase transformations.
19. MULLIN, J. W. and SÖHNEL, O.: *Chem. Eng. Sci.* **32** (1977) 683–686. Expressions of supersaturation in crystallisation studies.
20. OSTWALD, Wilhelm: *Z. Phys. Chem. (Leipzig)* **34** (1900) 493–503. Über die vermeintliche Isomeric des roten und gelben Quecksilberoxyds und die Oberflaschen spannung fester Körper.
21. MIERS, H. A. and ISAAC, F.: *J. Chem. Soc.* **89** (1906) 413–454. Refractive indices of crystallizing solutions.
22. SEIDELL, A. in LINKE, W. F. (ed.): *Solubilities of Inorganic and Metal Organic Compounds*, 4th. edition vol. 1 (van Nostrand, New York, 1958) vol. 2 (*Am. Chem. Soc.*, Washington, D.C., 1965).
23. STEPHEN, H and STEPHEN, T.: *Solubilities of Inorganic and Organic Compounds* (Pergamon Press, London, 1963).
24. BROUL, M., NYVLT, J. and SÖHNEL, O.: *Solubilities in Binary Aqueous Solutions* (Academia, Prague, 1981).
25. MOYERS, C. G. and ROUSSEAU, R. W. in ROUSSEAU, R. W.: *Handbook of Separation Process Technology* (John Wiley, New York)
26. American Petroleum Institute: *Selected Values of Properties of Hydrocarbons* Research Project No. 44 (Amer. Pet. Institute)
27. STRICKLAND-CONSTABLE, R. F.: *Kinetics and Mechanism of Crystallization*, (Academic Press, London, 1968)
28. KASHCHIEV, D.: *Nucleation — basic theory with applications*. (Butterworth-Heinemann, Oxford, 2000)
29. GARSIDE, J. and DAVEY, R. J.: *Chem. Eng. Commun.* **4** (1980) 393–424. Secondary contact nucleation: kinetics, growth and scale-up.
30. UBBLEOHDE, A. R.: *Melting and Crystal Structure* (Oxford University Press, Oxford, 1965).
31. GARTEN, V. A. and HEAD, R. B.: *Phil. Mag.* **8** (1963) 1793–1803 and **14** (1966) 1243–1253. Homogeneous nucleation and the phenomenon of crystalloluminescence.
32. BERGLUND, K. A. in JANČIČ, S. J. and DE JONG, E. J. (eds.): *Industrial Crystallisation 84* (Elsevier, Amsterdam, 1984)
33. MULLIN, J. W. and LECI, C. L.: *Phil. Mag.* **19** (1969) 1075–1077. Evidence of molecular cluster formation in supersaturated solutions of citric acid.
34. LARSON, M. A. and GARSIDE, J.: *Chem. Eng. Sci.* **41** (1986) 1285–1289. Solute clustering in supersaturated solutions.

This book belongs to Bradley Loren (bloren@mcandrews-ip.com) Copyright Elsevier 2024

Intas Exhibit 1032
Page 284 of 470
PGR2025-00043

35. NYVLT, J.: *Industrial Crystallization from Solutions* (Butterworth, London, 1971).
36. NYVLT, J., SÖHNEL, O., MATUCHOVA, M. and BROUL, M.: *The Kinetics of Industrial Crystallization* (Academia, Prague, 1985).
37. RANDOLPH, A. D and LARSON, M. A.: *Theory of Particulate Processes* (Academic Press, New York, 1971).
38. NIELSEN, A. E. and SÖHNEL, O.: *J. Cryst. Growth* **11** (1971) 233–242. Interfacial tensions, electrolyte crystal-aqueous solution, from nucleation data.
39. SÖHNEL, O. and MULLIN, J. W.: *J. Cryst. Growth* **44** (1978) 377–382. A method for the determination of precipitation induction periods.
40. MATZ, G.: *Kristallisation* 2nd. edition (Springer Verlag, Berlin, 1969).
41. JANČIČ, S. J. and GROOTSCHOLTEN, P. A. M.: *Industrial Crystallization* (Reidel, Dordecht, 1984).
42. LAUDICE, R. A.: The growth of single crystals (Prentice-Hall, Englewood Cliffs, N.J., 1970).
43. GARSIDE, J.: *Chem. Eng. Sci.* **40** (1985) 3–26. Industrial crystallisation from solution.
44. NIELSEN, A. E.: *J. Cryst. Growth* **67** (1984) 289–310. Electrolyte crystal growth mechanisms.
45. PAMPLIN, B. R. (ed): *Crystal Growth* 2nd. edition (Pergamon Press, Oxford, 1980).
46. KALDIS, E. and SCHEEL, H. J.: *Crystal Growth and Materials* (North-Holland, Amsterdam, 1977).
47. TENGLER, T. and MERSMANN, A.: *Germ. Chem. Eng.* **7** (1984) 248–259. Influence of temperature, saturation and flow velocity on crystal growth from solutions.
48. WÖHLK, W.: *Meszanordnungen zur Bestimmung von Kristallwachstumsgeschwindigkeiten*, (Fortschr. Ber. VDI Z., Reihe **3** 1982 no. 71).
49. WHITE, E. T., BENDIG L. L. and LARSON, M. A.: *A.I.Ch.E. Symp. Ser.* **72** No. 153 (1976) 41–47. Analysis and design of crystallization systems.
50. JONES, A. G. and MULLIN, J. W.: *Chem. Eng. Sci.* **29** (1974) 105–118. Programmed cooling crystallisation of potassium sulphate solutions.
51. JANSE, A. H. and DE JONG, E. J. in MULLIN, J. W. (ed): *Industrial Crystallization 75* (Plenum Publishing, London, 1976).
52. GARSIDE, J. and JANČIČ, S. J.: *AIChE J.* **25** (1979) 948–958. Measurement and scale-up of secondary nucleation kinetics for the potash alum-water system.
53. WHETSTONE, J.: *Trans. Faraday. Soc.* **51** (1955) 973–80 and 1142–53. The crystal habit modification of inorganic salts with dyes (in two parts).
54. GARRETT, D. E.: *Brit. Chem. Eng.* **4** (1959) 673–677. Industrial crystallisation: influence of chemical environment.
55. BOTSARIS, G. D. in JANČIČ, S. J. and DE JONG, E. J. (eds.): *Industrial Crystallization 81* (North-Holland, Amsterdam, 1982).
56. DAVEY, R. J. in JANČIČ, S. J. and DE JONG, E. J. (eds.): *Industrial Crystallization 78* (North-Holland, Amsterdam, 1979).
57. DEICHA, G.: *Lacunes des cristeaux et leurs inclusions fluides* (Masson, Paris, 1955).
58. POWERS, H. E. C.: *Sugar Technol. Rev.* **1** (1970) 85–190. Sucrose crystals: inclusions and structure.
59. WILCOX, W. R. and KUO, V. H. S.: *J. Cryst. Growth* **19** (1973) 221–229. Nucleation of monosodium urate crystals.
60. SASKA, M. and MYERSON, A. S.: *J. Crys. Growth* **67** (1984) 380–382. A crystal-growth model with concentration dependent diffusion.
61. PHOENIX, L.: *Brit. Chem. Eng.* **11** (1966) 34–38. How trace additives inhibit the caking of inorganic salts.
62. ARMSTRONG, A. J.: *Chem. Proc. Eng.* **51**(11)(1970) 59. Scraped surface crystallisers.
63. BUSHNELL, J. D. and EAGEN, J. F.: *Oil Gas Jl.* **73** (1975) 42, 80–84. Dewax process produces benefits.
64. BARDUHN, A. J.: *Chem. Eng. Prog.* **71** (1975) 11, 80–87. The status of freeze-desalination.
65. MULLIN, J. W. and WILLIAMS, J. R.: *Chem. Eng. Res. Des.* **62** (1984) 296–302. A comparison between indirect contact cooling methods for the crystallisation of potassium sulphate.
66. FINKELSTEIN, E.: *J. Heat Recovery Syst.* **3** (1983) 431–437. On solar ponds: critique, physical fundamentals and engineering aspects.
67. BAMFORTH, A. W.: *Industrial Crystallisation* (Leonard Hill, London, 1965).
68. SAEMAN, W. C.: *A.I.Ch.E.Jl.* **2** (1956) 107–112. Crystal size distribution in mixed systems.
69. MULLIN, J. W. and NYVLT, J.: *Chem. Eng. Sci.* **26** (1971) 369–377. Programmed cooling of batch crystallizers.
70. ROBINSON, J. and ROBERTS, J. E.: *Can. J. Chem. Eng.* **35** (1957) 105–112. A mathematical study of crystal growth in a cascade of agitators.
71. ABEGG, C. F. and BALAKRISHNAM, N. S.: *A.I.Ch.E. Symp. Ser.* **72** No. 153 (1976) 88–94. The tanks-in-series concept as a model for imperfectly mixed crystallizers.
72. TOUSSAINT, A. G. and DONDERS, A. J. M.: *Chem. Eng. Sci.* **29** (1974) 237–245. The mixing criterion in crystallisation by cooling.
73. WHITE, E. T. and RANDOLPH, A. D.: *AIChE Jl* **33** (1984) 686–689. Graphical solution of the material balance constraint for MSMPR crystallizers.

This book belongs to Bradley Loren (bloren@mcandrews-ip.com) Copyright Elsevier 2024

Intas Exhibit 1032
Page 285 of 470
PGR2025-00043

74. GRIFFITHS, H.: *Trans. Instn. Chem. Engrs.* **25** (1947) 14–18. Crystallisation.
75. MULLIN, J. W. and NYVLT, J.: *Trans. Instn. Chem. Engrs.* **48** (1970) 7–14. Design of classifying crystalisers.
76. MERSMANN, A. and KIND, M.: *Intl Chem. Eng.* **29** (1989) 616–626. Modeling of chemical process equipment: the design of crystallizers.
77. DE JONG, E. J.: *Intl Chem. Eng.* **24** (1984) 419–431. Development of crystallizers.
78. BENNETT, R. C., FIEDELMAN, H. and RANDOLPH, A. D.: *Chem. Eng. Prog.* **69** (July, 1973) 86–93. Crystallizer influenced nucleation.
79. MOLINARI, J. G. D. in ZEIF, M. and WILCOX, W. R. (eds.): *Fractional Solidification* (Dekker, New York, 1967) 393–400.
80. GEL'PERIN, N. I. and NOSOV, G. A.: *Sov. Chem. Ind.* (Eng. Transl.) **9** (1977) 713–717. Fractional crystallisation of melts in drum crystallizers.
81. PONOMARENKO, K., POTEBYNA, G. F. and BEI, V. I.: *Theor. Found. Chem. Eng.* (Engl. Transl.) **13** (1980) 724–729. Crystallization of melts on a thin moving wall.
82. WINTERMANTEL, K.: *Chem. Ing. Tech.* **58** (1986) 6, 498–499. Effective separation power in freezing out layers of crystals from melts and solutions - a unified presentation.
83. ATWOOD, G. R. in Reference 42a, 112–121. The progressive mode of multistage crystallisation.
84. RITTNER, S. and STEINER, R.: *Chem. Ing. Tech.* **57** (1985) 2, 91–102. Melt crystallisation of organic substances and its large scale application.
85. FISCHER, O., JANČIČ, S. J. and SAXER, K. in JANČIČ, S. J. and DE JONG, E. J. (eds.): *Industrial Crystallization 84* (Elsevier, Amsterdam, 1984).
86. GATES, W. C. and POWERS, J. E.: *AIChE Jl* **16** (1970) 648–657. Determination of the mechanics causing and limiting separation by column crystallization.
87. HENRY, J. D. and POWERS, J. E.: *AIChE Jl* **16** (1970) 1055–1063. Experimental and theoretical investigation of continuous flow column crystallisation.
88. MCKAY, D. L. in ZEIT, F. and WILCOX, W. R. (eds.): *Fractional Solidification* (Marcel Dekker, New York, 1967) 427–439.
89. BRODIE, J. A.: *Mech. Chem. Trans. Inst. Engrs. Australia* **7** (1971) 1, 37–44. A continuous multistage melt purification process.
90. TAKEGAMI, K., NAKAMARU, N. and MORITA, M. in JANČIČ, S. J. and DE JONG, E. J. (eds.): *Industrial Crystallization 84* (Elsevier, Amsterdam, 1984). 143–146.
91. MORITOKI, M.: *Int. Chem. Eng.* **20** (1980) 394–401. Crystallization and sweating of p-cresol by application of high pressure.
92. SHEARON, W. H. and DUNWOODY, W. B.: *Ind. Eng. Chem.* **45** (1953) 496–504. Ammonium nitrate.
93. NUNELLY, L. M. and CARTNEY, F. T.: *Ind. Eng. Chem. Prod. Res. Dev.* **21** (1982) 617–620. Granulation of urea by the falling-curtain process.
94. MULLIN, J. W.: Sublimation in *Ullmann's Encyclopedia of Industrial Chemistry* (VCH Verlagsgesellschaft mbH, D-6940 Weinheim, 1988).
95. HOLDEN, C. A. and BRYANT, H. S.: *Sep. Sci.* **4** (1969) (1) 1–13. Purification by sublimation.
96. KEMP, S. D. in CREMER, H. W. and DAVIES, T. (eds.): *Chemical Engineering Practice*, **6**, (Butterworth, London, 1958) 567–600. Sublimation and vacuum freeze drying.
97. KUDELA, L. and SAMPSON, M. J.: *Chem. Eng. (N. Y.)* **93** (1986) 12, 93–98. Understanding sublimation technology.
98. RUTNER, E., GOLDFINGER, P. and HIRTH, J. P. (eds.): *Condensation and Evaporation of Solids* (Gordon and Breach, New York, 1964).
99. FAKTOR, M. M. and GARRETT, I.: *Growth of Crystals from the Vapour* (Chapman and Hall, London, 1974).
100. GILLOT, J. and GOLDBERGER, W. M.: *Chem. Eng. Prog. Symp. Ser.* **65** (1969) (91) 36–42. Separation by thin-film fractional sublimation.
101. VITOVEC, J., SMOLIK, J. and KUGLER, K.: *Collect. Czech. Chem. Commun.* **43** (1978) 396–400. Separation of sublimable compounds by partial crystallisation from their vapour mixture.
102. EGGERS, H. H., OLLMANN, D., HEINZ, D., DROBOT, D. W. and NIKOLAJEW, A. W.: *Z. Phys. Chem. (Leipzig)* **267** (1986) 353–363. Sublimation und Desublimation im System $AlCl_3$–$FeCl_3$.
103. MATSOUKA, M. in JANČIČ, S. J. and DE JONG, E. J. (eds.): *Industrial Crystallization 84* (Elsevier, Amsterdam 1984) 357–360. Rates of nucleation and growth of organic condensates of mixed vapours.
104. SHERWOOD, T. K. and JOHANNES, C.: *AIChE Jl.* **8** (1962) 590–593. The maximum rate of sublimation of solids.
105. PLEWES, A. C. and KLASSEN, J.: *Can. J. Technol.* **29** (1951) 322. Mass transfer rates from the solid to the gas phase.
106. UEDA, H. and TAKASHIMA, Y.: *J. Chem. Eng. Japan* **10** (1977) 6–12. Desublimation of two-component systems.
107. STRICKLAND-CONSTABLE, R. F.: *Kinetics and Mechanism of Crystallization* (Academic Press, London, 1968).

This book belongs to Bradley Loren (bloren@mcandrews-ip.com) Copyright Elsevier 2024

Intas Exhibit 1032
Page 286 of 470
PGR2025-00043

108. BILIK, R. J. and KRUPICZKA, R.: *Chem. Eng. Jl.* **26** (1983) 169–180. Heat transfer in the desublimation of phthalic anhydride.
109. CIBOROWSKI, J. and WRENSKI, S.: *Chem. Eng. Sci.* **17** (1962) 481–489. Condensation of subliminable materials in a fluidized bed.
110. KNUTH, M. and WEINSPACH, P. M.: *Chem. Ing. Tech.* **48** (1976) 893. Experimentelle Untersuchung des Wärme und Stoffübergangs an die Partikeln einer Wirbelschicht bei der Desublimation.
111. MATZ, G.: *Chem. Ing. Tech.* **30** (1958) 319–329. Fleitzbett-Sublimation.
112. CEDRO, V.: letter to *Chem. Eng. (N. Y.)* **93** (1986) 21, 5. Fluid beds and sublimation.
113. WINTERMANTEL, K., HOLZKNECH, H. and THOMA, P.: *Chem.Eng. Technol.* **10** (1987) 205–210. Density of sublimed layers.
114. BAILEY, A. E.: *Solidification of Fats and Waxes* (Interscience, New York, 1950).
115. GORDON, L., SALUTSKY, M. L. and WILLARD, H. H.: *Precipitation from Homogeneous Solution* (Wiley-Interscience, New York, 1959).
116. JOY, E. F. and PAYNE, J. H.: *Ind. Eng. Chem.* **47** (1955) 2157–2161. Fractional precipitation or crystallisation systems.
117. SALUTSKY, M. L. and SITES, J. G.: *Ind. Eng. Chem.* **47** (1955) 2162–2166. Ra-Ba separation process.
118. VAN PELT, W. H. S. M. and VAN NISTELROOY, M. G. J.: Food Eng. (November, 1975) 77–79. Procedure for the concentration of beer.
119. THIJSSEN, H. A. C. in SPICER, A. (ed.): *Advances in Preconcentration and Dehydration of Foods* (Wiley-Interscience, New York, 1974).
120. HEIST, J. A.: *AIChE Symp. Ser.* **77** (1984) (209) 259–272. Freeze crystallisation: waste water recycling and reuse.
121. OMRAN, A. M.: and KING, C. J.: *AIChE Jl.* **20** (1974) 799–801. Kinetics of ice crystallisation in sugar solutions and fruit juices.
122. POLOAKOFF, M., MEEHAN, N. J. and ROSS, S. K.: *Chem. & Industry* **10** (1999) 750–752 A supercritical success story.
123. JESSOP, P. G. and LEITNER, W. (eds): *Chemical Synthesis using supercritical fluids* (Wiley-VCH, Weinheim 1999)
124. MCHUGH, M. A. and KRUKONIS, V. J.: *Supercritical Fluid Extraction: Principles and Practice* (2nd edition) (Butterworth-Heinemann, Boston, 1994)
125. DARR, J. A. and POLIAKOFF, M.: *Chem. Rev.* **99** (1999) 495. New directions in inorganic and metal-organic coordination chemistry in supercritical fluids.
126. JESSOP, P. G., IKARIYA, T. and NOYORI, R.: *Chem. Rev.* **99** (1999) 475. Homogeneous catalysis in supercritical fluids.
127. BAIKER, A.: *Chem. Rev.* **99** (2) (1999) 453–473. Supercritical fluids in heterogeneous catalysis.

15.11. NOMENCLATURE

		Units in SI System	Dimensions in **M**, **N**, **L**, **T**, $\boldsymbol{\theta}$
A	crystal surface area	m^2	$\mathbf{L}^2$
A'	heat transfer area	m^2	$\mathbf{L}^2$
a_o	amount of component **A** in original solid	kg	**M**
B	secondary nucleation rate	$1/m^3$ s	$\mathbf{L}^{-3}\mathbf{T}^{-1}$
b	kinetic order of nucleation or exponent in equation 15.11	—	—
b_o	amount of component **B** in original solid	kg	**M**
C	concentration of solute	$kmol/m^3$	$\mathbf{NL}^{-3}$
C^*	saturated concentration of solute	$kmol/m^3$	$\mathbf{NL}^{-3}$
C_p	specific heat capacity	J/kg K	$\mathbf{L}^2\mathbf{T}^{-2}\boldsymbol{\theta}^{-1}$
c	solution concentration	kg/kg	—
c^*	equilibrium concentration	kg/kg	—
c_i	concentration at interface	kg/kg	—
c_{io}	initial concentration of impurity	kg/kg	—
c_{in}	impurity concentration after stage n	kg/kg	—
c_r	solubility of particles of radius r	kg/kg	—

This book belongs to Bradley Loren (bloren@mcandrews-ip.com) Copyright Elsevier 2024
Intas Exhibit 1032
Page 287 of 470
PGR2025-00043

		Units in SI System	Dimensions in **M**, **N**, **L**, **T**, $\boldsymbol{\theta}$
c_s	slurry concentration or magma density	kg/m^3	$\mathbf{MT}^{-3}$
D	molecular diffusivity	m^2/s	$\mathbf{L}^2\mathbf{T}^{-1}$
d	characteristic size of crystal	m	**L**
d'	characteristic dimension of vaporisation chamber	m	**L**
d_D	dominant size of crystal size distribution	m	**L**
d_p	product crystal size	m	**L**
d_s	size of seed crystals	m	**L**
E	mass of solvent evaporated/mass of solvent in initial solution	kg/kg	—
e	evaporation coefficient (equation 15.49)	—	—
F	fraction of liquid removed after each decantation	—	—
F'	pre-exponential factor in equation 15.9	1/m^3 s	$\mathbf{L}^{-3}\mathbf{T}^{-1}$
ΔG	excess free energy	J	$\mathbf{ML}^2\mathbf{T}^{-2}$
G'	flowrate of inert gas	kg/s	$\mathbf{MT}^{-1}$
G_d	overall growth rate	m/s	$\mathbf{LT}^{-1}$
ΔG_v	free energy change per unit volume	J/m^3	$\mathbf{ML}^{-1}\mathbf{T}^{-2}$
H_f	heat of fusion	J/kg	$\mathbf{L}^2\mathbf{T}^{-2}$
i	order of integration or relative kinetic order	—	—
J	rate of nucleation	1/m^3 s	$\mathbf{L}^{-3}\mathbf{T}^{-1}$
j	exponent in equation 15.11	—	—
K_b	birthrate constant	—	—
K_G	overall crystal growth coefficient	kg/s	$\mathbf{MT}^{-1}$
K_N	primary nucleation rate constant	1/m^{3}s	$\mathbf{L}^{-3}\mathbf{T}^{-1}$
k	Boltzmann constant	1.38×10^{23} J/K	$\mathbf{ML}^2\mathbf{T}^{-2}\boldsymbol{\theta}^{-1}$
k_1	constant in equation 15.33	1/m^{3}s	$\mathbf{L}^{-3}\mathbf{T}^{-1}$
k_2	constant in equation 15.34	m/s	$\mathbf{LT}^{-1}$
k_3	constant in equation 15.35	m$^{-(i+3)}$ s$^{(i-1)}$	$\mathbf{L}^{-(i+3)}\mathbf{T}^{(i-1)}$
k_4	constant in equation 15.38	m$^{-(i+3)}$ s$^{(i-1)}$	$\mathbf{L}^{-(i+3)}\mathbf{T}^{(i-1)}$
k_d	diffusion mass transfer coefficient	kg/m^{2}s	$\mathbf{ML}^{-2}\mathbf{T}^{-1}$
k_r	integration or reaction mass transfer coefficient	kg/m^{2}s	$\mathbf{ML}^{-2}\mathbf{T}^{-1}$
l	exponent in equation 15.11	—	—
M	molecular weight of solute in solution	kg/kmol	$\mathbf{MN}^{-1}$
M'	molecular weight	kg/kmol	$\mathbf{MN}^{-1}$
M_g	molecular weight of inert gas	kg/kmol	$\mathbf{MN}^{-1}$
M_s	molecular weight of sublimed material	kg/kmol	$\mathbf{MN}^{-1}$
m	particle mass or mass deposited in time t	kg	**M**
m_s	mass of seeds	kg	**M**
N	rotational speed of impeller	Hz	$\mathbf{T}^{-1}$
n	order of nucleation process or number of stages	—	—
n'	population density of crystals	m^{-4}	$\mathbf{L}^{-4}$
n_i	moles of ions/mole of electrolyte	—	—
n°	population density of nuclei	m^{-4}	$\mathbf{L}^{-4}$
P	vapour pressure	N/m^2	$\mathbf{ML}^{-1}\mathbf{T}^{-2}$
P'	crystal production rate	kg/s	$\mathbf{MT}^{-1}$
P_g	partial pressure of inert gas	N/m^2	$\mathbf{ML}^{-1}\mathbf{T}^{-2}$
P_s	vapour pressure at surface	N/m^2	$\mathbf{ML}^{-1}\mathbf{T}^{-2}$
P_s'	partial pressure of vaporised material	N/m^2	$\mathbf{ML}^{-1}\mathbf{T}^{-2}$
P_t	total pressure	N/m^2	$\mathbf{ML}^{-1}\mathbf{T}^{-2}$
Q	heat load	W	$\mathbf{ML}^2\mathbf{T}^{-3}$

This book belongs to Bradley Loren (bloren@mcandrews-ip.com) Copyright Elsevier 2024

Intas Exhibit 1032
Page 288 of 470
PGR2025-00043

		Units in SI System	Dimensions in **M**, **N**, **L**, **T**, $\boldsymbol{\theta}$
q	heat of crystallisation	J/kg	$\mathbf{L}^2\mathbf{T}^{-2}$
R	Universal Gas Constant	8314 J/kmol K	$\mathbf{MN}^{-1}\mathbf{L}^2\mathbf{T}^{-2}\boldsymbol{\theta}^{-1}$
R	molecular mass of hydrate/molecular mass of anhydrous salt	—	—
R_G	mass deposition rate	kg/m^{2}s	$\mathbf{ML}^{-2}\mathbf{T}^{-1}$
Re	Reynolds' number ($ud'\rho_v/\mu$)	—	—
r	radius of particle or equivalent sphere	m	**L**
r'	particle size in equilibrium with bulk solution	m	**L**
r_c	critical size of nucleus	m	**L**
S	supersaturation ratio	—	—
S'	mass sublimation rate	kg/s	$\mathbf{MT}^{-1}$
Sc	Schmidt Number ($\mu/\rho_v D$)	—	—
s	order of overall crystal growth	—	—
T	temperature	K	$\boldsymbol{\theta}$
ΔT_m	logarithmic mean temperature difference	deg K	$\boldsymbol{\theta}$
T_M	melting point	K	$\boldsymbol{\theta}$
T_s	surface temperature	K	$\boldsymbol{\theta}$
t	time	S	**T**
t_b	batch time	s	**T**
t_i	induction period	s	**T**
t_r	residence time	s	**T**
U	overall coefficient of heat transfer	W/m^{2}K	$\mathbf{MT}^{-3}\theta^{-1}$
u	gas velocity	m/s	$\mathbf{LT}^{-1}$
u'	mean linear growth velocity	m/s	$\mathbf{LT}^{-1}$
V'	volume of suspension of crystals	m^3	$\mathbf{L}^3$
V_L	volume of liquor in vessel	m^3	$\mathbf{L}^3$
V_W	volume of wash water	m^3	$\mathbf{L}^3$
v	molar volume	m^3/kmol	$\mathbf{N}^{-1}\mathbf{L}^3$
v'	maximum theoretical vaporisation rate	kg/m^{2}s	$\mathbf{ML}^{-2}\mathbf{T}^{-1}$
v_g	molar volume of gas	m^3/kmol	$\mathbf{N}^{-1}\mathbf{L}^3$
v_1	molar volume of liquid	m^3/kmol	$\mathbf{N}^{-1}\mathbf{L}^3$
v_s	molar volume of solid	m^3/kmol	$\mathbf{N}^{-1}\mathbf{L}^3$
w_1	initial mass of solvent in liquor	kg	**M**
w_2	final mass of solvent in liquor	kg	**M**
x	solute concentration in terms of mole fraction	—	—
x'	effective film thickness	m	**L**
x_c	amount of component **A** in crystallised solid	kg	**L**
y	yield of crystals	kg	**M**
y_c	amount of component **B** in crystallised solid	kg	**M**
z	kmol of gas produced by 1 kmol of electrolyte	—	—
z_1, z_2	functions in equation 15.6	1/K	$\boldsymbol{\theta}^{-1}$
α	shape factor in equation 15.16	—	—
β	shape factor in equation 15.16	—	—
ϕ	relative supersaturation	—	—
γ	ion activity coefficient	—	—
$\gamma\pm$	mean activity coefficient	—	—
φ	degree of supersaturation/equilibrium saturation	—	—
λ	latent heat of vaporisation of solvent	J/kg	$\mathbf{L}^2\mathbf{T}^{-2}$
λ_f	latent heat of fusion	J/kg	$\mathbf{L}^2\mathbf{T}^{-2}$
λ_s	latent heat of sublimation	J/kg	$\mathbf{L}^2\mathbf{T}^{-2}$
λ_v	latent heat of vaporisation per unit mass	J/kg	$\mathbf{L}^2\mathbf{T}^{-2}$

This book belongs to Bradley Loren (bloren@mcandrews-ip.com)
Copyright Elsevier 2024
Intas Exhibit 1032
Page 289 of 470
PGR2025-00043

		Units in SI System	Dimensions in **M**, **N**, **L**, **T**, $\boldsymbol{\theta}$
λ'_v	latent heat of vaporisation per mole	J/kmol	$\mathbf{MN}^{-1}\mathbf{L}^2\mathbf{T}^{-2}$
μ	fluid viscosity	Ns/m^2	$\mathbf{ML}^{-1}\mathbf{T}^{-1}$
ρ	density of crystal	kg/m^3	$\mathbf{ML}^{-3}$
ρ_g	density of inert gas	kg/m^3	$\mathbf{ML}^{-3}$
ρ_s	density of solid or sublimed material	kg/m^3	$\mathbf{ML}^{-3}$
ρ_v	density of vapour	kg/m^3	$\mathbf{ML}^{-3}$
σ	interfacial tension of crystallisation surface	J/m^2	$\mathbf{MT}^{-2}$

This book belongs to Bradley Loren (bloren@mcandrews-ip.com)

Copyright Elsevier 2024

Intas Exhibit 1032
Page 290 of 470
PGR2025-00043

CHAPTER 16

Drying

16.1. INTRODUCTION

The drying of materials is often the final operation in a manufacturing process, carried out immediately prior to packaging or dispatch. Drying refers to the final removal of water, or another solute, and the operation often follows evaporation, filtration, or crystallisation. In some cases, drying is an essential part of the manufacturing process, as for instance in paper making or in the seasoning of timber, although, in the majority of processing industries, drying is carried out for one or more of the following reasons:

(a) To reduce the cost of transport.
(b) To make a material more suitable for handling as, for example, with soap powders, dyestuffs and fertilisers.
(c) To provide definite properties, such as, for example, maintaining the free-flowing nature of salt.
(d) To remove moisture which may otherwise lead to corrosion. One example is the drying of gaseous fuels or benzene prior to chlorination.

With a crystalline product, it is essential that the crystals are not damaged during the drying process, and, in the case of pharmaceutical products, care must be taken to avoid contamination. Shrinkage, as with paper, cracking, as with wood, or loss of flavour, as with fruit, must also be prevented. With the exception of the partial drying of a material by squeezing in a press or the removal of water by adsorption, almost all drying processes involve the removal of water by vaporisation, which requires the addition of heat. In assessing the efficiency of a drying process, the effective utilisation of the heat supplied is the major consideration.

16.2. GENERAL PRINCIPLES

The moisture content of a material is usually expressed in terms of its water content as a percentage of the mass of the dry material, though moisture content is sometimes expressed on a wet basis, as in Example 16.3. If a material is exposed to air at a given temperature and humidity, the material will either lose or gain water until an equilibrium condition is established. This equilibrium moisture content varies widely with the moisture content and the temperature of the air, as shown in Figure 16.1. A non-porous insoluble solid, such as sand or china clay, has an equilibrium moisture content approaching zero

This book belongs to Bradley Loren (bloren@mcandrews-ip.com) Copyright Elsevier 2024

Intas Exhibit 1032
Page 291 of 470
PGR2025-00043

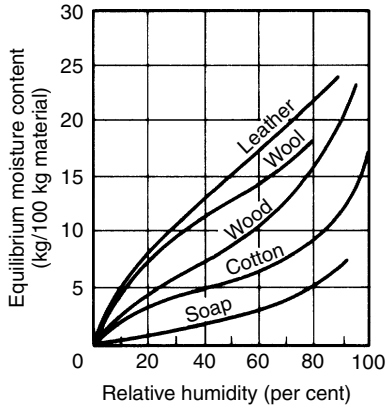


Figure 16.1. Equilibrium moisture content of a solid as a function of relative humidity at 293 K

for all humidities and temperatures, although many organic materials, such as wood, textiles, and leather, show wide variations of equilibrium moisture content. Moisture may be present in two forms:

Bound moisture. This is water retained so that it exerts a vapour pressure less than that of free water at the same temperature. Such water may be retained in small capillaries, adsorbed on surfaces, or as a solution in cell walls.

Free moisture. This is water which is in excess of the equilibrium moisture content.

The water removed by vaporisation is generally carried away by air or hot gases, and the ability of these gases to pick up the water is determined by their temperature and humidity. In designing dryers using air, the properties of the air–water system are essential, and these are detailed in Volume 1, Chapter 13, where the development of the humidity chart is described. For the *air–water system*, the following definitions are of importance:

Humidity $\mathscr{H}$, mass of water per unit mass of dry air.

Since:
$$\frac{\text{moles of water vapour}}{\text{moles of dry air}} = \frac{P_w}{(P - P_w)}$$

then:
$$\mathscr{H} = \frac{18P_w}{29(P - P_w)}$$

where P_w is the partial pressure of water vapour and P is the total pressure.

Humidity of saturated air $\mathscr{H}_0$. This is the humidity of air when it is saturated with water vapour. The air then is in equilibrium with water at the given temperature and pressure.

Percentage humidity

$$= \frac{\text{Humidity of air}}{\text{Humidity of saturated air}} \times 100 = \frac{\mathscr{H}}{\mathscr{H}_0} \times 100$$

This book belongs to Bradley Loren (bloren@mcandrews-ip.com) Copyright Elsevier 2024

Intas Exhibit 1032
Page 292 of 470
PGR2025-00043

Percentage relative humidity, $\mathscr{R}$

$$= \frac{\text{Partial pressure of water vapour in air}}{\text{Vapour pressure of water at the same temperature}} \times 100$$

The distinction between *percentage humidity* and *percentage relative humidity* is of significance though, the difference in the values of the two quantities does not usually exceed 7 to 8 per cent. Reference may be made here to Volume 1, Section 13.2.1.

Humid volume, is the volume of unit mass of dry air and its associated vapour. Then, under ideal conditions, at atmospheric pressure:

$$\text{humid volume} = \frac{22.4}{29}\left(\frac{T}{273}\right) + \frac{22.4\mathscr{H}}{18}\left(\frac{T}{273}\right) \text{ m}^3/\text{kg}$$

where T is in degrees K,

or :

$$\frac{359}{29}\left(\frac{T}{492}\right) + \frac{359\mathscr{H}}{18}\left(\frac{T}{492}\right) \text{ ft}^3/\text{lb}$$

where T is in degrees Rankine.

Saturated volume is the volume of unit mass of dry air, together with the water vapour required to saturate it.

Humid heat is the heat required to raise unit mass of dry air and associated vapour through 1 degree K at constant pressure or $1.00 + 1.88\mathscr{H}$ kJ/kg K.

Dew point is the temperature at which condensation will first occur when air is cooled.

Wet bulb temperature. If a stream of air is passed rapidly over a water surface, vaporisation occurs, provided the temperature of the water is above the dew point of the air. The temperature of the water falls and heat flows from the air to the water. If the surface is sufficiently small for the condition of the air to change inappreciably and if the velocity is in excess of about 5 m/s, the water reaches the wet bulb temperature θ_w at equilibrium.

The rate of heat transfer from gas to liquid is given by:

$$Q = hA(\theta - \theta_w) \tag{16.1}$$

The mass rate of vaporisation is given by:

$$\begin{aligned} G_v &= \frac{h_D A M_w}{\mathbf{R}T}(P_{w0} - P_w) \\ &= \frac{h_D A M_A}{\mathbf{R}T}[(P - P_w)_{\text{mean}}(\mathscr{H}_w - \mathscr{H})] \\ &= h_D A \rho_A (\mathscr{H}_w - \mathscr{H}) \end{aligned} \tag{16.2}$$

The rate of heat transfer required to effect vaporisation at this rate is given by:

$$G_v = h_D A \rho_A (\mathscr{H}_w - \mathscr{H})\lambda \tag{16.3}$$

This book belongs to Bradley Loren (bloren@mcandrews-ip.com) Copyright Elsevier 2024

Intas Exhibit 1032
Page 293 of 470
PGR2025-00043

At equilibrium, the rates of heat transfer given by equations 16.1 and 16.3 must be equal, and hence:

$$\mathscr{H} - \mathscr{H}_w = -\frac{h}{h_D \rho_A \lambda}(\theta - \theta_w) \tag{16.4}$$

In this way, it is seen that the wet bulb temperature θ_w depends only on the temperature and humidity of the drying air.

In these equations:

h is the heat transfer coefficient,
h_D is the mass transfer coefficient,
A is the surface area,
θ is the temperature of the air stream,
θ_w is the wet bulb temperature,
P_{w0} is the vapour pressure of water at temperature θ_w,
M_A is the molecular weight of air,
M_w is the molecular weight of water,
$\mathbf{R}$ is the universal gas constant,
T is the absolute temperature,
$\mathscr{H}$ is the humidity of the gas stream,
$\mathscr{H}_w$ is the humidity of saturated air at temperature θ_w,
ρ_A is the density of air at its mean partial pressure, and
λ is the latent heat of vaporisation of unit mass of water.

Equation 16.4 is identical with equation 13.8 in Volume 1, and reference may be made to that chapter for a more detailed discussion.

16.3. RATE OF DRYING

16.3.1. Drying periods

In drying, it is necessary to remove free moisture from the surface and also moisture from the interior of the material. If the change in moisture content for a material is determined as a function of time, a smooth curve is obtained from which the rate of drying at any given moisture content may be evaluated. The form of the drying rate curve varies with the structure and type of material, and two typical curves are shown in Figure 16.2. In curve 1, there are two well-defined zones: AB, where the rate of drying is constant and BC, where there is a steady fall in the rate of drying as the moisture content is reduced. The moisture content at the end of the constant rate period is represented by point B, and this is known as the *critical moisture content*. Curve 2 shows three stages, DE, EF and FC. The stage DE represents a constant rate period, and EF and FC are falling rate periods. In this case, the Section EF is a straight line, however, and only the portion FC is curved. Section EF is known as the first falling rate period and the final stage, shown as FC, as the second falling rate period. The drying of soap gives rise to a curve of type 1, and sand to a curve of type 2. A number of workers, including SHERWOOD[1] and NEWITT and co-workers[2–7], have contributed various theories on the rate of drying at these various stages.

This book belongs to Bradley Loren (bloren@mcandrews-ip.com) Copyright Elsevier 2024

Intas Exhibit 1032
Page 294 of 470
PGR2025-00043

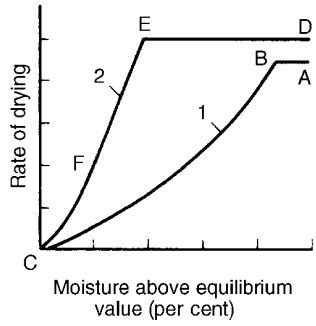


Figure 16.2. Rate of drying of a granular material

Constant rate period

During the constant rate period, it is assumed that drying takes place from a saturated surface of the material by diffusion of the water vapour through a stationary air film into the air stream. GILLILAND[8] has shown that the rates of drying of a variety of materials in this stage are substantially the same as shown in Table 16.1.

Table 16.1. Evaporation rates for various materials under constant conditions[8]

Material	Rate of evaporation	
	(kg/m^2 h)	(kg/m^2 s)
Water	2.7	0.00075
Whiting pigment	2.1	0.00058
Brass filings	2.4	0.00067
Brass turnings	2.4	0.00067
Sand (fine)	2.0–2.4	0.00055–0.00067
Clays	2.3–2.7	0.00064–0.00075

In order to calculate the rate of drying under these conditions, the relationships obtained in Volume 1 for diffusion of a vapour from a liquid surface into a gas may be used. The simplest equation of this type is:

$$W = k_G A(P_s - P_w) \tag{16.5}$$

where k_G is the mass transfer coefficient.

Since the rate of transfer depends on the velocity u of the air stream, raised to a power of about 0.8, then the mass rate of evaporation is:

$$W = k_G A(P_s - P_w)u^{0.8} \tag{16.6}$$

where: A is the surface area,
P_s is the vapour pressure of the water, and
P_w is the partial pressure of water vapour in the air stream.

This book belongs to Bradley Loren (bloren@mcandrews-ip.com) Copyright Elsevier 2024
Intas Exhibit 1032
Page 295 of 470
PGR2025-00043

This type of equation, used in Volume 1 for the rate of vaporisation into an air stream, simply states that the rate of transfer is equal to the transfer coefficient multiplied by the driving force. It may be noted, however, that $(P_s - P_w)$ is not only a driving force, but it is also related to the capacity of the air stream to absorb moisture.

These equations suggest that the rate of drying is independent of the geometrical shape of the surface. Work by POWELL and GRIFFITHS[9] has shown, however, that the ratio of the length to the width of the surface is of some importance, and that the evaporation rate is given more accurately as:

(a) For values of $u = 1–3$ m/s:

$$W = 5.53 \times 10^{-9} L^{0.77} B(P_s - P_w)(1 + 61u^{0.85}) \text{ kg/s} \tag{16.7}$$

(b) For values of $u < 1$ m/s:

$$W = 3.72 \times 10^{-9} L^{0.73} B^{0.8}(P_s - P_w)(1 + 61u^{0.85}) \text{ kg/s} \tag{16.8}$$

where: P_s, the saturation pressure at the temperature of the surface (N/m^2),
P_w, the vapour pressure in the air stream (N/m^2), and
L and B are the length and width of the surface, respectively (m).

For most design purposes, it may be assumed that the rate of drying is proportional to the transfer coefficient multiplied by $(P_s - P_w)$. CHAKRAVORTY[10] has shown that, if the temperature of the surface is greater than that of the air stream, then P_w may easily reach a value corresponding to saturation of the air. Under these conditions, the capacity of the air to take up moisture is zero, while the force causing evaporation is $(P_s - P_w)$. As a result, a mist will form and water may be redeposited on the surface. In all drying equipment, care must therefore be taken to ensure that the air or gas used does not become saturated with moisture at any stage.

The rate of drying in the constant rate period is given by:

$$W = \frac{\mathrm{d}w}{\mathrm{d}t} = \frac{hA\Delta T}{\lambda} = k_G A(P_s - P_w) \tag{16.9}$$

where: W is the rate of loss of water,
h is the heat transfer coefficient from air to the wet surface,
ΔT is the temperature difference between the air and the surface,
λ is the latent heat of vaporisation per unit mass,
k_G is the mass transfer coefficient for diffusion from the wet surface through the gas film,
A is the area of interface for heat and mass transfer, and
$(P_s - P_w)$ is the difference between the vapour pressure of water at the surface and the partial pressure in the air.

This book belongs to Bradley Loren (bloren@mcandrews-ip.com) Copyright Elsevier 2024

Intas Exhibit 1032
Page 296 of 470
PGR2025-00043

It is more convenient to express the mass transfer coefficient in terms of a humidity difference, so that $k_G A(P_s - P_w) \simeq kA(\mathscr{H}_s - \mathscr{H})$. The rate of drying is thus determined by the values of h, ΔT and A, and is not influenced by the conditions inside the solid. h depends on the air velocity and the direction of flow of the air, and it has been found that $h = CG'^{0.8}$ where G' is the mass rate of flow of air in kg/s m^2. For air flowing parallel to plane surfaces, SHEPHERD *et al.*[11] have given the value of C as 14.5 where the heat transfer coefficient is expressed in W/m^2 K.

If the gas temperature is high, then a considerable proportion of the heat will pass to the solid by radiation, and the heat transfer coefficient will increase. This may result in the temperature of the solid rising above the wet bulb temperature.

First falling-rate period

The points B and E in Figure 16.2 represent conditions where the surface is no longer capable of supplying sufficient free moisture to saturate the air in contact with it. Under these conditions, the rate of drying depends very much on the mechanism by which the moisture from inside the material is transferred to the surface. In general, the curves in Figure 16.2 will apply, although for a type 1 solid, a simplified expression for the rate of drying in this period may be obtained.

Second falling-rate period

At the conclusion of the first falling rate period it may be assumed that the surface is dry and that the plane of separation has moved into the solid. In this case, evaporation takes place from within the solid and the vapour reaches the surface by molecular diffusion through the material. The forces controlling the vapour diffusion determine the final rate of drying, and these are largely independent of the conditions outside the material.

16.3.2. Time for drying

If a material is dried by passing hot air over a surface which is initially wet, the rate of drying curve in its simplest form is represented by BCE, shown in Figure 16.3

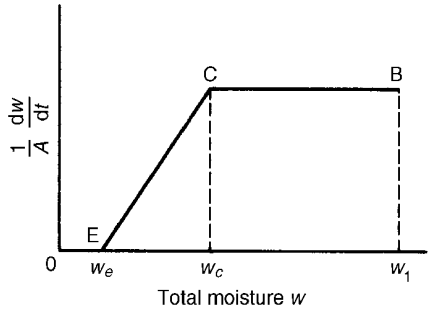


Figure 16.3. The use of a rate of drying curve in estimating the time for drying

This book belongs to Bradley Loren (bloren@mcandrews-ip.com) Copyright Elsevier 2024
Intas Exhibit 1032
Page 297 of 470
PGR2025-00043

where: w is the total moisture,
w_e is the equilibrium moisture content (point E),
$w - w_e$ is the free moisture content, and
w_c is the critical moisture content (point C).

Constant-rate period

During the period of drying from the initial moisture content w_1 to the critical moisture content w_c, the rate of drying is constant, and the time of drying t_c is given by:

$$t_c = \frac{w_1 - w_c}{R_c A} \tag{16.10}$$

where: R_c is the rate of drying per unit area in the constant rate period, and
A is the area of exposed surface.

Falling-rate period

During this period the rate of drying is, approximately, directly proportional to the free moisture content $(w - w_e)$, or:

$$-\left(\frac{1}{A}\right)\frac{\mathrm{d}w}{\mathrm{d}t} = m(w - w_e) = mf \quad \text{(say)} \tag{16.11}$$

Thus:
$$-\frac{1}{mA}\int_{w_e}^{w}\frac{\mathrm{d}w}{(w - w_e)} = \int_0^{t_f}\mathrm{d}t$$

or:
$$\frac{1}{mA}\ln\left[\frac{w_c - w_e}{w - w_e}\right] = t_f$$

and:
$$t_f = \frac{1}{mA}\ln\left(\frac{f_c}{f}\right) \tag{16.12}$$

Total time of drying

The total time t of drying from w_1 to w is given by $t = (t_c + t_f)$.

The rate of drying R_c over the constant rate period is equal to the initial rate of drying in the falling rate period, so that $R_c = mf_c$.

Thus:
$$t_c = \frac{(w_1 - w_c)}{mAf_c} \tag{16.13}$$

and the total drying time,
$$t = \frac{(w_1 - w_c)}{mAf_c} + \frac{1}{mA}\ln\left(\frac{f_c}{f}\right)$$
$$= \frac{1}{mA}\left[\frac{(f_1 - f_c)}{f_c} + \ln\left(\frac{f_c}{f}\right)\right] \tag{16.14}$$

This book belongs to Bradley Loren (bloren@mcandrews-ip.com) Copyright Elsevier 2024

Intas Exhibit 1032
Page 298 of 470
PGR2025-00043

Example 16.1

A wet solid is dried from 25 to 10 per cent moisture under constant drying conditions in 15 ks (4.17 h). If the critical and the equilibrium moisture contents are 15 and 5 per cent respectively, how long will it take to dry the solid from 30 to 8 per cent moisture under the same conditions?

Solution

For the first drying operation:

$$w_1 = 0.25 \text{ kg/kg}, w = 0.10 \text{ kg/kg}, w_c = 0.15 \text{ kg/kg and } w_e = 0.05 \text{ kg/kg}$$

Thus: $f_1 = (w_1 - w_e) = (0.25 - 0.05) = 0.20$ kg/kg

$$f_c = (w_c - w_e) = (0.15 - 0.05) = 0.10 \text{ kg/kg}$$

$$f = (w - w_e) = (0.10 - 0.05) = 0.05 \text{ kg/kg}$$

From equation 16.14, the total drying time is:

$$t = (1/mA)[(f_1 - f_c)/f_c + \ln(f_c/f)]$$

or: $$15 = (1/mA)[(0.20 - 0.10)/0.10 + \ln(0.10/0.05)]$$

and: $$mA = 0.0667(1.0 + 0.693) = 0.113 \text{ kg/s}$$

For the second drying operation:

$$w_1 = 0.30 \text{ kg/kg}, w = 0.08 \text{ kg/kg}, w_c = 0.15 \text{ kg/kg and } w_e = 0.05 \text{ kg/kg}$$

Thus: $f_1 = (w_1 - w_e) = (0.30 - 0.05) = 0.25$ kg/kg

$$f_c = (w_c - w_e) = (0.15 - 0.05) = 0.10 \text{ kg/kg}$$

$$f = (w - w_e) = (0.08 - 0.05) = 0.03 \text{ kg/kg}$$

The total drying time is then:

$$t = (1/0.113)[(0.25 - 0.10)/0.10 + \ln(0.10/0.03)]$$
$$= 8.856(1.5 + 1.204)$$
$$= \underline{23.9 \text{ ks } (6.65 \text{ h})}$$

Example 16.2

Strips of material 10 mm thick are dried under constant drying conditions from 28 to 13 per cent moisture in 25 ks (7 h). If the equilibrium moisture content is 7 per cent, what is the time taken to dry 60 mm planks from 22 to 10 per cent moisture under the same conditions assuming no loss from the edges? All moistures are given on a wet basis.

The relation between E, the ratio of the average free moisture content at time t to the initial free moisture content, and the parameter J is given by:

E	1	0.64	0.49	0.38	0.295	0.22	0.14
J	0	0.1	0.2	0.3	0.5	0.6	0.7

This book belongs to Bradley Loren (bloren@mcandrews-ip.com) Copyright Elsevier 2024

Intas Exhibit 1032
Page 299 of 470
PGR2025-00043

It may be noted that $J = kt/l^2$, where k is a constant, t the time in ks and $2l$ the thickness of the sheet of material in millimetres.

Solution

For the 10 mm strips

Initial free moisture content $= (0.28 - 0.07) = 0.21$ kg/kg.

Final free moisture content $= (0.13 - 0.07) = 0.06$ kg/kg.

Thus: when $t = 25$ ks, $E = (0.06/0.21) = 0.286$

and from Figure 16.4, a plot of the given data,

$$J = 0.52$$

Thus: $$0.52 = (k \times 25)/(10/2)^2$$

and: $$k = 0.52$$

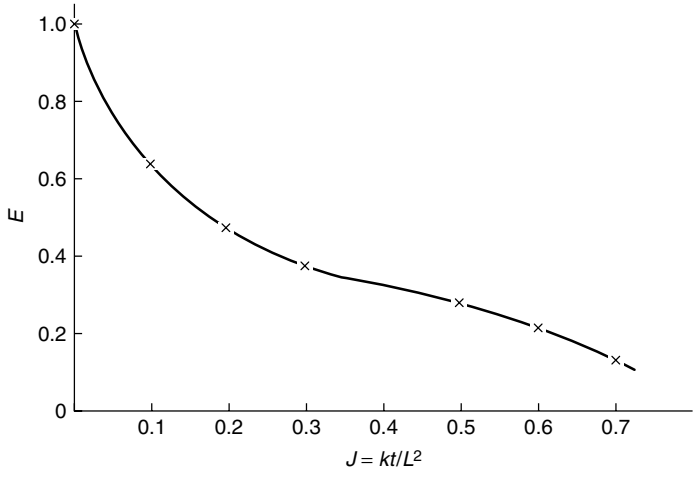


Figure 16.4. Drying data for Example 6.2

For the 60 mm planks

Initial free moisture content $= (0.22 - 0.07) = 0.15$ kg/kg.

Final free moisture content $= (0.10 - 0.07) = 0.03$ kg/kg.

$$E = (0.03/0.15) = 0.20$$

From Figure 16.4: $J = 0.63$

and hence: $t = Jl^2/k$

$= 0.63(60/2)^2/0.52 = \underline{\underline{1090 \text{ ks}}}$ (12.6 days)

This book belongs to Bradley Loren (bloren@mcandrews-ip.com) Copyright Elsevier 2024

Intas Exhibit 1032
Page 300 of 470
PGR2025-00043

Example 16.3

A granular material containing 40 per cent moisture is fed to a countercurrent rotary dryer at a temperature of 295 K and is withdrawn at 305 K, containing 5 per cent moisture. The air supplied, which contains 0.006 kg water vapour/kg dry air, enters at 385 K and leaves at 310 K. The dryer handles 0.125 kg/s wet stock.

Assuming that radiation losses amount to 20 kJ/kg dry air used, determine the mass flowrate of dry air supplied to the dryer and the humidity of the exit air.

The latent heat of water vapour at 295 K = 2449 kJ/kg, specific heat capacity of dried material = 0.88 kJ/kg K, the specific heat capacity of dry air = 1.00 kJ/kg K, and the specific heat capacity of water vapour = 2.01 kJ/kg K.

Solution

This example involves a heat balance over the system. 273 K will be chosen as the datum temperature, and it will be assumed that the flowrate of dry air = G kg/s.

Heat in:

(a) *Air*

G kg/s dry air enter with $0.006G$ kg/s water vapour and hence the heat content of this stream

$$= [(1.00G) + (0.006G \times 2.01)](385 - 273) = 113.35G \text{ kW}$$

(b) *Wet solid*

0.125 kg/s enter containing 0.40 kg water/kg wet solid, assuming the moisture is expressed on a wet basis.

Thus: $$\text{mass flowrate of water} = (0.125 \times 0.40) = 0.050 \text{ kg/s}$$

and: $$\text{mass flowrate of dry solid} = (0.125 - 0.050) = 0.075 \text{ kg/s}$$

Hence:

the heat content of this stream $= [(0.050 \times 4.18) + (0.075 \times 0.88)](295 - 273) = 6.05$ kW

Heat out:

(a) *Air*

Heat in exit air $= [(1.00\ G) + (0.006\ G \times 2.01)](310 - 273) = 37.45G$ kW.

Mass flowrate of dry solids = 0.075 kg/s containing 0.05 kg water/kg wet solids.

Hence:

$$\text{water in the dried solids leaving} = (0.05 \times 0.075)/(1 + 0.05) = 0.0036 \text{ kg/s}$$

and:

$$\text{the water evaporated into gas steam} = (0.050 - 0.0036) = 0.0464 \text{ kg/s}.$$

Assuming evaporation takes place at 295 K, then:

$$\text{heat in the water vapour} = 0.0464[2.01(310 - 295) + 2449 + 4.18(295 - 273)]$$
$$= 119.3 \text{ kW}$$

This book belongs to Bradley Loren (bloren@mcandrews-ip.com) Copyright Elsevier 2024

Intas Exhibit 1032
Page 301 of 470
PGR2025-00043

and:

$$\text{the total heat in this stream} = (119.30 + 37.45G) \text{ kW}.$$

(b) *Dried solids*

The dried solids contain 0.0036 kg/s water and hence heat content of this stream is:

$$= [(0.075 \times 0.88) + (0.0036 \times 4.18)/(305 - 273)] = 2.59 \text{ kW}$$

(c) *Losses*

These amount to 20 kJ/kg dry air or $20m$ kW.

Heat balance

$$(113.35\ G + 6.05) = (119.30 + 37.45\ G + 2.59 + 20\ G)$$

and:

$$G = \underline{\underline{2.07 \text{ kg/s}}}$$

$$\text{Water in the outlet air stream} = (0.006 \times 2.07) + 0.0464 = 0.0588 \text{ kg/s}$$

and:

$$\text{the humidity } \mathscr{H} = (0.0588/2.07) = \underline{\underline{0.0284 \text{ kg/kg dry air}}}$$

16.4. THE MECHANISM OF MOISTURE MOVEMENT DURING DRYING

16.4.1. Diffusion theory of drying

In the general form of the curve for the rate of drying of a solid shown in Figure 16.2, there are two and sometimes three distinct sections. During the constant-rate period, moisture vaporises into the air stream and the controlling factor is the transfer coefficient for diffusion across the gas film. It is important to understand how the moisture moves to the drying surface during the falling-rate period, and two models have been used to describe the physical nature of this process, the diffusion theory and the capillary theory. In the diffusion theory, the rate of movement of water to the air interface is governed by rate equations similar to those for heat transfer, whilst in the capillary theory the forces controlling the movement of water are capillary in origin, arising from the minute pore spaces between the individual particles.

Falling rate period, diffusion control

In the falling-rate period, the surface is no longer completely wetted and the rate of drying steadily falls. In the previous analysis, it has been assumed that the rate of drying per unit effective wetted area is a linear function of the water content, so that the rate of drying is given by:

$$\left(\frac{1}{A}\right)\frac{\mathrm{d}w}{\mathrm{d}t} = -m(w - w_e) \qquad \text{(equation 16.11)}$$

In many cases, however, the rate of drying is governed by the rate of internal movement of the moisture to the surface. It was initially assumed that this movement was a process

This book belongs to Bradley Loren (bloren@mcandrews-ip.com) Copyright Elsevier 2024

Intas Exhibit 1032
Page 302 of 470
PGR2025-00043

of diffusion and would follow the same laws as heat transfer. This approach has been examined by a number of workers, and in particular by SHERWOOD[12] and NEWMAN[13].

Considering a slab with the edges coated to prevent evaporation, which is dried by evaporation from two opposite faces, the Y-direction being taken perpendicular to the drying face, the central plane being taken as $y = 0$, and the slab thickness $2l$, then on drying, the moisture movement by diffusion will be in the Y-direction, and hence from Volume 1, equation 10.66:

$$\frac{\partial C_w}{\partial t} = D_L \frac{\partial^2 C_w}{\partial y^2}$$

where C_w is the concentration of water at any point and any time in the solid, and D_L is the coefficient of diffusion for the liquid.

If w is the liquid content of the solid, integrated over the whole depth, w_1 the initial content, and w_e the equilibrium content, then:

$$\frac{(w - w_e)}{(w_1 - w_e)} = \frac{\text{Free liquid content at any time}}{\text{Initial free liquid content}}$$

SHERWOOD[12] and NEWMAN[13] have presented the following solution assuming an initially uniform water distribution and zero water-concentration at the surface once drying has started:

$$\frac{(w - w_e)}{(w_1 - w_e)} = \frac{8}{\pi^2}\left\{e^{-D_L t(\pi/2l)^2} + \frac{1}{9}e^{-9D_L t(\pi/2l)^2} + \frac{1}{25}e^{-25D_L t(\pi/2l)^2} + \cdots\right\} \quad (16.15)$$

This equation assumes an initially uniform distribution of moisture, and that the drying is from both surfaces. When drying is from one surface only, then l is the total thickness. If the time of drying is long, then only the first term of the equation need be used and thus, differentiating equation 16.15 gives:

$$\frac{dw}{dt} = -\frac{2D_L}{l^2}\, e^{-\frac{D_L t\pi^2}{4l^2}}(w_1 - w_e) \quad (16.16)$$

In the drying of materials such as wood or clay, the moisture concentration at the end of the constant rate period is not uniform, and is more nearly parabolic. Sherwood has presented an analysis for this case, and has given experimental values for the drying of brick clay.

In this case, it is assumed that the rate of movement of water is proportional to a concentration gradient, and capillary and gravitational forces are neglected. Water may, however, flow from regions of low concentration to those of high concentration if the pore sizes are suitable, and for this and other reasons, CEAGLSKE and HOUGEN[14,15] have proposed a capillary theory which is now considered.

16.4.2. Capillary theory of drying

Principles of the theory

The capillary theory of drying has been proposed in order to explain the movement of moisture in the bed during surface drying. The basic importance of the pore space between

This book belongs to Bradley Loren (bloren@mcandrews-ip.com) Copyright Elsevier 2024

Intas Exhibit 1032
Page 303 of 470
PGR2025-00043

granular particles was first pointed out by SLICHTER[16] in connection with the movement of moisture in soils, and this work has been modified and considerably expanded by HAINES[17]. The principles are now outlined and applied to the problem of drying. Considering a systematic packing of uniform spherical particles, these may be arranged in six different regular ways, ranging from the most open to the closest packing. In the former, the spheres are arranged as if at the corners of a cube with each sphere touching six others. In the latter arrangement, each sphere rests in the hollow of three spheres in adjacent layers, and touches twelve other spheres. These configurations are shown in Figure 16.5. The densities of packing of the other four arrangements will lie between those illustrated.

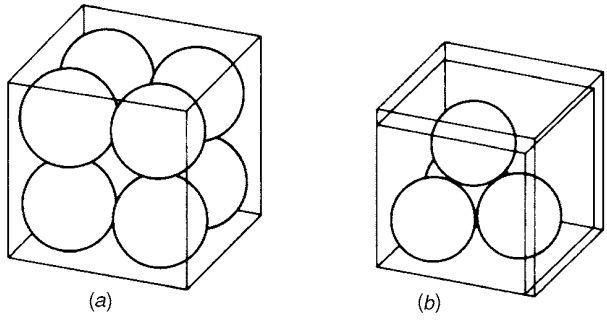


Figure 16.5. Packing of spherical particles. (*a*) Cubic arrangement, one sphere touching six others. (*b*) Rhombohedral packing, one sphere touching twelve others, with layers arranged in rhombic formation

In each case, a regular group of spheres surrounds a space which is called a pore, and the bed is made up of a series of these elemental groupings. The pores are connected together by passages of various sizes, the smallest portions of which are known as *waists*. The size of a pore is defined as the diameter of the largest sphere which can be fitted into it, and the size of a waist as the diameter of the inscribed circle. The sizes of the pores and waists will differ for each form of packing, as shown in Table 16.2.

Table 16.2. Properties of packing of spheres of radius r

Packing arrangement	Pore space (per cent total volume)	Radius of pore	Radius of waist	Value of x in equation 16.20 for:	
				limiting suction potential of pores	entry suction potential of waists
Cubical	47.64	$0.700r$	$0.414r$	2.86	4.82
Rhombohedral	25.95	$0.288r$	$0.155r$	6.90	12.90

The continuous variation in the diameter of each passage is the essential difference between a granular packing and a series of capillary tubes. If a clean capillary of uniform

This book belongs to Bradley Loren (bloren@mcandrews-ip.com) Copyright Elsevier 2024
Intas Exhibit 1032
Page 304 of 470
PGR2025-00043

diameter $2r'$ is placed in a liquid, the level will rise in the capillary to a height h_s given by:

$$h_s = \left(\frac{2\sigma}{r'\rho g}\right)\cos\alpha \tag{16.17}$$

where: ρ is the density of the liquid,
σ is the surface tension, and
α is the angle of contact.

A negative pressure, known as a *suction potential*, will exist in the liquid in the capillary. Immediately below the meniscus, the suction potential will be equivalent to the height of the liquid column h_s and, if water is used, this will have the value:

$$h_s = \frac{2\sigma}{r'\rho g} \tag{16.18}$$

If equilibrium conditions exist, the suction potential h_1 at any other level in the liquid, a distance z_1 below the meniscus, will be given by:

$$h_s = h_1 + z_1 \tag{16.19}$$

Similarly, if a uniform capillary is filled to a height greater than h_s, as given by equation 16.17, and its lower end is immersed, the liquid column will recede to this height.

The non-uniform passages in a porous material will also display the same characteristics as a uniform capillary, with the important difference that the rise of water in the passages will be limited by the pore size, whilst the depletion of saturated passages will be controlled by the size of the waists. The height of rise is controlled by the pore size, since this approximates to the largest section of a varying capillary, whilst the depletion of water is controlled by the narrow waists which are capable of a higher suction potential than the pores.

The theoretical suction potential of a pore or waist containing water is given by:

$$h_t = \frac{x\sigma}{r\rho g} \tag{16.20}$$

where: x is a factor depending on the type of packing, shown in Table 16.2, and
r is the radius of the spheres.

For an idealised bed of uniform rhombohedrally packed spheres of radius r, for example, the waists are of radius $0.155r$, from Table 16.2, and the maximum theoretical suction potential of which such a waist is capable is:

$$\frac{2\sigma}{0.155r\rho g} = \frac{12.9\sigma}{r\rho g}$$

from which $x = 12.9$.

The maximum suction potential that can be developed by a waist is known as the *entry suction potential*. This is the controlling potential required to open a saturated

This book belongs to Bradley Loren (bloren@mcandrews-ip.com) Copyright Elsevier 2024

Intas Exhibit 1032
Page 305 of 470
PGR2025-00043

pore protected by a meniscus in an adjoining waist and some values for x are given in Table 16.2.

When a bed is composed of granular material with particles of mixed sizes, the suction potential cannot be calculated and it must be measured by methods such as those given by HAINES[17] and OLIVER and NEWITT[3].

Drying of a granular material according to the capillary theory

If a bed of uniform spheres, initially saturated, is to be surface dried in a current of air of constant temperature, velocity and humidity, then the rate of drying is given by:

$$\frac{\mathrm{d}w}{\mathrm{d}t} = k_G A(P_{w0} - P_w) \tag{16.21}$$

where P_{w0} is the saturation partial pressure of water vapour at the wet bulb temperature of the air, and P_w is the partial pressure of the water vapour in the air stream. This rate of drying will remain constant so long as the inner surface of the "stationary" air film remains saturated.

As evaporation proceeds, the water surface recedes into the waists between the top layer of particles, and an increasing suction potential is developed in the liquid. When the menisci on the cubical waists, that is the largest, have receded to the narrowest section, the suction potential h_s at the surface is equal to $4.82\sigma/r\rho g$, from Table 16.2. Further evaporation will result in h_s increasing so that the menisci on the surface cubical waists will collapse, and the larger pores below will open. As h_s steadily increases, the entry suction of progressively finer surface waists is reached, so that the menisci collapse into the adjacent pores which are thereby opened.

In considering the conditions below the surface, the suction potential h_1 a distance z_1 from the surface is given by:

$$h_s = h_1 + z_1 \qquad \text{(equation 16.19)}$$

The flow of water through waists surrounding an open pore is governed by the size of the waist as follows:

(a) If the size of the waist is such that its entry suction potential exceeds the suction potential at that level within the bed, it will remain full by the establishment of a meniscus therein, in equilibrium with the effective suction potential to which it is subjected. This waist will then protect adjoining full pores which cannot be opened until one of the waists to which it is connected collapses.
(b) If the size of the waist is such that its entry suction potential is less than the suction potential existing at that level, it will in turn collapse and open the adjoining pore. In addition, this successive collapse of pores and waists will progressively continue so long as the pores so opened expose waists having entry suction potentials of less than the suction potentials existing at that depth.

As drying proceeds, two processes take place simultaneously:

(a) The collapse of progressively finer surface waists, and the resulting opening of pores and waists connected to them, which they previously protected, and

This book belongs to Bradley Loren (bloren@mcandrews-ip.com) Copyright Elsevier 2024

Intas Exhibit 1032
Page 306 of 470
PGR2025-00043

(b) The collapse of further full waists within the bed adjoining opened pores, and the consequent opening of adjacent pores.

Even though the effective suction potential at a waist or pore within the bed may be in excess of its entry or limiting suction potential, this will not necessarily collapse or open. Such a waist can only collapse if it adjoins an opened pore, and the pore in question can only open upon the collapse of an adjoining waist.

Effect of particle size. Reducing the particle size in the bed will reduce the size of the pores and the waists, and will increase the entry suction potential of the waists. This increase means that the percentage variation in suction potentials with depth is reduced, and the moisture distribution is more uniform with small particles.

As the pore sizes are reduced, the frictional forces opposing the movement of water through these pores and waists may become significant, so that equation 16.19 is more accurately represented by:

$$h_s = h_1 + z_1 + h_f \tag{16.22}$$

where h_f, the frictional head opposing the flow over a depth z_1 from the surface, will depend on the particle size. It has been found[2] that, with coarse particles when only low suction potentials are found, the gravity effect is important though h_f is small, whilst with fine particles h_f becomes large.

(a) For particles of 0.1–1 mm radius, the values of h_1 are independent of the rate of drying, and vary appreciably with depth. Frictional forces are, therefore, negligible whilst capillary and gravitational forces are in equilibrium throughout the bed and are the controlling forces. Under such circumstances the percentage moisture loss at the critical point at which the constant rate period ends is independent of the drying rate, and varies with the depth of bed.
(b) For particles of 0.001–0.01 mm radius, the values of h_1 vary only slightly with rate of drying and depth, indicating that both gravitational and frictional forces are negligible whilst capillary forces are controlling. The critical point here will be independent of drying rate and depth of bed.
(c) For particles of less than 0.001 mm (1 μm) radius, gravitational forces are negligible, whilst frictional forces are of increasing importance and capillary and frictional forces may then be controlling. In such circumstances, the percentage moisture loss at the critical point diminishes with increased rate of drying and depth of bed. With beds of very fine particles an additional factor comes into play. The very high suction potentials which are developed cause a sufficient reduction of the pressure for vaporisation of water to take place inside the bed. This internal vaporisation results in a breaking up of the continuous liquid phase and a consequent interruption in the free flow of liquid by capillary action. Hence, the rate of drying is still further reduced.

Some of the experimental data of Newitt *et al.*[2] are illustrated in Figure 16.6.

Freeze drying

Special considerations apply to the movement of moisture in freeze drying. Since the water is frozen, liquid flow under capillary action is impossible, and movement must be

This book belongs to Bradley Loren (bloren@mcandrews-ip.com) Copyright Elsevier 2024

Intas Exhibit 1032
Page 307 of 470
PGR2025-00043

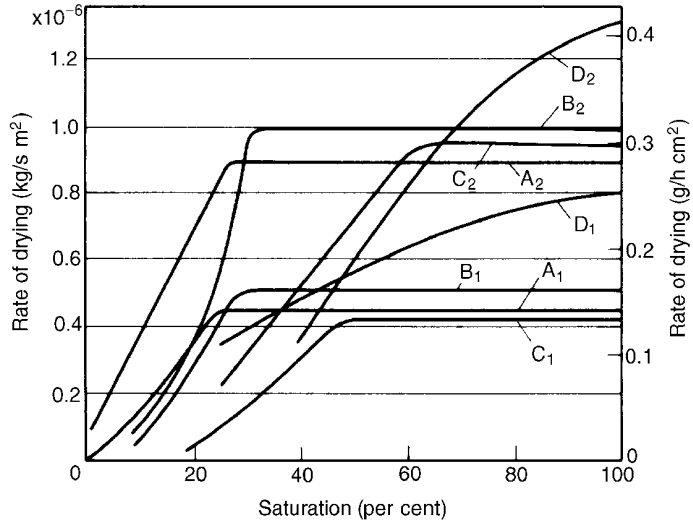


Figure 16.6. Rates of drying of various materials as a function of percentage saturation. A–60 μm glass spheres, bed 51 mm deep. B–23.5 μm silica flour, bed 51 mm deep. C–7.5 μm silica flour, bed 51 mm deep. D–2.5 μm silica flour, bed 65 mm deep. Subscripts: 1. Low drying rate 2. High drying rate

by vapour diffusion, analogous to the "second falling rate period" of the normal case. In addition, at very low pressures the mean free path of the water molecules may be comparable with the pore size of the material. In these circumstances the flow is said to be of the 'Knudsen' type, referred to in Volume 1, Section 10.1.

16.5. DRYING EQUIPMENT

16.5.1. Classification and selection of dryers

Because of the very wide range of dryer designs available, classification is a virtually impossible task. PARKER[18] takes into account, however, the means by which material is transferred through the dryer as a basis of his classification, with a view to presenting a guide to the selection of dryers. Probably the most thorough classification of dryer types has been made by KRÖLL[19] who has presented a decimalised system based on the following factors:

(a) Temperature and pressure in the dryer,
(b) The method of heating,
(c) The means by which moist material is transported through the dryer,
(d) Any mechanical aids aimed at improving drying,
(e) The method by which the air is circulated,
(f) The way in which the moist material is supported,
(g) The heating medium, and
(h) The nature of the wet feed and the way it is introduced into the dryer.

This book belongs to Bradley Loren (bloren@mcandrews-ip.com) Copyright Elsevier 2024
Intas Exhibit 1032
Page 308 of 470
PGR2025-00043

In selecting a dryer for a particular application, as SLOAN[20] has pointed out, two steps are of primary importance:

(a) A listing of the dryers which are capable of handling the material to be dried,
(b) Eliminating the more costly alternatives on the basis of annual costs, capital charges + operating costs. A summary of dryer types, together with cost data, has been presented by BACKHURST and HARKER[21] and the whole question of dryer selection is discussed further in Volume 6.

Once a group of possible dryers has been selected, the choice may be narrowed by deciding whether batch or continuous operation is to be employed and, in addition to restraints imposed by the nature of the material, whether heating by contact with a solid surface or directly by convection and radiation is preferred.

In general, continuous operation has the important advantage of ease of integration into the rest of the process coupled with a lower unit cost of drying. As the rate of throughput of material becomes smaller, however, the capital cost becomes the major component in the total running costs and the relative cheapness of batch plant becomes more attractive. This is illustrated in Figure 16.7 which is taken from the work of KEEY[22]. In general, throughputs of 5000 kg/day (0.06 kg/s) and over are best handled in batches whilst throughputs of 50,000 kg/day (0.06 kg/s) and over are better handled continuously. The ease of construction of a small batch dryer compared with the sophistication of the

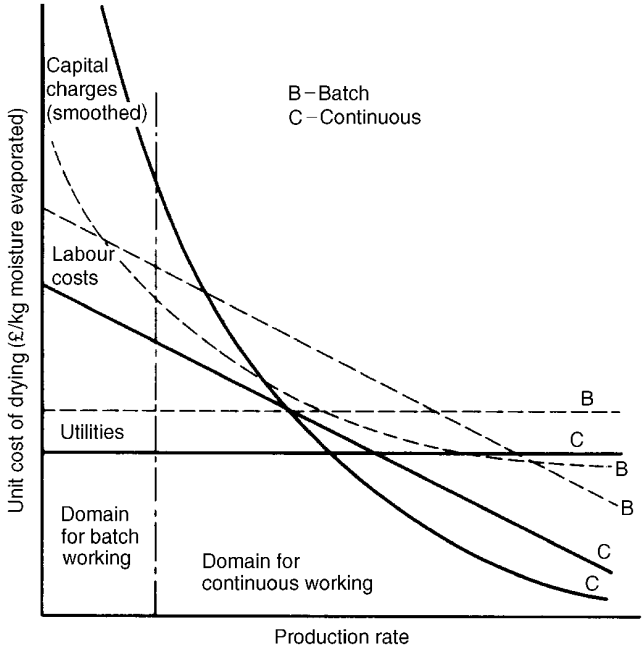


Figure 16.7. Variation of unit costs of drying with production rate[22]

This book belongs to Bradley Loren (bloren@mcandrews-ip.com) Copyright Elsevier 2024
Intas Exhibit 1032
Page 309 of 470
PGR2025-00043

continuous dryer should also be taken into account. In addition, a batch dryer is much more versatile and it can often be used for different materials. The humidity may be controlled during the drying operation, and this is especially important in cases where the humidity has to be maintained at different levels for varying periods of time.

Direct heating, in which the material is heated primarily by convection from hot gases has several advantages. Firstly, directly heated dryers are, in general, less costly, mainly because of the absence of tubes or jackets within which the heating medium must be contained. Secondly, it is possible to control the temperature of the gas within very fine limits, and indeed it is relatively simple to ensure that the material is not heated beyond a specified temperature. This is especially important with heat-sensitive materials. Against this, the overall thermal efficiency of directly heated dryers is generally low due to the loss of energy in the exhaust gas and, where an expensive solvent is evaporated from the solid, the operation is often difficult and costly. Losses also occur in the case of fluffy and powdery materials, and further problems are encountered where either the product or the solvent reacts with oxygen in the air.

A major cost in the operation of a dryer is in heating the air or gas. Frequently, the hot gases are produced by combustion of a fuel gas or atomised liquid, and considerable economy may be effected by using a combined heat and power system in which the hot gases are first passed through a turbine connected to an electrical generator.

Many of these disadvantages may be overcome by modifications to the design, although these increase the cost, and often an indirectly heated dryer may prove to be more economical. This is especially the case when thermal efficiency, solvent recovery or maximum cleanliness is of paramount importance and, with indirectly heated dryers, there is always the danger of overheating the product, since the heat is transferred through the material itself.

The maximum temperature at which the drying material may be held is controlled by the thermal sensitivity of the product and this varies inversely with the time of retention. Where lengthy drying times are employed, as for example in a batch shelf dryer, it is necessary to *operate under vacuum* in order to maintain evaporative temperatures at acceptable levels. In most continuous dryers, the retention time is very low, however, and operation at atmospheric pressure is usually satisfactory. As noted previously, dryer selection is considered in some detail in Volume 6.

16.5.2. Tray or shelf dryers

Tray or shelf dryers are commonly used for granular materials and for individual articles. The material is placed on a series of trays which may be heated from below by steam coils and drying is carried out by the circulation of air over the material. In some cases, the air is heated and then passed once through the oven, although, in the majority of dryers, some recirculation of air takes place, and the air is reheated before it is passed over each shelf. As air is passed over the wet material, both its temperature and its humidity change. This process of air humidification is discussed in Volume 1, Chapter 13.

If air of humidity $\mathscr{H}_1$ is passed over heating coils so that its temperature rises to θ_1, this operation may be represented by the line AB on the humidity chart shown in Figure 16.8. This air then passes over the wet material and leaves at, say 90 per cent relative humidity,

This book belongs to Bradley Loren (bloren@mcandrews-ip.com) Copyright Elsevier 2024

Intas Exhibit 1032
Page 310 of 470
PGR2025-00043

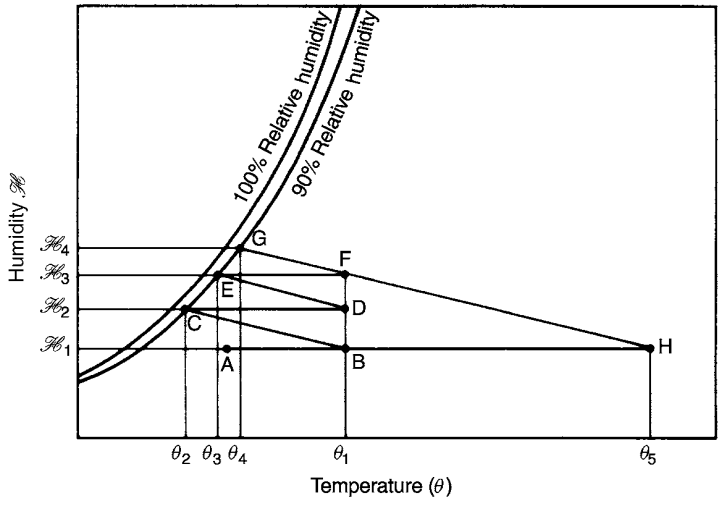


Figure 16.8. Drying with reheating of air

with its temperature falling to some value θ_2. This change in the condition of the air is shown by the line BC, and the humidity has risen to $\mathscr{H}_2$. The wet-bulb temperature of the air will not change appreciably and therefore BC will coincide with an adiabatic cooling line. Each kg of air removes $(\mathscr{H}_2 - \mathscr{H}_1)$ kg of water, and the air required to remove a given amount of water from the material may easily be found. If the air at θ_2 is now passed over a second series of heating coils and is heated to the original temperature θ_1, the heating operation is shown by the line CD. This reheated air can then be passed over wet material on a second tray in the dryer, and pick up moisture until its relative humidity rises again to 90 per cent at a temperature θ_3. This is at point E. In this way each kilogram of air has picked up water amounting to $(\mathscr{H}_3 - \mathscr{H}_1)$ kg of water. Reheating in this way may be effected a number of times, as shown in Figure 16.8, so that the moisture removed per kilogram of air can be considerably increased compared with that for a single pass. Thus, for three passes of air over the material, the total moisture removed is $(\mathscr{H}_4 - \mathscr{H}_1)$ kg/kg air.

If the air of humidity $\mathscr{H}_1$ had been heated initially to a temperature θ_5, the same amount of moisture would have been removed by a single passage over the material, assuming that the air again leaves at a relative humidity of 90 per cent.

This reheating technique has two main advantages. Firstly, very much less air is required, because each kilogram of air picks up far more water than in a single stage system, and secondly, in order to pick up as much water in a single stage, it would be necessary to heat the air to a very much higher temperature. This reduction in the amount of air, needed simplifies the heating system, and reduces the tendency of the air to carry away any small particles.

A modern tray dryer consists of a well-insulated cabinet with integral fans and trays which are stacked on racks, or loaded on to trucks which are pushed into the dryer. Tray areas are 0.3–1 m^2 with a depth of material of 10–100 mm, depending on the particle size of the product. Air velocities of 1–10 m/s are used and, in order to conserve heat,

This book belongs to Bradley Loren (bloren@mcandrews-ip.com) Copyright Elsevier 2024
Intas Exhibit 1032
Page 311 of 470
PGR2025-00043

85–95 per cent of the air is recirculated. Even at these high values, the steam consumption may be 2.5–3.0 kg/kg moisture removed. The capacity of tray dryers depends on many factors including the nature of the material, the loading and external conditions, although for dyestuffs an evaporative capacity of 0.03–0.3 kg/m^2 ks (0.1–1 kg/m^2 h) has been quoted with air at 300–360 K[22].

Example 16.4

A 100 kg batch of granular solids containing 30 per cent moisture is to be dried in a tray drier to 15.5 per cent of moisture by passing a current of air at 350 K tangentially across its surface at a velocity of 1.8 m/s. If the constant rate of drying under these conditions is 0.0007 kg/s m^2 and the critical moisture content is 15 per cent, calculate the approximate drying time. Assume the drying surface to be 0.03 m^2/kg dry mass.

Solution

$$\text{In 100 kg feed, mass of water} = (100 \times 30/100) = 30 \text{ kg}$$

and:

$$\text{mass of dry solids} = (100 - 30) = 70 \text{ kg}$$

For b kg water in the dried solids: $100b/(b + 70) = 15.5$

and the water in the product, $b = 12.8$ kg

Thus: initial moisture content, $w_1 = (30/70) = 0.429$ kg/kg dry solids

final moisture content, $w_2 = (12.8/70) = 0.183$ kg/kg dry solids

and water to be removed $= (30 - 12.8) = 17.2$ kg

The surface area available for drying $= (0.03 \times 70) = 2.1$ m^2 and hence the rate of drying during the constant period $= (0.0007 \times 2.1) = 0.00147$ kg/s.

As the final moisture content is above the critical value, all the drying is at this constant rate and the time of drying is:

$$t = (17.2/0.00147) = 11{,}700 \text{ s or } \underline{\underline{11.7 \text{ ks}}} \ (3.25 \text{ h})$$

16.5.3. Tunnel Dryers

In tunnel dryers, a series of trays or trolleys is moved slowly through a long tunnel, which may or may not be heated, and drying takes place in a current of warm air. Tunnel dryers are used for drying paraffin wax, gelatine, soap, pottery ware, and wherever the throughput is so large that individual cabinet dryers would involve too much handling. Alternatively, material is placed on a belt conveyor passing through the tunnel, an arrangement which is well suited to vacuum operation. In typical tunnel arrangements, shown in Figure 16.9,

This book belongs to Bradley Loren (bloren@mcandrews-ip.com) Copyright Elsevier 2024

Intas Exhibit 1032
Page 312 of 470
PGR2025-00043

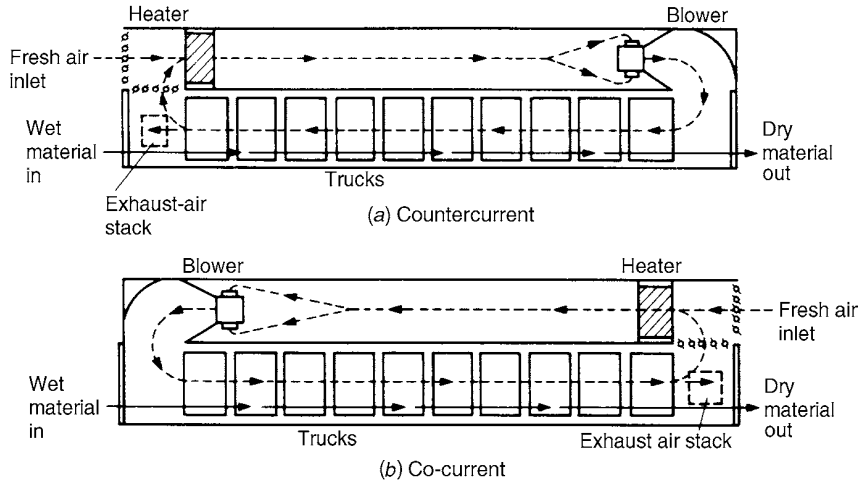


Figure 16.9. Arrangements for tunnel dryers

the construction is of block or sheet metal and the size varies over a wide range, with lengths sometimes exceeding 30 m.

16.5.4. Rotary Dryers

For the continuous drying of materials on a large scale, 0.3 kg/s (1 tonne/h) or greater, a rotary dryer, which consists of a relatively long cylindrical shell mounted on rollers and driven at a low speed, up to 0.4 Hz is suitable. The shell is supported at a small angle to the horizontal so that material fed in at the higher end will travel through the dryer under gravity, and hot gases or air used as the drying medium are fed in either at the upper end of the dryer to give co-current flow or at the discharge end of the machine to give countercurrent flow. One of two methods of heating is used:

(a) Direct heating, where the hot gases or air pass through the material in the dryer.
(b) Indirect heating, where the material is in an inner shell, heated externally by hot gases. Alternatively, steam may be fed to a series of tubes inside the shell of the dryer.

The shell of a rotary dryer is usually constructed by welding rolled plate, thick enough for the transmission of the torque required to cause rotation, and to support its own weight and the weight of material in the dryer. The shell is usually supported on large tyres which run on wide rollers, as shown in Figure 16.10, and although mild steel is the usual material of construction, alloy steels are used, and if necessary the shell may be coated with a plastics material to avoid contamination of the product.

With countercurrent operation, since the gases are often exhausted by a fan, there is a slight vacuum in the dryer, and dust-laden gases are in this way prevented from escaping.

This book belongs to Bradley Loren (bloren@mcandrews-ip.com) Copyright Elsevier 2024
Intas Exhibit 1032
Page 313 of 470
PGR2025-00043

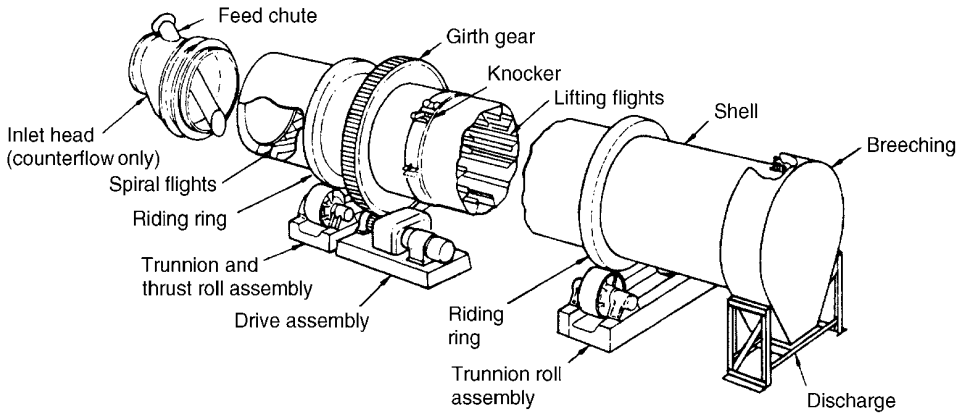


Figure 16.10. Rotary dryer, 0.75 m diameter × 4.5 m long for drying dessicated coconut[21]

This arrangement is suitable for sand, salt, ammonium nitrate and other inorganic salts, and is particularly convenient when the product is discharged at a high temperature. In this case, gas or oil firing is used and, where air is used as a drying medium, this may be filtered before heating, in order to minimise contamination of the product. As the gases leaving the dryer generally carry away very fine material, some form of cyclone or scrubber is usually fitted. Since the hot gases come into immediate contact with the dried material, the moisture content may be reduced to a minimum, though the charge may become excessively heated. Further, since the rate of heat transfer is a minimum at the feed end, a great deal of space is taken up with heating the material.

With co-current flow, the rate of passage of the material through the dryer tends to be greater since the gas is travelling in the same direction. Contact between the wet material and the inlet gases gives rise to rapid surface drying, and this is an advantage if the material tends to stick to the walls. This rapid surface drying is also helpful with materials containing water of crystallisation. The dried product leaves at a lower temperature than with countercurrent systems, and this may also be an advantage. The rapid lowering of the gas temperature as a result of immediate contact with the wet material also enables heat sensitive materials to be handled rather more satisfactorily.

Since the drying action arises mainly from direct contact with hot gases, some form of lifter is essential to distribute the material in the gas stream. This may take the form of flights, as shown in Figure 16.11, or of louvres. In the former case, the flights lift the material and then shower it across the gas stream, whilst in the latter the gas stream enters the shell along the louvres. In Figure 16.12 it may be seen that, in the rotary louvre dryer, the hot air enters through the louvres, and carries away the moisture at the end of the dryer. This is not strictly a co-current flow unit, but rather a through circulation unit, since the material continually meets fresh streams of air. The rotation of the shell, at about 0.05 Hz (3 rpm), maintains the material in agitation and conveys it through the dryer. Rotary dryers are 0.75–3.5 m in diameter and up to 9 m in length[23].

The thermal efficiency of rotary dryers is a function of the temperature levels, and ranges from 30 per cent in the handling of crystalline foodstuffs to 60–80 per cent in the

This book belongs to Bradley Loren (bloren@mcandrews-ip.com) Copyright Elsevier 2024
Intas Exhibit 1032
Page 314 of 470
PGR2025-00043

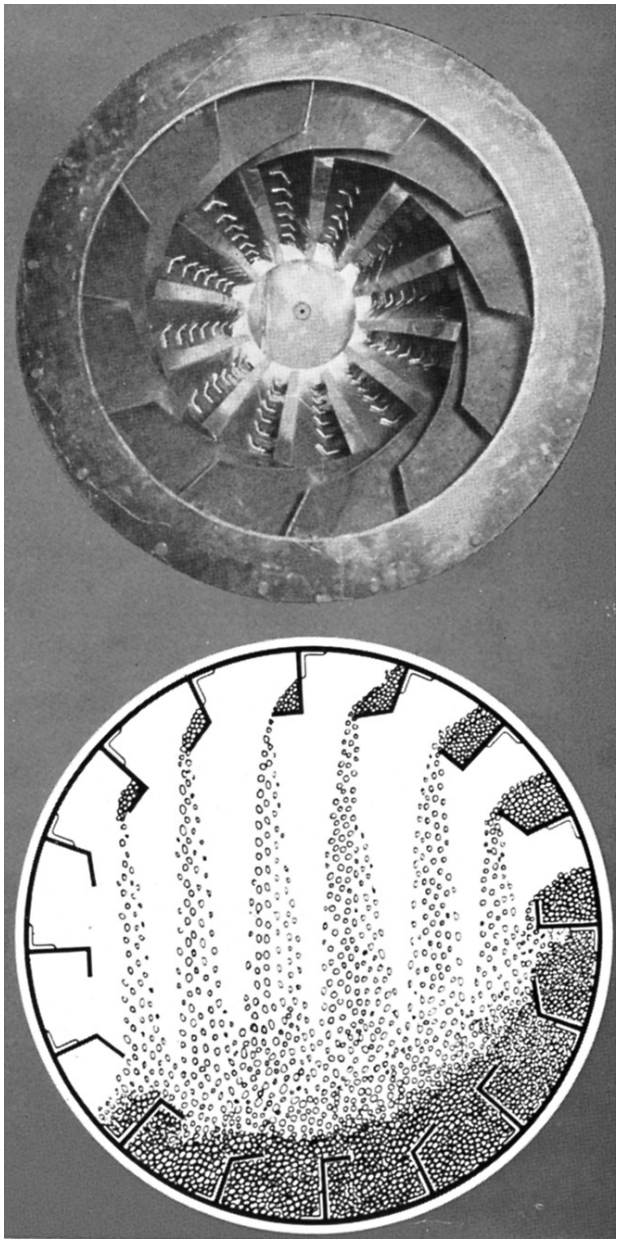


Figure 16.11. Helical and angled lifting flights in a rotary dryer

This book belongs to Bradley Loren (bloren@mcandrews-ip.com)
Copyright Elsevier 2024
Intas Exhibit 1032
Page 315 of 470
PGR2025-00043

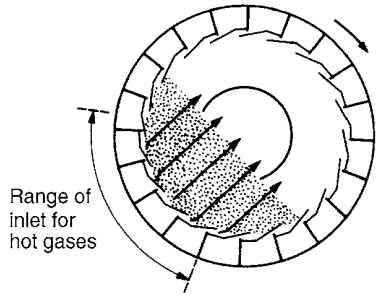


Figure 16.12. Air flow through a rotary louvre dryer

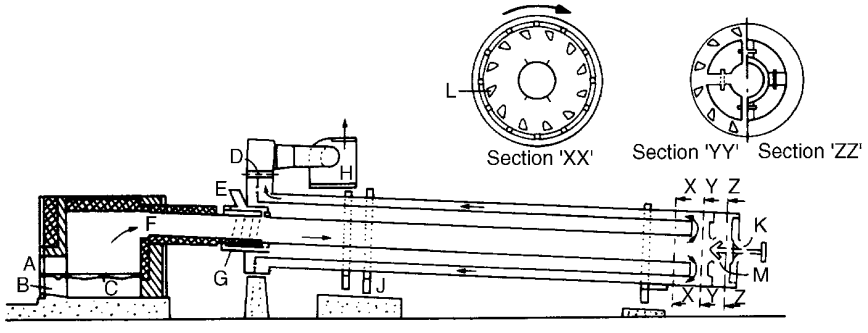


Figure 16.13. Indirectly heated rotary dryer. A–Firing door. B–Air regulator. C–Furnace. D–Control valves. E–Feed chute. F–Furnace flue. G–Feed screw. H–Fan. J–Driving gear. K–Discharge bowl. L–Duct lifters. M–By-pass valve

case of inert materials. Evaporative capacities of 0.0015–0.0080 kg/m^3 s may be achieved and these are increased by up to 50 per cent in louvre dryers.

In one form of *indirectly heated dryer*, shown in Figure 16.13, hot gases pass through the innermost cylinder, and then return through the annular space between the outer cylinders. This form of dryer can be arranged to give direct contact with the wet material during the return passage of the gases. Flights on the outer surface of the inner cylinder, and the inner surface of the outer cylinder, assist in moving the material along the dryer. This form of unit gives a better heat recovery than the single flow direct dryer, though it is more expensive. In a simpler arrangement, a single shell is mounted inside a brickwork chamber, through which the hot gases are introduced.

The steam-tube dryer, shown in Figure 16.14, incorporates a series of steam tubes, fitted along the shell in concentric circles and rotating with the shell. These tubes may be fitted with fins to increase the heat transfer surface although material may then stick to the tubes. The solids pass along the inclined shell, and leave through suitable ports at the other end. A small current of air is passed through the dryer to carry away the moisture, and the air leaves almost saturated. In this arrangement, the wet material comes in contact with very humid air, and surface drying is therefore minimised. This type of unit has a high thermal efficiency, and can be made from corrosion resisting materials without difficulty.

This book belongs to Bradley Loren (bloren@mcandrews-ip.com) Copyright Elsevier 2024

Intas Exhibit 1032
Page 316 of 470
PGR2025-00043

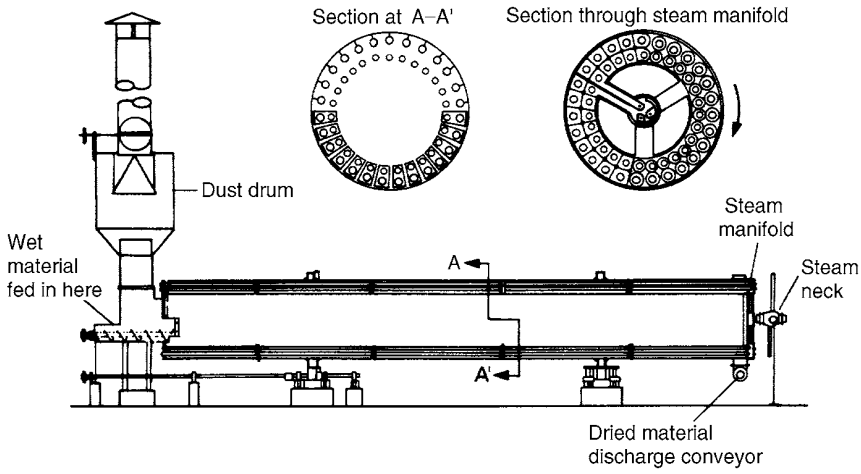


Figure 16.14. Steam-tube rotary dryer

Design considerations

Many of the design problems associated with rotary dryers have been discussed by FRIEDMAN and MARSHALL[24], by PRUTTON *et al.*[25] and by MILLER *et al.*[26].

Heat from the air stream passes to the solid material during its fall through the air stream, and also from the hot walls of the shell, although the first mechanism is much the more important. The heat transfer equation may be written as:

$$Q = UaV\Delta T \tag{16.23}$$

where: Q is the rate of heat transfer,
U is the overall heat transfer coefficient,
V is the volume of the dryer,
a is the area of contact between the particles and the gas per unit volume of dryer, and
ΔT is the mean temperature difference between the gas and material.

The combined group Ua has been shown[25,26] to be influenced by the feed rate of solids, the air rate and the properties of the material, and a useful approximation is given by:

$$Ua = \bar{\kappa} G'^{n}/D \tag{16.24}$$

where $\bar{\kappa}$ is a dimensional coefficient. Typical values for a 300 mm diameter dryer revolving at 0.08–0.58 Hz (5–35 rpm) show that $n = 0.67$ for specific gas rates in the range 0.37–1.86 kg/m^2, as given by SAEMAN[27]. The coefficient $\bar{\kappa}$ is a function of the number of flights and, using SI units, this is given approximately by:

$$\bar{\kappa} = 20(n_f - 1) \tag{16.25}$$

This book belongs to Bradley Loren (bloren@mcandrews-ip.com) Copyright Elsevier 2024
Intas Exhibit 1032
Page 317 of 470
PGR2025-00043

Equation 16.25 was derived for a 200 mm diameter dryer with between 6 and 16 flights[28]. Combining equations 16.24 and 16.25 gives:

$$Ua = 20(n_f - 1)G'^{0.67}/D \tag{16.26}$$

and hence for a 1 m diameter dryer with 8 flights, Ua would be about 140 W/m^3 K for a gas rate of 1 kg/m^2 s.

SAEMAN[27] has investigated the countercurrent drying of sand in a dryer of 0.3 m diameter and 2.0 m long with 8 flights rotating at 0.17 Hz (10 rpm) and has found that the volumetric heat transfer coefficient may be correlated in terms of the hold-up of solids, as shown in Figure 16.15, and is independent of the gas rate in the range 0.25–20 kg/m^2 s.

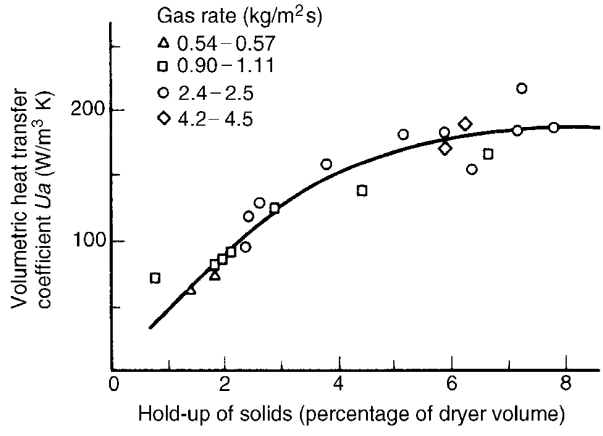


Figure 16.15. Correlation of volumetric heat-transfer coefficients with hold-up[27]

Other typical values of heat transfer coefficients achieved in drying operations are:

Application	*Parameter*	*Value*		*Reference*
Heated surface (fairly dry solid)	U	5–12	W/m^{2}K	28
Unagitated dryers	U	5–29	W/m^{2}K	29
Moderate agitation	U	29–85	W/m^{2}K	29
High agitation	U	85–140	W/m^{2}K	29
Cake-encrusted heating surface	U	5–29	W/m^{2}K	29
Light powdery materials	$U\Delta T$	950	W/m^2	24
Coarse granular materials	$U\Delta T$	6300	W/m^2	24

The hold-up in a rotary dryer varies with the feed rate, the number of flights, the shell diameter and the air rate. For zero air flow, FRIEDMAN and MARSHALL[24] give the hold-up as:

$$X = \frac{25.7F'}{SN^{0.9}D} \quad \text{per cent of dryer volume} \tag{16.27}$$

This book belongs to Bradley Loren (bloren@mcandrews-ip.com) Copyright Elsevier 2024
Intas Exhibit 1032
Page 318 of 470
PGR2025-00043

where: D is the diameter of the drum (m),
F' is the feed rate ($m^3/s\ m^2$),
S is the slope of the dryer (m/m length),
N is the rate of rotation (Hz), and
X is the holdup, expressed as a percentage of the drum volume.

As the air flowrate is increased, X changes and an empirical relation for the hold-up X_a with air flow is:

$$X_a = X \pm KG' \tag{16.28}$$

although the values of K are poorly defined. X_a usually has a value of about 3 per cent, when working with a slope of about 0.1. In equation 16.28, the positive sign refers to countercurrent flow and the negative sign to co-current flow.

A more general approach has been made by SHARPLES *et al.*[30] who have solved differential moisture and heat-balance equations coupled with expressions for the forward transport of solids, allowing for solids being cascaded out of lifting baffles. Typical results, shown in Figure 16.16, were obtained using a 2.6 m diameter dryer, 16 m long with a 1° slope (60 mm/m). Commercial equipment is available with diameters up to 3 m and lengths up to 30 m, and hence the correlations outlined in this section must be used with caution beyond the range used in the experimental investigations.

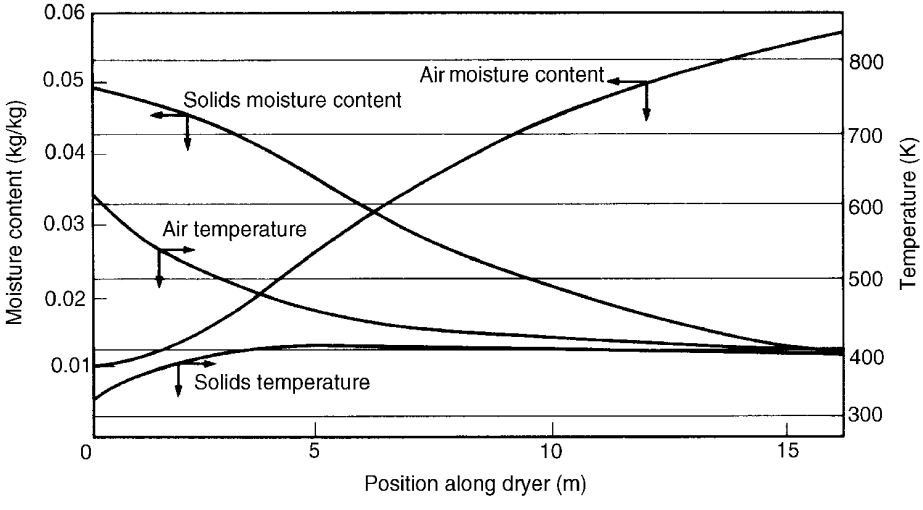


Figure 16.16. Conditions in a 2.6 m diameter × 16 m long rotary dryer with 1° slope. Co-current drying of 11.3 kg/s of fertiliser granules with 9.1 kg/s of air[30]

In general, the allowable mass velocity of the gas in a direct-contact rotary dryer depends on the dust content of the solids and is 0.55–7.0 kg/m^2 s with coarse particles. Inlet gas temperatures are typically 390–450 K for steam-heated air and 800–1100 K for flue gas, and the peripheral speed of the shell is 0.3–0.4 m/s.

This book belongs to Bradley Loren (bloren@mcandrews-ip.com) Copyright Elsevier 2024
Intas Exhibit 1032
Page 319 of 470
PGR2025-00043

Example 16.5

A flow of 0.35 kg/s of a solid is to be dried from 15 per cent to 0.5 per cent moisture on a dry basis. The mean heat capacity of the solids is 2.2 kJ/kg deg K and it is proposed that a co-current adiabatic dryer should be used with the solids entering at 300 K and, because of the heat sensitive nature of the solids, leaving at 325 K. Hot air is available at 400 K with a humidity of 0.01 kg/kg dry air and the maximum allowable mass velocity of the air is 0.95 kg/m^{2}s. What diameter and length should be specified for the proposed dryer?

Solution

With an inlet air temperature and humidity of 400 K and 0.01 kg/kg dry air respectively from Figure 13.4 in Volume 1, the inlet wet-bulb temperature = 312 K. If, not unreasonably, it is assumed that the number of transfer units is 1.5, then for adiabatic drying the outlet air temperature, T_0 is given by:

$$1.5 = \ln((400 - 312)/(T_0 - 312) \text{ and } T_0 = 331.5 \text{ K}.$$

The solids outlet temperature will be taken as the maximum allowable, 325 K.

From the steam tables in the Appendix, the latent heat of vaporisation of water at 312 K is 2410 kJ/kg. Again from steam tables, the specific heat capacity of water vapour = 1.88 kJ/kg K and that of the solids will be taken as 2.18 kJ/kg K.

For a mass flow of solids of 0.35 kg/s and inlet and outlet moisture contents of 0.15 and 0.005 kg/kg dry solids respectively, the mass of water evaporated = $0.35(0.15 - 0.005) = 0.0508$ kg/s.

For unit mass of solids, the heat duty includes:

heat to the solids = $2.18(325 - 300) = 54.5$ kJ/kg
heat to raise the moisture to the dew point = $(0.15 \times 4.187(312 - 300)) = 7.5$ kJ/kg
heat of vaporisation = $2410(0.15 - 0.005) = 349.5$ kJ/kg
heat to raise remaining moisture to the solids outlet temperature
$= (0.005 \times 4.187)(325 - 312) = 0.3$ kJ/kg
and heat to raise evaporated moisture to the air outlet temperature
$= (0.15 - 0.005)1.88(331.5 - 312) = 5.3$ kJ/kg
a total of $(54.5 + 7.5 + 349.5 + 0.3 + 5.3) = 417.1$ kJ/kg
or: $(417.1 \times 0.35) = 146$ kW

From Figure 13.4 in Volume 1, the humid heat of the entering air is 1.03 kJ/kg K and making a heat balance:

$$G_1\ (1 + \mathscr{H}_1) = Q/C_{p_1}(T_1 - T_2)$$

where: G_1 (kg/s) is the mass flowrate of inlet air,

$\mathscr{H}_1$ (kg/kg) is the humidity of inlet air,

Q (kW) is the heat duty,

C_{p_1} (kJ/kg K) is the humid heat of inlet air

and: T_1 and T_2 (K) are the inlet and outlet air temperatures respectively.

In this case:

$$G_1(1 + 0.01) = 146/(1.03(400 - 331.5)) = 2.07 \text{ kg/s}$$

and: mass flowrate of dry air, $G_a = (2.07/1.01) = 2.05$ kg/s

This book belongs to Bradley Loren (bloren@mcandrews-ip.com) Copyright Elsevier 2024

Intas Exhibit 1032
Page 320 of 470
PGR2025-00043

The humidity of the outlet air is then:

$$\mathscr{H}_2 = 0.01 + (0.0508/2.05) = 0.0347 \text{ kg/kg}$$

At a dry bulb temperature of 331.5 K, with a humidity of 0.0347 kg/kg, the wet-bulb temperature of the outlet air, from Figure 13.4 in Volume 1, is 312 K, the same as the inlet, which is the case for adiabatic drying.

The dryer diameter is then found from the allowable mass velocity of the air and the entering air flow and for a mass velocity of 0.95 kg/m^{2}s, the cross sectional area of the dryer is:

$$(2.07/0.95) = 2.18 \text{ m}^2$$

equivalent to a diameter of $[(4 \times 2.18)/\pi]^{0.5} = \underline{\underline{1.67 \text{ m}}}$

With a constant drying temperature of 312 K:

at the inlet: $\Delta T_1 = (400 - 312) = 88$ deg K

and at the outlet: $\Delta T_2 = (331.5 - 312) = 19.5$ deg K

and the logarithmic mean, $\Delta T_m = (88 - 19.5)/\ln(88/19.5) = 45.5$ deg K.

The length of the dryer, L is then: $L = Q/(0.0625\pi DG'^{0.67}\Delta T_m)$

where D (m) is the diameter

and G' (kg/m^{2}s) is the air mass velocity.

In this case: $L = 146/[0.0625\pi \times 1.67(0.95)^{0.67} \times 45.5)] = \underline{\underline{10.1 \text{ m}}}$

This gives a length/diameter ratio of $(10.1/1.67) = 6$, which is a reasonable value for rotary dryers.

16.5.5. Drum dryers

If a solution or slurry is run on to a slowly rotating steam-heated drum, evaporation takes place and solids may be obtained in a dry form. This is the basic principle used in all drum dryers, some forms of which are illustrated in Figure 16.17. The feed to a single drum dryer may be of the dip, pan, or splash type. The dip-feed system, the earliest design, is still used where liquid can be picked up from a shallow pan. The agitator prevents settling of particles, and the spreader is sometimes used to produce a uniform coating on the drum. The knife, which is employed for removing the dried material, functions in a similar manner to the doctor blade on a rotary filter. If the material is dried to give a free-flowing powder, this comes away from the drum quite easily. The splash-feed type is used for materials, such as calcium arsenate, lead arsenate, and iron oxide, where a light fluffy product is desired. The revolving cylinder throws the liquor against the drum, and a uniform coating is formed with materials which do not stick to the hot surface of the drum.

Double drum dryers may be used in much the same way, and Figure 16.17 shows dip-feed and top-feed designs. Top-feed gives a larger capacity as a thicker coating is obtained. It is important to arrange for a uniform feed to a top-feed machine, and this may be effected by using a perforated pipe for solutions and a travelling trough for suspensions.

This book belongs to Bradley Loren (bloren@mcandrews-ip.com) Copyright Elsevier 2024

Intas Exhibit 1032
Page 321 of 470
PGR2025-00043

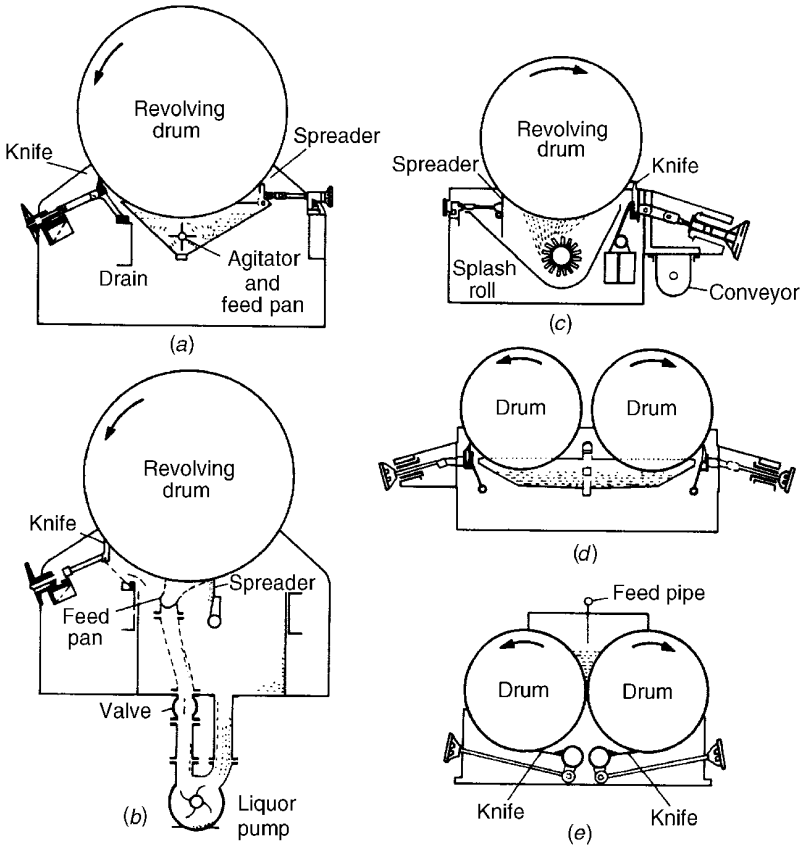


Figure 16.17. Methods of feeding drum dryers. (*a*) Single drum, dip-feed. (*b*) Single drum, pan-feed. (*c*) Single drum, splash-feed. (*d*) Double drum, dip-feed. (*e*) Double drum, top-feed

Drums are usually made from cast iron, although chromium-plated steel or alloy steel is often used where contamination of the product must be avoided, such as with pharmaceuticals or food products. Arrangements must be made for accurate adjustment of the separation of the drums, and the driving gears should be totally enclosed. A range of speeds is usually obtained by selecting the gears, rather than by fitting a variable speed drive. Removal of the steam condensate is important, and an internal syphon is often fitted to keep the drum free of condensate. In some cases, it is better for the drums to be rotated upwards at the point of closest proximity, and the knives are then fitted at the bottom. By this means, the dry material is kept away from the vapour evolved. Some indication of the sizes of this type of dryer is given in Table 16.3, and it may be noted that the surface of each drum is limited to about 35 m^2. This, coupled with developments in the design of spray dryers, renders the latter more economically attractive, especially where large throughputs are to be handled. For steam-heated drum dryers, normal evaporative capacities are proportional to the active drum area and are 0.003–0.02 kg/m^2 s, although higher rates are claimed for grooved drum dryers.

This book belongs to Bradley Loren (bloren@mcandrews-ip.com) Copyright Elsevier 2024

Intas Exhibit 1032
Page 322 of 470
PGR2025-00043

Table 16.3. Sizes of double drum dryers

Drum dimensions Diameter (m) × Length (m)	Length (m)	Width (m)	Height (m)	Mass (kg)
0.61 × 0.61	3.5	2.05	2.3	3,850
0.61 × 0.91	3.8	2.05	2.4	4,170
0.81 × 1.32	5.0	2.5	2.8	7,620
0.81 × 1.83	5.5	2.5	2.8	8,350
0.81 × 2.28	5.9	2.5	2.8	8,890
0.81 × 2.54	6.25	2.5	2.8	9,300
0.81 × 3.05	6.7	2.5	2.8	10,120
1.07 × 2.28	6.4	3.0	3.0	14,740
1.07 × 2.54	6.7	3.0	3.0	15,420
1.07 × 3.05	7.2	3.0	3.0	16,780
1.52 × 3.66	7.9	4.1	4.25	27,220

The solid is usually in contact with the hot metal for 6–15 s, short enough to prevent significant decomposition of heat sensitive materials, and heat transfer coefficients are 1–2 kW/m^2 K.

When the temperature of the drying material must be kept as low as possible, vacuum drying is used, and one form of vacuum dryer is shown in Figure 16.18. The dried material is collected in two screw conveyors and carried usually to two receivers so that one can be filled while the other is emptied.

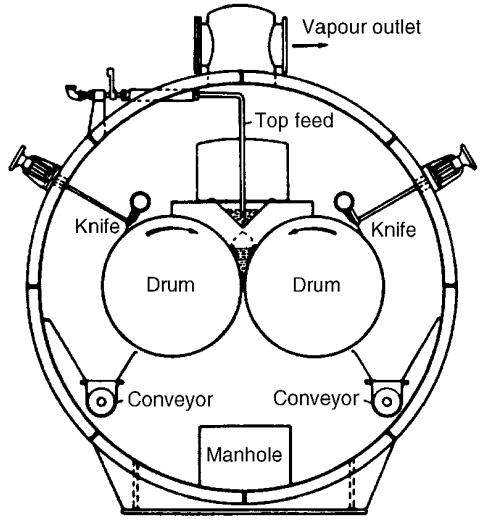


Figure 16.18. Vacuum drum dryer

16.5.6. Spray dryers

Water may be evaporated from a solution or a suspension of solid particles by spraying the mixture into a vessel through which a current of hot gases is passed. In this way, a

This book belongs to Bradley Loren (bloren@mcandrews-ip.com) Copyright Elsevier 2024
Intas Exhibit 1032
Page 323 of 470
PGR2025-00043

large interfacial area is produced and consequently a high rate of evaporation is obtained. Drop temperatures remain below the wet bulb temperature of the drying gas until drying is almost complete, and the process thus affords a convenient means of drying substances which may deteriorate if their temperatures rise too high, such as milk, coffee, and plasma. Furthermore, because of the fine state of subdivision of the liquid, the dried material is obtained in a finely divided state.

In spray drying, it is necessary to atomise and distribute, under controlled conditions, a wide variety of liquids, the properties of which range from those of solutions, emulsions, and dispersions, to slurries and even gels. Most of the atomisers commonly employed are designed for simple liquids, that is mobile Newtonian liquids. When atomisers are employed for slurries, pastes, and liquids having anomalous properties, there is a great deterioration in performance and, in many cases, atomisers may be rapidly eroded and damaged so as to become useless. There is therefore much to be gained by considering various types and designs of atomiser so that a suitable selection can be made for the given duty.

The performance of a spray dryer or reaction system is critically dependent on the drop size produced by the atomiser and the manner in which the gaseous medium mixes with the drops. In this context an atomiser is defined as a device which causes liquid to be disintegrated into drops lying within a specified size range, and which controls their spatial distribution.

Atomisers

Atomisers are classified in Table 16.4[31] according to the three basic forms of energy commonly employed — pressure energy, centrifugal kinetic energy, and gaseous energy. Where greater control is required over disintegration or spatial dispersion, combinations of atomiser types may be employed, and, for example, swirl-spray nozzles or spinning discs may be incorporated in a blast atomiser, their primary functions being to produce thin liquid sheets which are then eventually atomised by low, medium or high velocity gas streams.

The fundamental principle of disintegrating a liquid consists in increasing its surface area until it becomes unstable and disintegrates. The theoretical energy requirement is the increase in surface energy plus the energy required to overcome viscous forces, although in practice this is only a small fraction of the energy required. The process by which drops are produced from a liquid stream depends upon the nature of the flow in the atomiser, that is whether it is laminar or turbulent, the way in which energy is imparted to the liquid, the physical properties of the liquid, and the properties of the ambient atmosphere. The basic mechanism is, however, unaffected by these variables and consists essentially of the breaking down of unstable threads of liquid into rows of drops and conforms to the classical mechanism postulated by LORD RAYLEIGH[32]. This theory states that a free column of liquid is unstable if its length is greater than its circumference, and that, for a non-viscous liquid, the wavelength of that disturbance which will grow most rapidly in amplitude is 4.5 times the diameter. This corresponds to the formation of droplets of diameter approximately 1.89 times that of the jet d_j. WEBER[33] has shown that the

This book belongs to Bradley Loren (bloren@mcandrews-ip.com) Copyright Elsevier 2024

Intas Exhibit 1032
Page 324 of 470
PGR2025-00043

Table 16.4. Classification of atomisers[31]

Pressure used in pressure atomisers	Centrifugal energy used in rotary atomisers	Gaseous energy used in twin-fluid or blast atomisers
Fan-spray nozzles 0.25–1.0 MN/m^2	Spinning cups 6–30 m/s	External mixing (fluid pressures independent)
Impact nozzles Impinging jet nozzles 0.25–1.0 MN/m^2 Impact plate nozzles Up to 3.0 MN/m^2 Deflector nozzles 7.0 MN/m^2	Spinning discs Flat discs Saucer-shaped discs Radial-vaned discs Multiple discs 30–180 m/s	Internal mixing (fluid pressures interdependent)
Swirl-spray nozzles Hollow cone, full cone 0.4–70 MN/m^2		Low velocity Gas velocity 30–120 m/s Gas–liquid ratio 2–25 kg/kg
Divergent pintle nozzles 0.25–7.0 MN/m^2 Fixed or vibrating pintle		Medium velocity Gas velocity 120–300 m/s Gas–liquid ratio 0.2–1 kg/kg
		High velocity Gas velocity sonic or above Gas–liquid ratio 0.2–1 kg/kg

optimum wavelength for the disruption of jets of viscous liquid is:

$$\lambda_{\text{opt}} = \sqrt{(2\pi d_j)}\left[1 + \frac{3\mu}{\sqrt{(\rho\sigma d_j)}}\right]^{0.5} \tag{16.29}$$

A uniform thread will break down into a series of drops of uniform diameter, each separated by one or more satellite drops. Because of the heterogeneous character of the atomisation process, however, non-uniform threads are produced and this results in a wide range of drop sizes. An example of a part of a laminar sheet collapsing into a network of threads and drops is shown in Figure 16.19. Only when the formation and disintegration of threads are controlled can a homogeneous spray cloud be produced. One method by which this can be achieved is by using a rotary cup atomiser operating within a critical range of liquid flow rates and rotor speeds, although, as shown later, this range falls outside that normally employed in practice.

Although certain features are unique to particular atomiser types, many of the detailed mechanisms of disintegration are common to most forms of atomiser[34]. The most effective way of utilising energy imparted to a liquid is to arrange that the liquid mass has a large specific surface before it commences to break down into drops. Thus the primary function of an atomiser is to transpose bulk liquid into thin liquid sheets. Three modes of disintegration of such spray sheets have been established[35], namely *rim*, *perforated sheet*, and *wave*. Because of surface tension, the free edge of any sheet contracts into a thick rim, and *rim disintegration* occurs as it breaks up by instabilities analogous to those

This book belongs to Bradley Loren (bloren@mcandrews-ip.com) Copyright Elsevier 2024

Intas Exhibit 1032
Page 325 of 470
PGR2025-00043

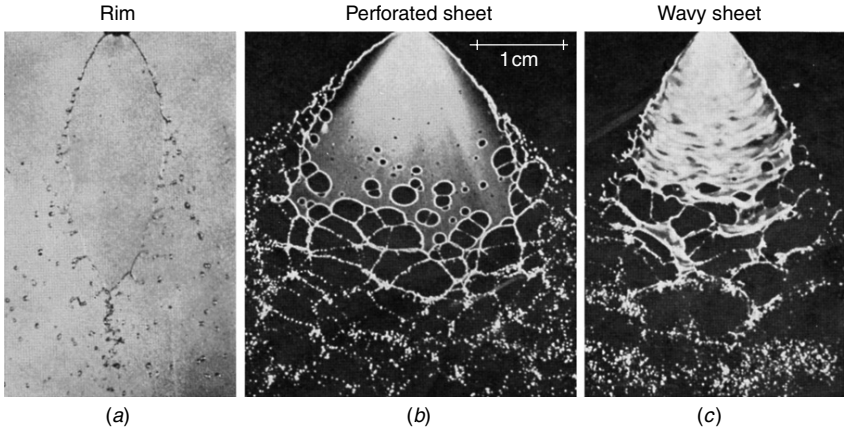


Figure 16.19. Modes of disintegration of liquid films

of free jets. Figure 16.19*a* illustrates a fan spray sheet and shows that, as the liquid in each edge moves along the curved boundary, the latter becomes disturbed and disintegrates. When this occurs, the resulting drops sustain the direction of flow of the edge at the point at which the drops are formed, and remain attached to the receding surface by thin threads which rapidly disintegrate into streams of drops.

In *perforated-sheet disintegration* shown in Figure 16.19*b*, small holes suddenly appear in the sheet as it advances into the atmosphere. They rapidly grow in size[36] until the thickening rims of adjacent holes coalesce to form threads of varying diameter. The threads finally break down into drops.

Disintegration can also occur through the superimposition of a wave motion on the sheet, as shown in Figure 16.19*c*. Sheets of liquid corresponding to half or full wavelengths of liquid are torn off and tend to draw up under the action of surface tension, although these may suffer disintegration by air action or liquid turbulence before a regular network of threads can be formed.

In a *pressure atomiser*, liquid is forced under pressure through an orifice, and the form of the resulting liquid sheet can be controlled by varying the direction of flow towards the orifice. By this method, flat and conical spray sheets can be produced. From the Bernoulli equation, given in Volume 1, Chapter 6, the mass rate of flow through a nozzle may be derived as:

$$G = C_D \rho A_N \sqrt{[2(-\Delta P)]\rho} \tag{16.30}$$

For a given nozzle and fluid, and an approximately constant coefficient of discharge, C_D, then:

$$G = \text{constant } \sqrt{(-\Delta P)} \tag{16.31}$$

The capacity of a nozzle is conveniently described by the *flow number*, **FN** a dimensional constant defined by:

$$\mathbf{FN} \equiv \frac{\text{Volumetric flow (gal/h)}}{\sqrt{\text{Pressure (lb/in}^2)}} = 2.08 \times 10^6 \frac{\text{Volume flow (m}^3/\text{s)}}{\sqrt{\text{Pressure (kN/m}^2)}} \tag{16.32}$$

This book belongs to Bradley Loren (bloren@mcandrews-ip.com) Copyright Elsevier 2024

Intas Exhibit 1032
Page 326 of 470
PGR2025-00043

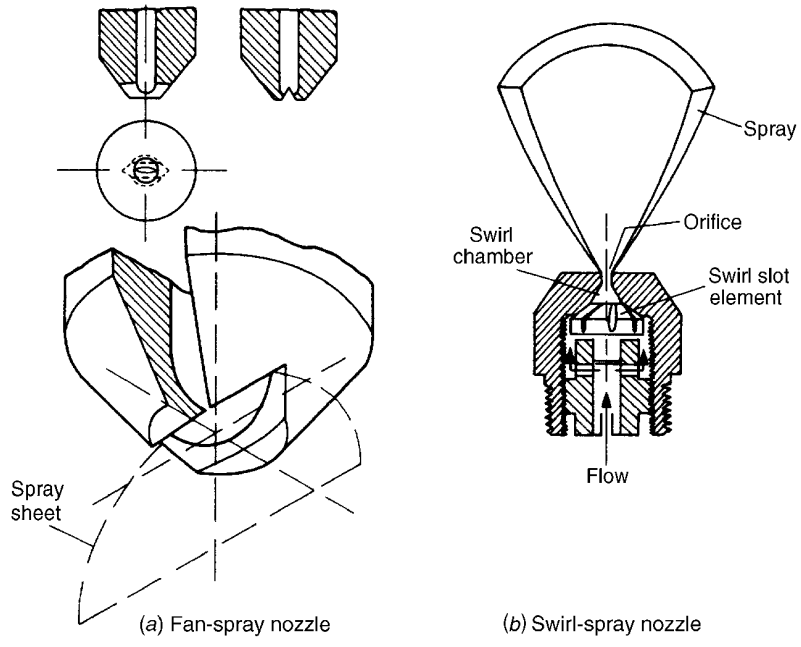


Figure 16.20. Pressure atomisers

In the fan-spray drop nozzle shown in Figure 16.20*a*, two streams of liquid are made to impinge behind an orifice by specially designed approach passages, and a sheet is formed in a plane perpendicular to the plane of the streams. The orifice runs full and, since the functional portion is sharp-edged, high discharge coefficients are obtained which are substantially constant over wide ranges of Reynolds number.

The influence of conditions on the droplet size where the spray sheet disintegrates through aerodynamic wave motion may be represented by the following expression proposed by DOMBROWSKI and MUNDAY[34] for ambient densities around normal atmospheric conditions:

$$d_m = \left(\frac{0.000156}{C_D}\right)\left[\frac{\mathbf{FN}\sigma\rho}{\sin\phi(-\Delta P)}\right]^{1/3}\rho_A^{-1/6} \tag{16.33}$$

where **FN** is given in equation 16.32, ϕ is the half-angle of the sheet, $-\Delta P$ is in kN/m^2 and all other quantities are expressed in SI units.

The principle of operation of the impinging jet nozzle resembles that of the fan spray nozzle with the exception that two or more independent jets are caused to impinge in the atmosphere. In impact atomisers, one jet is caused to strike against a solid surface, and for two jets impinging at 180°[34], using SI units:

$$d_m = 1.73\left(\frac{d_j^{0.75}}{u_l^{0.5}}\right)\left[\frac{\sigma}{\rho}\right]^{0.25} \tag{16.34}$$

This book belongs to Bradley Loren (bloren@mcandrews-ip.com) Copyright Elsevier 2024
Intas Exhibit 1032
Page 327 of 470
PGR2025-00043

With this atomiser, the drop size is effectively independent of viscosity, and the size spectrum is narrower than with other types of pressure nozzle.

When liquid is caused to flow through a narrow divergent annular orifice or around a pintle against a divergent surface on the end of the pintle, a conical sheet of liquid is produced where the liquid is flowing in radial lines. Such a sheet generally disintegrates by an aerodynamic wave motion. The angle of the cone and the root thickness of the sheet may be controlled by the divergence of the spreading surface and the width of the annulus. For small outputs this method is not so favourable because of difficulties in making an accurate annulus. A conical sheet is also produced when the liquid is caused to emerge from an orifice with a tangential or swirling velocity resulting from its path through one or more tangential or helical passages before the orifice. Figure 16.20*b* shows a typical nozzle used for a spray dryer. In such swirl-spray nozzles the rotational velocity is sufficiently high to cause the formation of an air core throughout the nozzle, resulting in low discharge coefficients for this type of atomiser.

Several empirical relations have been proposed to express drop size in terms of the operating variables. One suitable for small atomisers with 85° spray cone angles, at atmospheric pressure is[34]:

$$d_m = 0.0134 \left(\frac{\mathbf{FN}^{0.209} (\mu/\rho)^{0.215}}{(-\Delta P)^{0.348}} \right) \tag{16.35}$$

where $-\Delta P$ is in kN/m^2, **FN** is given in equation 16.32, and all other quantities are in SI units.

Pressure nozzles are somewhat inflexible since large ranges of flowrate require excessive variations in differential pressure. For example, for an atomiser operating satisfactorily at 275 kN/m^2, a pressure differential of 17.25 MN/m^2 is required to increase the flowrate to ten times its initial value. These limitations, inherent in all pressure-type nozzles, have been overcome in swirl spray nozzles by the development of spill, duplex, multi-orifice, and variable port atomisers, in which ratios of maximum to minimum outputs in excess of 50 can be easily achieved[34].

In a *rotary atomiser*, liquid is fed on to a rotating surface and spread out by centrifugal force. Under normal operating conditions the liquid extends from the periphery in the form of a thin sheet which breaks down some distance away from the periphery, either freely by aerodynamic action or by the action of an additional gas blast. Since the accelerating force can be controlled independently, this type of atomiser is extremely versatile and it can handle successfully a wide range of feed rates with liquids having a wide range of properties. The rotating component may be a simple flat disc though slippage may then occur, and consequently it is more usual to use bowls, vaned discs, and slotted wheels, as shown in Figure 16.21. Diameters are 25–460 mm and small discs rotate at up to 1000 Hz while the larger discs rotate at up to 200 Hz with capacities of 1.5 kg/s. Where a coaxial gas blast is used to effect atomisation, lower speeds of the order of 50 Hz may be used. At very low flowrates, such as 30 mg/s, the liquid spreads out towards the cup lip where it forms a ring. As liquid continues to flow into the ring, its inertia increases, overcomes the restraining surface tension and viscous forces and is centrifuged off as discrete drops of uniform size, which initially remain attached to the rim by a fine attenuating thread. When the drop is finally detached, the thread breaks down into a chain of small satellite drops.

This book belongs to Bradley Loren (bloren@mcandrews-ip.com) Copyright Elsevier 2024

Intas Exhibit 1032
Page 328 of 470
PGR2025-00043

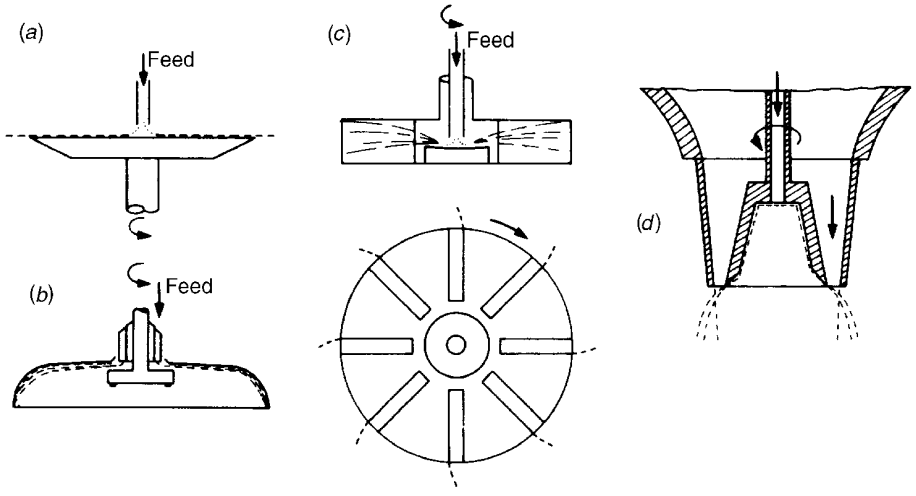


Figure 16.21. Characteristic rotary atomisers: (*a*) Sharp-edge flat disc; (*b*) Bowl; (*c*) Vaned disc; (*d*) Air-blast bowl atomiser

Since the satellite drops constitute only a small proportion of the total liquid flowrate, a cup operating under these conditions effectively produces a monodisperse spray. Under these conditions the drop size from sharp-edged discs has been given by WALTON and PREWETT[37] as:

$$d_m = \left(\frac{0.52}{N}\right)\sqrt{\left(\frac{\sigma}{D\rho}\right)} \tag{16.36}$$

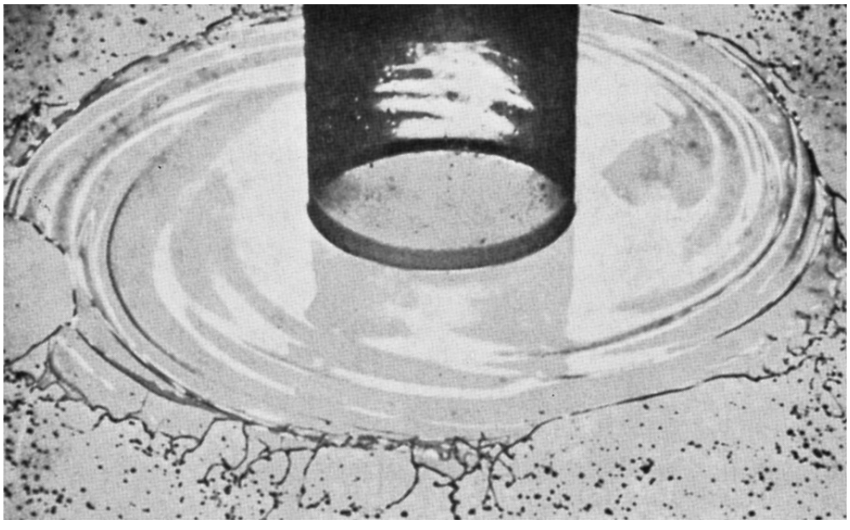
When the liquid flowrate is increased, the retaining threads grow in thickness and form long jets. As they extend into the atmosphere, these jets are stretched and finally break down into strings of drops. Under more practical ranges of flowrate, the jets are unable to remove all the liquid, the ring is forced away and a thin sheet extends around the cup lip and eventually breaks up into a polydisperse spray, as shown in Figure 16.22.

A far greater supply of energy for disintegration of the liquid jet can be provided by using a high-speed gas stream which impinges on a liquid jet or film. By this means a greater surface area is formed and drops of average size less than 20 μm can be produced. This is appreciably smaller than is possible by the methods previously described, although the energy requirements are much greater. The range of flowrates which can be used is wide, because the supply of liquid and the energy for atomisation can be controlled independently. Gas velocities ranging from 50 m/s to sonic velocity are common, and sometimes the gas is given a vortex motion.

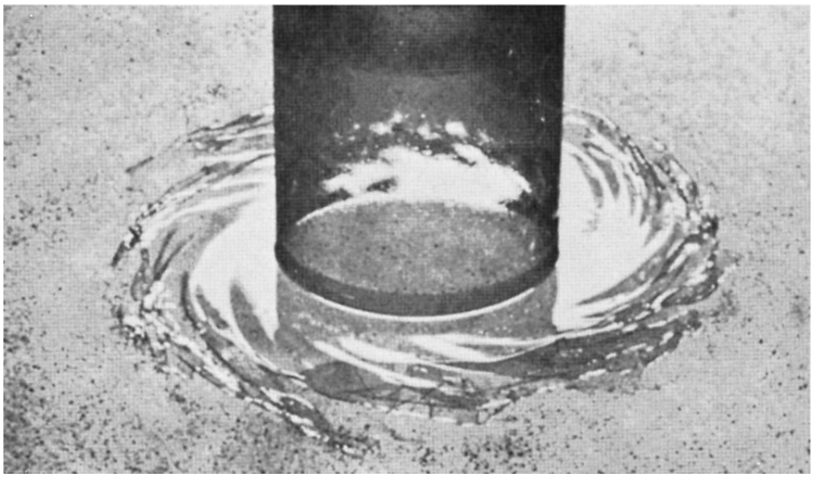
Break-up of the jet occurs as follows. Ligaments of liquid are torn off, which collapse to form drops. These may be subsequently blown out into films, which in turn further collapse to give a fine spray. Generally, this spray has a small cone angle and is capable of penetrating far greater distances than the pressure nozzle. Small atomisers of this type have been used in spray-drying units of low capacities.

This book belongs to Bradley Loren (bloren@mcandrews-ip.com) Copyright Elsevier 2024

Intas Exhibit 1032
Page 329 of 470
PGR2025-00043



(*a*) low speed



(*b*) high speed

Figure 16.22. Spray sheet from a rotating cup

Where the gas is impacted on to a liquid jet, the mean droplet size is given approximately by[34]:

$$d_s = \frac{0.585}{u_r}\sqrt{\left(\frac{\sigma}{\rho}\right)} + 0.0017\left(\frac{\mu}{\sqrt{(\sigma\rho)}}\right)^{0.45}\left(\frac{1000}{j}\right)^{1.5} \qquad (16.37)$$

This book belongs to Bradley Loren (bloren@mcandrews-ip.com) Copyright Elsevier 2024

Intas Exhibit 1032
Page 330 of 470
PGR2025-00043

where: d_s is the surface mean diameter (m),
j is the volumetric ratio of gas to liquid rates at the pressure of the surrounding atmosphere,
u_r is the velocity of the gas relative to the liquid (m/s),
μ is the liquid viscosity (Ns/m^2),
ρ is the liquid density (kg/m^3), and
σ is the surface tension (N/m).

As FRASER *et al.* point out, more efficient atomisation is achieved if the liquid is spread out into a film before impact[36].

Drying of drops

The amount of drying that a drop undergoes depends upon the rate of evaporation and the contact time, the latter depending upon the velocity of fall and the length of path through the dryer. The terminal velocity and the transfer rate depend upon the flow conditions around the drop. Because of the nature of the flow pattern, the latter also varies with angular position around the drop, although no practical design method has incorporated such detail and the drop is always treated as if it evaporates uniformly from all its surface.

There are two main periods of evaporation. When a drop is ejected from an atomiser its initial velocity relative to the surrounding gas is generally high and very high rates of transfer are achieved. The drop is rapidly decelerated to its terminal velocity, however, and the larger proportion of mass transfer takes place during the free-fall period. Little error is therefore incurred in basing the total evaporation time on this period.

An expression for the evaporation time for a pure liquid drop falling freely in air has been presented by MARSHALL[38,39]. For drop diameters less than 100 μm this may be simplified to give:

$$t = \frac{\rho\lambda(d_0^2 - d_t^2)}{8k_f\Delta T} \tag{16.38}$$

Sprays generally contain a wide range of drop sizes, and a stepwise procedure can be used[39] to determine the size spectrum as evaporation proceeds.

When single drops containing solids in suspension or solutions are suspended in hot gas streams, it is found that evaporation initially proceeds in accordance with equation 16.38 for pure liquid, although when solids deposition commences, a crust or solid film is rapidly formed which increases the resistance to transfer. Although this suggests the existence of a falling rate period similar to that found in tray-drying, the available published data indicate that it has little effect on the total drying time. As a result of crust formation, the dried particles may be in the form of hollow spheres.

Industrial spray dryers

Spray dryers are used in a variety of applications where a fairly high grade product is to be made in granular form. In the drying chamber the gas and liquid streams are brought into contact, and the efficiency of mixing depends upon the flow patterns induced in the chamber. Rotating disc atomisers are most commonly used. Countercurrent dryers give

This book belongs to Bradley Loren (bloren@mcandrews-ip.com) Copyright Elsevier 2024
Intas Exhibit 1032
Page 331 of 470
PGR2025-00043

the highest thermal efficiencies although product temperatures are higher in these units. This limits their use to materials which are not affected by overheating. Co-current dryers suffer from relatively low efficiencies, although they have the advantage of low product temperatures unless back-mixing occurs. In the case of materials which are extremely sensitive to heat, great care has to be taken in the design of the chamber to avoid overheating. Combustion gases are frequently used directly although, in some cases, such as the preparation of food products, indirectly heated air is used. Maximum temperatures are then normally limited to lower values than those with direct heating. Typical flow arrangements in spray drying are shown in Figure 16.23.

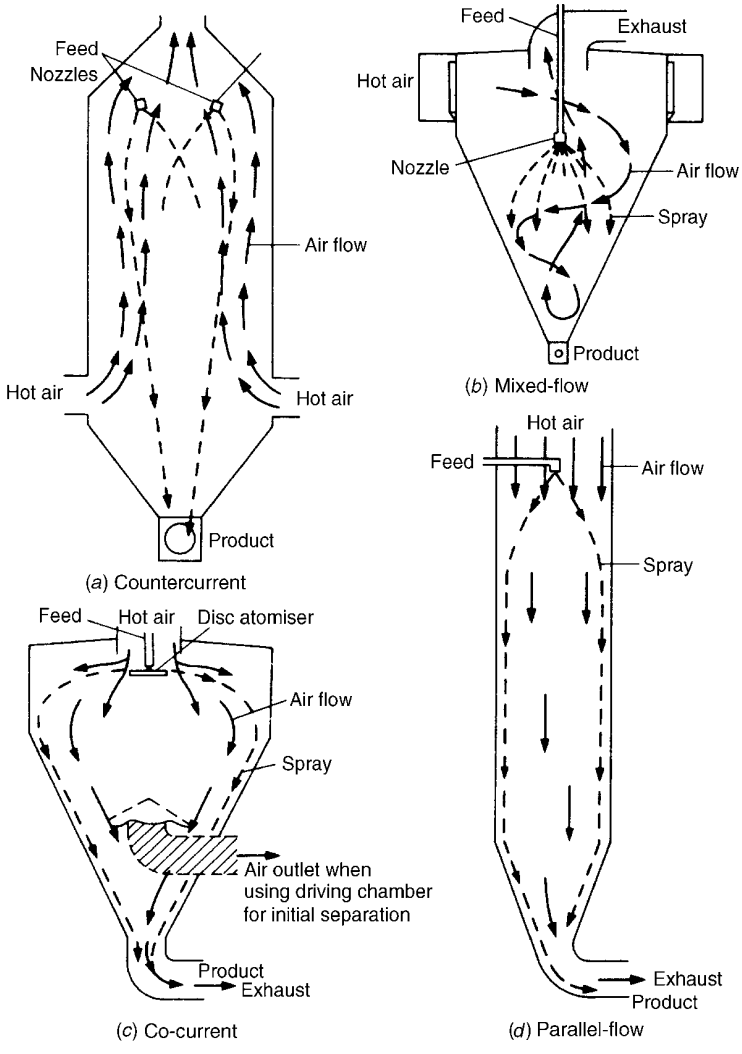


Figure 16.23. Flow arrangements in spray-drying[21]

This book belongs to Bradley Loren (bloren@mcandrews-ip.com) Copyright Elsevier 2024

Intas Exhibit 1032
Page 332 of 470
PGR2025-00043

The drying time and size of the particles are directly related to the droplet size, and therefore the initial formation of the spray is of great importance. The factors which govern the choice of atomisers for any specific drying application are principally dependent upon the characteristics of the liquid feed and upon the required drying characteristics of the drying chamber. A general guide is given in Table 16.5.

Table 16.5. Choice of atomiser

	Atomiser			
	Pressure	Rotary	Twin-fluid	Spinning-cup plus gas blast
Drying chamber				
Co-current	*	*	*	*
Countercurrent	*		*	
Feed				
Low viscosity solutions	*		*	
High viscosity solutions			*	*
Slurries		*	*	*
Pastes		*	*	*
Flexibility	Flowrate $\alpha\sqrt{(-\Delta P)}$	Flowrate independent of cup speed	Liquid flow independent of gas energy	Liquid flow independent of cup speed and gas energy

Pressure nozzles are most suited to low viscosity liquids and, where possible, viscous liquids should be preheated to ensure the minimum viscosity at the nozzle. Because of their simplicity, pressure nozzles are also employed to atomise viscous liquids with a kinematic viscosity up to 0.01 m^2/s, depending upon the nozzle capacity. Under these conditions, injection pressures of up to 50 MN/m^2 may be required to produce the required particle size. With slurries, the resulting high liquid velocities may cause severe erosion of the orifice and thus necessitate frequent replacement.

Spinning discs are very suitable for slurries and pastes, while high viscosity liquids tend to produce a stringy product. Care must also be taken in design to minimise incrustation around the lip and subsequent out-of-balance as drying takes place.

The simple gas atomiser is inherently fairly flexible although it has not yet found widespread application. This is a result of its tendency to produce a dusty product containing a large proportion of very small particles.

Often, little difficulty is experienced in removing the majority of the dried product, though in most cases the smaller particles that may be carried over in the exit gases must be reclaimed. Cyclones are the simplest form of separator though bag filters or even electrostatic precipitators may be required. With heat-sensitive materials, and in cases where sterility is of prime importance, more elaborate methods are required. For example, cooling streams of air may be used to aid the extraction of product while maintaining the required low temperature. Mechanical aids are often incorporated to prevent particles adhering to the chamber walls, and, in one design, the cooling air also operates a revolving device which sweeps the walls.

In some cases all the product is conveyed from the dryer by the exhaust gases and collected outside the drying chamber. This method is liable to cause breakage of the

This book belongs to Bradley Loren (bloren@mcandrews-ip.com) Copyright Elsevier 2024

Intas Exhibit 1032
Page 333 of 470
PGR2025-00043

particles though it is particularly suited for heat-sensitive materials which may deteriorate if left in contact with hot surfaces inside the dryer.

Spray drying has generally been regarded as a relatively expensive process, especially when indirect heating is used. The data given in Table 16.6 taken from GROSE and DUFFIELD[40] using 1990 costs, illustrate the cost penalties associated with indirect heating or with low inlet temperatures in direct heating.

Table 16.6. Operating costs for a spray dryer evaporating 0.28 kg/s (1 tonne/h) of water[40]

Basis: Air outlet temperature, 353 K
Cost of steam, £10/Mg
Cost of fuel oil, £150/Mg
Cost of power, £0.054/kWh (£15.0×10^{-6}/kJ)

	Air inlet temperature (K)	Steam flow (kg/s)	Oil flow (kg/s)	Power consumption (kW)	Cost (£/100 h)			Cost (£/Mg)
					Fuel	Power	Total	Total
Air heated:								
Indirectly	453	0.708	—	71	2550	384	2934	8150
Direct combustion	523	—	0.033	55	1800	296	2096	5820
Direct combustion	603	—	0.031	47	1650	254	1904	5300

QUINN[41] has drawn attention to the advantages with larger modern units using higher air inlet temperatures, 675 K for organic products and 925 K for inorganic products.

In spray dryers, using either a nozzle or rotating disc as the atomiser[41], volumetric evaporative capacities are 0.0003–0.0014 kg/m^3 s for cross-and co-current flows, with drying temperatures of 420–470 K. For handling large volumes of solutions, spray dryers are unsurpassed, and it is only at feed rates below 0.1 kg/s, that a drum dryer becomes more economic. Indeed the economy of spray drying improves with capacity until, at evaporative capacities of greater than 0.6 kg/s, the unit running cost is largely independent of scale.

In the jet spray dryer, cold feed is introduced[42] into preheated primary air which is blown through a nozzle at velocities up to 400 m/s. Very fine droplets are obtained with residence times of around 0.01 s, and an air temperature of 620 K. This equipment has been used for evaporating milk without adverse effect on flavour and, although operating costs are likely to be high, the system is well suited to the handling of heat-sensitive materials.

16.5.7. Pneumatic dryers

In pneumatic dryers, the material to be dried is kept in a state of fine division, so that the surface per unit volume is high and high rates of heat transfer are obtained. Solids are introduced into the dryer by some form of mechanical feeder, such as a rotating star wheel, or by an extrusion machine arranged with a high-speed guillotine to give short lengths of material, such as 5–10 mm. Hot gases from a furnace, or more frequently from an oil burner, are passed into the bottom of the dryer, and these pick up the particles and carry them up the column. The stream of particles leaves the dryer through a cyclone

This book belongs to Bradley Loren (bloren@mcandrews-ip.com) Copyright Elsevier 2024

Intas Exhibit 1032
Page 334 of 470
PGR2025-00043

separator and the hot gases pass out of the system. In some instances, final collection of the fine particles is by way of a series of bag filters. The time of contact of particles with the gases is small, typically 5 s, even with a lengthy duct — and the particle temperature does not approach the temperature of the hot gas stream. In some cases the material is recycled, especially where bound moisture is involved. Evaporative capacities, which are high, are greatly affected by the solids–air ratio. Typical thermal and power requirements are given by QUINN[43] as 4.5 MJ/kg moisture evaporated and 0.2 MJ/kg, respectively.

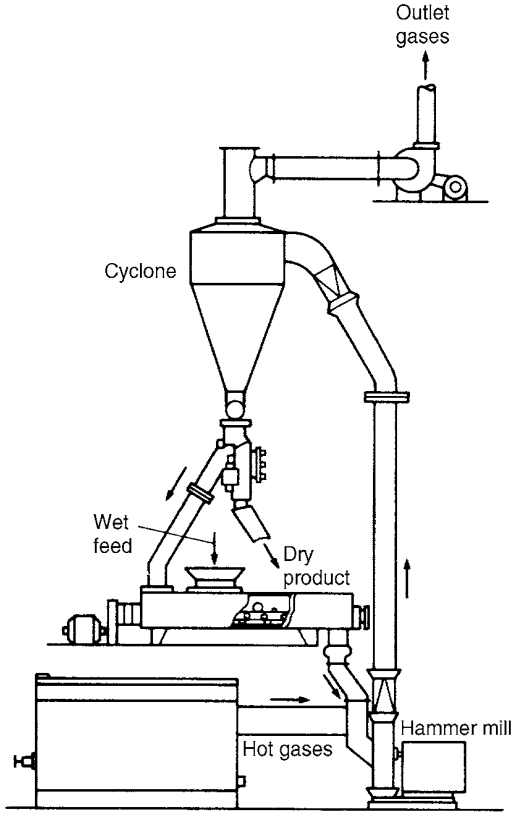


Figure 16.24. Air-lift dryer with an integral mill

A typical installation with the associated equipment is shown in Figure 16.24. Wet feed is delivered on to a bed of previously dried material in a double-paddle mixer to produce a friable mixture. This then passes to a cage mill where it comes into contact with hot gases from the furnace. Surface and some inherent moisture is immediately flash evaporated. The cage mill breaks up any agglomerates to ensure uniform drying of each individual particle. Gases and product are drawn up the drying column, where inherent moisture continues to be evaporated, before passing into the cyclone collector. Separated solids discharge through a rotary air lock into a dry divider which is set to recycle an

This book belongs to Bradley Loren (bloren@mcandrews-ip.com) Copyright Elsevier 2024
Intas Exhibit 1032
Page 335 of 470
PGR2025-00043

adequate percentage of solids for conditioning the new wet feed in the double paddle mixer. Gases from the cyclone are vented to atmosphere through a suitable dust collector or wet scrubber. The system operates under suction and dust is therefore reduced to a minimum. A direct oil or gas fired furnace is generally employed and the heat input is controlled according to the vent stack gas temperature. Indirect heating may be used where contamination of the product is undesirable.

Materials handled include food products, chalk, coal, organic chemicals, clays, spent coffee grounds, sewage sludge and chicken manure. Where exhaust gases have unpleasant odours, after-burners can be supplied to raise the temperature and burn off the organic and particulate content causing the problem.

Convex dryers are continuously operating pneumatic dryers with an inherent classifying action in the drying chamber which gives residence times for the individual particles differing according to particle size and moisture content. Such units offer the processing advantages of short-time, co-current dryers and are used primarily for drying reasonably to highly free-flowing moist products that can be conveyed pneumatically and do not tend to stick together. By virtue of the pronounced classifying action, such dryers are also well suited to the drying of thermally sensitive moist materials with widely differing particle sizes where the large particles have to be completely dried without any overheating of the small ones. Basically, this form of pneumatic dryer consists of a truncated cyclone with a bottom outlet that acts as a combined classifier and dryer.

16.5.8. Fluidised bed dryers

The principles of fluidisation, discussed in Chapter 6, are applied in this type of dryer, shown typically in Figure 16.25. Heated air, or hot gas from a burner, is passed by way of a plenum chamber and a diffuser plate, fitted with suitable nozzles to prevent any back-flow of solids, into the fluidised bed of material, from which it passes to a dust separator. Wet material is fed continuously into the bed through a rotary valve, and this mixes immediately with the dry charge. Dry material overflows through a downcomer to an integral after-cooler. An alternative design of this type of dryer is one in which a thin bed is used.

QUINN[43] points out that, whilst it would seem impossible to obtain very low product moisture levels when the incoming feed is very wet and at the same time ensure that the feed point is well away from the discharge point, this is not borne out by operating experience. Mixing in the bed is so rapid that it may be regarded as homogeneous, and baffles or physical separation between feed and discharge points are largely ineffective. The very high mass-transfer rates achieved make it possible to maintain the whole bed in a dry condition. Some rectangular fluidised-bed dryers have separately fluidised compartments through which the solids move in sequence. The residence time is very similar for all particles and the units, known as *plug-flow* dryers, often employ cold air to effect product cooling in the last stage.

Many large-scale uses include the drying of fertilisers, plastics materials, foundry sand, and inorganic salts, and AGARWAL, DAVIS, and KING[44] describe a plant consisting of two units, each drying 10.5 kg/s of fine coal. Small fluidised-bed dryers also find use in, for example, the drying of tablet granulations in the pharmaceutical industry[45].

This book belongs to Bradley Loren (bloren@mcandrews-ip.com) Copyright Elsevier 2024

Intas Exhibit 1032
Page 336 of 470
PGR2025-00043

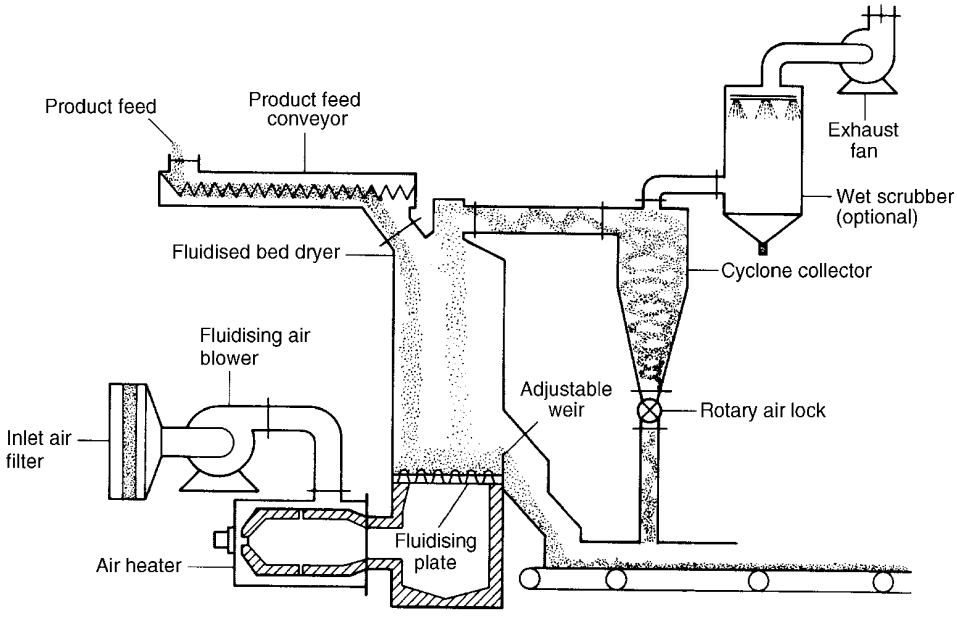


Figure 16.25. Flow diagram for a typical continuous fluidised-bed dryer

Dryers with grid areas of up to 14 m^2 have been built[46] and evaporative capacities vary from 0.02 kg/s m^2 grid area for the low-temperature drying of food grains to 0.3 kg/s m^2 for the drying of pulverised coal by direct contact with flue gases[44]. Specific air rates are usually 0.5–2.0 kg/s m^2 grid area and the total energy demand is 2.5–7.5 MJ/kg moisture evaporated. The exit gas is nearly always saturated with vapour for all allowable fluidisation velocities.

The choice between spray, pneumatic and fluidised dryers depends very much on the properties of the particles and some guidance in this respect is given in Table 16.7.

Table 16.7. Selection of spray, pneumatic and fluidised-bed dryers

Particle property	Spray dryer	Pneumatic dryer	Fluidised-bed dryer
Initial moisture greater than 80 per cent	Yes	No	No
Too dry to pump	No	Yes	Yes
Wet enough to pump but moisture less than 80 per cent	Yes	Yes	No
Solids in dissolved state	Yes	No	No
Partially dry but sticky particles	Yes	No	No
Fragile particles	Yes	No	Possible
Very small particles	Yes	Yes	No
Residence time (s)	3–10	1–10, often less than 1	Widely variable, greater than 10
Heat sensitive material	Yes	Yes	No
Relative drying speed	Third	First	Second

This book belongs to Bradley Loren (bloren@mcandrews-ip.com) Copyright Elsevier 2024
Intas Exhibit 1032
Page 337 of 470
PGR2025-00043

Design considerations

A simple, concise method for the preliminary sizing of a fluidised bed dryer has been proposed by CLARK[47] and this is now considered.

The minimum bed diameter is a function of the operating velocity, the particle characteristics and the humidity of the drying gas. The hot gas at the inlet rapidly loses heat and gains moisture as it passes through the bed which it eventually leaves at the bed temperature T_b and with a relative humidity $\mathscr{R}$, which is approximately equal to the relative humidity which would be in equilibrium with the dried product at the bed temperature. The operating velocity may be taken as twice the minimum fluidising velocity, obtained from the equations in Section 6.1.3, by laboratory tests, or more conveniently from Figure 16.26.

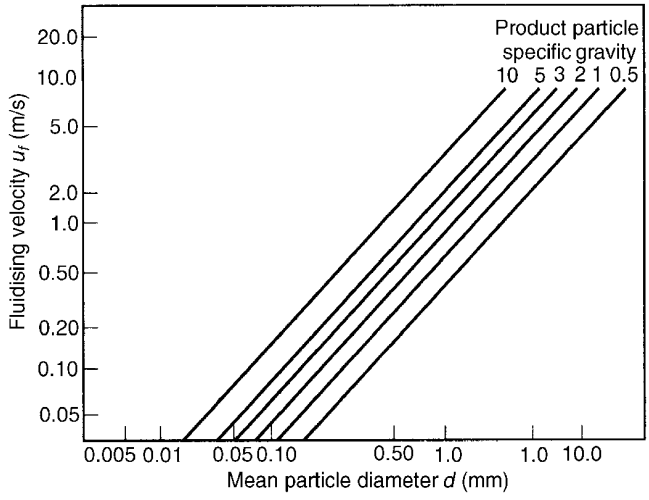


Figure 16.26. Superficial operating velocity in fluidised bed dryers[47]

For drying media other than air at approximately atmospheric pressure, the velocity obtained from Figure 16.26 should be multiplied by $0.00975\ \rho^{-0.29}\mu^{-0.43}$ where ρ and μ are the density (kg/m^3) and the viscosity (Ns/m^2) of the fluidising gas.

From a mass balance across the bed:

$$(\mathscr{R}100)(P_w/P) = [W + (G/(1+\mathscr{H}).\mathscr{H}]\big/[W + (G/(1+\mathscr{H})(0.625+\mathscr{H})] \quad (16.39)$$

where: $\mathscr{R}$ = exit gas relative humidity (per cent),
P_w = vapour pressure of water at the exit gas temperature (N/m^2),
P = total static pressure of gases leaving the bed (N/m^2),
W = evaporative capacity (kg/s),
G = inlet flow of air (kg/s), and
$\mathscr{H}$ = humidity of inlet air (kg/kg dry air)

This book belongs to Bradley Loren (bloren@mcandrews-ip.com) Copyright Elsevier 2024
Intas Exhibit 1032
Page 338 of 470
PGR2025-00043

The term $G/(1+\mathscr{H})$ is in effect the flow of dry air, and 0.625 is approximately the ratio of molecular masses in the case of water and air.

Values of P_w may be obtained from Figure 16.27 and, for indirect heating, $\mathscr{H}$ is the humidity of the ambient air. For direct heating, $\mathscr{H}$ may be obtained from Figure 16.28 which assumes that the air at 293 K, with a humidity of 0.01 kg/kg, is heated by the combustion of methane.

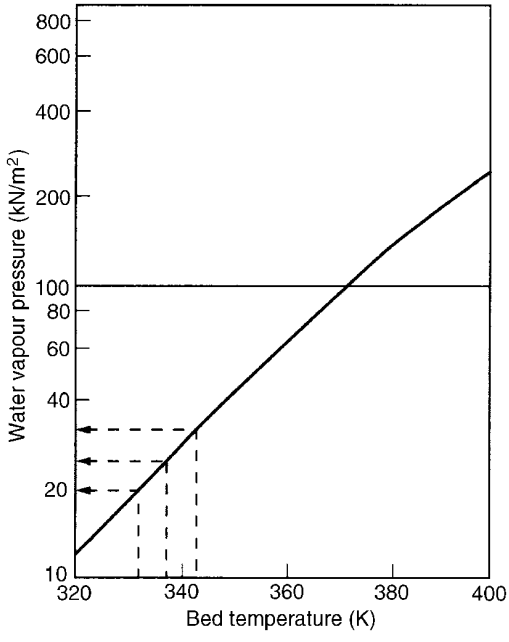


Figure 16.27. Water vapour pressure at the bed exit[47]

A heat balance (in W) across the bed gives:

$$C_m G(T_m - T_b) = \lambda_b W + C_f F(T_b - T_f) \tag{16.40}$$

where:
C_m = mean thermal capacity of the gas between T_m and T_b (J/kg deg K) (1000 J/kg deg K for air),
$C_f = [(X_f c_x + c_s)/(X_f + 1)]$ average thermal capacity of the wet solid between T_f and T_b (J/kg deg K),
X_f = moisture content of wet feed (kg/kg dry solid),
C_x = heat capacity of liquid being evaporated (J/kg deg K),
C_s = heat capacity of dry solid (J/kg deg K),
λ_b = mean latent heat of liquid at T_b (J/kg),
T_m, T_b, T_f = temperatures of inlet gas, bed and wet feed respectively (K), and
F = rate of wet solid feed (kg/s)

This book belongs to Bradley Loren (bloren@mcandrews-ip.com) Copyright Elsevier 2024
Intas Exhibit 1032
Page 339 of 470
PGR2025-00043

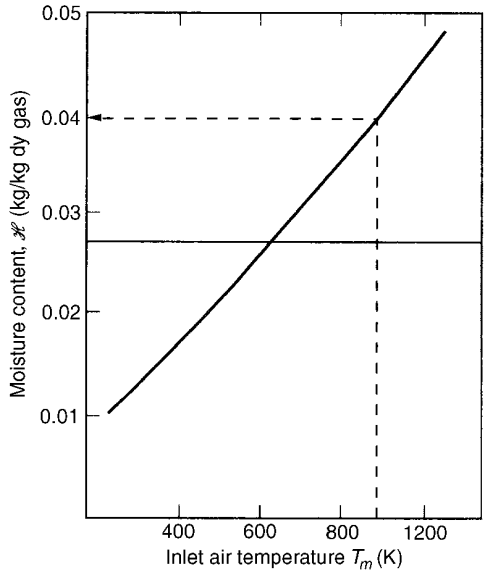


Figure 16.28. Moisture content of the inlet air[47]

Values of G and T_b are obtained from equations 16.39 and 16.40 and the bed diameter is then obtained from:

$$D^2 = \frac{(G + 1.58\ W)T_b}{278u_f}\ \text{m}^2 \tag{16.41}$$

noting that : $$\frac{\text{Mean molecular weight of inlet air}}{\text{molecular weight of water}} = \frac{29}{18} \approx 1.58$$

and:

$$\frac{\pi}{4}\left\{\frac{(\text{molecular weight or air}) \times (\text{datum temperature})}{\text{kilomolecular volume}}\right\} = \frac{\pi}{4}\left(\frac{29 \times 273}{22.4}\right)$$

$$= 278 \text{ kg deg K/m}^3$$

Example 16.6

A granular material of density 5000 kg/m^3 is to be dried in a fluidised bed dryer using directly heated air at 811 K. The particle size is 0.5 mm and 1.26 kg/s of water is to be removed from 12.6 kg/s of solid feed at 293 K. What diameter of bed should be specified?

$\lambda_b = 2325$ kJ/kg, ambient air is at 293 K, $\mathscr{H} = 0.01$ kg/kg and $C_f = 1.67$ kJ/kg deg K

Solution

From Figure 16.28: $\mathscr{H} = 0.036$ kg/kg at 811 K

This book belongs to Bradley Loren (bloren@mcandrews-ip.com) Copyright Elsevier 2024

Intas Exhibit 1032
Page 340 of 470
PGR2025-00043

and the right-hand side of equation 16.39 is:

$$= (1.26 + 0.0347\ G)/(1.26 + 0.638\ G)$$

Taking $\mathscr{R}$ as 90 per cent and P as 101.3 kN/m^2, then, for assumed values of T_b of 321, 333 and 344 K:

$$P_w = 13, 20 \text{ and } 32 \text{ kN/m}^2, \text{ respectively}$$

and:
$$G = 27.8, 12.9 \text{ and } 6.02 \text{ kg/s, respectively.}$$

Using equation 16.40, for $T_b = 321$, 333 and 344 K,

$$G = 7.16, 7.8 \text{ and } 7.54 \text{ kg/s respectively.}$$

Plotting G against T_b for each equation on the same axis, then:

$$G = 8.3 \text{ kg/s when } T_b = 340 \text{ K.}$$

From Figure 16.27, $u_f = 0.61$ m/s. Hence, in equation 16.41:

$$D^2 = 340(8.3 + (1.58 \times 1.26))/(278 \times 0.61)$$

and:
$$\underline{\underline{D = 4.60 \text{ m}}}$$

This is a very large diameter bed and it may be worthwhile increasing the fluidising velocity provided any increased elutriation is acceptable. If u_f is increased to 1.52 m, the diameter then becomes 2.88 m with a subsequent reduction in capital costs.

One development in the field of fluidised bed drying is what is known as *sub-fluidised conditioning*. A fluidised-bed dryer normally works with a maximum residence time of some 1200 s. If this is increased, then the spread of product residence times increases excessively due to the fact that axial and longitudinal mixing occur in the bed during the fluidisation process and, the more vigorous the fluidisation, the greater the spread of residence times. If fluidisation continues for too long, breakage and other product damage is likely to occur. A solution to this problem, developed by Ventilex, is sub-fluidised conditioning where forward movement of the product is created by a shaking mechanism in which the product is kept at the threshold of fluidisation. As a result, there is little or no axial or longitudinal mixing and the spread of residence time is kept to a minimum. In essence, this process provides a situation which approaches that of ideal plug flow, and many products can be conditioned by this combination of fluidised and sub-fluidised techniques. In addition, even less air is required for drying and thus small auxiliary equipment is required and energy requirements are less. Nominal bed thicknesses are 150–250 mm and long residence times, of up to 7 ks, are possible with a minimal time spread. In the drying of drugs, nuts, meats and rice, no degradation takes place and, in this respect, the process is comparable with traditional installations such as conveyor dryers, with the added benefits of fluidisation. The system is also applicable to the drying of minerals such as china clay and sand, and also to animal wastes and sludges. A typical installation together with a flow diagram is shown in Figure 16.29.

This book belongs to Bradley Loren (bloren@mcandrews-ip.com) Copyright Elsevier 2024

Intas Exhibit 1032
Page 341 of 470
PGR2025-00043

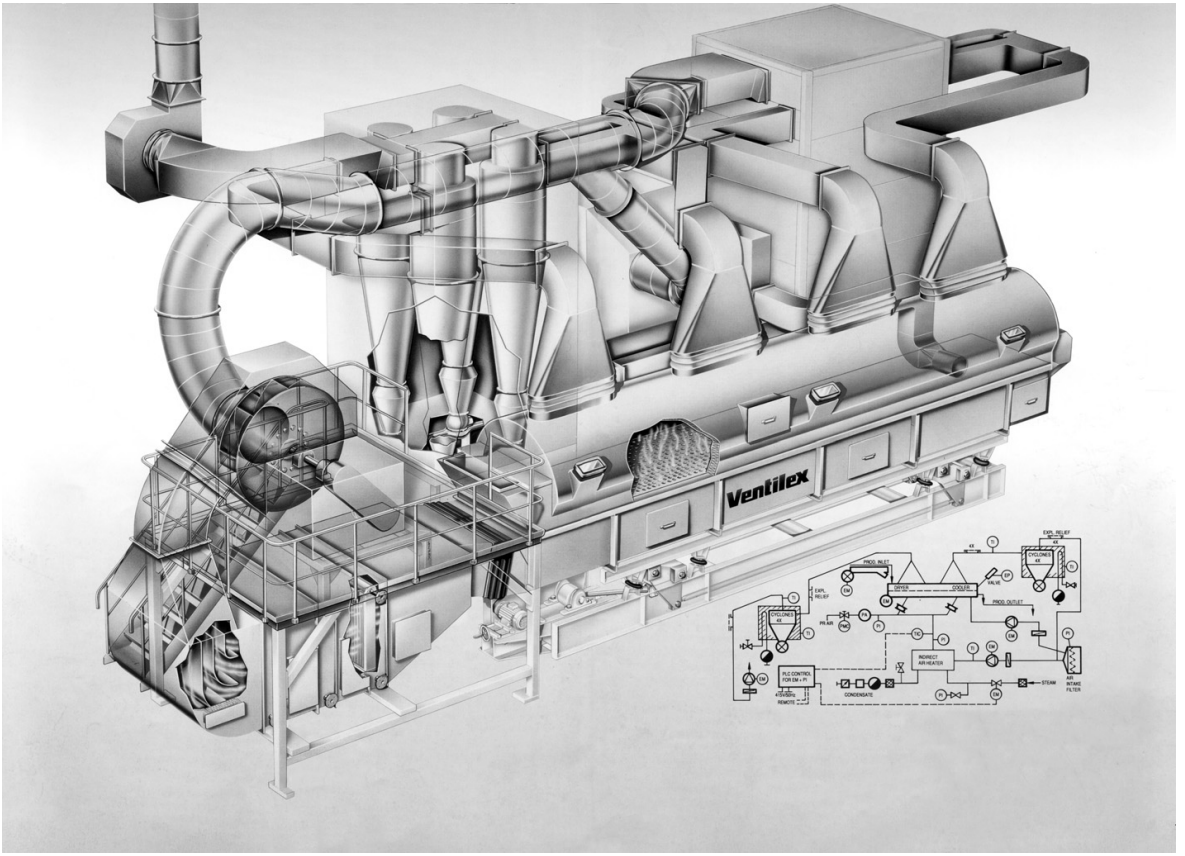


Figure 16.29. Unit for sub-fluidised drying

This book belongs to Bradley Loren (bloren@mcandrews-ip.com)

Copyright Elsevier 2024

Intas Exhibit 1032
Page 342 of 470
PGR2025-00043

16.5.9. Turbo-shelf dryers

The handling of sticky materials can present difficulties, and one type of dryer which is useful for this type of material is the turbo-dryer. As shown in Figure 16.30, wet solid is fed in a thin layer to the top member of a series of annular shelves each made of a number of segmental plates with slots between them. These shelves rotate and, by means of suitably placed arms, the material is pushed through a slot on to a shelf below. After repeated movements, the solid leaves at the bottom of the dryer. The shelves are heated by a row of steam pipes, and in the centre there are three or more fans which suck the hot air over the material and remove it at the top.

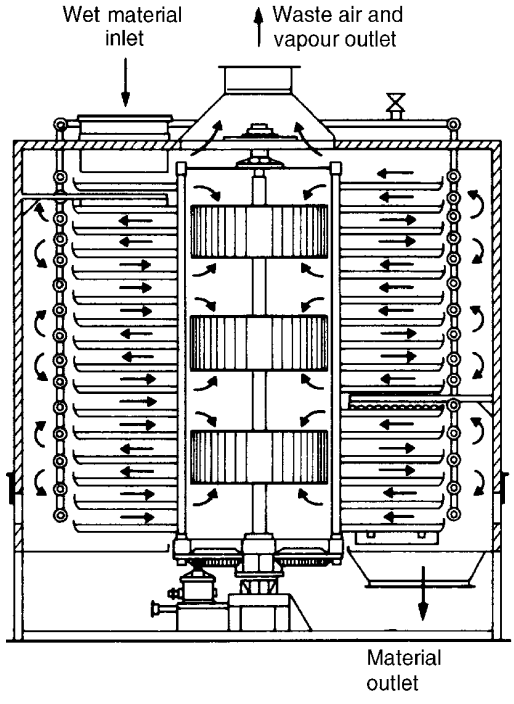


Figure 16.30. Turbo-shelf dryer

The accelerated drying induced by the raking of the material gives evaporative capacities of 0.0002–0.0014 kg/s m^2 shelf area which are comparable with those obtained by through circulation on perforated belts. Shelf areas are 0.7–200 m^2 in a single unit and the dryer may easily be converted to closed-circuit operation, either to prevent emission of fumes or in order to recover valuable solvents. Typical air velocities are 0.6–2.5 m/s, and the lower trays are often used to cool the dry solids. A turbo-dryer combines cross-circulation drying, as in a tray dryer, with drying by showering the particles through the hot air as they tumble from one tray to another.

This book belongs to Bradley Loren (bloren@mcandrews-ip.com) Copyright Elsevier 2024
Intas Exhibit 1032
Page 343 of 470
PGR2025-00043

16.5.10. Disc dryers

A disc dryer provides a further way in which pasty and sticky materials may be handled, and it can also cope satisfactorily with materials which tend to form a hard crust or pass through a rheologically-difficult phase during the drying operation.

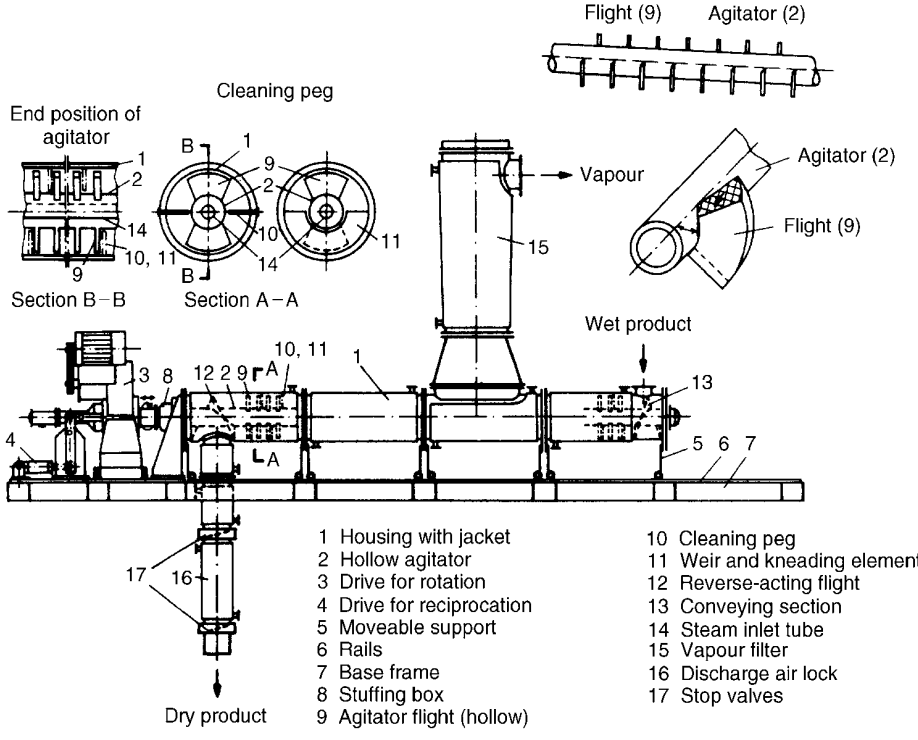


Figure 16.31. Arrangement of a disc dryer

As shown in Figure 16.31, a single-agitator disc contact dryer, consists of a heated cylindrical housing (1) assembled from unit sections, and a heated hollow agitating rotor (2) which has a simultaneous rotating and oscillating movement produced by means of a rotating drive (3) and a reciprocating drive (4). The drive (3 and 4) and stuffing box (8) are located at the dry product end, and the stuffing box is protected by a reverse acting flight (12). The wet product is introduced, drawn in by the screw flight (13) and continuously conveyed through the dryer. The vapour passes through the vapour filter (15) to the condenser. This vapour filter system has a back-scavenging action, and is specially designed for removing dust from vapour in vacuum drying plants. The hollow agitator (2) is fitted, over its whole length, with heated flights, which are arranged equidistantly in pairs. Between every two axially neighbouring agitator flights, there are, projecting inwards from the housing fixed wiping pegs (10) or annular weir/kneading elements (11) which extend inward to the agitator core.

This book belongs to Bradley Loren (bloren@mcandrews-ip.com) Copyright Elsevier 2024
Intas Exhibit 1032
Page 344 of 470
PGR2025-00043

The self-cleaning of the heating surfaces is achieved by the combined rotating-reciprocating movement of the agitator. The stationary elements (10 and 11) clean the faces of the agitator flights, at the end of each oscillating movement, during one rotation of the agitator. By the forward and backward movement, the edges of the agitator flights (9) clean the inner surface of the housing and the fixed elements projecting inwards to the core of the agitator clean the agitator (2). In all, about 95 per cent of the heating surface is cleaned.

The rotating and reciprocating motions need not be synchronised, because the individual agitator flights (9) oscillate only between two adjacent fixed elements (10 and 11). This is so that the speed of rotation, the frequency of reciprocation and the forward and backward speed of reciprocation can be adjusted independently of one another over a wide range of settings. The housing sections (1) which are supported by frames (5) on rails, can be drawn forward when cleaning is necessary. The transport of pasty products through the dryer may be achieved by the differential forward and backward oscillatory motion, combined with the action of the bevelled edges of the agitator flights.

Contivac dryers, for example, have heating surfaces of 4–60 m^2 and volumes of 0.1–3 m^3. They may be operated under vacuum or up to 400 kN/m^2 with heating fluids at 330 K–670 K. The evaporative capacity is 0.03–0.55 kg/s and the agitator speed ranges from 0.1 Hz (6 rpm) for rheologically difficult materials, to 1 Hz (60 rpm) for easier applications.

Operating on a similar principle is the *Buss paddle* dryer which effects batch drying of liquids, pasty and sandy materials. The paddle dryer, which is the main element of the drying unit. It consists of a horizontal, cylindrical housing which contains a paddle agitator in the form of a hollow shaft carrying agitator arms. The jacket, the hollow shaft and the agitator arms are steam-heated. The paddle agitator is driven by an electric motor and gear unit. A built-on torque bracket with a microswitch protects the paddle agitator against overloading. The product to be dried is passed through the charging nozzle into the paddle dryer, where it is distributed uniformly by the rotating paddle agitator. The drying proceeds under vacuum while intensive intermixing by the agitator causes continual renewal of the product particles in contact with the heated surfaces. This guarantees efficient heat transfer and uniform product quality. Vapours are purged of dust in passing through a vapour filter and are then fed to a condenser. Non-condensable gases are drawn off by the vacuum system. The vapour filter is equipped with a removable filter insert and, to prevent excessive pressure drop across the fabric from thick, and possibly moist dust build-up on the filter sacks, these are provided with a reverse jet arrangement, that is the individual filter sacks are cleaned in turn automatically during operation by short though powerful countercurrent blasts of steam blown through the filter sack. This serves to blow and shake off the dust layer and keep the filter sack dry. After the drying process is complete, the dried material may be cooled by applying cooling water to the dryer jacket and paddle agitator. The dryer is emptied by the arms of the paddle agitator, which are designed to move the material in the vessel towards the outlet when rotated backwards. The discharge outlet is specially constructed to prevent the formation of a plug of material. At 373 K, an evaporation rate of over 4 g/s m^2 can be achieved for a steam consumption of 1.5 kg/kg of evaporated water.

This book belongs to Bradley Loren (bloren@mcandrews-ip.com) Copyright Elsevier 2024

Intas Exhibit 1032
Page 345 of 470
PGR2025-00043

16.5.11. Centrifuge dryers

Where a product of a high quality and purity is required, this can, in many cases, be achieved only by washing the solids during a centrifugation process in order to flush out the suspension mother liquor or to dissolve salt crystals. The washed crystals are then usually dried in a separate physical unit operation involving different equipment and problems can be encountered due to the exposure to the atmosphere of the wet cake as it is transferred between the centrifuge and the dryer. These problems may be largely eliminated by using a combined centrifuge–dryer which it is claimed, has the following advantages:

(a) It is hermetically sealed from the environment and is therefore easy to inert.
(b) There is no human contact with the product at any stage of the operation and no possibility of foreign materials being introduced.
(c) The handling of the product is simple and gentle.
(d) Drying times can be reduced by using a jet-pulsed bed drying technique.
(e) The unit can be emptied completely with no residual cake in the basket or on the wall of the drum.

All these advantages are inherent in the FIMA, TZT centrifuge–dryer which is operated as follows.

The feed suspension is introduced into the centrifuge through a hollow drive shaft, and the liquid from the suspension is separated from the crystals and discharged from a sealed filter basket by passing it though a metal filter which retains the solids inside a sealed chamber. Any contaminants are then washed away from the filling pipe, the centrifuge basket and the separated solids by introducing wash liquid through the hollow drive shaft. This operation may be repeated as required. One advantage of the TZT system is that, with no internal pipes or structures that might accumulate unwashed solids, all the separated solids make contact with the wash water. The ring of separated solids is then removed from the wall of the centrifuge by introducing powerful gas blasts beneath the filter medium and the wet en-masse solids accumulate at the bottom of the filter drum. The drying process is achieved by rotating the drum at slow speeds and injecting heated drying gas as process into the closed centrifuge chamber. The moisture-laden gas leaves passing through the filter medium so that the solids are retained within the basket. Such a process is extremely gentle to the solids and dries at low product temperatures even when using higher gas temperatures as a result of the cooling effect of the surface evaporation of the moisture. Dry powder is discharged from the unit by opening the sealing centrifuge housing and fluidising the solids which then enter an integrated powder conveying system. In this system the gas used for drying may be recycled in a closed gas loop, or it may be discharged to atmosphere in an open system.

Units of this type have a capacity of 20–400 kg in terms of filling mass, filter areas of 0.37–2.4 m^2 and drum diameters of 400–1300 mm and lengths of 300–600 mm.

Although this is, in essence a batch operation, close reproducibility between batches overcomes many of the problems associated with batch identification which can be a problem with more conventional drying equipment.

This book belongs to Bradley Loren (bloren@mcandrews-ip.com) Copyright Elsevier 2024

Intas Exhibit 1032
Page 346 of 470
PGR2025-00043

16.6. SPECIALISED DRYING METHODS

16.6.1. Solvent drying

Two processes are used here:

Superheated-solvent drying in which a material containing non-aqueous moisture is dried by contact with superheated vapours of its own associated liquid, and,

Solvent dehydration in which water-wet substances are exposed to an atmosphere of a saturated organic solvent vapour.

The first of these has advantages where a material containing a flammable liquid such as butanol is involved. Drying is effected with a gas with an air–moisture ratio of 90 kg/kg moisture in order to ensure that the composition is well below the lower explosive limit. The heat requirement is as great as those for superheated solvent drying at the same gas outlet temperature of 400 K[48]. Superheated solvent drying in a fluidised bed has been used for the drying of polypropylene pellets to eliminate the need for water-washing and for fractionating. A flowsheet of the installation is shown[49] in Figure 16.32.

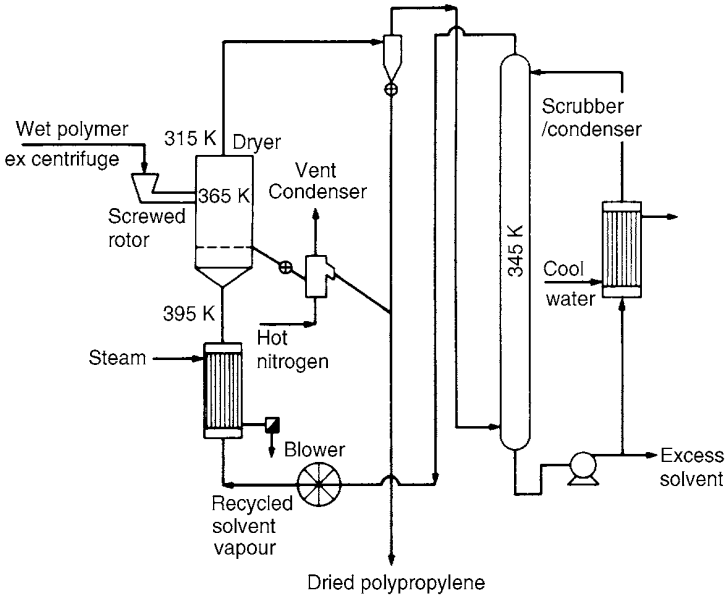


Figure 16.32. Flowsheet for drying polypropylene by fluidising with a hot stream of solvent vapour[49]

The most important applications of solvent dehydration lie within the field of kiln drying for seasoning timber where substantial reductions in drying times have been achieved[50].

16.6.2. Superheated steam drying

The replacement of air by superheated steam to take up evaporating moisture is attractive in that it provides a high temperature heat source which also gives rise to a much higher

This book belongs to Bradley Loren (bloren@mcandrews-ip.com) Copyright Elsevier 2024

Intas Exhibit 1032
Page 347 of 470
PGR2025-00043

driving force for mass transfer since it does not become saturated at relatively low moisture contents as is the case with air. In the drying of foodstuffs, a further advantage is the fact that the steam is completely clean and there is much less oxidation damage. In the seasoning of timber, for example, drying times can be reduced quite significantly. Although the principles involved have been understood for some considerable time, as BASEL and GRAY[49] points out, applications have been limited to due to corrosion problems and the lack of suitable equipment. A flowsheet of a batch dryer using superheated steam is shown in Figure 16.33. The dryer is initially filled with air circulated by a blower, together with evaporated moisture. Any excess moisture is vented to atmosphere so that the air is gradually replaced by steam. For an evaporation rate of 10 kg/m^3 volume of the dryer chamber, the composition of the gas phase would reach about 90 per cent steam in about 600 s.

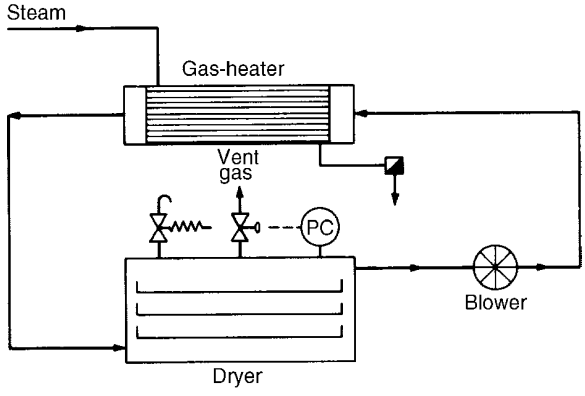


Figure 16.33. Superheated-steam dryer

As LUIKOV[51] reports, superheated steam drying may also be used to dry wet material by heating it in a sealed autoclave, and periodically releasing the steam which is generated. This pressure release causes flash evaporation of moisture throughout the whole extent of the material, thus avoiding drying stresses and severe moisture gradients. Such an operation has been applied to the drying of thermal insulating materials by BOND *et al.*[52] who have investigated the drying of paper. In this work, impinging jets of superheated steam were used at 293–740 K during the constant drying period, with jet Reynolds numbers, 100–12000. Above 450 K, steam drying was found to be much faster than air drying for the same mass velocity of gas. The specific blower power was found to be much lower than for air drying at temperatures of industrial importance. It was concluded that steam-impingement drying can lead to significant reductions in both capital investment and energy costs.

In tests on the drying of sand, WENZEL and WHITE[53] found that the use of steam rather than air did not alter the general characteristics of the drying process, and that the drying rate during the constant rate period was determined by the heat transfer rate. In these tests, the heat transferred by radiation from the steam and surrounding surfaces was 7.5–31

This book belongs to Bradley Loren (bloren@mcandrews-ip.com) Copyright Elsevier 2024
Intas Exhibit 1032
Page 348 of 470
PGR2025-00043

per cent of the total heat transferred, and coefficients of convective heat transfer were 13–100 W/m^{2}K. It was concluded that higher drying rates and greater thermal efficiencies are possible when drying with superheated steam as opposed to air, and that the choice of steam drying must depend on a balance between the savings in operating costs and the higher capital investment attributable to the higher temperatures and pressures.

SCHWARTZE and BRÖCKER[54], who has made a theoretical study of the evaporation of water into mixtures of superheated steam and air, has calculated the inversion temperature above which the evaporation rate into pure superheated steam is higher than that into dry air under otherwise similar conditions. The data obtained are given in Figure 16.34 which shows quite clearly the enhanced evaporation rates at gas temperatures above about 475 K. This inversion temperature is given by the point of intersection of the curves for evaporation rate with dry air and superheated steam. The Nusselt and Sherwood equations for heat and mass transfer coefficients for the relevant geometrical configuration, given in Volume 1, were used to calculate the evaporation rates, and these were found to be in excellent agreement with experimental data in the literature. TAYLOR and KRISHNA[55] points out that this approach may be used for a wide range of applications, and VIDAURRE and MARTINEZ[56] show that the model may be extended to include specialised applications, such as the evaporation of multicomponent liquids.

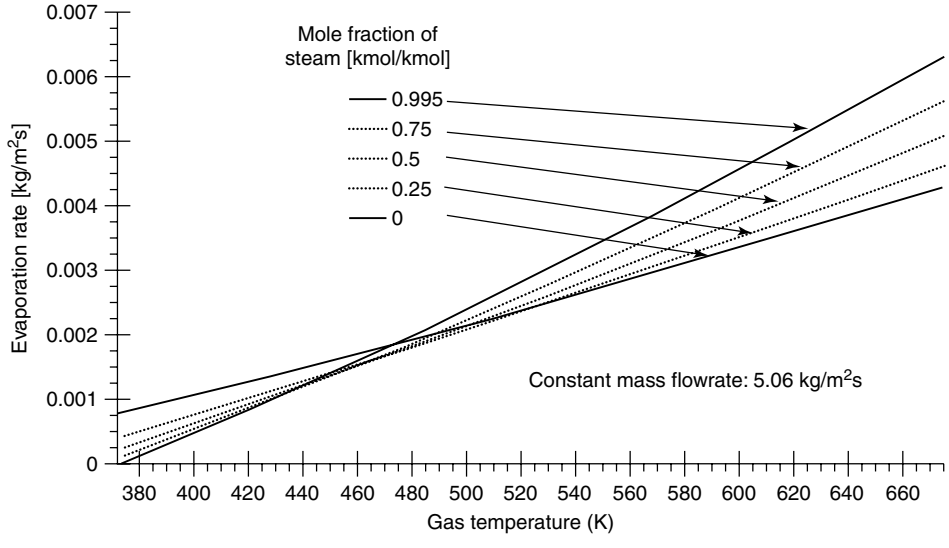


Figure 16.34. Inversion temperature with superheated steam drying[54]

16.6.3. Freeze drying

In this process, the material is first frozen and then dried by sublimation in a very high vacuum, 10–40 N/m^2, at a temperature of 240–260 K. During the sublimation of the ice, a dry surface layer is left, though this is not free to move because it has been frozen,

This book belongs to Bradley Loren (bloren@mcandrews-ip.com) Copyright Elsevier 2024
Intas Exhibit 1032
Page 349 of 470
PGR2025-00043

and a honeycomb structure is formed. With normal vacuum drying of biological solutions containing dissolved salts, a high local salt concentration is formed at the skin, although with freeze drying this does not occur because of the freezing of the solid. Thus, freeze drying is useful not only as a method of working at low temperatures, but also as a method of avoiding surface hardening.

As described by CHAMBERS[57], heat has to be supplied to the material to provide the heat of sublimation. The rate of supply of heat should be such that the highest possible water vapour pressure is obtained at the ice surface without danger of melting the material. During this stage, well over 95 per cent of the water present should be removed, and in order to complete the drying, the material should be allowed to rise in temperature, to say ambient temperature. The great attraction of this technique is that it does not harm heat-sensitive materials, and it is suitable for the drying of penicillin and other biological materials. Initially, high costs restricted the application of the process though economic advances have reduced these considerably and foodstuffs are now freeze-dried on a large scale. MAGUIRE[58] has estimated a total cost of £0.06/kg of water evaporated, in a plant handling 0.5–0.75 kg/s (2–3 tonne/h) of meat.

A typical layout of a freeze-drying installation is shown in Figure 16.35. Heat is supplied either by conduction, or by radiation from hot platens which interleave with trays containing the product, and the sublimed moisture condenses on to a refrigerated coil at the far end of the drying chamber. The use of dielectric-heating has been investigated[59], though uneven loading of the trays can lead to scorching, and ionisation of the residual gases in the dryer results in browning of the food.

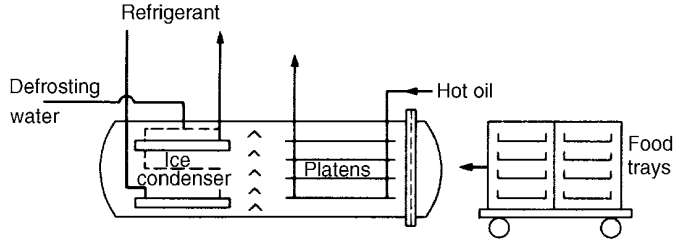


Figure 16.35. Flowsheet of freeze-drying plant

Continuous freeze-drying equipment has been developed[60], and chopped meat and vegetables may be dried in a rotating steam-jacketed tube enclosed in the vacuum chamber. A model of the freeze-drying process has been presented by DYER and SUNDERLAND[61], and further details are given in Section 15.8 on freeze crystallisation.

16.6.4. Flash drying

Conventional drying consists of mixing and heating the solids to achieve even drying, and simultaneously transporting the vapours away from the surface of the solids so as to maintain a high rate of mass transfer. Although these two stages can be achieved

This book belongs to Bradley Loren (bloren@mcandrews-ip.com) Copyright Elsevier 2024

simultaneously by contacting the solids with a hot gas stream, heat-sensitive materials, such as foods and pharmaceuticals, may suffer thermal degradation, and other solids may lose some of their water of hydration when subjected to high temperatures. This problem may often be overcome by using a flash drying technique to ensure that the solids are in contact with hot gas in a highly turbulent environment for only a very short time, perhaps only for a few seconds.

A typical flash-drying process consists of a modified pneumatic conveyor in which the wet solids are introduced into a pipe through which they are transported in a high velocity hot gas stream. In such a process, sticky sludges must first be mixed with dry solids so that the resultant mixture breaks up into smaller particles in the gas stream. Such a process can be used for a wide range of applications[62]. In the drying of the gypsum by-product of flue gas desulphurisation, for example, operating at a minimum solids temperature allows the gypsum to retain its water of hydration, and in the conversion of sewerage sludge into dry fertiliser flash drying prevents the fertilizer from oxidising. Because waste flue gases can often be used as the drying medium, little or no external heat energy is required and, when the dried sludge is burned as a fuel, the heat generated provides much of the energy required for drying.

Even when back-mixed with dry solids, some materials are too sticky or paste-like to feed to a flash dryer, though these can often be handled in a spin dryer consisting of a high shear agitator inside a specially designed drying chamber. In this way, the wet paste may be subjected simultaneously to high shear to break up the solid mass, and to gas at a high velocity to dry the smaller particles. As the particles become small enough and dry enough, they are carried out of the chamber with the spent air and, as with conventional flash drying, the contact time is but a few seconds.

Neither flash nor spin-drying produces highly uniform particles and, even though the bulk of the particles remain at or near the wet bulb temperature, small particles are often over-dried and overheated. Particles of uniform size can be formed by spray drying, however, although it is then necessary that the feed should be in the form of a pumpable liquid which can be atomised so that the particles are evenly exposed to the hot air.

16.6.5. Partial-recycle dryers

The majority of drying operations depend on direct heating using a high flowrate of hot air and/or combustion products which is passed once through or over the wet material and then exhausted to the atmosphere. A variation of this arrangement is the closed-loop system where the entire air or gas stream is confined and recycled after condensing out the vapour. Such a system is justified only where the vaporised liquid or gas has to be recovered for economic or environmental reasons. In addition to the once-through and the closed-loop systems, there is a third class of dryers which incorporates the partial-recycle mode of operation. In this system, a substantial proportion, typically 40–60 per cent, of the outlet air is returned to the dryer in order to minimise the heating requirements and the amount of effluent treatment required. Conveyor, flash-pneumatic conveying-, fluidised-bed, rotary, spray and tray types of direct dryers can all be designed for closed-loop or partial-recycle operation and Cook[63] has claimed that recycling part of the exhaust stream has the following advantages:

This book belongs to Bradley Loren (bloren@mcandrews-ip.com) Copyright Elsevier 2024

Intas Exhibit 1032
Page 351 of 470
PGR2025-00043

(a) smaller collectors are needed for removing dried product from the exhaust gases,
(b) less heat is lost in the exhausts which leave, typically, at 340–420 K,
(c) since the total volume of exhaust gases is reduced, the cost of preventing undesirable gases or particles from entering the atmosphere is reduced,
(d) when using direct burners to heat the air, the level of oxygen content is minimised, thus enabling sensitive products to be handled and reducing potential fire and/or explosion hazards.

In conveyor and tray types of dryer, air is often recirculated inside the drying vessel in an attempt to save energy or to maintain a relatively high moisture content in the drying air. In other direct dryers such as flash, fluidised-bed, rotary and spray units, any recycle of exhaust air must be returned to the dryer using external ducting, the cost of which is offset by the net savings from the lower volumes of exhaust streams which have to be handled.

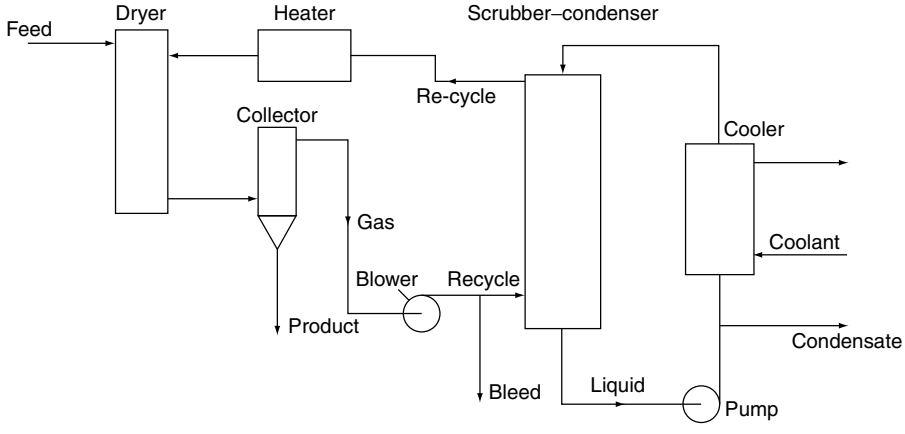


Figure 16.36. Partial-recycle drying systems

As shown in Figure 16.36, in a partial-recycle drying process, the total airflow leaving the dryer is first passed to a particulate or dust collector in order to remove entrained product or fines, and is then split into two streams — a bleed stream which is vented to atmosphere and a recycle stream which is returned to the system. The bleed stream is large enough to carry all of the moisture that has entered the system, and the recycle portion is returned to the inlet of either the heater or the drying vessel. In the condensing operation, shown in Figure 16.36, the exhaust stream from the dust collector is passed through a condenser, usually a wet scrubber, to remove most of the entrained moisture before it is returned to the inlet of the heater or the dryer. The bleed stream may also be passed through the condenser for gas-cleaning prior to discharge to atmosphere, thus removing moisture and thereby reducing the load on the condenser. Although condensers minimise the amount of bleed to the atmosphere and the moisture content of the drying air, they also cool the recycle stream and this increases costs due to the need to reheat the stream. The total volume of the bleed must be balanced by the heater output and any

This book belongs to Bradley Loren (bloren@mcandrews-ip.com) Copyright Elsevier 2024
Intas Exhibit 1032
Page 352 of 470
PGR2025-00043

leakage into the system, noting that moisture can enter the dryer from three sources — the feed, combustion air and the supply air — and can leave in the bleed in the product and as condensate, if any. It may be noted that, in Figure 16.36, the scrubber–condenser also serves as a collector for particulates. If an oxygen content of less than 21 per cent by volume or a temperature above 270–640K is required, then a direct-fired heater may be used. If non-aqueous solvents are to be evaporated in the dryer, the effluent may require incineration or other treatment prior to discharge to the atmosphere, and dual blowers are often needed to maintain the required pressures throughout the system.

COOK[63] has presented data on the performance of a partial-recycle units based on a direct-fired burner using natural gas. These are compared with the once-through operation in Table 16.8.

Table 16.8. Comparison of Once-Through with Partial-Recycle Operation

Example	Recycle mode	Burner outlet temperature (K)	Recycle (per cent)	Bleed (per cent)	Moisture (kg/kg air)	Heat Load (MW)	Air flow (m^3/s)
1	condensing	1090	46.0	54.0	0.206	2.74	8.14
2	condensing	810	19.7	80.3	0.173	2.83	8.22
3	condensing	1370	58.9	41.1	0.222	2.68	8.11
4	bleed only	1160	46.0	54.0	0.325	2.52	7.92
5	bleed only	858	25.4	74.6	0.206	2.68	8.14
6	once-through	700	0.0	100.0	0.148	2.90	8.28

(Dryer inlet = 700 K, dryer outlet = 365 K)

In these systems, the total collection efficiencies of the dry product are 85 per cent for the drying vessel, 90 per cent for the cyclone collector and 98 per cent for the scrubber-condenser. The net efficiency of the system may be as high as 99.97 per cent if the scrubber effluent is considered as product. All the runs are based on 1.25 kg/s product and 0.75 kg/s evaporation at an elevation of 300 m above sea level. The total air flow is measured at the outlet before the stream is split into the recycle and bleed portions and, for such flows, the design of suitable fans is outlined by JORGENSEN[64]. The calculations outlined here may be confirmed by the use of psychometric charts, and this procedure has been considered in some detail by COOK and DUMOUNT[65].

In recent years, air-recycling in drying systems has become more widely adopted as a means of reducing total dryer discharges to the atmosphere. It would seem that this trend is likely to continue because of environmental concerns and the ever-increasing costs of treating emissions.

16.7. THE DRYING OF GASES

The drying of gases is carried out on a very large scale. The most important applications of the process are:

(a) in order to reduce the tendency of the gas to cause corrosion,
(b) preparation of dry gas for use in a chemical reaction, and
(c) reduction of the humidity of air in air-conditioning plants.

This book belongs to Bradley Loren (bloren@mcandrews-ip.com) Copyright Elsevier 2024

Intas Exhibit 1032
Page 353 of 470
PGR2025-00043

The problems involved in the drying or dehumidification of gases are referred to in Volume 1, Chapter 13, and the most important methods available are now summarised.

Cooling. A gas stream may be dehumidified by bringing it into contact with a cold liquid or a cold solid surface. If the temperature of the surface is lower than the dew point of the gas, condensation will take place, and the temperature of the surface will tend to rise by virtue of the liberation of latent heat: It is therefore necessary to remove heat constantly from the surface. Because a far larger interfacial surface can be produced with a liquid, it is usual to spray a liquid into the gas and then to cool it again before it is recycled. In many cases, countercurrent flow of the gas and liquid is obtained by introducing the liquid at the top of a column and allowing the gas to pass upwards.

Compression. The humidity of a gas may be reduced by compressing it, cooling it down to near its original temperature, and then draining off the water which has condensed. During compression, the partial pressure of the water vapour increases and condensation occurs as soon as the saturation value is exceeded.

Liquid absorbents. If the partial pressure of the water in the gas is greater than the equilibrium partial pressure at the surface of a liquid, condensation will take place as a result of contact between the gas and liquid. Thus, water vapour is frequently removed from a gas by bringing it into contact with concentrated sulphuric acid, phosphoric acid, or glycerol. Concentrated solutions of salts, such as calcium chloride, are also effective. The process may be carried out either in a packed column or in a spray chamber. Regeneration of the liquid is an essential part of the process, and this is usually effected by evaporation.

Solid adsorbents and absorbents. The use of silica gel or solid calcium chloride to remove water vapour from gases is a common operation in the laboratory. Moderately large units can be made, although the volume of packed space required is generally large because of the comparatively small transfer surface per unit volume. If the particle size is too small, the pressure drop through the material becomes excessive. The solid desiccants are regenerated by heating.

Gas is frequently dried by using a calcium chloride liquor containing about 0.56 kg calcium chloride/kg solution. The extent of recirculation of the liquor from the base of the tower is governed by heating effects, since the condensation of the water vapour gives rise to considerable heating. It is necessary to install heat exchangers to cool the liquor leaving the base of the tower.

In the contact plant for the manufacture of sulphuric acid, sulphuric acid is itself used for drying the air for the oxidation of the sulphur. When drying hydrocarbons such as benzene, it is sometimes convenient to pass the material through a bed of solid caustic soda, although, if the quantity is appreciable, this method is expensive.

The great advantage of materials such as silica gel and activated alumina is that they enable the gas to be almost completely dried. Thus, with silica gel, air may be dried down to a dew point of 203 K. Small silica gel containers are frequently used to prevent moisture condensation in the low pressure lines of pneumatic control installations.

16.8. FURTHER READING

BACKHURST, J. R. and HARKER, J. H.: *Process Plant Design* (Heinmann, London, 1973).

BACKHURST, J. R., HARKER, J. H., and PORTER, J. E.: *Problems in Heat and Mass Transfer* (Edward Arnold, London, 1974).

This book belongs to Bradley Loren (bloren@mcandrews-ip.com) Copyright Elsevier 2024

Intas Exhibit 1032
Page 354 of 470
PGR2025-00043

BAILEY, A. G.: *Electrostatic Spraying of Liquids* (John Wiley, New York, 1988).
BARCLAY, S. F.: *A Study of Drying* (Inst. Energy, London, 1957).
BRIDGMAN, M. J.: *Drying—Principles and Practice in the Process Industries* (Caxton, Christchurch, 1966).
BROWN, W. H.: *An Introduction to the Seasoning of Timber* (Pergamon Press, Oxford, 1965).
BRUIN, S. (ed): *Preconcentration and Drying of Food Materials* (Elsevier, London, 1988).
BUTCHER, C.: *Chem. Engr. London* No 450 (July 1988) 16. Fluid bed dryers.
CLARKE, R. J. and MACRAE, R. (eds): *Coffee*, Vol. 2: *Technology* (Elsevier, London, 1987).
KEEY, R. B.: *Drying Principles and Practice* (Pergamon Press, Oxford, 1972).
KEEY, R. B.: *Introduction to Industrial Drying Operations* (Pergamon Press, Oxford, 1978).
KEEY, R. B.: *Drying of Loose and Particulate Materials* (Hemisphere Publishing Corporation, London and Washington DC, 1991).
LUIKOV, A. V.: *Heat and Mass Transfer in Capillary-porous Bodies* (Pergamon Press, Oxford, 1966).
MASTERS, K.: *Spray Drying Handbook* (George Godwin, London, 1985).
MCCABE, W. L., SMITH J. C. and HARRIOTT, P.: *Unit Operations of Chemical Engineering*. 4th edn (McGraw-Hill, New York, 1984).
MUJUMDER, A. S. (ed): *Handbook of Industrial Drying*. (Marcel Dekker, London, 1987).
NONHEBEL, G.: *Gas Purification Processes* (Newnes, London, 1964).
NONHEBEL, G. and MOSS, A. A. H.: *Drying of Solids in the Chemical Industry* (Butterworth, London, 1971).
THIJSSEN, H. A. C. and RULKENS, W. H.: *Recent Developments in Freeze Drying* (Int. Inst. Refrigeration, Lausanne, 1969).
VANÉCÉK, J., MARKVART, M. and DRBOHLAV, R.: *Fluidized Bed Drying* (Leonard Hill, London, 1966).
WALAS, S. M.: *Chemical Process Equipment: Selection and Design* (Butterworth, London, 1989).
WILLIAMS-GARDNER, A.: *Industrial Drying* (George Godwin, London, 1971).

16.9. REFERENCES

1. SHERWOOD, T. K.: *Trans. Am. Inst. Chem. Eng.* **32** (1936) 150. The air drying of solids.
2. PEARSE, J. F., OLIVER, T. R., and NEWITT, D. M.: *Trans. Inst. Chem. Eng.* **27** (1949) 1. The mechanism of the drying of solids. Part I. The forces giving rise to movement of water in granular beds, during drying.
3. OLIVER, T. R. and NEWITT, D. M.: *Trans. Inst. Chem. Eng.* **27** (1949) 9. The mechanism of drying of solids. Part II. The measurement of suction potentials and moisture distribution in drying granular solids.
4. NEWITT, D. M. and COLEMAN, M.: *Trans. Inst. Chem. Eng.* **30** (1952) 28. The mechanism of drying of solids. Part III. The drying characteristics of China clay.
5. CORBEN, R. W. and NEWITT, D. M.: *Trans. Inst. Chem. Eng.* **33** (1955) 52. The mechanism of drying of solids. Part VI. The drying characteristics of porous granular material.
6. KING, A. R. and NEWITT, D. M.: *Trans. Inst. Chem. Eng.* **33** (1955) 64. The mechanism of drying of solids. Part VII. Drying with heat transfer by conduction.
7. CORBEN, R. W.: *University of London*, Ph.D. Thesis (1955). The mechanism of drying of solids. Part IV. A study of the effect of granulation on the rate of drying of a porous solid.
8. GILLILAND, E. R.: *Ind. Eng. Chem.* **30** (1938) 506. Fundamentals of drying and air conditioning.
9. POWELL, R. W. and GRIFFITHS, E.: *Trans. Inst. Chem. Eng.* **13** (1935) 175. The evaporation of water from plane and cylindrical surfaces.
10. CHAKRAVORTY, K. R.: *J. Imp. Coll. Chem. Eng. Soc.* **3** (1947) 46. Evaporation from free surfaces.
11. SHEPHERD, C. B., HADLOCK, C., and BREWER, R. C.: *Ind. Eng. Chem.* **30** (1938) 388. Drying materials in trays. Evaporation of surface moisture.
12. SHERWOOD, T. K.: *Ind. Eng. Chem.* **21** (1929) 12, 976. The drying of solids I, II.
13. NEWMAN, A. B.: *Trans. Am. Inst. Chem. Eng.* **27** (1931) 203. The drying of porous solids: diffusion and surface emission equations.
14. CEAGLSKE, N. H. and HOUGEN, O. A.: *Trans. Am. Inst. Chem. Eng.* **33** (1937) 283. The drying of granular solids.
15. CEAGLSKE, N. H. and HOUGEN, O. A.: *Ind. Eng. Chem.* **29** (1937) 805. Drying granular solids.
16. SLICHTER, C. S.: *U.S. Geol. Survey, 19th Annual Report* (1897-8) Part 2, 301. Theoretical investigation of the motion of ground waters.
17. HAINES, W. B.: *J. Agric. Science* **17** (1927) 264. Studies in the physical properties of soils. IV. A further contribution to the theory of capillary phenomena in soil.
18. PARKER, N. H.: *Chem. Eng. Albany* **70** No. 13 (24 June 1963) 115. Aids to dryer selection.
19. KRÖLL, K.: *Trockner, einteilen, ordnen, benennen, benummern, Schilde Schriftenreihe* **6** (Schilde Bad-Hersfeld, 1965).

This book belongs to Bradley Loren (bloren@mcandrews-ip.com) Copyright Elsevier 2024

Intas Exhibit 1032
Page 355 of 470
PGR2025-00043

20. SLOAN, C. E.: *Chem Eng. Albany* **74** No. 13 (19 June 1967) 169. Drying systems and equipment.
21. BACKHURST, J. R. and HARKER, J. H.: *Process Plant Design* (Heinemann, London 1973).
22. KEEY, R. B.: *Drying Principles and Practice* (Pergamon Press, Oxford, 1972).
23. ERISMAN, J. L.: *Ind. Eng. Chem.* **30** (1938) 996. Roto-louvre dryer.
24. FRIEDMAN, S. J. and MARSHALL, W. R.: *Chem. Eng. Prog.* **45** (1949) 482, 573. Studies in rotary drying.
25. PRUTTON, C. F., MILLER, C. O., and SCHUETTE, W. H.: *Trans. Am. Inst. Chem. Eng.* **38** (1942) 123, 251. Factors influencing the performance of rotary dryers.
26. MILLER, C. O., SMITH, B. A., and SCHUETTE, W. H.: *Trans. Am. Inst. Chem. Eng.* **38** (1942) 841. Factors influencing the performance of rotary dryers.
27. SAEMAN, W. C.: *Chem. Eng. Prog.* **58**, No. 6 (June 1962) 49–56. Air-solids interaction in rotary dryers and coolers.
28. FISHER, J. J.: *Ind. Eng. Chem.* **55** No. 2 (1963) 18. Low temperature drying in vacuum tumblers.
29. LAPPLE, W. C., CLARK, W. E. and DYBDAL, E. C.: *Chem. Eng. Albany* **62** No. 11 (1955) 177. Drying. Design and costs.
30. SHARPLES, K., GLIKEN, P. G. and WARNE, R.: *Trans. Inst. Chem. Eng.* **42** (1964) T275. Complete simulation of rotary dryers.
31. FRASER, R. P., EISENKLAM, P., and DOMBROWSKI, N.: *Brit. Chem. Eng.* **2** (1957) 414–17, 496–501, 536–43, and 610–13. Liquid atomisation in chemical engineering.
32. RAYLEIGH, Lord: *Proc. Lond. Math. Soc.* **10** (1878-9) 4–13. On the instability of jets.
33. WEBER, C.: *Z. angew. Math. Mech.* **11** (1931) 136–54. Zum Zerfall eines Flüssigkeitsstrahles.
34. DOMBROWSKI, N. and MUNDAY, G.: in *Biochemical and Biological Engineering Science*. Vol. 2. Ch. 16 Spray drying (Academic Press, 1967).
35. DOMBROWSKI, N. and FRASER, R. P.: *Phil. Trans.* **247A** (1954) 101. A photographic investigation into the disintegration of liquid sheets.
36. FRASER, R. P., EISENKLAM, P., DOMBROWSKI, N., and HASSON, D.: *A.I.Ch.E.Jl.* **8** (1962) 672–80. Drop formation from rapidly moving liquid sheets.
37. WALTON, W. H. and PREWETT, W. C.: *Proc. Phys. Soc.* **628** (1949) 341. The production of sprays and mists of uniform drop size by means of spinning disc type sprayers.
38. MARSHALL, W. R.: *Chem. Eng. Prog.* Monogr. Ser. No. 2, **50** (1954). Atomization and spray drying.
39. MARSHALL, W. R.: *Trans. Am. Soc. Mech. Eng.* **77** (1955) 1377. Heat and mass transfer in spray drying.
40. GROSE, J. W. and DUFFIELD, G. H.: *Chem. and Ind.* (1954) 1464. Chemical engineering methods in the food industry.
41. QUINN, J. J.: *Ind. Eng. Chem.* **57**, No. 1 (Jan. 1965) 35–37. The economics of spray drying.
42. BRADFORD, P. and BRIGGS, S. W.: *Chem. Eng. Prog.* **59**, No. 3 (1963) 76. Equipment for the food industry — 3. Jet spray drying.
43. QUINN, M. F.: *Ind. Eng. Chem.* **55**, No. 7 (July, 1963) 18–24. Fluidized bed dryers.
44. AGARWAL, J. C., DAVIS, W. L., and KING, D. T.: *Chem. Eng. Prog.* **58**, No. 11 (Nov. 1962) 85–90. Fluidized-bed coal dryer.
45. SCOTT, M. W., LIEBERMAN, H. A., RANKELL, A. S., CHOW, F. S., and JOHNSTON, G. W.: *J. Pharm. Sci.* **52**, No. 3 (Mar 1963) 284–91. Drying as a unit operation in the pharmaceutical industry. I. Drying of tablet granulations in fluidized beds.
46. VANĚČEK, V., MARKVART, M. and DRBOHLAV, R.: *Fluid Bed Drying* (Leonard Hill, 1966).
47. CLARK, W. E.: *Chem. Eng. Albany* **74** No. 6 (13 March 1967) 177. Fluid-bed drying.
48. CHU JU CHIN, LANE, A. M. and CONKER, D.: *Ind. Eng. Chem.* **45** (1953) 1586. Evaporation of liquids into their superheated vapours.
49. BASEL, L. and GRAY, E.: *Chem. Eng. Prog.* **58** (June 1962) 67. Superheated solvent drying in a fluidized bed.
50. ELLWOOD, E. L., GOTTSTEIN, J. W., and KAUMAN, W. G.: A Laboratory Study of the Vapour Drying Process. CSIRO Forest Prod. Div., Paper 14 (1961) 111.
51. LUIKOV, A. V.: *Heat and Mass Transfer in Capillary-porous Bodies* (Pergamon Press, Oxford, 1966). Oxford, 1966).
52. BOND, J. F., MUJUMDAR, A. S., VAN HEININGEN, A. R. P. and DOUGLAS, W. J. M.: *Can J. Chem. Eng.* **72** (1994) 452–456. Drying paper by impinging jets of superheated steam.
53. WENZEL, L. and WHITE, R. R.: *Ind. Eng. Chem. Proc. Des. Dev.* **9** (1970) 207–214. Drying granular solids by superheated steam.
54. SCHWARTZE, J. P. and BRÖCKER, S.: *Int. J. Heat Mass Trans.* **43** (2000) 1791–1800. The evaporation of water into air of different humidities and the inversion temperature phenomenon.
55. TAYLOR, R. and KRISHNA, R.: *Multicomponent Mass Transfer.* (Wiley, New York, 1993)
56. VIDAURRE, M. and MARTINEZ, J.: *A.I.Ch.E.Jl* **43** (3) (1997) 681–692. Continuous drying of a solid wetted with ternary mixtures.
57. CHAMBERS, H. H.: *Trans. Inst. Chem. Eng.* **27** (1949) 19. Vacuum freeze drying.

This book belongs to Bradley Loren (bloren@mcandrews-ip.com) Copyright Elsevier 2024

Intas Exhibit 1032
Page 356 of 470
PGR2025-00043

58. MAGUIRE, J. F.: *Food Eng.* **34**, No. 8 (Aug. 1962) 54–5 and **34**, No. 9 (Sept. 1962) 48–52. Freeze drying moves ahead in U.S.
59. HARPER, J. C., CHICHESTER, C.O., and ROBERTS, T. E.: *Agric. Eng.* **43** (1962) 78, 90. Freeze-drying of foods.
60. MAISTER, H. G., HEGER, E. N., and BOGARD, W. M.: *Ind. Eng. Chem.* **50** (1958) 623. Continuous freeze-drying of *Serratia marcescens*.
61. DYER, D. F. and SUNDERLAND, J. E.: *Chem. Eng. Sci.* **23** (1968) 965. The role of convection in drying.
62. FRANCE, S.: *Chem. Eng. Albany* (December 1996) 83–84. Delicately drying solids - in a flash.
63. COOK, E. M.: *Chem. Eng. Albany* (April 1996) 82–89. Process calculations for partial-recycle dryers.
64. JORGENSEN, R. (ed.): *Fan Engineering* (8th edn.) (Buffalo Forge Co., Buffalo, New York, 1983).
65. COOK, E. M. and DUMOUNT, H. D.: *Process Drying Practice* (McGraw-Hill, New York, 1991).

16.10. NOMENCLATURE

		Units in SI System	Dimensions in **M**, **N**, **L**, **T**, $\boldsymbol{\theta}$
A	Area for heat transfer or evaporation	m^2	$\mathbf{L}^2$
A_N	Area of nozzle or jet normal to direction of flow	m^2	$\mathbf{L}^2$
a	Surface area per unit volume	m^2/m^3	$\mathbf{L}^{-1}$
B	Width of surface	m	**L**
C	Coefficient	$kg^{0.2}/m^{0.4}s^{0.2}$	$\mathbf{M}^{0.2}\ \mathbf{L}^{-0.4}\ \mathbf{T}^{-0.2}$
C_D	Coefficient of discharge	—	—
C_w	Water concentration of a point in solid	kg/m^3	$\mathbf{ML}^{-3}$
C_f	Heat capacity of wet material	J/kg K	$\mathbf{L}^2\ \mathbf{T}^{-2}\ \boldsymbol{\theta}^{-1}$
C_m	Mean heat capacity of gas	J/kg K	$\mathbf{L}^2\ \mathbf{T}^{-2}\ \boldsymbol{\theta}^{-1}$
C_s	Heat capacity of dry solid	J/kg K	$\mathbf{L}^2\ \mathbf{T}^{-2}\ \boldsymbol{\theta}^{-1}$
C_x	Heat capacity of liquid evaporated	J/kg K	$\mathbf{L}^2\ \mathbf{T}^{-2}\ \boldsymbol{\theta}^{-1}$
D	Diameter of drum or disc	m	**L**
D_L	Diffusion coefficient (liquid phase)	m^2/s	$\mathbf{L}^2\ \mathbf{T}^{-1}$
d	Particle diameter	m	**L**
d_j	Nozzle or jet diameter	m	**L**
d_m	Main drop diameter	m	**L**
d_s	Surface-mean diameter of drop	m	**L**
d_t	Diameter of evaporating drop at time t	m	**L**
d_o	Initial diameter of drop	m	**L**
F	Wet solid feed rate	kg/s	$\mathbf{MT}^{-1}$
F'	Volumetric rate of feed per unit cross-section	m^3/sm^2	$\mathbf{LT}^{-1}$
f	Free moisture content	kg	**M**
f_c	Free moisture content at critical condition	kg	**M**
f_1	Initial free moisture content	kg	**M**
FN	Flow number of nozzle (equation 16.32)	—	—
G	Mass flow in jet or nozzle *or* of gas	kg/s	$\mathbf{MT}^{-1}$
G_v	Mass rate of evaporation	kg/s	$\mathbf{MT}^{-1}$
G'	Mass rate of flow of air per unit cross-section	kg/m^2 s	$\mathbf{ML}^{-2}\ \mathbf{T}^{-1}$
g	Acceleration due to gravity	m/s^2	$\mathbf{LT}^{-2}$
$\mathscr{H}$	Humidity	kg/kg	—
$\mathscr{H}_s$	Humidity of saturated air at surface temperature	kg/kg	—
$\mathscr{H}_w$	Humidity of saturated air at temperature $\boldsymbol{\theta}_w$	kg/kg	—
$\mathscr{H}_0$	Humidity of saturated air	kg/kg	—
h	Heat transfer coefficient	W/m^2K	$\mathbf{MT}^{-3}\boldsymbol{\theta}^{-1}$
h_D	Mass transfer coefficient	m/s	$\mathbf{LT}^{-1}$
h_f	Friction head over a distance z_1 from surface	m	**L**
h_s	Suction potential immediately below meniscus	m	**L**
h_t	Theoretical suction potential of pore or waist	m	**L**
h_1	Suction potential at distance z_1 below meniscus	m	**L**
j	Volumetric gas/liquid ratio	—	—
K	Coefficient	m^2s/kg	$\mathbf{M}^{-1}\ \mathbf{L}^2\ \mathbf{T}$

This book belongs to Bradley Loren (bloren@mcandrews-ip.com) Copyright Elsevier 2024

Intas Exhibit 1032
Page 357 of 470
PGR2025-00043

		Units in SI System	Dimensions in **M**, **N**, **L**, **T**, $\boldsymbol{\theta}$
K'	Coefficient	$s^{1.8}/m^{1.5}$	$\mathbf{L}^{-1.8}\ \mathbf{T}^{1.8}$
K''	Transfer coefficient ($h_D\rho_A$)	$kg/m^2\ s$	$\mathbf{ML}^{-2}\ \mathbf{T}^{-1}$
k_G	Mass transfer coefficient	s/m	$\mathbf{L}^{-1}\ \mathbf{T}$
k_f	Thermal conductivity of gas film at interface	W/mK	$\mathbf{MLT}^{-3}\boldsymbol{\theta}^{-1}$
L	Length of surface	m	**L**
l	Half thickness of slab	m	**L**
M_A	Molecular weight of air	kg/kmol	$\mathbf{MN}^{-1}$
M_w	Molecular weight of water	kg/kmol	$\mathbf{MN}^{-1}$
m	Ratio of rate of drying per unit area to moisture content	$m^{-2}s^{-1}$	$\mathbf{L}^{-2}\ \mathbf{T}^{-1}$
N	Revolutions per unit time	Hz	$\mathbf{T}^{-1}$
n	Index	—	—
n_f	Number of flights	—	—
P	Total pressure	N/m^2	$\mathbf{ML}^{-1}\ \mathbf{T}^{-2}$
P_s	Vapour pressure of water at surface of material	N/m^2	$\mathbf{ML}^{-1}\ \mathbf{T}^{-2}$
P_w	Partial pressure of water vapour	N/m^2	$\mathbf{ML}^{-1}\ \mathbf{T}^{-2}$
P_{wo}	Partial pressure at surface of material at wet bulb temperature	N/m^2	$\mathbf{ML}^{-1}\ \mathbf{T}^{-2}$
$-\Delta P$	Pressure drop across nozzle	N/m^2	$\mathbf{ML}^{-1}\ \mathbf{T}^{-2}$
Q	Rate of heat transfer	W	$\mathbf{ML}^2\ \mathbf{T}^{-3}$
R_c	Rate of drying per unit area for constant rate period	$kg/m^2\ s$	$\mathbf{ML}^{-2}\ \mathbf{T}^{-1}$
R	Universal gas constant	8314 J/kmol K	$\mathbf{MN}^{-1}\ \mathbf{L}^2\ \mathbf{T}^{-2}\boldsymbol{\theta}^{-1}$
$\mathscr{R}$	Exit gas relative humidity (per cent)	—	—
r	Radius of sphere	m	**L**
r'	Radius of capillary	m	**L**
S	Slope of drum	—	—
T	Absolute temperature	K	$\boldsymbol{\theta}$
T_b	Bed temperature	K	$\boldsymbol{\theta}$
T_f	Temperature of wet solids feed	K	$\boldsymbol{\theta}$
T_m	Mean temperature of inlet gas	K	$\boldsymbol{\theta}$
ΔT	Temperature difference	K	$\boldsymbol{\theta}$
t	Time	s	**T**
t_c	Time of constant rate period of drying	s	**T**
t_f	Time of drying in falling rate period	s	**T**
U	Overall heat transfer coefficient	$W/m^2\ K$	$\mathbf{MT}^{-3}\boldsymbol{\theta}^{-1}$
u	Gas velocity	m/s	$\mathbf{LT}^{-1}$
u_f	Fluidising velocity	m/s	$\mathbf{LT}^{-1}$
u_l	Liquid velocity in jet or spray	m/s	$\mathbf{LT}^{-1}$
u_r	Velocity of gas relative to liquid	m/s	$\mathbf{LT}^{-1}$
V	Volume	m^3	$\mathbf{L}^3$
W	Mass rate of evaporation	kg/s	$\mathbf{MT}^{-1}$
w	Total moisture	kg	**M**
w_c	Critical moisture content	kg	**M**
w_e	Equilibrium moisture content	kg	**M**
w_1	Initial moisture content	kg	**M**
X	Hold-up of drum	—	—
X_a	Hold-up of drum with air flow	—	—
X_f	Moisture content of wet feed	kg/kg	—
x	Factor depending on type of packing	—	—
y	Distance in direction of diffusion	m	**L**
z_1	Distance below meniscus	m	**L**
α	Angle of contact	—	—
$\bar{\kappa}$	Coefficient	$kg^{1-n}\ m^{2n}\ s^{n-3}/K$	$\mathbf{M}^{1-n}\ \mathbf{L}^{2n}\ \mathbf{T}^{n-3}\boldsymbol{\theta}^{-1}$
$\boldsymbol{\theta}$	Gas temperature	K	$\boldsymbol{\theta}$
θ_s	Surface temperature	K	$\boldsymbol{\theta}$
θ_w	Wet bulb temperature	K	$\boldsymbol{\theta}$
λ	Latent heat vaporisation per unit mass	J/kg	$\mathbf{L}^2\ \mathbf{T}^{-2}$

This book belongs to Bradley Loren (bloren@mcandrews-ip.com) Copyright Elsevier 2024

Intas Exhibit 1032
Page 358 of 470
PGR2025-00043

		Units in SI System	Dimensions in **M**, **N**, **L**, **T**, $\boldsymbol{\theta}$
λ_b	Mean latent heat vaporisation per unit mass of T_b	kJ/kg	$\mathbf{L}^2\ \mathbf{T}^{-2}$
λ_{opt}	Optimum wavelength for jet disruption	m	**L**
μ	Viscosity	Ns/m^2	$\mathbf{ML}^{-1}\ \mathbf{T}^{-1}$
ρ	Density	kg/m^3	$\mathbf{ML}^{-3}$
ρ_A	Density of air at its mean partial pressure	kg/m^3	$\mathbf{ML}^{-3}$
σ	Surface tension	J/m^2	$\mathbf{MT}^{-2}$
ϕ	Half-angle of spray cone or sheet	—	—

This book belongs to Bradley Loren (bloren@mcandrews-ip.com)
Copyright Elsevier 2024
Intas Exhibit 1032
Page 359 of 470
PGR2025-00043

CHAPTER 17

Adsorption

17.1. INTRODUCTION

Although adsorption has been used as a physical-chemical process for many years, it is only over the last four decades that the process has developed to a stage where it is now a major industrial separation technique. In adsorption, molecules distribute themselves between two phases, one of which is a solid whilst the other may be a liquid or a gas. The only exception is in adsorption on to foams, a topic which is not considered in this chapter.

Unlike *absorption*, in which solute molecules diffuse from the bulk of a gas phase to the bulk of a liquid phase, in *adsorption*, molecules diffuse from the bulk of the fluid to the surface of the solid adsorbent forming a distinct adsorbed phase.

Typically, gas adsorbers are used for removing trace components from gas mixtures. The commonest example is the drying of gases in order to prevent corrosion, condensation or an unwanted side reaction. For items as diverse as electronic instruments and biscuits, sachets of adsorbent may be included in the packaging in order to keep the relative humidity low. In processes using volatile solvents, it is necessary to guard against the incidental loss of solvent carried away with the ventilating air and recovery may be effected by passing the air through a packed bed of adsorbent.

Adsorption may be equally effective in removing trace components from a liquid phase and may be used either to recover the component or simply to remove a noxious substance from an industrial effluent.

Any potential application of adsorption has to be considered along with alternatives such as distillation, absorption and liquid extraction. Each separation process exploits a difference between a property of the components to be separated. In distillation, it is volatility. In absorption, it is solubility. In extraction, it is a distribution coefficient. Separation by adsorption depends on one component being more readily adsorbed than another. The selection of a suitable process may also depend on the ease with which the separated components can be recovered. Separating *n*- and *iso*-paraffins by distillation requires a large number of stages because of the low relative volatility of the components. It may be economic, however, to use a selective adsorbent which separates on the basis of slight differences in mean molecular diameters, where for example, *n*- and *iso*-pentane have diameters of 0.489 and 0.558 nm respectively. When an adsorbent with pore size of 0.5 nm is exposed to a mixture of the gases, the smaller molecules diffuse to the adsorbent surface and are retained whilst the larger molecules are excluded. In another stage of the process, the retained molecules are desorbed by reducing the total pressure or increasing the temperature.

This book belongs to Bradley Loren (bloren@mcandrews-ip.com) Copyright Elsevier 2024

Intas Exhibit 1032
Page 360 of 470
PGR2025-00043

Most commercial processes for producing nitrogen and oxygen from air use the cryogenic distillation of liquefied air. There is also interest in adsorptive methods, particularly for moderate production rates. Some adsorbents take up nitrogen preferentially and can be used to generate an oxygen-rich gas containing 95 mole per cent of oxygen. Regeneration of the adsorbent yields a nitrogen-rich gas. It is also possible to separate the gases using an adsorbent with 0.3 nm pores. These allow oxygen molecules of 0.28 nm in size to diffuse rapidly on to the adsorption surface, whereas nitrogen molecules of 0.30 nm will diffuse more slowly. The resulting stream is a nitrogen-rich gas of up to 99 per cent purity. An oxygen stream of somewhat lower purity is obtained from the desorption stage.

Other applications of commercial adsorbents are given in Table 17.1, taken from the work of CRITTENDEN[1]. Some typical solvents which are readily recovered by adsorptive techniques are listed in Table 17.2, taken from information supplied by manufacturers.

All such processes suffer one disadvantage in that the capacity of the adsorbent for the adsorbate in question is limited. The adsorbent has to be removed at intervals from the process and regenerated, that is, restored to its original condition. For this reason, the adsorption unit was considered in early industrial applications to be more difficult to integrate with a continuous process than, say, a distillation column. Furthermore, it was difficult to manufacture adsorbents which had identical adsorptive properties from batch to batch. The design of a commercial adsorber and its operation had to be sufficiently flexible to cope with such variations.

These factors, together with the rather slow thermal regeneration that was common in early applications, resulted in the adsorber being an unpopular option with plant designers. Since a greater variety of adsorbents has become available, each tailor-made for a specific application, the situation has changed, particularly as faster alternatives to thermal regeneration are often possible.

Adsorption occurs when molecules diffusing in the fluid phase are held for a period of time by forces emanating from an adjacent surface. The surface represents a gross discontinuity in the structure of the solid, and atoms at the surface have a residue of molecular forces which are not satisfied by surrounding atoms such as those in the body of the structure. These residual or van der Waals forces are common to all surfaces and the only reason why certain solids are designated "adsorbents" is that they can be manufactured in a highly porous form, giving rise to a large internal surface. In comparison the external surface makes only a modest contribution to the total, even when the solid is finely divided. Iron oxide particles with a radius of 5 μm and a density of 5000 kg/m^3 have an external surface of 12,000 m^2/kg. A typical value for the total surface of commercial adsorbents is 400,000 m^2/kg.

The adsorption which results from the influence of van der Waals forces is essentially physical in nature. Because the forces are not strong, the adsorption may be easily reversed. In some systems, additional forces bind absorbed molecules to the solid surface. These are chemical in nature involving the exchange or sharing of electrons, or possibly molecules forming atoms or radicals. In such cases the term *chemisorption* is used to describe the phenomenon. This is less easily reversed than physical adsorption, and regeneration may be a problem. Chemisorption is restricted to just one layer of molecules on the surface, although it may be followed by additional layers of physically adsorbed molecules.

When molecules move from a bulk fluid to an adsorbed phase, they lose degrees of freedom and the free energy is reduced. Adsorption is always accompanied by the

This book belongs to Bradley Loren (bloren@mcandrews-ip.com) Copyright Elsevier 2024

Intas Exhibit 1032
Page 361 of 470
PGR2025-00043

Table 17.1. Typical applications of commercial adsorbents[1]

Type	Typical applications
Silica gel	Drying of gases, refrigerants, organic solvents, transformer oils; desiccant in packings and double glazing; dew point control of natural gas.
Activated alumina	Drying of gases, organic solvents, transformer oils; removal of HCl from hydrogen; removal of fluorine and boron-fluorine compounds in alkylation processes.
Carbons	Nitrogen from air; hydrogen from syn-gas and hydrogenation processes; ethene from methane and hydrogen; vinyl chloride monomer (VCM) from air; removal of odours from gases; recovery of solvent vapours; removal of SO_x and NO_x; purification of helium; clean-up of nuclear off-gases; decolourising of syrups, sugars and molasses; water purification, including removal of phenol, halogenated compounds, pesticides, caprolactam, chlorine.
Zeolites	Oxygen from air; drying of gases; removing water from azeotropes; sweetening sour gases and liquids; purification of hydrogen; separation of ammonia and hydrogen; recovery of carbon dioxide; separation of oxygen and argon; removal of acetylene, propane and butane from air; separation of xylenes and ethyl benzene; separation of normal from branched paraffins; separation of olefins and aromatics from paraffins; recovery of carbon monoxide from methane and hydrogen; purification of nuclear off-gases; separation of cresols; drying of refrigerants and organic liquids; separation of solvent systems; purification of silanes; pollution control, including removal of Hg, NO_x and SO_x from gases; recovery of fructose from corn syrup.
Polymers and resins	Water purification, including removal of phenol, chlorophenols, ketones, alcohols, aromatics, aniline, indene, polynuclear aromatics, nitro- and chlor-aromatics, PCB, pesticides, antibiotics, detergents, emulsifiers, wetting agents, kraftmill effluents, dyestuffs; recovery and purification of steroids, amino acids and polypeptides; separation of fatty acids from water and toluene; separation of aromatics from aliphatics; separation of hydroquinone from monomers; recovery of proteins and enzymes; removal of colours from syrups; removal of organics from hydrogen peroxide.
Clays (acid-treated and pillared)	Treatment of edible oils; removal of organic pigments; refining of mineral oils; removal of polychlorobiphenyl (PCB).

This book belongs to Bradley Loren (bloren@mcandrews-ip.com) Copyright Elsevier 2024

Intas Exhibit 1032
Page 362 of 470
PGR2025-00043

Table 17.2. Properties of some solvents recoverable by adsorptive techniques

	Molecular weight (kg/kmol)	Specific heat capacity at 293 K (kJ/kg K)	Density at 293 K (kg/m^3)	Latent heat evaporation (kJ/kg)	Boiling point (K)	Explosive limits in air at 293 K (per cent by volume)		Solubility in water at 293 K (kg/m^3)
						low	high	
acetone	58.08	2.211	791.1	524.6	329.2	2.15	13.0	∞
allyl alcohol	58.08	2.784	853.5	687	369.9	2.5	18	∞
n-amyl acetate	130.18	1.926	876	293	421.0	3.6	16.7	1.8
iso-amyl acetate	130.18	1.9209	876	289	415.1	3.6	—	2.5
n-amyl alcohol	88.15	2.981	817	504.9	410.9	1.2	—	68
iso-amyl alcohol	88.15	2.872	812	441.3	404.3	1.2	—	32
amyl chloride	106.6	—	883	—	381.3	—	—	Insol.
amylene	70.13	1.181	656	314.05	309.39	1.6	—	Insol.
benzene	78.11	1.720	880.9	394.8	353.1	1.4	4.7	0.8
n-butyl acetate	116.16	1.922	884	309.4	399.5	1.7	15	10
iso-butyl acetate	116.16	1.921	872	308.82	390.2	2.4	10.5	6.7
n-butyl alcohol	74.12	2.885	809.7	600.0	390.75	1.45	11.25	78
iso-butyl alcohol	74.12	2.784	805.7	578.6	381.8	1.68	—	85
carbon disulphide	76.13	1.005	1267	351.7	319.25	1.0	50	2
carbon tetrachloride	153.84	0.846	1580	194.7	349.75	Non-flammable		0.084
cellosolve	90.12	2.324	931.1	—	408.1	—	—	∞
cellosolve methyl	76.09	2.236	966.3	565	397.5	—	—	∞
cellosolve acetate	132.09	—	974.8	—	426.0	—	—	230
chloroform	119.39	0.942	1480	247	334.26	Non-flammable		8
cyclohexane	84.16	2.081	778.4	360	353.75	1.35	8.35	Insol.
cyclohexanol	100.16	1.746	960	452	433.65	—	—	60
cyclohexanone	98.14	1.813	947.8	—	429.7	3.2	9.0	50
cymene	134.21	1.666	861.2	283.07	449.7	—	—	Insol.
n-decane	142.28	2.177	730.1	252.0	446.3	0.7	—	Insol.
dichloroethylene	96.95	1.235	1291	305.68	333.0	9.7	12.8	Insol.
ether (diethyl)	74.12	2.252	713.5	360.4	307.6	1.85	36.5	69
ether (di-*n*-butyl)	130.22	—	769.4	288.1	415.4	—	—	3
ethyl acetate	88.10	2.001	902.0	366.89	350.15	2.25	11.0	79.4
ethyl alcohol	56.07	2.462	789.3	855.4	351.32	3.3	19.0	∞
ethyl bromide	108.98	0.812	1450	250.87	311.4	6.7	11.2	9.1
ethyl carbonate	118.13	1.926	975.2	306	399.0	—	—	V.sl.sol.
ethyl formate	74.08	2.135	923.6	406	327.3	2.7	16.5	100
ethyl nitrite	75.07	—	900	—	290.0	3.0	—	Insol.
ethylene dichloride	96.97	1.298	1255.0	323.6	356.7	6.2	15.6	8.7
ethylene oxide	44.05	—	882	580.12	283.5	3.0	80	∞
furfural	96.08	1.537	1161	450.12	434.8	2.1	—	83
n-heptane	100.2	2.123	683.8	318	371.4	1.0	6.0	0.052
n-hexane	86.17	2.223	659.4	343	341.7	1.25	6.9	0.14
methyl acetate	74.08	2.093	927.2	437.1	330.8	4.1	13.9	240
methyl alcohol	32.04	2.500	792	1100.3	337.7	6.72	36.5	67.2
methyl cyclohexanol	114.18	—	925	—	438.0	—	—	11
methyl cyclohexanone	112.2	1.842	924	—	438.0	—	—	30
methyl cyclohexane	98.18	1.855	768	323	373.9	1.2	—	Insol.
methyl ethyl ketone	72.10	2.085	805.1	444	352.57	1.81	11.5	265
methylene chloride	84.93	1.089	1336	329.67	313.7	Non-flammable		20
monochlorobenzene	112.56	1.256	1107.4	324.9	404.8	—	—	0.49
naphthalene	128.16	1.683	1152	316.1	491.0	0.8	—	0.04
nonane	128.25	2.106	718	274.2	422.5	0.74	2.9	Insol.
octane	114.23	2.114	702	296.8	398.6	0.95	3.2	0.015
paraldehyde	132.16	1.825	904	104.75	397.0	1.3	—	120
n-pentane	72.15	2.261	626	352	309.15	1.3	8.0	0.36

(*continued overleaf*)

This book belongs to Bradley Loren (bloren@mcandrews-ip.com) Copyright Elsevier 2024

Intas Exhibit 1032
Page 363 of 470
PGR2025-00043

Table 17.2. (*continued*)

	Molecular weight (kg/kmol)	Specific heat capacity at 293 K (kJ/kg K)	Density at 293 K (kg/m^3)	Latent heat evaporation (kJ/kg)	Boiling point (K)	Explosive limits in air at 293 K (per cent by volume) low	high	Solubility in water at 293 K (kg/m^3)
iso-pentane	72.09	2.144	619	371.0	301.0	1.3	7.5	Insol.
pentachloroethane	202.33	0.900	1678	182.5	434.95	Non-flammable		0.5
perchloroethylene	165.85	0.879	1662.6	209.8	393.8	Non-flammable		0.4
n-propyl acetate	102.3	1.968	888.4	336.07	374.6	2.0	8.0	18.9
iso-propyl acetate	102.3	2.181	880	332.4	361.8	2.0	8.0	29
n-propyl alcohol	60.09	2.453	803.6	682	370.19	2.15	13.5	∞
iso-propyl alcohol	60.09	2.357	786.3	667.4	355.4	2.02	—	∞
propylene dichloride	112.99	1.398	1159.3	302.3	369.8	3.4	14.5	2.7
pyridine	79.10	1.637	978	449.59	388.3	1.8	12.4	∞
tetrachloroethane	167.86	1.130	1593	231.5	419.3	Non-flammable		3.2
tetrahydrofuran	72.10	1.964	888	410.7	339.0	1.84	11.8	∞
toluene	92.13	1.641	871	360	383.0	1.3	7.0	0.47
trichloroethylene	131.4	0.934	1465.5	239.9	359.7	Non-flammable		1.0
xylene	106.16	1.721	897	347.1	415.7	1.0	6.0	Insol.
water	18	4.183	998	2260.9	373.0	Non-flammable		∞

liberation of heat. For physical adsorption, the amount of heat is similar in magnitude to the heat of condensation. For chemisorption it is greater and of an order of magnitude normally associated with a chemical reaction. If the heat of adsorption cannot be dispersed by cooling, the capacity of the adsorbent will be reduced as its temperature increases.

It is often convenient to think of adsorption as occurring in three stages as the adsorbate concentration increases. Firstly, a single layer of molecules builds up over the surface of the solid. This monolayer may be chemisorbed and associated with a change in free energy which is characteristic of the forces which hold it. As the fluid concentration is further increased, layers form by physical adsorption and the number of layers which form may be limited by the size of the pores. Finally, for adsorption from the gas phase, capillary condensation may occur in which capillaries become filled with condensed adsorbate, and its partial pressure reaches a critical value relative to the size of the pore.

Although the three stages are described as taking place in sequence, in practice, all three may be occurring simultaneously in different parts of the adsorbent since conditions are not uniform throughout. Generally, concentrations are higher at the outer surface of an adsorbent pellet than in the centre, at least until equilibrium conditions have been established. In addition, the pore structure will consist of a distribution of pore sizes and the spread of the distribution depends on the origin of the adsorbent and its conditions of manufacture.

17.2. THE NATURE OF ADSORBENTS

Adsorbents are available as irregular granules, extruded pellets and formed spheres. The size reflects the need to pack as much surface area as possible into a given volume of bed and at the same time minimise pressure drop for flow through the bed. Sizes of up to about 6 mm are common.

This book belongs to Bradley Loren (bloren@mcandrews-ip.com) Copyright Elsevier 2024

Intas Exhibit 1032
Page 364 of 470
PGR2025-00043

To be attractive commercially, an adsorbent should embody a number of features:

(a) it should have a large internal surface area.
(b) the area should be accessible through pores big enough to admit the molecules to be adsorbed. It is a bonus if the pores are also small enough to exclude molecules which it is desired not to adsorb.
(c) the adsorbent should be capable of being easily regenerated.
(d) the adsorbent should not age rapidly, that is lose its adsorptive capacity through continual recycling.
(e) the adbsorbent should be mechanically strong enough to withstand the bulk handling and vibration that are a feature of any industrial unit.

17.2.1. Molecular sieves

An increase in the use of adsorbers as a means of separation on a large scale is the result of the manufacturers' skill at developing and producing adsorbents which are tailored for specific tasks. First, by using naturally occurring zeolites and, later, synthesised members of that family of minerals, it has been possible to manufacture a range of adsorbents known collectively as *molecular sieves*. These have lattice structures composed of tetrahedra of silica and alumina arranged in various ways. The net effect is the formation of a cage-like structure with windows which admit only molecules less than a certain size as shown in Figure 17.1. By using different source materials and different conditions of manufacture, it is possible to produce a range of molecular sieves with access dimensions of 0.3 nm–1 nm. The dimensions are precise for a particular sieve because they derive from the crystal structure of that sieve. Some of the molecules admitted by different molecular sieves are given in Table 17.3 which is taken from the work of BARRER[2]. The crystallites of a sieve are about 10 μm in size and are aggregated for commercial use by mixing with a clay binder and extruding as pellets or rolling into spheres. The pelletising creates two other sets of pores, between crystallites and between pellets. Neither may add significantly to the adsorptive surface though each will influence rates of diffusion and pressure drop. It has been estimated by YANG[3] that there are about forty naturally occurring zeolites and that some one hundred and fifty have been synthesised.

The manufacture of molecular sieves has been reviewed in the literature, and particularly by BRECK[4], BARRER[5] and ROBERTS[6].

17.2.2. Activated carbon

In some of the earliest recorded examples of adsorption, activated carbon was used as the adsorbent. Naturally occurring carbonaceous materials such as coal, wood, coconut shells or bones are decomposed in an inert atmosphere at a temperature of about 800 K. Because the product will not be porous, it needs additional treatment or *activation* to generate a system of fine pores. The carbon may be produced in the activated state by treating the raw material with chemicals, such as zinc chloride or phosphoric acid, before carbonising. Alternatively, the carbon from the carbonising stage may be selectively

This book belongs to Bradley Loren (bloren@mcandrews-ip.com) Copyright Elsevier 2024

Intas Exhibit 1032
Page 365 of 470
PGR2025-00043

Table 17.3. Classification of some molecular sieves[2]

	Molecular Size Increasing ⟶									
Type 5	He, Ne, A, CO H_2, O_2, N_2, NH_3, H_2O Size limit for Ca- and Ba-mordenites and levynite about here (~0.38 nm)	Kr, Xe CH_4 C_2H_6 CH_3OH CH_3CN CH_3NH_2 CH_3Cl CH_3Br CO_2 C_2H_2 CS_2	C_3H_8 *n*-C_4H_{10} *n*-C_7H_{16} *n*-$C_{14}H_{30}$ etc. C_2H_5Cl C_2H_5Br C_2H_5OH $C_2H_5NH_2$ CH_2Cl_2 CH_2Br_2 CHF_2Cl CHF_3 $(CH_3)_2NH$ CH_3I B_2H_6	CF_4 C_2F_6 CF_2Cl_2 CF_3Cl $CHFCl_2$	SF_6 *iso*-C_4H_{10} *iso*-C_5H_{12} *iso*-C_8H_{18} etc. $CHCl_3$ $CHBr_3$ CHI_3 $(CH_3)_2CHOH$ $(CH_3)_2CHCl$ *n*-C_3F_8 *n*-C_4F_{10} *n*-C_7F_{16} B_5H_9	$(CH_3)_3N$ $(C_2H_5)_3N$ $C(CH_3)_4$ $C(CH_3)_3Cl$ $C(CH_3)_3Br$ $C(CH_3)_3OH$ CCl_4 CBr_4 $C_2F_2Cl_4$	C_6H_6 $C_6H_5CH_3$ $C_6H_4(CH_3)_2$ Cyclohexane Thiophen Furan Pyridine Dioxane $B_{10}H_{14}$	Naphthalene Quinoline, 6-decyl- 1, 2, 3, 4- tetrahydro- naphthalene, 2-butyl-1- hexyl indan $C_6F_{11}CF_3$	1, 3, 5 triethyl benzene 1, 2, 3, 4, 5, 6, 7, 8, 13, 14, 15, 16-decahydro-chrysene	(*n*-$C_4F_9)_3N$
Type 4	Size limit for Na-mordenite and Linde sieve 4 A about here (~0.4 nm)	Size limit for Ca-rich chabazite, Linde sieve 5 A, Ba-zeolite and gmelinite about here (~0.49 nm)								
Type 3							Size limit for Linde sieve 10X about here (~0.8 nm)			
Type 2								Size limit for Linde sieve 13X about here (~1.0 nm)		
Type 1										

This book belongs to Bradley Loren (bloren@mcandrews-ip.com)

Copyright Elsevier 2024

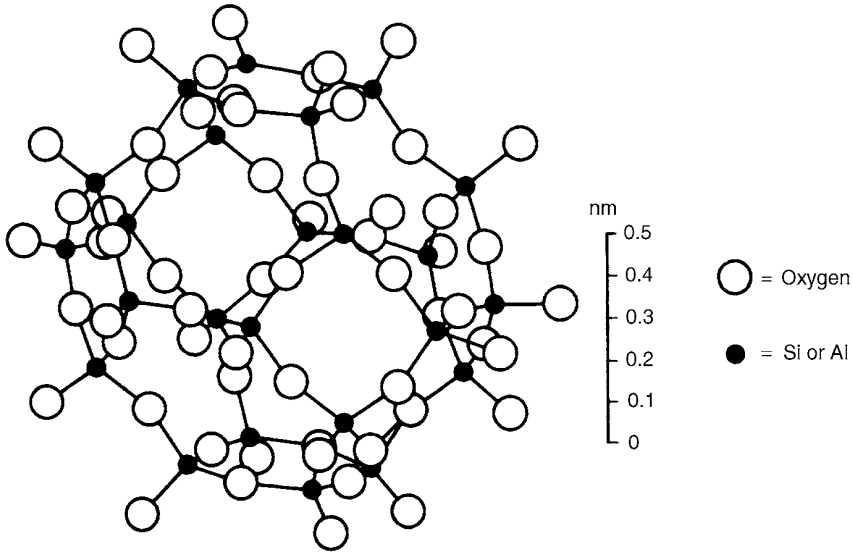


Figure 17.1. A cubo-octahedral unit composed of SiO_4 and AlO_4 tetrahedra[2]

oxidised at temperatures in excess of 1000 K in atmospheres of materials such as steam or carbon dioxide.

Activated carbon has a typical surface area of 10^6 m^2/kg, mostly associated with a set of pores of about 2 nm in diameter. There is likely to be another set of pores of about 1000 nm in diameter, which do not contribute to the surface area. There may even be a third, intermediate set of pores which is particularly developed in carbons intended for use with liquids, as shown in Figure 17.2 which is taken from the work of SCHWEITZER[7].

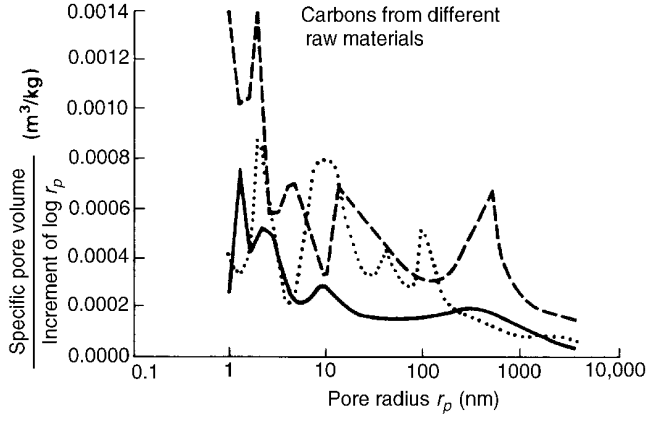


Figure 17.2. Typical pore volume distributions for three activated carbons used for liquid-phase processes[7]

This book belongs to Bradley Loren (bloren@mcandrews-ip.com) Copyright Elsevier 2024
Intas Exhibit 1032
Page 367 of 470
PGR2025-00043

Activated carbon may be used as a powder, in which form it is mixed in with the liquid to be treated, and then removed by filtration. It may also be used in granular form. When the use of carbon is low, it is normally economic to regenerate it, and this is usually the case with powder. Granular carbon is normally regenerated after use. Because it has a low affinity for water, activated carbon may preferentially adsorb components from aqueous solution or from moist gases.

By carefully choosing the starting material and the activating process, it has been possible in recent years to generate in carbon a pore system with a narrow span of pore sizes. With a mean pore diameter of perhaps 0.6 nm, such products are known as carbon molecular sieves.

17.2.3. Silica gel

When a silicate solution such as sodium silicate is acidified, a gel of polymeric colloidal silicilic acid is formed as an agglomerate of micro-particles. When the gel is heated, water is expelled leaving a hard, glassy structure with voids between the micro-particles equivalent to a mean pore diameter of about 3 nm and an internal surface of about 500,000 m^2/kg. As discussed by Everett and Stone[8] these properties may be varied by controlling the pH of the solution from which the gel is precipitated.

Silica gel is probably the adsorbent which is best known. Small sachets of gel are often included in packages of material that might deteriorate in a damp atmosphere. Sometimes a dye is added in the manufacturing process so that the gel changes colour as it becomes saturated.

Unlike the activated carbons, the surface of silica gel is hydrophilic and it is commonly used for drying gases and also finds applications where there is a requirement to remove unsaturated hydrocarbons. Silica gels are brittle and may be shattered by the rapid release of the heat of adsorption that accompanies contact with liquid water. For such applications, a tougher variety is available with a slightly lower surface area.

17.2.4. Activated alumina

When an adsorbent is required which is resistant to attrition and which retains more of its adsorptive capacity at elevated temperatures than does silica gel, activated alumina may be used. This is made by the controlled heating of hydrated alumina. Water molecules are expelled and the crystal lattice ruptures along planes of structural weakness. A well-defined pore structure results, with a mean pore diameter of about 4 nm and a surface area of some 350,000 m^2/kg. The micrograph shown in Figure 17.3 taken from the work of Bowen *et al.*[9] shows, at the higher magnification, the regular hexagonal disposition of the pores at the thin edges of particles of alumina.

Activated alumina has a high affinity for water in particular, and for hydroxyl groups in general. It cannot compete in terms of capacity or selectivity with molecular sieves although its superior mechanical strength is important in moving-bed applications. As a powder, activated alumina may be used as a packing for chromatographic columns, as described in Chapter 19.

This book belongs to Bradley Loren (bloren@mcandrews-ip.com) Copyright Elsevier 2024

Intas Exhibit 1032
Page 368 of 470
PGR2025-00043

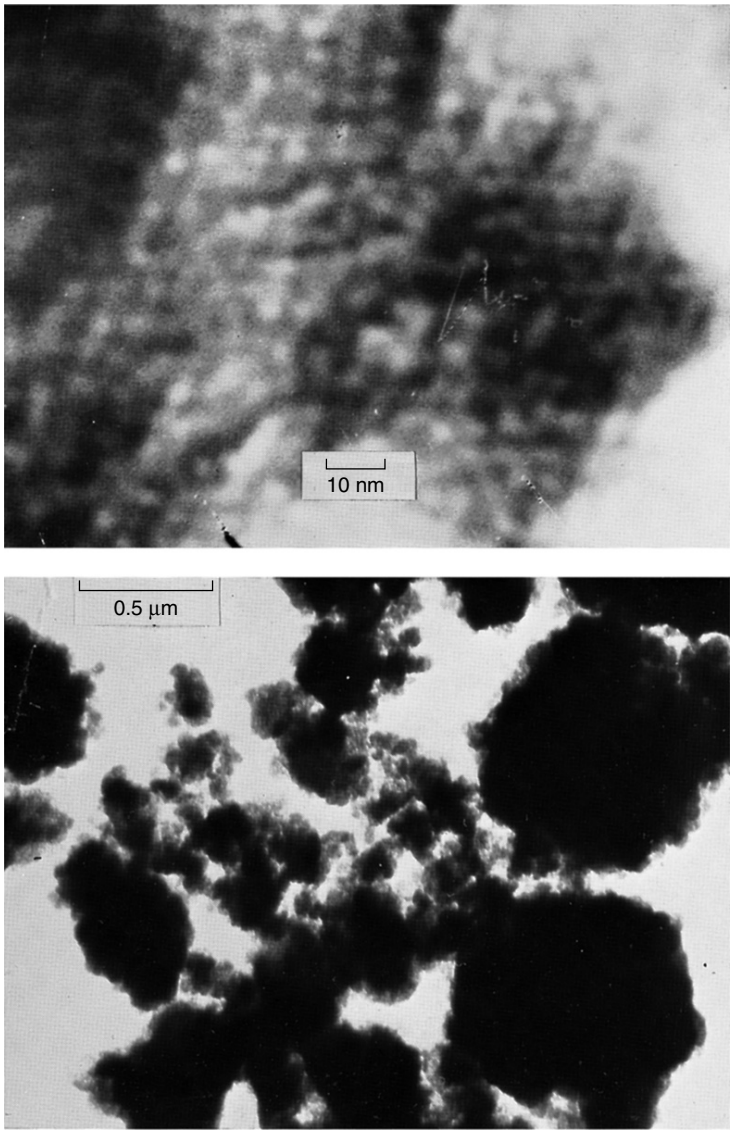


Figure 17.3. Electron micrographs of a commercial activated alumina at two magnifications[9]

17.3. ADSORPTION EQUILIBRIA

Much of the early work on the nature of adsorbents sought to explain the equilibrium capacity and the molecular forces involved. Adsorption equilibrium is a dynamic concept achieved when the rate at which molecules adsorb on to a surface is equal to the rate at which they desorb. The physical chemistry involved may be complex and no single theory

This book belongs to Bradley Loren (bloren@mcandrews-ip.com) Copyright Elsevier 2024
Intas Exhibit 1032
Page 369 of 470
PGR2025-00043

of adsorption has been put forward which satisfactorily explains all systems. Fortunately for the engineer, what is needed is an accurate representation of equilibrium, the theoretical minutiae of which is not of concern. For this reason, some of the earliest theories of adsorption are still the most useful, even though the assumptions on which they were based were seen in later years to be not entirely valid. Most theories have been developed for gas–solid systems because the gaseous state is better understood than the liquid. Statistical theories are being developed which should apply equally well to gas–solid and liquid–solid equilibria, though these are not yet at a stage when they can be applied easily and confidently to the design of equipment.

The capacity of an adsorbent for a particular adsorbate involves the interaction of three properties — the concentration C of the adsorbate in the fluid phase, the concentration C_s of the adsorbate in the solid phase and the temperature T of the system. If one of these properties is kept constant, the other two may be graphed to represent the equilibrium. The commonest practice is to keep the temperature constant and to plot C against C_s to give an adsorption isotherm. When C_s is kept constant, the plot of C against T is known as an adsorption isostere. In gas–solid systems, it is often convenient to express C as a pressure of adsorbate. Keeping the pressure constant and plotting C_s against T gives adsorption isobars. The three plots are shown for the ammonia-charcoal system in Figure 17.4 which is taken from the work of BRUNAUER[10].

17.3.1. Single component adsorption

Most early theories were concerned with adsorption from the gas phase. Sufficient was known about the behaviour of ideal gases for relatively simple mechanisms to be postulated, and for equations relating concentrations in gaseous and adsorbed phases to be proposed. At very low concentrations the molecules adsorbed are widely spaced over the adsorbent surface so that one molecule has no influence on another. For these limiting conditions it is reasonable to assume that the concentration in one phase is proportional to the concentration in the other, that is:

$$C_s = K_a C \tag{17.1}$$

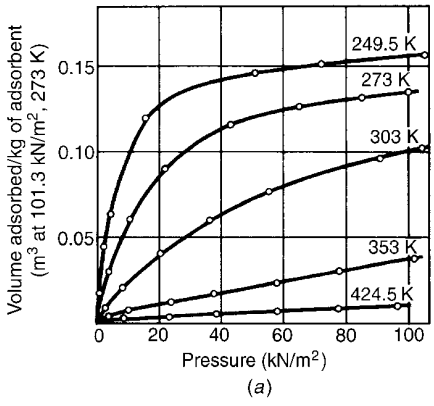
This expression is analogous to Henry's Law for gas–liquid systems even to the extent that the proportionality constant obeys the van't Hoff equation and $K_a = K_0 \, \mathrm{e}^{-\Delta H/\mathbf{R}T}$ where ΔH is the enthalpy change per mole of adsorbate as it transfers from gaseous to adsorbed phase. At constant temperature, equation 17.1 becomes the simplest form of adsorption isotherm. Unfortunately, few systems are so simple.

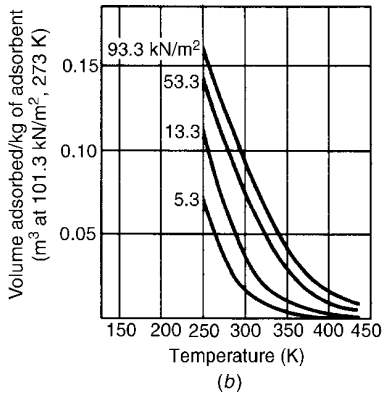
17.3.2. The Langmuir isotherm

At higher gas phase concentrations, the number of molecules absorbed soon increases to the point at which further adsorption is hindered by lack of space on the adsorbent surface. The rate of adsorption then becomes proportional to the empty surface available, as well as to the fluid concentration. At the same time as molecules are adsorbing, other molecules

This book belongs to Bradley Loren (bloren@mcandrews-ip.com) Copyright Elsevier 2024

Intas Exhibit 1032
Page 370 of 470
PGR2025-00043





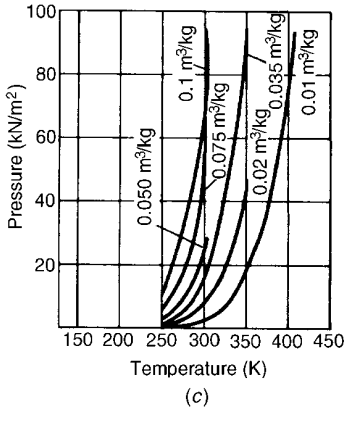


Figure 17.4. Equilibrium data for the adsorption of ammonia on charcoal[10]
(*a*) Adsorption isotherm (*b*) Adsorption isobar (*c*) Adsorption isostere

This book belongs to Bradley Loren (bloren@mcandrews-ip.com)
Copyright Elsevier 2024
Intas Exhibit 1032
Page 371 of 470
PGR2025-00043

will be desorbing if they have sufficient activation energy. At a fixed temperature, the rate of desorption will be proportional to the surface area occupied by adsorbate. When the rates of adsorption and desorption are equal, a dynamic equilibrium exists. For adsorption which is confined to a mono-molecular layer, the equilibrium may be written as:

$$k_0 a_0 C = k_0(1 - a_1)C = k_1' a_1$$

or:

$$a_1 = \frac{B_0 C}{1 + B_0 C} \tag{17.2}$$

where: a_0 is the fraction of empty surface,
a_1 is the fraction of surface occupied by a monolayer of adsorbed molecules,
$B_0 = k_0/k_1'$,
k_0 is the velocity constant for adsorption on to empty surface, and
k_1' is the velocity constant for desorption from a monolayer.

Equation 17.2 has been developed for adsorption from the gas phase. It is convenient to also express it in terms of partial pressures, which gives:

$$\frac{C_s}{C_{sm}} = \frac{B_1 P}{1 + B_1 P} \tag{17.3}$$

where: C_s is the concentration of the adsorbed phase,
C_{sm} is the concentration of the adsorbed phase when the monolayer is complete,
$B_1 = B_0/\mathbf{R}T$,and
P is the partial pressure of adsorbate in the gas phase
.

Equations 17.2 and 17.3 have the form of the LANGMUIR[11] equation, developed in 1916, which describes the adsorption of gases on to plane surfaces of glass, mica and platinum. A number of assumptions is implicit in this development. As well as being limited to monolayer adsorption, the Langmuir equation assumes that:

(a) these are no interactions between adjacent molecules on the surface.
(b) the energy of adsorption is the same all over the surface.
(c) molecules adsorb at fixed sites and do not migrate over the surface.

When $B_1 P \ll 1$, equation 17.3 reverts to the form of Henry's Law, as given in equation 17.1. Equation 17.3 can be rewritten in linear form to give:

$$\frac{P}{C_s} = \frac{P}{C_{sm}} + \frac{1}{B_1 C_{sm}} \tag{17.4}$$

so that a plot of P/C_s against P will be a straight line when applied to a system that behaves in accordance with the Langmuir isotherm.

It has been shown experimentally, however, that many systems do not follow this isotherm and efforts continue to find an improved equation.

This book belongs to Bradley Loren (bloren@mcandrews-ip.com) Copyright Elsevier 2024

Intas Exhibit 1032
Page 372 of 470
PGR2025-00043

17.3.3. The BET isotherm

In 1938, BRUNAUER, EMMETT and TELLER[12] and EMMETT and DE WITT[13] developed what is now known as the BET theory. As in the case in Langmuir's isotherm, the theory is based on the concept of an adsorbed molecule which is not free to move over the surface, and which exerts no lateral forces on adjacent molecules of adsorbate. The BET theory does, however, allow different numbers of adsorbed layers to build up on different parts of the surface, although it assumes that the net amount of surface which is empty or which is associated with a monolayer, bilayer and so on is constant for any particular equilibrium condition. Monolayers are created by adsorption on to empty surface and by desorption from bilayers. Monolayers are lost both through desorption and through the adsorption of additional layers. The rate of adsorption is proportional to the frequency with which molecules strike the surface and the area of that surface. From the kinetic theory of gases, the frequency is proportional to the pressure of the molecules and hence:

The rate of adsorption on to empty surface $= k_0 a_0 P$, and
the rate of desorption from a monolayer $= k_1' a_1$

Desorption is an activated process. If E_1 is the excess energy required for one mole in the monolayer to overcome the surface forces, the proportion of molecules possessing such energy is $e^{-E_1/\mathbf{R}T}$. Hence the rate of desorption from a monolayer may be written as:

$$A_1' e^{-E_1/\mathbf{R}T} a_1$$

where A_1' is the frequency factor for monolayer desorption.

The dynamic equilibrium of the monolayer is given by:

$$k_0 a_0 P + A_2' e^{-E_2/\mathbf{R}T} a_2 = k_1 a_1 P + A_1' e^{-E_1/\mathbf{R}T} a_1 \tag{17.5}$$

where A_2' is the frequency factor for description from a bilayer, thus creating a monolayer.

Applying similar arguments to the empty surface, then:

$$k_0 a_0 P = A_1' e^{-E_1/\mathbf{R}T} a_1 \tag{17.6}$$

From equations 17.5 and 17.6:

$$k_1 a_1 P = A_2' e^{-E_2/\mathbf{R}T} a_2$$

$$a_1 = \frac{k_0}{A_1'} e^{E_1/\mathbf{R}T} a_0 P = \alpha_0 a_0 \tag{17.7}$$

and:

$$a_2 = \frac{k_1}{A_2'} e^{E_2/\mathbf{R}T} a_1 P = \beta a_1 \tag{17.8}$$

The BET theory assumes that the reasoning used for one or two layers of molecules may be extended to n layers. It argues that energies of activation after the first layer are all equal to the latent heat of condensation, so that:

$$E_2 = E_3 = E_4 = \cdots = E_n = \lambda_M$$

This book belongs to Bradley Loren (bloren@mcandrews-ip.com) Copyright Elsevier 2024

Intas Exhibit 1032
Page 373 of 470
PGR2025-00043

Hence it may be assumed that β is constant for layers after the first and:

$$a_i = \beta^{i-1} a_1 = B_2 \beta^i a_0$$

where $B_2 = \alpha_0/\beta$, and a_i is the fraction of the surface area containing i layers of adsorbate.

Since $a_0, a_1, \ldots$ are fractional areas, their summation over n layers will be unity and:

$$\begin{aligned} 1 &= a_0 + \sum_{i=1}^{n} a_i \\ &= a_0 + \sum_{i=1}^{n} B_2 \beta^i a_0 \end{aligned} \tag{17.9}$$

The total volume of adsorbate associated with unit area of surface is given by:

$$v_s = v_s^1 \sum_{i=1}^{n} i a_i = v_s^1 \sum_{i=1}^{n} i B_2 \beta^i a_0 \tag{17.10}$$

where v_s^1 is the volume of adsorbate in a unit area of each layer.

Since v_s^1 does not change with n, a geometrically plane surface is implied. Strictly, equation 17.10 is not applicable to highly convex or concave surfaces. Equations 17.9 and 17.10 may be combined to give:

$$\frac{v_s}{v_s^1} = \frac{\sum_{i=1}^{n} i B_2 \beta^i a_0}{a_0 + \sum_{i=1}^{n} B_2 \beta^i a_0} \tag{17.11}$$

The numerator of equation 17.11 may be written as:

$$B_2 a_0 \beta \frac{\mathrm{d}}{\mathrm{d}\beta} \left(\sum_{i=1}^{n} \beta^i \right) = B_2 a_0 \beta \frac{\mathrm{d}}{\mathrm{d}\beta} \left\{ \left(\frac{1 - \beta^n}{1 - \beta} \right) \beta \right\}$$

and the denominator as:

$$a_0 \left[1 + B_2 \beta \left(\frac{1 - \beta^n}{1 - \beta} \right) \right]$$

Substituting these values into equation 17.11 and rearranging gives:

$$\frac{v_s}{v_s^1} = \frac{B_2 \beta}{1 - \beta} \frac{[1 - (n+1)\beta^n + n\beta^{n+1}]}{[1 + (B_2 - 1)\beta - B_2 \beta^{n+1}]} \tag{17.12}$$

On a flat unrestricted surface, there is no theoretical limit to the number of layers that can build up. When $n = \infty$, equation 17.12 becomes:

$$\frac{v_s}{v_s^1} = \frac{B_2 \beta}{(1 - \beta)(1 - \beta + B_2 \beta)} \tag{17.13}$$

This book belongs to Bradley Loren (bloren@mcandrews-ip.com) Copyright Elsevier 2024

Intas Exhibit 1032
Page 374 of 470
PGR2025-00043

When the pressure of the adsorbate in the gas phase is increased to the saturated vapour pressure, condensation occurs on the solid surface and v_s/v_s^1 approaches infinity. In equation 17.13, this condition corresponds to putting $\beta = 1$. It may be noted that putting $\beta = 1/(1 - B_2)$ is not helpful.

Hence from equation 17.8:

$$1 = \frac{k_1}{A_2'} e^{\lambda_M/\mathbf{R}T} \cdot P^0$$

where: λ_M is the molar latent heat and
P^0 is the saturated vapour pressure.

Hence, from equation 17.8, $\beta = P/P^0$.

Equation 17.12 may be rewritten for unit mass of adsorbent instead of unit surface. This is known as the limited form of the BET equation which is:

$$\frac{V_s}{V_s^1} = B_2 \frac{P}{P^0} \frac{[1 - (n+1)(P/P^0)^n + n(P/P^0)^{n+1}]}{(1 - P/P^0)[1 + (B_2 - 1)(P/P^0) - B_2(P/P^0)^{n+1}]} \tag{17.14}$$

where V_s^1 is the volume of adsorbate contained in a monolayer spread over the surface area present in unit mass of adsorbent.

When $n = 1$, adsorption is confined to a monolayer and equation 17.14 reduces to the Langmuir equation.

When $n = \infty$, $(P/P^0)^n$ approaches zero and equation 17.13 may be rearranged in a convenient linear form to give:

$$\frac{P/P_0}{V(1 - P/P_0)} = \frac{1}{V^1 B_2} + \frac{B_2 - 1}{V^1 B_2} \left(\frac{P}{P^0} \right) \tag{17.15}$$

where V and V^1 are the equivalent gas phase volumes of V_s and V_s^1.

If a plot of the left-hand term against P/P^0 is linear, the experimental data may be said to fit the infinite form of the BET equation. From the slope and the intercept, V^1 and B_2 may be calculated.

The advantage of equation 17.14 is that it may be fitted to all known shapes of adsorption isotherm. In 1938, a classification of isotherms was proposed which consisted of the five shapes shown in Figure 17.5 which is taken from the work of BRUNAUER *et al.*[14]. Only gas–solid systems provide examples of all the shapes, and not all occur frequently. It is not possible to predict the shape of an isotherm for a given system, although it has been observed that some shapes are often associated with a particular adsorbent or adsorbate properties. Charcoal, with pores just a few molecules in diameter, almost always gives a Type I isotherm. A non-porous solid is likely to give a Type II isotherm. If the cohesive forces between adsorbate molecules are greater than the adhesive forces between adsorbate and adsorbent, a Type V isotherm is likely to be obtained for a porous adsorbent and a Type III isotherm for a non-porous one.

In some systems, three stages of adsorption may be discerned. In the activated alumina-air-water vapour system at normal temperature, the isotherm is found to be of Type IV. This consists of two regions which are concave to the gas concentration axis separated by a region which is convex. The concave region that occurs at low gas concentrations is usually associated with the formation of a single layer of adsorbate molecules over the

This book belongs to Bradley Loren (bloren@mcandrews-ip.com) Copyright Elsevier 2024

Intas Exhibit 1032
Page 375 of 470
PGR2025-00043

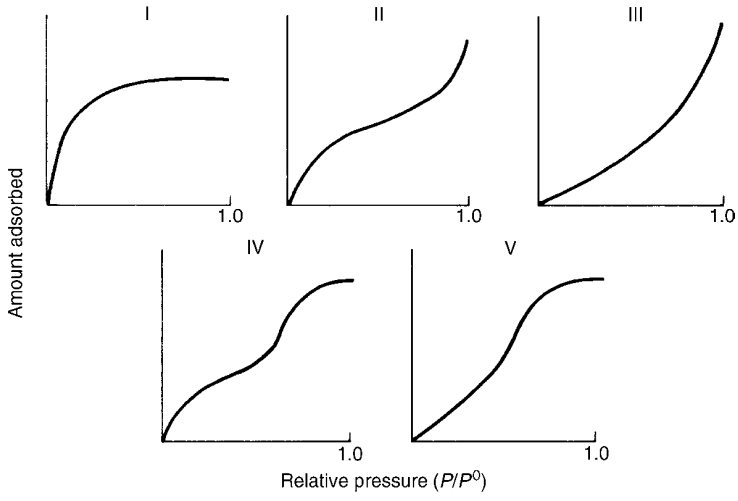


Figure 17.5. Classification of isotherms into five types of BRUNAEUR, DEMING, DEMING and TELLER[14]

surface. The convex portion corresponds to the build-up of additional layers, whilst the other concave region is the result of condensation of adsorbate in the pores — so called *capillary condensation* as discussed earlier in this Section.

At low gas concentrations, whilst the monolayer is still incomplete, the absorbed molecules are relatively immobile. In the multilayer region, the adsorbed molecules behave more like a liquid film. The amount of capillary condensation that occurs depends on the pore sizes and their distribution, as well as on the concentration in the gas phase.

When $n = 1$, equation 17.14 represents a Type I isotherm.

When $n = \infty$, equation 17.14 represents a Type II, and the rarer Type III isotherm by choosing a suitable value for B_2. As B_2 is increased, the point of inflexion or "knee" of Type II becomes more prominent. This corresponds to an increasing tendency for the monolayer to become complete before a second layer starts. In the extreme case of an adsorbent whose surface is very uniform from an energy point of view, the adsorbate builds up in well-defined layers. This gives rise to a stepped isotherm, in which each step corresponds to another layer. When B_2 is less than 2, there is no point of inflexion and Type III isotherms are obtained. The condition $1 > B_2 > 0$ often corresponds to a tendency for molecules to adsorb in clusters rather than in complete layers.

The success of the BET equation in representing experimental data should not be regarded as a measure of the accuracy of the model on which it is based. Its capability of modelling the mobile multilayers of a Type IV isotherm is entirely fortuitous because, in the derivation of the equation, it is assumed that adsorbed molecules are immobile.

Example 17.1

Spherical particles of 15 nm diameter and density 2290 kg/m^3 are pressed together to form a pellet. The following equilibrium data were obtained for the sorption of nitrogen at 77 K. Obtain estimates

This book belongs to Bradley Loren (bloren@mcandrews-ip.com) Copyright Elsevier 2024

Intas Exhibit 1032
Page 376 of 470
PGR2025-00043

of the surface area of the pellet from the adsorption isotherm and compare the estimates with the geometric surface. The density of liquid nitrogen at 77 K is 808 kg/m^3.

P/P^0	0.1	0.2	0.3	0.4	0.5	0.6	0.7	0.8	0.9
m^3 liq $N_2 \times 10^6$/kg solid	66.7	75.2	83.9	93.4	108.4	130.0	150.2	202.0	348.0

where P is the pressure of the sorbate and P^0 is its vapour pressure at 77 K.

Use the following data:

$$\text{density of liquid nitrogen} = 808 \text{ kg/m}^3$$

$$\text{area occupied by one adsorbed molecule of nitrogen} = 0.162 \text{ nm}^2$$

$$\text{Avogadro Number} = 6.02 \times 10^{26} \text{ molecules/kmol}$$

Solution

For 1 m^3 of pellet with a voidage ε, then:

$$\text{Number of particles} = (1-\varepsilon)/(\pi/6)(15 \times 10^{-9})^3$$

$$\text{Surface area per unit volume} = (1-\varepsilon)\pi(15 \times 10^{-9})^2/(\pi/6)(15 \times 10^{-9})^3$$

$$= 6(1-\varepsilon)/(15 \times 10^{-9}) \text{ m}^2/\text{m}^3$$

1 m^3 of pellet contains 2290 $(1-\varepsilon)$ kg solid and hence:

$$\text{specific surface} = 6(1-\varepsilon)/[(15 \times 10^{-9}(1-\varepsilon)2290]$$

$$= \underline{\underline{1.747 \times 10^5 \text{ m}^2/\text{kg}}}$$

(a) *Using the BET isotherm*

$$(P/P^0)/[V(1-P/P^0)] = 1/V'B + (B-1)(P/P^0)/V'B \qquad \text{(equation 17.15)}$$

where V and V' are the liquid volumes of adsorbed nitrogen.

From the adsorption data given:

(P/P^0)	0.1	0.2	0.3	0.4	0.5	0.6
V (m^3 liquid N_2/kg solid $\times 10^6$)	66.7	75.2	83.9	93.4	108.4	130.0
$((P/P^0)/V) \times 10^{-6}$	1500	2660	3576	4283	4613	4615
$(P/P^0)/[V(1-P/P^0)]$	1666	3333	5109	7138	9226	11538

Plotting $(P/P^0)/[V(1-P/P^0)]$ against (P/P^0), as shown in Figure 17.6, then:

$$\text{intercept, } 1/V'B = 300, \text{ and slope, } (B-1)/V'B = 13{,}902$$

This book belongs to Bradley Loren (bloren@mcandrews-ip.com) Copyright Elsevier 2024

Intas Exhibit 1032
Page 377 of 470
PGR2025-00043

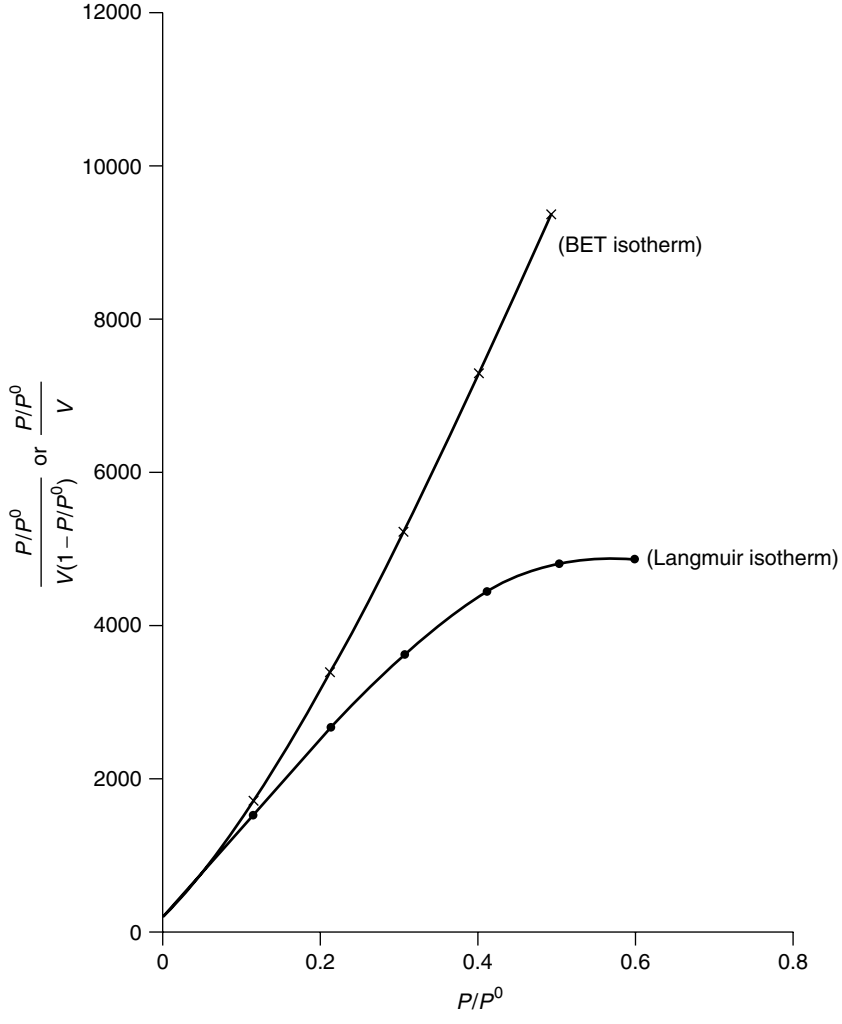


Figure 17.6. Adsorption isotherms for Example 17.1.

from which:

$$B = (13{,}902/300) + 1 = 47.34$$

and:

$$V' = 1/(300 \times 47.34) = 70.4 \times 10^{-6}\ \text{m}^3/\text{kg}.$$

$$\text{The total surface area} = [(70.4 \times 10^{-6} \times 808 \times 6.2 \times 10^{26} \times 0.162 \times 10^{-18})]/28$$

$$= \underline{\underline{2.040 \times 10^5\ \text{m}^2/\text{kg}}}.$$

This book belongs to Bradley Loren (bloren@mcandrews-ip.com) Copyright Elsevier 2024

Intas Exhibit 1032
Page 378 of 470
PGR2025-00043

(b) *Using the Langmuir form of the isotherm:*

Assuming this applies at low concentrations then, expressing pressure as the ratio P/P^0, and the amount adsorbed as a volume of liquid adsorbate, equation 17.4 becomes:

$$(P/P^0)/V = (P/P^0)/V' + 1/(B_2V')$$

Thus, a plot of $(P/P^0)/V$ against (P/P^0) will have a slope of $(1/V')$.

Thus, from Figure 17.6:

$$1/V' = 13{,}902$$

and:

$$V' = 71.9 \times 10^{-6}\text{m}^3/\text{kg}$$

which agrees with the value from the BET isotherm.

It may be noted that areas calculated from the isotherm are some 20 per cent greater than the geometric surface, probably due to the existence of some internal surface within the particles.

17.3.4. The Gibbs isotherm

An entirely different approach to equilibrium adsorption is to assume that adsorbed layers behave like liquid films, and that the adsorbed molecules are free to move over the surface. It is then possible to apply the equations of classical thermodynamics. The properties which determine the free energy of the film are pressure and temperature, the number of molecules contained and the area available to the film. The Gibbs free energy G may be written as:

$$G = F(P, T, n_s, A_s) \tag{17.16}$$

Hence:

$$\mathrm{d}G = \left(\frac{\partial G}{\partial P}\right)_{T,n_s,A_s} ; \mathrm{d}P + \left(\frac{\partial G}{\partial T}\right)_{P,n_s,A_s} ; \mathrm{d}T + \left(\frac{\partial G}{\partial n_s}\right)_{T,P,A_s} ; \mathrm{d}n_s + \left(\frac{\partial G}{\partial A_s}\right)_{T,P,n_s} \mathrm{d}A_s \tag{17.17}$$

At constant temperature and pressure this becomes:

$$\mathrm{d}G = \left(\frac{\partial G}{\partial n_s}\right) \mathrm{d}n_s + \left(\frac{\partial G}{\partial A_s}\right) \mathrm{d}A_s \tag{17.18}$$

$$= \mu_s \, \mathrm{d}n_s - \Gamma \, \mathrm{d}A_s \tag{17.19}$$

where: μ_s is the free energy per mole or chemical potential of the film, and
Γ is defined as a two-dimensional or spreading pressure.

The total Gibbs free energy may be written as:

$$G = \mu_s n_s - \Gamma A_s \tag{17.20}$$

so that:

$$\mathrm{d}G = \mu_s \, \mathrm{d}n_s + n_s \, \mathrm{d}\mu_s - \Gamma \, \mathrm{d}A_s - A_s \, \mathrm{d}\Gamma \tag{17.21}$$

A comparison of equations 17.19 and 17.21 shows that:

$$\mathrm{d}\Gamma = \frac{n_s}{A_s} \mathrm{d}\mu_s$$

This book belongs to Bradley Loren (bloren@mcandrews-ip.com) Copyright Elsevier 2024

Intas Exhibit 1032
Page 379 of 470
PGR2025-00043

If the gas phase is ideal and equilibrium exists between it and the sorbed phase then, by definition:

$$\mathrm{d}\mu_s = \mathrm{d}\mu_g = \mathbf{R}T\,\mathrm{d}(\ln P) \tag{17.22}$$

where μ_g is the chemical potential of the gas.

Substituting for $\mathrm{d}\mu_s$ gives:

$$\mathrm{d}\Gamma = \frac{n_s}{A_s}\mathbf{R}T\,\mathrm{d}(\ln P) \tag{17.23}$$

Equation 17.23 has the form of an adsorption isotherm since it relates the amount adsorbed to the corresponding pressure. This is known as the *Gibbs Adsorption Isotherm*. For it to be useful, an expression is required for Γ. Assuming an analogy between adsorbed and liquid films, HARKINS and JURA[15] have proposed that:

$$\Gamma = \alpha_1 - \beta_1 a_m \tag{17.24}$$

where α_1, β_1, are constants, $a_m = A_s/\mathbf{N}n_s$, the area per molecule of adsorbate and $\mathbf{N}$ is the Avogadro number. Substituting for $\mathrm{d}\Gamma$ in equation 17.23 and integrating, at constant A_s, from some condition P_1, n_{s_1} at which the adsorbed film becomes mobile, to an arbitrary coverage n_s at pressure P, gives:

$$\ln\frac{P}{P_1} = \frac{1}{\mathbf{R}T}\frac{\beta_1 A_s^2}{2\mathbf{N}}\left(\frac{1}{n_{s_1}^2} - \frac{1}{n_s^2}\right) \tag{17.25}$$

Equation 17.25 may be rewritten as:

$$\ln\frac{P}{P^0} = L' - \frac{M'}{V^2} \tag{17.26}$$

where V is the volume occupied in the gas phase by n_s moles of sorbate at a temperature T and pressure P.

Thus:
$$L' = \ln\frac{P_1}{P^0} + \frac{1}{\mathbf{R}T}\frac{\beta_1 A_s^2}{2\mathbf{N}}\frac{1}{n_{s_1}^2} \tag{17.27a}$$

and:
$$M' = \frac{1}{\mathbf{R}T}\frac{\beta_1 A_s^2}{2\mathbf{N}}\frac{1}{\rho_g^2} \tag{17.27b}$$

where ρ_g is the molar density of the gas phase. Equation 17.26 is the *Harkins-Jura (H–J) equation*, which may be used to correlate adsorption data and to obtain an estimate of the surface area of an adsorbent.

The H–J model may be criticised because the comparison between an adsorbed film on a solid surface and a liquid film on a liquid surface does not stand detailed examination. Other equations of state have been used instead of equation 17.24. These are discussed in more detail by RUTHVEN[16].

Although making fundamentally different assumptions about the static or mobile nature of an adsorbed layer, the BET and H–J equations may often represent a set of experimental data equally well. As pointed out by GARG and RUTHVEN[17], their respective assumptions lead one to expect that the BET equation may be applied to low surface coverage when

This book belongs to Bradley Loren (bloren@mcandrews-ip.com) Copyright Elsevier 2024

Intas Exhibit 1032
Page 380 of 470
PGR2025-00043

it is thought that adsorbed molecules do not move. The H–J equation may be applied to the middle range of relative pressures (P/P^0) corresponding to the completion of a monolayer and the formation of additional mobile layers. Neither theory, it seems, is equipped to deal with the filling of micropores that occurs with the onset of capillary condensation at higher relative pressures. For this condition, a third theory of adsorption has been shown to be useful.

17.3.5. The potential theory

In this theory the adsorbed layers are considered to be contained in an *adsorption space* above the adsorbent surface. The space is composed of equipotential contours, the separation of the contours corresponding to a certain adsorbed volume, as shown in Figure 17.7. The theory was postulated in 1914 by POLANYI[18], who regarded the potential of a point in adsorption space as a measure of the work carried out by surface forces in bringing one mole of adsorbate to that point from infinity, or a point at such a distance from the surface that those forces exert no attraction. The work carried out depends on the phases involved. Polanyi considered three possibilities: (a) that the temperature of the system was well below the critical temperature of the adsorbate and the adsorbed phase could be regarded as liquid, (b) that the temperature was just below the critical temperature and the adsorbed phase was a mixture of vapour and liquid, (c) that the temperature was above the critical temperature and the adsorbed phase was a gas. Only the first possibility, the simplest and most common, is considered here.

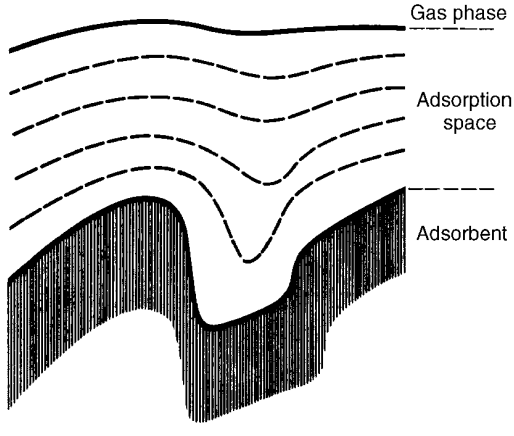


Figure 17.7. The concept of adsorption space used by Polanyi[18]

At temperatures below the critical point, the pressure at the adsorbent surface is the saturated vapour pressure of the liquid adsorbate, P^0. At the limit of adsorption space, the pressure exerted by the adsorbate molecules in the gas phase is P. For an ideal gas, the work done bringing a mole to the adsorbent surface is given by:

$$\varepsilon_p = \mathbf{R}T \ln P^0/P \tag{17.28}$$

This book belongs to Bradley Loren (bloren@mcandrews-ip.com) Copyright Elsevier 2024
Intas Exhibit 1032
Page 381 of 470
PGR2025-00043

The potential theory postulates a unique relationship between the adsorption potential ε_p and the volume of adsorbed phase contained between that equipotential surface and the solid. It is convenient to express the adsorbed volume as the corresponding volume in the gas phase.

Hence: $$\varepsilon_p = \mathrm{f}(V) \tag{17.29}$$

where the function is assumed to be independent of temperature. Equations 17.28 and 17.29 may be combined to give an adsorption isotherm equation, although this is not explicit until the form of $\mathrm{f}(V)$ has been specified. The form may be expressed graphically by plotting $\mathbf{R}T \ln P^0/P$ against V, giving what is called a characteristic curve as shown in Figure 17.8. The curve is valid for a particular adsorbent and adsorbate at any temperature and its validity may often be extended to other adsorbates on the same adsorbent. The adsorption potential must then be rewritten as:

$$\varepsilon_p = \beta_2 \mathrm{f}_1(V) \tag{17.30}$$

where β_2 is a coefficient of affinity. For many adsorbates, β_2 is proportional to the molar volume V'_M of the liquid adsorbate at a temperature T. Values of β_2 for some hydrocarbons, relative to benzene, are given in Table 17.4 which is taken from the work

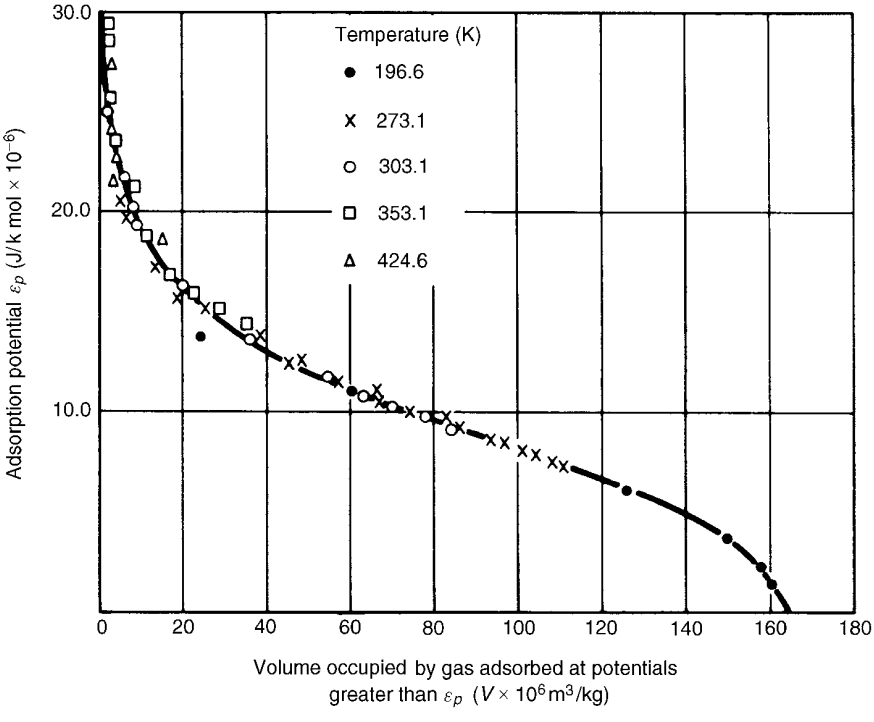


Figure 17.8. Characteristic curve for the adsorption of carbon dioxide on to charcoal[10]

This book belongs to Bradley Loren (bloren@mcandrews-ip.com) Copyright Elsevier 2024
Intas Exhibit 1032
Page 382 of 470
PGR2025-00043

Table 17.4. Values of coefficients of affinity relative to $\beta_2 = 1$ for benzene, and of $V'_M/V'_{M(\text{benzene})}$

Vapour	β_2 expt	$V'_M/V'_{M(\text{benzene})}$
C_6H_6	1	1
C_5H_{12}	1.12	1.28
C_6H_{12}	1.04	1.21
C_7H_{16}	1.50	1.65
$C_6H_5CH_3$	1.28	1.19
CH_3Cl	0.56	0.59
CH_2Cl_2	0.66	0.71
$CHCl_3$	0.88	0.90
CCl_4	1.07	1.09
C_2H_5Cl	0.78	0.80
CH_3OH	0.40	0.46
C_2H_5OH	0.61	0.65
HCOOH	0.60	0.63
CH_3COOH	0.97	0.96
$(C_2H_5)_2O$	1.09	1.17
CH_3COCH_3	0.88	0.82
CS_2	0.70	0.68
CCl_3NO	1.28	1.12
NH_3	0.28	0.30

of YOUNG and CROWELL[19], with relative molar volumes listed for comparison. For the same volume V of adsorbates 1 and 2:

$$\frac{\varepsilon_{p1}}{\varepsilon_{p2}} = \frac{\beta_{21}}{\beta_{22}} = \frac{V'_{M1}}{V'_{M2}} \tag{17.31}$$

so that the pressures exerted by a particular volume of adsorbate on the same adsorbent are related by:

$$\left(\frac{T}{V'_M}\ln\frac{P^0}{P}\right)_1 = \left(\frac{T}{V'_M}\ln\frac{P^0}{P}\right)_2 \tag{17.32}$$

Thus, from adsorption data for one gas, data for other gases on the same adsorbent may be found. Several other methods of plotting the characteristic curve have been proposed[3].

17.4. MULTICOMPONENT ADSORPTION

The three isotherms discussed, BET, (H–J based on Gibbs equation) and Polanyi's potential theory involve fundamentally different approaches to the problem. All have been developed for gas–solid systems and none is satisfactory in all cases. Many workers have attempted to improve these and have succeeded for particular systems. Adsorption from gas mixtures may often be represented by a modified form of the single adsorbate equation. The Langmuir equation, for example, has been applied to a mixture of n'' components[11].

This book belongs to Bradley Loren (bloren@mcandrews-ip.com) Copyright Elsevier 2024

Intas Exhibit 1032
Page 383 of 470
PGR2025-00043

The volume of the ith component V_i which is adsorbed at a partial pressure P_i is given by:

$$\frac{V_i}{V_i^1} = \frac{B_i P_i}{1 + \sum_{j=1}^{n''} B_j P_j} \tag{17.33}$$

where V_i^1 is the volume of i contained in a monolayer.

Thermodynamic arguments indicate that V^1 should be the same for all species. A mean value V^1 is used, which for a binary mixture is given by:

$$\frac{1}{V^1} = \frac{y_1}{V_1^1} + \frac{y_2}{V_2^1} \tag{17.34}$$

where y_1, y_2 are mole fractions.

Equation 17.33 has a limited application. A fuller discussion of adsorption from gas mixtures can be found in the literature[3,16,19,20].

17.5. ADSORPTION FROM LIQUIDS

Adsorption from liquids is less well understood than adsorption from gases. In principle the equations derived for gases ought to be applicable to liquid systems, except when capillary condensation is occurring. In practice, some offer an empirical fit of the equilibrium data. One of the most popular adsorption isotherm equations used for liquids was proposed by FREUNDLICH[21] in 1926. Arising from a study of the adsorption of organic compounds from aqueous solutions on to charcoal, it was shown that the data could be correlated by an equation of the form:

$$C_s' = \alpha_2 (C^*)^{1/n} \tag{17.35}$$

where: C_s' is mass of adsorbed solute per unit mass of charcoal, and
C^* is the concentration of solute in solution in equilibrium with that on the solid.
α_2 and n are constants, the latter normally being greater than unity.

Although this was proposed originally as an empirical equation, the Freundlich isotherm was shown later to have some thermodynamic justification by GLUECKAUF and COATES[22]. It has also been modified for binary mixtures. In gas–solid systems, it is convenient to measure the amount adsorbed by noting the changes in pressures and volume of the gas phase, or the change in the mass of the solid. Neither approach is practicable in liquid–solid systems because the volume changes in the liquid phase are small, and because of the difficulty of distinguishing between the adsorbed phase and liquid clinging to the solid that is removed from solution. Instead, the amount adsorbed is calculated from the changes in concentration of a known volume of liquid after it has attained equilibrium with a known amount of adsorbent. Adsorption from solutions of non-electrolytes has been discussed by KIPLING[23].

17.6. STRUCTURE OF ADSORBENTS

The equilibrium capacity of an adsorbent for different molecules is one factor affecting its selectivity. Another is the structure of the system of pores which permeates the adsorbent.

This book belongs to Bradley Loren (bloren@mcandrews-ip.com) Copyright Elsevier 2024

Intas Exhibit 1032
Page 384 of 470
PGR2025-00043

This determines the size of molecules that can be admitted and the rate at which different molecules diffuse towards the surface. Molecular sieves, with their precise pore sizes, are uniquely capable of separating on the basis of molecular size. In addition, it is sometimes possible to exploit the different rates of diffusion of molecules to bring about their separation. A particularly important example referred to earlier, concerns the production of oxygen and nitrogen from air.

Although it is sometimes possible to view pores with an electron microscope and to obtain a measure of their diameter, it is difficult by this means to measure the distribution of sizes and impossible to measure the associated surface area. Adsorptive methods are used instead, employing some of the theories of adsorption explained previously.

17.6.1. Surface area

The simplest measure of surface area is that obtained by the so-called *point B method*. Many isotherms of Type II or IV show a straight section at intermediate relative pressures. The more pronounced the section, the more complete is the adsorbed monolayer before multilayer adsorption begins. As may be seen from Figure 17.9, the lower limit of the straight section is the point B which was identified by EMMETT[24] and YANG[3] as corresponding to a complete monolayer. This interpretation is accepted as a convenient empiricism.

The BET isotherm, represented by equation 17.14, may be rearranged as:

$$\frac{\phi_1}{V_s} = \frac{1}{V_s^1 B_2} + \frac{\theta_1}{V_s^1} \tag{17.36}$$

where:

$$\phi_1 = \frac{P/P^0[1 - (P/P^0)^n - n(P/P^0)^n(1 - P/P^0)]}{(1 - P/P^0)^2}$$

$$\theta_1 = \frac{P}{P^0}\frac{[1 - (P/P^0)^n]}{(1 - P/P^0)^n}$$

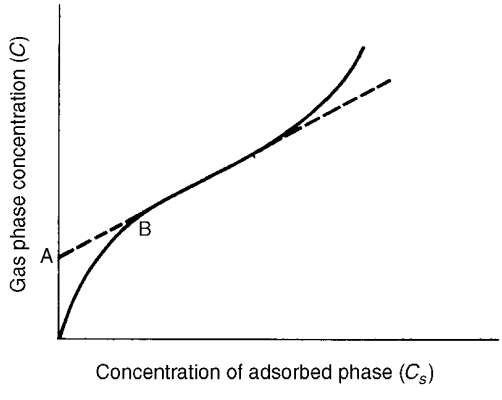


Figure 17.9. The "point B" method of estimating surface area

This book belongs to Bradley Loren (bloren@mcandrews-ip.com) Copyright Elsevier 2024
Intas Exhibit 1032
Page 385 of 470
PGR2025-00043

For a given value of n, a plot of ϕ_1/V_s against θ_1 should give a straight line from the slope of which V_s^1 may be calculated. The simpler, infinite, form of the BET isotherm is given by equation 17.15. The appropriate plot gives a straight line, from the slope and intercept of which V_1 may be calculated. Equation 17.15 is most likely to apply at low relative pressures.

Equation 17.26, derived by HARKINS and JURA[15] may be plotted as ln (P/P_0) against $1/V^2$ to give a straight line. The slope is proportional to A_s^2. The constant of proportionality may be found by using the same adsorbate on a solid of known surface area. Since the equation was derived for mobile layers and makes no provision for capillary condensation, it is most likely to fit data in the intermediate range of relative pressures.

17.6.2. Pore sizes

Having obtained a measure of surface area, a mean pore size may be calculated by simplifying the pore system into n_p cylindrical pores per unit mass of adsorbent, of mean length L_p and mean pore radius r_p.

Hence: Pore volume $V_p = n_p \pi r_p^2 L_p$

Surface area $A_p = 2n_p \pi r_p L_p$

and:
$$r_p = \frac{2V_p}{A_p} \tag{17.37}$$

This expression has been generalised by EVERETT and STONE[8] for any shape of capillary by including a shape factor γ which takes a value that depends on the geometry of the capillary. This is unity for parallel sided fissures as well as for cylindrical pores.

Where there is a wide distribution of pore sizes and, possibly, quite separately developed pore systems, a mean size is not a sufficient measure. There are two methods of finding such distributions. In one a porosimeter is used, and in the other the hysteresis branch of an adsorption isotherm is utilised. Both require an understanding of the mechanism of capillary condensation.

The regions of Type IV and Type V isotherms which are concave to the gas-concentration axis at high concentrations correspond to the bulk condensation of adsorbate in the pores of the adsorbent. An equation relating volume condensed to partial pressure of adsorbate and pore size, may be found by assuming transfer of adsorbate to occur in three stages:

(i) transfer from the gas to a point above the meniscus in the capillary.
(ii) condensation on the meniscus.
(iii) transfer from a plane surface source of liquid adsorbate to the gas-phase in order to maintain the first stage.

At equilibrium the free energy changes associated with the second and third stages are zero. For the first stage at, constant temperature T:

$$\Delta G = \int_{P^0}^{P_m} V \, \mathrm{d}P = n_s \mathbf{R} T \ln \frac{P_m}{P^0} \tag{17.38}$$

This book belongs to Bradley Loren (bloren@mcandrews-ip.com) Copyright Elsevier 2024

Intas Exhibit 1032
Page 386 of 470
PGR2025-00043

where: n_s is the number of moles condensed,
P_m is the vapour pressure over the meniscus, and
P^0 is the vapour pressure over the plane surface.

Another expression for ΔG may be obtained from consideration of the interfacial changes that occur as the capillaries fill. This takes the form:

$$\Delta G = \Delta A_p(\sigma_{sl} - \sigma_{sv}) = -\Delta A_p \sigma_{lv} \cos\phi \tag{17.39}$$

where: σ represents surface tensions at the three interfaces of the solid (s), liquid (l) and vapour (v),
ϕ is the interfacial angle between liquid and solid, and
ΔA_p is the change in interfacial area.

Hence:

$$n_s \mathbf{R}T \ln \frac{P_m}{P^0} = -\Delta A_p \sigma_{lv} \cos\phi \tag{17.40}$$

If the transfer of $\mathrm{d}n_s$ moles results in a change in interfacial area $\mathrm{d}A_p$, then:

$$\frac{\mathrm{d}n_s}{\mathrm{d}A_p} = -\frac{\sigma_{lv}\cos\phi}{\mathbf{R}T\ln(P_m/P^0)} = \frac{1}{V_M}\frac{\mathrm{d}V}{\mathrm{d}A_p} \tag{17.41}$$

where: $\mathrm{d}V$ is the volume occupied by $\mathrm{d}n_s$ moles in the vapour phase, and
V_M is the molar volume.

Thus:

$$\frac{\mathrm{d}V}{\mathrm{d}A_p} = \frac{V_M \sigma_{lv}\cos\phi}{\mathbf{R}T\ln(P^0/P_m)} \tag{17.42}$$

The left-hand side of equation 17.42 is a characteristic dimension of the pores in which condensation or evaporation occurs at an adsorbate pressure P_m. This depends on the geometry of the pores, as well as whether adsorption or desorption is occurring. Figure 17.10 illustrates the conditions in a cylindrical pore. For desorption occurring from the free surface of condensate:

$$\mathrm{d}V = \mathrm{d}(\pi r_p^2 L_p) = \pi r_p^2 \,\mathrm{d}L_p$$

$$\mathrm{d}A_p = (2\pi r_p L_p) = 2\pi r_p \,\mathrm{d}L_p$$

Hence:

$$\frac{\mathrm{d}V}{\mathrm{d}A_p} = \frac{r_p}{2} \tag{17.43}$$

and:

$$r_p = \frac{2V_M}{\mathbf{R}T}\frac{\sigma_{lv}\cos\phi}{\ln P^0/P} \tag{17.44}$$

Equation 17.44 is known as the *Kelvin equation*, and is considered to be valid for desorption.

This book belongs to Bradley Loren (bloren@mcandrews-ip.com) Copyright Elsevier 2024

Intas Exhibit 1032
Page 387 of 470
PGR2025-00043

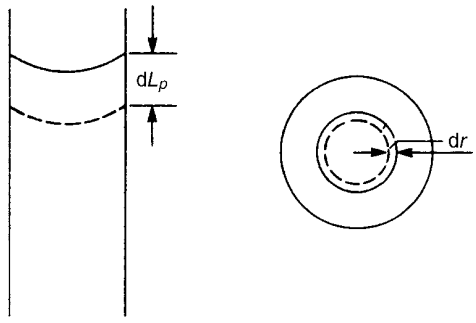


Figure 17.10. The capillary condensation equation applied to a cylindrical pore (*a*) for desorption (*b*) for adsorption

For adsorption on to existing layers of adsorbate on the cylindrical surface of the pores:

$$\mathrm{d}V = \mathrm{d}[\pi(r_p^2 - r^2)L_p] = -2\pi r L_p \,\mathrm{d}r$$
$$\mathrm{d}A_p = \mathrm{d}[2\pi r L_p] = 2\pi L_p \,\mathrm{d}r$$

Therefore:

$$r_p' = \frac{V_M}{\mathbf{R}T}\frac{\sigma_{lv}\cos\phi}{\ln P^0/P} \tag{17.45}$$

where r_p' is the net radius of the pore.

Equation 17.45 is known as the *Cohan equation*[25]. Together with equation 17.44, this offers an explanation of the hysteresis effect which many isotherms exhibit at high relative concentrations of 0.4–0.95. Figure 17.11 shows an isotherm for nitrogen on activated-alumina. A difference between adsorption and desorption conditions over the middle-to-high range of relative pressures may be noted. When applied to this range, equation 17.44 or equation 17.45 may be used to estimate the distribution of pore sizes contained within the adsorbent. A method, such as that of CRANSTON and INKLEY[26] leads to the distribution shown in Figure 17.12.

Interpretation of the pore radii calculated in this way is complicated by the fact that adsorption is occurring on the surface of pores which are, as yet, too big for condensation to occur. Radii given by equations 17.44 or 17.45 are net values, and an allowance has to be made for any adsorbed layers present when condensation occurs.

The actual structure of an adsorbent may be very different from a model assuming independent cylindrical pores. It may be possible to allow for the difference by including a geometric factor in the simple equations, or it may be necessary to "view" the surface using, for example, a scanning electron microscope. Sometimes the results are a pleasing confirmation of the simple assumptions. Figure 17.3 shows a transmission electron micrograph of an activated alumina similar to that which gave rise to Figures 17.11 and 17.12. The thin edges of particles are sufficiently transparent to the electron beam to show up parallel sets of pores on a hexagonal array, and about 4 nm in diameter, very close to

This book belongs to Bradley Loren (bloren@mcandrews-ip.com) Copyright Elsevier 2024

Intas Exhibit 1032
Page 388 of 470
PGR2025-00043

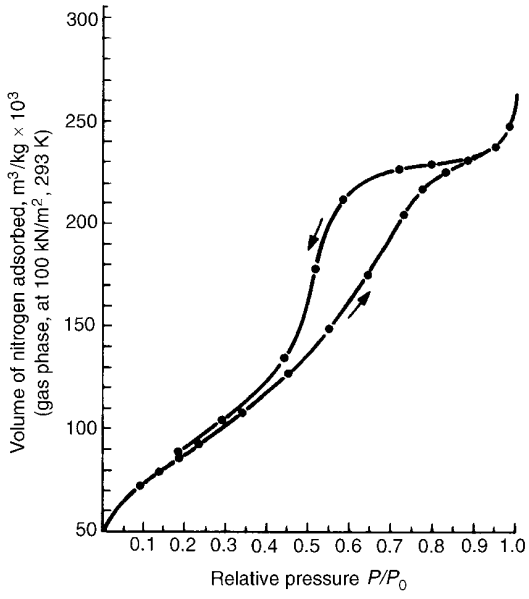


Figure 17.11. Nitrogen isotherm for activated alumina determined at the boiling point of liquid nitrogen

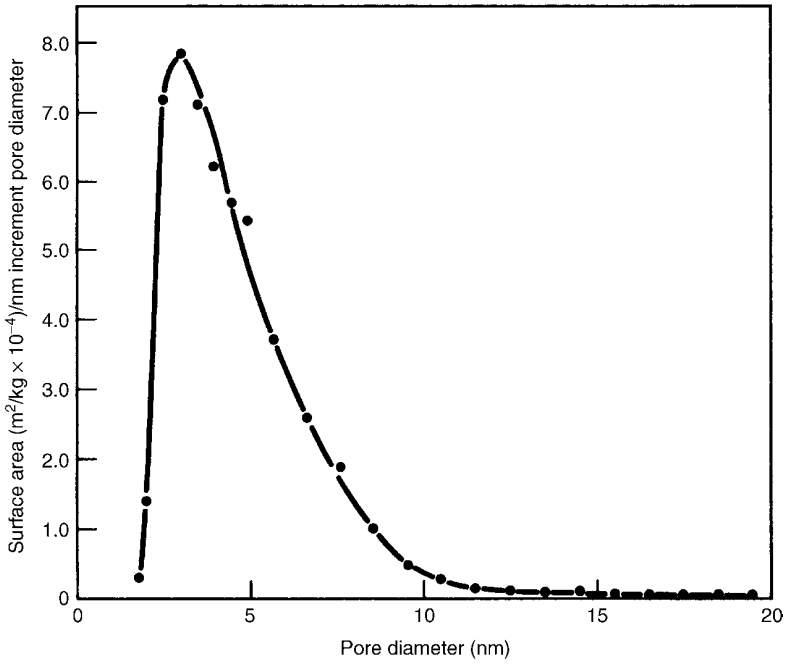


Figure 17.12. Pore size distribution of an activated alumina calculated from the isotherm by the method of Cranston and Inkley[26]

This book belongs to Bradley Loren (bloren@mcandrews-ip.com) Copyright Elsevier 2024

Intas Exhibit 1032
Page 389 of 470
PGR2025-00043

the peak in Figure 17.12. The physical structure of an adsorbent is an important factor in determining the rate at which adsorbate molecules diffuse to the adsorbent surface.

Example 17.2

Data taken from the adsorption leg of the isotherm of Figure 17.11 are listed in the first two columns of the following table. Test the applicability of the following equilibrium theories: (a) Langmuir (b) infinite BET and (c) Harkins and Jura. From (a) and (b) obtain estimates of the surface area of the adsorbent and compare the values with that obtained by the "point B" method. One molecule of nitrogen adsorbed on alumina occupies 0.162 nm^2.

The Avogadro Number is 6.02×10^{26} molecules/kmol.

P/P^0 (—)	$V \times 10^2$ ($m^3 N_2$/kg alumina at 293 K and 10^5 N/m^2)	$\frac{P}{P^0}\frac{1}{V}$ (kg/m^3)	$\frac{P}{P^0}\frac{1}{V}\frac{1}{(1-P/P^0)}$ (kg/m^3)	$\frac{1}{V^2}$ (kg^2/m^6)
0.05	6.6	0.76	0.80	230
0.10	7.4	1.35	1.50	183
0.15	8.1	1.85	2.18	152
0.20	8.8	2.27	2.88	129
0.25	9.4	2.66	3.55	113
0.30	10.2	2.94	4.20	96
0.35	10.9	3.21	4.94	84
0.40	11.7	3.42	5.73	73
0.50	13.8			53
0.60	16.5			37
0.87	19.6			26
0.80	22.1			20

Solution

(a) For $n = 1$, equation 17.14 may be written in a Langmuir form to give:

$$\frac{P/P^0}{V} = \frac{P/P^0}{V^1} + \frac{1}{B_2 V^1}$$

where V is the gas phase volume equivalent to the amount adsorbed.

The data, which are plotted as $(P/P^0)/V$ against P/P^0 in Figure 17.13, may be seen to conform to a straight line only at low values of P/P^0, suggesting that more than one layer of molecules is adsorbed.

From the slope of the line, $1/V^1 = 12.56$, hence $V^1 = 7.96 \times 10^{-2}$ m^3/kg

The surface area occupied by this adsorbed volume $= \frac{7.96 \times 10^{-2}}{24} \times 6.02 \times 10^{26} \times 0.162 \times 10^{-18}$

$= \underline{\underline{323{,}000 \text{ m}^2/\text{kg}}}$

This book belongs to Bradley Loren (bloren@mcandrews-ip.com) Copyright Elsevier 2024

(b) $$\frac{P/P^0}{V(1-P/P^0)} = \frac{1}{V^1 B_2} + \frac{B_2 - 1}{V^1 B_2}(P/P^0) \qquad \text{(equation 17.15)}$$

The left-hand side of equation 17.15 is plotted against P/P^0 in Figure 17.13. The data conform to a straight line over a wider range of relative pressure than was the case in (a).

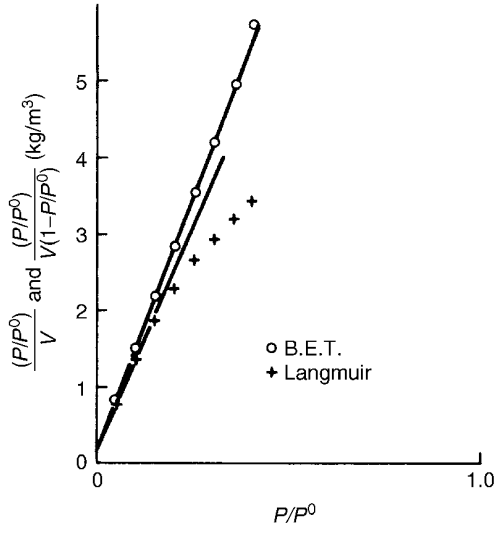


Figure 17.13. Langmuir and BET plots for Example 17.2

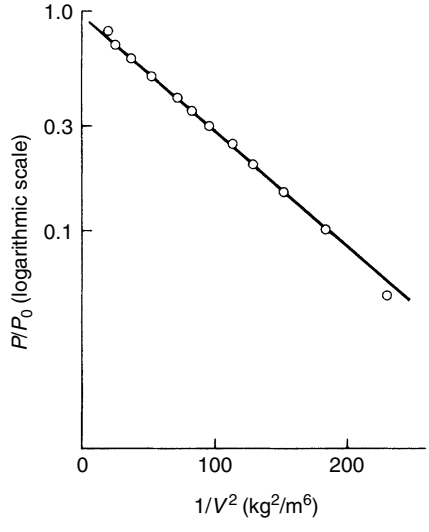


Figure 17.14. Harkins–Jura plot for Example 17.2

This book belongs to Bradley Loren (bloren@mcandrews-ip.com)
Copyright Elsevier 2024
Intas Exhibit 1032
Page 391 of 470
PGR2025-00043

$$\text{Slope}, \left(\frac{B_2 - 1}{V^1 B_2}\right) = 14.05$$

$$\text{Intercept}, \left(\frac{1}{V^1 B_2}\right) = 0.2$$

Hence: $B_2 = 71.2$ and $V^1 = 7.02 \times 10^{-2}$ m^3/kg
Surface area = 285,000 m^2/kg
From Figure 17.11, point B corresponds to about 7.5×10^{-2} m^3/kg or 305,000 m^2/kg

(c) According to equation 17.26, a plot of $\ln(P/P^0)$ against $1/V^2$ should be linear. Figure 17.14 shows that agreement in the middle range of relative pressure is good.

17.7. KINETIC EFFECTS

In much of the early theory used to describe adsorption in different kinds of equipment, it was assumed that equilibrium was achieved instantly between the concentrations of adsorbate in the fluid and in the adsorbed phases. Whilst it may be useful to make this assumption because it leads to relatively straightforward solutions and shows the interrelationship between system parameters, it is seldom true in practice. In large-scale plant particularly, performance may fall well short of that predicted by the equilibrium theory.

There are several resistances which may hinder the movement of a molecule of adsorbate from the bulk fluid outside a pellet to an adsorption site on its internal surface, as shown in Figure 17.15. Some of these are sequential and have to be traversed in series, whilst others derive from possible parallel paths. In broad terms, a molecule, under the influence of concentration gradients, diffuses from the turbulent bulk fluid through a laminar boundary layer around a solid pellet to its external surface. It then diffuses, by various possible mechanisms, through the pores or the lattice vacancies in the pellet until it is held by an adsorption site. During desorption the process is reversed.

In the process of being adsorbed, molecules lose degrees of freedom and a heat of adsorption is released. All the resistances to mass transfer also affect the transfer of heat out of the pellet, though to a different extent. If the heat cannot disperse fast enough,

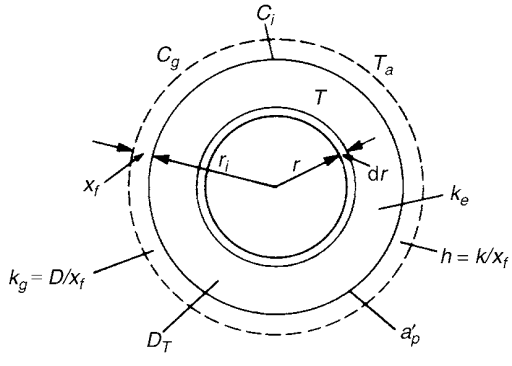


Figure 17.15. Adsorbate and energy transport in a spherical pellet

This book belongs to Bradley Loren (bloren@mcandrews-ip.com) Copyright Elsevier 2024

Intas Exhibit 1032
Page 392 of 470
PGR2025-00043

the temperature of the adsorbent increases and the effective capacity of the equipment is reduced.

17.7.1. Boundary film

There have been many studies of the effect of boundary films on mass and heat transfer to single pellets and in packed beds, including the work of RANZ and MARSHALL[27] and DWIVEDI and UPADHEY[28]. Other theories of mass and heat transfer are discussed in Volume 1, Chapter 10, although only the steady-state film-theory is considered here. It is assumed that the difference in concentration and temperature between the bulk fluid and the external surface of a pellet is confined to a narrow laminar boundary-layer in which the possibility of accumulation of adsorbate or of heat is neglected.

Adsorbate is transferred to an adsorbent at a rate which depends upon a'_p the external surface area of the solid and upon ΔC, the concentration difference across the boundary film.

Thus: $$\text{Rate of mass transfer} = k_g a'_p \Delta C$$

where k_g is a mass transfer coefficient.
The rate at which heat is generated by mass transfer into the pellet is given approximately by:

$$\text{Rate of liberation of heat} = k_g a'_p \Delta C \Delta H$$

where ΔH is the heat of adsorption. When the temperature of the pellet has increased to the extent that heat is lost as fast as it is generated, then:

$$k_g a'_p \Delta C \Delta H = h a'_p \Delta T \tag{17.46}$$

where h is a heat transfer coefficient
Since $k_g = D/x_f$ and $h = k/x_f$ then:

$$\Delta T = \frac{D}{k} \Delta H \Delta C \tag{17.47}$$

which may be written as:

$$\Delta T = \frac{1}{\rho c_{pg}} \frac{Pr}{Sc} \Delta H \Delta C \tag{17.48}$$

where: D = fluid diffusivity,
k = fluid thermal conductivity,
x_f = thickness of boundary film,
Pr = Prandtl Number $c_{pg}\mu/k$, and
Sc = Schmidt Number $\mu/\rho D$

For gas mixtures, the ratio Pr/Sc is about 0.2–5. $\Delta H/\rho c_{pg}$ is normally large. It follows that a small value of ΔC corresponds to a large value of ΔT. Generally, the boundary film does not offer much resistance to mass transfer, except in relative terms during the

This book belongs to Bradley Loren (bloren@mcandrews-ip.com) Copyright Elsevier 2024

Intas Exhibit 1032
Page 393 of 470
PGR2025-00043

unsteady state conditions that exist when a pellet is first exposed to a fluid. The boundary film may, however, offer a significant resistance to heat transfer.

A re-evaluation of published data for mass transfer carried out by WAKAO and FUNAZKRI[29] indicates that, for the range $3 < Re < 10^4$:

$$Sh = 2.0 + 1.1Sc^{1/3}Re^{0.6} \tag{17.49}$$

where Sh is the Sherwood number ($k_g d_p/D$)
Re is the Reynolds number based on the superficial velocity through the bed, and pellet diameter. Equation 17.49 assumes that axial diffusion in the bed has been allowed for, which is not the case in most of the earlier work.

The corresponding equation for heat transfer, neglecting radiation, is:

$$Nu = 2.0 + 1.1Pr^{1/3}Re^{0.6} \tag{17.50}$$

where Nu is the Nusselt number hd_p/k.

17.7.2. Intra-pellet effects

After passing through the boundary layer, the molecules of adsorbate diffuse into the complex structure of the adsorbent pellet, which is composed of an intricate network of fine capillaries or interstitial vacancies in a solid lattice. The problem of diffusion through a porous solid has attracted a great deal of interest over the years and there is a fairly good understanding of the mechanisms involved, at least for gas phase diffusion. Here, diffusion within a single cylindrical pore is considered and, then, the pore is related to the pellet as a whole.

Molecules entering a pore move randomly between the pore-wall and the pore-space. Sometimes molecules are more closely associated with the wall and may be thought of as diffusing over the surface, subject to a surface concentration-difference and a surface diffusion-coefficient. At other times, molecules move in pore-space, where their behaviour depends on the mean free path of the gas and on the pore diameter. The mean free path λ, which is the average distance between collisions of gas molecules, may be predicted using the kinetic theory of gases, and given by GLASSTONE and LEWIS[30] as:

$$\lambda = \frac{1}{\sqrt{2}n'\pi\sigma^2} \tag{17.51}$$

where: n' = number of molecules in unit volume of gas phase,
σ = collision diameter.

At atmospheric pressure and 293 K:

$$n' = \frac{6 \times 10^{26}}{24.0} = 2.5 \times 10^{25} \text{ molecules/m}^3$$

The collision diameter of most molecules is about 0.2 nm.

Hence: $\lambda = 225$ nm.

This book belongs to Bradley Loren (bloren@mcandrews-ip.com) Copyright Elsevier 2024

In pores that are appreciably smaller than the mean free path, molecules tend to collide with the pore walls rather than with other molecules. Having collided with the wall, the molecules are momentarily retained and then released in a random direction. The coefficient, D_k, which controls this *Knudsen diffusion*, considered by SATTERFIELD[31], and in Volume 1, Chapter 3, may be derived from the kinetic theory to give:

$$D_k = \frac{2}{3}\left(\frac{8k'_B T}{\pi m_M}\right) r_p \tag{17.52}$$

or:

$$D_k = 1.0638\left(\frac{\mathbf{R}T}{M}\right) r_p \tag{17.53}$$

where: r_p is the pore radius
m_M is the mass of a molecule, and
M is the molecular weight.

The flux due to Knudsen diffusion is given by:

$$N_{Ak} = -D_k \frac{\partial C_A}{\partial l} \tag{17.54}$$

where l is the distance into the pore.

When the mean free path is small compared with pore diameter, the dominating experience of molecules is that of collision with other molecules in the gas phase. In that respect, the situation is much the same as that which exists in the bulk gas. The appropriate diffusion coefficient D_m may be obtained from published experimental values, or calculated from a theoretical expression. For molecular diffusion in a binary gas, the Chapman and Enskog equation may be used, as discussed by BIRD, STEWART and LIGHTFOOT[32]. This takes the form:

$$D_m = \frac{1.88 \times 10^{-4} T^{3/2}}{P\sigma_{AB}^2 \Omega_{AB}} \left(\frac{1}{M_A} + \frac{1}{M_B}\right)^{1/2} \tag{17.55}$$

where: D_m is the diffusion coefficient (m^2/s),
M_A, M_B are molecular weights of **A** and **B**,
P is the pressure (N/m^2),
T is the temperature (K),
σ_{AB} is a collision diameter (nm), and
Ω_{AB} is a dimensionless collision integral.

Bird Stewart and Lightfoot have published tables which give values of Ω and σ.

The contribution to the total flux that comes from bulk diffusion is given by:

$$N_{Am} = -D_m \frac{\partial C_A}{\partial l} \tag{17.56}$$

The total diffusion in any one adsorbent is complicated by the fact that there is no sudden transition from Knudsen to molecular diffusion at a particular pore size, and most

This book belongs to Bradley Loren (bloren@mcandrews-ip.com) Copyright Elsevier 2024

Intas Exhibit 1032
Page 395 of 470
PGR2025-00043

adsorbents contain a range of pore sizes. Methods of obtaining a value for an average coefficient have been suggested. For example, EVANS *et al.*[33] have suggested that, in a binary system:

$$\frac{1}{D_{\text{av}}} = \frac{1}{D_k} + \frac{1}{D_m}\left[1 - \left(1 + \frac{N_B}{N_A}\right) y_A\right] \tag{17.57}$$

where y_A is the mole fraction of one component. The final bracket allows for deviations from equimolecular counterdiffusion. Whilst both Knudsen and molecular diffusion may be regarded as alternative mechanisms in a particular pore, a third mechanism, namely surface diffusion, is a possible additional route by which molecules may enter a pellet. Surface diffusion is sometimes likened to movement in a liquid film, the surface diffusion coefficient D_s increasing with surface coverage until the monolayer is complete and then remaining constant. Since it exists in parallel with other forms of diffusion, surface diffusion is additive in its effect and:

$$\alpha D_T = \alpha D_{\text{av}} + (1 - \alpha) J D_s \tag{17.58}$$

where: α is pore volume per unit volume of pellet[34], and
J is a factor which has been shown to decrease with temperature.

Surface diffusion is only significant when the pores are small and $D_{\text{av}} = D_k$.
There is an energy of activation E_s for surface diffusion which leads to a temperature dependence of an Arrhenius kind and:

$$D_s = D_{s_0}\, \mathrm{e}^{-E_s/\mathbf{R}T} \tag{17.59}$$

Equation 17.59 has been confirmed experimentally, suggesting that molecules move over a surface by "hopping" to adjacent adsorption sites. It may be assumed that this process involves a lower energy of activation than that required for complete desorption. The molecule will continue to "hop" until it finds a vacant adsorption site, thus explaining the increase of surface diffusion coefficient with coverage.

The Einstein equation for surface diffusion gives $D_s = \lambda_A^2/2\,\delta t$, where λ_A is the average distance between vacant adsorption sites and δt is the residence time on a site.

Experimental measurements of surface diffusion are usually calculated by subtracting from the measured total diffusion that predicted theoretically for Knudsen and molecular diffusion.

Using the total diffusion coefficient defined in equation 17.58, the flux into a pore may be written as:

$$N_A = -D_T \frac{\partial C_A}{\partial l} \tag{17.60}$$

The total diffusional flow into a pellet must allow for the fraction of pellet which is pore, and the tortuous path through the pore system.

In terms of an effective diffusivity D_e and a mean concentration gradient across a porous medium of thickness L, the flux through the medium may be written as:

$$N_A = D_e(-\Delta C_A)/L \tag{17.61}$$

This book belongs to Bradley Loren (bloren@mcandrews-ip.com) Copyright Elsevier 2024

Intas Exhibit 1032
Page 396 of 470
PGR2025-00043

N_A, which refers to unit superficial area, may be expressed in terms of an interstitial flow N_{Ai} and voidage ε as:

$$N_A = \varepsilon N_{Ai} \tag{17.62}$$

A third flux N_{Ac} may be defined which refers to the actual flow of molecules along the tortuous path of a pore of length L_e.

Thus: $$N_{Ac} = D_T(-\Delta C_A/L_e) \tag{17.63}$$

The velocity of **A** along the direct axial path $= N_{Ai}/\bar{C}_A$
The velocity of **A** through a tortuous pore $= N_{Ac}/\bar{C}_A$
where $\bar{C}_A$ is the mean molar concentration of **A**.
The tortuous and direct paths are equivalent if the time taken for **A** to traverse each is the same.

Thus: $$\frac{L}{N_{Ai}/\bar{C}_A} = \frac{L_e}{N_{Ac}/\bar{C}_A} \tag{17.64}$$

Hence: $$N_{Ac} = N_{Ai}\frac{L_e}{L} = \frac{N_A}{\varepsilon}\frac{L_e}{L}$$

Substituting in equation 17.63: $$N_A = D_T\varepsilon\frac{(-\Delta C_A)}{L}\left(\frac{L}{L_e}\right)^2 \tag{17.65}$$

From equations 17.61 and 17.65: $$D_e = \frac{D_T\varepsilon}{(L_e/L)^2} = \frac{D_T\varepsilon}{\tau^2} \tag{17.66}$$

where τ is the tortuosity (actual pore length/superficial diffusion path) and τ^2 is a tortuosity factor.

Values of τ^2 of 2–6 are common. Occasionally, much higher values are quoted which are more likely to indicate shortcomings in the theory rather than highly tortuous paths. There is some confusion in the literature between τ^2 and τ, as discussed by EPSTEIN[35].

17.7.3. Adsorption

The final stage in getting a molecule from the bulk phase outside a pellet on to the interior surface is the adsorption step itself. Where adsorption is physical in nature, this step is unlikely to affect the overall rate. An equilibrium state is likely to exist between adsorbate molecules immediately above a surface and those on it. An adsorption isotherm such as equation 17.4 or 17.35 may be applied.

When chemisorption is involved, or when some additional surface chemical reaction occurs, the process is more complicated. The most common combinations of surface mechanisms have been expressed in the *Langmuir–Hinshelwood* relationships[36]. Since the adsorption process results in the net transfer of molecules from the gas to the adsorbed phase, it is accompanied by a bulk flow of fluid which keeps the total pressure constant. The effect is small and usually neglected. As adsorption proceeds, diffusing molecules may be denied access to parts of the internal surface because the pore system becomes blocked at critical points with condensate. Complex as the situation may be in theory,

This book belongs to Bradley Loren (bloren@mcandrews-ip.com) Copyright Elsevier 2024
Intas Exhibit 1032
Page 397 of 470
PGR2025-00043

it may often be simplified by selecting what is termed the *controlling resistance*. This relates to the step whose resistance is overwhelmingly large in comparison with that for the other layers. The whole of the difference in adsorbate concentration, from its value in the bulk gas to its value at the adsorbent surface, occurs across the controlling resistance. It may be, however, that rate control is mixed, involving two or more resistances.

The relative importance of the boundary-film and intra-pellet diffusion in mass transfer is measured by the *Biot number*. On the assumption that there is no accumulation of adsorbate at the external surface of a pellet, then:

$$k_g(C_g - C_i) = D_e \left.\frac{\partial C}{\partial r}\right|_{r=r_i}$$

$$\frac{k_g r_i}{D_e} = \frac{1}{(1 - C_i/C_g)} \left.\frac{\partial (C/C_g)}{\partial (r/r_i)}\right|_{r=r_i} \tag{17.67}$$

where the left-hand dimensionless group Bi is the *Biot number*. A high value of Bi indicates that intra-pellet diffusion is controlling the rate of transport.

The discussion so far has concentrated on mass transfer. The transfer of the heat liberated on adsorption or consumed on desorption may also limit the rate process or the adsorbent capacity. Again the possible effects of the boundary-film and the intra-pellet thermal properties have to be considered. A Biot number for heat transfer is hr_i/k_e. In general, this is less than that for mass transfer because the boundary layer offers a greater resistance to heat transfer than it does to mass transfer, whilst the converse is true in the interior of the pellet.

17.8. ADSORPTION EQUIPMENT

The scale and complexity of an adsorption unit varies from a laboratory chromatographic column a few millimeters in diameter, as used for analysis, to a fluidised bed several metres in diameter, used for the recovery of solvent vapours, from a simple container in which an adsorbent and a liquid to be clarified are mixed, to a highly-automated moving-bed of solids in plug-flow.

All such units have one feature in common in that in all cases the adsorbent becomes saturated as the operation proceeds. For continuous operation, the spent adsorbent must be removed and replaced periodically and, since it is usually an expensive commodity, it must be regenerated, and restored as far as possible to its original condition.

In most systems, regeneration is carried out by heating the spent adsorbent in a suitable atmosphere. For some applications, regeneration at a reduced pressure without increasing the temperature is becoming increasingly common. The precise way in which adsorption and regeneration are achieved depends on the phases involved and the type of fluid–solid contacting employed. It is convenient to distinguish three types of contacting:

(a) Those in which the adsorbent and containing vessel are fixed whilst the inlet and outlet positions for process and regenerating streams are moved when the adsorbent becomes saturated. The fixed bed adsorber is an example of this arrangement. If

This book belongs to Bradley Loren (bloren@mcandrews-ip.com) Copyright Elsevier 2024

Intas Exhibit 1032
Page 398 of 470
PGR2025-00043

continuous operation is required, the unit must consist of at least two beds, one of which is on-line whilst the other is being regenerated.

(b) Those in which the containing vessel is fixed, though the adsorbent moves with respect to it. Fresh adsorbent is fed in and spent adsorbent removed for regeneration at such a rate as to confine the adsorption within the vessel. This type of arrangement includes fluidised beds and moving beds with solids in plug flow.

(c) Those in which the adsorbent is fixed relative to the containing vessel which moves relative to fixed inlet and outlet positions for process and regenerating fluids. The rotary-bed adsorber is an example of such a unit.

17.8.1. Fixed or packed beds

When used as part of a commercial operation with gas or liquid mixtures, the single pellets discussed in the context of *rate processes* are consolidated in the form of packed beds. Usually the beds are stationary and the feed is switched to a second bed when the first becomes saturated. Whilst there are applications for moving-beds, as discussed later, only fixed-bed equipment will be considered, here as this is the most widely used type.

Figure 17.16*a* depicts the way in which adsorbate is distributed along a bed, during an adsorption cycle. At the inlet end of the bed, the adsorbent has become saturated and is

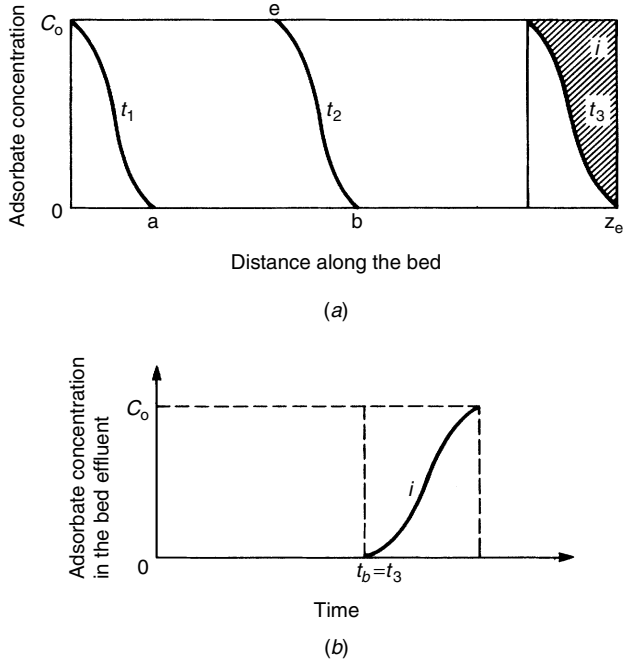


Figure 17.16. The distribution of adsorbate concentration in the fluid phase through a bed (*a*) Development and progression of an adsorption wave along a bed. (*b*) Breakthrough curve

This book belongs to Bradley Loren (bloren@mcandrews-ip.com) Copyright Elsevier 2024

in equilibrium with the adsorbate in the inlet fluid. At the exit end, the adsorbate content of the adsorbent is still at its initial value. In between, there is a reasonably well-defined mass-transfer zone in which the adsorbate concentration drops from the inlet to the exit value. This zone progresses through the bed as the run proceeds. At t_1 the zone is fully formed, t_2 is some intermediate time, and t_3 is the breakpoint time t_b at which the zone begins to leave the column. For efficient operation the run must be stopped just before the breakpoint. If the run extends for too long, the breakpoint is exceeded and the effluent concentration rises sharply, as is shown in the breakthrough curve of Figure 17.16*b*.

A mass balance of adsorbate in the fluid flowing through an increment dz of bed as shown in Figure 17.17 gives:

$$\underset{\text{INPUT}}{uA\varepsilon C} - \underset{\text{OUTPUT}}{\left[uA\varepsilon C + \frac{\partial(uA\varepsilon C)}{\partial z}\,\mathrm{d}z\right]} = \underset{\text{ACCUMULATION}}{\frac{\partial(\varepsilon AC\,\mathrm{d}z)}{\partial t}} + \underset{\text{LOSS BY ADSORPTION}}{\text{Loss}} \tag{17.68}$$

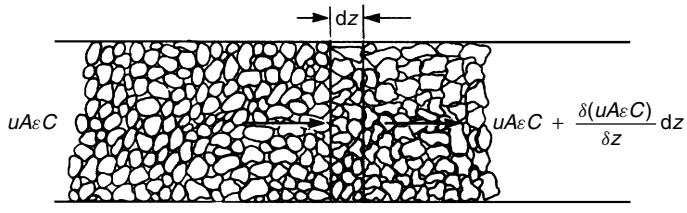


Figure 17.17. Conservation of adsorbate across an increment of a packed bed

The rate of loss by adsorption from the fluid phase equals the rate of gain in the adsorbed phase and:

$$\text{Rate of adsorption} = \frac{\partial[(1-\varepsilon)AC_s\,\mathrm{d}z]}{\partial t}$$

The equations may be rearranged to give:

$$\left(\frac{\partial(uC)}{\partial z}\right)_t + \left(\frac{\partial C}{\partial t}\right)_z = -\frac{1}{m}\left(\frac{\partial C_s}{\partial t}\right)_z \tag{17.69}$$

where:
$$m = \frac{\varepsilon}{1-\varepsilon}$$

When the adsorbate content of the inlet stream is small, the fluid velocity is virtually constant along the bed.

Therefore:
$$u\left(\frac{\partial C}{\partial z}\right)_t + \left(\frac{\partial C}{\partial t}\right)_z = -\frac{1}{m}\left(\frac{\partial C_s}{\partial t}\right)_z \tag{17.70}$$

which may be simplified further by substituting to give:

$$\chi = \frac{z}{mu} \quad \text{and} \quad t_1 = \left(t - \frac{z}{u}\right)$$

This book belongs to Bradley Loren (bloren@mcandrews-ip.com) Copyright Elsevier 2024

Intas Exhibit 1032
Page 400 of 470
PGR2025-00043

so that:
$$\frac{\partial C}{\partial \chi} = -\frac{\partial C_s}{\partial t_1} \tag{17.71}$$

Equation 17.70 includes explicitly the interpellet voidage. The intra-pellet voidage α contributed by the pores is subsumed in the term C_s, which is the mean adsorbate content on the pellet. C_s varies along the bed although it is assumed to be constant at any radius at a particular distance from the inlet.

If α is included in the conservation equation, then this becomes:

$$u\frac{\partial C}{\partial z} + \frac{\partial C}{\partial t} = -\frac{1}{m}\frac{\partial}{\partial t}[(1-\alpha)C_s' + \alpha C'] \tag{17.72}$$

where: C' is the mean adsorbate concentration in the fluid phase which is present in the pore volume of the pellet, and
C_s' is the mean adsorbate concentration in the adsorbed phase in a pellet,

C' is not equal to C, except in equilibrium operation, although it is likely to be in equilibrium with C_s' through an adsorption isotherm $C' = \mathrm{f}(C_s')$. C is normally expressed in moles per unit volume of fluid. In equation 17.70, consistent units for C_s are moles per unit volume of pellet. In practice, C_s is often quoted as mass of adsorbate per unit mass of adsorbate-free adsorbent (C_s'').

It then follows that:
$$C_s'' = \frac{M}{\rho_p}C_s$$

where: M is the molecular weight of adsorbate, and
ρ_p is the pellet density.

The latter may be related to true solid density ρ_s by:
$$\rho_p = (1-\alpha)\rho_s$$

and to the bed density, ρ_B, by:
$$\rho_B = (1-\varepsilon)\rho_p$$

Whilst it is convenient to refer to pellet mean concentrations when analysing the performance of agglomerates of pellets such as is found in a packed bed, in reality, both C_s and C decrease from the outside of the pellet to the centre, as shown in Figure 17.18.

Another important approximation implicit in equation 17.70 is that radial and longitudinal dispersions may be neglected. Radial concentration gradients are likely to be small. It has been shown that because of the greater bed voidage at the wall, and within about three pellet diameters of it, a peak in longitudinal velocity occurs near the wall and the breakthrough for wall-flow is earlier. For a bed/pellet diameter ratio of greater than 20, the effect is small. At low Reynolds numbers longitudinal dispersion may become important. This gives rise to axial mixing, which elongates the mass transfer zone and reduces separation efficiency. When it is necessary to take longitudinal dispersion into account, a form of Fick's Law is assumed to apply and the term $D_L(\partial^2 C/\partial z^2)$ is added to the left-hand side of equation 17.70. Values of D_L may be calculated from published

This book belongs to Bradley Loren (bloren@mcandrews-ip.com) Copyright Elsevier 2024
Intas Exhibit 1032
Page 401 of 470
PGR2025-00043

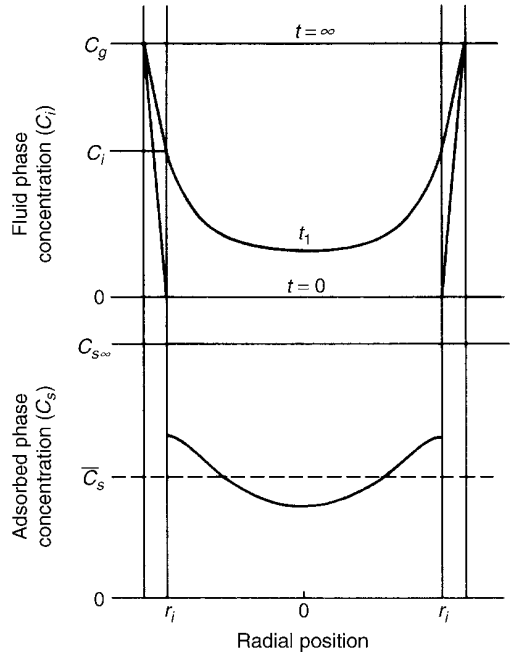


Figure 17.18. Distribution of adsorbate through a spherical pellet

correlations of Peclet Numbers. For gases, EDWARDS and RICHARDSON[37] have shown that:

$$\frac{1}{Pe} = \frac{0.73\varepsilon}{Re\,Sc} + \frac{1}{2\left(1 + \dfrac{9.5\varepsilon}{Re\,Sc}\right)} \tag{17.73}$$

where:

$$Pe = \frac{2ur_i}{D_L}$$

In liquids the effects of longitudinal dispersion are small, even at low Reynolds Numbers.

Many solutions are available for equation 17.70 and its refinements. Three cases are considered to illustrate the range of solutions. Firstly, it is assumed that the bed operates isothermally and that equilibrium is maintained between adsorbate concentrations in the fluid and on the solid. Secondly, the non-equilibrium isothermal case is considered and, finally, the non-equilibrium non-isothermal case.

17.8.2. Equilibrium, isothermal adsorption in a fixed bed, single adsorbate

At all positions in the bed, concentrations in the fluid and adsorbed phases are related by the adsorption isotherm. This implies that there is no resistance to the transfer of molecules of adsorbate from bulk fluid to adsorption site.

This book belongs to Bradley Loren (bloren@mcandrews-ip.com) Copyright Elsevier 2024

Intas Exhibit 1032
Page 402 of 470
PGR2025-00043

If the adsorption isotherm is written as $C_s = \mathrm{f}(C)$, equation 17.69 may be rewritten as:

$$u\frac{\partial C}{\partial z} + \frac{\partial C}{\partial t} = -\frac{1}{m}\frac{\partial C_s}{\partial C}\frac{\partial C}{\partial t}$$

$$= -\frac{1}{m}\mathrm{f}'(C)\frac{\partial C}{\partial t} \tag{17.74}$$

Also:
$$\left(\frac{\partial C}{\partial t}\right)_z = -\left(\frac{\partial C_s}{\partial z}\right)_t \cdot \left(\frac{\partial z}{\partial t}\right)_c$$

and:
$$\left\{u - \left[1 + \frac{1}{m}\mathrm{f}'(C)\right]\frac{\partial z}{\partial t}\right\}\frac{\partial C}{\partial z} = 0$$

Hence:
$$\left(\frac{\partial z}{\partial t}\right)_c = \frac{u}{1 + \dfrac{1}{m}\mathrm{f}'(C)} \tag{17.75}$$

Equation 17.75 is important as it illustrates, for the equilibrium case, a principle that applies also to the non-equilibrium cases more commonly encountered. The principle concerns the way in which the shape of the adsorption wave changes as it moves along the bed. If an isotherm is concave to the fluid concentration axis it is termed *favourable*, and points of high concentration in the adsorption wave move more rapidly than points of low concentration. Since it is physically impossible for points of high concentration to overtake points of low concentration, the effect is for the adsorption zone to become narrower as it moves along the bed. It is, therefore, termed *self-sharpening*.

An isotherm which is convex to the fluid concentration axis is termed *unfavourable*. This leads to an adsorption zone which gradually increases in length as it moves through the bed. For the case of a linear isotherm, the zone goes through the bed unchanged. Figure 17.19 illustrates the development of the zone for these three conditions.

Whilst the simple theory predicts that the adsorption zone associated with a favourable isotherm reduces to a step change in concentration, in practice finite resistance to mass transfer and the effect of longitudinal diffusion will result in a zone of finite and constant width being propagated. The property is important because it leads to simplified methods of sizing fixed beds. Figure 17.20 taken from the work of Bowen and Rimmer[38] shows a typical isotherm for activated alumina and water. This has sections concave to the gas concentration axis at high and low concentrations and the middle section is convex. From the predictions of the equilibrium solutions, it might be expected that the portions of the adsorption wave corresponding to the extremes of the concentration range would sharpen as they moved through the column. The middle of the range should become longer. Experimental results are shown in Figure 17.21. These were obtained from a narrow, jacketed, laboratory column operating essentially isothermally, though not under equilibrium conditions. The figure does show the tendency for high and low concentrations to develop a constant pattern and for the middle range to spread as the wave progresses. In order to predict the breakpoint, only the leading zone has to be considered. Equation 17.75 may be integrated at constant C to give:

$$\frac{ut}{1 + \dfrac{1}{m}\mathrm{f}'(C)} = z - z_0 \tag{17.76}$$

This book belongs to Bradley Loren (bloren@mcandrews-ip.com) Copyright Elsevier 2024

Intas Exhibit 1032
Page 403 of 470
PGR2025-00043

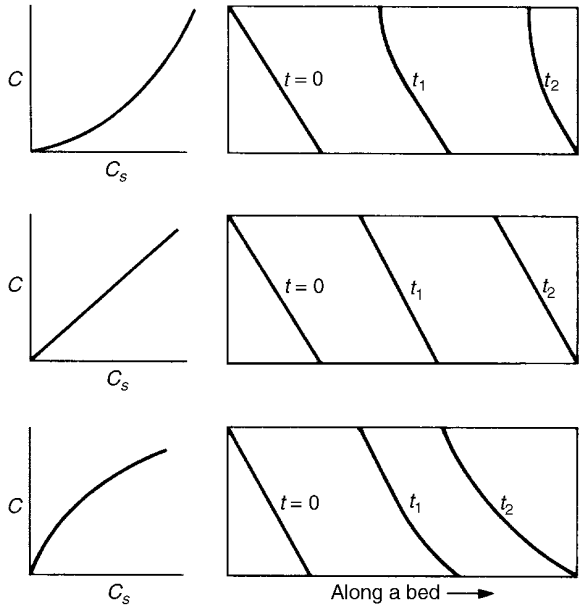


Figure 17.19. Effect of the shape of the isotherm on the development of an adsorption wave through a bed with the initial distribution of adsorbate shown at $t = 0$

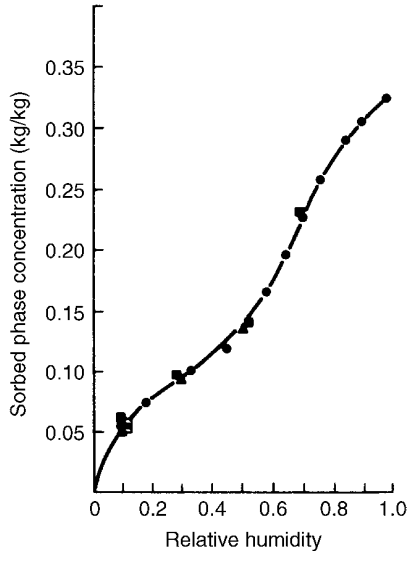


Figure 17.20. Adsorption isotherm for water vapour on activated alumina, plotted as a function of the relative humidity. Temperatures: ● 303 K, ■ 308 K, ▲ 315 K, □ 325 K, ○ 335 K

This book belongs to Bradley Loren (bloren@mcandrews-ip.com)
Copyright Elsevier 2024
Intas Exhibit 1032
Page 404 of 470
PGR2025-00043

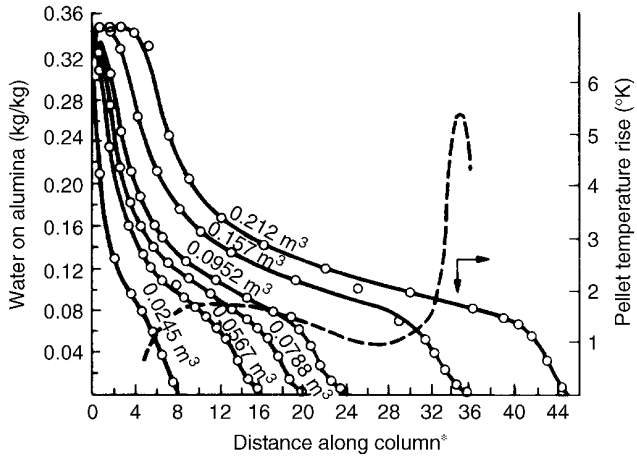


Figure 17.21. Distribution of adsorbate along a column operating quasi-isothermally with a Type IV isotherm. The dotted line is the temperature distribution at the breakpoint of a column of length 36 units. Air flow 8.8×10^{-6} m^3/s. Temperature of jacket 303 K. Relative humidity of feed 95 per cent. The volumes to breakpoint of each bed are indicated on the curves.

*Each unit of distance is the length of bed containing 1 g of adsorbent[38]

where z_0 is the position of C initially. For a bed initially free of adsorbate, z_0 is zero for all values of C.

The condition for which the bed is likely to operate at near equilibrium is when the feed rate is low. This is also the condition when longitudinal dispersion may be significant. Equilibrium solutions have been found by LAPIDUS and AMUNDSON[39] and by LEVENSPIEL and BISCHOFF[40] for this case. These take the form:

$$\frac{C}{C_0} = \frac{1}{2} \cdot \left\{ 1 + \text{erf} \left[\left(\frac{uz}{4D_L} \right)^{1/2} \frac{(t - t_{\min})}{(t\, t_{\min})^{1/2}} \right] \right\} \tag{17.77}$$

where $t_{\min}$ is the minimum time, under given flow conditions, to saturate a bed of unit cross-section and length z. C_0 is the constant concentration of adsorbate in the fluid entering the bed. The minimum time is given by:

$$t_{\min} = \left(1 + \frac{1}{m} \frac{C_{s\infty}}{C_0} \right) \frac{z}{u} \tag{17.78}$$

where $C_{s\infty}$ is the concentration of adsorbed phase in equilibrium with C_0.

Example 17.3

A solvent contaminated with 0.03 kmol/m^3 of a fatty acid is to be purified by passing it through a fixed bed of activated carbon which will adsorb the acid but not the solvent. If the operation is essentially isothermal and equilibrium is maintained between the liquid and the solid, calculate the length of a bed of 0.15 m diameter to give 3600 s (1 h) of operation when the fluid is fed at 1×10^{-4} m^3/s. The bed is initially free of adsorbate, and the intergranular voidage is 0.4. Use an equilibrium, fixed-bed theory to obtain an answer for three types of isotherm:

This book belongs to Bradley Loren (bloren@mcandrews-ip.com) Copyright Elsevier 2024

Intas Exhibit 1032
Page 405 of 470
PGR2025-00043

(a) $C_s = 10\ C$
(b) $C_s = 3.0\ C^{0.3}$ — use the mean slope
(c) $C_s = 10^4\ C^2$ — take the breakthrough concentration as 0.003 kmol/m^3.

C and C_s refer to concentrations (kmol/m^3) in the gas phase and the adsorbent, respectively.

Solution

From equation 17.76:

$$ut/\left(1 + \frac{1}{m}\mathrm{f}'(C)\right) = (z - z_0)$$

For case (a):

$C_s = 10C$ which represents a linear isotherm.

All concentrations move at the same velocity. If $z_0 = 0$ at $t = 0$ for all concentrations, the adsorption wave propagates as a step change from the inlet to the outlet concentration,

$$\mathrm{f}'(C_s) = 10$$

$$u = 1 \times 10^{-4}/[(\pi/4)(0.15^2\varepsilon)] \text{ m/s}$$

where ε is the intergranular voidage $= 0.4$.

$$m = \varepsilon/(1 - \varepsilon) = (0.4/0.6)$$

$$t = 3600\text{s}$$

Thus:
$$z = \left(\frac{4 \times 10^{-4}}{\pi \times 0.15^2 \times 0.4}\right)\left(\frac{3600}{1 + 10(0.6/0.4)}\right)$$

$$= \underline{\underline{3.18 \text{ m}}}$$

It may be noted that, when the adsorption wave begins to emerge from the bed, the bed is saturated in equilibrium with the inlet concentration.

Hence:
$$uA\varepsilon t C_0 = zA[\varepsilon C_0 + (1 - \varepsilon)C_s^*]$$

which is the same as that obtained by applying equation 17.76 to a linear isotherm.

For case (b):

$C_s = 3C^{0.3}$ which represents a favourable isotherm.

As C increases, f(C) decreases and points of higher concentrations are predicted to move a greater distance in a given time than lower concentrations. It is not possible for points of higher concentrations to overtake lower concentrations, and if $z_0 = 0$ for all concentrations, the adsorption wave will propagate as a step change similar to case *a*.

Hence:
$$z = ut \Big/ \left[1 + \frac{1}{m}\frac{C_s^*}{C_0}\right]$$

$$= \left(\frac{4 \times 10^{-4}}{\pi \times 0.15^2 \times 0.4}\right)\left(\frac{3600}{1 + (0.6/0.4)(3/C_0^{0.7})}\right)$$

$$= \underline{\underline{0.95 \text{ m}}}$$

This book belongs to Bradley Loren (bloren@mcandrews-ip.com) Copyright Elsevier 2024

Intas Exhibit 1032
Page 406 of 470
PGR2025-00043

For case (c):

$$C_s = 10^4 C^2 \quad \text{which represents an unfavourable isotherm.}$$

$$f'(C) = 2 \times 10^4\ C.$$

As C increases, $f'(C)$ increases such that, in a given time, z for lower concentrations is greater than for higher concentrations. Following the progress of the breakpoint concentration, $C = 0.003$ kmol/m^3, then:

$$f'(0.003) = 60$$

Hence:

$$z = \left(\frac{4 \times 10^{-4}}{\pi \times 0.15^2 \times 0.4}\right)\left(\frac{3600}{1 + (0.60/0.40)60}\right)$$

$$= \underline{\underline{0.55 \text{ m}}}$$

At breakpoint, the bed is far from saturated and:

$$\text{saturation} = \frac{100 u A \varepsilon t C_0}{z A C_0 \varepsilon \left[1 + \frac{1}{m} \cdot \frac{C_s^*}{C_0}\right]} = \frac{100 u t}{z\left[1 + \frac{1}{m} \cdot \frac{C_s^*}{C_0}\right]}$$

$$= 100\left(\frac{4 \times 10^{-4} \times 3600}{\pi \times 0.15^2 \times 0.4}\right) \Big/ \left[0.55(1 + (0.6/0.4)(9/0.03))\right]$$

$$= \underline{\underline{20.5 \text{ per cent}}}$$

17.8.3. Non-equilibrium adsorption — isothermal operation

Isothermal operation in a fixed bed may be achieved in a well-cooled laboratory column and also in large-scale equipment if the concentration of adsorbate is low and the release of heat of adsorption is not great. A third and rather specialised situation in which isothermal conditions may exist is that in which a component is adsorbed on to a surface already covered with a second component. If this second component is displaced by the first, its heat of desorption will "consume" the heat released when the adsorption of the first component occurs.

Constant patterns analysis

A constant wave-pattern develops when adsorption is governed by a favourable isotherm. In Figure 17.16*a*, a typical wave is assumed to move a distance dz in a time dt. If the wave is already fully developed, it will retain its shape. A mass balance gives:

$$\varepsilon u A C_0\, \mathrm{d}t = A[(1 - \varepsilon)C_{s\infty} + \varepsilon C_0]\, \mathrm{d}z$$

$$\frac{\mathrm{d}z}{\mathrm{d}t} = \frac{u}{1 + \frac{1}{m}\frac{C_{s\infty}}{C_0}} \tag{17.79}$$

This book belongs to Bradley Loren (bloren@mcandrews-ip.com) Copyright Elsevier 2024

Intas Exhibit 1032
Page 407 of 470
PGR2025-00043

where equation 17.79 is similar in form to the equilibrium equation 17.75, and identical to it if the isotherm is linear.

The mass balance may be carried out at any level of concentration within the zone to give:

$$\frac{\mathrm{d}z}{\mathrm{d}t} = \frac{u}{1 + \dfrac{1}{m}\dfrac{C_s}{C}} \tag{17.80}$$

For a constant pattern wave, all concentrations within the wave have the same velocity.

Therefore:
$$\frac{C_s}{C} = \frac{C_{s\infty}}{C_0} \tag{17.81}$$

This is the *constant-pattern simplification* that enables many solutions to be obtained from what might otherwise be complex rate equations. It represents a condition that is approached as the wave becomes fully developed and leads to what are termed *asymptotic solutions*.

Representing the mass balance in a fixed bed by:

$$\left(\frac{\partial C_s}{\partial \chi}\right)_{t_1} = -\left(\frac{\partial C_s}{\partial t_1}\right)_{\chi} \qquad \text{(equation 17.71)}$$

and assuming a general rate expression:

$$\frac{\partial C_s}{\partial t_1} = \mathrm{G}(C, C_s) \tag{17.82}$$

where G denotes a function.

The constant pattern assumption gives:

$$\frac{\partial C_s}{\partial t_1} = \mathrm{G}_1(C_s) = \mathrm{G}_2(C) = -\frac{\partial C}{\partial \chi} \tag{17.83}$$

Equation 17.83 may be integrated to give, at constant χ to give:

or, at constant t_1 to give:
$$\left.\begin{aligned} \int \frac{\mathrm{d}C_s}{\mathrm{G}_1(C_s)} &= \left[\int \frac{dC_s}{\mathrm{G}_1(C_s)}\right]_{t_1=0} + t_1 \\ \int \frac{\mathrm{d}C_s}{\mathrm{G}_2(C)} &= \left[\int \frac{\mathrm{d}C_s}{\mathrm{G}_2(C)}\right]_{x=0} - \chi \end{aligned}\right\} \tag{17.84}$$

If, for example, a rate expression may be written as:

$$\frac{\partial C_s}{\partial t_1} = k_g^0(C - C^*) \tag{17.85}$$

where C^* is the fluid concentration in equilibrium with the mean solid concentration C_s, then, assuming a Langmuir equilibrium relationship similar to equation 17.3:

$$C_s = \frac{C_{sm} B_3 C^*}{1 + B_3 C^*} \tag{17.86}$$

This book belongs to Bradley Loren (bloren@mcandrews-ip.com) Copyright Elsevier 2024

Intas Exhibit 1032
Page 408 of 470
PGR2025-00043

Substituting in equation 17.85 for C and C^*, from equations 17.81 and 17.86, respectively, gives the expression for $G_1(C_s)$ for the particular case.

Rosen's solutions

Rate equations, such as equation 17.85, make no attempt to distinguish mechanisms of transfer within a pellet. All such mechanisms are taken into account within the rate constant $\boldsymbol{k}$. A more fundamental approach is to select the important factors and combine them to form a rate equation, with no regard to the mathematical complexity of the equation. In most cases this approach will lead to the necessity for numerical solutions although for some limiting conditions, useful analytical solutions are possible, particularly that presented by ROSEN[41].

A mass balance for diffusion of adsorbate into a spherical pellet may be written as:

$$\underbrace{\left[-4\pi r^2 D_e \frac{\partial C_r}{\partial r}\right]}_{\text{IN}} - \underbrace{\left[-4\pi r^2 D_e \frac{\partial C_r}{\partial r} + \frac{\partial\left(-4\pi r^2 D_e \dfrac{\partial C_r}{\partial r}\right)\mathrm{d}r}{\partial r}\right]}_{\text{OUT}} = \underbrace{\left[4\pi r^2\,\mathrm{d}r \frac{\partial C_r}{\partial t} + 4\pi r^2\,\mathrm{d}r \frac{\partial C_{sr}}{\partial t}\right]}_{\text{ACCUMULATION}} \qquad (17.87)$$

where C_r and C_{sr} are concentrations of adsorbate at a radius r.

If there is equilibrium between fluid in the pores and the adjacent surface, and if the equilibrium is linear then:

$$C_{sr} = K_a C_r \qquad (17.88)$$

Hence the mass balance may be written as:

$$\frac{\partial C_r}{\partial t} = \frac{D_e}{1 + K_a}\left(\frac{\partial^2 C_r}{\partial r^2} + \frac{2}{r}\frac{\partial C_r}{\partial r}\right) \qquad (17.89)$$

The total adsorbate in the pellet at any particular time may be written as:

$$4\pi \int (r^2 C_r + r^2 K_a C_r)\,\mathrm{d}r$$

so that the mean concentration C_s is given by:

$$C_s = \frac{3}{r_i^3}(1 + K_a)\int r^2 C_r\,\mathrm{d}r \qquad (17.90)$$

The rate at which adsorbate enters a pellet may be expressed in terms of the concentration driving force across the boundary film to give:

$$\frac{4}{3}\pi r_i^3 \frac{\partial C_s}{\partial t} = 4\pi r_i^2 k_g (C - C_i)$$

Thus:

$$\frac{\partial C_s}{\partial t} = \frac{3k_g}{r_i}(C - C_i) \qquad (17.91)$$

where C_i is in equilibrium with the solid concentration at $r = r_i$.

This book belongs to Bradley Loren (bloren@mcandrews-ip.com) Copyright Elsevier 2024

Intas Exhibit 1032
Page 409 of 470
PGR2025-00043

Solutions have been found by Rosen, using the fixed-bed equation 17.70 together with equations 17.90 and 17.91. The general solution takes the form:

$$\frac{C}{C_0} = \tfrac{1}{2} + \mathrm{F}(\lambda', \tau', \psi) \tag{17.92}$$

where the length parameter is:

$$\lambda' = \frac{3D_e K_a z}{mur_i^2} \tag{17.93}$$

the time parameter is:

$$\tau' = \frac{2D_e}{r_i^2}\left(t - \frac{z}{u}\right) \tag{17.94}$$

and the resistance parameter is:

$$\psi = \frac{D_e K_a}{r_i k_g} \tag{17.95}$$

Solutions are available in tabulated and graphical form. Except for small values of λ', the solution has the following convenient form:

$$\frac{C}{C_0} = \frac{1}{2}\left\{1 + \mathrm{erf}\left[\frac{\left(3\dfrac{\tau'}{2\lambda'} - 1\right)}{2\sqrt{[(1+5\psi)/5\lambda']}}\right]\right\} \tag{17.96}$$

RUTHVEN[16] gives a useful summary of other solutions.

Example 17.4

A bed is packed with dry silica gel beads of mean diameter 1.72 mm to a density of 671 kg of gel/m^3 of bed. The density of a bead is 1266 kg/m^3 and the depth of packing is 0.305 m. Humid air containing 0.00267 kg of water/kg of dry air enters the bed at the rate of 0.129 kg of dry air/m^2 s. The temperature of the air is 300 K and the pressure is 1.024×10^5 N/m^2. The bed is assumed to operate isothermally. Use the method of Rosen to find the effluent concentration as a function of time. Equilibrium data for the silica gel are given by the curve in Figure 17.22. An appropriate value of k_g, the film mass transfer coefficient, is 0.0833 m/s.

Solution

The length parameter λ' is calculated from equation 17.83:

$$\lambda' = \frac{3D_e K_a z}{mur_i^2}$$

$$K_a = \left(\frac{0.084}{0.00267}\right) \times \left(\frac{1266}{1.186}\right) = 3.36 \times 10^4$$

This book belongs to Bradley Loren (bloren@mcandrews-ip.com) Copyright Elsevier 2024

Intas Exhibit 1032
Page 410 of 470
PGR2025-00043

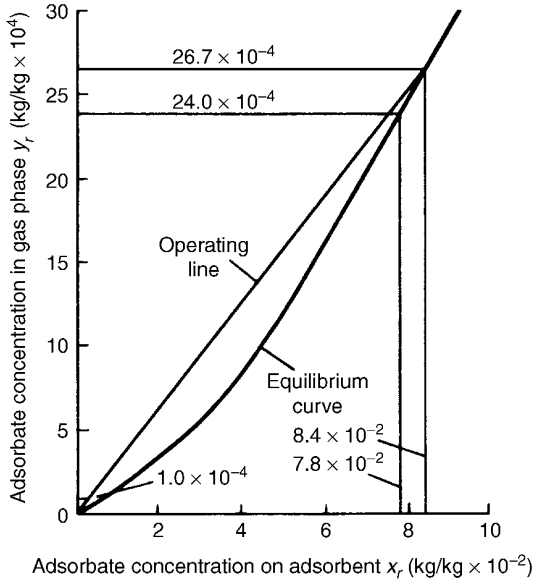


Figure 17.22. Adsorption isotherm for water vapour in air on silica gel

where K_a is obtained from the mean slope of the isotherm between its origin and the point corresponding to the inlet concentration. This slope has been multiplied by the ratio of bead to gas densities to give K_a in the same units as equation 17.88.

$$m = \frac{\varepsilon}{1-\varepsilon} = \frac{1266-671}{671} = 0.89$$

where ε is the volume (and area) voidage between beads.

$$\varepsilon = \frac{1266-671}{1266} = 0.47$$

$$u = \frac{0.129}{0.47 \times 1.186} = 0.233 \text{ m/s}$$

where u is the interstitial velocity of the air.

$$r_i = 0.86 \text{ mm}$$

$$z = 0.305 \text{ m}$$

D_e is the diffusivity of sorbate referred to the sorbed phase (and this has a value of 10^{-10}–10^{-11} m^2/s). Substituting values gives $\lambda' = 18{,}500 - 1850$. The use of equation 17.96 is valid for large values of λ'. From equations 17.93 and 17.94:

$$\frac{\tau'}{\lambda'} = \frac{2\left(t - \frac{z}{u}\right)mu}{3K_a z} = \left(\frac{2 \times 0.89}{3 \times 3.36 \times 10^4}\right)\left(\frac{0.233t}{0.305} - 1\right)$$

This book belongs to Bradley Loren (bloren@mcandrews-ip.com) Copyright Elsevier 2024

Intas Exhibit 1032
Page 411 of 470
PGR2025-00043

where t is expressed in hours.

Thus:
$$t = 20.55\frac{\tau'}{\lambda'} + \frac{1}{2750}$$

From equations 17.93 and 17.95:

$$\frac{\psi}{\lambda'} = \frac{mur_i}{3zk_g}$$

$$k_g = 0.0833 \text{ m/s (given)}$$

Thus:
$$\frac{\psi}{\lambda'} = \frac{(0.89 \times 0.233 \times 0.00086)}{(3 \times 0.305 \times 0.0833)}$$

$$= 2.36 \times 10^{-3}$$

For the relative values of λ' and ψ/λ', equation 17.96 may be rewritten as:

$$\frac{C}{C_0} = \frac{1}{2}\left[1 + \text{erf}\left(\frac{(3\tau'/2\lambda' - 1)}{2\sqrt{(\psi/\lambda')}}\right)\right]$$

$$= \frac{1}{2}[1 + \text{erf}E]$$

where:
$$E = \frac{(3\tau'/2\lambda' - 1)}{2\sqrt{(\psi/\lambda')}}$$

For selected values of C/C_0, the value of E may be found from the tables of error functions given in the Appendix in Volume 1. From E a ratio τ/λ' may be calculated and hence a corresponding time. These calculations are summarised as follows:

$\frac{C}{C_0}$	erf E	E	$\frac{\tau'}{\lambda'}$	t (h)
0.024	−0.952	−1.40	0.576	11.8
0.045	−0.910	−1.20	0.589	12.1
0.079	−0.842	−1.00	0.602	12.4
0.24	−0.520	−0.50	0.635	13.0
0.50	0	0	0.667	13.7
0.715	0.430	0.40	0.693	14.2
0.92	0.840	1.00	0.732	15.0

17.8.4. Non-equilibrium adsorption — non-isothermal operation

When the effects of heats of adsorption cannot be ignored — the situation in most industrial adsorbers — equations representing heat transfer have to be solved simultaneously with those for mass transfer. All the resistances to mass transfer will also affect heat transfer although their relative importance will be different. Normally, the greatest resistance to mass transfer is found within the pellet and the smallest in the external boundary film. For heat transfer, the thermal conductivity of the pellet is normally greater than that of the boundary film so that temperatures through a pellet are fairly uniform. The temperature

This book belongs to Bradley Loren (bloren@mcandrews-ip.com) Copyright Elsevier 2024

Intas Exhibit 1032
Page 412 of 470
PGR2025-00043

difference between bulk conditions outside a pellet and conditions within it occurs almost wholly across the boundary film.

The effects of non-isothermal adsorption in fixed beds have been examined by LEAVITT[42]. Non-isothermal adsorption of a single adsorbate from a carrier fluid leads to the complex wave front shown in Figure 17.23. As adsorption proceeds, the leading edge of the adsorption wave meets adsorbent that is essentially free of adsorbate. Adsorption occurs and the temperature of the adsorbent increases until a dynamic equilibrium is established between fluid and adsorbed phase at the prevailing temperature. These conditions persist through a first plateau zone until the rate of adsorption falls to a point where the temperature of the plateau zone cannot be sustained. As the temperature falls, more adsorption occurs until the second plateau zone is formed, in equilibrium with the incoming stream. The net result is that adiabatic, or near adiabatic, conditions can lead to the formation of two transfer zones separated by a zone in which conditions remain constant.

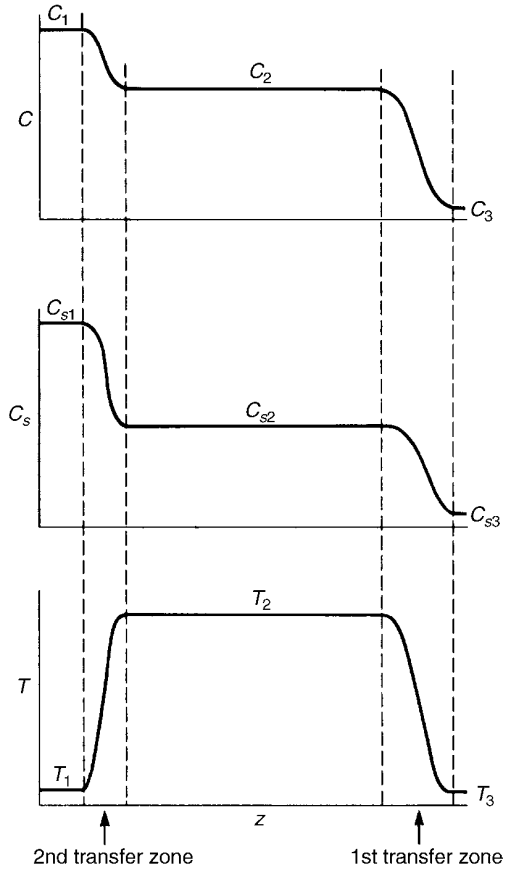


Figure 17.23. Idealised distributions of temperature and concentrations during adiabatic adsorption

This book belongs to Bradley Loren (bloren@mcandrews-ip.com) Copyright Elsevier 2024

Intas Exhibit 1032
Page 413 of 470
PGR2025-00043

The adiabatic profile may be further complicated by the shape of the isotherm. Under isothermal conditions, a favourable isotherm produces a single transfer zone, although an isotherm with favourable and unfavourable sections may generate a more complex profile, as shown in Figure 17.21.

A heat balance over an increment of bed $\mathrm{d}z$ may be written as:

$$(\mathrm{IN} - \mathrm{OUT}) = -\frac{\partial}{\partial z}(u\varepsilon A\rho_g c_{pg}(T - T_0))\,\mathrm{d}z - U_0\pi d_b\,\mathrm{d}z(T - T_a) \tag{17.97}$$

where: d_b is the diameter of the containing vessel,
T_a is the temperature of the surroundings,
T_0 is the reference temperature, and
U_0 is the overall coefficient for heat transfer between the containing vessel and the surroundings

ACCUMULATION:

$$= \frac{\partial}{\partial t}(\varepsilon A\,\mathrm{d}z\rho_g c_{pg}(T - T_0) + (1 - \varepsilon)A\,\mathrm{d}z\rho_p c_{ps}(T - T_0)) + \frac{\partial}{\partial t}(W\,\mathrm{d}z c_{pw}(T - T_0)) \tag{17.98}$$

where W is the mass per unit length of containing vessel.

LOSS BY ADSORPTION:

$$= (1 - \varepsilon)A\,\mathrm{d}z\frac{\partial(C_s\Delta H)}{\partial t} = (1 - \varepsilon)A\,\mathrm{d}z\frac{\partial(C_s\Delta H)}{\partial T}\frac{\partial T}{\partial t} \tag{17.99}$$

where ΔH is the heat of adsorption, a negative quantity.

Hence: $$\frac{\partial(u\varepsilon A\rho_g c_{pg}(T - T_0))}{\partial z}\mathrm{d}z + U_0\pi d_b\,\mathrm{d}z(T - T_a) + \frac{\partial}{\partial t}(\varepsilon A\,\mathrm{d}z\rho_g C_{pg}(T - T_0)$$
$$+(1 - \varepsilon)A\,\mathrm{d}z\rho_p c_{ps}(T - T_0) + W\,\mathrm{d}z c_{pw}(T - T_0)) + (1 - \varepsilon)A\,\mathrm{d}z\frac{\partial(C_s\Delta H)}{\partial T}\frac{\partial T}{\partial t} = 0$$

For a cylindrical bed:

$$u\frac{\partial T}{\partial z} + \frac{4U_0}{\varepsilon d_b}\frac{(T - T_a)}{\rho_g c_{pg}} + \left(1 + \frac{1 - \varepsilon}{\varepsilon}\frac{\rho_p c_{ps}}{\rho_g c_{pg}} + \frac{4W c_{pw}}{\varepsilon\pi d_b^2\rho_g c_{pg}} + \frac{1 - \varepsilon}{\varepsilon}\frac{1}{c_{pg}}\frac{\partial(C_s\Delta H)}{\partial T}\right)\frac{\partial T}{\partial t} = 0 \tag{17.100}$$

For the particular case of adiabatic operation with no sinks for heat in the wall, $U_0 = 0$ and $W = 0$.

Since: $$\frac{\partial T}{\partial z} = -\left(\frac{\partial T}{\partial t}\right)\left(\frac{\partial t}{\partial z}\right)$$

This book belongs to Bradley Loren (bloren@mcandrews-ip.com) Copyright Elsevier 2024

Intas Exhibit 1032
Page 414 of 470
PGR2025-00043

Then:

$$\left.\frac{\partial z}{\partial t}\right|_T = u_T = \frac{u}{1 + \frac{1}{m} \cdot \left(\frac{\rho_p c_{ps}}{\rho_g c_{pg}} + \frac{1}{\rho_g c_{pg}} + \frac{\partial (C_s \Delta H)}{\partial T}\right)} \tag{17.101}$$

where u_T is the velocity of a point of constant temperature. If the thermal wave is coherent, that is all points travel at the same velocity, then u_T is the thermal wave velocity. This may be compared with the concentration wave velocity u_c, where:

$$u_c = \frac{u}{1 + \frac{1}{m}\frac{\partial C_s}{\partial C}} \qquad \text{(equation 17.75)}$$

If the velocities of the thermal and concentration waves are equal, then from equations 17.75 and 17.101:

$$\frac{\partial C_s}{\partial C} = \frac{\rho_p c_{ps}}{\rho_g c_{pg}} + \frac{1}{\rho_g c_{pg}} + \frac{\partial (C_s \Delta H)}{\partial T} \tag{17.102}$$

When equation 17.102 is applied to the finite difference between inlet concentration and plateau, and between plateau and exit concentration, as shown in Figure 17.23, it becomes:

$$\frac{C_{s1} - C_{s2}}{C_1 - C_2} = \frac{\rho_p c_{ps}}{\rho_g c_{pg}} + \frac{1}{\rho_g c_{pg}} \left(\frac{(C_s \Delta H)_1 - (C_s \Delta H)_2}{T_1 - T_2}\right) \tag{17.103}$$

$$\frac{C_{s2} - C_{s3}}{C_2 - C_3} = \frac{\rho_p c_{ps}}{\rho_g c_{pg}} + \frac{1}{\rho_g c_{pg}} \left(\frac{(C_s \Delta H)_2 - (C_s \Delta H)_3}{T_2 - T_3}\right) \tag{17.104}$$

In equations 17.103 and 17.104, c_{ps} and c_{pg} are the mean specific heats over the ranges of temperature and concentrations encountered. Properties with subscripts 1 and 3 are known from inlet and exit conditions respectively. If the plateau values represented by subscript 2 are in equilibrium, then the values C_2, C_{s2} and T_2 may be found from the equations for any known form of the adsorption isotherm $C_{s2} = \mathrm{f}(C_2)$.

Equation 17.102 was derived on the assumption that concentration and thermal waves propagated at the same velocity. AMUNDSON *et al.*[43] showed that it was possible for the temperatures generated in the bed to propagate as a pure thermal wave leading the concentration wave. A simplified criterion for this to occur can be obtained from equations 17.75 and 17.101. Since there is no adsorption term associated with a pure thermal wave, and if changes within the bed voids are small, then:

$$u_T = \frac{m \rho_g c_{pg}}{\rho_p c_{ps}} u \tag{17.105}$$

Also:

$$u_c = m \frac{\Delta C}{\Delta C_s} u \tag{17.106}$$

For a bed initially free of adsorbate, the thermal wave propagates more quickly than the concentration wave if:

$$\frac{\rho_g}{\rho_p}\frac{c_{pg}}{c_{ps}} > \frac{C_1}{C_{s1}} \tag{17.107}$$

This book belongs to Bradley Loren (bloren@mcandrews-ip.com) Copyright Elsevier 2024

Intas Exhibit 1032
Page 415 of 470
PGR2025-00043

Since C_1/C_{s1} increases with temperature, u_c (non-isothermal) $> u_c$ (isothermal). It has been estimated that the rear wave moves at about two-thirds of the velocity of the front wave, so a more cautious criterion than equation 17.107 is given by:

$$\frac{\rho_g c_{pg}}{\rho_p c_{ps}} > \frac{3}{2}\frac{C_1}{C_{s1}} \tag{17.108}$$

where C_{s1} is a function of C_1 and the maximum temperature $T_{2\max}$ of the plateau zone.

Equation 17.101 may be rearranged to give:

$$T_2 = T_1 + \frac{[(\Delta H)C_s]_2 - [(\Delta H)C_s]_1}{\rho_g c_{pg}\dfrac{\Delta C_s}{\Delta C} - \rho_p c_{ps}} \tag{17.109}$$

T_2 is a maximum when C_{s2} is zero.

Hence:
$$T_{2\max} = T_1 + \frac{[(-\Delta H)C_s]_1}{\rho_g c_{pg}(C_s/C)_1 - \rho_p c_{ps}} \tag{17.110}$$

When equilibrium between the fluid and the solid cannot be assumed, it may still be possible to obtain analytical solutions for beds operating non-isothermally. In general, however, it will be necessary to look for numerical solutions. This problem has been summarised by RUTHVEN[16].

17.9. REGENERATION OF SPENT ADSORBENT

Most theory concerning the dynamics of an industrial adsorption unit is directed at sizing a bed for a given adsorption duty. In the design of a complete adsorption unit, however, it is most important to ensure that the spent adsorbent can be regenerated in a given time and that the total inventory of adsorbent is kept to a minimum. If spent adsorbent could be regenerated instantly, all units would consist of a single cylindrical-bed packed with a depth of pellets just sufficient to accommodate the adsorption zone. In practice, units vary in size and configuration because regeneration takes a finite time and what is an optimum arrangement for one application is not necessarily the optimum case for another.

In an ideal fixed-bed adsorber, the adsorption stage continues until the adsorbate wave is about to emerge from the bed and the effluent concentration begins to rise, as shown in Figure 17.16*b*. Conditions behind the adsorption zone are such that the adsorbent is more or less in equilibrium with the feed. The equilibrium condition has then to be changed for regeneration to occur. This is usually brought about by changing the temperature or the pressure so that the driving force, which had previously resulted in the movement of adsorbate from fluid to solid, is now reversed.

17.9.1. Thermal swing

The simplest and the most common way of regenerating an adsorbent in industrial applications is by heating. The vapour pressure exerted by the adsorbed phase increases with

This book belongs to Bradley Loren (bloren@mcandrews-ip.com) Copyright Elsevier 2024

Intas Exhibit 1032
Page 416 of 470
PGR2025-00043

temperature, so that molecules desorb until a new equilibrium with the fluid phase is established. Figure 17.24 depicts adsorption isotherms for a lower temperature T_1 and a higher temperature T_2. For a fixed concentration C in the fluid phase, the adsorbate concentration falls from C_{s1} to C_{s2} when the temperature is increased.

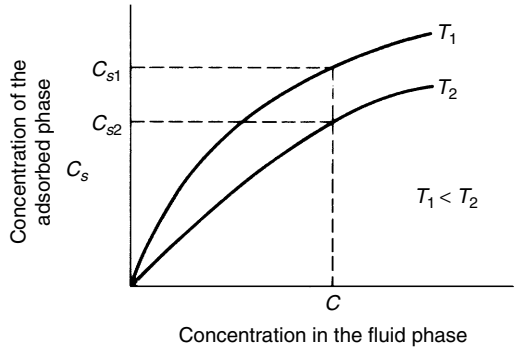


Figure 17.24. Thermal regeneration utilises the change in concentration that follows from a change in temperature

An adsorption unit using thermal swing regeneration usually consists of two packed beds, one on-line and one regenerating, as shown in Figure 17.25. Regenerating consists of heating, and purging to remove adsorbate. The arrangement is flexible and robust. The desorption temperature depends on the properties of the adsorbent and the adsorbates. Manufacturers normally recommend the best regenerating temperature for their particular adsorbent. Exceeding this temperature may accelerate the ageing processes which cause pores to coalesce and capacity to be reduced. Too low a temperature may result in incomplete regeneration so that the effluent concentration in subsequent adsorption stages will be higher than its design value. Hot spots may develop in the operation of a fixed bed, so particular care has to be taken to control temperature when handling flammable materials.

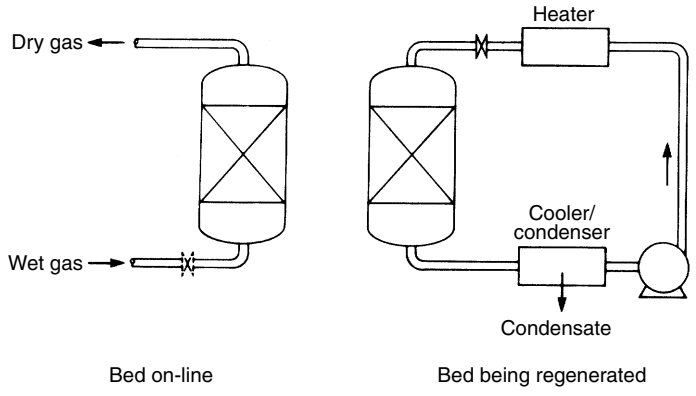
The relatively poor conductivity of a packed bed makes it difficult to get the heat of regeneration into the bed, either from a jacket or from coils embedded in the packing. This is more easily achieved by preheating the purge stream. Even in the best conditions, it takes time for the temperature of the bed to rise to the required level. Thermal regeneration is normally associated with long cycle times, measured in hours. Such cycles require large beds and, since the adsorption wave occupies only a small part of the bed on-line, the utilisation of the total adsorbent in the unit is low.

It is good operating practice to regenerate a bed in the reverse direction to that followed during adsorption. This ensures that the adsorbent at the end of the bed, which controls the quality of the treated stream, is that which is most thoroughly regenerated. CARTER[44] has quantified the effect and showed that regeneration is achieved in a shorter time in this way.

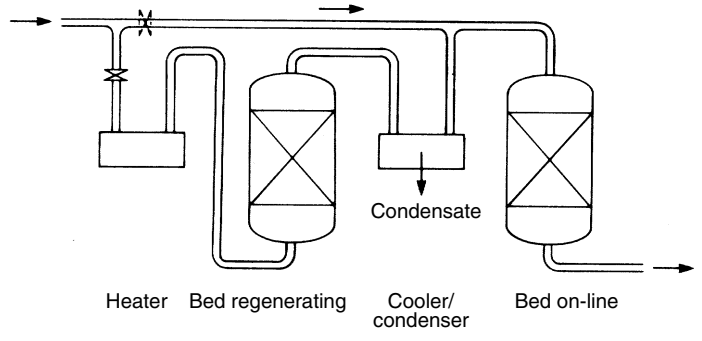
17.9.2. Plug-flow of solids

Better utilisation of adsorbent would be achieved if a unit could be designed in which adsorbent were removed for regeneration as soon as it became saturated, and even better

This book belongs to Bradley Loren (bloren@mcandrews-ip.com) Copyright Elsevier 2024
Intas Exhibit 1032
Page 417 of 470
PGR2025-00043



(*a*)



(*b*)

Figure 17.25. Typical arrangement of a two bed dryer. (*a*) Separate regeneration (*b*) Integrated regeneration

if the advancing adsorption wave were presented with only sufficient fresh adsorbent to contain the wave. Both characteristics are possible if the adsorbent moves countercurrent to the fluid at such a rate that the adsorption zone is stationary.

The earliest application of a moving bed in which solids moved with respect to the containing vessel was reported in the late 1940s. A typical application was the recovery of ethylene from gas composed mainly of hydrogen and methane, and with some propane and butane. The unit shown diagrammatically in Figure 17.26, taken from the work of BERG[45], is known as the *hypersorber*.

The mixture to be separated is fed to the centre of the column down which activated carbon moves slowly. Immediately above the feed, the rising gas is stripped of ethylene and heavier components leaving hydrogen, methane and any non-adsorbed gases to be discharged as a top-product. The adsorbent with its adsorbate continues down the column into an enriching section where it meets an upwards stream of recycled top-product. The

This book belongs to Bradley Loren (bloren@mcandrews-ip.com) Copyright Elsevier 2024

Intas Exhibit 1032
Page 418 of 470
PGR2025-00043

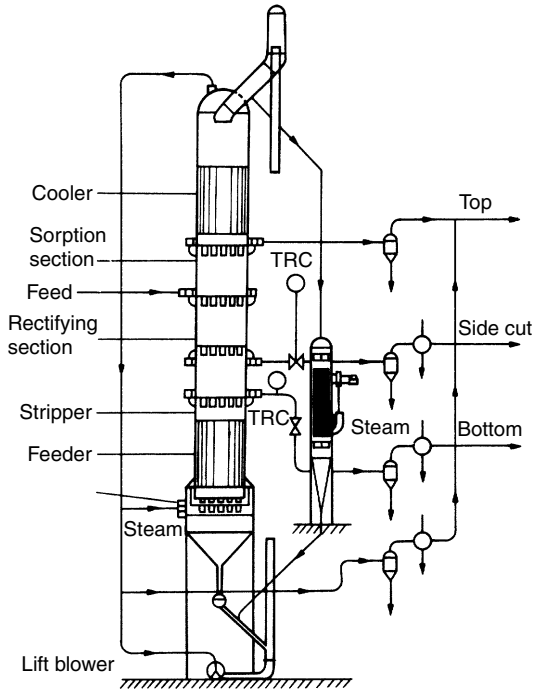


Figure 17.26. The hypersorber[45]

least-strongly adsorbed ethylene is desorbed and recovered in a side stream. The heavy components continue downwards on the carbon until these are also desorbed by steam, to be recovered as a bottom product. The carbon, now stripped of all the adsorbates, is lifted to the top of the column where it is cooled before the cycle starts again.

The rate at which the carbon is circulated may be controlled at entry to the lift-pipe. In normal operation, regenerating conditions do not maintain the carbon in its initial highly active state. Consequently, a small proportion of the regenerated carbon is steam-treated in a small column at a temperature of about 870 K. Some large hypersorbers, about 25 m high and 1.4 m in diameter, have been built for commercial operation. It seems that the units were beset from the beginning with problems of solids-handling. There was difficulty in maintaining an even flow of adsorbent and the problem of solids attrition and their subsequent loss as fines. Recently developed adsorbents, which are more selective and therefore more attractive as separating agents are, if anything, less resistant to attrition, and are unsuitable for moving-solid applications as a result.

In the 1960s there were attempts to use a moving bed of carbon to remove sulphur dioxide from flue gas on a pilot scale. As described by KATELL[46] and CARTELYOU[47], this *Reinluft* process was abandoned because of the problems caused by the carbon igniting in the presence of oxygen.

In order to design moving-bed equipment, the velocity of the adsorption zone relative to the solid has to be calculated. This gives the velocity at which the solids must move in

This book belongs to Bradley Loren (bloren@mcandrews-ip.com) Copyright Elsevier 2024
Intas Exhibit 1032
Page 419 of 470
PGR2025-00043

plugflow in order that the zone remains within the equipment. The depth of packing, z_a, should be sufficient to contain the zone. A mass balance across an increment dz gives:

$$u\varepsilon A\,\mathrm{d}C = k_g A(1-\varepsilon)a_p(C - C_i)\,\mathrm{d}z \tag{17.111}$$

C_i is an interfacial concentration which, in general, will not be known. It is often possible to express the rate of transfer of adsorbate in terms of an overall driving force $(C - C^*)$. In this case, equation 17.111 may be rearranged and integrated to give:

$$z_a = \frac{mu}{k_g^0 a_p}\int_{C_B}^{C_E}\frac{\mathrm{d}C}{C - C^*} \tag{17.112}$$

where C^* is the fluid concentration in equilibrium with the mean concentration of the adsorbed phase, at any instant, and k_g^0 is an overall mass transfer coefficient.

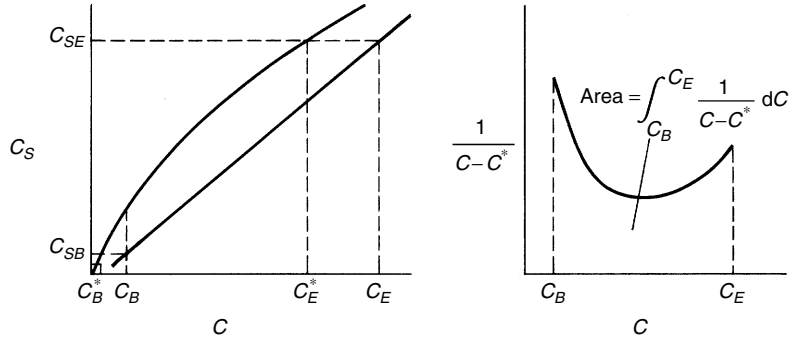


Figure 17.27. Graphical calculation of the number of transfer units

The integral in equation 17.112 may be evaluated numerically or graphically as shown in Figure 17.27. This is the *number of transfer units*, and the group outside the integral is the *height of a transfer unit*. The integral in equation 17.112 covers the whole concentration span of the adsorption process. If, instead, the limits are taken as from C_B to an arbitrary concentration C, then the length z' corresponding to C is given by:

$$z' = \frac{mu}{k_g^0 a_p}\int_{C_B}^{C}\frac{\mathrm{d}C}{C - C^*} \tag{17.113}$$

and:

$$\frac{z'}{z_a} = \frac{\displaystyle\int_{C_B}^{C}\frac{\mathrm{d}C}{C - C^*}}{\displaystyle\int_{C_B}^{C_E}\frac{\mathrm{d}C}{C - C^*}} \tag{17.114}$$

In Figure 17.28, C/C_E is plotted as a function of z'/z_a, and the unsaturated fraction i of the adsorption zone may then be found. Since the zone in a moving bed is essentially the

This book belongs to Bradley Loren (bloren@mcandrews-ip.com) Copyright Elsevier 2024

Intas Exhibit 1032
Page 420 of 470
PGR2025-00043

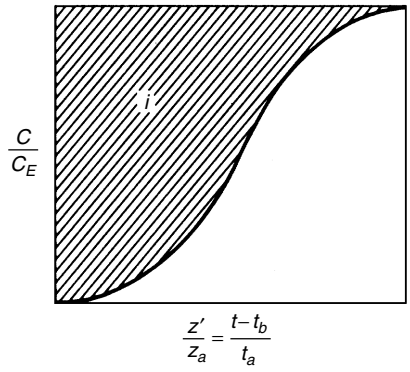


Figure 17.28. Dimensionless breakthrough curve showing fractional unsaturation of the adsorption zone

same as that which develops in a fixed bed, the time to break-point for the latter case, t_b, may be found from:

$$uA\varepsilon C_0 t_b = (z' - iz_a)C_{s\infty}\, A(1-\varepsilon) \tag{17.115}$$

The shape of the breakthrough wave, subsequent to the breakpoint, may then be determined from:

$$z' = \frac{(t - t_b)}{t_a} z_a \tag{17.116}$$

where t_a is the time for the adsorption zone to move its own length, and z' is measured from the inlet of the adsorption zone.

The method, which is illustrated in Example 17.5, applies only to isothermal beds in which the zone becomes fully-developed quite soon after the flow begins.

Example 17.5

An adsorption unit is to be designed to dry air using silica gel. A moving-bed design is considered in which silica gel moves down a cylindrical column in plug flow while air flows up the column. Air enters the unit at the rate of 0.129 kg of dry air/m^{2}s and with a humidity of 0.00267 kg water/kg dry air. It leaves essentially bone dry. There is equilibrium between air and gel at the entrance to and the exit from the adsorption zone. Experiments were carried out to find the relative resistances of the external gas film and pellet diffusion. Referred to a driving force expressed as mass ratios then:

(a) for the gas film, the coefficient $k_g a_z = 31.48 G'^{0.55}$ kg/m^{3}s
where G' is the mass flowrate of dry air per unit cross-section of bed.
(b) for pellet diffusion, solid-film coefficent $k_p a_z = 0.964$ kg/m^{3}s

where a_z is the external area of adsorbent per unit volume of bed

(a) Using the transfer-unit concept, calculate the minimum length of packing which will reduce the moisture content of the air to 0.0001 kg water/kg dry air. At what rate should the gel travel through the bed?

This book belongs to Bradley Loren (bloren@mcandrews-ip.com) Copyright Elsevier 2024

Intas Exhibit 1032
Page 421 of 470
PGR2025-00043

The properties of the gel and the condition of the air are as given in Example 17.4.

(b) After operating for some time, the gel jams and the unit continues operating as a fixed bed. How long after jamming will it be before the moisture content of the effluent rises to half the inlet value?

Solution

(a) The bed must be long enough to contain the adsorption zone. From equation 17.112 the number of transfer units may be written as: $\int \mathrm{d}y_r/(y_r - y_r^*)$ and the height of a transfer unit in appropriate units is $G'/k_g^0 a_z$, where k_g^0 is the overall mass transfer coefficient.

The integral may be evaluated graphically from a plot of $1/(y_r - y_r^*)$ against y_r over the concentration range of the adsorption zone.

A mass balance over a part of the bed gives an operating line:

$$y_r = \frac{G'_s}{G'}x_r + \left(y_{r\text{in}} - \frac{G'_s}{G'}x_{r\text{out}}\right)$$

This line, together with the equilibrium line, is similar to that shown in Figure 17.27. Corresponding values of y and y^* may be measured and the integral evaluated. The pinches between the operating and equilibrium lines which occur at each end of the zone prevent the end concentration from being used as the limits of the integration. If the lower limit of $y_r = 0.0001$ and the upper limit 0.0024, then from a graphical construction:

$$\int_{0.0001}^{0.0024} \frac{\mathrm{d}y_r}{y_r - y_r^*} = 10.95 \text{ transfer units}$$

The height of a transfer unit is: $\dfrac{G'}{k_g^0 a_z}$ (from equation 17.112)

k_g^0 may be evaluated from the film coefficients, as discussed in Chapter 12.

When the zone is fully developed, each part will move at the same constant velocity. If $\mathrm{f}'(C)$ is the mean slope of the isotherm over the range of concentrations of interest, then, in appropriate units:

$$[\mathrm{f}'(C)]_{\text{mean}} = \frac{(8.4 \times 10^{-2} \times 1266)}{(2.67 \times 10^{-3} \times 1.186)}$$

$$m = \frac{\varepsilon}{1 - \varepsilon} = \left(\frac{0.47}{0.53}\right) = 0.89$$

The inter-pellet air velocity = 0.233 m/s. The velocity u_c with which the adsorption wave moves through the column may be obtained from equation 17.79.

Hence: $u_c = 6.2 \times 10^{-6}$ m/s

$$G'_s = u_c(1 - \varepsilon)\rho_p$$

and: $$= 6.2 \times 10^{-6}(0.53)1266$$

$$= \underline{\underline{4.16 \times 10^{-3} \text{ kg/m}^2\text{s}}}$$

The rate at which clean adsorbent must be added and spent adsorbent removed in order to maintain steady state may also be found from an overall balance:

This book belongs to Bradley Loren (bloren@mcandrews-ip.com) Copyright Elsevier 2024

Intas Exhibit 1032
Page 422 of 470
PGR2025-00043

$$G'_s(0.084 - 0) = 0.129(0.00267)$$

$$G'_s = 4.11 \times 10^{-3} \text{ kg/m}^2\text{s}$$

(b) When the gel stops moving, the bed behaves as a fixed-bed already at its breakpoint. The concentration of water in the effluent begins to rise.
The time t_a for the adsorption zone to move its own length z_a is given by:

$$t_a = \frac{z_a}{u_c} = 8.3 \text{ h}$$

The time taken for a point at a distance z' into the zone to emerge is given by:

$$t = \frac{z'}{z_a} t_a$$

where:

$$\frac{z'}{z_a} = \int_{y_r^B}^{y_r} \frac{\mathrm{d}y_r}{y_r - y_r^*} \Bigg/ \int_{y_r^B}^{y_r^E} \frac{\mathrm{d}y_r}{y_r - y_r^*}$$

The results for graphical integration are tabulated below.

$$\frac{1}{k_g^0 a_z} = \frac{1}{k_g a_z} + \frac{m'}{k_p a_z}$$

where m' is the slope of the operating line $= \left(\frac{0.00267}{0.084}\right) = 0.0318$, as shown in Figure 17.22.

$$k_g a_z = 31.48 G'^{0.55} = 10.21 \text{ kg/m}^3 \text{ s}$$

Hence:

$$k_g^0 a_z = 7.64 \text{ kg/m}^3 \text{ s}$$

and:

$$\frac{G'}{k_g^0 a_z} = \left(\frac{0.129}{7.64}\right) = 0.0169 \text{ m}$$

The length of the adsorption zone $= (10.95 \times 0.0169) = 0.185$ m

Hence the minimum length of bed to contain the adsorption zone is 0.185 m. In practice, a somewhat greater length would be used to allow for variations in the length of the zone that might result from fluctuations in operating conditions. The data are summarised as follows:

y_r	y_r^*	$\frac{1}{y_r - y_r^*}$	$\int_{y_r^B}^{y_r} \frac{\mathrm{d}y_r}{y_r - y_r^*}$	$\frac{z'}{z_a}$	$\frac{y_r}{y_{r0}}$	t (h)
0.0001	0.00005	20,000	0	0	0.038	0
0.0002	0.00010	10,000	1.50	0.137	0.075	0.8
0.0006	0.00032	3570	4.00	0.362	0.225	3.1
0.0010	0.00062	2630	5.18	0.473	0.374	4.1
0.0014	0.00100	2500	6.13	0.560	0.525	4.5
0.0018	0.00133	3700	7.38	0.674	0.674	5.8
0.0022	0.00204	6250	9.33	0.852	0.825	7.1
0.0024	0.00230	10,000	10.95	1.000	0.899	7.7

By interpolation, $y_r/y_{r0} = 0.5$ when $t \approx$ 4.4 h.

This book belongs to Bradley Loren (bloren@mcandrews-ip.com) Copyright Elsevier 2024

Intas Exhibit 1032
Page 423 of 470
PGR2025-00043

17.9.3. Rotary bed

Because of the difficulty of ensuring that the solid moves steadily and at a controlled rate with respect to the containing vessel, other equipment has been developed in which solid and vessel move together, relative to a fixed inlet for the feed and a fixed outlet for the product. Figure 17.29 shows the principle of operation of a rotary-bed adsorber used, for example, for solvent recovery from air on to activated-carbon. The activated-carbon is contained in a thick annular layer, divided into cells by radial partitions. Air can enter through most of the drum circumference and passes through the carbon layer to emerge free of solvent. The clean air leaves the equipment through a duct connected along the axis of rotation. As the drum rotates, the carbon enters a section in which it is exposed to steam. Steam flows from the inside to the outside of the annulus so that the inner layer of carbon, which determines the solvent content of effluent air, is regenerated as thoroughly as possible. Steam and solvent pass to condensers and the solvent recovered, either by decanting or by a process such as distillation. In the particular equipment shown, there is no separate provision for cooling the regenerated adsorbent; instead it is allowed to cool in contact with vapour-laden air and the adsorptive capacity may be lower as a result[16].

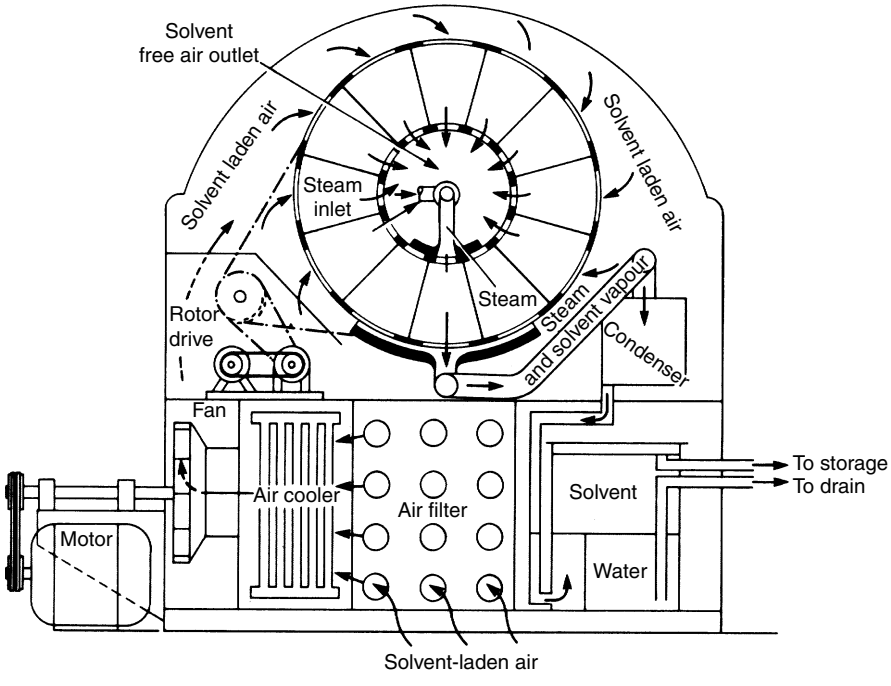


Figure 17.29. Rotary-bed adsorber

17.9.4. Moving access

In an interesting alternative to a moving-bed or a moving-container adsorber, a multiway valve effectively changes the position of the inlet and outlet valves relative to a fixed bed.

This book belongs to Bradley Loren (bloren@mcandrews-ip.com) Copyright Elsevier 2024

Intas Exhibit 1032
Page 424 of 470
PGR2025-00043

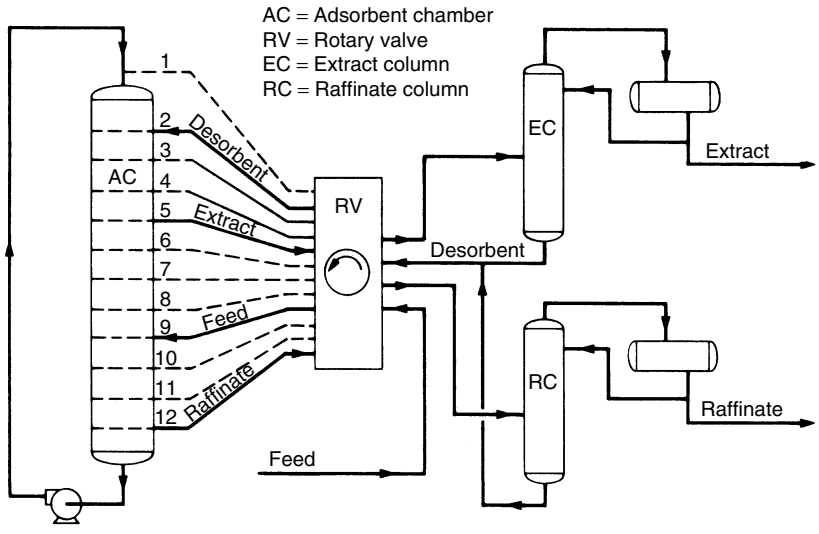


Figure 17.30. Sorbex: a number of small beds used with a rotary valve to simulate a moving bed

Such a system is shown diagrammatically in Figure 17.30 which shows a unit consisting of twelve small beds housed in one column. It may be assumed that it is fed with a mixture containing components **A** and **B**, the former being the more strongly absorbed of the two, with the desorption carried out using a third component **D**, the most strongly adsorbed component of all, and therefore capable of displacing **B** and **A** in that order. The valve rotates in a stepwise fashion, at regular intervals, with the positions of the inlets and the outlets for the process and regenerating streams moving to each numbered position in turn, thus simulating the behaviour of a moving bed as shown in Figure 17.31. As described by BROUGHTON[48] and JOHNSON and KABZA[49], the arrangement was developed by Universal Oil Products under the general name "Sorbex". The unit currently operates in the liquid phase, chiefly for separating *p*-xylene from C_8 aromatics, normal from branched and cyclo-paraffins, or olefins from mixture with paraffins. In principle, the unit may be used for gas-phase separations although, in either phase, success depends crucially on the proper working of the rotary valve.

17.9.5. Fluidised beds

Although the moving packed-bed has not yet achieved commercial success, another arrangement in which the solid moves with respect to the containing vessel, the fluidised bed, has fared better. Behaving essentially as a stirred tank reactor, the fluidised bed does not gives the ideal configuration for use as an adsorber. The solid is thoroughly mixed, so that the condition of the effluent is controlled by the mean adsorbate concentration on the solid, rather than by the initial concentration as in the case of a fixed bed. Nevertheless, there are other considerations which outweigh this disadvantage. Solid is easily added to and removed from fluidised bed. The pressure drop through a fluidised bed is effectively

This book belongs to Bradley Loren (bloren@mcandrews-ip.com) Copyright Elsevier 2024

Intas Exhibit 1032
Page 425 of 470
PGR2025-00043

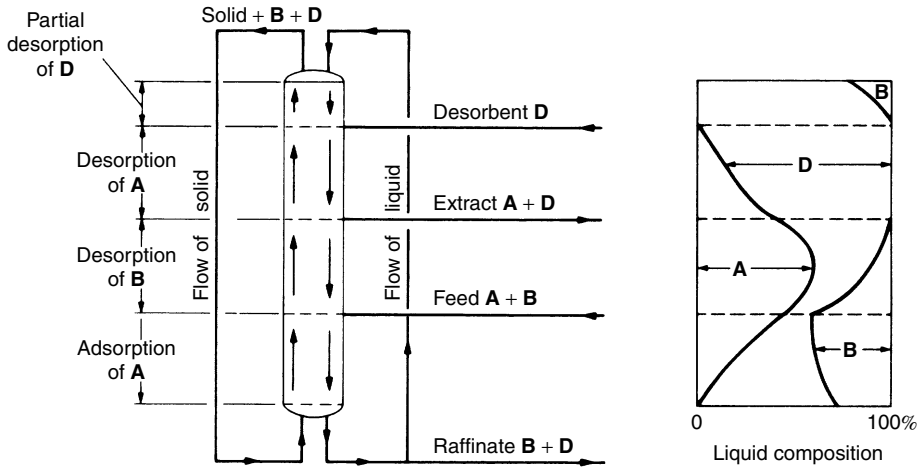


Figure 17.31. The moving-bed equivalent of the Sorbex process

constant over a wide range of fluid flowrates, and this makes it possible to treat materials at high flowrates in relatively compact equipment.

If the mean residence time in the fluidised bed is sufficiently long, it may be regarded as a single stage, from which streams of fluid and solid leave in equilibrium.

17.9.6. Compound beds

There is sometimes an advantage in using two kinds of adsorbent in an adsorption bed. Near the inlet would be an adsorbent with a high capacity at high concentrations, although it may have an unfavourable isotherm so that, on its own, the adsorption zone would then be unduly long, particularly if large pellets were used to minimise the pressure drop. If it is followed by a second bed of adsorbent with a highly favourable isotherm and a low mass transfer resistance, a short mass transfer zone will be sufficient to effect the required separation.

17.9.7. Pressure-swing regeneration

In thermal-swing regeneration, the bed may need a substantial time to reach the regeneration temperature. The high temperatures may also affect the product and accelerate the ageing processes in the adsorbent.

An alternative is to use pressure rather than temperature as the thermodynamic variable to be changed with adsorption taking place at high pressure and desorption at low pressure — hence the description *pressure–swing adsorption*. An arrangement utilising this principle was proposed by SKARSTROM[50,51]. Figure 17.32 shows a typical arrangement of a unit consisting of two fixed beds, one adsorbing and one regenerating. These functions are later reversed. A simple cycle consists of four steps. In step 1, high-pressure feed flows through bed A. Part of its effluent is expanded to the lower pressure, and then passed

This book belongs to Bradley Loren (bloren@mcandrews-ip.com) Copyright Elsevier 2024

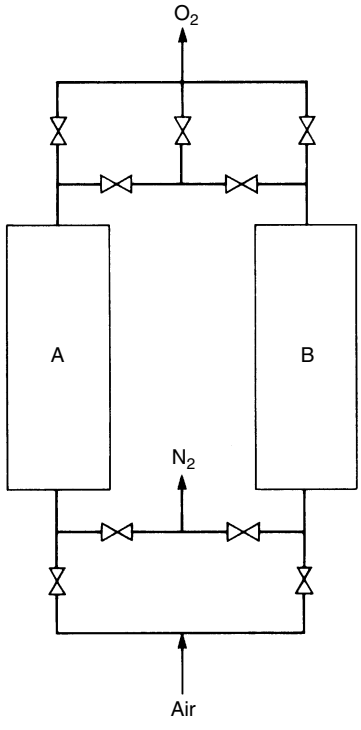


Figure 17.32. A two-bed unit using pressure swing regeneration for separating oxygen and nitrogen on a small scale

through bed B which it regenerates. In step 2, B is repressurised to the feed pressure using feed gas, while A is blown down to the purge pressure. Steps 3 and 4 follow the sequence of 1 and 2 except that the functions of beds A and B are reversed.

In large-scale equipment, more than two beds may be used so that pressure energy is better utilised. The regenerating effect of the purge stream depends on its volume rather than on its mass, so only a fraction of the high pressure effluent, say 20 per cent, is needed to achieve effective regeneration. Because changes in pressure can be brought about more rapidly than changes in temperature, pressure-swing regeneration can be used with shorter cycle-times than was possible with thermal-swing. This, in turn, allows smaller beds to be used and consequently a smaller inventory of adsorbent is needed in the system.

Pressure-swing regeneration is useful when the stream to be treated is needed at pressures above atmospheric, as for example in the case of instrument air. Pressure-swing units are compact and can readily be made portable. When the process stream is at atmospheric pressure or below, it may be possible to regenerate using a partial vacuum. When Skarstrom was patenting his "heatless" adsorber, GUERIN DE MONTGAREUIL and DOMINE[52] were patenting a system using vacuum regeneration. The original aim of both patents was to separate oxygen and nitrogen from air. With the range of adsorbents then available, neither process was particularly successful for that particular application. Skarstrom's equipment was, however, found to be suitable for the drying of gases, and,

This book belongs to Bradley Loren (bloren@mcandrews-ip.com) Copyright Elsevier 2024

Intas Exhibit 1032
Page 427 of 470
PGR2025-00043

after some modifications, the Guerin-Domine process was applied successfully to the separation of air on a large scale.

A mathematical description of a pressure swing system has been presented by SHENDALMAN and MITCHELL[53] who assumed that isothermal equilibrium adsorption takes place and that the isotherm is linear, with the feed consisting of a single adsorbate at low concentration in a non-adsorbed carrier gas.

The mass conservation equation for the adsorber, over an increment dz of bed may be written as:

$$\frac{\partial(uC)}{\partial z} + \frac{\partial C}{\partial t} + \frac{1}{m}\frac{\partial C_s}{\partial t} = 0 \qquad \text{(equation 17.69)}$$

where m is the interpellet void ratio, $\varepsilon/(1-\varepsilon)$.

For an ideal gas:
$$C = \frac{yP}{\mathbf{R}T}$$

where y is the mole fraction of the adsorbate and P is the total pressure.
If the adsorbed phase is in linear equilibrium with the gas, then:

$$C_s = \frac{K_a y P}{\mathbf{R}T}$$

where K_a is the equilibrium constant.
Substituting in equation 17.69:

$$\frac{\partial(uyP)}{\partial z} + \frac{\partial P}{\partial t} + \frac{K_a}{m}\frac{\partial(yP)}{\partial t} = 0 \qquad (17.118)$$

Neglecting the pressure gradient $\partial P/\partial z$:

$$\frac{\partial u}{\partial z} + u\frac{\partial \ln y}{\partial z} + \left(1 + \frac{K_a}{m}\right)\frac{\partial \ln P}{\partial t} + \left(1 + \frac{K_a}{m}\right)\frac{\partial \ln y}{\partial t} = 0 \qquad (17.119)$$

For a pure carrier gas, $y = 1$ and $K_a = 0$, and therefore:

$$\frac{\partial u}{\partial z} + \frac{\partial \ln P}{\partial t} = 0 \qquad (17.120)$$

Substituting in equation 17.119:

$$u\frac{\partial \ln y}{\partial z} + \frac{K_a}{m}\frac{\partial \ln P}{\partial t} + \left(1 + \frac{K_a}{m}\right)\frac{\partial \ln y}{\partial t} = 0 \qquad (17.121)$$

By the method of characteristics[54], equation 17.121 may be reduced to an ordinary differential equation to give:

$$\frac{dz}{u} = \frac{dt}{\left(1 + \frac{K_a}{m}\right)} = -\frac{d\ln y}{\left(\frac{K_a}{m}\right)\left(\frac{d\ln P}{dt}\right)} \qquad (17.122)$$

from which:
$$\frac{dz}{dt} = \frac{u}{1 + \frac{1}{m}K_a} \qquad (17.123)$$

Equation 17.123 is a particular case of equation 17.75.

This book belongs to Bradley Loren (bloren@mcandrews-ip.com) Copyright Elsevier 2024

Intas Exhibit 1032
Page 428 of 470
PGR2025-00043

The left-hand side of equation 17.123 is the velocity of a point of fixed concentration on the adsorption wave. For a linear isotherm and if longitudinal diffusion is neglected, all points of concentration will move at the same velocity. Changing the pressure will affect u and, to a lesser extent, K_a.

Pressure-swing regeneration is achieved by using a part of the high-pressure adsorber effluent for purging. The volume of purge must be such that the distance the adsorption wave moves at high pressure is completely reversed in the same time at low pressure. The requirement is normally satisfied by using a fraction of the high pressure effluent which is equal to the ratio of the low pressure to the high pressure.

The second characteristic that follows from equation 17.122 is:

$$\frac{\mathrm{d}\ln y}{\mathrm{d}\ln P} = \frac{-\frac{1}{m}K_a}{1+\frac{K_a}{m}} \tag{17.124}$$

where m is the inter-pellet void ratio $\varepsilon/(1-\varepsilon)$.
Integrating between the high and low pressure gives:

$$\frac{y_H}{y_L} = \left(\frac{P_L}{P_H}\right)^{(K_a/m)/[1+(K_a/m)]} \tag{17.125}$$

This relates the change in effluent concentration to the pressure ratio.

The change in the position of the characteristic that results from a pressure-swing is given by integrating equation 17.120 from the closed end of the bed where $u = 0$, $z = 0$.

Thus: $$u = -\left(\frac{\partial \ln P}{\partial t}\right) z \tag{17.126}$$

From equation 17.123: $$u = \left(1+\frac{K_a}{m}\right)\frac{\mathrm{d}z}{\mathrm{d}t} = -\left(\frac{\mathrm{d}\ln P}{\mathrm{d}t}\right) z$$

which, on integration gives: $$\frac{z_H}{z_L} = \left(\frac{P_L}{P_H}\right)^{1/(1+K_a/m)} \tag{17.127}$$

where z_H represents the distance moved by the adsorption front during the high pressure stage.

The net distance moved by the front, from the beginning of one position of low pressure to the next is given by:

$$\Delta z = z_L - z'_L = z_L - \left(\frac{P_H}{P_L}\right)^{1/(1+K_a/m)} z_H \tag{17.128}$$

If Δz is negative, insufficient regeneration is occurring to sustain a condition of cyclic steady-state.

This book belongs to Bradley Loren (bloren@mcandrews-ip.com) Copyright Elsevier 2024

Intas Exhibit 1032
Page 429 of 470
PGR2025-00043

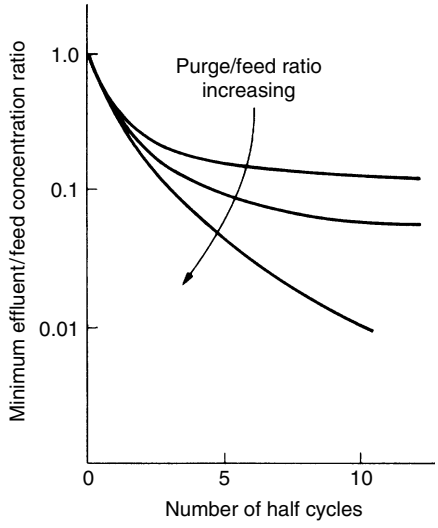


Figure 17.33. Effect of cycling and purge/feed volumetric ratio on minimum effluent/feed concentration ratio, using pressure-swing regeneration

Figure 17.33 shows how the purge–feed volumetric ratio and cycling affect effluent concentration. Ratios of 1.1–1.5 are normal.

17.9.8. Parametric pumping

When operated in a conventional mode, a fixed bed is fed with the stream to be processed until the breakpoint is reached. Thus, maximum use is made of the adsorptive capacity of the bed, without exceeding it. Regeneration is accomplished by changing a variable, such as temperature, pressure or concentration, and purging the bed in a countercurrent manner.

As described by WILHELM *et al.*[55], an alternative operating procedure has been developed in order to improve the separation obtained, where separation is defined as the ratio of concentrations in the upper and lower reservoirs, or in a reservoir and the feed. The technique has become known as *parametric pumping* because changing an operating parameter, such as temperature, may be considered as *pumping* the adsorbate into a reservoir at one end of a bed and, by difference, depleting the adsorbate in a reservoir at the other end.

Direct mode of operation

Figure 17.34*a* shows a simple one-bed unit, operating in batch mode, and heated and cooled through a jacket. The arrangement is known as the *direct thermal mode* because heat is supplied to the whole length of bed at the same instant. Finite resistances to heat transfer will mean, however, that, in practice, the bed takes a finite time to reach the required temperature.

This book belongs to Bradley Loren (bloren@mcandrews-ip.com) Copyright Elsevier 2024

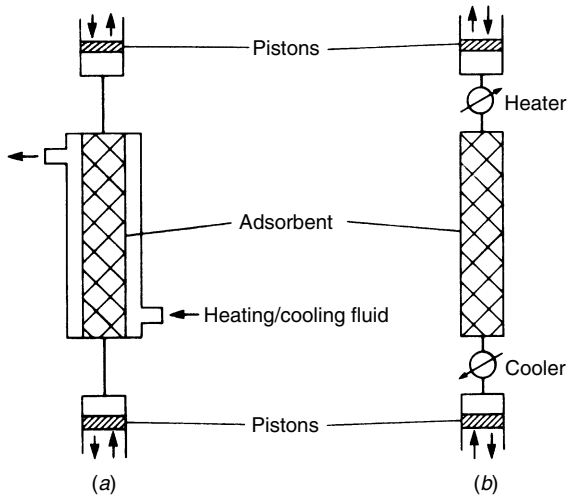


Figure 17.34. Parametric pumping, batch operation (*a*) Direct thermal mode (*b*) Recuperative thermal mode

To illustrate the principle, a number of assumptions will be made which are not realised in practice, although they enable the source of the separation to be identified. It is assumed that there is equilibrium at all times between fluid and the solid with which it is in contact. It is assumed that changes in temperature can be achieved instantaneously. It is further assumed that the adsorption front travels at such a velocity at the higher temperature that it traverses the length of the bed in the time allowed for upwards flow of the fluid. At the lower temperature, it is assumed that the adsorption wave travels half the distance in the same time with flow downwards. Each change may be regarded as taking place in two steps — first the temperature is changed and the new equilibrium established and then the pistons move to reverse the direction of flow. This simplified process is illustrated in Figure 17.35.

When the temperature of the bed is changed, the mass of adsorbate in an increment of bed dz is conserved. Hence, for the first change from hot to cold:

$$A\,\mathrm{d}z[\varepsilon C_F + (1-\varepsilon)C_{sF}] = A\,\mathrm{d}z[\varepsilon C_c + (1-\varepsilon)C_{sc}] \tag{17.129}$$

For equilibrium operation and a linear isotherm, $C_{sc} = K_c C_c$ and $C_{sF} = K_H C_F$, and hence:

$$\frac{C_F}{C_c} = \frac{1 + \dfrac{1}{m}K_c}{1 + \dfrac{1}{m}K_H} \tag{17.130}$$

It may be seen from equation 17.123 that the right-hand side of equation 17.130 is the ratio of zone velocities, and:

$$\frac{C_F}{C_c} = \frac{u_H}{u_c} \tag{17.131}$$

It was assumed that $u_H/u_c = 2$, and hence $C_F = 2C_c$, $C_H = 2C_F$, $C_c = 2C_{cc}$ and so on.

This book belongs to Bradley Loren (bloren@mcandrews-ip.com) Copyright Elsevier 2024
Intas Exhibit 1032
Page 431 of 470
PGR2025-00043

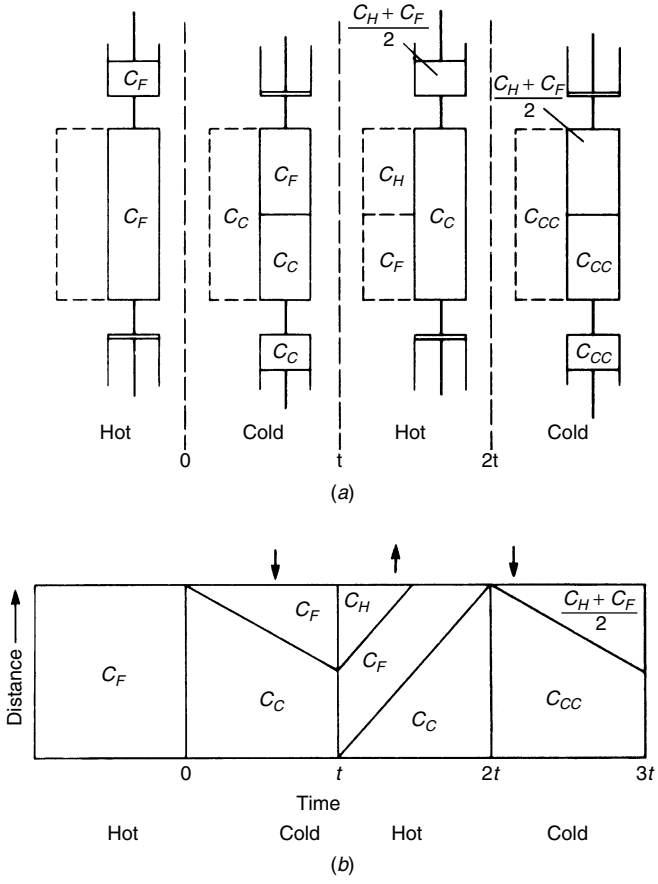


Figure 17.35. Ideal parapump, direct heating (*a*) Dotted section represents the condition immediately after a temperature change but before the pistons move (*b*) Position of the wave-front against time

In equation 17.129, C_s is the mean adsorbate concentration over a pellet of adsorbent. It may be desirable to include the intra-pellet voidage α and intra-pellet concentrations C'_F, C'_{sF} and so on to give:

$$\varepsilon C_F + (1-\varepsilon)\alpha C'_F + (1-\varepsilon)(1-\alpha)C'_{sF} = \varepsilon C_c + (1-\varepsilon)\alpha C'_c + (1-\varepsilon)(1-\alpha)C'_{sc}$$

At equilibrium: $$C_F = C'_F, \quad C_c = C'_c,$$

$$C'_{sF} = K_H C_F, \quad C'_{sc} = K_c C_c$$

Hence equation 17.130 becomes:

$$\frac{C_F}{C_c} = \frac{1 + \frac{1}{m}[\alpha + (1-\alpha)K_c]}{1 + \frac{1}{m}[\alpha + (1-\alpha)K_H]} \tag{17.132}$$

This book belongs to Bradley Loren (bloren@mcandrews-ip.com) Copyright Elsevier 2024

Intas Exhibit 1032
Page 432 of 470
PGR2025-00043

It may be seen that even with only the two cycles shown, a significant difference has been achieved between the concentrations of the material in the two reservoirs $[0.5(C_H + C_F)/C_{cc} = 6]$. Separation is sometimes defined as the ratio of the upper reservoir concentration to that of the feed. In this case a value of 3/2 is obtained. Continuing the cycling process will increase the degree of separation without limit in this ideal case. In practice, thermal lags and diffusional processes make it impossible to sustain sharp differences of concentration, though separations giving a 100,000-fold change in concentrations have been achieved.

The process described so far has made maximum use of the adsorptive capacity of the bed in upwards flow. If the flow were continued beyond that point, the contents of the lower reservoir would pass unchanged into the top reservoir and the separation would be reduced. It may be more convenient, however, to use a shorter time for upwards flow. The effect of allowing the process to continue only until the concentration wave has reached two-thirds of the way along the bed is shown in Figure 17.36. As in Figure 17.35, $u_H = 2u_c$. After the second up-flow stage, the average concentration in the material that has left the top of the bed is given by:

$$\tfrac{1}{2}[(C_{HH} + C_H)/2 + C_F] = 2C_F \tag{17.133}$$

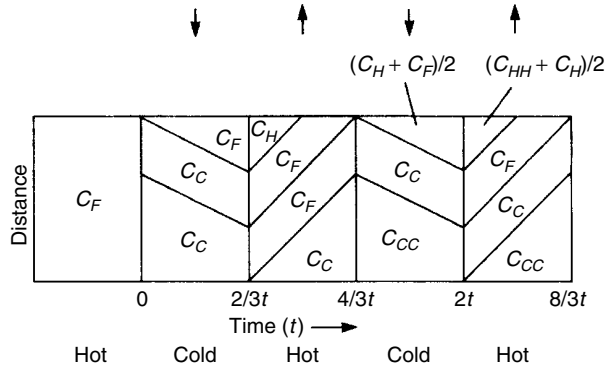


Figure 17.36. Effect of cycle-time on separation

The separation between upper and lower reservoirs in this case is 8. This compares with a value of 7 shown in Figure 17.35*b* after the same number of flow-reversals. The degree of separation depends on frequency of cycling as well as the total number of cycles.

Recuperative mode

Figure 17.34*b* shows an alternative method of supplying heat in thermal parametric-pumping. Heat is supplied in upwards flow by passing feed from the lower reservoir

This book belongs to Bradley Loren (bloren@mcandrews-ip.com) Copyright Elsevier 2024
Intas Exhibit 1032
Page 433 of 470
PGR2025-00043

through a heat exchanger. Cold operation in downward flow is achieved by cooling the feed from the top reservoir. Clearly, even when this method is idealised, the thermal wave takes a finite time to travel the length of the bed. The method is known as the *indirect* or *recuperative mode*, and is shown in Figure 17.34*b* as applied to a batch process.

The velocity with which a pure thermal wave travels through an insulated packed bed may be obtained from equation 17.100 by putting $U_0 = 0$ and $(\partial/\partial T)(C_s \Delta H) = 0$ to give:

$$\frac{u}{u_T} = \left[1 + \left(\frac{1}{m}\frac{\rho_p c_{ps}}{\rho_g c_{pg}}\right) + \left(\frac{4W c_{pw}}{\varepsilon \pi d_p^2 \rho_g c_{pg}}\right)\right] \tag{17.134}$$

It has been assumed that the gas and solid have the same temperature at any point, and that the fluid concentration is constant throughout a pellet at a value equal to that immediately outside the pellet. Within the limits of these assumptions, the thermal wave velocity u_T is independent of temperature. As discussed in Section 17.8.4, the velocity of the thermal wave relative to that of the concentration wave can be positive, as it normally is in liquids, negative or zero.

Figure 17.37 shows a thermal wave plotted as a dotted line of distance against time. The velocity u_c of the concentration wave depends on where it is in relation to the thermal wave, as can be seen by comparison with the full line in the Figure 17.37.

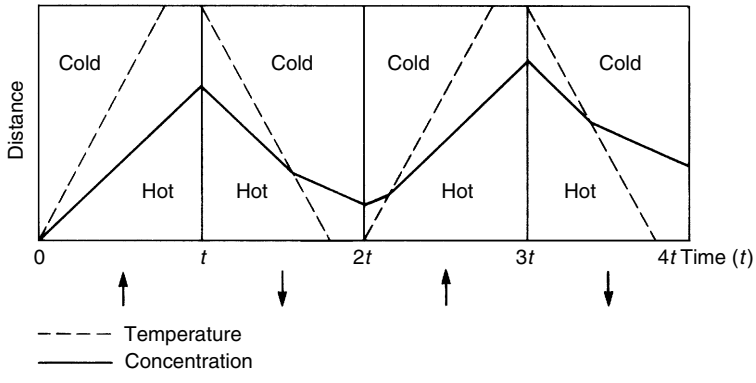


Figure 17.37. Wave propagation in recuperative mode

It may be shown that the ratio of the concentration in a hot zone to that in a cold zone for recuperative parametric pumping is given by:

$$\frac{C_H}{C_c} = \frac{1/u_c - 1/u_T}{1/u_H - 1/u_T} \tag{17.135}$$

For 'instant' heating and cooling, u_T equals infinity and equation 17.135 becomes equivalent to equation 17.131 for the direct-heating mode.

The net movement upwards of a concentration wave is greater in the direct mode. Fewer cycles are needed to achieve a given separation. Nevertheless, the recuperative mode is probably the more convenient method to use on a commercial scale. Indeed,

This book belongs to Bradley Loren (bloren@mcandrews-ip.com) Copyright Elsevier 2024
Intas Exhibit 1032
Page 434 of 470
PGR2025-00043

its equivalent is the only mode that can be used when other parameters, such as pH or pressure, are changed instead of temperature.

Many workers have demonstrated the effectiveness of parametric pumping in order to achieve separations in laboratory-scale equipment. It is mainly liquid systems that have been studied, using either temperature or pH as the control variable. Pressure parametric-pumping is described in a US patent and is discussed by YANG[3].

The principles of separation have been discussed using equilibrium theory. Finite resistances to heat and mass transfer will reduce the separation achieved.

17.9.9. Cycling-zone adsorption (CZA)

When parametric pumping was being developed, an alternative parameter-swinging technique was proposed by PIGFORD *et al.*[56] which is called *cycling-zone adsorption*. Instead of reversing the flow through a single bed as temperature is changed, a number of beds is used, connected in series, alternatively hot and cold. As with parametric pumping, heat may be supplied in the feed stream to each bed or through a jacket. The reversals of temperature remain, though each reversal of direction of the parametric pump corresponds to an additional stage of CZA. Figure 17.38 illustrates a two-bed unit. Given the same assumptions of ideality and, in particular, equilibrium and instant temperature changes, the sequence of events giving rise to concentration peaks and troughs in the effluent is shown in Figure 17.39. The effluent is switched between high and low concentration reservoirs.

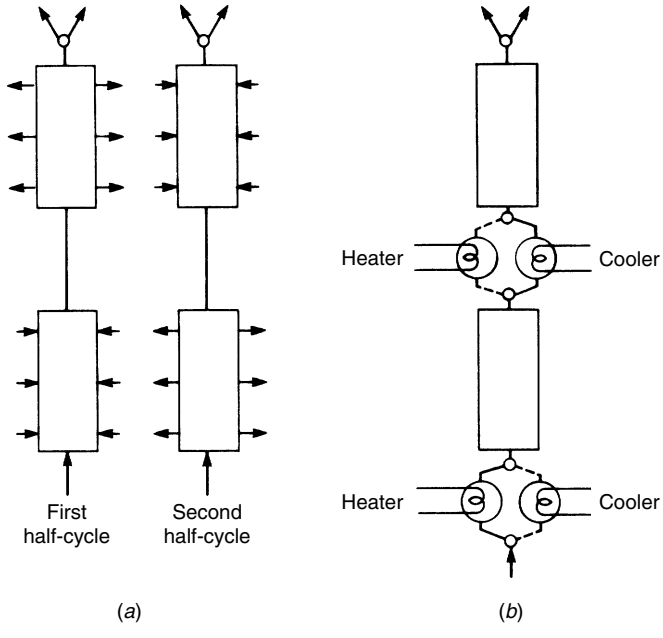


Figure 17.38. A two-bed cycling zone adsorption unit (*a*) Direct heating mode (*b*) Recuperative heating mode

This book belongs to Bradley Loren (bloren@mcandrews-ip.com) Copyright Elsevier 2024

Intas Exhibit 1032
Page 435 of 470
PGR2025-00043

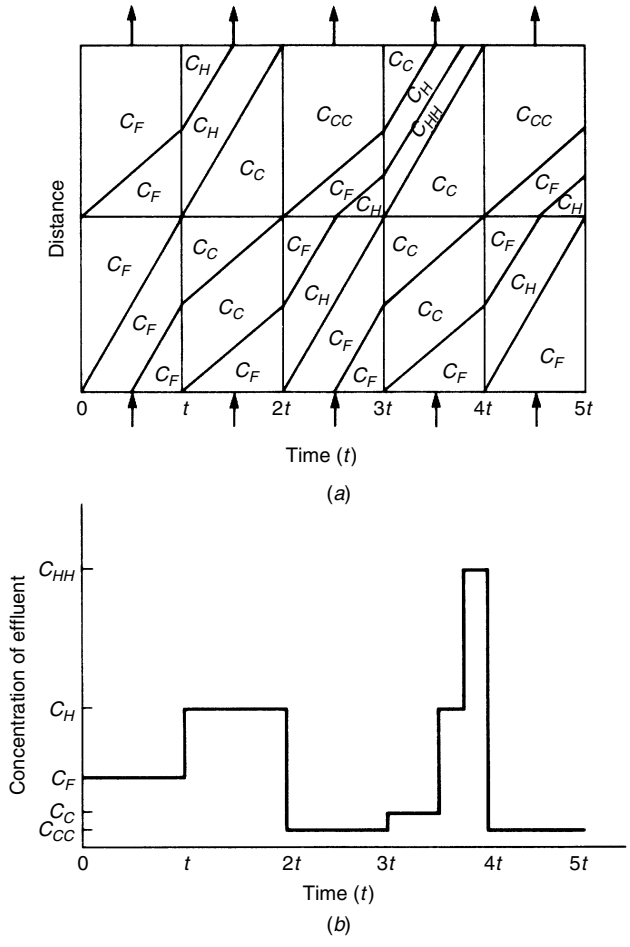


Figure 17.39. Direct mode cycling zone adsorption (*a*) Progression of concentration bands through a two-bed unit (*b*) Effluent concentration

In the example considered, the separation between highest and lowest effluent concentrations, after four temperature reversals, is $C_{HH}/C_{cc} = 16$, on the basis of the earlier assumptions. A single bed operating in a similar way would produce a separation of C_H/C_c equal to only 4. There is no theoretical limit to the separation that may be achieved by adding further stages. Clearly, there are practical considerations which will limit the number, such as pressure drop and total capital cost.

The other factor affecting separation will be the frequency with which the temperatures are changed. The maximum time for one stage will be the time taken for the feed to break through a hot bed. The minimum time will be determined by the fact that, if there are too many temperature changes, the concentration bands will pass through unchanged.

The principle temperature-cycling of separation has been described. Pressure-cycling has been described by PLATT and LAVIE[57].

This book belongs to Bradley Loren (bloren@mcandrews-ip.com) Copyright Elsevier 2024

Intas Exhibit 1032
Page 436 of 470
PGR2025-00043

Further discussions of pressure swing adsorption, parametric pumping and cycling-zone adsorption have been presented by YANG[3], SCHWEITZER[7] and WANKAT[58].

17.10. FURTHER READING

Adsorption and Ion Exchange: *A.I.Ch.E. Symposium Series* No 259 **83** (1987) (see also numbers 14, 24, 69, 74, 80, 96, 117, 120, 134, 152, 165, 219, 233, 242).

Adsorption and its Applications in Industry and Environmental Protection Vol 1 Applications in Industry Vol II Applications in Environmental Protection (Elsevier, Amsterdam, 1999).

COONEY, D. O.: *Adsorption Design for Wastewater Treatment* (CRC Press, Lewis Publishers, Boca Raton, 1998).

CHEREMISINOFF, N. P. and CHEREMISINOFF, P. N.: *Carbon Adsorption for Pollution Control* (Prentice Hall, Englewood Cliff, New Jersey, 1993).

KARGER, J. and RUTHVEN, D. M.: *Diffusion in Zeolites and other Microporous Solids* (John Wiley & Sons, New York, 1992).

LE VAN, M. D., (ed.) *Fundamentals of Adsorption V* (Kluwer Academic Publishers, Norwell, 1996).

PERRY, R. H., GREEN, D. W., and MALONEY, J. O. (eds.): *Perry's Chemical Engineers' Handbook*. 7th edn (McGraw-Hill Book Company, New York, 1997).

RUTHVEN, D. M.: *Principles of Adsorption and Adsorption Processes* (Wiley, 1984).

RUTHVEN D. M., FAROOQ S. and KNAEBEL K. S.: *Pressure Swing Adsorption* (VCH Publishers, New York, 1994).

SLEJKO, F. L.: *Adsorption Technology* (Marcel Dekker, New York, 1985).

SUZUKI, M. (ed.): *Fundamentals of Adsorption IV* (Kodansha, Tokyo, 1993).

SUZUKI, M.: *Adsorption Engineering* (Elsevier, Amsterdam, 1990).

THOMAS, W. J. and CRITTENDEN, B. D.: *Adsorption, Technology and Design* (Butterworth-Heinemann, Oxford, 1998).

TIEN, Chi: *Adsorption Calculations and Modeling* (Butterworth, Boston, 1994).

VALENZUELA, D. Y. and MYERS A. I.: *Adsorption Equilibrium Data Handbook* (Prentice Hall, EngIewood Cliffs, 1989).

WANKAT, P. C.: *Large Scale Adsorption and Chromatography (2* vols*)* (CRC Press Boca Raton, 1986).

YANG, R. T.: *Gas Separation by Adsorption Processes* (Butterworth, London 1987).

YANG, R. T.: *Gas Separation by Adsorption Processes* (Series on Chemical Engineering, Vol 1) (World Scientific Publishing Co, 1997).

17.11. REFERENCES

1. CRITTENDEN, B.: *The Chemical Engineer* No. 452 (Sept. 1988). 21. Selective adsorption.
2. BARRER, R. M.: *Brit. Chem. Eng*. **4** (1959) 267. New selective sorbents: porous crystals as molecular filters.
3. YANG, R. T.: *Gas Separation by Adsorption Processes* (Butterworth, London, 1987).
4. BRECK, D. W.: *Zeolite Molecular Sieves* (Wiley, New York, 1974).
5. BARRER, R. M.: *Zeolites and Clay Minerals* (Academic Press, London, 1978).
6. ROBERTS, C. W.: *Properties and Applications of Zeolites* (Chemical Society, London, 1979).
7. SCHWEITZER, P. A. (ed.): *Handbook of Separation Techniques for Chemical Engineers* 2nd edn. (McGraw-Hill, New York, 1988).
8. EVERETT, D. H. and STONE, F. S. (eds): *The Structure and Properties of Porous Materials* (Butterworth, Oxford, 1958).
9. BOWEN, J. H., BOWREY, R. and MALIN, A. S.: *J. Catalysis* **7** (March 1967) 457. A study of the surface area and structure of activated alumina by direct observation.
10. BRUNAUER, S.: *The Adsorption of Gases and Vapours* (Oxford U.P., Oxford, 1945).
11. LANGMUIR, I.: *J. Am. Chem. Soc*. **40** (1918) 1361. The adsorption of gases on plane surfaces of glass, mica and platinum.
12. BRUNAUER, S., EMMETT, P. H. and TELLER, E.: *J. Am. Chem. Soc*. **60** (1938) 309. Adsorption of gases in multimolecular layers (for errata see reference 13).
13. EMMETT, P. H. and DE WITT, T.: *Ind. Eng. Chem. (Anal.)* **13** (1941) 28. Determination of surface areas.
14. BRUNAUER, S., DEMING, L. S., DEMING, W. E. and TELLER, E.: *J. Am. Chem. Soc*. **62** (1940) 1723. On a theory of the van der Waals adsorption of gases.
15. HARKINS, W. D. and JURA, G.: *J. Chem. Phys*. **11** (1943) 431. An adsorption method for the determination of the area of a solid without the assumption of a molecular area and the area occupied by nitrogen molecules on the surface of solids. *J. Amer. Chem. Soc*. **66** (1944) 1366. Surface of solids. Part XIII.

This book belongs to Bradley Loren (bloren@mcandrews-ip.com) Copyright Elsevier 2024

Intas Exhibit 1032
Page 437 of 470
PGR2025-00043

16. RUTHVEN, D. M.: *Principles of Adsorption and Adsorption Processes* (Wiley, New York, 1984).
17. GARG, D. R. and RUTHVEN, D. M.: *A.I.Ch.E. Jl* **21** (1975) 200. Linear driving force approximation for diffusion controlled adsorption in molecular sieve columns.
18. POLANYI, M.: *Trans. Farad. Soc* **28** (1932) 316. Theory of adsorption of gases — introductory paper.
19. YOUNG, D. M. and CROWELL, A. D.: *Physical Adsorption of Gases* (Butterworth, 1962).
20. MERSMANN, A., MUNSTERMANN, U. and SCHADL, J.: *Germ. Chem. Eng*., **7** (1984) 137. Separation of gas mixtures by adsorption.
21. FREUNDLICH, H.: *Colloid and Capillary Chemistry* (Methuen, London, 1926).
22. GLUECKAUF, E., and COATES, J. I.: *J. Chem. Soc*. (1947) 1315. Theory of chromatography.
23. KIPLING, J. J.: *Adsorption from Solutions of Non-Electrolytes* (Academic Press, 1965).
24. EMMETT, P. H.: *Advances in Colloid Science* **1** (1942) 1. The measurement of the surface areas of finely divided or porous solids by low temperature adsorption isotherms.
25. COHAN, L. H.: *J. Am. Chem. Soc*. **60** (1938) 433. Sorption hysteresis and vapour pressure of concave surfaces.
26. CRANSTON, R. W. and INKLEY, F. A.: *Advances in Catalysis* **9** (1957) 143. The determination of pore structures from nitrogen adsorption isotherms.
27. RANZ, W. E. and MARSHALL, W. R.: *Chem. Eng. Prog*. **48** (4) (1952) 173. Evaporation from drops. Part II.
28. DWIVEDI, P. N. and UPADHEY, S. N.: *Ind. Eng. Chem. Proc. Des. Dev*. **16** (1977) 157. Particle–fluid mass transfer in fixed and fluidized beds.
29. WAKAO, N. and FUNAZKRI, T.: *Chem. Eng. Sci*. **33** (1978) 1375. Effect of fluid dispersion coefficients on particle–fluid mass transfer coefficients in packed beds.
30. GLASSTONE, S. and LEWIS, D.: *Elements of Physical Chemistry* (Macmillan, 1970).
31. SATTERFIELD, C. N.: *Mass transfer in Heterogeneous Catalysis* (MIT Press, Boston, 1970).
32. BIRD, R. B., STEWART, W. E. and LIGHTFOOT, E. N.: *Transport Phenomena* (Wiley, New York, 1960).
33. EVANS, R. B., WATSON, G. M. and MASON, E. A.: *J. Chem. Phys*. **33** (1961) 2076. Gaseous diffusion in porous media at uniform pressure.
34. SCHNEIDER, P. and SMITH, J. M.: *A.I.Ch.E. Jl* **14** (1968) 762. Adsorption rate constants from chromatography.
35. EPSTEIN, N.: *Chem. Eng. Sci*. **44** (1989) 777. On tortuosity and the tortuosity factor in flow and diffusion through porous media.
36. HINSHELWOOD, C. N.: *The Kinetics of Chemical Change* (Clarendon Press, Oxford, 1940).
37. EDWARDS, M. F. and RICHARDSON, J. F.: *Chem. Eng. Sci*. **23** (1968) 109. Gas dispersion in packed beds.
38. BOWEN, J. H. and RIMMER, P. G.: *Trans. Inst. Chem. Eng*., **50** (1972) 168. Design of fixed bed sorbers using a quadratic driving force equation.
39. LAPIDUS, L. and AMUNDSON, N. R.: *J. Phys. Chem*. **56** (1952) 373. Mathematics of adsorption in fixed beds — The rate determining steps in radial adsorption analysis; *ibid* **56** (1952) 984. The effect of longitudinal diffusion in ion exchange and chromatographic columns.
40. LEVENSPIEL, O. and BISCHOFF, K. B.: In *Advances in Chemical Engineering* Vol. 4 DREW, T. B., HOOPES, J. W. and VERMEULEN, T. (eds.) (Academic Press, 1963) 95. Patterns of flow in chemical process vessels.
41. ROSEN, J. B.: *J. Chem. Phys*. **20** (1965) 387. Kinetics of fixed bed systems for solid diffusion into spherical particles.
42. LEAVITT, F. W.: *Chem. Eng. Prog*. **58** (8) (1962) 54. Nonisothermal adsorption in large fixed beds.
43. AMUNDSON, N. R., ARIS, R. and SWANSON, R.: *Proc. Roy. Soc*. **286A** (1965) 129. On simple exchange waves in fixed beds.
44. CARTER, J. W.: *A.I.Ch.E. Jl*. **21** (1975) 380. On the regeneration of fixed adsorber beds.
45. BERG, C.: *Chem. Eng. Prog*. **47** (11) (1951) 585. Hypersorption design.
46. KATELL, S.: *Chem. Eng. Prog*. **62** (Oct. 1966) 67. Removing sulphur dioxide from flue gases.
47. CARTELYOU, C. G.: *Chem. Eng. Prog*. **65** (9) (1969) 69. Commercial processes for SO_2 removal.
48. BROUGHTON, D. B.: *Chem. Eng. Prog*. **64** (8) (1968) 60. Molex, history of a process.
49. JOHNSON, J. A. and KABZA, R. G.: *I. Chem. E. Annual Research Meeting, Swansea* (1990) Sorbex: Industrial scale adsorptive separation.
50. SKARSTROM, C. W.: *Annals N Y Acad. Sci*. **72** (1959) 751. Use of adsorption phenomena in automatic plant-type gas analysis.
51. SKARSTROM, C. W.: *US Patent* 2944627 (1960). Method and apparatus for fractionating a gaseous mixture by adsorption.
52. GUERIN DE MONTGAREUIL, P. and DOMINE, D.: *US Patent* 3155468 (1964). Process for separating a binary gaseous mixture by adsorption.
53. SHENDALMAN, L. H. and MITCHELL, J. E.: *Chem. Eng. Sci*. **27** (1972) 1449. A study of heatless adsorption in the model system CO_2 in He.
54. ACRIVOS, A.: *Ind. Eng. Chem*. **45** (1956) 703. Method of characteristics technique. Application to heat and mass transfer problems.

This book belongs to Bradley Loren (bloren@mcandrews-ip.com) Copyright Elsevier 2024

Intas Exhibit 1032
Page 438 of 470
PGR2025-00043

55. WILHELM, R. H., RICE, A. W., ROLKE, R. W. and SWEED, N. H.: *Ind. Eng. Chem. (Fund)* **7** (1968) 337. Parametric pumping.
56. PIGFORD, R. L., BAKER, B. and BLUM, D.: *Ind. Eng. Chem. (Fund)* **8** (1969) 144. An equilibrium theory of the parametric pump.
57. PLATT, D. and LAVIE, R.: *Chem. Eng. Sci*. **40** (1985) 733. Pressure cycle zone adsorption.
58. WANKAT, P. C.: *Cyclic Separations—Parametric Pumping, Pressure Swing Adsorption and Cycling Zone Adsorption* (A.I.Ch.E. Modular Instruction Series, Module B6.11, 1986).

17.12. NOMENCLATURE

		Units in SI System	Dimensions in **M**, **N**, **L**, **T**, $\boldsymbol{\theta}$
A	Superficial cross-sectional area of bed	m^2	$\mathbf{L}^2$
A_p	Interfacial area for condensate in a pore	m^2	$\mathbf{L}^2$
A_s	Area of an adsorbed film	m^2	$\mathbf{L}^2$
A_1', A_2'	Arrhenius frequency factors for desorption	$kmol/m^2s$	$\mathbf{NL}^{-2}\ \mathbf{T}^{-1}$
a_m	Area occupied by one molecule in an adsorbed film	m^2	$\mathbf{L}^2$
a_p	External area of adsorbent per unit volume of adsorbent	m^{-1}	$\mathbf{L}^{-1}$
a_p'	External surface of a pellet	m^2	$\mathbf{L}^2$
a_z	External area of adsorbent per unit volume of bed	m^{-1}	$\mathbf{L}^{-1}$
a_0, a_1, a_2	Fraction of the adsorbent surface covered by no adsorbate, one, two layers	—	—
B_0, B_1, B_i, B_j	Constants in Langmuir-type equations	various	
B_2	α_0/β in equation 17.9	—	—
C	Concentration of adsorbate in the fluid	$kmol/m^3$	$\mathbf{NL}^{-3}$
C_B	Concentration of adsorbate **B** in the fluid	$kmol/m^3$	$\mathbf{NL}^{-3}$
C_c	Concentration of adsorbate after 1 cold stage	$kmol/m^3$	$\mathbf{NL}^{-3}$
C_c'	Concentration of adsorbate within a pore after 1 cold stage	$kmol/m^3$	$\mathbf{NL}^{-3}$
C_{cc}	Concentration of adsorbate after two cold stages	$kmol/m^3$	$\mathbf{NL}^{-3}$
C_E	Concentration of adsorbate at the emergence of the adsorption zone	$kmol/m^3$	$\mathbf{NL}^{-3}$
C_F	Concentration of adsorbate in feed conditions	$kmol/m^3$	$\mathbf{NL}^{-3}$
C_i	Concentration of adsorbate at the exterior surface of a pellet	$kmol/m^3$	$\mathbf{NL}^{-3}$
C_H, C_{HH}	Concentration of adsorbate after one, two hot stages	$kmol/m^3$	$\mathbf{NL}^{-3}$
C_0	Concentration of adsorbate initially or at inlet	$kmol/m^3$	$\mathbf{NL}^{-3}$
C_p'	Concentration of adsorbate in feed conditions within a pore	$kmol/m^3$	$\mathbf{NL}^{-3}$
C_r, C_{sr}	Concentration of adsorbate at radius r in the fluid, or in adsorbed phases	$kmol/m^3$	$\mathbf{NL}^{-3}$
C_s	Concentration of adsorbed phase	$kmol/m^3$	$\mathbf{NL}^{-3}$
C_s'	Concentration of adsorbed phase within a pore	$kmol/m^3$	$\mathbf{NL}^{-3}$
C_s''	Mass concentration of adsorbed phase referred to adsorbate free adsorbent	kg/m^3	$\mathbf{ML}^{-3}$
$\bar{C}_s$	Mean concentration of adsorbed phase	$kmol/m^3$	$\mathbf{NL}^{-3}$
C_{sc}'	Concentration of adsorbed phase in a pore after one cold stage	$kmol/m^3$	$\mathbf{NL}^{-3}$
C_{SF}'	Concentration of adsorbed phase in a pore in feed conditions	$kmol/m^3$	$\mathbf{NL}^{-3}$
C_{sm}	Concentration of adsorbed phase in a monolayer	$kmol/m^3$	$\mathbf{NL}^{-3}$
$C_{s\infty}$	Ultimate or maximum concentration of adsorbed phase	$kmol/m^3$	$\mathbf{NL}^{-3}$

This book belongs to Bradley Loren (bloren@mcandrews-ip.com) Copyright Elsevier 2024

Intas Exhibit 1032
Page 439 of 470
PGR2025-00043

		Units in SI System	Dimensions in **M**, **N**, **L**, **T**, $\boldsymbol{\theta}$
C^*	Concentration of adsorbate in equilibrium with $\bar{C}_s$	kmol/m^3	$\mathbf{NL}^{-3}$
c_{pg}	Specific heat capacity of the gas phase	J/kg K	$\mathbf{L}^2\mathbf{T}^{-2}\boldsymbol{\theta}^{-1}$
c_{ps}	Specific heat capacity of the adsorbent with adsorbate	J/kg K	$\mathbf{L}^2\mathbf{T}^{-2}\boldsymbol{\theta}^{-1}$
c_{pw}	Specific heat capacity of the wall	J/kg K	$\mathbf{L}^2\mathbf{T}^{-2}\boldsymbol{\theta}^{-1}$
D	Diffusivity	m^2/s	$\mathbf{L}^2\mathbf{T}^{-1}$
D_{av}	Average diffusivity	m^2/s	$\mathbf{L}^2\mathbf{T}^{-1}$
D_e	Effective diffusivity	m^2/s	$\mathbf{L}^2\mathbf{T}^{-1}$
D_k	Knudsen diffusivity	m^2/s	$\mathbf{L}^2\mathbf{T}^{-1}$
D_L	Longitudinal diffusivity	m^2/s	$\mathbf{L}^2\mathbf{T}^{-1}$
D_M	Molecular diffusivity	m^2/s	$\mathbf{L}^2\mathbf{T}^{-1}$
D_s	Surface diffusivity	m^2/s	$\mathbf{L}^2\mathbf{T}^{-1}$
D_{s0}	Surface diffusivity in standard conditions	m^2/s	$\mathbf{L}^2\mathbf{T}^{-1}$
D_T	Total diffusivity	m^2/s	$\mathbf{L}^2\mathbf{T}^{-1}$
d_b	Bed diameter	m	**L**
d_p	Pellet diameter	m	**L**
E	Argument of an error function	—	—
E_s	Energy of activation in surface diffusion	J/kmol	$\mathbf{MN}^{-1}\mathbf{L}^2\mathbf{T}^{-2}$
$E_0, E_1 \ldots E_n$	Energy of activation of desorption from empty surface, monolayer etc.	J/kmol	$\mathbf{MN}^{-1}\mathbf{L}^2\mathbf{T}^{-2}$
F	A function in equation 17.92	—	—
$f'(C)$	Slope of an adsorption isotherm	—	—
G	Function in equation 17.82	—	—
G	Gibbs free energy of an adsorbed film *or*	J	$\mathbf{ML}^2\mathbf{T}^{-2}$
	Mass flowrate of fluid	kg/s	$\mathbf{MT}^{-1}$
G', G'_s	Mass flowrate per unit cross sectional area of fluid, solid	kg/m^{2}s	$\mathbf{ML}^{-2}\mathbf{T}^{-1}$
G_1, G_2	Functions in equation 17.83	—	—
H	Enthalpy per kmol	J/kmol	$\mathbf{MN}^{-1}\mathbf{L}^2\mathbf{T}^{-2}$
h	Film heat transfer coefficient	W/m^2 K	$\mathbf{MT}^{-3}\boldsymbol{\theta}^{-1}$
i	Unsaturated fraction of an adsorption zone	—	—
J	A factor in equation 17.58	—	—
K	An equilibrium constant based on activities	various	
K_a, K_c, K_H	Adsorption equilibrium constants	—	—
K_0	Adsorption equilibrium constant at a standard condition	—	—
k	Thermal conductivity of fluid	W/mK	$\mathbf{MLT}^{-3}\boldsymbol{\theta}^{-1}$
$\boldsymbol{k}$	Reaction rate constant (1st order)	s^{-1}	$\mathbf{T}^{-1}$
k_B	Boltzmann constant	1.3805×10^{-23}J/K	$\mathbf{ML}^2\mathbf{T}^{-2}\boldsymbol{\theta}^{-1}$
k_e	Effective thermal conductivity of solid	W/mK	$\mathbf{MLT}^{-3}\boldsymbol{\theta}^{-1}$
k_g	Film mass transfer coefficient	m/s	$\mathbf{LT}^{-1}$
k_g^o	Overall mass transfer coefficient	m/s	$\mathbf{LT}^{-1}$
k_p	Mass transfer coefficient based on 'solid film'	m/s	$\mathbf{LT}^{-1}$
$\boldsymbol{k}_0, \boldsymbol{k}_1$	Adsorption velocity constants for empty surface, monolayer	kmol/Ns	$\mathbf{M}^{-1}\mathbf{NL}^{-1}\mathbf{T}$
$\boldsymbol{k}'_1, \boldsymbol{k}'_2$	Desorption velocity constants for monolayer, bilayer	kmol/m^{2}s	$\mathbf{NL}^{-2}\mathbf{T}^{-1}$
L	Length of porous medium	m	**L**
L'	Constant in equation 17.26	—	—
L_e	Length of porous path	m	**L**
L_p	Mean length of a pore	m	**L**
l	Distance into a pore	m	**L**
M	Molecular weight	kg/kmol	$\mathbf{MN}^{-1}$
M'	Constant in equation 17.26	m^{-6}	$\mathbf{L}^{-6}$
M_A, M_B	Molecular weights of **A**, **B**	kg/kmol	$\mathbf{MN}^{-1}$

This book belongs to Bradley Loren (bloren@mcandrews-ip.com) Copyright Elsevier 2024

Intas Exhibit 1032
Page 440 of 470
PGR2025-00043

		Units in SI System	Dimensions in **M**, **N**, **L**, **T**, $\boldsymbol{\theta}$
m	Inter-pellet void ratio $\varepsilon/(1-\varepsilon)$	—	—
m'	Slope of an operating line	—	—
m_M	Mass of one molecule	kg	**M**
N	Avogadro number (6.023×10^{26} molecules per kmol *or* 6.023×10^{23} molecules per mol)	kmol^{-1}	$\mathbf{N}^{-1}$
N_A, N_B	Flux of molecular species **A**, **B**	$\text{kmol/m}^2\text{s}$	$\mathbf{NL}^{-2}\mathbf{T}^{-1}$
N_{AC}	Interstitial flux of **A**	$\text{kmol/m}^2\text{s}$	$\mathbf{NL}^{-2}\mathbf{T}^{-1}$
N_{Ai}	Flux along a tortuous pore	$\text{kmol/m}^2\text{s}$	$\mathbf{NL}^{-2}\mathbf{T}^{-1}$
Nu	Nusselt number (hd_p/k)	—	—
n	Number of adsorbed layers	—	—
n	Index in the Freundlich equation 17.35	—	—
n'	Number of molecules per unit volume of gas	m^{-3}	$\mathbf{L}^{-3}$
n''	Number of components in equation 17.33	—	—
n_0	Initial number of mols of adsorbate	kmol	**N**
n_p	Number of pores	—	—
n_s	Number of mols of adsorption in a film or capillary	kmol	**N**
n_{s1}	Number of mols of adsorbate at pressure P_1	kmol	**N**
P	Total pressure	N/m^2	$\mathbf{ML}^{-1}\mathbf{T}^{-2}$
$\bar{P}$	Mean pressure	N/m^2	$\mathbf{ML}^{-1}\mathbf{T}^{-2}$
P^0	Vapour pressure of the adsorbed phase	N/m^2	$\mathbf{ML}^{-1}\mathbf{T}^{-2}$
P_A	Partial pressure of **A**	N/m^2	$\mathbf{ML}^{-1}\mathbf{T}^{-2}$
Pe	Peclet number (ud_p/D_L)	—	—
P_H/P_L	High/low pressure ratio	—	—
P_m	Vapour pressure over a meniscus	N/m^2	$\mathbf{ML}^{-1}\mathbf{T}^{-2}$
Pr	Prandtl number ($c_p\mu/k$)	—	—
P_1	Pressure at which the adsorbed film becomes mobile	N/m^2	$\mathbf{ML}^{-1}\mathbf{T}^{-2}$
R	Gas constant	8314 J/kmol K	$\mathbf{MN}^{-1}\mathbf{L}^2\mathbf{T}^{-2}\boldsymbol{\theta}^{-1}$
r	Radius within a spherical pellet or pore	m	**L**
r_i	Outer radius of a spherical pellet	m	**L**
r_p	Radius of a pore	m	**L**
r_p'	Net radius of a pore allowing for adsorbed layers	m	**L**
Sc	Schmidt number ($\mu/\rho D$)	—	—
Sh	Sherwood number ($k_g d_p/D$)	—	—
T	Absolute temperature	K	$\boldsymbol{\theta}$
T_a	Ambient temperature	K	$\boldsymbol{\theta}$
T_0	Initial or reference temperature	K	$\boldsymbol{\theta}$
t	Time	s	**T**
t_a	Time for an adsorption zone to move its own length	s	**T**
t_b	Time to breakpoint	s	**T**
t_1	Time parameter in equation 17.71	s	**T**
t_{min}	Minimum time to saturate unit cross section of a bed of length, z	s	**T**
U_0	Overall heat transfer coefficient	W/m^2 K	$\mathbf{MT}^{-3}\boldsymbol{\theta}^{-1}$
u	Interpellet velocity of fluid	m/s	$\mathbf{LT}^{-1}$
u_c, u_H	Velocity of a point on an adsorption wave at lower/higher temperatures	m/s	$\mathbf{LT}^{-1}$
u_T	Velocity of a point on a thermal wave	m/s	$\mathbf{LT}^{-1}$
V	Volume of fluid *or* volume per unit mass of adsorbent	m^3 (m^3/kg)	$\mathbf{L}^3$ ($\mathbf{M}^{-1}\mathbf{L}^3$)
V^1	Volume in the gas phase equivalent to an adsorbed monolayer	m^3	$\mathbf{L}^3$
V_i	Volume of ith component	m^3	$\mathbf{L}^3$
V_0	Initial volume of solution	m^3	$\mathbf{L}^3$

This book belongs to Bradley Loren (bloren@mcandrews-ip.com) Copyright Elsevier 2024

Intas Exhibit 1032
Page 441 of 470
PGR2025-00043

		Units in SI System	Dimensions in **M**, **N**, **L**, **T**, $\boldsymbol{\theta}$
V_p	Volume of a pore	m^3	$\mathbf{L}^3$
V_s	Volume of the adsorbed phase	m^3	$\mathbf{L}^3$
V_M	Molar volume of adsorbate	m^3/kmol	$\mathbf{N}^{-1}\mathbf{L}^3$
V'_m	Molar volume of liquid adsorbate	m^3/kmol	$\mathbf{N}^{-1}\mathbf{L}^3$
V_s^1	Volume of the adsorbed phase in a monolayer	m^3	$\mathbf{L}^3$
v_s	Volume of adsorbate on unit area of surface	m^3/m^2	**L**
v_s^1	Volume of adsorbate on unit area of monolayer	m^3/m^2	**L**
W	Mass per unit length of containing vessel	kg/m	$\mathbf{ML}^{-1}$
x_f	Thickness of boundary film	m	**L**
x_r	Mass ratio of adsorbed phase to adsorbent	—	—
y	Mole fraction of adsorbate in the fluid phase	—	—
y_H, y_L	Mole fractions in the effluent during high, low pressure stages of PSA	—	—
y_r	Mass ratio of adsorbate to carrier fluid	—	—
y_r^B, y_r^E	y_r at breakpoint, after emergence of adsorption zone	—	—
y_r^*	y_r in equilibrium with mean concentration of adsorbed phase	—	—
z	Distance along a bed	m	**L**
z'	Position of concentration C	m	**L**
z_a	Length of an adsorption zone	m	**L**
z_e	Length of a fixed bed	m	**L**
z_H	Distance moved by an adsorption zone at high pressure	m	**L**
z_L, z'_L	Distances moved by an adsorption zone in successive low pressure stages	m	**L**
z_0	Initial position of a point on the adsorption wave	m	**L**
α	Intra-pellet void fraction	—	—
α_0, α_1, α_2	Constants in equations 17.7, 17.24, 17.35	various	
β, β_1, β_2	Constants in equations 17.8, 17.24, 17.30	various	
Γ	Two dimensional spreading pressure	N/m	$\mathbf{MT}^{-2}$
Δ	Change in property	—	—
ε	Interpellet void fraction	—	—
ε_p	Adsorption potential	J/kmol	$\mathbf{MN}^{-1}\mathbf{L}^2\mathbf{T}^{-2}$
$\boldsymbol{\theta}_1$	Constant in equation 17.36	m^3	$\mathbf{L}^3$
Ω	Collision integral	—	—
λ	Mean free path of a gas molecule	m	**L**
λ_A	Average distance between adsorption sites	m	**L**
λ_M	Molar latent heat	J/kmol	$\mathbf{MN}^{-1}\mathbf{L}^2\mathbf{T}^{-2}$
λ'	Length parameter in equation 17.93	—	—
μ	Viscosity	Ns/m^2	$\mathbf{ML}^{-1}\mathbf{T}^{-1}$
μ_g	Chemical potential of a gas	J/kmol	$\mathbf{MN}^{-1}\mathbf{L}^2\mathbf{T}^{-2}$
μ_s	Chemical potential of an adsorbed film	J/kmol	$\mathbf{MN}^{-1}\mathbf{L}^2\mathbf{T}^{-2}$
ρ_B	Mass or molar density of a packed bed	kg/m^3 ($kmol/m^3$)	$\mathbf{ML}^{-3}$ ($\mathbf{NL}^{-3}$)
ρ_g	Mass (or molar) density of a gas	kg/m^3 ($kmol/m^3$)	$\mathbf{ML}^{-3}$ ($\mathbf{NL}^{-3}$)
ρ_p	Mass (or molar density) of an adsorbent pellet	kg/m^3 ($kmol/m^3$)	$\mathbf{ML}^{-3}$ ($\mathbf{NL}^{-3}$)
ρ_s	Mass (or molar) density of a solid	kg/m^3 ($kmol/m^3$)	$\mathbf{ML}^{-3}$ ($\mathbf{NL}^{-3}$)
σ_{AB}	Collision diameter between **A** and **B** molecules	m	**L**
σ_{sl}, σ_{sv}, σ_{lv}	Surface tensions at three interfaces in a solid–liquid–gas system	N/m	$\mathbf{MT}^{-2}$
ϕ	Interfacial angle between liquid and solid	—	—
ϕ_1	Constant in equation 17.36	m^3	$\mathbf{L}^3$
τ	Tortuosity, L/L_e	—	—
τ'	Time parameter in equation 17.94	—	—
φ	A resistance parameter in equation 17.95	—	—
χ	Time parameter in equations 17.71 and 17.83	s	T

This book belongs to Bradley Loren (bloren@mcandrews-ip.com) Copyright Elsevier 2024

Intas Exhibit 1032
Page 442 of 470
PGR2025-00043

CHAPTER 19

Chromatographic Separations

19.1. INTRODUCTION

Chromatographic methods of separation are distinguished by their high *selectivity*, that is their ability to separate components of closely similar physical and chemical properties. Many mixtures which are difficult to separate by other methods may be separated by chromatography. The range of materials which can be processed covers the entire spectrum of molecular weights, from hydrogen to proteins.

Chromatography plays several roles in the process industries. The design of a new plant begins with a proposed chemical route from starting materials to finished product, already tested at least on a small laboratory scale. In many cases, *analytical chromatography* will have been used in the laboratory to separate and identify the products in the mixtures produced by the proposed chemical process. In the biotechnology area, for example, the original starting material may be a natural product or a complex synthetic mixture which has been analysed by chromatography. Information on the choice of chromatographic stationary and mobile phases and operating conditions is therefore often already available and provides a basis for initial scale−up to an intermediate laboratory scale, *preparative chromatography*, and for the subsequent design of the commercial separation process, *production* or *large-scale chromatography*, as shown in Figure 19.1.

Chromatography also plays two other roles in process engineering. First, the detailed design of each unit operation in a process requires a knowledge of a variety of physical and chemical properties of the materials involved. Chromatographic techniques can provide rapid and accurate methods of measuring a great variety of thermodynamic, kinetic and other physico-chemical properties[1]. Secondly, chromatography is widely used for routine chemical analysis in quality control and for automated analysis of process streams in process control (*process chromatography*)[2,3]. This chapter, however, is concerned mainly with production chromatography as a unit operation whose use is increasing as the demand for high purity materials grows.

In chromatography the components of a mixture are separated as they pass through a column. The column contains a *stationary phase* which may be a packed bed of solid particles or a liquid with which the packing is impregnated. The mixture is carried through the column dissolved in a gas or liquid stream known as the *mobile phase, eluent* or *carrier*. Separation occurs because the differing distribution coefficients of the components of the mixture between the stationary and mobile phases result in differing velocities of travel.

Chromatographic methods are classified according to the nature of the mobile and stationary phases used. The terms *gas chromatography* (GC) and *liquid*

This book belongs to Bradley Loren (bloren@mcandrews-ip.com) Copyright Elsevier 2024

Intas Exhibit 1032
Page 443 of 470
PGR2025-00043

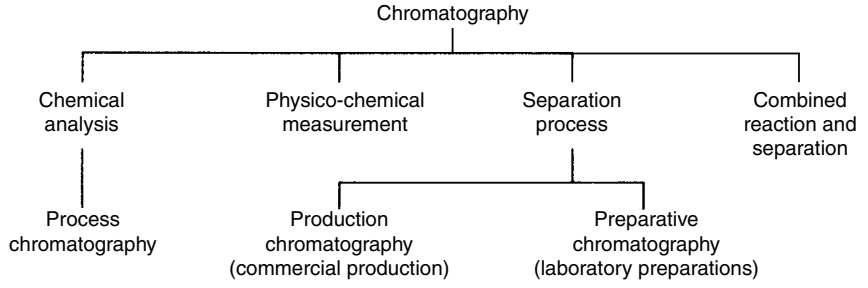


Figure 19.1. Uses of chromatography

chromatography (LC) refer to the nature of the mobile phase. The different types of stationary phase are described in Section 19.4.

Both GC and LC may be operated in one of several modes. The principal modes currently used for large-scale separations are elution, selective adsorption or desorption, and simulated countercurrent chromatography. In addition, reaction and separation can be combined in a single column with unique advantages. Elution is the most used and best developed form of the technique and is described first.

19.2. ELUTION CHROMATOGRAPHY

19.2.1. Principles

For convenience, the term *solute* is used to refer to a component of the feed mixture to be separated, regardless of the nature of the mobile and stationary phases: when the stationary phase is a solid surface, the "solute" might be better described as an adsorbate.

In elution chromatography, a discrete quantity (batch or "sample") of feed mixture is introduced into the column at the inlet. The mobile-phase flow causes the band of feed to migrate and split progressively into its component solute-bands or peaks, as shown in Figure 19.2. Emergence of the bands at the column outlet is monitored by a suitable detector, and the components are collected in sequence. The velocity at which each band travels through the column is normally less than that of the mobile phase and depends on the distribution coefficient of solute between the two phases. A solute 1 will travel faster than a solute 2, as shown in Figure 19.2 if it has a lower affinity for the stationary phase, or a higher affinity for the mobile phase, than solute 2. The principle is one of differential migration. This is the basis of the use of chromatography for (i) measurement of distribution coefficients from migration velocities and (ii) chemical analysis and separation of mixtures.

Continuous production is achieved in elution chromatography by repetitive batch injection or *cyclic batch elution*. The injection cycle is timed so that the emergence of the last-eluted component of one batch at the column exit is immediately followed by the emergence of the first-eluted component to be collected from the next batch as shown, for example, in Figure 19.2*b*. At any one time there is more than one batch moving through the column.

This book belongs to Bradley Loren (bloren@mcandrews-ip.com) Copyright Elsevier 2024

Intas Exhibit 1032
Page 444 of 470
PGR2025-00043

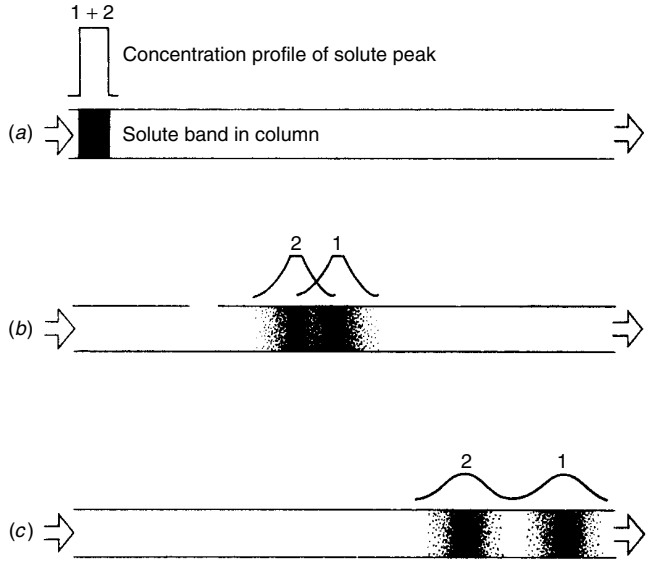


Figure 19.2. Separation of a mixture of two solute components 1 and 2 by elution chromatography. (*a*) Shows the solute band immediately after entry of the band into the column. (*b*) and (*c*) show the band separating into two component bands as it passes through the column

19.2.2. Retention theory

The theory of retention permits the calculation of the time the solute is *retained* in the column between injection and elution. The *retention time* t_R is defined, as shown in Figure 19.3, in terms of a solute concentration–time plot, knwon as the *chromatogram* registered by a detector at the column outlet. A part of this time t_M is required by the solute simply to pass through the mobile phase from inlet to outlet. The *adjusted retention time* t'_R represents the extra retention due to repeated partitioning or distribution of the solute between mobile and stationary phases as the band migrates along the column. An analogy for the principle of retention by repeated partitioning has been well put by BAILEY and OLLIS[4]: "Imagine a number of coachmen who start together down a road lined with pubs. Obviously those with the greatest thirst will complete the journey last, while those with no taste for ale will progress rapidly!" This analogy provides a good basis for a simple physical argument which leads to an equation for the retention time of a solute.

The average molecule of a given solute moves repeatedly in and out of the stationary phase during its passage through the column. The molecule spends some of its time being swept along by the mobile phase and some of its time "sitting in a pub", that is in the stationary phase. If R is the ratio of the total time spent by this average molecule in the mobile phase to the total time spent in the mobile and stationary phases, then:

$$R = \frac{t_M}{t_R} \tag{19.1}$$

$$= \frac{u_R}{u} \tag{19.2}$$

This book belongs to Bradley Loren (bloren@mcandrews-ip.com) Copyright Elsevier 2024

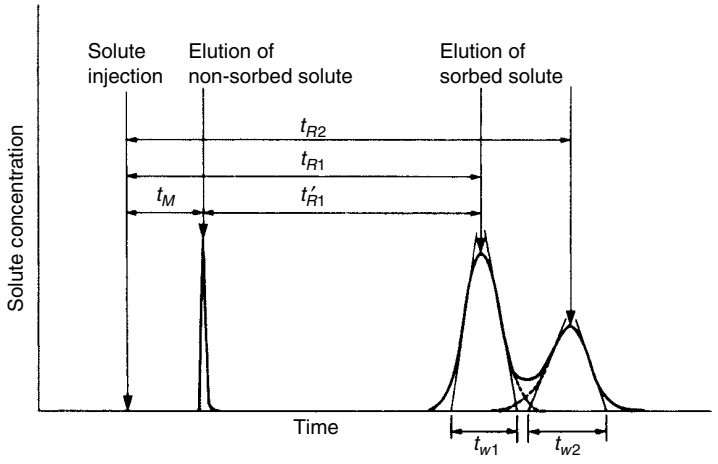


Figure 19.3. Chromatogram obtained by elution chromatography of a mixture of two solutes. The retention time t_R is the time taken by a solute to pass through the column. t_M is the mobile-phase holdup and is measured as the retention time of a non-sorbed solute. t'_R is the adjusted retention time, the total time spent by the solute in the stationary phase; it is equal to $t_R - t_M$. t_W is the width of a solute band at the baseline, i.e., the distance between the points of intersection of the baseline with tangents at the points of inflexion on the sides of the band

Here u_R is the velocity at which the solute band moves along the column and u is the velocity of the mobile phase; that is, $u = (\text{superficial velocity})/\varepsilon$, where superficial velocity is volumetric flow rate divided by cross-sectional area of column and ε is the fractional volume of column occupied by mobile phase. Most column packings are porous, in which case ε includes both interstitial and pore (intraparticle) voidage, as defined in the note to Table 19.1, and here u is less than the interstitial velocity.

Table 19.1. Contributions to plate height

Term in equation 19.10	Mechanism
$A = 2\lambda d_p$	Inequalities in patterns of flow in column packing.
$B/u = 2\gamma D_m/u$	Axial diffusion in mobile phase.
$C_s u = \frac{2}{3}\frac{k' d_f^2}{(1+k')D_s}u$	Lack of equilibrium between solute in the two phases due to slow mass transfer in stationary phase film.
$C_m u = \frac{\omega d_p^2}{D_m}u$	Slow mass transfer of solute in mobile phase during passage of solute to and from interface with stationary phase (includes diffusion through stagnant mobile phase in intra-particle* pores).

*Note. *Intra*-particle pores are pores *within* the particle. Inter-particle (interstitial) voidage refers to space *between* the particles, i.e. in the interstices of the packing.

The crux of the argument is that the average molecule is representative of a large number of identical molecules of the solute. Hence R, defined previously as the fractional time the average molecule spends in the mobile phase, may also be viewed as the fraction

This book belongs to Bradley Loren (bloren@mcandrews-ip.com) Copyright Elsevier 2024

Intas Exhibit 1032
Page 446 of 470
PGR2025-00043

of the total number of molecules that are in the mobile phase at equilibrium; that is:

$$R = \frac{n_m}{n_m + n_s} \tag{19.3}$$

or:

$$R = \frac{1}{1 + k'} \tag{19.4}$$

where k' is the mass distribution coefficient, n_s/n_m, usually known as the *capacity factor*. n_m and n_s are the numbers of mols of solute in the mobile and stationary phases, respectively, in an elemental height of column. Equating the expressions from equations 19.2 and 19.4 for R:

$$u_R = u/(1 + k') \tag{19.5}$$

or:

$$t_R = t_M(1 + k') \tag{19.6}$$

Equation 19.6 is often expressed in an alternative form. If q and c are the concentrations of solute in the stationary and mobile phases, respectively, and $K(= q/c)$ is the distribution coefficient of solute between the two phases, then:

$$\frac{n_s}{n_m} = \frac{1 - \varepsilon}{\varepsilon} K \tag{19.7}$$

and:

$$t_R = t_M \left(1 + \frac{1 - \varepsilon}{\varepsilon} K\right) \tag{19.8}$$

This equation allows the retention time (or solute band velocity) to be calculated from the equilibrium distribution coefficient K, and vice versa.

Equation 19.8 is the basic retention equation of elution chromatography. It is founded on the assumptions that the distribution isotherm, the plot of q against c at constant temperature, is linear and that equilibrium of the solute between phases is achieved instantaneously throughout the column.

More rigorous treatments of retention theory start from conservation of mass over a differential length of column[5,6]. They require the same assumptions as the simpler analysis presented here and lead to the same result, equation 19.8.

19.3. BAND BROADENING AND SEPARATION EFFICIENCY

The equations in the previous section relate only to the average molecule and so describe only the mean retention of a band. The mean retention is that of the peak of the band, as shown in Figure 19.3 if the band is symmetrical. In practice there is a spread of time about this mean due to several processes which tend to broaden the bands as they migrate through the column, as shown in the sequence (*a*)–(*c*) of Figure 19.2.

The band broadening may be characterised by a plate height, and its causes provide a basis for understanding why modern chromatography is such an efficient separation technique.

This book belongs to Bradley Loren (bloren@mcandrews-ip.com) Copyright Elsevier 2024

Intas Exhibit 1032
Page 447 of 470
PGR2025-00043

19.3.1. Plate height

In a hypothetical ideal column, a solute band would retain its initial profile unaltered as it migrated along the column. In a real, non-ideal, column an initially narrow band broadens by dispersion as it migrates. The band width is proportional to the square root of the distance travelled along the column.

The rate at which the band broadens depends on the *inefficiency* of the column. This is more precisely defined as the *height equivalent to a theoretical plate (HETP)*, discussed in detail in Chapter 11. MARTIN and SYNGE[7] introduced the concept when describing their invention of liquid chromatography in 1941. The HETP is defined as a unit of column length sufficient to bring the solute in the mobile phase issuing from it into equilibrium with that in the stationary phase throughout the unit. Plate models[6,8], using this concept, show that the HETP **H** of a column of length L may be determined by injecting a very small sample of solute, measuring its retention t_R and band width t_w at the column outlet as shown in Figure 19.3, and using the relation:

$$\mathbf{H} = \frac{L}{N} = \frac{L}{16(t_R/t_w)^2} \tag{19.9}$$

The greater the ratio t_R/t_w, then the greater the number of theoretical plates N in the column.

To maximise separation efficiency requires low H and high N values. In general terms this requires that the process of repeated partitioning and equilibration of the migrating solute is accomplished rapidly. The mobile and stationary phases must be mutually well-dispersed. This is achieved by packing the column with fine, porous particles providing a large surface area between the phases (0.5–4 m^2/g in GC, 200–800 m^2/g in LC). Liquid stationary phases are either coated as a very thin film (0.05–1 μm) on the surface of a porous *solid support* (GC) or chemically bonded to the support surface as a monomolecular layer (LC).

19.3.2. Band broadening processes and particle size of packing

There are several band-broadening processes operating in a chromatographic column. Each contributes a term to the plate height. Many equations for **H** have been proposed[9] since the original one of VAN DEEMTER, ZUIDERWEG and KLINKENBERG[10]. A widely used modern version of this equation is:

$$\mathbf{H} = A + \frac{B}{u} + C_s u + C_m u \tag{19.10}$$

The terms arise from the mechanisms of dispersion, or band-broadening, listed in Table 19.1.

In gas chromatography the B and C terms are usually larger than the A term. A plot of plate height against velocity shows a minimum.

Diffusion rates in liquids (LC) are typically three to four orders of magnitude less than in gases (GC). The lower mobile-phase diffusivity D_m affects two of the plate-height terms in liquid chromatography given in Table 19.1. First, the B/u term is small. Secondly, the $C_m u$ term is large. The $C_s u$ term is small in many LC applications where the stationary phase is only a monolayer of "liquid" bonded to the surface of a solid

This book belongs to Bradley Loren (bloren@mcandrews-ip.com) Copyright Elsevier 2024

Intas Exhibit 1032
Page 448 of 470
PGR2025-00043

support. Thus, overall, the A and C terms tend to be dominant in LC. C_m would be larger than in GC if the low value of diffusivity D_m were not compensated by a small particle diameter d_p. This is why much smaller particles (3–8 μm in analytical applications) are used in *high performance liquid chromatography* (HPLC) than in gas chromatography (120–300 μm). Smaller particles, however, entail much higher pressure drops, in the region of 40–400 bar (4–40 MN/m^2), across the column. Indeed, the abbreviation HPLC is often regarded as meaning *high pressure liquid chromatography*.

For reasons explained in Section 19.5.3, large-scale LC employs larger particles (10–70 μm) than analytical HPLC. This increases the $C_m u$ term by deepening the intraparticle pores containing stagnant mobile phase to be penetrated by the solute. (See note to Table 19.1). *Pellicular* packings, in which each particle contains only a superficially porous layer with an inner solid core, have been used, though the present trend is towards totally porous particles of 15–25 μm.

19.3.3. Resolution

The *resolution* between two solute components achieved by a column depends on the opposed effects of (a) the increasing separation of band centres and (b) the increasing band width as bands migrate along the column. The resolution R_s is defined by:

$$R_s = \frac{t_{R2} - t_{R1}}{\frac{1}{2}(t_{w1} + t_{w2})} \tag{19.11}$$

where t_{R1} and t_{R2} are the retention times of the two components, and t_{w1} and t_{w2} are the widths of the bands measured as defined in Figure 19.3. For the two bands in Figure 19.3. R_s is 1.26.

The resolution equation (19.11) may be expressed in a more useful form by introducing a *separation (selectivity) factor*:

$$\alpha = k'_2/k'_1 \tag{19.12}$$

Equations 19.6 and 19.12 may be manipulated to give:

$$t_{R2} - t_{R1} = t_M \left[2k' \left(\frac{\alpha + 1}{\alpha - 1} \right) \right] \tag{19.13}$$

where k' is the mean capacity factor, $\frac{1}{2}(k'_1 + k'_2)$. This equation is used to substitute for the numerator in equation 19.11; equation 19.9 is similarly used to substitute for t_{w1} and t_{w2} is the denominator. The result is:

$$R_s = \left(\frac{(\alpha - 1)}{2(\alpha + 1)} \right) \left(\frac{k'}{1 + k'} \right) \sqrt{\mathbf{N}} \tag{19.14}$$

This is an important basic equation for elution chromatography. Although the equation needs modification to cope with the wide, concentrated, feed bands of preparative and production chromatography[11], it shows how separation is controlled by the parameters α, k' and **N**. The great power of chromatography as a separation process lies in the high values that can readily be achieved for α and **N**.

This book belongs to Bradley Loren (bloren@mcandrews-ip.com) Copyright Elsevier 2024

Intas Exhibit 1032
Page 449 of 470
PGR2025-00043

19.3.4. The separating power of chromatography

The selectivity or separation factor, α, is a ratio of mass distribution coefficients given in equation 19.12, and so is a thermodynamic rather than a kinetic factor. The value of α depends mainly on the nature of the two solutes, on the stationary phase and, in liquid chromatography, the mobile phase. It is the analogue of the relative volatility α in distillation, considered in Chapter 11. If a liquid mixture has two components for which α is close to unity, that is $\alpha - 1 \ll 1$, they are difficult to separate by distillation because α cannot be controlled without introducing another constituent, as in azeotropic or extractive distillation, whose presence changes α. Judicious choice of the stationary phase and in liquid chromatography the mobile phase too, can greatly enhance $(\alpha - 1)$ with a corresponding beneficial effect, as shown by equation 19.14, on resolution.

A second reason why very high resolution can be obtained in chromatography is that very large numbers of theoretical plates are readily achieved. If the column is well packed with particles having a narrow spread of sizes, the plate height is about twice the particle diameter[9,12]. A typical large-scale GC or LC column will contain of $10^3 - 10^4$ plates.

Equation 19.14 also shows that resolution increases with increasing capacity factor k'. Diminishing returns apply at high k' and values of 1–5 are generally advocated.

19.4. TYPES OF CHROMATOGRAPHY

To separate compounds effectively requires an appropriate choice of the chromatographic mobile and stationary phases. Much chemical ingenuity has been exercised in devising a great many different types of chromatography, and only those relevant to production chromatography are described. The applications of GC and LC are distinguished in general terms, and then the principal types of GC, LC and their more recent stable-mate, supercritical fluid chromatography (SFC) are outlined.

19.4.1. Comparison of gas and liquid chromatography

A solute travelling along a GC column is in its vapour form while it is the mobile phase. Its retention is therefore inversely proportional to its vapour pressure. For optimum capacity factor k' (Section 19.3.4) and production economics, solutes usually need to be subjected to chromatography at a temperature within 20–30 K of their boiling point[12,13]. Although extreme column temperatures have been used for chemical analysis, the range of stability of organic liquid phases restricts normal large-scale operation to solutes boiling at 270–520 K. Thus GC is best suited to separating materials of molecular weight below about 300. The column temperature must be chosen to match the materials being separated and close control is required for reproducible retention times.

In LC the mobile phase is a liquid and so has a density some three orders of magnitude greater than in GC. The denser mobile phase has a much greater solubilising capacity for compatible solutes, permitting higher molecular weight materials to be separated without

This book belongs to Bradley Loren (bloren@mcandrews-ip.com) Copyright Elsevier 2024

Intas Exhibit 1032
Page 450 of 470
PGR2025-00043

excessive retention. Liquid chromatography is therefore used to separate liquid or solid mixtures of higher boiling point than those in GC, though there is some overlap in the ranges of molecular weight appropriate to each method. LC is the preferred method also for heat-sensitive materials because the advantage of lower retention allows operation at lower temperatures. Room temperature is often used and precise temperature control is not as important as in GC.

Unlike GC, LC requires no vaporiser to inject the materials to be separated into the mobile phase. Low energy consumption is often advanced as a virtue of LC., although the overall energy consumption in LC may be at least as high as in GC if the eluted components have to be separated from the mobile phase itself. This separation is usually achieved by evaporation or distillation, taking advantage of the normally large difference in volatility between the solute and mobile phase, which is frequently an organic solvent or water. The solvent must be of very high purity and completely free of non-volatile residues in order to avoid contaminating the product.

19.4.2. Gas chromatography (GC)

The principal types of chromatography involved in large-scale separations are summarised in Table 19.2, and some explanatory comments are pertinent.

Gas chromatography (GC) employs a gaseous mobile phase, known as the *carrier gas*. In *gas–liquid chromatography* (GLC) the stationary phase is a liquid held on the surface and in the pores of a nominally inert solid support. By far the most commonly used support is diatomaceous silica, in the form of pink crushed firebrick, white diatomite filter aids or proprietary variants. Typical surface areas of 0.5–4 m^2/g give an equivalent film thickness of 0.05–1 μm for normal liquid/support loadings of 5–50 per cent by mass.

In *gas–solid chromatography* (GSC) the stationary phase is a solid adsorbent, such as silica or alumina. The associated virtues associated therewith, namely, cheapness and longevity, are insufficiently appreciated. The disadvantages, surface heterogeneity and irreproducibility, may be overcome by surface modification or coating with small amounts of liquid to reduce heterogeneity and improve reproducibility[14,15]. Porous polymers, for example polystyrene and divinyl benzene, are also available. Molecular sieves, discussed in Chapter 17, are used mainly to separate permanent gases.

19.4.3. Liquid chromatography (LC)

Many forms of liquid chromatography have been developed in order to separate different types of compound, as shown in Table 19.2.

Bonded-phase chromatography (BPC) is an improved form of the now virtually extinct liquid–liquid chromatography. The problem of mutual dissolution of the two liquid phases, and hence progressive loss of stationary phase during service, is solved by chemically bonding the stationary liquid as a monomolecular layer to the surface of a solid support. The support is usually silica gel, a porous, amorphous, rigid solid form of silica. Surface areas are 200–800 m^2/g and average pore diameters are 5–25 nm. BPC exists in two forms. In *normal-phase* BPC the mobile phase is less polar than the stationary phase. The stationary phase is a polar-bonded organic which brings about retention of moderately to

This book belongs to Bradley Loren (bloren@mcandrews-ip.com) Copyright Elsevier 2024

Intas Exhibit 1032
Page 451 of 470
PGR2025-00043

This book belongs to Bradley Loren (bloren@mcandrews-ip.com)

Table 19.2. Main types of chromatography for large-scale separation

	Name	Mobile phase	Stationary phase	Materials separated
Gas chromatography (GC)	Gas–Liquid (GLC)	Gas, e.g. N_2, H_2, He	Liquid-film coated on solid support	Gases and adequately volatile liquids (mol. wt. <300) of adequate thermal stability, e.g. hydrocarbons and their derivatives, solvents, inorganic gases, essential oils, some steroids and vitamins.
	Gas–Solid (GSC)	Gas, e.g. N_2, H_2, He	Solid adsorbent, e.g. alumina	
Liquid chromatography (LC)	Normal bonded phase (NP-BPC)	Nonpolar or slightly polar solvent, e.g. heptane/ dichloromethane	Polar organic group, usually monolayer, e.g. $-C_2H_4CN$, chemically bonded to silica surface.	Almost every possible type of nonionic compound of mol. wt. 100–3000, and many synthetic or biopolymers of higher mol. wt. Some forms of RP-BPC suitable for ionic compounds.
	Reverse bonded phase (RP-BPC)	Polar solvents, e.g. water/ methanol, acetonitrile.	Nonpolar (sometimes polar) organic moiety, usually monolayer, e.g. n-C_8, n-C_{18}, chemically bonded to silica surface.	
	Liquid–solid (LSC) (adsorption)	Polar or nonpolar solvent	Solid adsorbent, usually silica or alumina.	
	Ion-exchange (IEC)	Aqueous buffer or salt solution, sometimes with organic solvent modifier.	Organic polymer (e.g. poly-styrene-divinylbenzene) surface derivatised with ionic functional groups. (See also Section 19.6.2).	Organic or inorganic ions, e.g. rare earth elements, pharmaceuticals, amino acids, peptides, nucleic acids, proteins. Saccharides.
	Size exclusion (SEC) (gel permeation GPC)	Organic or aqueous	Porous gels of silica, synthetic polymers or biopolymers with exclusion limits from 10^2 upto 10^8	Mainly synthetic and biopolymers of mol.wt >2000, but also smaller molecules.
	Affinity (AC)	Aqueous, usually buffered	Specific affine ligand bonded to support matrix. (See also Section 19.6.2).	Proteins (enzymes, antibodies, antigens, lectins), peptides, nucleic acids, oligonucleotides, viruses, cells.
	Hydrophobic interaction (HIC)	Aqueous, usually buffered	Apolar ligand (e.g. octylamino) bonded to support matrix. A form of AC: ligand complexes with apolar (hydrocarbon) sites on protein solute.	Usually proteins.
Supercritical fluid chromatography (SFC)		Supercritical fluid, e.g. CO_2	Liquid film coated on solid support; solid adsorbent; or bonded phase.	Materials of mol. wt. overlapping with both GC and LC.
Chiral chromatography (form of GC, LC or SFC)		Gas, liquid or supercritical fluid	Chiral stationary phase (GC, LC and SFC); or nonchiral stat. phase with chiral eluent (in LC)	Racemates are separated into their enantionomers.

Copyright Elsevier 2024

Intas Exhibit 1032
Page 452 of 470
PGR2025-00043

strongly polar solutes. In *reverse-phase* BPC, the mobile phase is more polar than the stationary phase, which retains a great variety of solutes less polar than in the normal phase mode. Because of the cheapness and versatility of the often water-based mobile phase, the reverse-phase technique is now dominant amongst analytical and preparative LC methods. In larger scale separations, the superior and milder surface chemistry of reverse-phase BPC may need to be balanced against the even cheaper *liquid–solid (adsorption) chromatography* (LSC) packings.

The other LC techniques listed in Table 19.2 rely on mechanisms other than solution, and simple adsorption and need more explanation.

Ion-exchange chromatography (IEC) is carried out with packings that possess charge-bearing functional groups. The most common retention mechanism is simple ion-exchange of solute ions X and mobile phase ions Y with the charged groups R of the stationary phase:

$$X^- + R^+Y^- = Y^- + R^+X^- \quad \text{(anion exchange)}$$

$$X^+ + R^-Y^+ = Y^+ + R^-X^+ \quad \text{(cation exchange)}$$

Solute ions X that compete weakly with mobile phase eluent ions Y for ion exchanger sites R will be retained only slightly on the column. Solute ions that interact strongly with the ion-exchanger elute later in the chromatogram.

The ion-exchangers used in LC consist either of an organic polymer with ionic functional groups, or silica coated with an organic polymer with ionic functional groups. The types of functional groups used are the same as described in Chapter 18. Since IEC can be carried out with an aqueous mobile phase near physiological conditions, it is an important technique in the purification of sensitive biomolecules such as proteins.

Size exclusion or *gel permeation chromatography* (SEC, GPC) differs from all other methods in separating according to molecular size, rather than structural characteristics such as functional groups. The particulate packing contains pores of well-defined size. Solute molecules, too large to enter the pores, are totally excluded from the interior of the particles and elute first. Their molecular weights are said to exceed the *exclusion limit*. Smaller molecules permeate the particles to a varying extent, depending on molecular size, and are retained to varying extents in order of size. The technique is complementary to other methods which separate on the basis of molecular structural difference. SEC is often the first step in the resolution of a complex mixture by more than one LC method.

Affinity chromatography depends on the specific adsorption which results from molecular "recognition". The "lock-and-key" mechanism shown in Figure 19.4 involves a number of co-operating interactions within regions of high complementarity on two molecules. One of the two molecules is chemically bonded to the support *matrix* and forms the *ligand*. The other molecule is then the *ligate*, that is the solute subjected to chromatography. Because the adsorption complex results from a multisite mechanism, the interaction is very specific to the two molecular species concerned. *Bio-affinity chromatography* uses the variety of such complexes that occur in biological systems, for example, antibody–antigen, enzyme–inhibitor, enzyme–cofactor and hormone–receptor complexes, and specific base sequences for binding nucleic acids. In each case either component of the pair may be bound to the matrix in order to chromatograph the other. The principle of affinity chromatography is not restricted to purely biological *ligands*;

This book belongs to Bradley Loren (bloren@mcandrews-ip.com) Copyright Elsevier 2024

Intas Exhibit 1032
Page 453 of 470
PGR2025-00043

synthetic ligands, which are usually less *group-specific*, may be dyes, metal chelates or electron donors or acceptors[16]. All of these techniques have been almost exclusively applied to biological *ligates* (Table 19.2).

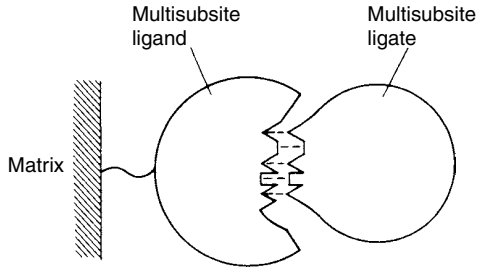


Figure 19.4. Principle of molecular recognition used in affinity chromatography[17]

19.4.4. Supercritical fluid chromatography (SFC)

Supercritical fluid chromatography (SFC) is intermediate between GC and LC. The mobile phase is a supercritical fluid, usually carbon dioxide at near ambient temperatures. As with LC, SFC is suitable for separating higher molecular weight materials than GC, and the low operating temperature is advantageous for heat-sensitive materials, as in LC. SFC separations, however, may be performed two or three times faster than LC because materials have higher diffusivities in a supercritical fluid than in a liquid, and so suffer less band-broadening from the effect of the $C_m u$ term in equation 19.10 and Table 19.1. A supercritical fluid may readily be separated from the required products merely by reducing the pressure, avoiding the costs of the mobile phase separation that are a main disadvantage of LC. Carbon dioxide is a particularly attractive mobile phase for large-scale separations because it is non-toxic, environmentally acceptable and cheap, and has a very convenient temperature and pressure at its critical point. Pure carbon dioxide is a non-polar mobile phase of low solvating power, however, and exclusive reliance on it has restricted SFC to niche applications involving a rather narrow range of low polarity compounds. This position now appears to be changing as a result, in part, of mixing polar organic solvents with carbon dioxide in the mobile phase. The applications of SFC may soon expand to match those of its more-established relative, supercritical fluid extraction, as discussed in Section 13.8.1[18–21].

19.4.5. Chiral chromatography

The optical activity of biologically-active chemicals is important to their activity and toxicology. Pure enantiomers, or optical isomers, of pharmaceuticals and agrochemicals can in many cases be made by enantiospecific synthesis. An alternative method is to use a less complicated synthesis followed by chromatographic resolution of the racemic mixture into its enantiomers.

This book belongs to Bradley Loren (bloren@mcandrews-ip.com) Copyright Elsevier 2024

Intas Exhibit 1032
Page 454 of 470
PGR2025-00043

Since all the physical properties of two given enantiomers are the same in the absence of a chiral, or optically active, medium, their chromatographic resolution needs a different approach from the relatively simple separation of geometrical isomers, stereoisomers or positional isomers. Two methods are used. The older technique of *indirect resolution*, requires conversion of the enantiomers to diastereoisomers using a suitable chiral reagent, followed by separation of the diastereoisomers on a non-chiral GC or LC stationary phase. This technique has now been largely superseded by *direct resolution*, using either a chiral mobile phase (in LC) or a chiral stationary phase. A variety of types of chiral stationary phase have been developed for use in GC, LC and SFC[21−23].

19.5. LARGE–SCALE ELUTION (CYCLIC BATCH) CHROMATOGRAPHY

19.5.1. Introduction

The three main modes of chromatographic operation are elution chromatography, selective adsorption/desorption, and simulated countercurrent chromatography. Of these, elution chromatography, used as a cyclic batch process, was the first to be developed for large-scale separations.

The distinction between preparative and production chromatography is sometimes drawn in terms of the scale of operation though it is really a matter of purpose. The term *preparative chromatography* is used to refer to the technical preparation of limited quantities of material in the laboratory, and *production chromatography* to continuous production for commercial purposes, where economics are important. The two are compared in Table 19.3.

Table 19.3. Comparison of production, preparative and analytical chromatography

		Production	Preparative	Analytical
Performance criteria and basis for design		Product cost, that is throughput (cost/yr.), for specified purity	Throughput for specified purity, or simple diameter scale-up of known analytical separation	Resolution and speed of analysis
Processing rate	GC	0.1–1.5 kg/h (100 mm dia.) 1–15 kg/h (300 mm dia.)	0.1 g–1 kg batch	—
	LC	0.02–0.3 kg/h (100 mm dia.) 0.2–3.0 kg/h (300 mm dia.)	0.01 g–0.2 kg batch	—
Column diameter	GC	>80 mm	5–120 mm	0.1–5 mm
	LC	>30 mm	3–40 mm	0.3–5 mm
Column length	GC	1–8 m	0.6–8 m	>0.5 m
	LC	0.2–2 m	0.1–2 m	>0.03 m
Particle size	GC	150–500 μm	100–400 μm	80–250 μm
	LC*	20–70 μm	8–60 μm	3–8 μm

* Except LC of proteins, etc. which are 30–300 μm.

Since elution is basically a batch technique, continuous production requires cyclic batch operation under automatic control. This is achieved, first, by using repetitive automatic

This book belongs to Bradley Loren (bloren@mcandrews-ip.com) Copyright Elsevier 2024

injection of successive batches of the mixture to be separated and, secondly, by recycling the mobile phase, unless this is water or carbon dioxide.

19.5.2. Gas chromatography equipment

Figure 19.5 shows the general flow scheme of a production gas-chromatograph. The *carrier gas* (mobile phase) which is normally nitrogen, hydrogen or helium flows continuously. The feed mixture to be separated is vaporised and periodically injected into the gas stream. The duration of the injection period is usually 10–180 s. The feed band entering the column then has a rectangular concentration–time profile and is far larger in both duration and concentration than in analytical chromatography. As the separated fractions elute from the column, they are passed in turn to individual fraction collectors controlled by appropriate valve sequencing. Here they are condensed by cooling and any aerosol formed is trapped. The carrier gas is completely cleaned of traces of solute by passage through a packed bed of molecular sieve or activated carbon, recompressed to a pressure of, typically, 2–6 bar (200–600 kN/m^2) and recycled.

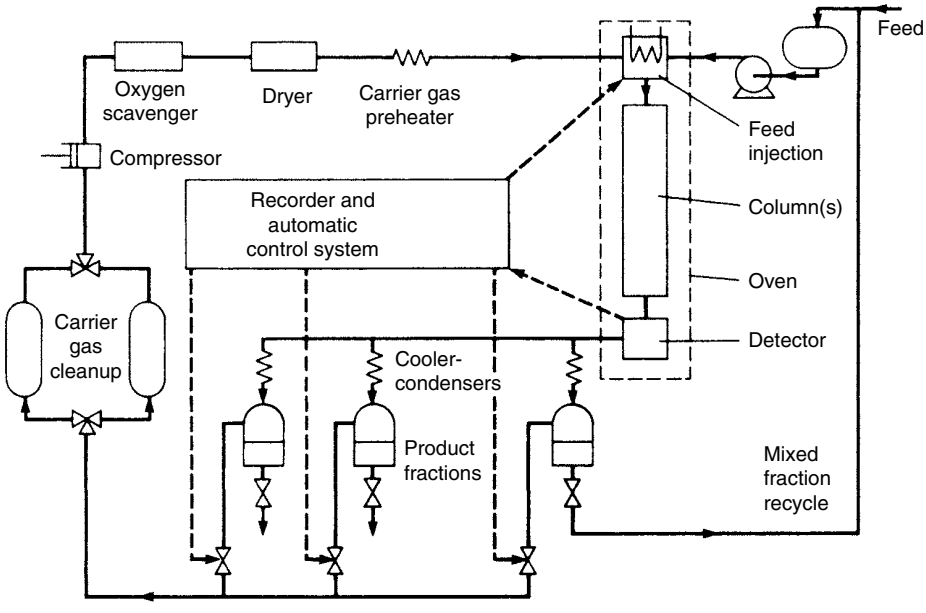


Figure 19.5. Production gas-chromatograph

The duration of the injection is a substantial fraction of the cycle time. An effective technique, therefore, is to run the feed vaporiser continuously and to direct the vapour/carrier mixture to one of, say, 2–5 parallel columns in sequence[24–26].

Production experience with large-scale gas-chromatography has been accumulated mainly since the mid-1970s, with columns up to about 400 mm diameter and throughputs

This book belongs to Bradley Loren (bloren@mcandrews-ip.com) Copyright Elsevier 2024

Intas Exhibit 1032
Page 456 of 470
PGR2025-00043

up to about 100 tonne/yr, separating a variety of organic compounds[12,27−32]. These developments have been summarised elsewhere[33]. Several detailed descriptions have been given of equipment of various sizes[12,26,34−36]. There are many preparative chromatographs on the market and one company has offered production units with column diameters up to 600 mm[32,37]. For a 400 mm unit total production costs (capitalised plus direct operating costs) were projected in 1987 as £3.5/kg for a production rate of 10 kg/h[32]. Elf Aquitaine has devised an interesting process using a molecular sieve as stationary phase to separate 100,000 tonne/year of a light naphtha into an *n*-paraffin product that may be used as a petroleum feedstock and a high octane fraction, rich in *iso*-paraffins, for use in lead-free petrol[38].

19.5.3. Liquid chromatography equipment

Very large LC columns up to 1.2 m in diameter have been used on occasion since the 1940s. These were low pressure units with very large packing particles and were therefore relatively slow and inefficient. The use of smaller particles and higher velocities, both requiring large column pressure differences (40–400 bar), has been a key factor in the development of modern HPLC since 1967 (Section 19.3.2.) The other two factors were improved stationary phases (Section 19.4.3) and better detectors.

Since about 1977 an increasing number of manufacturers have been marketing production and preparative units based on HPLC methodology, with diameters now up to 600 mm and even, in one case, 2 m. By using pressures over 10 bar, these units can operate with relatively small particles in the size range 10–70 μm. This is larger than the 3–8 μm particles of analytical HPLC, not only because of pressure limitations in large diameter columns (a stainless steel column of 400 mm diameter with a wall thickness of 200 mm can withstand little more than 100 bar), but also because of loss of column efficiency associated with fluid frictional heating in fine packing interstices[39]. For these reasons the particle size should be not less than about 20 μm in columns over 100 mm diameter[39,40], although the optimum size is still a matter of discussion.

Particle size also determines the technique used in packing the column. Rigid particles larger than 25 μm may be packed dry, as in GC. Smaller particles tend to clump if dry-packed and need to be packed suspended as a liquid slurry under high pressure. Over 30 mm in diameter require physical compression at least when packing, and preferably during operation, to create and maintain a compact, uniform bed free of voids, having good efficiency. Various patented axial or radial bed compression systems are in use in commercial equipment, as shown, for example, in Figure 19.6.

The general flow scheme of a production liquid chromatograph is similar to that of the corresponding GC unit, shown in Figure 19.5, with four main differences. First, thermostatting requirements for the column are less strict, and may sometimes even be dispensed with. Secondly, the feed is injected as a liquid, and not vaporised. Thirdly, if the product is to be separated from the mobile-phase solvent, distillation or evaporation and solvent recycle are incorporated in the loop[28,41,42]. Finally, the liquid streams are filtered to ensure column longevity, and de-aerated to prevent air bubbles forming.

Commercial LC units, available from a number of manufacturers, have been surveyed[39]. Some of the largest scale applications are summarised by WANKAT[43]

This book belongs to Bradley Loren (bloren@mcandrews-ip.com) Copyright Elsevier 2024

Intas Exhibit 1032
Page 457 of 470
PGR2025-00043



Figure 19.6. Stainless steel columns for liquid chromatography[37]. Two are 450 mm dia., one 150 mm dia. and two 110 mm dia. Pressure rating 70 bar. The devices below each column permit axial bed compression by piston

and many more applications exist for pharmaceuticals, biochemicals, fine chemicals and industrial chemicals. Production costs were estimated in 1987 at £20–170/kg for production rates of 0.06–2.3 kg/h in 150–450 mm diameter columns[44].

19.5.4. Process design and optimisation

The design of a production chromatograph is a complex exercise because of the many process variables involved. Some of the published work on optimisation proceeds from the unsatisfactory notion that a large-scale chromatograph is little more than a scaled-up analytical one into which large samples are injected. Thus the sample size is commonly chosen as the largest which does not excessively degrade resolution.

This book belongs to Bradley Loren (bloren@mcandrews-ip.com) Copyright Elsevier 2024

While this approach simplifies scale-up in preparative work, it does not lead to optimum large scale performance, especially when production economics are taken into account. The best criteria of performance for design purposes are, in preparative applications, the throughput for a specified product purity and, in production applications, the product cost, that is (throughput)/(processing cost per unit time), for a specified product purity[28,45−47]. On this basis it may be shown that performance is improved, first, by controlling the feed band-width and concentration independently and, secondly, by injecting much wider bands than used in analysis and restricting the column length so that the feed components are incompletely resolved at the column outlet; the mixed (overlapping) fractions are then recycled to the feedstock[47,48]. The method is illustrated in Figure 19.7.

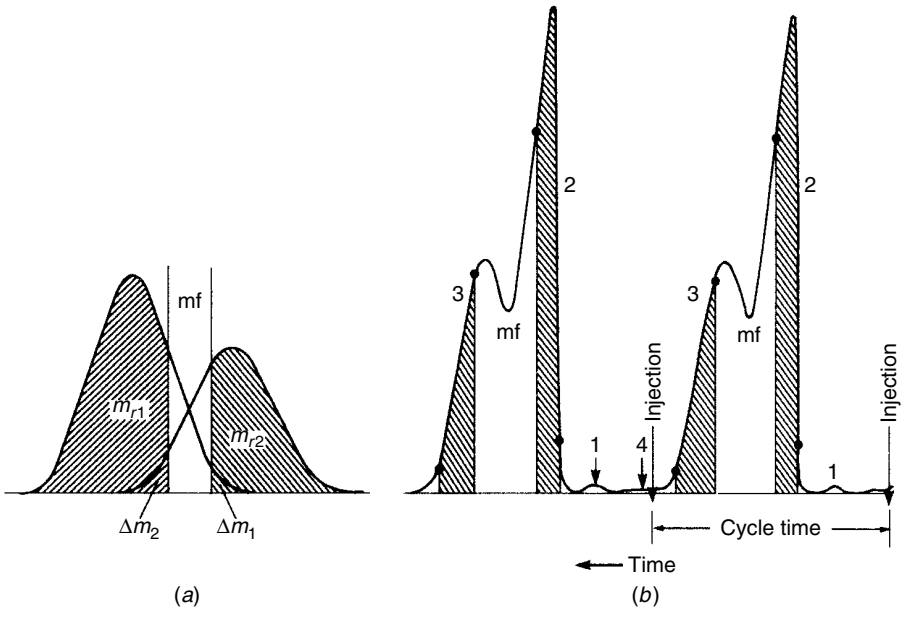


Figure 19.7. Cyclic batch elution chromatography: obtaining high product purity and high throughput by using incomplete resolution (overlapping bands) and recycling the mixed fraction (mf) to the feedstock (*a*) Control of band separation and cut points determines fractional impurities $\Delta m_2/m_{r1}$ and $\Delta m_1/m_{r2}$.[49] (*b*) Chromatogram for separation of pure cis- and trans- 1,3-pentadiene. Components: 1, isoprene; 2, trans- 1,3-pentadiene; 3, cis-1,3-pentadiene; 4, cyclo-pentadiene. Component 1 is eluted at almost the same time as component 4 of the previous injection[12]

Information on process design and optimisation is available in the literature already cited and in references for GC[49−50] and for LC[42,51−57]. The flow chart for design calculations shown in Figure 19.8 demonstrates the large number of variables involved and the relations between them. The problem of maintaining column efficiency as the column diameter increases, once a major difficulty in scale-up, is now generally regarded as solved by using a narrow particle-size range, good packing technique and efficient distributors[12,32,33,51].

This book belongs to Bradley Loren (bloren@mcandrews-ip.com) Copyright Elsevier 2024
Intas Exhibit 1032
Page 459 of 470
PGR2025-00043

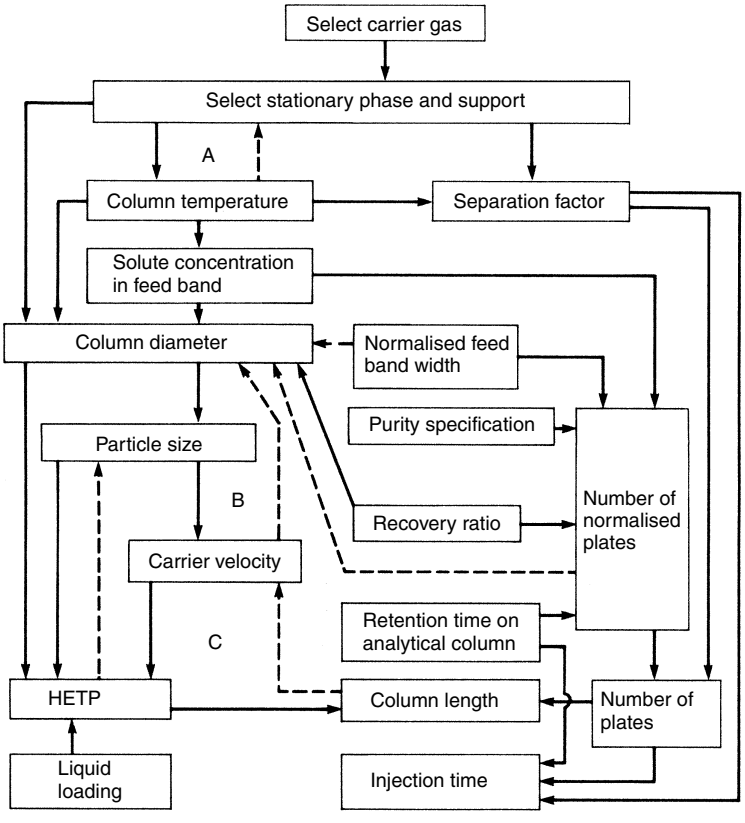


Figure 19.8. Flow chart for design of production and preparative gas chromatographs[13]. Feedback is shown by broken lines. A, B and C are principal calculation loops

19.6. SELECTIVE ADSORPTION OF PROTEINS

Chromatography is now an integral and indispensable part of the biotechnology industry. Most regulatory authorities expect at least one chromatographic step to be used in producing a protein-based pharmaceutical. Other techniques cannot provide the purity levels now required, which may sometimes reach 99.999 per cent. Moreover, other techniques, such as fractional precipitation, electrophoresis, isoelectric focusing and ultrafiltration, involve heat generation or strong shear forces. Chromatography usually permits milder processing conditions close to physiological, so avoiding denaturation, the unfolding of the protein molecule, and retaining biological activity.

19.6.1. Principles

Although elution chromatography is an efficient technique for resolving most mixtures, it is less appropriate for biological macromolecules such as proteins and nucleic acids.

This book belongs to Bradley Loren (bloren@mcandrews-ip.com) Copyright Elsevier 2024

Proteins contain a variety of functional groups and interact with the stationary phase at a number of simultaneous sites on the protein molecule, each more or less affected by change in *eluent*, or mobile-phase, pH or ionic strength. The equilibrium constant for the dissociation of the adsorption complex thus contains a product of many eluent-sensitive concentration terms, and the equilibrium position is very sensitive to elution conditions. Under the elution conditions, some proteins in a mixture may be tightly bound by the stationary phase ($t'_R \to \infty$) while others are unretained ($t'_R \approx 0$). Differential migration (Section 19.2.1) is replaced by extreme retention values.

This very large selectivity or relative retention, makes normal *isocratic elution* (constant eluent composition) inappropriate. Instead, *gradient elution* or stepwise elution are used. The eluent pH or ionic strength is changed either in a continuous gradient or in a series of steps to desorb and so elute one protein, or group of proteins, at a time. An example of stepwise elution is shown in Figure 19.9.

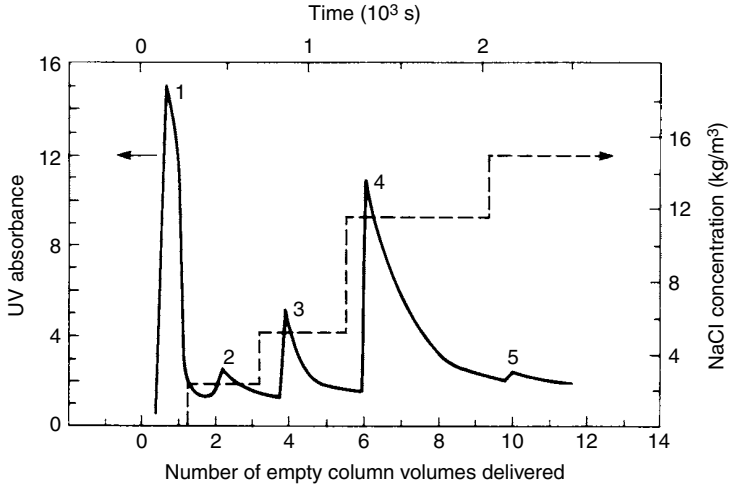


Figure 19.9. Chromatogram for stepwise elution of bovine serum albumin on a Vistec diethyl aminoethyl cellulose ion-exchanger, using stepwise increases in sodium chloride concentration in the mobile phase to achieve selective desorption. Proteins: 1, serum fraction not adsorbed by column (includes γ-gobulin); 2,3, transferrin, and so on; 4,5 albumin[57]

For large-scale separations, a further operational change is commonly adopted. Maximum production requires that the width of the protein band fed to the column be increased so that protein is adsorbed on the whole of the column packing before desorption[58]. The procedure is then essentially the same as the adsorption–desorption techniques described in Chapter 17, where both adsorption and desorption are pursued to breakthrough[59]. This procedure may be termed *selective adsorption* or *desorption* to distinguish it from elution, or differential migration. Although in principle a form of adsorption, the procedure is usually regarded as a form of chromatography because it uses the high-selectivity technology of the latter.

Affinity chromatography is conducted in the selective-adsorption mode, whereas ion-exchange chromatography is usually carried out in the selective-desorption mode. The

This book belongs to Bradley Loren (bloren@mcandrews-ip.com) Copyright Elsevier 2024
Intas Exhibit 1032
Page 461 of 470
PGR2025-00043

reason is that affinity chromatography, being the more highly selective, normally relies on specificity in the adsorption step. Ion-exchange chromatography usually gives a multi-component adsorption which is resolved in the desorption step. Both procedures involve a cyclic batch process. Various aspects of the process have been analysed theoretically and optimised[59−63].

19.6.2. Practice

Large-scale separation of proteins may be carried out by *ion-exchange* (IEC), *affinity* (AC), *hydrophobic-interaction, size-exclusion* or *reverse-bonded-phase* (RP-BPC) chromatography, as given in Table 19.2. Whereas IEC and AC are best conducted in the selective-adsorption or desorption mode of operation, RP-BPC and SEC are conducted in the elution mode, often by gradient elution. RP-BPC has the disadvantages that the organic solvents often added to the aqueous eluent tend to denature proteins, and that the silica in the bonded-phase packing is chemically stable only at pH of 2–8.

Protein separations by IEC, AC and SEC differ from other separations in using soft polysaccharide-gel packings. Agarose, dextran and cellulose have the desired properties of hydrophilicity, to avoid denaturation, and large pore size, to permit access of the large protein molecules to the high interior surface area, but are soft and will not tolerate high pressure drops across the column. Particle sizes are therefore commonly quite large, and usually 30–300 μm. Improved, more rigid, supports are now widely available[64,65].

Chromatography is currently used in the downstream processing, or bioseparation, of biological macromolecules produced both from natural sources, such as albumin and various factors from blood plasma, and by biotechnology, as with monoclonal antibodies and recombinant DNA products like interferons, insulin, vaccines, growth hormones and tissue plasminogen activator. Downstream processing, which can account for 50–80 per cent of total production costs, involves integrated product separation and recovery trains[66,67]. Frequently both IEC, AC and SEC steps are included. Two examples are shown in Figure 19.10. In this context, one advantage of IEC and AC is that they can effect concentration from dilute solution at the same time as separation. This results from tight binding in the adsorption stage, coupled with freedom to control concentration in the desorption stage.

19.6.3. Expanded bed adsorption

A recent innovation in downstream processing is to use an expanded bed for adsorption. An expanded bed occurs over a narrow range of flow velocity, and is intermediate between a fixed bed and a fluidised bed. It resembles a fluidised bed in having a greater voidage than a fixed bed. This has the great advantage that crude, particulate-containing feedstocks will pass through the expanded bed without the suspended solids causing the blockages that would normally result with a packed bed. Proteins, for example, may be removed from fermentation broths and preparations of disrupted cells by adsorption in an expanded bed of a suitable adsorbent. After washing, the flow velocity is reduced so that the adsorbent settles into a fixed bed, and the proteins are recovered by changing the eluent, or mobile phase, composition. This technique can simplify downstream processing by replacing the

This book belongs to Bradley Loren (bloren@mcandrews-ip.com) Copyright Elsevier 2024

Intas Exhibit 1032
Page 462 of 470
PGR2025-00043

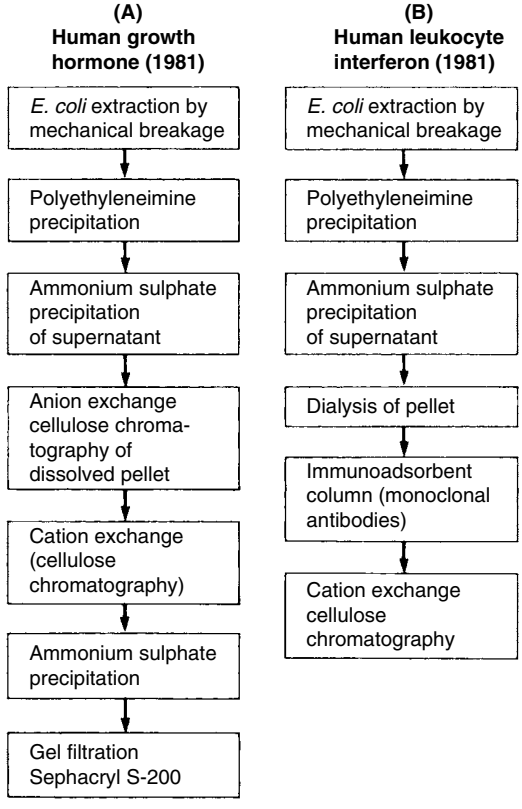


Figure 19.10. Summary of purification processes for two human proteins synthesised in recombinant *E. coli*[68]. The term gel filtration is sometimes used as an alternative to size-exclusion chromatography

early filtration, centrifugation and concentration steps with a single process. An expanded bed is preferred to a fully fluidised bed in this application because it suffers less bed-wide axial mixing, especially if suitable steps are taken to stabilise the bed in order to reduce axial mixing. A stable expanded bed resembles a fixed bed in providing many theoretical plates to the incoming protein which is thereby captured efficiently. The technique is variously called *expanded-bed adsorption* and *expanded-bed chromatography*[69].

19.7. SIMULATED COUNTERCURRENT TECHNIQUES

The preference for operating processes continuously wherever possible has led to the development of alternative modes of operation to cyclic-batch elution-chromatography and selective adsorption/desorption. There are several truly continuous modes, such as so-called *countercurrent chromatography* (CCC) using centrifugal fields[70], the continuous rotating annulus[71] and cross-flow devices[71]. These have recently seen extensive development at the preparative scale though not yet at larger scales. The production scale,

This book belongs to Bradley Loren (bloren@mcandrews-ip.com) Copyright Elsevier 2024

Intas Exhibit 1032
Page 463 of 470
PGR2025-00043

however, is now well established in pseudo-continuous schemes which use a simulated moving-bed for countercurrent operation. In these, the solid or liquid "stationary phase" is in effect a moving bed flowing countercurrently to the liquid or gaseous "mobile phase". The feed mixture to be separated is fed continuously to a point in the middle of the column. The ratio of the flowrates of the two phases is chosen so that the feed splits into two fractions moving in opposite directions from the feed point. The basic principle of these moving-bed schemes has been described in Section 17.9, as shown in Figure 17.31.

The original moving-bed process was the *hypersorber*, described in Section 17.9.2. This is no longer used due to problems of solids-attrition and high rates of axial mixing[43,71]. These problems are nowadays avoided by simulating the movement of the bed using a fixed bed, and periodically moving the positions of entrance and exit of the process streams. The process is thus periodical rather than truly continuous.

The two main forms of simulated countercurrent/moving-bed processes are *Simulated Moving Bed Chromatography* (SMB) and the *Semi-Continuous Chromatographic Refiner* (SCCR). Both are now well established industrially, with at least 227 SMB trains of units world-wide by 2000. These are well suited to large-scale separation of simple binary mixtures where the purity requirements for the product are high, but not so demanding as to warrant use of elution chromatography or selective adsorption. Examples include the separation of xylenes, sugars and pharmaceutical enantiomers.

The SMB process was invented by Broughton in 1961 and developed by Universal Oil Products under the general name "Sorbex". Initially used for separating *n*-paraffins in bulk, it is now used for a variety of individual-isomer separations and class separations, and is currently attracting considerable interest for separating pharmaceutical enantiomers. The SMB process is described in Section 17.9.4 and in a growing literature[21,22,71–74].

The *Semi-Continuous Chromatographic Refiner* (SCCR), developed by Ganetsos and Barker[71], uses an array of twelve column sections (each, for example, 76 mm i.d. × 610 mm long) mounted in a circle. The column sections are connected in series (at top and bottom alternately) to form a closed loop (12×0.61 m $= 7.32$ m long). The loop is shown diagrammatically in Figure 19.11. Valved inlet and outlet ports are provided at top and bottom of each column section. The array is fixed, but countercurrent operation is simulated by periodically shifting the five process stream ports and the carrier fluid locks to the next adjacent column sections in one direction, the same as for fluid flow, round the array. This simulates bed movement in the opposite direction. The rate of port advancement is less than the velocity of the less strongly adsorbed component 1 through the bed, but greater than that of the more strongly adsorbed component 2. The components are therefore collected at ports at opposite "ends" of the loop.

Compared with elution chromatography, the advantage of both the SMB and SCCR forms of simulated countercurrent operation is that each product is taken off as soon as it is separated. The disadvantages are mechanical complexity and the fact that the number of pure products readily obtainable from one column is limited to two at most. Elution chromatography allows many components to be separated on one column. If no components are taken off before reaching the column exit, however, any components that are much more easily separated than the key components occupy space in

This book belongs to Bradley Loren (bloren@mcandrews-ip.com) Copyright Elsevier 2024

Intas Exhibit 1032
Page 464 of 470
PGR2025-00043

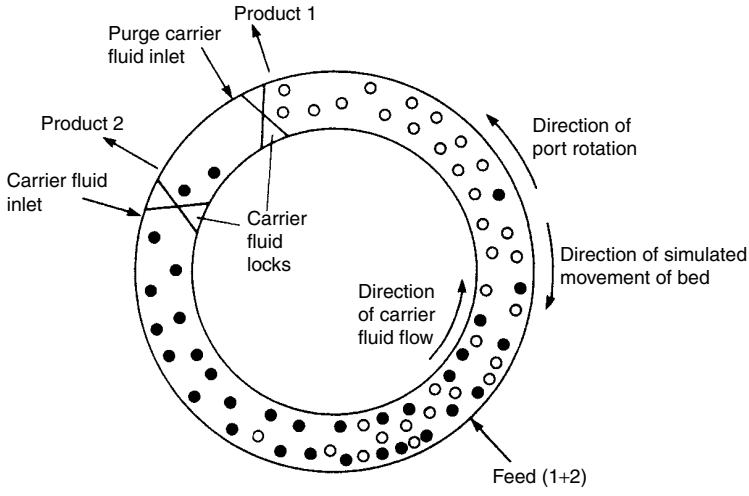


Figure 19.11. Diagrammatic representation of the principle of operation of a *Semi-Continuous Chromatographic Refiner*[75]. Open and closed circles show schematically the concentrations of the two components being separated. The distance from feed point to product 1 offtake and from feed point to carrier fluid inlet must be sufficient to allow the required purity levels to be achieved against the usual band-spreading process

the column, even after they have separated, and so raise the cycle time between injections and reduce throughput. This often-cited problem of elution chromatography may be overcome either by using column-switching methods[43] or by adopting window-diagram techniques. The latter permit the compositions of mixed stationary or mixed mobile phases to be chosen to optimise band spacing in the elution sequence[76]. Either approach allows the whole column to be engaged in separation at all times, as in simulated countercurrent operation.

19.8. COMBINED REACTION AND SEPARATION

When chemical reactions are carried out in chromatographic columns, reaction and separation occur simultaneously. The immediate advantages of combining these processes in a single column are that the reaction products are obtained in high purity, and both the capital and energy costs of the process can be lower than when the operations are conducted separately. A more subtle but important advantage is that, when the reaction is equilibrium-limited, much higher conversions than the equilibrium values can be achieved. If the reaction is of the type $\mathbf{A} \rightleftharpoons \mathbf{B} + \mathbf{C}$, on-column separation of **B** and **C** prevents the reverse reaction, so that **A** can be converted entirely into $\mathbf{B} + \mathbf{C}$.

Several types of reaction may be carried out in a chromatographic reactor. The reaction can be chemical or biochemical, taking place on the stationary phase, in the mobile phase, or both. The stationary phase must be chosen to have a good retention (affinity) for at least one component of the reaction system, and in some cases it has to act as a catalyst or catalyst support. Chromatographic reactors are particularly suited to enzyme-catalysed reactions such as the inversion of sucrose and biosynthesis of dextran, to various

This book belongs to Bradley Loren (bloren@mcandrews-ip.com) Copyright Elsevier 2024

Intas Exhibit 1032
Page 465 of 470
PGR2025-00043

dissociation, isomer-interconversion and catalytic-cracking reactions, and to the selective production of intermediate species in reaction sequences, or where side reactions would otherwise interfere with production. Both elution-chromatography and simulated-moving-bed modes of operation are employed and have been extensively analysed[71,77,78].

19.9. COMPARISON WITH OTHER SEPARATION METHODS

In general, chromatography is a powerful but relatively expensive separation technique whose advantages and disadvantages need to be evaluated carefully in selecting a separation system. The expense arises chiefly from the packings and the need in many cases to recycle the mobile phase. GLC and some LC and SFC packings need occasional replacement. Published cost data are as yet limited.

The most obvious virtue of chromatographic methods is their great separating power. This results from the very small plate height and the enhanced relative volatility permitted by adding a third component, the stationary phase, to the mixture to be separated, as discussed in Section 19.3.4. Thus, gas chromatography employs columns typically an order of magnitude shorter than those required for the same separation by distillation[79]. On the other hand, GC throughputs are much less than in distillation for the same column diameter, unless the separation is difficult (low relative volatility), in which case the throughput in distillation is reduced by the need for a high reflux ratio. Overall, the balance of advantage probably lies with GC for difficult separations where the relative volatility, before enhancement with stationary phase, is less than about 1.2, while distillation is to be preferred when it is greater than 1.6. Chromatographic methods in general are advantageous for difficult separations and for separations where high product purities are specified.

The same advantages are exhibited by LC in comparison with techniques such as fractional crystallisation, liquid extraction, ultrafiltration and adsorption. It has already been pointed out (Section 19.6) that LC now plays a major part in bioseparations, where the technique needs to be integrated into the process train as part of a systems approach.

In choosing suitable methods to separate a given mixture of compounds, the general characteristics favouring a chromatographic method are:

(a) It can achieve difficult separations, as discussed in Section 19.3.4.
(b) It can meet high product purity specifications[46].
(c) It can separate heat-sensitive compounds (permitted by low residence times and absence of reflux, together with low temperatures in LC and SFC).
(d) It has relatively low energy consumption (cf. distillation).
(e) It can split an n-component mixture into n pure components in one column instead of $(n - 1)$ columns (cf. distillation and other countercurrent processes).
(f) Product is often recovered in a non-toxic carrier or solvent (in GC, SFC, and LC with aqueous mobile phase) from which it is readily separated, if necessary.
(g) The technique is very versatile, and an appropriate type of chromatography may be chosen for most separations.
(h) It is well suited, though not restricted, to low volume, high value separations.

This book belongs to Bradley Loren (bloren@mcandrews-ip.com) Copyright Elsevier 2024

Intas Exhibit 1032
Page 466 of 470
PGR2025-00043

In this chapter the three main modes of large-scale chromatographic operation, and combined reaction and separation. Many useful but small-scale chromatographic methods have been omitted, as well as allied separation techniques which combine aspects of chromatographic principles or practice with aspects of adsorption, extraction, sedimentation or electrophoresis. Such is the pace of invention that novel processes related to chromatography are still being developed and described in the literature.

19.10. FURTHER READING

BRAITHWAITE, A. and SMITH, F. J.: *Chromatographic Methods*, 4th edn. (Chapman and Hall, 1986).

CONDER, J. R., in *New Developments in Gas Chromatography* (ed. Purnell, J. H.) pp. 137–186, Production-Scale Gas Chromatography (Wiley, 1973).

GANETSOS, G. and BARKER, P. E.: *Preparative And Production Scale Chromatography* (Marcel Dekker, 1993)

HAMADA, J. S.: *J. Chromatogr.* **760** (1997) 81. Large-scale high-performance liquid chromatography of enzymes for food applications. (Review)

SKEA, W. M. in *High Performance Liquid Chromatography* (eds. BROWN, P. R. and HARTWICK, R. A.), Chapter 12: Process High Performance Liquid Chromatography (Wiley, 1989).

SNYDER, L. R. and KIRKLAND, J. J.: *Introduction to Modern Liquid Chromatography*, 2nd edn. (Wiley, 1979).

SOFER, G. K. and NYSTRÖM, L. E.: *Process Chromatography* (Academic Press, 1989)

SUBRAMANIAN, G. (ed.): *Preparative and Process-Scale Liquid Chromatography* (Ellis Horwood, 1991)

SUBRAMANIAN, G. (ed.): *Process-Scale Liquid Chromatography* (VCH Verlagsgesellschaft, 1995)

YAMAMOTO, S., NAKANISHI, K. and MATSUNO, R.: *Ion-Exchange Chromatography of Proteins* (Marcel Dekker, 1988). Chapter 9: Large Scale Operation.

19.11. REFERENCES

1. CONDER, J. R. and YOUNG, C. L.: *Physicochemical Measurement by Gas Chromatography* (Wiley, 1979).
2. SYNOVEC, R. E., MOORE, L. K., RENN, C. N. and HANCOCK, D. O.: *Internat. Lab.* (Dec. 1989), 16. New directions in process liquid chromatography.
3. GUIOCHON, G. and GUILLEMIN, C. L.: *Quantitative Gas Chromatography for Laboratory Analysis and On-Line Process Control* (Elsevier, 1988).
4. BAILEY, J. E. and OLLIS, D. F.: *Biochemical Engineering Fundamentals*, 2nd edn. (McGraw-Hill, 1986).
5. LITTLEWOOD, A. B.: *Gas Chromatography*, 2nd edn. (Academic Press, 1970).
6. GLUECKAUF, E.: *Trans. Faraday Soc.* **51** (1955) 34. Theory of chromatography, Part 9: the theoretical plate concept in column separation.
7. MARTIN, A. J. P. and SYNGE, R. L. M.: *Biochem. J.* **35** (1941) 1358. A new form of chromatography employing two liquid phases.
8. PURNELL, J. H.: *Gas Chromatography* (Wiley, 1962).
9. JÖNSSON, J. Å., in *Chromatographic Theory and Basic Principles* (JÖNSSON, J. Å. ed.), Chapter 3, Dispersion and Peak Shapes in Chromatography (Marcel Dekker, 1987).
10. VAN DEEMTER, J. J., ZUIDERWEG, F. J. and KLINKENBERG, A.: *Chem. Eng. Sci.* **5** (1956) 271. Longitudinal diffusion and resistance to mass transfer as causes of nonideality in chromatography.
11. CONDER, J. R. and PURNELL, J. H.: *Chem. Eng. Sci.* **25** (1970) 353. Separation and throughput in production and preparative chromatography.
12. ROZ, B., BONMATI, R., HAGENBACH, G. and VALENTIN, P.: *J. Chromatog. Sci.* **14** (1976) 367. Practical operation of prep-scale gas chromatographic units.
13. CONDER, J. R.: *J. Chromatog.* **256** (1983) 381. Design procedure for preparative and production gas chromatography.
14. PHILLIPS, C. S. G. and SCOTT, C. G., in *Progress in Gas Chromatography* (PURNELL, J. H. ed.), pp. 121–152, Modified Solids for Gas–Solid Chromatography (Wiley, 1968).
15. AL-THAMIR, W. K., LAUB, R. J. and PURNELL, J. H.: *J. Chromatog.* **142** (1977) 3. Gas chromatographic separation of all C_1–C_4 hydrocarbons by multi-substrate gas–solid–liquid chromatography.
16. MOHR, P. and POMMERENING, K.: *Affinity Chromatography* (Marcel Dekker, 1985).
17. PORATH, J.: *J. Chrom.* **218** (1981) 241. Development of modern bioaffinity chromatography.

This book belongs to Bradley Loren (bloren@mcandrews-ip.com) Copyright Elsevier 2024

Intas Exhibit 1032
Page 467 of 470
PGR2025-00043

18. PERRUT, M.: *J. Chromatogr.* **A, 658** (1994) 293. Advances in supercritical fluid chromatographic processes. (Review).
19. JUSFORGUES, P.: In *Process-Scale Liquid Chromatography*, SUBRAMANIAN, G. (ed.) (VCH Verlagsgesellschaft, 1995) Chapter 7. Separation in large scale industrial supercritical fluid chromatography.
20. BEVAN, C. D., MELLISH, C. J.: In *Process-Scale Liquid Chromatography*, SUBRAMANIAN, G. (ed.) (VCH Verlagsgesellschaft, 1995) Chapter. 8. Scaling-up of supercritical fluid chromatography to large-scale applications.
21. SCHULTE, M. and STRUBE, J.: *J. Chromatogr*. **A, 906** (2001) 399. Preparative enantioseparation by simulated moving bed chromatography.
22. FRANCOTTE, E.: *J. Chromatogr*. **A, 906** (2001) 379. Enantioselective chromatography as a powerful alternative for the preparation of drug enantiomers.
23. WHITE, C. A.: In *Preparative and Process-Scale Liquid Chromatography*, SUBRAMANIAN, G. (ed.) (Ellis Horwood, 1991) Chapter 13. An Introduction to large-scale enantioseparation.
24. RENDELL, M.: *Process Engineering* (April 1975) 66. The real future for large-scale chromatography.
25. SAID, A. S.: *American Laboratory* (June 1983) 17; *ibid*: (August 1983) 38. Calculations of a continuous and preparative gas chromatograph.
26. SHINGARI, M. K., CONDER, J. R. and FRUITWALA, N. A.: *J. Chromatog.* **285** (1984) 409. Construction and operation of a pilot scale production gas chromatograph for separating heat-sensitive materials.
27. RYAN, J. M. and DIENES, G. L.: *Drug. and Cosmetic Industry* **99** (4) (1966) 60. Plant-scale gas chromatography.
28. TIMMINS, R. S., MIR, L. and RYAN, J. M.: *Chem. Engg. Albany*, **76** (19 May, 1969) 170. Large-scale chromatography: new separation tool.
29. VALENTIN, P., HAGENBACH, G., ROZ, B. and GUIOCHON, G.: In *Gas Chromatography* 1972, PERRY, S.G., ed. (Institute of Petroleum, 1973) p. 157, New Advances in the Operation of Large-Scale Gas Chromatographic Units.
30. BONMATI, R. and GUIOCHON, G.: *Perfumer and Flavourist* **3** (October, 1978) 17. Gas chromatography as an industrial process operation — application to essential oils.
31. SAKODYNSKII, K. I., VOLKOV, S. A., KOVANKO, Y. A., ZELVENSKII, V. U., REZNIKOV, V. I. and AVERIN, V. A., *J. Chromatog.* **204** (1981) 167. Design of and experience in operating technological preparative installations.
32. HILAIREAU, P. and COLIN, H.: *Chromatogr. Soc. Bull.* **26** (1987) 10. Gas chromatography: a real industrial separation process.
33. CONDER, J. R.: *Manuf. Chemist.* **55** (1984) 38. GC scales up to production.
34. CAREL, A. B., CLEMENT, R. E. and PERKINS, G.: *J. Chromatog. Sci.* **7** (1969) 218. Construction and operation of a gas chromatograph using sectional one foot diameter columns.
35. CAREL, A. B. and PERKINS, G.: *Analyt. Chim.* **34** (1966) 83. Gas chromatographic fractionation as a supplement and replacement for laboratory distillation.
36. GYIMESI, J. and SZEPESY, L.: *Chromatographia* **9** (1976) 195. Experiences with the development and operation of a large scale preparative gas chromatograph.
37. Literature of Prochrom SA (later Separex), B.P.9, 54250 Champigneulles, France.
38. BERNARD, J. R., GOURLIA, J-P. and GUTTIERREZ, J.: *Chem. Eng. Albany* **88** (18 May, 1981) 92. Separating paraffin isomers using chromatography.
39. VERZELE, M., DE CONINCK, M., VINDEVOGEL, J. and DEWAELE, C.: *J. Chromatog.* **450** (1988) 47. Column hardware in preparative liquid chromatography.
40. DONE, J. N.: *J. Chromatog.* **125** (1976) 43. Sample loading and efficiency in adsorption, partition and bonded-phase high-speed liquid chromatography.
41. PIRKLE, W. H.: cited in ref. (42).
42. HAYWOOD, P. A. and MUNRO, G., in *Developments in Chromatography*, Vol. 2 (KNAPMAN, C. E. H. ed.), Chapter 2, Preparative Scale Liquid Chromatography (Applied Science, 1980).
43. WANKAT, P. C.: In *Handbook of Separation Process Technology*, ROUSSEAU, R. W., ed. (Wiley, 1987) Chapter 14, Large-Scale Chromatography.
44. JONES, K.: *Symposium on Advances in Chromatography* (Chromatographic Society and Royal Society of Chemistry), Warrington, November 1986, reported in *Chrom. Soc. Bull.* **25** (1987) 23. Large-Scale HPLC.
45. HUPE, K. P.: *J. Chromatog. Sci.* **9** (1971) 11. Efficiency of production GLC.
46. CONDER, J. R.: In *New Developments in Gas Chromatography*, PURNELL, J. H., ed. (Wiley, 1973) 137–186, Production-Scale Gas Chromatography.
47. GAREIL, P. and ROSSET, R.: *Analysis* **10** (1982) 397. La chromatographie en phase liquide préparative par développment par élution.
48. CONDER, J. R. and SHINGARI, M. K.: *J. Chromatog. Sci.* **11** (1973) 525. Throughput and band overlap in production and preparative chromatography.

This book belongs to Bradley Loren (bloren@mcandrews-ip.com) Copyright Elsevier 2024

Intas Exhibit 1032
Page 468 of 470
PGR2025-00043

49. CHEH, C. H.: *J. Chromatogr*. **A, 658** (1994) 283. Advances in preparative gas chromatography for hydrogen isotope separation.
50. CONDER, J. R.: *Chromatographia* **8** (1975) 60. Performance optimisation for production gas chromatography.
51. MOSCARIELLO, J., PURDOM, G., COFFMAN, J., ROOT, T. W. and LIGHTFOOT, E. N.: *J. Chromatogr.* **A, 908** (2001) 131. Characterising the performance of industrial-scale columns.
52. KNOX, J. H. and PYPER, H. M.: *J. Chromatog.* **363** (1986) 1. Framework for maximising throughput in preparative liquid chromatography.
53. GRUSHKA, E., ed.: *Preparative-Scale Chromatography* (Dekker, 1989). Reprinted from *Sep. Sci. Technol.* **22** (Nos. 8–10), (1987) 1791–2110. (Several articles in this volume deal with optimisation).
54. COX, G. B. and SNYDER, L. R.: *LC-GC* **6** (1988) 894. Preparative and process-scale HPLC.
55. GOLSHAN-SHIRAZI, S. and GUIOCHON, G.: *J. Chromatog.* **A, 658** (1994) 149. Modelling of preparative liquid chromatography.
56. NICOUD, R. M. and PERRUT, M.: in COSTA, C. A. and CABRAL, J. S. (eds.) *Chromatographic and Membrane Processes in Biotechnology* (Kluwer Academic Publishers, 1991) p.381. Operating modes, scale-up and optimisation of chromatographic processes.
57. PORSCH, B.: *J. Chromatogr.* **A, 658** (1994) 179. Some specific problems in the practice of preparative high performance liquid chromatography.
58. LEAVER, G., CONDER, J. R. and HOWELL, J. A.: *Sep. Sci. Tech.* **22** (1987) 2037. A method development study of the production of albumin from animal blood by ion-exchange chromatography.
59. CHASE, H. A.: *J. Chromatog.* **297** (1984) 179. Prediction of the performance of preparative affinity chromatography.
60. ARNOLD, F. H., CHALMERS, J. J., SAUNDERS, M. S., CROUGHAN, M. S., BLANCH, H. W. and WILKE, C. R.: *ACS Sympos. Ser.* **271** (1985), Chap. 7. A rational approach to the scale-up of affinity chromatography.
61. HORSTMAN, B. J. and CHASE, H. A.: *Chem. Eng. Res. Des.* **67** (1989) 243. Modelling the affinity adsorption of immunoglobulin G to protein A immobilised to agarose matrices.
62. FERNANDEZ, M. A., LAUGHINGHOUSE, W. S., and CARTA, G.: *J. Chromatogr*. **A**, **746** (1996) 184–198. Characterisation of protein adsorption by composite silicapolyacrylamide gel anion exchanges II: mass transfer in packed columns and predictability of breakthrough behaviour.
63. CONDER, J. R. and HAYEK, B. O.: *Biochem. Eng. J.* **6** (2000) 225. Adsorption and desorption kinetics of bovine serum albumin in ion-exchange and hydrophobic interaction chromatography on silica matrices.
64. LEONARD, M.: *J. Chromatogr.* B, **699** (1997) 3. New packing materials for protein chromatography.
65. ROPER, D. K. and LIGHTFOOT, E. N.: *J. Chromatogr*. A, **702** (1995) 3. Separation of biomolecules using adsorptive membranes.
66. STOWELL, J. D. BAILEY, P. J. and WINSTANLEY, D. J. (eds.): *Bioactive Microbial Products* 3: *Downstream Processing* (Academic Press, 1986).
67. VERRALL, M. S. and HUDSON, M. J. (eds.): *Separations for Biotechnology* (Ellis Horwood, 1987).
68. MCGREGOR, W. C.: *Ann. N. Y. Acad. Sci.* **413** (1983) 231. Large scale isolation and purification of proteins from recombinant *E. coli.*
69. ANSPACH, F. B., CURBELO, D., HARTMANN, R., GARKE, G. and DECKWER, W. D.: *J. Chromatogr.* A, **865** (1999) 129. Expanded-bed chromatography in primary protein purification.
70. MENET, J. M. and THIÉBAUT, D.: *Countercurrent Chromatography* (Marcel Dekker, 1999).
71. GANETSOS, G. and BARKER, P. E.: *Preparative and Production Scale Chromatography* (Marcel Dekker, 1993).
72. PYNNONEN, B.: *J. Chromatogr.* **A, 827** (1998) 143. Simulated moving-bed processing: escape from the high-cost box.
73. CHARTON, F. and NICOUD, R. M.: *J. Chromatogr.* **A, 702** (1995) 97. Complete design of a simulated moving bed.
74. AZEVEDO, D. C. S., PAIS, L. S. and RODRIGUES, A. E.: *J. Chromatogr*. **A, 865** (1999) 187. Enantiomers separation by simulated moving-bed chromatography.
75. BARKER, P. E., in *Developments in Chromatography Vol*. 1 (ed. KNAPMAN, C. E. H.), Chapter 2, Developments in Continuous Chromatographic Refining (Applied Science, 1978).
76. PURNELL, J. H.: *Phil. Trans. Roy. Soc. Lond.* **A305** (1982) 657. The current chromatographic scene.
77. COCA, J., ADRIO, G., JENG C. Y. and LANGER, S. H.: In *Preparative and Production-scale Chromatography*, GANETSOS, G. and BARKER, P. E. (eds.) (Marcel Dekker, 1993), Chapter 19. Gas and liquid chromatographic reactors.
78. ADACHI, S.: *J. Chromatogr.* **A, 658** (1994) 271. Simulated moving-bed chromatography for continuous separation of two components and its application to bioreactors.
79. CONDER, J. R. and FRUITWALA, N. A.: *Chem. Eng. Sci.* **36** (1981) 509. Comparison of plate numbers and column lengths in chromatography and distillation.

This book belongs to Bradley Loren (bloren@mcandrews-ip.com) Copyright Elsevier 2024

Intas Exhibit 1032
Page 469 of 470
PGR2025-00043

19.12. NOMENCLATURE

		Units in SI System	Dimensions in **M, N, L, T**
A	Coefficient in equation 19.10 (Table 19.1)	m	**L**
B	Coefficient of $1/u$ in equation 19.10 (Table 19.1)	m^2s	$\mathbf{L}^2\ \mathbf{T}^{-1}$
C_s, C_m	Coefficient of u in equation 19.10 (Table 19.1)	s	**T**
c	Concentration of solute in mobile phase	kg/m^3	$\mathbf{ML}^{-3}$
D_m	Diffusivity of solute in mobile phase	m^2s	$\mathbf{L^2\ T^{-1}}$
D_s	Diffusivity of solute in stationary phase	m^2s	$\mathbf{L}^2\ \mathbf{T}^{-1}$
d_f	Effective thickness of stationary liquid "film"	m	**L**
d_p	Diameter of packing particles	m	**L**
H	Plate height	m	**L**
K	Distribution coefficient of solute between the two phases	—	—
k'	Capacity factor (mass distribution coefficient, $= n_s/n_m$); mean capacity factor for two solutes	—	—
L	Column length	m	**L**
N	Number of theoretical plates in column	—	—
n_m, n_s	Number of moles of solute in equilibrated mobile and stationary phases in elemental length of column	kmol	**N**
q	Concentration of solute in/on stationary phase	kg/m^3	$\mathbf{ML}^{-3}$
R	Retention ratio (equation 19.1)	—	—
R_s	Resolution	—	—
t_M	Mobile phase hold-up time in column	s	**T**
t_R	Retention time of solute in column	s	**T**
t'_R	Adjusted retention time, $= t_R - t_M$	s	**T**
t_w	Band width measured at base (Figure 19.3)	s	**T**
u	Average mobile-phase velocity, = (superficial velocity)/ε	m/s	$\mathbf{LT}^{-1}$
u_R	Velocity of migration of solute band	m/s	$\mathbf{LT}^{-1}$
α	Separation factor (selectivity factor) (equation 19.12)	—	—
γ	Obstruction (labyrinth) factor for diffusion through packed bed	—	—
ε	Packing voidage (interstitial plus intraparticle)	—	—
λ	"Eddy diffusion" constant in packed bed	—	—
ω	Packing geometry factor	—	—

This book belongs to Bradley Loren (bloren@mcandrews-ip.com) Copyright Elsevier 2024

Intas Exhibit 1032
Page 470 of 470
PGR2025-00043